UNIVERSITÀ DELLA CALABRIA

Dipartimento di Biologia, Ecologia e Scienze della Terra (DiBEST)

Dottorato di Ricerca in

Scienze e Ingegneria dell'Ambiente, delle Costruzioni e dell'Energia

CICLO

XXX

Compositional and textural study of beach sands from active volcanic areas (southern Tyrrhenian sea)

Settore Scientifico Disciplinare

GEO 02 – GEOLOGIA STRATIGRAFICA E SEDIMENTOLOGIA

Coordinatore: Ch. Prof. Salvatore CRITELLI

Firma

Tutors: Prof.ssa Rosanna De Rosa

Firma

Prof.ssa Emilia LE PERA

Firma

Co-Tutor: Prof.ssa Kathleen M. MARSAGLIA

Firma

Dottorando: Consuele MORRONE

Firma

TABLE OF CONTENTS

ABSTRACT iv
-INTRODUCTION- 1
-Chapter 1- Provenance Study- 6
1.1 - Factors that control sediment and texture composition - 6
1.1.1 – Climate - 7
1.1.2 – Slope gradient - 9
1.1.3 – Transport influence - 10
1.2 - Volcaniclastic particles - 12
1.2.1 - Volcaniclastic particles in provenance studies - 16
1.2.2 - Volcaniclastic rocks as oil reservoirs - 19
1.3 - Relationship between provenance and tectonic setting - 20
-Chapter 2 -Study areas- 21
2.1 - Geological setting of Aeolian Province - 21
2.1.1 – Petrography and classification of Aeolian islands source rocks - 25
2.1.1.a - Alicudi Island - 25
2.1.1b - Filicudi Island - 27
2.1.1c – Salina Island - 28
2.1.1d - Lipari Island – 30
2.1.1e - Vulcano Island - 31
2.1.1f - Panarea Island – 32
2.1.1g - Stromboli Island - 34
2.2 - Geological setting of Campania Province - 35
2.2.1 – Petrography and classification of Campania province source rocks - 40
2.2.1a – Phlegrean Fields – 41
2.2.1b – Mount Vesuvius – 43
2.2.1c – Volturno River drained source rocks – 47
-Chapter 3 - Sample locations- 50
3.1 – Aeolian Islands- 50
3.1a - Alicudi island - 51
3.1b - Filicudi island - 53
3.1c - Salina island - 55
3.1d - Lipari island - 57
3.1e - Vulcano island - 59
3.1f - Panarea island - 60
3.1g - Stromboli island – 62

3.2 – Campanian Province - 64
Chapter 4 Methods and Results 69
4.1 – Sieving analysis -..... 69
4.1.1 – Aeolian Islands sieving analysis results-..... 70
4.1.1a - Alicudi island – 70
4.1.1b - Filicudi island –..... 71
4.1.1c - Salina island – 72
4.1.1d – Lipari island –..... 73
4.1.1e – Vulcano island – 74
4.1.1f – Panarea island – 75
4.1.1g – Stromboli island – 76
4.1.2 – Campania province sieving analysis results-..... 78
4.1.2a – Volturno-Licola coastal stretch –..... 78
4.1.2b – Bacoli-Naples coastal stretch – 80
4.1.2c – Portici-Sorrento coastal stretch –..... 83
4.2 - Polarizing microscope and Electron Microprobe analyses – 86
4.2.1 – Grain types and modal composition -..... 89
4.2.1a - Volcanic lithic fragments - 90
4.2.1b - Minor constituents - 91
4.2.1.1 – Aeolian Islands – 91
4.2.1.1a - Monomineralic components -..... 91
4.2.1b – Modal composition –..... 92
4.2.1.2 – Campanian province - 106
4.2.1.2a - Monomineralic components and lithic fragments -..... 106
4.2.1.2c – Heavy minerals study – 121
4.2.2 - Roundness study (optical microscope) –..... 126
4.2.2.1 – Aeolian Islands -..... 127
4.2.2.2 – Campania province -..... 144
4.3 – ROUNDNESS STUDY- (IMAGE ANALYSIS) - 154
4.3.1 – Thin section image analysis results-..... 156
4.3.2 – Bulk granular sample results-..... 169
4.4 – Aeolian Islands GIS analysis (SGI calculation) - 183
4.4.1 – Alicudi island drainage basins characteristics -..... 184
4.4.2 – Filicudi island drainage basins characteristics - 186
4.4.3 – Salina island drainage basins characteristics -..... 188
4.4.4 – Lipari island drainage basins characteristics -..... 192

4.4.5 – Vulcano island drainage basins characteristics - 194
4.4.6 – Panarea island drainage basins characteristics - 197
4.4.7 – Stromboli island drainage basins characteristics - 200
-Chapter 5 – Discussion - 203
-Chapter 6 – Conclusions- 218
- Future work – 221
-References- 222
-Petrographic PLATES- 239
APPENDIX A (point counting raw data) 258
APPENDIX B (recalculated petrographic parameters) 334
APPENDIX C (roundness recalculated parameters [optical microscope]) 342

ABSTRACT

The main goal of this research focuses on the provenance, compositional and textural investigation of modern sand supplied from volcanic terrains (southern Tyrrhenian sea). This is a contribution to quantify the controls on volcaniclastic sand composition among volcanic areas with different tectonic settings and compositions. Specifically, an important aim of this research is to quantitatively compare the relation between areal distribution, texture and composition of “source” lithotypes – which are the clastic debris producer – with respect to texture and composition of "volcano-derived" sediments.

The study area covers the coastal perimeter/stretch of two Italian volcanic provinces in the southern Tyrrhenian sea: Aeolian islands and Campania province. Particular attention has been given to the factors that control the relationships between grain rounding, grain-size, sand composition, texture and source rocks. This research provide a good opportunity to define the provenance signatures of detritus eroded from lavas with different compositions, pyroclastic and minor sedimentary rocks. Different sandy petrofacies for the studied areas of Campania province have been formalized.

In order to investigate on provenance, pre-burial processes, composition and texture of modern sand supplied from volcanic terrains, different studies have been carried out through:

- Sieving analyses;
- Polarizing microscope and Electron Microprobe;
- Image analysis (roundness study);
- Geographic Information System analysis (SGI calculation).

There is a clear differences between Aeolian Islands costal beach sand and Campania coastal beach sand in terms of detritus maturity. Grain-size distribution within Aeolian beach sediment show a tendency towards coarser sand fraction to gravel, whereas Campania coastal samples show a tendency towards medium to fine sand fractions; this indicates a varied physical disintegration of the source rocks.

The major components of Aeolian islands and Campania beach sands are monomineralic grains, sedimentary and volcanic lithic fragments with lesser amounts of calcareous bioclasts. Samples from Aeolian islands and Portici Sorrento coastal stretch have an high percentage of volcanic lithic fragments (Lvl > Lvmi> Lvv), whereas samples from Pozzuoli, display an average percentage among Lvl~Lvmi~Lvv. Three

different petrofacies have been defined along Campania coastal stretch: sedimentary (Apennines), Vesuvian and Phlegrean fields petrofacies.

Stromboli, Vulcano, Alicudi and Filicudi sands have a dual basaltic/shoshonitic and andesitic composition "signatures". Panarea, Lipari and Salina sands have a wider range of composition "signatures" ranging from basalts to rhyolites. there is evidence that, on Aeolian islands, sand composition does accurately reflect bedrock composition except in the case of source areas dominated by pumice outcrops (e.g. Lipari islands), whereas in more protected and quite beach-environment such as Pozzuoli bay, this grain types (pumice, associated to more evolved [acid] volcanism and then explosive volcanism) have been found and resulted to be texturally more preserved.

In the sandy detritus the persistence for the lithic grains is ranked as follows: Lvlblg, Lvmiblgl, Lvvblgl > Lvlbrgl, Lvmibrlgl, Lvvbrgl > Lvlclgl, Lvmiclgl, Lvvclgl > Lvf > Lvlgrgl, Lvmigrgl, Lvvgrgl, pumice. Thus, mafic source rocks will be overestimated and more acid source rocks will be underestimated in the stratigraphic record.

New volcanic lithic compounds have been introduced (*Lvlgrgl*, *Lvmigrgl*, *Lvvgrgl*) then who will study the ancient stratigraphic records will know that the Lvlgrgl means dacitic provenance.

New discriminating diagrams have been introduced which allow to obtain important information among the volcanic source rocks ranging from basic to acid composition.

Lvlblgl, Lvmiblgl, Lvvblgl (1); Lvlbrgl, Lvmibrgl, Lvvbrgl (2); *Lvlgrgl, Lvmigrgl, Lvvgrgl* (3) can be produced not only by basaltic, andesitic and dacitic source rocks but also by source rocks with the same SiO2 content belonging at different alkaline series (e.g. trachybasalt, shoshonite, latite, trachyandesite, trachydacite, trachyte).

Campania samples displaying an higher roundness degree which decrease towards Phlegrean Fields area from north (Volturno river-mouth) to south and, show an higher percentage of (3), (4), (5) and (6) roundness category, whereas Aeolian islands samples have an higher percentage of (1) and (2) roundness category.

There is a correlation between roundness and geographic location of the Aeolian islands beaches. Sand grains round more efficiently under gentler wave action of the eastern side whereas the more angular grains of the north-western beaches are immediately eroded from the nearby cliffs with null or quite minimal reworking.

A new methodological and research approach for roundness degree calculation have been tested by conducting image analysis.

By relating GIS, compositional and textural results, it is possible to affirm that lavas

source rocks have an higher propensity to create sandy detritus than pyroclastic source rocks. This finding has implications for the stratigraphic record especially for the sandy pumice clasts which could be underrepresented in older volcaniclastic deposits and overrepresented in other detritus size fractions.

This actualistic study helps in understanding factors controlling siliciclastic sediment composition and texture, in turn, will help in deciphering major controls on ancient volcaniclastic successions, especially those where volcanic terrains have been totally lost by erosion.

LIST OF TABLES

Table 2.1 - Age and composition of volcanism in Campania province (modified from Peccerillo 2005). 36

Table 3.1 – Table displaying name, latitude, longitude, localities and sampling environment of each sample collected on Alicudi island (UTM coordinates system). 51

Table 3.2 – Table displaying name, latitude, longitude, localities and sampling environment of each sample collected on Filicudi island (UTM coordinates system). 53

Table 3.3 – Table displaying name, latitude, longitude, localities and sampling environment of each sample collected on Filicudi island (UTM coordinates system). 55

Table 3.4 – Table displaying name, latitude, longitude, localities and sampling environment of each sample collected on Lipari island (UTM coordinates system). 57

Table 3.5 – Table displaying name, latitude, longitude, localities and sampling environment of each sample collected on Vulcano island (UTM coordinates system). 59

Table 3.6 – Table displaying name, latitude, longitude, localities and sampling environment of each sample collected on Panarea island (UTM coordinates system). 61

Table 3.7 – Table displaying name, latitude, longitude, localities and sampling environment of each sample collected on Stromboli island (UTM coordinates system). 62

Table 3.8 – Table displaying name, latitude, longitude, localities and sampling environment of each sample collected along Campania coastal strech (UTM coordinates system). Samples are grouped from north to south. 65

Table 3.8 (continued) – Table displaying name, latitude, longitude, localities and sampling environment of each sample collected along Campania coastal strech (UTM coordinates system). Samples are grouped from north to south. 66

Table 4.1 – Grain-size distribution. Vc: Very coarse; C: Coarse; m: Medium; f: Fine; Vf: Very fine. 70

Table 4.2 – Granulometric distribution. Vc: Very coarse; C: Coarse; m: Medium; f: Fine; Vf: Very fine. 71

Table 4.3 – Granulometric distribution. Vc: Very coarse; C: Coarse; m: Medium; f: Fine; Vf: Very fine. 72

Table 4.4 – Granulometric distribution. Vc: Very coarse; C: Coarse; m: Medium; f: Fine; Vf: Very fine (data are from Morrone et al., 2017). 73

Table 4.5 – Granulometric distribution. Vc: Very coarse; C: Coarse; m: Medium; f: Fine; Vf: Very fine..... 74

Table 4.6 – Granulometric distribution. Vc: Very coarse; C: Coarse; m: Medium; f: Fine; Vf: Very fine..... 75

Table 4.7 – Granulometric distribution. Vc: Very coarse; C: Coarse; m: Medium; f: Fine; Vf: Very fine..... 76

Table 4.8 – Granulometric distribution. Vc: Very coarse; C: Coarse; m: Medium; f: Fine; Vf: Very fine..... 78

Table 4.9 – Grain-size distribution. Vc: Very coarse; C: Coarse; m: Medium; f: Fine; Vf: Very fine..... 80

Table 4.10 – Grain-size distribution. Vc: Very coarse; C: Coarse; m: Medium; f: Fine; Vf: Very fine..... 83

Table 4.11 - Grain-size vs. sampling environments. HtB: high-tide berm; LtB: low-tide berm; Dn: dune; FB: fluvial bar; RM: river mouth; SDC: slope detrital cone; SwZ: swash zone; Cr: crater; Lc: lacustrine; LM: lake mouth; ShF: shoreface; Tot: total. 85

Table 4.12 - Key to counted parameters (modified from Marsaglia, 1992, 1993, Critelli et al., 2002; Dickinson, 1970). 88

Table 4 .13 – Degree of roundness class terminology and numerical indices. For this study was used the Folk's scale..... 89

Table 4.14 – Point-counting of heavy mineral analyses of 125 □m sand fraction (300 points) and grain percentages for each sample (data are from Le Pera and Morrone, 217). 123

Table 4.15 – Total mean roundness value of both volcanic lithic fragments and single crystal grains (TOT MR). GE = geographic exposure. SA = Salina island; L = Lipari island; V = Vulcano island; PN = Panarea island; STR = Stromboli island; AL = Alicudi island; Fi = Filicudi island. 141

Table 4.16 – Outcropping source rocks in the different drainage basins (geological map symbols are from Lucchi et al., 2013); ha = hectares 186

Table 4.17 – Lavas and pyroclastic rocks percentage calculated for each drainage basin and relative SGI values (e.g. Palomares and Arribas, 1993). L = lavas; P = Pyroclastic rocks; ha = hectares..... 186

Table 4.18 – Outcropping source rocks in the different drainage basins (geological map symbols are from Lucchi et al., 2013); ha = hectares..... 188

Table 4.19 – Lavas and pyroclastic rocks percentage calculated for each drainage basin and relative SGI values (e.g. Palomares and Arribas, 1993). L = lavas; P = Pyroclastic rocks.; ha = hectares..... 188

Table 4.20 – Outcropping source rocks in the different drainage basins (geological map symbols are from Lucchi et al., 2013); ha = hectares -(continued)-..... 190

Table 4.20 – Outcropping source rocks in the different drainage basins (geological map symbols are from Lucchi et al., 2013); ha = hectares -(continued)-..... 191

Table 4.20 – Outcropping source rocks in the different drainage basins (geological map symbols are from Lucchi et al., 2013); ha = hectares..... 192

Table 4.21 – Lavas and pyroclastic rocks percentage calculated for each drainage basin and relative SGI values (e.g. Palomares and Arribas, 1993). L = lavas; P = Pyroclastic rocks.; ha = hectares..... 192

Table 4.22 - Outcrop areas of each source rock concerning drainage systems. Bas-And: Basaltic Andesitic; And: Andesitic; Rhyol: Rhyolitic (modified from Morrone et al., 2017)..... 193

Table 4.23 - Basin areas, bedrock associations and Sand Generation Index for Lavas and Pyroclastic rocks. SGI: Sand Generation Index (e.g., Palomares & Arribas 1993); L: Lavas; P: Pyroclastic rocks; ha: hectares (modified from Morrone et al., 2017)..... 194

Table 4.24 – Outcropping source rocks in the different drainage basins (geological map symbols are from De Astis et al., 1994); L/P = lavas + pyroclasts; ha = hectares. 196

Table 4.25 – Lavas and pyroclastic rocks percentage calculated for each drainage basin and relative SGI values (e.g. Palomares and Arribas, 1993). L = lavas; P = Pyroclastic rocks.; ha = hectares..... 197

Table 4.26 – Outcropping source rocks in the different drainage basins (geological map symbols are from Lucchi et al., 2013); L = lavas; P = Pyroclastic rocks.; L/P = lavas + pyroclasts; S = sedimentary cover; ha = hectares. -(continued)- 198

Table 4.26 – Outcropping source rocks in the different drainage basins (geological map symbols are from Lucchi et al., 2013); L = lavas; P = Pyroclastic rocks.; L/P = lavas + pyroclasts; S = sedimentary cover; ha = hectares. 199

Table 4.27 – Lavas and pyroclastic rocks percentage calculated for each drainage basin and relative SGI values (e.g. Palomares and Arribas, 1993). L = lavas; P = Pyroclastic rocks.; ha = hectares. 199

Table 4.28 – Outcropping source rocks in the different drainage basins (geological map symbols are from Lucchi et al., 2013); L = lavas; P = Pyroclastic rocks.; L/P = lavas + pyroclasts; S = sedimentary cover; ha = hectares. –(continued)- 201

Table 4.28 – Outcropping source rocks in the different drainage basins (geological map symbols are from Lucchi et al., 2013); L = lavas; P = Pyroclastic rocks.; L/P = lavas + pyroclasts; S = sedimentary cover; ha = hectares. 202

Table 4.29 – Lavas and pyroclastic rocks percentage calculated for each drainage basin and relative SGI values (e.g. Palomares and Arribas, 1993). L = lavas; P = Pyroclastic rocks.; ha = hectares. 202

Table 5.1 – Differences between McBride and Picard (1987) and our roundness calculation technique. PN-11: tested sample. Key to grain shape categories. 1 = very angular; 2 = angular; 3 = sub-angular; 4 = sub-rounded; 5 = rounded; 6 = well rounded. 211

Table A-A - *Key to Grain Shape Categories. 1 = very angular; 2 = angular; 3 = sub-angular; 4 = sub-rounded; 5 = rounded; 6 = well rounded; Vc: very coarse sand fraction; C: coarse sand fraction; m: medium sand fraction; f: fine sand fraction; Vf: very fine sand fraction. 258

Table A-B -1- Qt: total quartz; F: feldspars; L: lithic fragments; Vc: very coarse sand fraction; C: coarse sand fraction; m: medium sand fraction; f: fine sand fraction; Vf: very fine sand fraction. 334

Table A-B -2- Lm: metamorphic lithics; Ls: sedimentary lithichs; Lv: volcanic lithics. Vc: very coarse sand fraction; C: coarse sand fraction; m: medium sand fraction; f: fine sand fraction; Vf: very fine sand fraction. 335

Table A-B -3- Lvl: lathwork texture; Lvmi: microlitic texture; Lvv: vitric texture. Vc: very coarse sand fraction; C: coarse sand fraction; m: medium sand fraction; f: fine sand fraction; Vf: very fine sand fraction. 336

Table A-B -4 - Lvf: felsitic texture; Lvmi: microlitic texture; Lvl: lathwork texture. Vc: very coarse sand fraction; C: coarse sand fraction; m: medium sand fraction; f: fine sand fraction; Vf: very fine sand fraction..... 337

Table A-B -5 - Pm: pumice grains; Lvl: lathwork texture; Lvmi: microlitic texture. Lvvbrgl: brown vitric texture; Lvvblgl: black vitric texture; Lvvclgl: colorless vitric texture. Vc: very coarse sand fraction; C: coarse sand fraction; m: medium sand fraction; f: fine sand fraction; Vf: very fine sand fraction. (Values are expressed as %)..... 338

Table A-B -6 - Lvvbrgl: brown vitric texture; Lvvblgl: black vitric texture; Lvvclgl: colorless vitric texture. BAS & AND: basaltic and andesitic provenance; ALT: altered volcanic grains; RIO & Dac: rhyolitic and dacitic provenance. Vc: very coarse sand fraction; C: coarse sand fraction; m: medium sand fraction; f: fine sand fraction; Vf: very fine sand fraction. (Values are expressed as %)..... 339

Table A-B -7- Bas_{Prov}: basaltic provenance; And_{Prov}: andesitic provenance; Dac_{Prov}: dacitic provenance. BAS & AND: basaltic and andesitic provenance; ALT: altered volcanic grains; RIO & Dac: rhyolitic and dacitic provenance. Vc: very coarse sand fraction; C: coarse sand fraction; m: medium sand fraction; f: fine sand fraction; Vf: very fine sand fraction. (Values are expressed as %)..... 340

Table A-B – 8 - VFR: volcanic rock fragments with all texture typologies accessory minerals; ACC: single grains of olivine, pyroxene, opaque; PLG: plagioclase. (Values are expressed as %)..... 341

Table A-C -1 – Key to grain shape categories. 1 = very angular; 2 = angular; 3 = sub-angular; 4 = sub-rounded; 5 = rounded; 6 = well rounded. Lvl = volcanic lithic with lathwork texture, Lvmi = volcanic lithic with microlitic texture, Lvv = volcanic lithic with vitric texture, Lvf = volcanic lithic with felsitic texture, Plag = plagioclase, Py = pyroxene; Ol = Olivine; Hb = hornblende (Lipari data are from Morrone et al., 2018). 343

Table A-C -2 – Key to grain shape categories. 1 = very angular; 2 = angular; 3 = sub-angular; 4 = sub-rounded; 5 = rounded; 6 = well rounded. Lvl = volcanic lithic with lathwork texture, Lvmi = volcanic lithic with microlitic texture, Lvv = volcanic lithic with vitric texture, Lvf = volcanic lithic with felsitic texture, Plag = plagioclase, Py = pyroxene; Ol = Olivine; Hb = hornblende (Lipari data are from Morrone et al., 2018). 344

Table A-C -3 – Key to grain shape categories. 1 = very angular; 2 = angular; 3 = sub-angular; 4 = sub-rounded; 5 = rounded; 6 = well rounded. Lvl = volcanic lithic with lathwork texture, Lvmi = volcanic lithic with microlitic texture, Lvv = volcanic lithic with vitric texture, Lvf =

volcanic lithic with felsitic texture, Pm: pumice grain; Plag = plagioclase, Py = pyroxene; K = k-feldspar. 345

Table A-C - 4 – Key to grain shape categories. 1 = very angular; 2 = angular; 3 = sub-angular; 4 = sub-rounded; 5 = rounded; 6 = well rounded. Lvl = volcanic lithic with lathwork texture, Lvmi = volcanic lithic with microlitic texture, Lvv = volcanic lithic with vitric texture, Lvf = volcanic lithic with felsitic texture, Pm: pumice grain; Plag = plagioclase, Py = pyroxene; Ol = Olivine. 346

Table A-C -5 – Key to grain shape categories. 1 = very angular; 2 = angular; 3 = sub-angular; 4 = sub-rounded; 5 = rounded; 6 = well rounded. Lss = siliciclastic sedimentary lithic; Lsc(xx) = crystalline carbonate sedimentary lithic; Lsc(micr) = micritic carbonate sedimentary lithic; Qm: monocrystalline quartz grain; Ca = calcite grain; K = K-feldspar. 347

Table A-C -6 – Key to grain shape categories. 1 = very angular; 2 = angular; 3 = sub-angular; 4 = sub-rounded; 5 = rounded; 6 = well rounded. Plag = plagioclase, Py = pyroxene; K = k-feldspar. 347

Table A-C – 7 – Key to grain shape categories. 1 = very angular; 2 = angular; 3 = sub-angular; 4 = sub-rounded; 5 = rounded; 6 = well rounded. Lvl = volcanic lithic with lathwork texture, Lvmi = volcanic lithic with microlitic texture, Lvv = volcanic lithic with vitric texture; Plag = plagioclase, Py = pyroxene; K = k-feldspar; Le = leucite. 349

LIST OF FIGURES

Figure 1.1 – Schematic representation of the system that influences the clastic sediments composition (modified from Johnsson, 1993)..... 6

Figure 1.2- Relationship between physical and chemical weathering based on climate parameters (modified from Louis Peltier, 1950). Studied areas are represented by rectangles (climatic data are from http://www.centrometeo.com). 7

Figure 1.3 – Stability series representation (modified from Goldich 1938) and alteration products. 8

Figure 1.4 - *Weathering-limited* and *transport-limited* erosion regimes: regolith thickness as a function of topography. 9

Figure 1.5 – This diagram shows the pre-burial process occurring in a stream based on grain-size and flow velocity (from Hjulström 1935). 12

Figure 1.6 – a) Classification and nomenclature of tuffs and ashes based on their fragmental composition (modified from Schmid, 1981); b) Classification of pyroclastic rocks and (c) pyroclastic sediments according to grain-size (modified from Fisher and Schminke, 1984). 15

Figure 1.7 – Panoramic view of bombs and lapilli field on Volcano island (Aeolian islands)... 15

Figure 1.8 - Tectonic setting of source terranes and volcaniclastic sedimentation (modified from Artemieva and Meissner, 2012); b) major types of magmatism associated with specific tectonic settings (modified from Wilson, 1995). 17

Figure 1.9 - Source rocks and volcaniclastic facies. (Chatam Islands volcanic complex in south Pacific Ocean, modified from James et al., 2011). 17

Figure 1.10 - During magmatic eruptions, several, and different, processes, give rise to a range of distinctive volcaniclastic facies (modified from Lucchi, 1980)..... 18

Figure 1.11 - Global oil and gas distribution in volcanic rock (modified from Zou Caineng et al., 2013). 19

Figure 2.1 - Location map of Aeolian volcanic islands and associated seamounts. TLF is the Tindari-Letojanni Fault system (modified from Lucchi et al., 2013). The red line highlights the ring-like structure. 21

Figure 2.2 - Schematic geodynamic setting of the Aeolian arc. A narrow Ionian plate is subducting beneath Calabria and the southern Tyrrhenian Sea. It is bounded to the west by the Tintari–Letojanni Fault (TLF) system (modified from Lucchi et al., 2013). 22

Figure 2.3 - Aeolian Arc subduction plan is localized along the Calabria's Ionian edge, immersion W-NW, inclination around 50°- 60° below the Tyrrhenian Sea (modified from Doglioni, 1999). 22

Figure 2.4 – a) Main tectonic lineaments that control the Aeolian Islands volcanism; b) temporal and spatial evolution, increase in K with age and from western to eastern islands; c) Depth of earthquakes between 1981 and 1986 (modified from De Astis et al., 2003)..... 23

Figure 2.5 – Temporal evolution of the volcanism of the Aeolian area, based on geochronogical data (modified from De Astis et al., 2003). 24

Figure 2.6 – a) K_2O Vs. SiO_2 classification diagrams for the Aeolian arc volcanics. Lines dividing arc tholeiitic (TH), calc-alkaline (CA), high-K calc-alkaline (HKCA) and shoshonitic (SHO) series (modified from Peccerillo et al., 2013); b) Sketch map of volcanic products series of the Marsili basin (Francalanci et al., 2007). 25

Figure 2.7 - K2O vs. SiO2 classification diagram for the Alicudi rocks (modified from Peccerillo and Taylor, 1976). 26

Figure 2.8 - (a) Total-alkali Vs. silica (TAS) and (b) potassium Vs. silica classification diagram for the Filicudi rocks (modified from Lucchi et al., 2013). 28

Figure 2.9 - Total alkali Vs. silica (TAS) diagram classification diagram for lavas and pyroclastic rocks from Salina island (modified from Lucchi et al., 2013). 29

Figure 2.10 - Total alkali Vs. silica (TAS) diagram classification diagram for lavas and pyroclastic rocks from Lipari island (modified from Lucchi et al., 2013). 31

Figure 2.11 - Total alkali Vs. silica (TAS) diagram classification diagram for lavas and pyroclastic rocks from Vulcano island (modified from Lucchi et al., 2013). 32

Figure 2.12 - Total alkali Vs. silica (TAS) diagram classification diagram for lavas and pyroclastic rocks from Panarea island (modified from Lucchi et al., 2013). The dashed line indicate the boundary between the alkaline and subalkaline fields of Irvine & Baragar (1971). 33

Figure 2.13 - Total alkali Vs. silica (TAS) diagram classification diagram for lavas and pyroclastic rocks from Stromboli island (modified from Lucchi et al., 2013). 34

Figure 2.14 - -- Location map of the Campania volcanoes (modified from Peccerillo 2005). ... 35

Figure 2.15 -- Geodynamic evolution model for the southern Italian Peninsula (modified from Peccerillo 2005). A) A continuous subduction zone of the Apulian-Ionian plate was active until about 0.8 Ma. B) Slab breakoff in the Apulian sector generated distension regime at the contact between Apulia and the southern Apennines; C) Sinking and rollback of the narrow Ionian slab generated suctioning of intraplate asthenosphere from the Apulia foreland; this was contaminated by sedimentary material and fluids from the subduction zone and generated a hybrid OIB-arc mantle wedge, whose melting gave the Campania volcanoes and Stromboli. .. 38

Figure 2.16 - -- Schematic geological map of the Campania Plain. The oldest volcanics of the area outcrop on lschia Island (modified from Scandone et al., 1991). 40

Figure 2.17 - --Geological and structural sketch map of Phlegrean fields (modified from Barberi et al., 1986)..... 42

Figure 2.18 - Plot of total alkalis vs. silica for Phlegrean Fields. Data are from Peccerillo, 2005 (a) and from Pappalardo and Mastrolorenzo, 2012 (b); c) schematic chronogram of Phlegrean Fields activity as recorded by stratigraphic successions (modified from Pappalardo and Mastrolorenzo, 2012). 43

Figure 2.19 - Schematic relationship between Vesuvius units and alluvial plain deposits (modified from Santacroce et al., 2003)..... 44

Figure 2.20 – Classification of Vesuvius volcanic products based on TAS diagram (a: modified from Peccerillo, 2005; b: modified from Santacroce et al., 2003). 45

Figure 2.21 -- Location map of Volturno River (modified from Corniello, 2010). 47

Figure 2.22 – Geological sketch map of the drained products of Volturno river. 1) Calcareous debris deposits; 2) Alluvial, lacustrine and marine clay - silt deposits or sand deposits; 3) Campania Ignimbrite, often covered by pyroclastic deposits; 4) Old tuffs; 5) Arenaceous-clayey-marly deposits; 6) Limestones and dolomite limestones; 7) Main faults; 8) Crater-shaped forms (modified from Corniello, 2010). 48

Figure 2.22 -- Campania Ignimbrite isopach map (in meters); 1: Carbonate mountains (modified from Corniello, 2010). 49

Figure 3.1 – Elevation model, map and sample location of Aeolian Islands. 50

Figure 3.2 – a) Qgis image showing the elevation classes, samples location and relative drainage basins of Alicudi island; b) very poorly sorted pocket beach (AL-5). 52

Figure 3.3 – Very poorly sorted beach (immature texture) ranging from gravel to sand in grain-size. Red circle shows the exact sampled point (AL-6). 52

Figure 3.4 – a) Qgis image showing the elevation classes, samples location and relative drainage basins of Filicudi island; b) very poorly sorted pocket beaches with an immature texture developed in correspondence of a slope detrital cones. 54

Figure 3.5 - Very poorly sorted beach with immature-texture on Filicudi islands. Circle: Fi-1 sample location..... 54

Figure 3.6 – Textural-maturity differences among Salina beaches. a) Well sorted sand (medium to fine sand, SA-14); b) very well sorted beach sand (medium to fine sand SA-3); c) very poorly sorted beach (boulders-pebbles, sand, SA-9); d) poorly sorted beach ranging from gravel to fine sand in grain-size (SA-12)..... 56

Figure 3.7 – Qgis image showing the elevation classes, samples location and relative drainage basins of Salina island. 56

Figure 3.8 – Poorly sorted beach ranging from very coarse to medium in grain-size on Salina island (Pollara, SA-5). 57

Figure 3.9 - Digital elevation map of Lipari island showing the boundaries of the drainage basins with respect to samples location (modified from Morrone et al., 2017). 58

Figure 3.11 – Qgis image showing the elevation classes, samples location and relative drainage basins of Vulcano island..... 60

Figure 3.12 – a) Well sorted (pocket) beach sand ranging from medium to coarse in grain-size, sampled on the eastern side of Vulcanello peninsula (V12); b) close-up of very poorly sorted beach ranging from coarse to medium in grain-size, it was sampled on the southernmost portion of Vulcano island (Gelso)..... 60

Figure 3.13 – Qgis image showing the elevation classes, samples location and relative drainage basins of Panarea island. 61

Figure 3.14 – Some sample sites and textural-maturity differences on Panarea beaches. a) Very well sorted sandy beach (PN-8); b) poorly sorted gravelly beach (PN-2), c) moderately sorted beach from Lisca Bianca islet ranging from very coarse to medium sand (PN-4); d) very poorly sorted beach consisting of cobbles and sand (PN-10). 62

Figure 3.15 – Qgis image showing the elevation classes, samples location and relative drainage basins of Stromboli island. STR-9 is the crater sample..... 63

Figure 3.16 – Some sample sites on Stromboli island. a) poorly sorted gravel-sandy beach near the main port (STR-1); b) very poorly sorted beach formed at the bottom of a slope detrital cone (STR-5); c) moderately sorted beach from Malpasso (STR-4); d) moderately sorted beach ranging from coarse to medium sand in grain-size (Ficogrande beach, STR-8)..... 63

Figure 3.17 – Digital elevation map of the Campanian province showing sample locations of both Mt. Vesuvius and Phlegrean Fields areas. 64

Figure 3.18 – a) Well sorted lake sand ranging from medium to very fine in grain size (PZ-20, Torrefumo); b) well sorted fluvial bar sand ranging from medium to very fine in grain-size (VO-1, Volturno river); c) very well sorted Volturno river mouth sand ranging from medium to very fine in grain-size (VO-3); d) moderately sorted slope detrital cone sand ranging from gravel to medium sand in grain-size (PZ-18)..... 67

Figure 3.19 – a) Very well sorted beach sand ranging from medium to fine in grain-size (PZ-13, Capo Miseno); b) very well sorted beach sand ranging from medium to very fine in grain-size (BC-2, Acqua Morta; 2); c) very well sorted beach sand showing an heavy mineral concentrations and a “traction carpet” ranging from medium to very fine in grain-size (VO-5, Castel Volturno); d) very well sorted sand ranging from medium to very fine in grain-size, it was sampled from dunal environment (Li-4, Licola mare)..... 68

Figure 3.20 – a) moderately sorted beach sand (TA-1). In the background is shown the Mt. Vesuvius (TA-1); b) poorly sorted crater sand (VE-2); c) very well sorted beach sand sampled from a dune (PZ-17); d) moderately sorted “black” beach sand from Sorrento (SO-3). 68

Figure 4.1 – Main step during sieving analyses..... 69

Figure 4.2 - Granulometric distribution. The particles diameter is shown on the x-axis, and the class weight on the y-axis. G: gravel; Vc: very coarse sand; C: coarse sand; m: medium sand; f: fine sand; Vf: very fine sand; S: silt..... 70

Figure 4.3 - Granulometric distribution. The particles diameter is shown on the x-axis, and the class weight on the y-axis. G: gravel; Vc: very coarse sand; C: coarse sand; m: medium sand; f: fine sand; Vf: very fine sand; S: silt..... 71

Figure 4.4 - Granulometric distribution. The particles diameter is shown on the x-axis, and the class weight on the y-axis. G: gravel; Vc: very coarse sand; C: coarse sand; m: medium sand; f: fine sand; Vf: very fine sand; S: silt..... 72

Figure 4.5 - Granulometric distribution. The particles diameter is shown on the x-axis, and the class weight on the y-axis. G: gravel; Vc: very coarse sand; C: coarse sand; m: medium sand; f: fine sand; Vf: very fine sand; S: silt (data are from Morrone et al., 2017)..... 73

Figure 4.6 - Granulometric distribution. The particles diameter is shown on the x-axis, and the class weight on the y-axis. G: gravel; Vc: very coarse sand; C: coarse sand; m: medium sand; f: fine sand; Vf: very fine sand; S: silt. 74

Figure 4.7 - Granulometric distribution. The particles diameter is shown on the x-axis, and the class weight on the y-axis. G: gravel; Vc: very coarse sand; C: coarse sand; m: medium sand; f: fine sand; Vf: very fine sand; S: silt. 75

Figure 4.8 - Granulometric distribution. The particles diameter is shown on the x-axis, and the class weight on the y-axis. G: gravel; Vc: very coarse sand; C: coarse sand; m: medium sand; f: fine sand; Vf: very fine sand; S: silt. 76

Figure 4.9 – Grain-size distribution. The particles diameter is shown on the x-axis, and the class weight on the y-axis. G: gravel; Vc: very coarse sand; C: coarse sand; m: medium sand; f: fine sand; Vf: very fine sand; S: silt. 79

Figure 4.10 – Grain-size distribution. The particles diameter is shown on the x-axis, and the class weight on the y-axis. G: gravel; Vc: very coarse sand; C: coarse sand; m: medium sand; f: fine sand; Vf: very fine sand; S: silt. 81

Figure 4.10 - (continued) – Grain-size distribution. The particles diameter is shown on the x-axis, and the class weight on the y-axis. G: gravel; Vc: very coarse sand; C: coarse sand; m: medium sand; f: fine sand; Vf: very fine sand; S: silt. 82

Figure 4.11 – Grain-size distribution. The particles diameter is shown on the x-axis, and the class weight on the y-axis. G: gravel; Vc: very coarse sand; C: coarse sand; m: medium sand; f: fine sand; Vf: very fine sand; S: silt. 83

Figure 4.11 - (continued) – Grain-size distribution. The particles diameter is shown on the x-axis, and the class weight on the y-axis. G: gravel; Vc: very coarse sand; C: coarse sand; m: medium sand; f: fine sand; Vf: very fine sand; S: silt. 84

Figure 4.12 – Most representative grain-size distributions from the two study areas. Campania province is dominated by medium and fine sand. The Aeolian Islands beaches sediments are mainly dominated by coarser fractions with respect to the Campania province beaches. Vc: very coarse; C: coarse; m: medium; f: fine..... 85

Figure 4.13 – Polarizing microscope connected to a point counter with automated stepper-stage. 87

Figure 4.14 - Grain roundness and sphericity classes used as visual comparator during point counting (modified from Powers 1953). 89

Figure 4.15 - Qt:F:L diagram. Qt: total quartz (monocrystalline + polycrystalline quartz); F: feldspars; L: all lithics. 93

Figure 4.16 – Single crystals vs. volcanic lithic grains in the medium sand fraction. a) Alicudi, (b) Stromboli, (c) Salina, (d) Panarea, (e) Filicudi islands sand samples. m= medium. 94

Figure 4.17 – Single crystals vs. lithic grains in the medium (a, c) and fine sand fractions (b, d). Lipari (a, b) and (b, c) Vulcano islands sand samples. m= medium; f= fine. Lipari data are from Morrone et al., 2018. 94

Figure 4.18 – Single crystals vs. lithic grains among the five sand fractions. a) Panarea; b) Salina; c) Alicudi; d) Filicudi; e) Stromboli crater sand; e) Stromboli beach sand. 95

Figure 4.19 – Main Stromboli streams from craters to beaches (torrential transport). High relief, it goes from 924 to 0 m.a.s.l. in short distances (about < 1.7 km minimum and < 3,5 km maximum). 96

Figure 4.20 – Ternary plot of relative proportions of Lm:Ls:Lv. Lm: metamorphic lithics; Ls: sedimentary lithics; Lv: volcanic lithics (modified from Marsaglia and Ingersoll, 1992). 97

Figure 4.21a – Ternary plot of relative proportions of Lvl:Lvmi:Lvv. Lvl: lathwork texture; Lvmi: microlitic texture; Lvv: vitric texture. Lipari data are from Morrone et al., 2017..... 97

Figure 4.21b – Grain-size vs. volcanic lithic texture. Vc: very coarse sand; C: coarse sand; m: medium sand; f: fine sand; Vf: very fine sand. 98

Figure 4.22 – Ternary plot of relative proportions of Lvf:Lvmi:Lvl. Lvf: volcanic lithic with felsitic texture; Lvmi: microlitic texture; Lvl: lathwork texture; Lipari data are from Morrone et al., 2017. 99

Figure 4.23 – Ternary plot of relative proportions of Lvvclgl:Lvvblgl:Lvvbrgl. Lvvclgl: vitric texture with colorless glass; Lvvblgl: vitric texture with black glass; Lvvbrgl: vitric texture with brown glass; Lipari data are from Morrone et al., 2017..... 100

Figure 4.24 – Ternary plot of relative proportions of Bas_{Prov}:And_{Prov}:Dac_{Prov}. Bas_{Prov}= Lvlblgl+Lvmiblgl; And_{Prov}= Lvlbrgl+Lvmibrgl; Dac_{Prov}= Lvlgrgl+Lvmigrgl. 101

Figure 4.25 – Ternary plot of relative proportions of BAS & AND:ALT/SUB:RIO & DAC. . 102

BAS & AND= Lvlblgl + Lvmiblgl + Lvvbl + Lvlbrgl + Lvmibrgl + Lvvbrgl; ALT/SUB= Lvlorgl + Lvmiorgl + Lvvorgl +Lvlalgl + Lvmialgl + Lvvalgl; RIO & DAC = Lvlgrgl + Lvmigrgl + Lvvgrgl + Lvlclgl + Lvmiclgl + Lvvclgl. al: altered glass in clay minerals and/or palagonite. 102

Figure 4.26 – Electron microprobe analyses of some grains found among Aeolian Islands beach sands. a) volcanic lithic grain having dacitic composition (SiO_2= 65.27; Na_2O+K_2O= 6.27) corresponding to a Lvmigrgl texture; b) volcanic lithic grain having dacitic composition (SiO_2= 70.57; Na_2O+K_2O= 7.20) corresponding to a Lvlgrgl texture; c) Enstatite basal section immersed in a glassy groundmass; d) Diopside single crystal in PN-2 sand sample. 103

Figure 4.27 – Electron microprobe analyses of some grains found among Aeolian Islands beach sands. a) Bytownite/anortite single crystal diagnostic of calc-alkaline magmas; b) Fe-Ti oxide (ilmenite) immersed in a glassy groundmass. 104

Figure 4.28 – a,b,d) ternary plot of relative proportions of BasProv:AndProv:DacProv. BasProv= Lvlblgl + Lvmiblgl; AndProv= Lvlbrgl + Lvmibrgl; DacProv= Lvlgrgl + Lvmigrgl. 105

Figure 4.29 – Ternary plot of relative proportions of volcanic rock fragments with all texture typologies (VFR), accessory minerals (ACC – single grains of olivine, pyroxene, opaque) and plagioclase (PLG). Shadow areas for andesitic source are from Mack & Jerzykiewicz (1989); shadow areas from Hawaiian Islands are from Marsaglia (1993). Lipari data are from Morrone et al., 2017. a) Lipari and Vulcano islands beach sand samples (medium and fine sand fraction); b) Salina, Filicudi and Alicudi islands medium sand fraction (for SA-1, Fi-3, AL-3 samples were plotted the 5 sand fractions); c) Panarea and Stromboli islands sand samples. 106

Figure 4.30 - Qt:F:L diagram (e.g. Dickinson, 1970). Qt: total quartz (monocrystalline + polycrystalline quartz); F: feldspars; L: all lithic fragments. 108

Figure 4.31 - Single crystals vs. lithic grains (% on y axis) in the medium sand fraction. The samples have been ordered from north (Volturno river mouth) to south (Sorrento) along Campania coastal stretch. a) from VO-1 to VO-10; b) from VO-11 to BC-3; c) from BC-1 to PZ-13; d) from PZ-10 to PZ-7; e) from PZ-6 to NA-3; f) from NA-2 to TA-1; g) from CA-3 to SO-1; h) Vesuvius craters samples. 110

Figure 4.32 – Single crystals vs. lithic grains among the five sand fractions. a) PZ-14 sand sample; b) PZ-8- sand sample; c) BC-1 sand sample. 111

Figure 4.33 – Ternary plot of relative proportions of Lm:Ls:Lv. Lm: metamorphic lithics; Ls: sedimentary lithics; Lv: volcanic lithics (modified from Marsaglia and Ingersoll, 1992). a) samples are from Volturno river mouth to Pozzuoli; b) samples are from Pozzuoli to Sorrento coastal stretch. 112

Figure 4.34 – Sedimentaclastic vs. volcaniclastic "SIGNAL" from Phlegran Fields to Volturno river mouth (from south to north). It is clearly evident how the volcaniclastic signal strongly decreases after Bacoli which probably marks the transition between volcanic and sedimentary petrofacies along the north Campania coastal stretch. 112

Figure 4.35 – Ternary plot of relative proportions of Lvl:Lvmi:Lvv. Lvl: lathwork texture; Lvmi: microlitic texture; Lvv: vitric texture. Samples goes from Volturno river-mouth to Sorrento village. 113

Figure 4.36 – Grain-size vs. volcanic lithic texture. Vc: very coarse sand; C: coarse sand; m: medium sand; f: fine sand; Vf: very fine sand. 114

Figure 4.37 – Ternary plot of relative proportions of Lvf:Lvmi:Lvl. Lvf: volcanic lithic with felsitic texture; Lvmi: microlitic texture; Lvl: lathwork texture. 115

Figure 4.38 – Ternary plot of relative proportions of Pm:Lvl:Lvmi. Pm: pumice grains; Lvl: lathwork texture; Lvmi: microlitic texture. 115

Figure 4.39 – Ternary plot of relative proportions of Lvvclgl:Lvvblgl:Lvvbrgl. Lvvclgl: vitric texture with colorless glass; Lvvblgl: vitric texture with black glass; Lvvbrgl: vitric texture with brown glass. Data are referred to entire Volturno-Sorrento coastal stretch. 117

Figure 4.40 – Ternary plot of relative proportions of Bas_{Prov}:And_{Prov}:Dac_{Prov}. Bas_{Prov}= Lvlblgl+Lvmiblgl; And_{Prov}= Lvlbrgl+Lvmibrgl; Dac_{Prov}= Lvlgrgl+Lvmigrgl. 118

Figure 4.41 – Ternary plot of relative proportions of BAS & AND:ALT:RIO & DAC. BAS & AND= Lvlblgl + Lvmiblgl + Lvvbl + Lvlbrgl + Lvmibrgl + Lvvbrgl; ALT= Lvlorgl + Lvmiorgl + Lvvorgl +Lvlalgl + Lvmialgl + Lvvalgl; RIO & DAC = Lvlgrgl + Lvmigrgl + Lvvgrgl + Lvlclgl + Lvmiclgl + Lvvclgl + Lvf. al: altered glass in clay minerals and/or palagonite..... 118

Figure 4.42 – Ternary plot of relative proportions of volcanic rock fragments with all texture typologies (VFR), accessory minerals (ACC – single grains of olivine, pyroxene, opaque) and plagioclase (PLG). Shadow areas for andesitic source are from Mack & Jerzykiewicz (1989); shadow areas from Hawaiian Islands are from Marsaglia (1993). 119

Figure 4.43 – Leucite and K-feldspar proportion vs. distance from Vesuvius volcanic edifice along Volturno river-mouth (north) to Sorrento village (south) coastal stretch. 120

Figure 4.44 – Heavy minerals samples location. Pozzuoli beaches: PZ-7, PZ-2 e PZ-12; Bacoli beache: BC-2; Volturno river-mouth area: VO-2 e VO-6. (modified from Le Pera and Morrone, 2018)..... 122

Figure 4.45 – Microprobe analysis of monomineralic and polymineralic grains. a) Spots 001, 002 and 003 show an opaque oxide with pseudobrookite composition [Fe_2TiO_5]. Spots 001 and 002 display pseudobrookite in monomineralic grain whereas spot 003 display pseudobrookite in volcanic lithic fragment [Op in Lvv]; b) Spots 008 shows an opaque oxide with pyrite composition [FeS_2] and spot 009 displays pseudobrookite in volcanic lithic fragment; c) Weathered volcanic lithic fragment or siliciclastic sedimentary polymineralic grain containing oxide opaque such as ilmenite [Fe_2+TiO_3]. d) Apatite and pseudobrookite in volcanic lithic fragment. Psbr = pseudobrookite, Pi = pyrite, Ilm = ilmenite, Qz = quartz, Ca = calcite, Apt = apatite. 124

Figure 4.46 – a) Relative abundances of opaques, pyroxene and amphibole in samples from Pozzuoli and Bacoli pocket beaches and of the Volturno river-mouth illustrating the difference between sedimentary provinces and the homogenization of the mineral association at delta environment. b) Different response to weathering of heavy minerals from Campania beach sands. c) Op= Opaques; To= Tourmaline; Py= Clinopyroxene; Anf= Amphibole; Bt= Biotite; Ru=Rutile; Gr= Garnet. Frequency and type of etched surface depends on crystal structure (etched morphology developed on cleavable pyroxenes and amphiboles, but less easily on other minerals) (modified from Le Pera and Morrone, 2018). 125

Figure 4.47 – Microphotographs showing the different roundness category. a) Very angular grain (1); b) angular grain (2); c) sub-angular grain (3); d) sub-rounded grain (4); e) rounded grain (5); f) well rounded grain (6)..... 127

Figure 4.48 – Mean roundness percentage of all grain typologies among Aeolian Islands. 128

Figure 4.49 – a) Torrential-type transport on Stromboli island; b) example of beach area calculation for STR-8 sample site on Stromboli island. 129

Figure 4.50 - Roundness degree among different grain types (single crystal grains and volcanic lithic fragments) vs. transport-distance on Stromboli island. 130

Figure 4.51 – Roundness degree vs. beach areas for Stromboli island beach sand (medium sand fraction). a) Single crystal grains roundness degree; b) Volcanic lithic fragments roundness degree. 131

Figure 4.52 – Roundness degree vs. beach areas for Panarea island beach sand (medium sand fraction). a) Volcanic lithic fragments roundness degree; b) single crystal grains roundness degree. 132

Figure 4.53 - Mean roundness vs. size of beaches area on Salina island (medium sand fraction). 133

Figure 4.54 – a) Single crystals Vs lithic grains; b,c) mean roundness vs. size of drainage basins (drainage basins area are from Morrone et al., 2017); d,e) mean roundness vs. size of beaches area (modified from Morrone et al., 2018)..... 134

Figure 4.55 - Mean roundness Vs size of beaches area on Vulcano island (medium sand fraction). 134

Figure 4.56 - Mean roundness vs. beaches area on Filicudi (upper) and Alicudi islands (lower). 136

Figure 4.57 - Mean roundness vs. grain-size for Alicudi (upper left), Filicudi (upper right), Panarea (lower left) and Salina islands (lower right). a) mean roundness degree among all grain types. 137

Figure 4.58 -- Mean roundness vs. grain-size for Stromboli beach sand (STR-1) and Stromboli crater sand (STR-9). a) mean roundness degree among all grain types; b) grain–size vs. mean roundness discriminated among the different volcanic lithic fragments; c) grain–size vs. mean roundness discriminated among single crystal grains. 138

Figure 4.59 – Geographic exposure of the developed sandy beaches among all the Aeolian Islands coastal perimeters. On the y axis is shown the sampled sandy beaches total number; on the x axis is shown the geographic exposure (NE = north-east, SE= south-east, SW = south-west, NW = north-west). 139

Figure 4.60 – Digital elevation map of Lipari island showing the different classes of slope, samples location and mean rounding of the analyzed sandy grain types (slope classes and hydrographic basins are from Morrone et al. 2017 and mean roundness data are from Morrone et al., 2018)..... 140

Figure 4.61 – Digital elevation map of Vulcano island showing the different classes of slope, samples location and mean rounding of the analyzed sandy grain types. 141

Figure 4.62 – Digital elevation map of Salina (upper) and Alicudi island (lower) showing the different classes of slope, samples location and mean rounding of the analyzed sandy grain types. 142

Figure 4.63 – Digital elevation map of Filicudi (upper) and Panarea island showing the different classes of slope, samples location and mean rounding of the analyzed sandy grain types. 143

Figure 4.64 – Digital elevation map of Stromboli island showing the different classes of slope, samples location and mean rounding of the analyzed sandy grain types. 144

Figure 4.65 – Mean roundness percentage of all grain typologies along Volturno-Sorrento coastal stretch. 145

Figure 4.66 – Mean roundness variation along Volturno-Sorrento coastal stretch (about 80 km from north to south Campania coastline). 146

Figure 4.67 – Mean roundness variation from Vesuvius crater to Portici, Torre del Greco, Torre Annunziata, Castellammare di Stabia (along about 15 km distance). 147

Figure 4.68 – Mean roundness vs. lithic fragments sand composition and their roundness variation along Volturno-Naples coastal stretch (about 46 km from north to south Campania coastline). 148

Figure 4.69 – Mean roundness vs. lithic fragments sand composition and their roundness variation along Portici-Sorrento coastal stretch (a), Castellammare di Stabia area (b) and Vesuvius crater sands (c)..... 149

Figure 4.71 – Mean roundness vs. single crystal grains sand composition and their roundness variation along Portici-Sorrento coastal stretch (a), Castellammare di Stabia area (b) and Vesuvius crater sands (c)..... 152

Figure 4.72 - Mean roundness degree vs. grain-size among all grain types. MR = mean roundness..... 153

Figure- 4.73 - Thin section (upper right) and bulk sample (upper left, lower) scanning method. 155

Figure 4.74 – Calibrated scale used to determine grains roundness class. 156

Figure 4.75 – AL-3-Vc thin section sample. a) Transmitted natural light scanned image; b) selected grains to analyzing; c) drawn grain boundaries by the software processing; d) circularity distribution values; e) roundness distribution values. Lower figure shows a close-up of the image processing steps..... 157

Figure 4.76 – AL-3-Vc sample. Red circle = circularity mean value; yellow triangle = roundness mean value; green square = optical microscope results plotted on Folk scale (upper). 158

Figure 4.77 – Fi--3-Vc thin section sample. a) Transmitted natural light scanned image; b) selected grains to analyzing; c) drawn grain boundaries by the software processing; d) circularity distribution values; e) roundness distribution values..... 158

Figure 4.78 – Fi-3-Vc sample. Red circle = circularity mean value; yellow triangle = roundness mean value; green square = optical microscope results plotted on Folk scale (upper). 159

Figure 4.79 – SA-1-Vc thin section sample. a) Transmitted natural light scanned image; b) selected grains to analyzing; c) drawn grain boundaries by the software processing; d) circularity distribution values; e) roundness distribution values..... 159

Figure 4.80 – SA-1-Vc sample. Red circle = circularity mean value; yellow triangle = roundness mean value; green square = optical microscope results plotted on Folk scale (upper). 160

Figure 4.81 – L2-m thin section sample. a) Transmitted natural light scanned image; b) selected grains to analyzing; c) drawn grain boundaries by the software processing; d) circularity distribution values; e) roundness distribution values. Red circle = circularity mean value; yellow triangle = roundness mean value; green square = optical microscope results plotted on Folk scale..... 161

Figure 4.82 – V5-m thin section sample. a) Transmitted natural light scanned image; b) selected grains to analyzing; c) drawn grain boundaries by the software processing; d) circularity distribution values; e) roundness distribution values. 162

Figure 4.83 – V5-m sample. Red circle = circularity mean value; yellow triangle = roundness mean value; green square = optical microscope results plotted on Folk scale (upper). 162

Figure 4.84 – PN-1-Vc thin section sample. a) Transmitted natural light scanned image; b) selected grains to analyzing; c) drawn grain boundaries by the software processing; d) circularity distribution values; e) roundness distribution values..... 163

Figure 4.85 – PN-1-Vc sample. Red circle = circularity mean value; yellow triangle = roundness mean value; green square = optical microscope results plotted on Folk scale (upper). 163

Figure 4.86 – STR-1-Vc thin section sample. a) Transmitted natural light scanned image; b) selected grains to analyzing; c) drawn grain boundaries by the software processing; d) circularity distribution values; e) roundness distribution values. 164

Figure 4.87 – STR-1-Vc sample. Red circle = circularity mean value; yellow triangle = roundness mean value; green square = optical microscope results plotted on Folk scale (upper). 164

Figure 4.88 – STR-9-Vc thin section sample. a) Transmitted natural light scanned image; b) selected grains to analyzing; c) drawn grain boundaries by the software processing; d) circularity distribution values; e) roundness distribution values. 165

Figure 4.89 – STR-9-Vc sample. Red circle = circularity mean value; yellow triangle = roundness mean value; green square = optical microscope results plotted on Folk scale (upper). 165

Figure 4.90 – a) VO-3-m sample; b) Li-1-m sample; c) BC-1-Vc sample; d) PZ-8-Vc sample; e) PZ-14-Vc sample; f) GA-1-m sample. Red circle = circularity mean value; yellow triangle = roundness mean value; green square = optical microscope results plotted on Folk scale. 167

Figure 4.91 – a) NA-1-m sample; b) PO-1-m sample; c) TG-1-m sample; d) TA-1-m sample; e) VE-1-m sample; f) CA-1-m sample; g) SO-1-m sample. Red circle = circularity mean value; yellow triangle = roundness mean value; green square = optical microscope results plotted on Folk scale..... 169

Figure 4.92 – Scanning method of a granular bulk sample. Image processing steps through ImageJ software. Real grains are on the upper left (pyroxene) and lower right (pumice). 170

Figure 4.93 –Example of a processed image (left) and scanned granular bulk sample (right). 171

Figure 4.94 –AL-3 sample image analyses results. a) Transmitted natural light scanned image; b) selected grains to analyzing; c) circularity distribution values; d) roundness distribution values..... 171

Figure 4.95 –Fi-3 sample image analyses results. a) Transmitted natural light scanned image; b) selected grains to analyzing; c) circularity distribution values; d) roundness distribution values. 172

Figure 4.96 (upper) - SA-1 sample image analyses results. Figure 4.97 (lower) L2 sample image analyses results. a) Transmitted natural light scanned image; b) selected grains to analyzing; c) circularity distribution values; d) roundness distribution values. 173

Figure 4.98 (upper) –V5 sample image analyses results. Figure 4.99 (lower) PN-1 sample image analyses results. a) Transmitted natural light scanned image; b) selected grains to analyzing; c) circularity distribution values; d) roundness distribution values. 174

Figure 4.100 (upper) –STR-1 sample image analyses results. Figure 4.101 (lower) STR-9 sample image analyses results. a) Transmitted natural light scanned image; b) selected grains to analyzing; c) circularity distribution values; d) roundness distribution values. 175

Figure 4.102 – VO-3 sample image analyses results. a) Transmitted natural light scanned image; b) selected grains to analyzing; c) circularity distribution values; d) roundness distribution values. 176

Figure 4.103 (upper) – Li-1 sample image analyses results. Figure 4.104 (lower) – PZ-8 sample image analyses results. a) Transmitted natural light scanned image; b) selected grains to analyzing; c) circularity distribution values; d) roundness distribution values. 177

Figure 4.105 (upper) – PZ-14 sample image analyses results. Figure 4.106 (lower) – GA-1 sample image analyses results. a) Transmitted natural light scanned image; b) selected grains to analyzing; c) circularity distribution values; d) roundness distribution values. 179

Figure 4.107 (upper) – NA-1 sample image analyses results. Figure 4.108 (lower) – PO-1 sample image analyses results. a) Transmitted natural light scanned image; b) selected grains to analyzing; c) circularity distribution values; d) roundness distribution values. 180

Figure 4.109 (upper) – TG-1 sample image analyses results. Figure 4.110 (lower) – TA-1 sample image analyses results. a) Transmitted natural light scanned image; b) selected grains to analyzing; c) circularity distribution values; d) roundness distribution values. 181

Figure 4.111 (upper) – VE-1 sample image analyses results. Figure 4.112 (lower) – CA-1 sample image analyses results. a) Transmitted natural light scanned image; b) selected grains to analyzing; c) circularity distribution values; d) roundness distribution values. 182

Figure 4.113 (lower) – SO-1 sample image analyses results. a) Transmitted natural light scanned image; b) selected grains to analyzing; c) circularity distribution values; d) roundness distribution values. 183

Figure 4.114 – Identified drainage basin (a,b), source rock lithologies (a) and grouped lithologies in lavas and pyroclastic rocks (b). 185

Figure 4.115 – Identified drainage basin (a,b), source rock lithologies (a) and grouped lithologies in lavas and pyroclastic rocks (b). 187

Figure 4.116 – Identified drainage basin (a,b), source rock lithologies (a) and grouped lithologies in lavas and pyroclastic rocks (b). 189

Figure 4.117 - TIN (triangular irregular network) of Lipari island showing the boundaries of the drainage basins with respect to samples (watershed) (modified from Morrone et al., 2017).... 193

Figure 4.118 – Identified drainage basin (a,b), source rock lithologies (a) and grouped lithologies in lavas and pyroclastic rocks (b). 195

Figure 4.119 – Identified drainage basin (a,b), source rock lithologies (a) and grouped lithologies in lavas and pyroclastic rocks (b). 198

Figure 4.120 – Identified drainage basin (a,b), source rock lithologies (a) and grouped lithologies in lavas and pyroclastic rocks (b) –(continued)- 200

Figure 4.120 – Identified drainage basin (a,b), source rock lithologies (a) and grouped lithologies in lavas and pyroclastic rocks (b). 201

Figure 5.1 - Campania petrofacies distribution based on sand composition along the studied coastal stretch. 206

Figure 5.2 - Sites showing heavy minerals “traction carpet” along Campania coastal stretch.. 210

Figure 5.3 – Mean roundness differences among Campania and Aeolian Islands sand samples. 212

Figure 5.4 – Mean roundness inherited from source rocks/crystalline habit. Pseudobrookite opaque minerals (red boundaries) and intra-crystalline apatite (green boundary). Yellow boundaries = glass. (BC-2, Campania coastal stretch). 214

Figure 5.5 – Real grains thin section scanned (on the left); red areas are grains (or grain parts) which have been recognized by the software (middle image); image processed and drawn by the software (on the right); red areas show errors in the roundness evaluation (not real grains), green areas represent the right grains analyzed. 216

PLATE I - Euhedral monocrystalline clinopyroxene with glassy rim and intracrystalline glass; (a) NX; (b) N//. (c) Lvvbrgl: Vitric volcanic lithic with brown glass; Sf: Devitrification with spherulitic texture (N//). (d) Vesiculated vitric lithic with black glass (Lvvblgl, N//). (e,f) Volcanic lithic with lathwork texture with brown glass (Lvlbrgl). Clearly visible are some phenocrysts of plagioclase (e: NX, f: N//), (modified from Morrone et al., 2017). 239

PLATE II - (a,b) Pl: grain of monocrystalline plagioclase; Lvldggl: volcanic lithic fragment with lathwork texture and dark gray glass; Lvmlblgl: volcanic lithic fragment with microlitic texture and black glass (a: NX, b: N//). (c,d) Volcanic lithic fragment with felsitic texture (*Lvf*, c: NX, d: N//). (e,f) Lvmlblgl: volcanic lithic fragment with microlitic texture with black glass; Pyc: angular monocrystalline clinopyroxene grains; Lvvclgl: vitric volcanic lithic colourless glass (e: NX, f: N//), (modified from Morrone et al., 2017). 240

PLATE III - (a,b) Lvldggl: volcanic lithic fragment with lathwork texture with dark grey glass; Pl: plagioclase; (a: NX, b: N//). (c,d) Lvvclgl: vitric volcanic lithic with colourless glass; Lvf: volcanic lithic fragment with felsitic texture; Lvlblgl: volcanic lithic fragment with lathwork texture with black glass (c: NX, d: N//). (e) Potassic fragment of a vitric volcanic lithic colourless glass (*Lvvclg*l) stained with sodium cobaltinitrite (N//). (f) Volcanic lithic fragment with microlitic texture with orange glass (*Lvmlorgl*, N//), (modified from Morrone et al., 2017). 241

PLATE IV - (a, b): Plagioclase with inter- and intra-crystalline orange glass (*Lvlorgl*, roundness category = 1, a: NX, b: N//); (c, d): euhedral olivine in *Lvlblgl* with roundness category = 2 (c: NX, d: N//); (e, f): *lathwork* volcanic lithic with grey glass (roundness category = 4, e: NX, f: N//). 242

PLATE V - (a, b): *microlitic* volcanic lithic with orange glass (*Lvlorgl*, roundness category = 3, a: NX, b: N//); (c, d): lathwork volcanic lithic with brown glass and plagioclase phenocrysts (*Lvlbrgl* showing an angular (2) roundness category, c: NX, d: N//); (e, f): *lathwork* volcanic lithic with grey (left) and brown (right) glassy groundmass (e: NX, f: N//). 243

PLATE VI - (a, b): volcanic lithic fragment with lathwork texture with orange glass; and pyroxene phenocrysts Pl: plagioclase; (a: NX, b: N//); (c, d): panoramic view of a Filicudi sand sample showing lithic fragments with *lathwork* texture, plagioclase and pyroxene phenocrysts (c: NX, d: N//); (e, f): volcanic lithic fragment with *lathwork* texture with black (left) and brown (right) glassy groundmass (e: NX, f: N//). 244

PLATE VII - (a, b): hornblende [001] and pyroxene single crystal grains; iddignsite in a glassy groundmass (right) (a: NX, b: N//); (c, d): very angular (1) biotite [010] single crystal grain (c: NX, d: N//); (e, f): plagioclase and pyroxene single crystal grains; sub-angular (3) to sub-rounded (4) oxides opaque minerals (e: NX, f: N//). 245

PLATE VIII - (a, b) [001] hornblende with angular roundness category (2) and volcanic lithic fragment with lathwork texture immersed in a grey groundmass *Lvlgrgl* (a: NX, b: N//); (c, d): sub-angular (3) pyroxene single crystal grain (right) and volcanic lithic fragments with *lathwork (grey)* and *microlitic* (brown) textures (c: NX, d: N//); (e, f): volcanic lithic with microlites

immersed in an orange groundmass (middle) and lathwork volcanic lithic with brown glass and plagioclase phenocryst (lower left) (e: NX, f: N//).....246

PLATE IX - (a): opaque mineral oxide with a rounded (5) roundness category (N//); (b): microlitic volcanic lithic with brown glass showing a sub-rounded (4) roundness category (N//); (c, d): sparitic limestone [Lsc(xx)] with a sub-rounded (4) roundness category (c: NX, d: N//); (e, f): micritic limestone [Lsc(micr)] showing a sub-angular (3) roundness category (e: NX, f: N//). 247

PLATE X - (a, b): Sanidine single crystal grain (stained) which shows a sub-rounded (4) roundness category (a: NX, b: N//); (c, d):calcareous bioclast (c: NX, d: N//); (e, f): very angular (1) well preserved pumice clast (e: NX, f: N//). 248

PLATE XI - (a, b): very angular (1) well preserved pumice grains from Torre Fumo like (a: NX, b: N//); (c, d) sub-angular (3) monocrystalline quartz (middle), sanidine single crystal grain (stained, lower left), sub-rounded (4) volcanic lithic with lathwork texture and brown groundmass (right) (c: NX, d: N//); (e, f): polycrystalline quartz and bioclast grains along Volturno-Licola coastal stretch (e: NX, f: N//). 249

PLATE XII - (a, b): Quartz and calcite in arenite (Rs: sedimentary rock fragments) (Rs (a: NX, b: N//); (c, d): sub-rounded (4) leucite single crystal grain stained with sodium cobaltinitrite (c: NX, d: N//); (e, f): polycrystalline quartz (Qp) and calcite (Ca) in arenite (Rs, fifth roundness category), calcite single crystal grain (upper right) (e: NX, f. N//). 250

PLATE XIII - (a, b): sub-angular (3) calcite single crystal grain (a: NX, b: N//); (c, d) sub-rounded (4) siliciclastic sedimentary lithic grain (Lss) (c: NX, d: N//); (e, f): altered volcanic lithic fragments (Lv alt) in palagonite and sericite (e: NX, f: N//). 251

PLATE XIV - (a, b): Chert grain (a: NX, b: N//); (c, d): sedimentary lithic grain with crystalline carbonate composition [Lss(xx)], siliciclastic sedimentary lithic (Lss), sedimentary lithic grain with micritic carbonate composition [Lss(micr)], polycrystalline quartz, angular (2) euhedral sanidine (right) single grain (c: NX, d: N//); (e, f): sub-angular brown garnet single grain (middle) (e: NX, f: N//). 252

PLATE XV - (a, b): rounded (5) monocrystalline quartz (a: NX, b: N//); (c, d): rounded (5) sedimentary lithic grain with micritic carbonate composition [Lss(micr)] (c: NX, d: N//); (e, f): calcite in a rounded (5) sedimentary rock fragment (Ca in Rs) (e: NX, f: N//).....253

PLATE XVI - (a, b): sub-rounded (4) volcanic lithic fragment with lathwork texture with black glass and plagioclase phenocrysts dispersed among sedimentary grains around Volturno-river

mouth (a: NX, b: N//); (c, d): Li-3 sample panoramic view showing an high amount of sedimentary lithic grains (c: NX, d: N//); (e, f): sub-angular leucite single crystal grain in the Vesuvius crater sand (e: NX, f: N//)..... 254

PLATE XVII - (a ,b): Volcanic lithic palagonitization (Lv alt) (a: NX, b: N//); (c, d): brown garnet in volcanic lithic with a brown glassy groundmass (Lvlbrgl) (c: NX, d: N//); (e, f): angular to sub-angular pyroxene single grains and *microlitic* volcanic lithic with orange glass and early plagonitization (middle grain) along Portici-Torre del Greco coastal stretch (e: NX, f: N//). 255

PLATE XVIII - (a ,b): Leucite and plagioclase phenocrysts in a brown glassy groundmass (*Lvlbrgl*) with a sub-angular (3) roundness category (a: NX, b: N//); (c, d): very angular (1) euhedral leucite with a glassy rim (c: NX, d: N//); (e, f): brown garnet in a volcanic lithic with a brown glassy groundmass (Lvlbrgl) (e: NX, f: N//)..... 256

PLATE XIX - (a ,b): Leucite phenocrysts in a black glassy groundmass (*Lvlblgl*) with a sub-angular (3) roundness category from a Sorrento beach (a: NX, b: N//); (c, d): sub-angular (3) calcite single crystal grain (middle), monocrystalline quartz (lower right), siliciclastic sedimentary lithic grain (upper left) and sedimentary lithic grain with crystalline carbonate composition [(upper right, [Lss(xx)] (c: NX, d: N//); (e, f): rounded grain containing calcite mineral (limestone grain) (e: NX, f: N//). 257

-INTRODUCTION-

On Earth, detrital sediments retain a record of eroded crustal material and knowledge of crusts of the past is gleaned from provenance studies. Principally, siliciclastic sediments are the domain of provenance studies estimating amounts, proportions, and rates of supply of sediments from multiple sources rocks. Therefore, provenance studies focus on types, identification, climatic conditions in source areas, quantitative distributions of source material and tectonic settings of source rocks. Generally speaking, the methodology survey depends of the investigators aims and the scientific matters they wants investigate, of course they are various and multidisciplinary (e.g. McBride and Picard, 1987; Johnsson and Basu, 1993; Palomares and Arribas, 1993; Critelli et al., 2003; Andò et al., 2012; Garzanti et al., 2015).

Relationships between source area and rock detrital component are related with provenance studies (e.g., Johnsson et al, 1993). Many studies that concerning clastic sediment petrography with sandy texture, have established a “first order” relationship between skeletal composition of terrigenous detritus and source area tectonic setting (Dickinson e Suczek, 1979; Dickinson et al., 1983; Marsaglia et al., 1996). The contribution of volcaniclastic sediments may reach as high as 5-10% of the total clastic flux on the Earth’s surface (e.g., Fisher and Schmincke, 1994).

The composition and texture of the detritus, supplied by volcanic rock, are a useful survey tool to understand the magmatic arc evolution and its activity (e.g., Dickinson, 1985), because of their homogeneous source rocks provenance lithotypes (e.g., Cawood, 1991; Heins and Kairo, 2007) and the relatively short distance between source area and depositional basin (e.g., Swindle et al., 1991). Spatial and temporal differences of primary volcaniclastic sediments (e.g., White and Houghton, 2006) between texture and composition of sandy particles, can be correlated to specific control factors: different geodynamic setting of volcanic arc (e.g., Dickinson, 1985; Cawood, 1991; Marsaglia, 1992; 1993; Morrone et al., 2017), different types of transport and basin sediment dispersal (Critelli et al., 2003; De Rosa et al., 1986; Zuffa, 1987; Smith and Lotosky, 1995; Marsaglia, 1992) and/or paleoclimatic/climatic influences on the volcanic detrital particles (Mack and Jerzykiewicz, 1989). Beach and fluvial sandy volcaniclastic detritus is directly produced by volcanic eruptions (pyroclastic detritus) or by erosion of pre-existent hypabyssal and/or volcanic rocks (epiclastic detritus) (i.e., Marsaglia, 1992; 1993; Critelli and Ingersoll, 1995; De Rosa, 1999; Critelli et al., 2002). Volcaniclastic associations often consist of pyroclastic/epiclastic detritus mixture (Cawood, 1991).

Biogenic processes, frequently play a significant role in mixing with volcaniclastic sediment (e.g., Marsaglia, 1993), or with pelagic sediment (Cawood, 1985).

Petrographic studies carried out on sandy-textured volcanic particles in the debris – both monomineralic and polymineralic – detect the potential controls that operate on the production and composition of the volcanoclastic sediment (e.g., Zuffa, 1985; 1987).

Different texture types of volcanic lithic (Dickinson, 1970; Marsaglia, 1992; 1993), and the different color and type of volcanic glass (Cawood, 1991; Marsaglia, 1992; 1993; De Rosa, 1999) may suggest a magmatic activity evolution of source area from basic to acid composition (e.g., Cawood, 1985), whereas paleovulcanic/neovulcanic grains are good markers to discriminate a coeval/non-coeval sedimentation with respect to eruptive activity (Critelli and Ingersoll, 1995; Critelli et al., 2002). In this volcano-derived detrital grains, secondary petrological ratios (e.g. Plagioclase/total Feldspar; Lvl:Lvmi:Lvv; Lvmi/Lvtot; Lvl/Lvtot; etc.) within primary petrological parameters (Quartz:Feldspar:Lithics; Q:F:L), can discriminate through provenances, tectonic setting of source area, such as backarc/forearc basin (Dickinson et al., 1983) or intra-oceanic hot spot (e.g., Ramalho, 2010). Specific studies on the composition of individual monomineralic volcanic grain categories such as pyroxene, outlined how the chemical pyroxene composition is related to magma type and tectonic setting (e.g., Leterrier et al., 1982), whereas chemistry of unweathered volcanic glassy grains are directly correlated to magmatic affinities of source areas (e.g., Cawood, 1991). The occurrence of volcanic colorless glass particles in the detritus, testifies convergent plate margin provenance and reflects the explosive nature of igneous activity (e.g., Fujioka et al., 1980; Cawood, 1985; Morrone et al., 2017) whereas orange-light brown glassy grains are peculiar of effusive Hawaiian fountains (e.g., Andronico et al., 2005).

The petrographic features of volcano-derived detritus have been clearly defined in previous studies relating sandstone composition to tectonic setting (e.g. Dickinson and Suczek, 1979; Critelli et al. 1990; Marsaglia and Ingersoll, 1992; Critelli and Ingersoll, 1995; Critelli et al., 2002). Both petrographic and geochemical investigations of volcanic sand and sandstone have distinguished between volcanogenic lithic fragments and monocrystalline grains of different provenances elucidating magmatic evolution of source areas (e.g. McCoy and Cornell, 1990; Cawood, 1991) and/or have focused on complex factors that control volcanic grain composition, including geomorphic processes, climate, depositional environment and particular source rocks (e.g. Jackson and Keller, 1970; Zuffa, 1985, 1987; Mack and Jerzykiewicz, 1989; Critelli et al., 1993;

Johnsson et al., 1993; Smith and Lotosky, 1995; King, 2003; White and Houghton, 2006). In this study we examine aspects of the pre-depositional and pre-burial parameters that affect the composition of volcaniclastic detritus in two different tectonic settings: the Aeolian Islands arc and the Campania magmatic province in southern Italy.

Because of weathering, transport, depositional and diagenetic processes the source rock signal often is scarcely preserved in sediments (e.g., Johnsson et al., 1993). The intensity and duration of these processes determine the preservation potential of original detrital signatures that can be easily overestimated or underestimated leading to disproportionate representation of parent source rocks in sediment (Morrone et al., 2017). When rock fragments are identifiable, even after their alteration given by weathering and diagenesis, they are infallible guides to source rocks. Provenance studies of modern detritus such as beach sands, allow understanding of pre-diagenetic processes and then catch important information on erosion and weathering type, transport in terms of both roundness and breakage (e.g., Picard and McBride, 1993) and continental deposition before being exported offshore (e.g., Marsaglia, 1993; Morrone et al., 2017; Ramalho et al., 2013).

The main goal of this research focuses on the provenance, compositional and textural investigation of modern sand supplied from volcanic terrains (southern Tyrrhenian sea). This is a contribution to quantify the controls on volcaniclastic sand composition among volcanic areas with different tectonic settings and compositions. Specifically, an important aim of this research is to quantitatively compare the relation between areal distribution, texture and composition of “source” lithotypes – which are the clastic debris producer – with respect to texture and composition of "volcano-derived" sediments.

The study area covers two Italian volcanic provinces in the southern Tyrrhenian sea: Aeolian islands and Campania province. The first comprises the coastal perimeters of all Aeolian islands: western, central and eastern sector which includes respectively Alicudi and Filicudi islands, Salina, Lipari and Vulcano islands, Panarea and Stromboli island. The second area includes Phlegrean Fields and Vesuvius coastal stretch. They have been chosen because these areas belong to two distinct magmatic and geodynamic provinces even if they are located geographically close in southern Tyrrhenian sea (e.g. Peccerillo 2003; 2005).

These areas provide a good opportunity for a detailed examination of the effects of multiple source lithology, climate, weathering, transport and depositional environment

on epiclastic sand composition (Ingersoll et al., 1993). This study demonstrates that there is great diversity in the types and abundances of modern volcaniclastic detritus produced in the studied areas. This detritus exhibits considerable diversity with regard to glass and mineral populations and textures of constituent volcanic components as seen in ancient equivalents (Mack and Jerzykiewicz 1989; Cather and Folk, 1991; Critelli and Ingersoll, 1995; Critelli et al., 2002). The difference between epiclastic, pyroclastic and autoclastic sand particles within volcanogenic debris is rarely obvious, especially after they are affected by sedimentary processes (e.g. Smith and Lotosky, 1995).

Detailed studies have been carried out, we have compared the samples among all the Aeolian islands coastal perimeters, and then between Campania province and Aeolian islands. Particular attention has been given to the factors that control the relationships between grain rounding, grain-size, sand composition, texture and source rocks. This research provide a good opportunity to define the provenance signatures of detritus eroded from lavas with different compositions, pyroclastic and minor sedimentary rocks. Different sandy petrofacies for the studied areas of Campania province have been formalized. In the Aeolian sedimentary provinces it was possible to carry out detailed study on pure volcaniclastic sands and then was useful to study all volcanic lithic types and understanding how particular lithic are diagnostic for some specific lithotypes of source rock and eruption style. Hence it was a useful study also for who conduct provenance research on ancient stratigraphic succession.

Furthermore, roundness studies on those sands have realized that allowed us acquiring important information on pre-depositional processes such as transport (e.g., breakage processes, roundness, geographic exposure, wave energy of the beaches and drainage basins width/area). The roundness study was carried out using three different methodologies such as image analysis through microscope, scanned thin sections and scanned bulk samples. In turn, then was possible to define which of those three methodologies have been more efficient to conduct in terms of both quality and time.

In addition, for the Aeolian province, the propensity to create sand of volcanic source rocks have been defined applying the concept of Sand Generation Index (SGI, sensu Palomares and Arribas, 1993) but never applied for volcanic source rocks before (Morrone et al., 2017). This kind of study can help to avoid making mistakes as well as underestimate or overestimate the contribution (or propensity to create detritus) gave by volcanic source rocks in stratigraphic record.

Thus, this research document the variability in composition and texture before the particles are buried by later pyroclastic events or reworked into the marine record environment. The relationships existing into the conversion process such as "volcanic rock → volcaniclastic sand" – deduced from this actualistic study – might supply a useful methodological and research contribute – to understanding provenance of ancient volcanogenic sequences in the stratigraphic record.

Moreover, in recent years, many works on volcaniclastic rocks (modern and ancient) and all that concerns their emplacement, indicate that this research field is strongly growing up. This is happening probably because it has been discovered that volcanic rocks can also serve as oil-reservoirs, in all of the World, but especially in China where this type of research is developing fast (e.g. Zou Caineng et al., 2013).

-Chapter 1- Provenance Study-

1.1 - Factors that control sediment and texture composition -

Clastic composition of sediments is controlled by several factors that play an important role in the dynamic systems of Earth's surface. These factors are closely related, and, in order to understand what information are contained in the compositional data, they should be considered as a whole, dependent on each other. The main factors include pre-burial factors such as the source rock composition and texture, changes induced by weathering, abrasion and mechanical breakage, hydrodynamic sorting and, post-burial effects, such as modifications induced by diagenetic environments. Each parameter is, in turn, controlled by tectonic setting, depositional environment and transport system energy, climate, vegetation, and slope gradient (e.g., Johnsson et al., 1993; fig. 1.1).

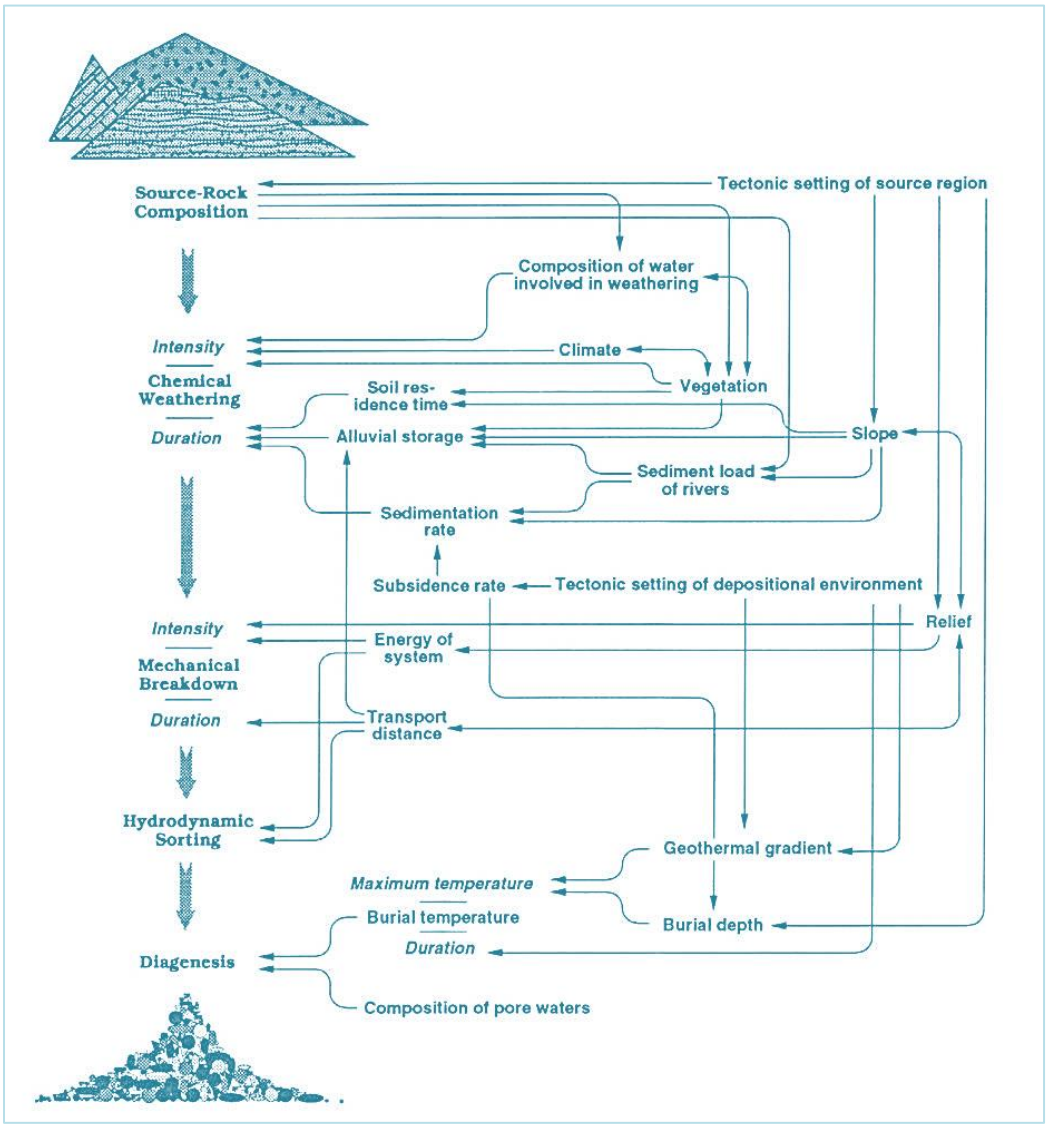

Figure 1.1 – Schematic representation of the system that influences the clastic sediments composition (modified from Johnsson, 1993).

1.1.1 – CLIMATE -

Climate plays a key role in influencing the clastic sediments composition (Krynine, 1935; Basu, 1976; Potter, 1978a; James et al., 1981; Mack, 1981; Suttner & Basu, 1981). It determines, primarily through precipitation, secondly with the temperatures, the intensity of the rock chemical weathering, whose alteration reactions take place in hydrated conditions. Tropical environments, with warm-humid climate, are characterized by a really strong chemical weathering, in fact, it's very difficult to determine the source provenance lithotypes (e.g., Heins and Kairo, 2007) only from the sediments composition. Under such climatic conditions, quartzose sand(stone) can be produced from different parental sources such as plutonic and metamorphic source rock (Potter, 1978a; Franzinelli & Potter, 1983; Basu, 1985; Johnsson et al., 1988; 1991).

In a temperate climate areas, chemical weathering is less intense than the tropical environment (fig. 1.2), and, for instance, Mann and Cavaroc (1973) have distinguished sands derived from different source rocks such as igneous, metamorphic and sedimentary source rocks. Generally, in arid environments, there is a direct correlation between source rock and sediment composition (Girty et al., 1988).

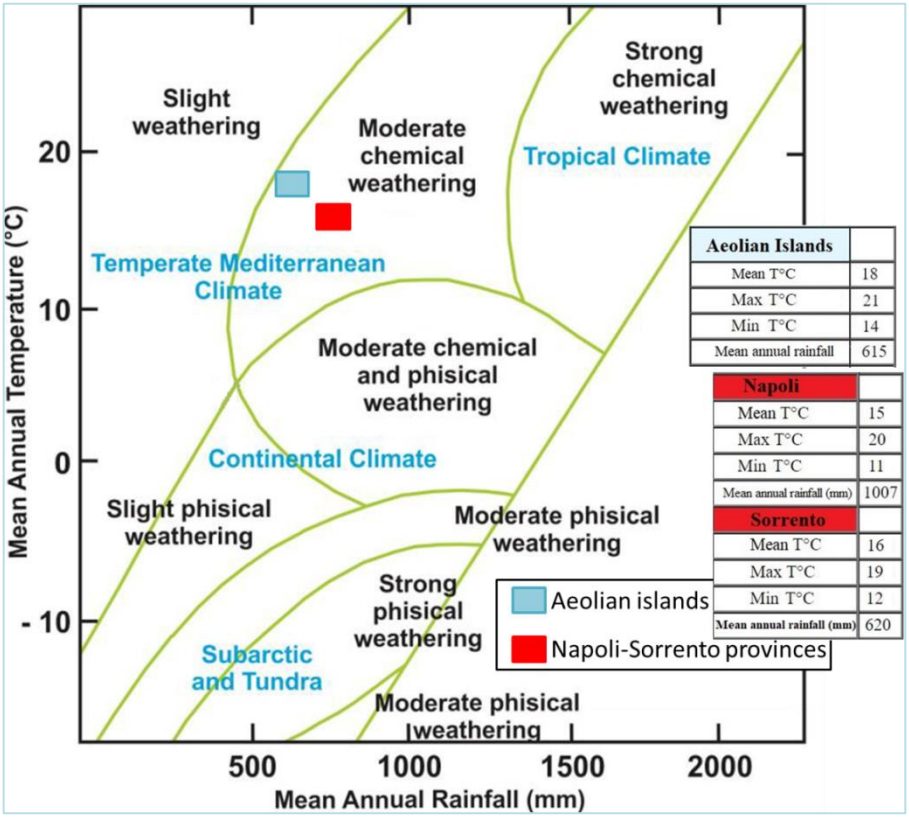

Figure 1.2- Relationship between physical and chemical weathering based on climate parameters (modified from Louis Peltier, 1950). Studied areas are represented by rectangles (climatic data are from http://www.centrometeo.com).

The weathering is the process that transform the source rocks in smaller fragments (clastic sediments) that become easy to remove and transport. There are three weathering main types: physical/mechanical weathering (without mineralogical variation), chemical weathering due to meteoric water that produce a mineralogical transformation into the source rocks, and biological weathering related to plants and animals activity. These organisms carry out a chemical and physical attack to the source rocks through organic acids and mechanical fracturing by roots (Scarciglia et al., 2005).

The weathering intensity also depends on the source rocks lithology, then depends on their fractures (e.g. frost weathering) and mineralogy. The source rocks have different reaction to weathering depending on their mineralogy. There are minerals more susceptible to alteration than others. Goldich (1938) argues that high temperature minerals are more unstable than low temperature minerals. The Goldich stability series is the inverse of what proposed by Bowen (1922) for magmatic crystallization (fig. 1.3).

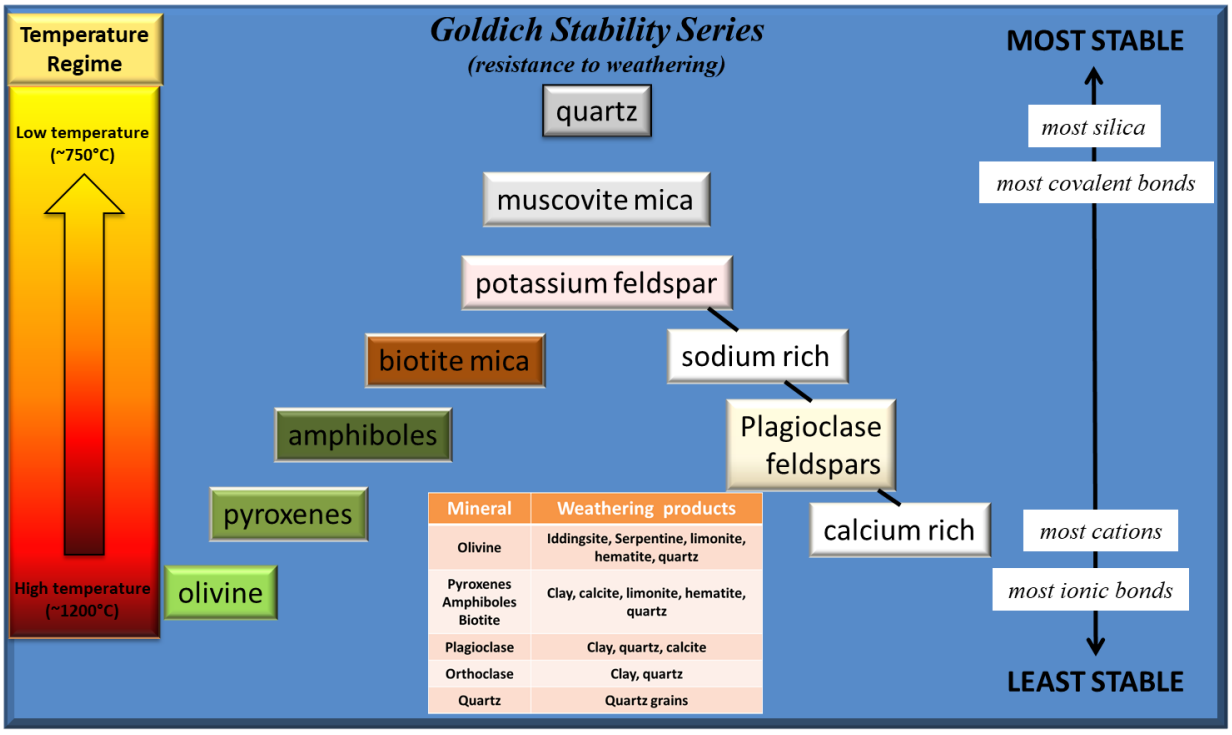

Figure 1.3 – Stability series representation (modified from Goldich 1938) and alteration products.

The methodological approach used by Basu (1976) and Suttner et al. (1981) in assessing the effects of weathering intensity on sediment composition, was carried out by comparing sediment produced by similar source rocks, under identical transport and depositional conditions, with different climate regimes. These authors suggest that sands derived from weathered granite source rocks in a semi-arid environment are different from sands derived from same source rocks in humid temperate areas.

Understanding the effects of weathering on sand composition is important not only to help constrain tectonic interpretation, but also to allow the use of sandstone composition as a paleoenvironmental indicator. In the depositional environment, sedimentation rate plays an important role: rapid sedimentation tends to isolate sediments quickly from the weathering environment and retard their alteration (Johnsson et al., 1990). These studies was really important because have provided a petrographic baseline in using compositional data to help in paleoclimatic deductions from clastic rocks (Krynine, 1950; Todd, 1968; Damuth & Fairbridge, 1970; Suttner & Dutta, 1986; Velbel & Saad, 1991).

1.1.2 – SLOPE GRADIENT -

The slope gradient is important because it can control the weathering efficiency in terms of duration and intensity (Carson & Kirkby, 1972; Stallard, 1985; 1988; Grantham & Velbel, 1988; Johnsson & Stallard, 1989; Johnsson et al., 1991). Erosion can be viewed as "transport-limited" or "weathering-limited" process (e.g., Carson and Kirkby, 1972). The weathered material is removed from the slope by transport processes. If the transport processes are quicker than weathering processes we have a "weathering-limited" erosion. On the contrary, it is called "transport-limited" erosion if the weathering rate is quicker than transport processes. The first condition is related to steep slopes gradients whereas the second is typical of lowland areas (fig. 1.4).

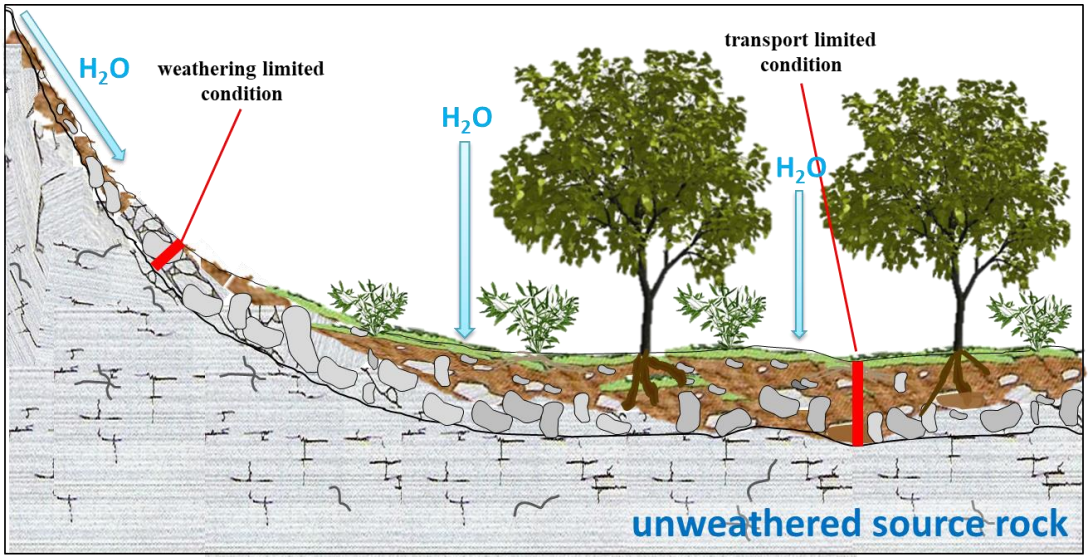

Figure 1.4 - *Weathering-limited* and *transport-limited* erosion regimes: regolith thickness as a function of topography.

The implications for these two types of erosion were derived from the chemical weathering studies and its products. Stallard (Stallard & Edmond, 1983; 1987; Stallard,

1985; 1988; Stallard et al., 1991) has marked different reactions in chemical weathering through suspend load test in tropical river draining areas with contrasting erosion. Same concepts have been applied to solid weathering products (Johnsson et al., 1988; 1991; Johnsson & Stallard, 1989; Stallard et al., 1991). In *transport-limited* conditions the weathering products have an higher interaction time with rainwater and groundwater. Soils are depleted in the soluble cationic components (leaching) when they are exposed for a long time in weathering environment and they have an increasing in stable minerals, especially quartz (figs. 1.3, 1.4). In *weathering-limited* condition the detritus persists a little time in the soil profile, then weathering products will not be completely leached, and will retain the cationic phases. Residual detritus will consist in an instable spectrum phases whose proportions reflect the bedrock composition (Johnsson, 1990; Johnsson et al., 1991). Slope gradient angles control the weathering depth: in low gradient slopes regolith thickness will be thicker than that of steep slope areas (fig. 1.4).

1.1.3 – TRANSPORT INFLUENCE -

Processes that affect sediments composition during transportation include abrasion, mechanical breakdown, hydrodynamic sorting and mixing effects, difficult to separate in natural systems.

1.1.3a - Abrasion and mechanical breakage -

The knowledge obtained in laboratory (Kuenen, 1959) suggests that the abrasion during river transport can be decisive in rounding the ruditic sediment, but it doesn't produce a significant rounding or a volumetric loss of labile sands constituents. Mechanical abrasion, however, seems to be important in aeolian and beach sand grains (Kuenen, 1960; 1964; Tentori et al., 2016; Morrone et al., 2018), and in removing quantitatively the least stable components mechanically, essentially lithic fragments from aeolian deposit (Dutta et al., 1993). Garzanti et al. (2015) argues that grain rounding is mainly due to aeolian and coastal reworking rather than to river transport.

The natural systems results are ambiguous in relation to the difficulty of separating the chemical weathering effects, during a protracted alluvial storage, mechanical breakdown and hydrodynamic sorting.

Some authors have stressed, through the study of river sands, an insignificant downstream enrichment of stable minerals (Russel, 1937; Pollak, 1961; Breyer & Bart, 1978). Others reported an increasing of quartz/feldspar ratios (Hayes, 1962), a decreasing of unstable lithic fragments (Cameron & Blatt, 1971; Shukis & Ethridge,

1975), an increasing of zircon, tourmaline and rutile, with respect to other heavy minerals (Hubert, 1962), and the progressive downstream destruction of least mechanically stable grains such as plagioclase (Pittman, 1969). McBride & Picard (1987), by comparing different source rock areas and corresponding grain types in the fluvial sands, have discovered that stable source rock lithotypes are overestimated in the sediments. Garzanti (1986) attributes to the feldspar mechanical breakage, along the cleavage planes, the feldspars elimination from the coarser grain-size classes, and their accumulation in the finer one, in deltaic sandstone from northern Italy.

1.1.3b – Hydrodynamic sorting

The hydrodynamic sorting produces substantial compositional differences between bed and suspended river load: the first consists of a higher minerals and lithic fragment variety, whereas the second it's generally constituted by clay minerals and monomineralic silt grains. In the bed load, sorting, deriving from density differences, can be produced where the hydrodynamic flow conditions change. Local heavy minerals concentrations may affect the local sediment composition, even if the local composition of entire sedimentary system is not quantitatively change (Garzanti, 1986; Garzanti et al., 2009; Garzanti et al., 2015). In a fluvial system, the sediment composition changing depend on new feed sources addition such as transverse drainages with respect to the main channel. For instance, Columbia river sands, display a quartz/feldspar ratio decreasing downstream, and a grain-size increasing; this suggests that downstream or hydrodynamic sorting dilution effects exceed those of chemical weathering abrasion (Kelley & Whetten, 1969; Whetten et al., 1969).

Mechanical effects of transport produce significant detritus changes even in the depositional environment and physical disintegration continues to be active during the final sediment burial. Kairo et al. (1993) display a correlation between sandstone composition and depositional environment through the petrographic study of a Pennsylvanian deltaic succession in Colorado. These authors attribute the compositional differences among sandstone depositional environments to mechanical breakage and hydrodynamic detritus sorting.

Grain-size, density and shape of sediments which are mobilized by water flows play a fundamental role in the transport evolution processes. These factors, related with tangential pressure exerted by water flow current on the particle, identify the values range that define the stability fields of some processes such as erosion, transport and deposition, expressed in a bi-dimensional diagram (e.g., Hjulström, 1935) (fig. 1.5).

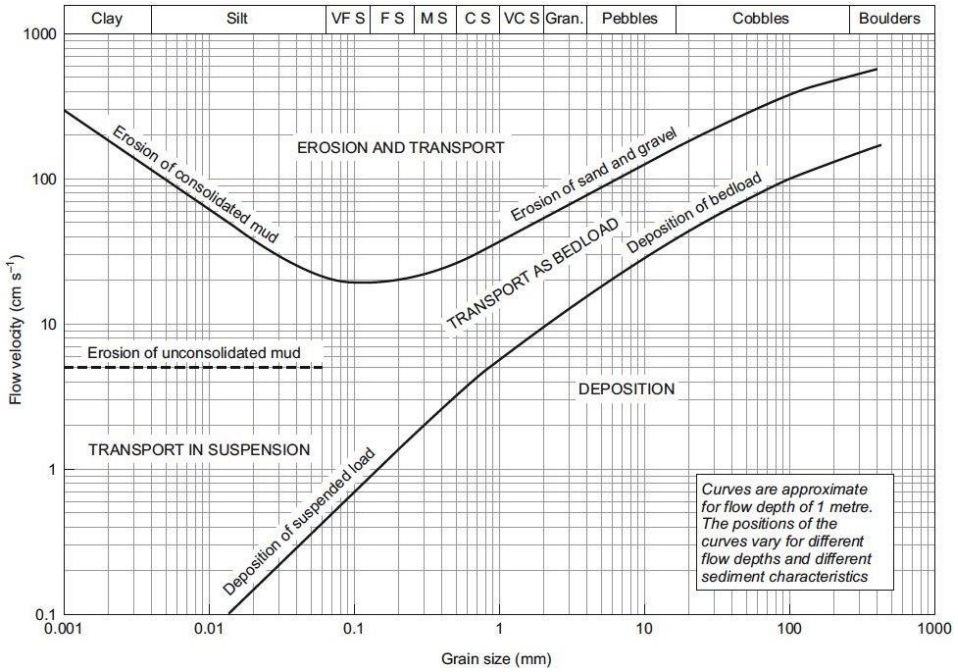

Figure 1.5 – This diagram shows the pre-burial process occurring in a stream based on grain-size and flow velocity (from Hjulström 1935).

Studies on mechanical processes, that induce compositional modification in the detritus, associated with grain-size distribution studies, are useful in interpreting the depositional environment of ancient sedimentary rocks in paleogeographic reconstruction of the source area/basin system.

1.2 - Volcaniclastic particles -

Fisher (1961) and Fisher and Smith (1991) were the first to introduce "volcaniclastic" term which includes the entire spectrum of clastic materials composed in dominantly or entirely of volcanic fragments, formed by any particle-forming mechanism (e.g. pyroclastic, hydroclastic, epiclastic, autoclastic), transported by any mechanism, deposited in any physiographic environment or mixed with any other detritus in any proportion (Gillespie and Styles, 1999). In addition to epiclastic volcaniclastic sediment supplied to basins by weathering and erosion of volcanic regions, large volume of volcaniclastics are also supplied directly to basin during explosive volcanism.

Volcanic particles are deposited as sediments: the principal differences with nonvolcanic sediments being in some of the physical processes by which the particles are formed. Some volcanic particles are generated by weathering and erosion (epiclastic) and therefore differ only in composition from nonvolcanic clasts. Other

volcanic particles are formed instantly by explosive processes. Volcaniclastic includes all volcanic particles regardless of their origin.

Generic types of volcaniclastic particles (Fisher and Schminke, 1984; Cas and Wright, 1987; Le Maitre et al., 1989):

- **Pyroclastic** particles (or pyroclasts): form by disintegration of magma, as gases are released by decompression and then ejected from a volcanic vent either in air or beneath water;
- **Hydroclasts:** form by steam explosions from magma-water interactions;
- **Autoclastic** fragments: form by mechanical friction during movement of lava and breakage of cool brittle outer margins, or gravity crumbling of spines and domes;
- **Alloclastic** fragments: form by disruption of pre-existing volcanic rocks by igneous processes beneath the Earth's surface;
- **Epiclasts:** are lithic clasts and minerals released by ordinary weathering processes from pre-existing consolidated rocks. Volcanic epiclasts are clasts of volcanic composition derived from erosion of volcanoes or ancient volcanic terrains.

Varieties of pyroclastic ejecta according to origin are different and, according to volcanology nomenclature, they can differentiated as follow (Fisher and Schminke, 1984; Cas and Wright, 1987; Le Maitre et al., 1989):

- **Essential** (or juvenile) are pyroclasts derived directly from erupting magma and consist of dense or inflated particles of chilled melt, or crystals (phenocrysts) in the magma prior to eruption (phenocrysts);
- **Cognate** (or accessory) are particles are fragmented comagmatic volcanic rocks from previous eruptions of the same volcano;
- **Accidental** are fragments (or "lithoclasts") are derived from the sub-volcanic basement rocks and therefore may be of any composition.

Names of pyroclasts and deposits according to grain size (fig. 6), are the same for both volcanology and sedimentology nomenclature:

- **Ash particles** are < 2 mm in diameter;

  Volcanic ash is composed of vitric, crystal or lithic particles (of juvenile, cognate or accidental origin) of various proportions. "**Tuff**" is the consolidated equivalent of ash. Reworked ash (or tuff) may be named according to the transport agent (fluvial tuff, aeolian tuff);

- **Lapilli** are fragments 2 mm to 64 mm in diameter (figs. 1.6, 1.7).

Lithified accumulations with more than 75% lapilli are termed *lapillistone*. *Lapilli-tuff* applies to lithified mixtures of ash and lapilli, where ash-size particles are 25-75% of the pyroclastic mixture. Lapilli are commonly angular to sub-rounded.

- **Bombs** or **blocks** are > 64 mm (figs. 1.6, 1.7).

Bombs are thrown from vents in a partly molten condition and solidify during flight or shortly after they land. Bombs are therefore almost exclusively juvenile.

Pumice and scoria (pyroclasts) that depend in part on their degree of vesicularity are named without reference to size, but usually are in the lapilli or larger size range.

- **Pumice** is a highly vesicular glass foam, generally of evolved and more rarely of basaltic composition with a density of <1 gm/cubic cm; bubble walls are composed of translucent glass.
- **Scoria** (also called **cinders**), usually mafic, are particles less inflated than pumice. They readily sink in water. They are generally composed of *tachylite*, that is, glass rendered nearly opaque by microcrystalline iron/titanium oxides.
- **Spatter** applies to bombs, usually basaltic, formed from lava blebs that readily weld (agglutinates) upon impact and contrasts with scoria that do not stick together. Scoria (or cinder) cones, for example, are composed largely of loose particles; spatter cones are composed mainly of agglutinated blebs or larger isolated lava tongues.

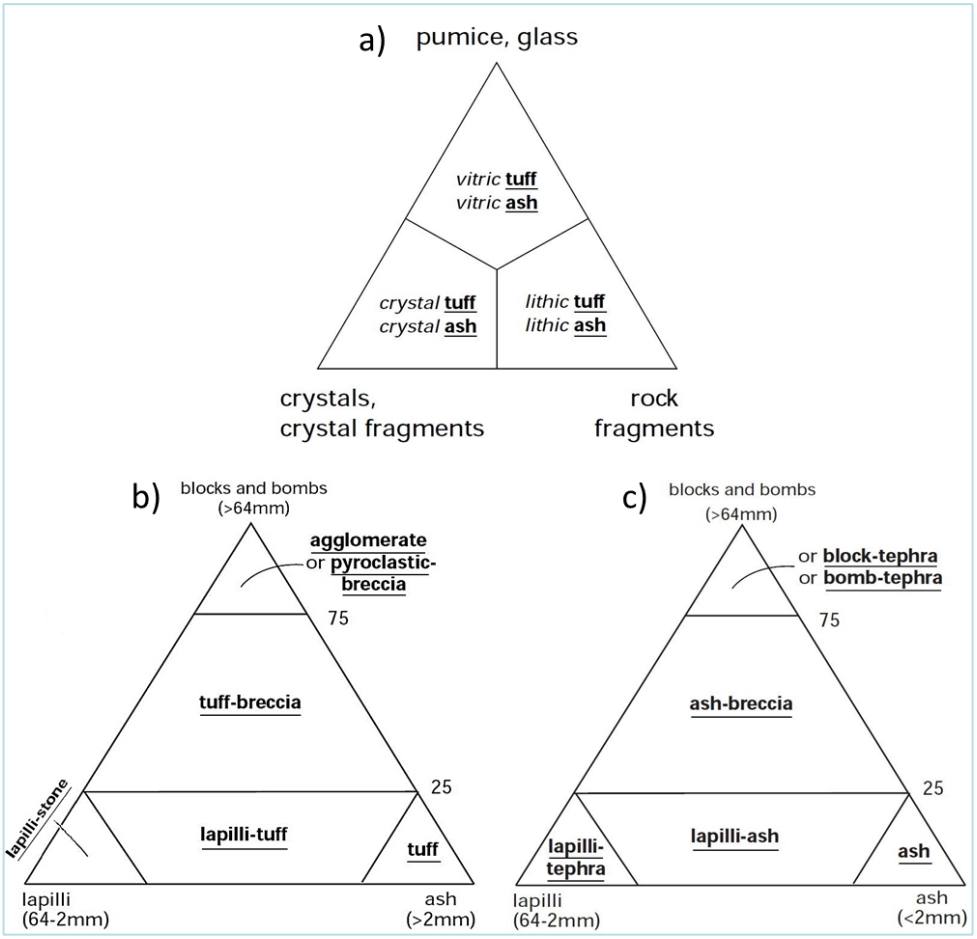

Figure 1.6 – a) Classification and nomenclature of tuffs and ashes based on their fragmental composition (modified from Schmid, 1981); b) Classification of pyroclastic rocks and (c) pyroclastic sediments according to grain-size (modified from Fisher and Schminke, 1984).

Figure 1.7 – Panoramic view of bombs and lapilli field on Volcano island (Aeolian islands).

Hence, blocks and bombs are volcanic equivalents of boulders, lapilli corresponds to gravel, ash is a volcanic analogue of sand and then tuff (lithified volcanic ash) is analogous to sandstone. This classification resembles classification principles of clastic sedimentary rocks.

Detrital grains derived from the erosion of ancient volcanic rocks are denominated "*paleovolcanic"* or "*non-coeval"* grains and provide information on the geological history of source areas. Whereas, *neo-volcanic* or "*coeval"* grains, are general volcanic grains which come from active volcanism deriving from subaerial or subaqueous activity during sedimentation. These grain-types supply information on source-area's geological setting and basin during deposition (Zuffa, 1985; 1987; Critelli and Ingersoll, 1995; Critelli et al., 2002).

1.2.1 - VOLCANICLASTIC PARTICLES IN PROVENANCE STUDIES -

Volcaniclastic sedimentation is characteristic of convergent plate margins in marine forearc sequences, in marine to nonmarine intra-arc grabens and in marine and nonmarine environments of backarc or inter-arc areas (fig. 1.8). In subduction settings, andesite to dacite magmas construct high-standing stratovolcanoes with large volumes and great heights, and therefore large reservoirs of sediment. They erode rapidly, providing large volumes of reworked pyroclastic and hydroclastic particles together with epiclastic volcanic debris that are deposited into surrounding basins.

In basin and tectonic analyses, volcanic sediments can be treated methodologically as non-volcanic sediments, but the close association of tectonism and volcanism provides an added dimension to the analytical importance of volcaniclastic sediments. Volcanism occurs at plate margins and in some instances within plates ("hot spots"), and sediments within those environments have a strong, and in some cases, an exclusive component of volcaniclastic particles (Fisher and Smith, 1991).

Source rocks controls on volcaniclastic sedimentation is very complex (e.g., Marsaglia, 1992, 1993; Morrone et al., 20017a): being volcanoes topographic highs, they are easily eroded, hydrotermally altered and also weathered (sand-grade ash particles reduced to clay in a few years). Thus the geological record is often biased towards the more distal parts of the "source rock/volcanic sediment system". Diagenesis is a major limiting factor in altering volcanic glass and crystals, destroying depositional textures and neoforming matrix (Johnsson et. al., 1993).

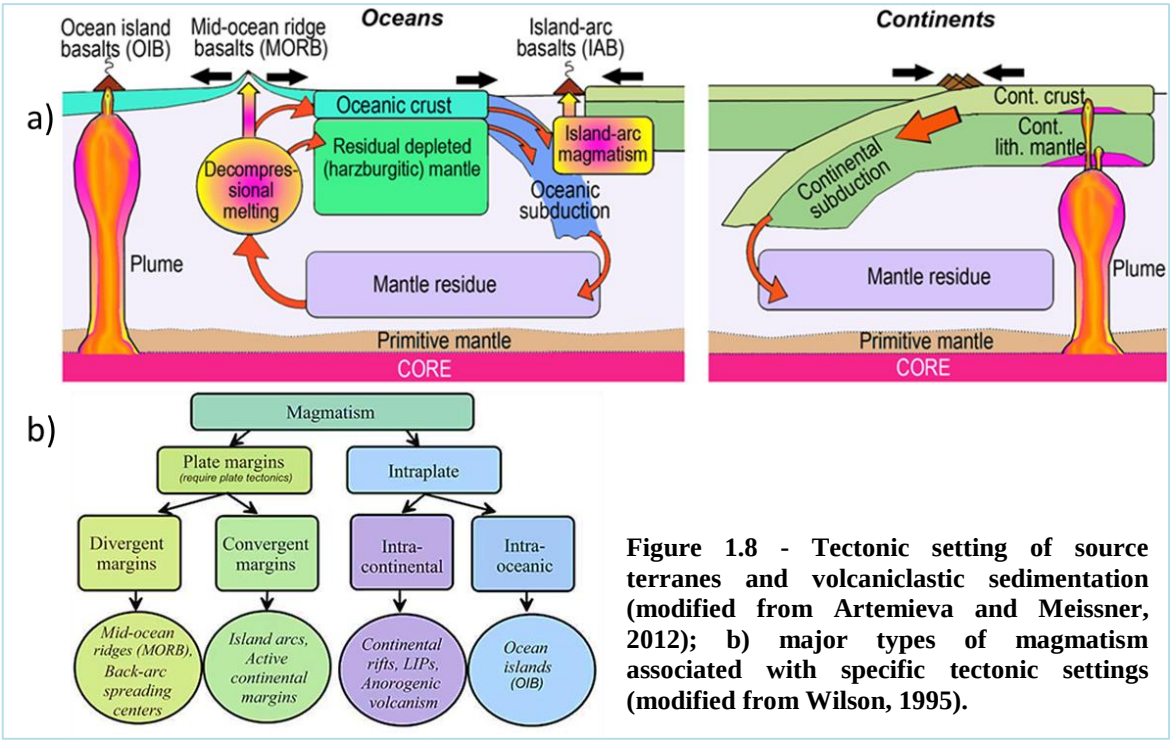

Figure 1.8 - Tectonic setting of source terranes and volcaniclastic sedimentation (modified from Artemieva and Meissner, 2012); b) major types of magmatism associated with specific tectonic settings (modified from Wilson, 1995).

Volcaniclastic facies are defined by distance from source, type of transporting agent, environment of deposition, and by composition. In volcanic settings, source rocks are not always only volcanic (single source rock), in fact volcanic/carbonate rocks are a recurrent association in tectonically active regions (dual source rocks). Rocks are volcaniclastic-carbonate successions with biotic growth during volcanic quiescence (fig. 1.9) (e.g. Cape Verde islands, Canary islands, Chatham islands, Campania province).

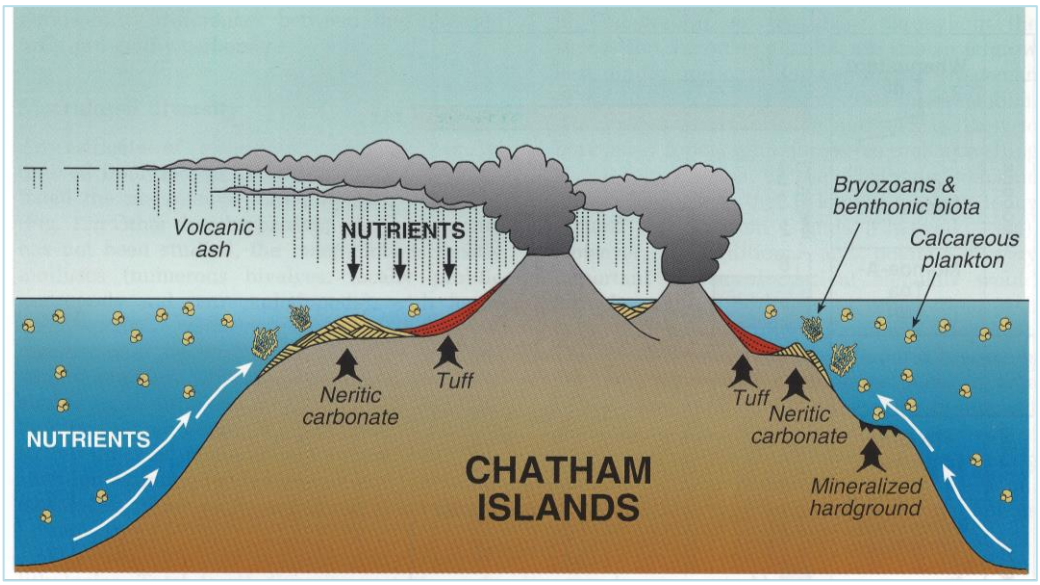

Figure 1.9 - Source rocks and volcaniclastic facies. (Chatam Islands volcanic complex in south Pacific Ocean, modified from James et al., 2011).

Solving paleotectonic and facies problems in most of the recent or ancient plate tectonic settings requires the establishment of penecontemporaneity of the volcaniclastic components in sedimentary rocks because volcanism is often the signature of tectonism (fig. 1.10). This may be difficult, however, because newly formed pyroclastic or hydroclastic particles and epiclastic particles derived from weathering of volcanic rocks (lava flows or lithified ash and volcanic breccia) or non-volcanic rocks are frequently mixed together by marine or non-marine transport processes (Fisher and Smith, 1991; figs. 1.9, 1.10).

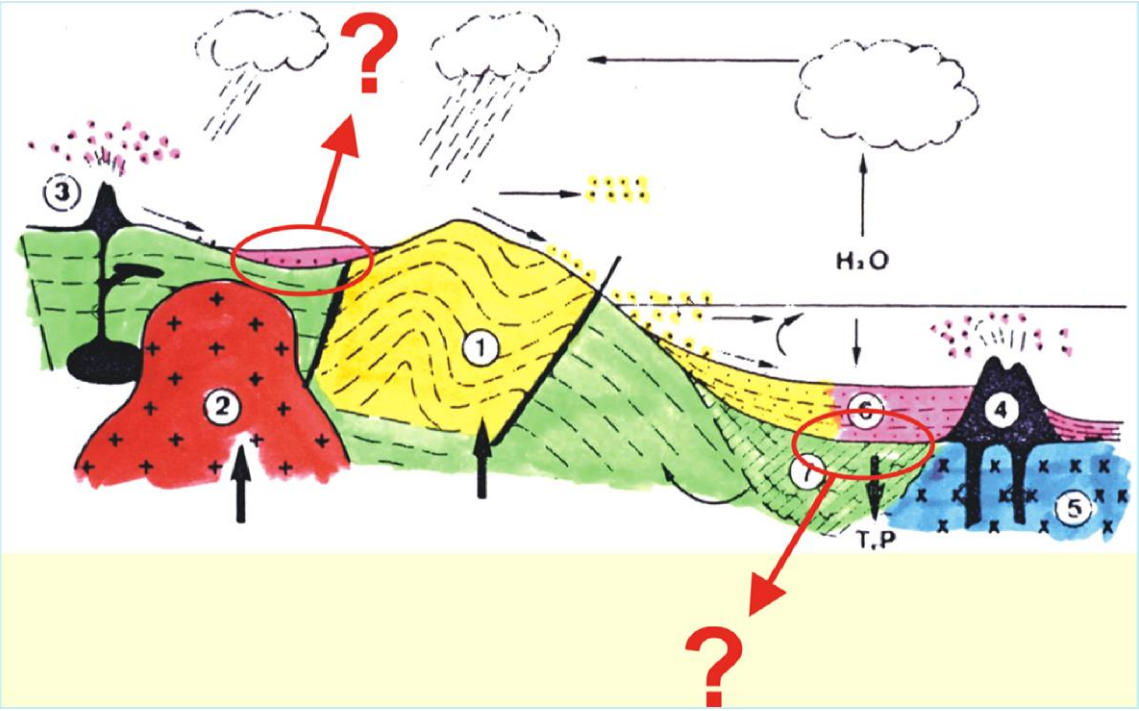

Figure 1.10 - During magmatic eruptions, several, and different, processes, give rise to a range of distinctive volcaniclastic facies (modified from Lucchi, 1980).

Volcaniclastic sediments are those composed by chiefly of grains of volcanic origin but «one of the most intricate task in optical analysis of volcaniclastic sand(stone) is the distinction of grains eroded from ancient volcanic rocks (i.e. *palaeovolcanic*, *non-coeval* grains) form grains generated by subaqueous and/or subaerial active volcanism during sedimentation such as *neovolcanic*, *coeval* grains» (Zuffa, 1985; 1987; Critelli and Ingersoll, 1995). Sand(stone) contains several types of volcanic grains which are of invaluable help for stratigraphic, paleogeographic and geodynamic reconstructions.

1.2.2 - VOLCANICLASTIC ROCKS AS OIL RESERVOIRS -

Fisher and Smith (1991) argue that the common belief among many petroleum geologists that regions of volcanic rocks are generally to be avoided as potential hydrocarbon reservoirs has greatly slowed the learning curve about volcaniclastic rocks. But they also say that many oil bearing basins occur within plate margins, and because most of the earth's volcanic action occurs at plate margins, there is hydrocarbon production in volcaniclastic rocks. In fact, in recent years many works on volcaniclastic rocks (modern and ancient) and all that concerns their emplacement was carried out indicating that this research field is strongly growing up. This is happening probably because it has been discovered that volcanic rocks can also serve as oil-reservoirs (e.g. Zou Caineng et al., 2013).

In this regard, Zou Caineng et al., (2013), in their book entitled "*Volcanic Reservoirs",* argue that, during the last 50 years, many volcanic rocks, as reservoir beds in hydrocarbon-bearing basins, have been widely discovered (fig. 1.11).

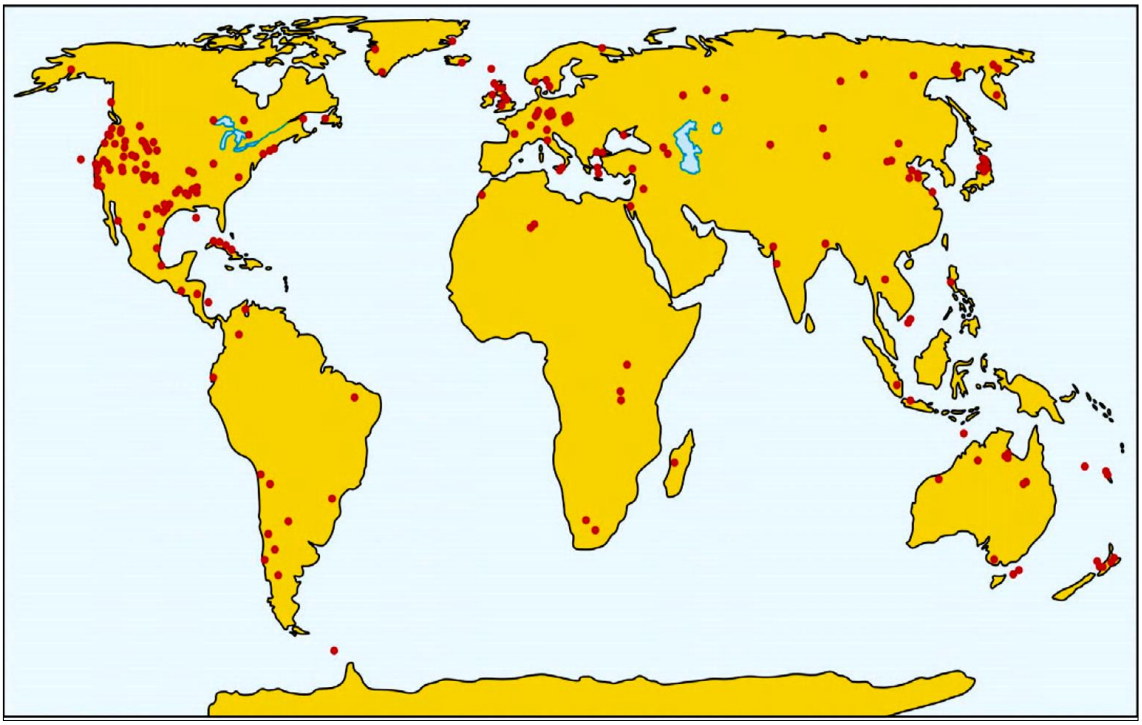

Figure 1.11 - Global oil and gas distribution in volcanic rock (modified from Zou Caineng et al., 2013).

Zou Caineng et al. (2013), focus on overseas volcanic reservoir exploration history and features of discovered oil and gas fields and some case studies. Moreover, discuss the generation period and distribution of volcanic rocks especially in hydrocarbon-bearing basins, based on the analyses of global volcanic rock distribution and tectonic

setting. They also discuss the development features, reservoir types, reservoir characteristics, and main controlling factors of favorable reservoir development of volcanic rocks in hydrocarbon-bearing basins. Hence, they summarize the assemblages of hydrocarbon accumulation in volcanic rock, as well as reservoir types and oil and gas distribution rules; point out that the assemblage of reservoir rock and effective source rock are the key to forming reservoirs; summarize relevant techniques in volcanic region prediction, play prediction, reservoir prediction, and fluid prediction.

Thus, volcanic reservoirs, considering volcanic rock as a reservoir type or being closely related to volcanism, are more complex than conventional sedimentary reservoirs in their unique hydrocarbon generation, migration, accumulation, and preservation. Their hydrocarbon accumulation may be independent of sedimentary rock, and as such they complement sedimentary reservoirs, which expands the province of oil and gas exploration (Zou Caineng et al., 2013).

1.3 - Relationship between provenance and tectonic setting -

In recent past, sandstone studies have focused particularly on the relationship between *petrofacies* and tectonic setting. Many authors agree that the detritus sandstone composition is significantly related to the tectonic setting of their source (Dickinson, 1974; Dickinson and Rich, 1972; Crook, 1974; Schwab, 1975; Dickinson and Suczek, 1979; Dickinson, 1982).

Sand composition is directly related to the source area in trench-arc systems (e.g., in the Aeolian Islands) due to the direct spatial relationship between source area and depositional basin where a rapid sedimentation occur (Harrold and Moore, 1975; Ingersoll and Suczek, 1979; Moore, 1979; Dickinson and Valloni, 1980; Valloni and Maynard, 1981; Enkeboll, 1982; Maynard et al., 1982; Valloni and Mezzadri, 1984; Yerino and Maynard, 1984; Valloni, 1985; Packer and Igersoll, 1986; Critelli et al., 1990; Cawood, 1991; Pirrie, 1991).

The study of several ancient and modern sandstone bodies has led to the *petrofacies* identification diagnostic of the different geodynamic setting which are really helpful in the paleogeographic and paleotectonic reconstructions (Dickinson & Suczek, 1979; Dickinson, 1985; Valloni & Zuffa, 1984; Girty, 1987; Ingersoll, 1990; Graham et al., 1991; Critelli & Ingersoll, 1995).

-Chapter 2 -Study areas-

2.1 - Geological setting of Aeolian Province -

The Aeolian archipelago, located between the Southern Tyrrhenian Sea backarc basin (Marsili oceanic basin) and the Calabrian Arc forearc region (figs 2.2, 2.3), it consists of seven main islands (Alicudi, Filicudi, Salina, Lipari, Vulcano, Panarea and Stromboli) forming a volcanic arc, and several seamounts (Eolo, Enarete, Sisifo, Lametini, Alcione and Palinuro) arranged approximately in a ring-like structure (fig. 2.1). The Aeolian arc is a most active volcanic structure, comprising a number of active (Stromboli and Vulcano) or dormant (Panarea and Lipari) volcanic islands together with extinct volcanoes (fig. 2.1). The Aeolian Islands were emplaced on thinned 20 km continental crust and so are considered examples of continental-arc volcanism (Barberi et al. 1973; Keller, 1982; Ventura et al. 1999; Trua et al., 2004; Nicolosi et al., 2006).

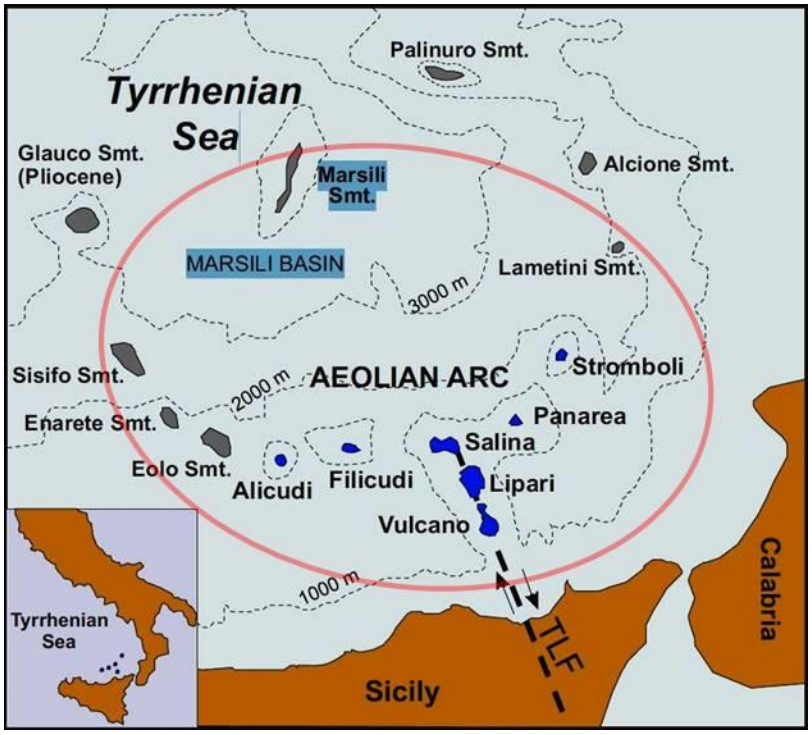

Figure 2.1 - Location map of Aeolian volcanic islands and associated seamounts. TLF is the Tindari-Letojanni Fault system (modified from Lucchi et al., 2013). The red line highlights the ring-like structure.

The geochemical affinity of these rocks and the occurrence of deep seismicity (up to 550 km) below the Southern Tyrrhenian Sea has led many authors to relate the Aeolian volcanic arc to the SE rollback of the Ionian slab below the Calabrian Arc (e.g. Patacca & Scandone, 1989; Faccenna et al. 2001; Gvirtzman & Nur, 2001; Chiarabba, De Gori & Speranza, 2008) (figs. 2.2, 2.3, 2.4).

The Aeolian Islands belong to a system "marginal arc-trench-basin" result of the collision between two converging plates such as the African and Eurasian plate. The volcanic front is represented by Aeolian Island, whereas the back-arc marginal basin is represented by the abyssal plain of the Tyrrhenian Sea (Alvarez et al., 1974; Doglioni et al., 1999) (figs. 2.2, 2.3).

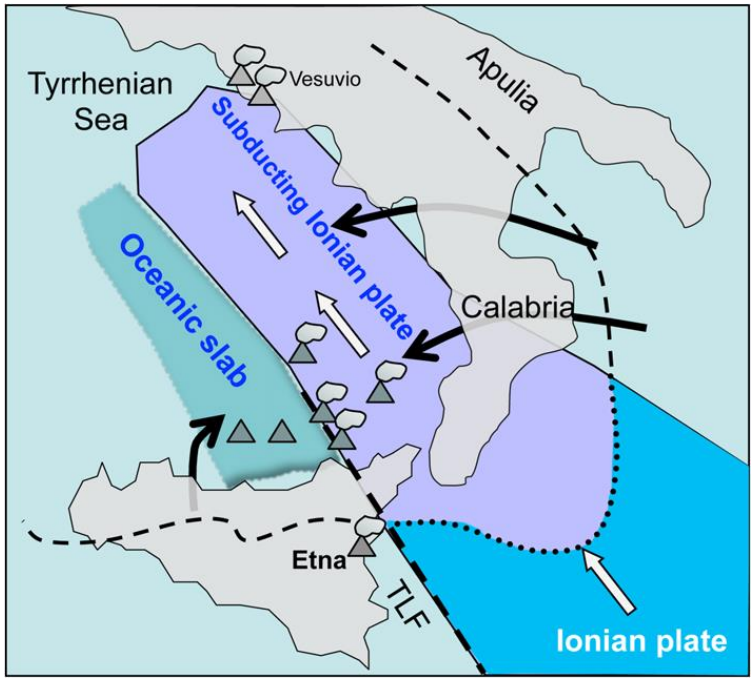

Figure 2.2 - Schematic geodynamic setting of the Aeolian arc. A narrow Ionian plate is subducting beneath Calabria and the southern Tyrrhenian Sea. It is bounded to the west by the Tintari–Letojanni Fault (TLF) system (modified from Lucchi et al., 2013).

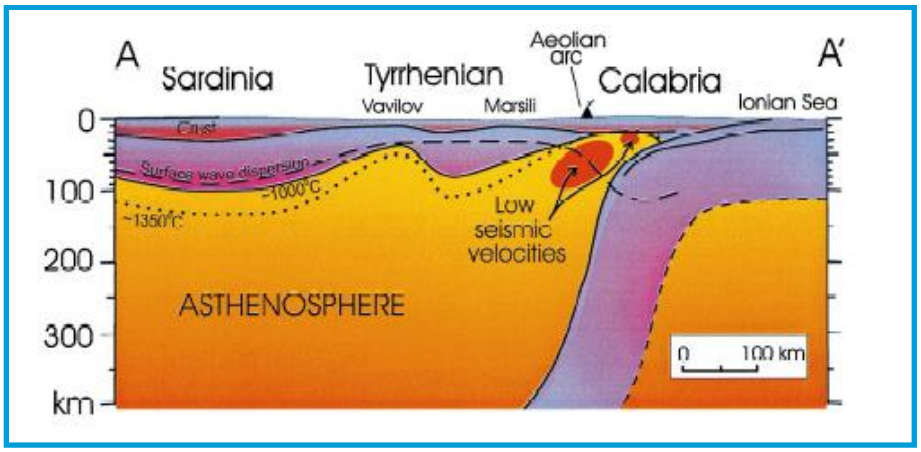

Figure 2.3 - Aeolian Arc subduction plan is localized along the Calabria's Ionian edge, immersion W-NW, inclination around 50°- 60° below the Tyrrhenian Sea (modified from Doglioni, 1999).

The Aeolian archipelago exhibits strong structural, volcanological and petrological variations (figs. 2.4, 2.5, 2.6). A first-order lithospheric fault system, the so-called *Tindari–Letojanni Fault*, divides the western and eastern sectors of the Aeolian arc (fig.

2.4). Traditionally, the Aeolian arc has been divided into three main sectors – the western, the central and the eastern arcs – which are characterized by first-order volcanological, magmatic and structural differences (De Astis et al., 2003; Peccerillo 2005; Ventura 2013). The western arc is formed by Alicudi and Filicudi, which are situated along east–west- to WNW–ESE-striking fault systems. A NNW–SSE compressive strain field due to the Africa–Eurasia convergence is active in this sector (Ventura 2013). The central islands of Vulcano and Lipari are located along the *Tindari-Letojanni Fault*, where a strike-slip strain regime is active. Salina is sited at the intersection between the east–west-trending structures of the western arc and the *Tindari–Letojanni Fault*. Panarea and Stromboli are situated along SW–NE-trending faults.

Active volcanoes are basically restricted to the central (Vulcano and Lipari) and eastern (Stromboli and Panarea) sectors of the Aeolian archipelago, where an extensional stress regime and a deep-focus earthquakes are detected as an effect of the north-westwards subduction of the Ionian lithospheric slab beneath the southern Tyrrhenian Sea (figs 2.2, 2.4). By contrast, no historical eruptions are recorded in the western Aeolian archipelago (Alicudi, Filicudi and Salina) where only shallow seismicity is detected in a compressional tectonic regime (fig. 2.4c).

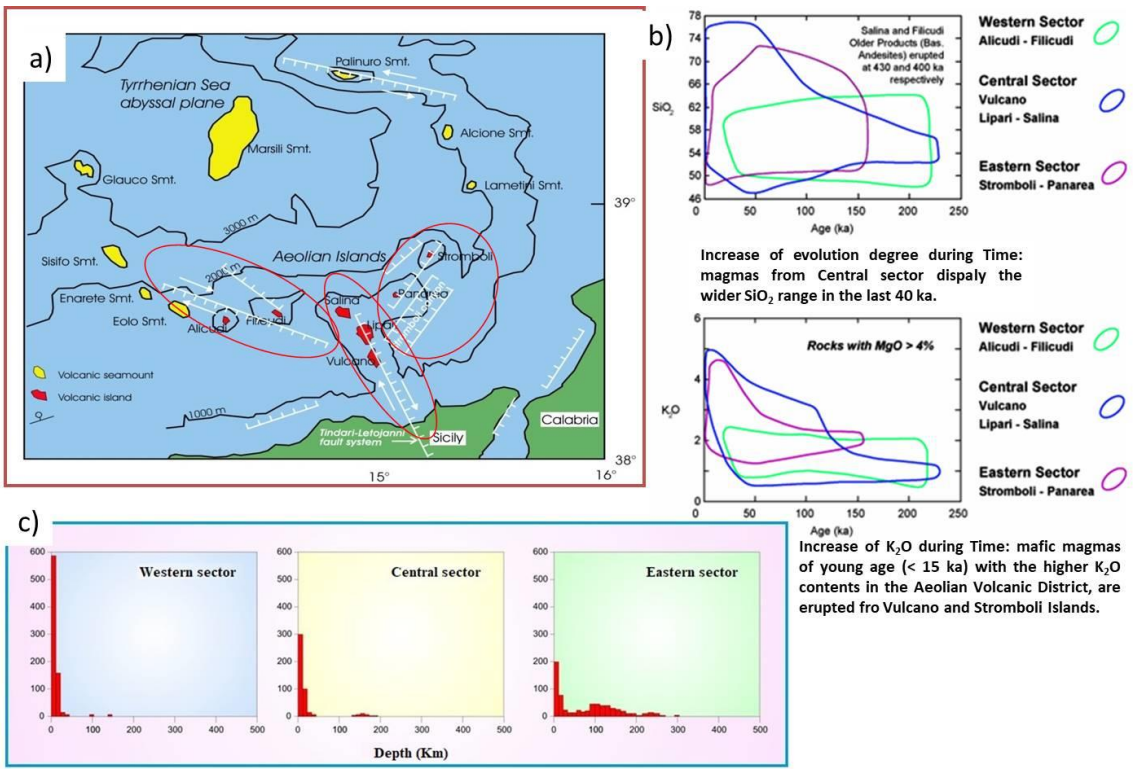

Figure 2.4 – a) Main tectonic lineaments that control the Aeolian Islands volcanism; b) temporal and spatial evolution, increase in K with age and from western to eastern islands; c) Depth of earthquakes between 1981 and 1986 (modified from De Astis et al., 2003).

Aeolian magmatic arc volcanism has migrated over the time from west to east (from Sisifo to Stromboli) and from north to south (from Salina to Lipari-Vulcano), historical activity is concentrated in the central and eastern sector (De Astis et al., 2003; De Rosa et al., 2003) (fig. 2.5).

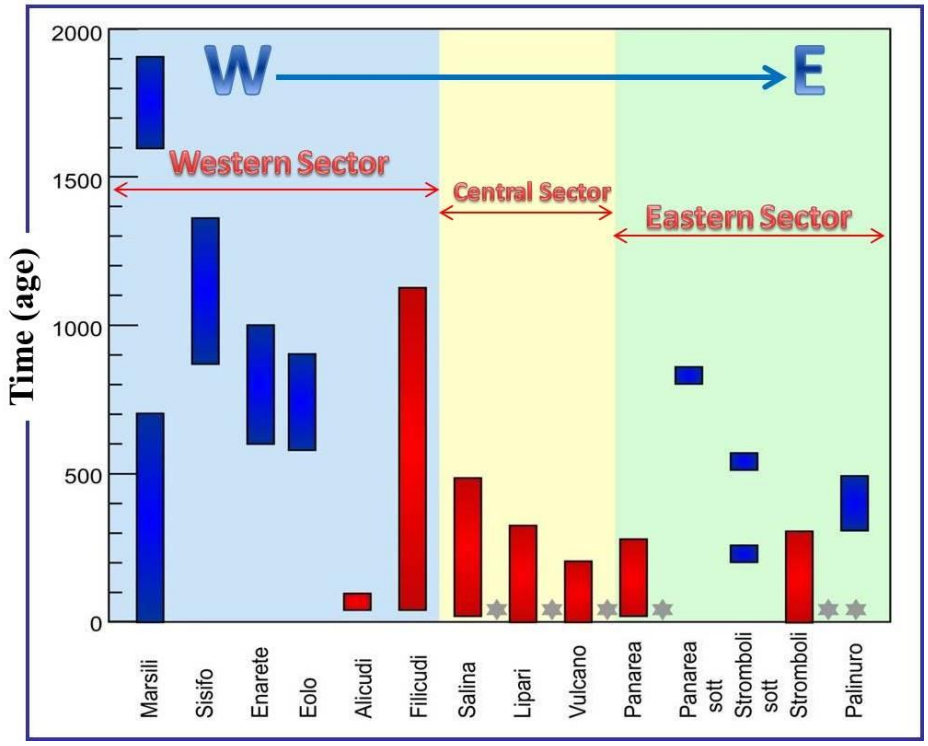

Figure 2.5 – Temporal evolution of the volcanism of the Aeolian area, based on geochronogical data (modified from De Astis et al., 2003).

Geophysical studies (De Astis et al., 2003; Panza et al., 2003) indicate that deep seismicity (up to 550 km) only occurs east of the Tindari–Letojanni Fault. In the western sector there are largely superficial and crustal earthquakes, in the south-central sector along the transcurrent fault, crustal earthquakes occur and the eastern sector is interested by deep earthquakes (Benioff's zone) with a few shallow earthquakes (fig. 2.2c). This is a consequence of the Ionian slab subduction beneath the Calabro–Peloritano basement and the southern Tyrrhenian Sea. Active Aeolian volcanism is therefore located above or at the margin of the deep seismicity zone.

The volcanic products, whose age ranges from 1.03 Ma to the present (Tranne et al. 2002; De Rosa et al., 2003; Lucchi et al. 2004; Lucchi, Tranne & Rossi, 2010), belong to the calc-alkaline, high-K calc-alkaline, shoshonitic and alkaline potassic associations (Barberi et al. 1973; Keller, 1982; Peccerillo, 2005) (fig. 2.6). Calc-alkaline (CA) and high-K calc-alkaline (HKCA) rocks occur throughout the arc but dominate at Alicudi, Filicudi, Salina, Lipari and Panarea. In contrast, shoshonites (SHO) are spatially

restricted to the central-eastern islands, where they generally appear during the mature to late stage of volcanic activity. The Marsili seamount has a CA basalt to basaltic andesite composition, with a few andesites (Trua et al. 2011). The degree of magma evolution increases from the external to the central islands; rhyolitic volcanism (SiO_2 70%) is present at Panarea and Salina, and becomes abundant at Lipari and Vulcano (Ellam et al., 1988; Francalanci et al., 1993; Crisci et al., 1991; Peccerillo and Wu, 1992; De Astis et al., 1997; Peccerillo, 2005) (figs. 2.4b, 2.6). Rhyolites characterize the younger stages of activity for all these volcanoes (Trua et al., 2004; Peccerillo, 2005). Thus, the geochemical data show an increase in potassium with the time, an increase in potassium ranging from the western to the eastern sector of the arc and an increase of the magma evolution degree with the time (fig. 2.4b).

The wide range of SiO_2 and K_2O explains the diversification of magmas and source rocks about the islands studied, especially Lipari and Salina islands.

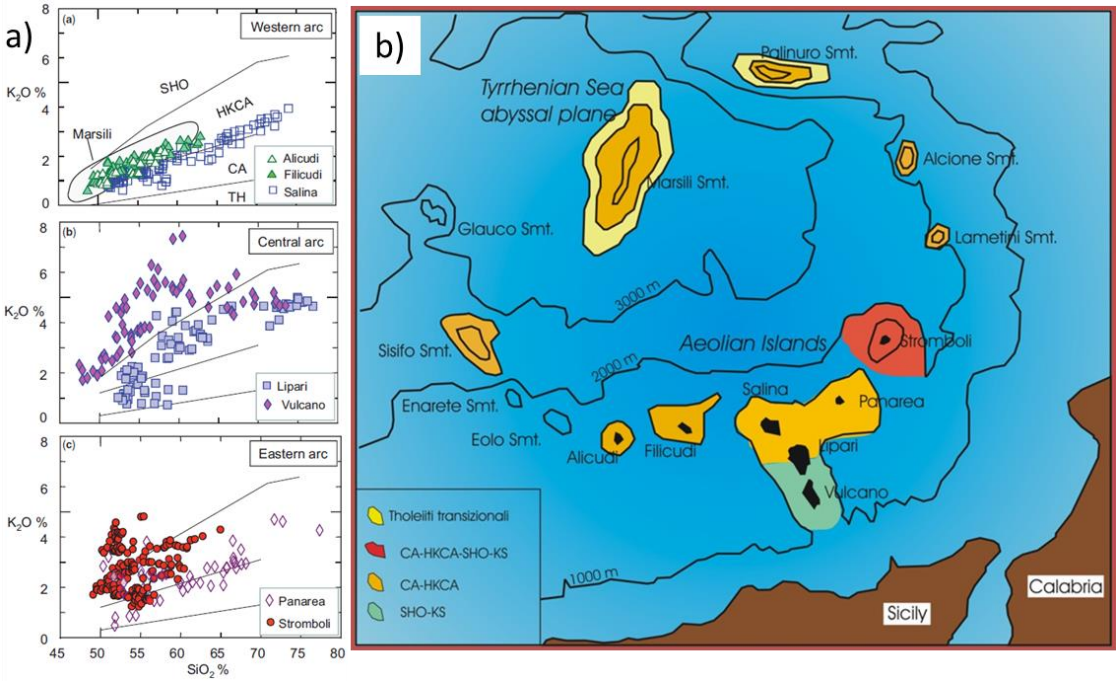

Figure 2.6 – a) K_2O Vs. SiO_2 classification diagrams for the Aeolian arc volcanics. Lines dividing arc tholeiitic (TH), calc-alkaline (CA), high-K calc-alkaline (HKCA) and shoshonitic (SHO) series (modified from Peccerillo et al., 2013); b) Sketch map of volcanic products series of the Marsili basin (Francalanci et al., 2007).

2.1.1 – Petrography and classification of Aeolian islands source rocks -

2.1.1.a - ALICUDI ISLAND -

The Alicudi volcano belongs to the western sector of the Aeolian archipelago, which extends from the Glauco seamount to the island of Filicudi (figs. 2.4a, 2.5).

Alicudi is a composite volcano made up predominantly of lavas and minor pyroclastic rocks. The volcanic products include calcalkaline basalts, basaltic andesites and andesites (fig. 2.7), which were erupted during three stages of activity separated by caldera collapses (Villari, 1980). Basalt and basaltic andesite lavas and minor pyroclastic rocks were emplaced during the first two stages, whereas the third stage was characterized by the outpouring of andesitic lava flows and domes. Rock ages range from 90 to ~30 ka, and represent the youngest activity in the western Aeolian arc (Gillot and Villari, 1980). All of the rocks from Alicudi are porphyritic, with phenocryst mineralogy dominated by plagioclase, pyroxene, and olivine. Plagioclase phenocrysts are abundant in the basalts, followed by olivine and clinopyroxene. Most of the plagioclase is complexly zoned and twinned, and ranges from bytownite to labradorite in composition. Olivine occurs as phenocrysts, microphenocrysts, and in the groundmass, often partially transformed to iddingsite. Clinopyroxenes are zoned and have diopsidic to salitic compositions. The groundmass consists of the same phases as the phenocrysts plus Fe–Ti oxides and orthopyroxene.

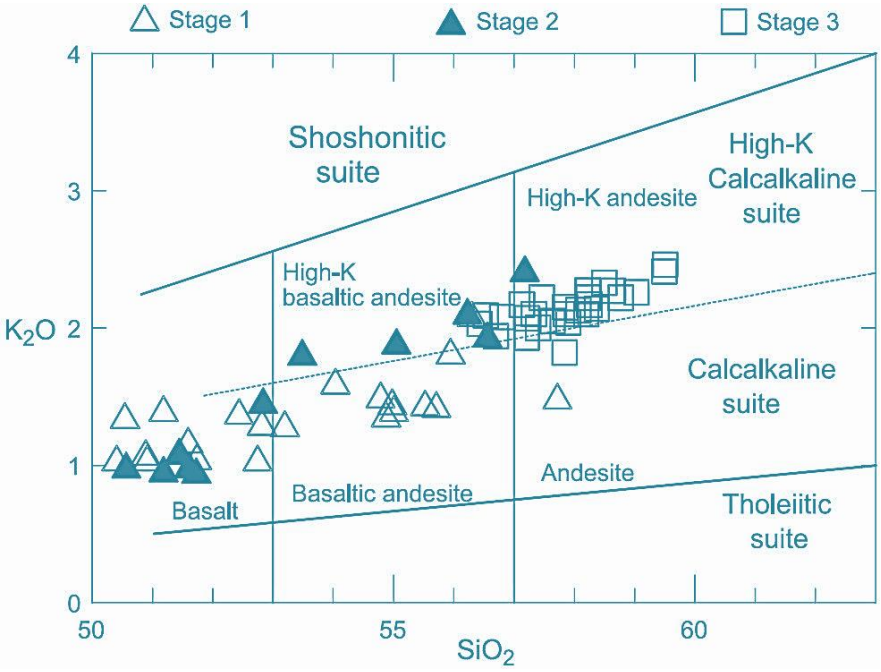

Figure 2.7 - K2O vs. SiO2 classification diagram for the Alicudi rocks (modified from Peccerillo and Taylor, 1976).

Basaltic andesites are texturally similar to the basalts, but the modal abundance of olivine is lower and orthopyroxene occurs along with brown hornblende as a microphenocryst phase. Glass is observed in the groundmass of some samples. High-K andesites have hypocrystalline porphyritic textures; the phenocryst mineralogy is still

dominated by plagioclase, with minor amounts of clino- and orthopyroxene, olivine, Fe–Ti oxides, and brown hornblende. The groundmass consists of the same phases as the phenocrysts set in a glass mesostasis. Xenoliths of magmatic and metamorphic origin are found in the Alicudi rocks, particularly in the mafic products of the first stage. Metamorphic xenoliths are mainly quartz-rich rocks. Most magmatic xenoliths are mafic to ultramafic in composition. Mafic enclaves have cumulate textures and compositionally range from gabbro to diorite, consisting of variable proportions of clinopyroxene, orthopyroxene, olivine and plagioclase. (Peccerillo et al., 2004, Lucchi et al., 2013).

2.1.1b - FILICUDI ISLAND -

Filicudi rock compositions range from basalts to dacites in the Total Alkali Silica (TAS) classification diagram (fig. 2.8a) and from calc-alkaline (CA) and high-K basalts to high-K dacites in the classification scheme of Peccerillo & Taylor (1976) (fig. 2.8b). The oldest exposed products are prevalently basalts and basaltic andesites (Paleo-Filicudi). Younger rocks are andesites and high-K andesites to dacites. All the Filicudi volcanics, except pumices, are highly porphyritic and display a holocrystalline or hypocrystalline seriate texture. Phenocryst mineralogy consists of plagioclase, clinopyroxene and olivine in the basaltic and basaltic andesitic rocks with sporadic accessory amounts of orthopyroxene microphenocrysts. Plagioclase is the dominant mineral phase in the high-K andesites, which also contain small amounts of clinopyroxene and orthopyroxene. Biotite, often partially or completely transformed into opaque minerals, is observed exclusively in the most-evolved andesites and dacites, together with brown hornblende. The groundmass generally contains the same mineral phases as the phenocrysts plus glass. Ti-magnetite, ilmenite and apatite are present in accessory amounts. Plagioclase is the most abundant mineral phase and consists of complexly zoned, sieve textured and/or variably twinned phenocrysts and microphenocrysts. Clinopyroxene is ubiquitous. It appears as colourless, euhedral to rounded, dusty and frittered phenocrysts and microphenocrysts. Composition is augitic or diopsidic. Olivine (Fo = 60–86 wt%) occurs as subhedral to euhedral phenocrysts with slight normal or reverse zoning. It often displays an iddingsitic rim or is mantled by clinopyroxene in the basalts and by orthopyroxene in the basaltic andesites. Orthopyroxene crystals are generally unzoned, sometimes with a reaction rim of clinopyroxene. Xenoliths of magmatic and metamorphic origin are frequently observed in the Filicudi lavas and pyroclastic deposits. Igneous xenoliths include medium to

coarse-grained gabbros and granodiorites, and lavas. Basalt and andesite lithic clasts show porphyritic textures and mineralogical composition similar to that of lavas. Metamorphic xenoliths, generally consisting of quartz, K-feldspar and plagioclase (Lucchi et al., 2013).

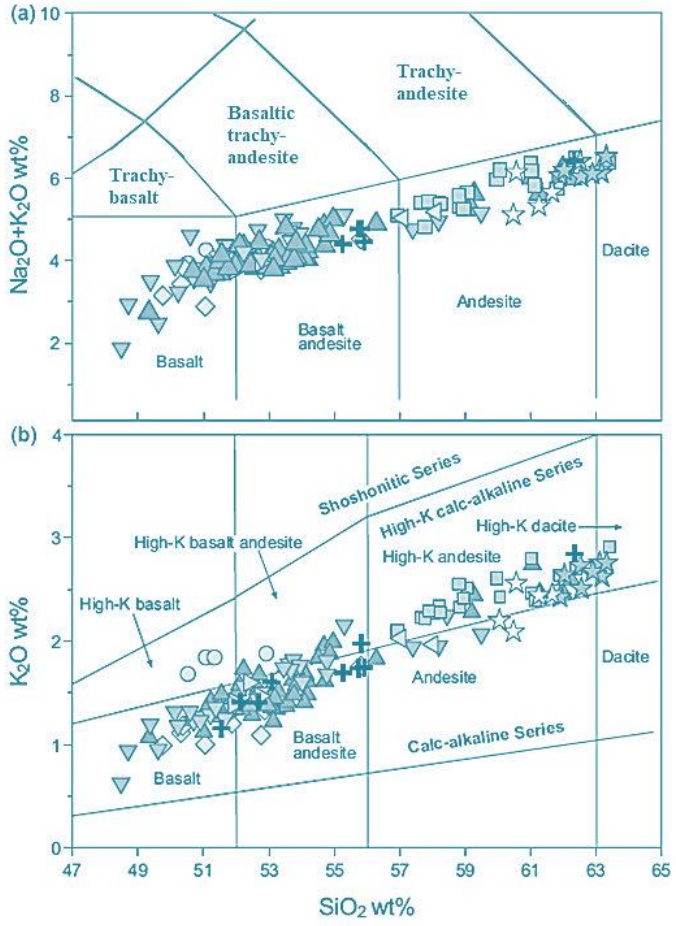

Figure 2.8 - (a) Total-alkali Vs. silica (TAS) and (b) potassium Vs. silica classification diagram for the Filicudi rocks.

2.1.1c – SALINA ISLAND -

According to Lucchi et al. (2013), the volcanic rocks of Salina, have a variable range in composition, from basaltic to rhyolitic (fig. 2.9). Basalt is by far the most abundant rock type on Salina. All Salina lavas typically exhibit holocrystalline, porphyritic textures with phenocryst contents of about 15–45 vol%. Scoria and pumice clasts have vitrophyric textures and generally contain less phenocrysts (5–25 vol%). Basalts of Salina are dominated by clear phenocrysts of plagioclase as well as olivine, often surrounded by thin rims of pigeonite, and clinopyroxene. The phenocrysts are typically enclosed within a groundmass of plagioclase, clinopyroxene, Ca-poor clinopyroxene (pigeonite) and Ti-magnetite.

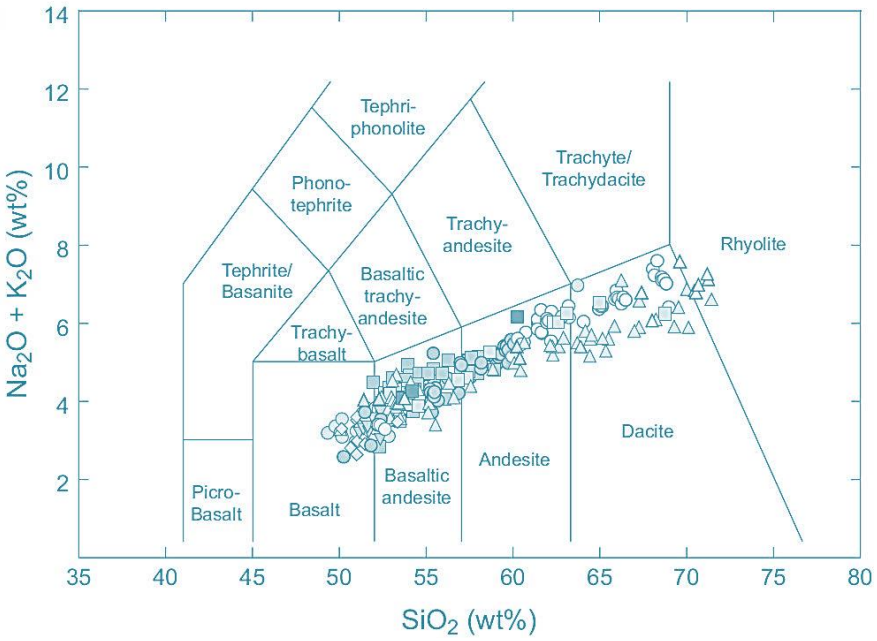

Figure 2.9 - Total alkali Vs. silica (TAS) diagram classification diagram for lavas and pyroclastic rocks from Salina island (modified from Lucchi et al., 2013).

Basaltic andesites contain less olivine and always moderate amounts of orthopyroxene and Ti-magnetite, which are ubiquitous in rocks. The groundmass of the basaltic andesites is typically pilotaxitic and composed of plagioclase, clinopyroxene, pigeonite and Ti-magnetite. In contrast to the basalts, plagioclase phenocrysts show complex zoning patterns and frequent sieve-textures. Olivine is always characterized by disequilibrium textures such as orthopyroxene or orthopyroxene-Ti-magnetite symplectite coronas. Orthopyroxene is often overgrown by clinopyroxene. Andesitic lavas and pyroclastic rocks are porphyritic, but generally contain fewer total phenocrysts than the basalts and basaltic andesites. The phenocryst mineralogy of the andesites consists of plagioclase, clinopyroxene, orthopyroxene and Ti-magnetite. Rare olivine crystals are resorbed and commonly surrounded by a breakdown rim of orthopyroxene with vermicular intergrowth of Ti-magnetite. Amphibole phenocrysts, which may be rimmed with fine-grained opaque aggregates. Apatite is present in trace amounts in the andesites. The phenocrysts are set in a pilotaxitic to hyalopilitic groundmass that consists of plagioclase, clinopyroxene (coexisting with either pigeonite or orthopyroxene) and Ti-magnetite. In the dacites rocks, the phenocryst mineralogy is similar to the intermediate rock types, although they contain higher modal proportions of orthopyroxene and amphibole, less clinopyroxene and they also tend to be less porphyritic. Amphibole is a conspicuous phenocryst phase. The phenocrysts are enclosed within a pilotaxitic or hyalopilitic to vitrophyric groundmass composed of

plagioclase, clinopyroxene, orthopyroxene, magnetite, rare late-stage biotite and, in some dacitic lavas, patches of coexisting quartz and alkali feldspar. The rhyolitic rocks restricted to the eruptive products of the Pollara tuff ring. Rhyolitic pumice clasts are characterized by a mineral assemblage that consists predominatly of plagioclase, amphibole and biotite, less-abundant clinopyroxene, orthopyroxene and rare xenocrystic olivine. Xenoliths are abundant and consist of granitoid basement rocks, metamorphic rocks and magmatic xenoliths (Keller 1980; Donato et al., 2006; Lucchi et al., 2013).

2.1.1d - LIPARI ISLAND –

The volcanic rocks of Lipari cover a wide compositional interval from calc-alkaline (CA) and high-K basaltic andesites to rhyolites, with a gap in the dacite field (fig. 2.10). Basaltic andesite lavas and scoriae have variably porphyritic (20 – 50%) with phenocrysts of plagioclase, diopsidic to augitic clinopyroxene and minor orthopyroxene and olivine. The orthopyroxene is mostly overgrown by clinopyroxene reaction rims. Olivine (Fo91 – 64) is generally transformed to iddingsite. Groundmass plagioclase displays an An_{68-48} composition, and clinopyroxene is pigeonitic. Andesite lavas and juvenile pyroclasts show variably porphyritic to porphyritic seriate textures (35–60% in lavas), with phenocrysts of plagioclase (An_{76-56}), augitic clinopyroxene, orthopyroxene and Fe-Ti oxides, set in a hyalopilitic to pilotaxitic groundmass containing plagioclase needles and Fe-Ti oxides. Ti-magnetite and apatite are the main accessory phases. The composition of plagioclase in the groundmass is An_{43} (Bargossi et al., 1989). Some andesites and dacites lavas contain abundant cordierite. These lavas exibit a seriate to highly porphyritic (up to 50%) texture and contain subhedral to anhedral zoned plagioclase, skeletal and stumpy orthopyroxene, clinopyroxene, cordierite, garnet and minor ilmenite, apatite, andalusite, spinel and sillimanite. Other dacitic lavas (e.g. Timpone del Corvo Formation) display porphyritic texture, with prevalent plagioclase phenocrysts and subordinate clinopyroxene, orthopyroxene and ilmenite. Groundmass is hyalopilitic to pilotaxitic or micro- to cripto-crystalline with plagioclase and Fe-Ti oxides. The pyroclastic rocks (e.g. M. Guardia Formation) are characterized by the occurrence of white pumiceous clasts (rhyolite), dark grey pumices (high-K andesite to latite) and light grey pumices (high-K dacite). The white pumices contain K-feldspar, plagioclase, horneblende, sporadic biotite and minor Ti-magnetite, apatite and zircon, whereas the dark pumices contain clinopyroxene, plagioclase and minor olivine, Ti-magnetite and apatite (De Rosa et al., 2003; Lucchi et al., 2013).

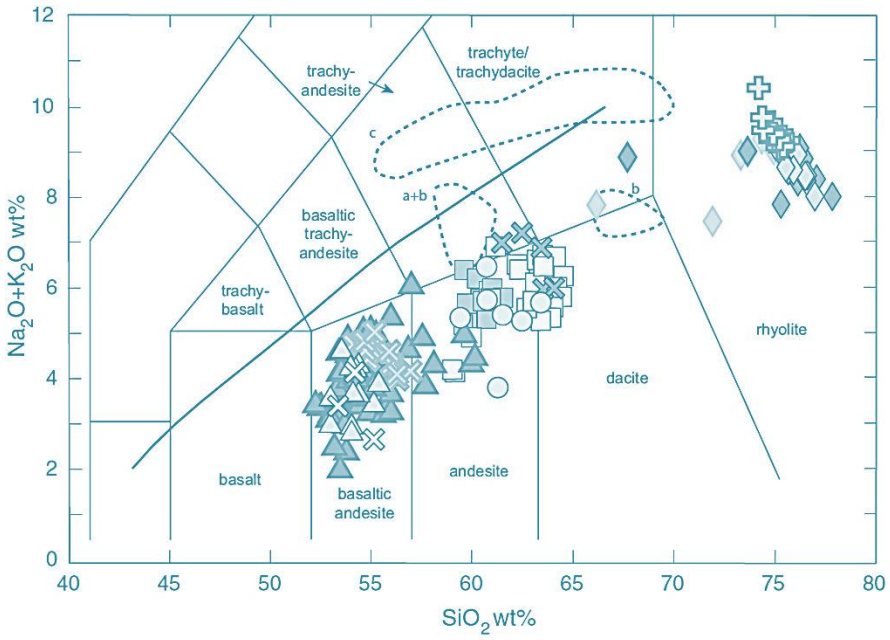

Figure 2.10 - Total alkali Vs. silica (TAS) diagram classification diagram for lavas and pyroclastic rocks from Lipari island (modified from Lucchi et al., 2013).

The rhyolite rocks are scarcely porphyritic with less than 5 vol% phenocrysts. K-feldspar is the main phase, followed by plagioclase (An_{25-20}) and hornblende. Biotite, Ti-magnetite, zircon and apatite are the main accessories. Some formations (e.g. Vallone del Gabellotto, Pomiciazzo, Pirrera) contain pyroclastic rocks and lavas which are aphyric to subaphyric, with eutaxitic texture. Magmatic and metamorphic xenoliths are documented in volcanic rocks from Lipari island (De Rosa et al., 2003; Gioncada et al., 2005; Davì et al., 2009; Lucchi et al., 2013).

2.1.1e - VULCANO ISLAND -

Vulcano rocks display a wide spectrum of compositions ranging from basalts to rhyolites with high-K calc-alkaline (HKCA) and shoshonitic (SHO) (fig. 2.11). The rocks from Vulcano show variable Porphyritic Index (PI, i.e. the total phenocryst content of the rock by volume), ranging from c. 2% to more than 60%. Some almost aphyric types are present. The groundmass is glassy to microcrystalline. The mafic rocks display plagioclase, Ca-rich clinopyroxene, Fe–Ti oxides and olivine mineral assemblage. Microphenocrysts of leucite, often transformed to analcite, are present in some KS rocks. Plagioclase and/or clinopyroxene phenocrysts are dominant in most of the mafic and intermediate rocks. Plagioclase, K-feldspar and biotite generally prevail in the more evolved rocks (e.g. trachytes), where brown amphibole rarely occurs. Apatite is commonly present in the mafic-intermediate rocks.

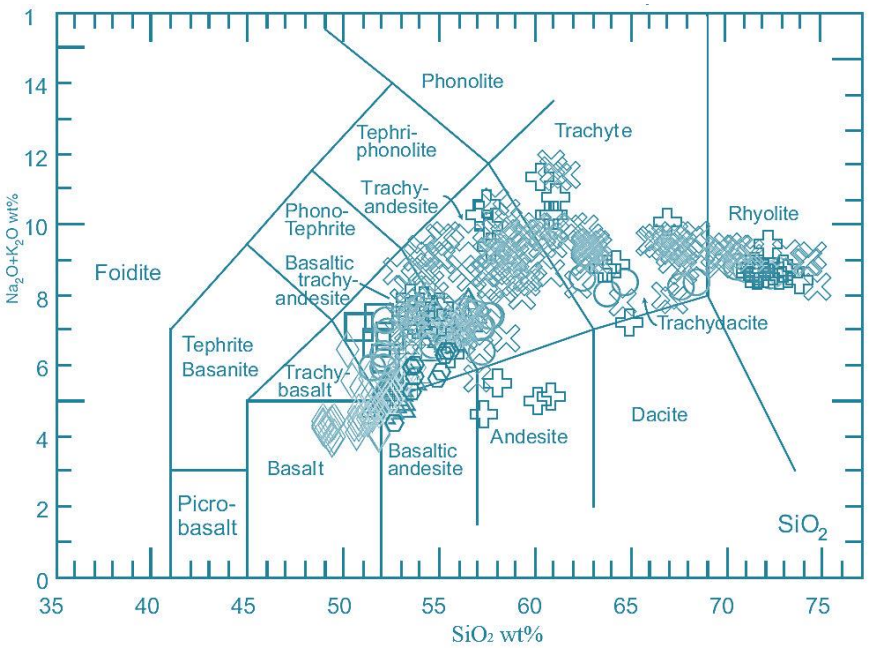

Figure 2.11 - Total alkali Vs. silica (TAS) diagram classification diagram for lavas and pyroclastic rocks from Vulcano island (modified from Lucchi et al., 2013).

Rhyolitic lava flows (e.g. La Fossa lithosome) are obsidianaceous and carry pinkreddish enclaves which are latitic to trachytic in composition, of variable shape and size and often showing embayments and rotational features. Even the products from the last eruption (1888–1890) contain plastically deformed magmatic enclaves (latites) in various stages of disaggregation and/or lava fragments of different composition, with clear evidence for both mingling and mixing (Lucchi et al., 2013).

2.1.1f - PANAREA ISLAND –

The Panarea volcanic rocks range from mafic to felsic, and from calc-alkaline and high-K calc-alkaline to shoshonitic (fig. 2.12). Dacites and high-K dacites are the most common rock types, followed by andesites. The basaltic rocks are limited on Panarea island. Most rocks have a variably porphyritic texture with phenocryst contents around 30–40%. The rhyolites are less porphyritic with phenocryst contents around 10%. Plagioclase is the dominant phenocrystic phase for all the rocks, followed by clinopyroxene and orthopyroxene. Amphibole, often transformed to opaque minerals, appears as phenocryst in the andesites and becomes more abundant in the dacites. Olivine occurs in the basaltic andesites. Biotite occurs as a phenocryst in some rhyolites (e.g. Basiluzzo) groundmass along with amphibole. Groundmasses range from hypocrystalline to glassy, and contain variable amounts of plagioclase, pyroxene, opaque minerals and a few biotite. Some rocks, especially dacites, have banded

groundmass given by the heterogeneous distribution of microliths. Rhyolites have a glassy, fluidal groundmass.

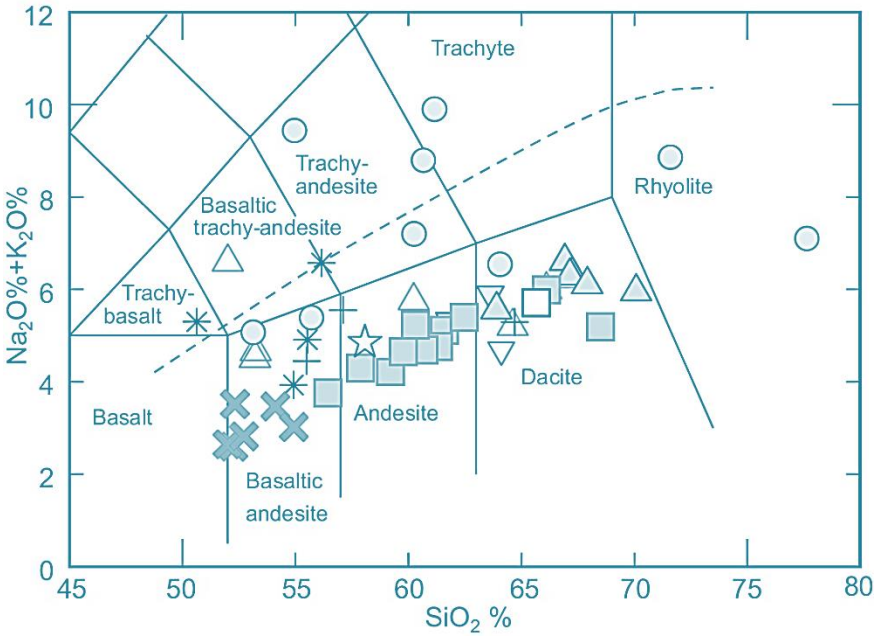

Figure 2.12 - Total alkali Vs. silica (TAS) diagram classification diagram for lavas and pyroclastic rocks from Panarea island (modified from Lucchi et al., 2013). The dashed line indicate the boundary between the alkaline and subalkaline fields of Irvine & Baragar (1971).

Plagioclase is complexly zoned and exhibits extremely variable An contents (An_{90}–An_{35} in the basaltic andesites; mostly An_{35}–An_{50} in the dacites). Clinopyroxene phenocrysts generally show a limited compositional variability but exhibit oscillatory zoning from augite to diopside. Orthopyroxene ranges between bronzite and hypersthene. Olivine phenocrysts have homogeneous compositions with $Fo_{78\ -\ 76}$ in basaltic andesites and $Fo_{74\ -\ 72}$ in the dacites (Calanchi et al., 2002; Cimarelli et al., 2008; Lucchi et al., 2013). Lucchi et al. (2013) have recognized distinctive characters by the main pyroclastic successions on Panarea island. Some pyroclastic products (e.g. Costa del Capraio Subsynthem are andesites to dacites. They are moderately porphyritic with c. 10–20% phenocrysts of plagioclase, clinopyroxene, amphibole, orthopyroxene and opaques, set in a vesicular hyalopilitic groundmass. Some scoriaes (e.g. Scoglio La Loca Subsynthem) are basalts to basaltic andesites, poorly porphyritic and vesicular, with phenocrysts of plagioclase and pale green clinopyroxene. Lucchi et al (2013) also have found metamorphic and magmatic xenoliths in many lava domes and flows. Metamorphic xenoliths mainly consist of quartzites and gneisses. Magmatic xenoliths include rock fragments and enclaves.

2.1.1g - STROMBOLI ISLAND -

The Stromboli rocks range from sub-alkaline to slightly alkaline and straddle the boundary between the two fields as shown in figure 2.13.

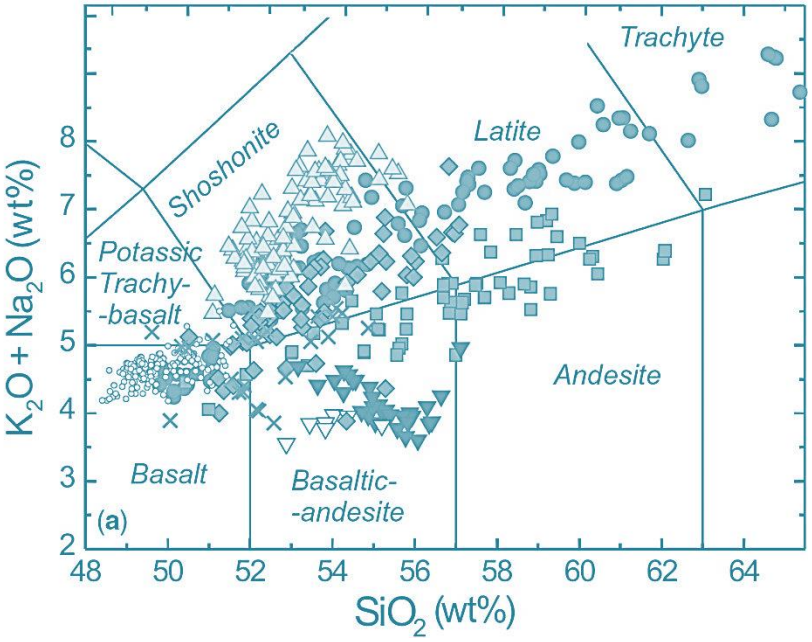

Figure 2.13 - Total alkali Vs. silica (TAS) diagram classification diagram for lavas and pyroclastic rocks from Stromboli island (modified from Lucchi et al., 2013).

Rocks generally have seriate porphyritic textures with variable phenocryst content (c. 5–55 vol%). The most abundant phenocryst and microphenocryst is plagioclase, with decreasing An component (from An_{90} to An_{45}) passing from less to more evolved magmas, followed by clinopyroxene. Olivine ($Fo_{62 - 91}$) is found in the basalts and intermediate rocks of the different series, while orthopyroxene occurs in the CA and HKCA rocks and as microphenocrysts in the evolved SHO products (latites). Hornblende is present in small amounts in the high-K andesites and is rare and deeply resorbed in the latites and thachytes. Biotite is c. 7 vol% of phenocrysts in the latites and c. 2 vol% in the trachytes. Leucite, generally transformed to analcime, appears both in the groundmass and as microphenocrysts of some of the KS lavas. Opaques are usually represented by Ti-magnetite, associated with ilmenite only in the CA rocks. Apatite is present as accessory phase, included in plagioclase and pyroxene. K-feldspar occurs in the lavas groundmass (KS). Phlogopite and biotite also occur in the groundmass vugs of KS rocks (Francalanci et al., 1989; 1993; 2004; Hornig-Kjarsgaard et al., 1993; Lucchi et al., 2013).

2.2 - Geological setting of Campania Province -

The Campania Province represents the southernmost sector of the volcanic belt along the Italian peninsula (fig. 2.14). It is formed by the active volcanoes of Somma-Vesuvio, Ischia and Campi Flegrei (Phlegraean Fields), and by the islands of Procida and Vivara. The Pontine Islands are also sometimes included in the Campania Province. Volcanic rocks range from mafic to felsic and mostly have silica undersaturated potassic to ultrapotassic compositions. Mafic rocks with K_2O contents close to calc-alkaline basalts have been found both as lavas and as lithic ejecta at Ventotene and Procida-Vivara. Pliocene (about 4.5 Ma) calc-alkaline rhyolites occur at Ponza, and 2 Ma old calc-alkaline basalts to andesites have been found by borehole drilling beneath the Campania Plain north of Campi Flegrei (Peccerillo 2005).

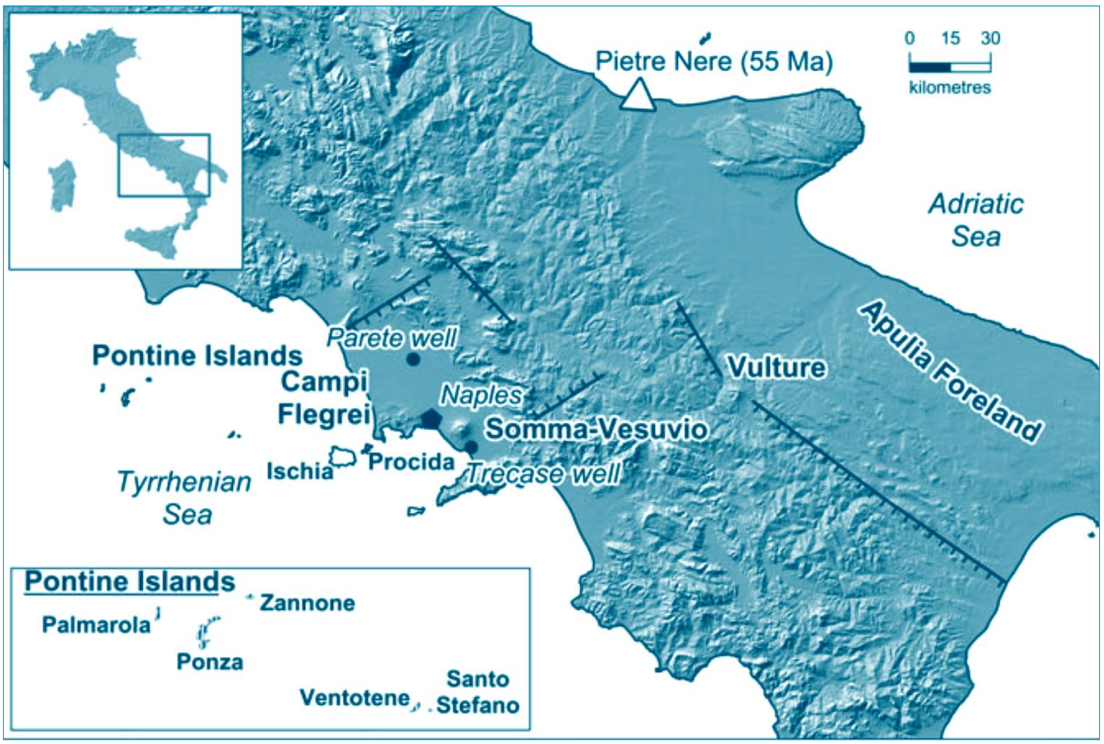

Figure 2.14 - -- Location map of the Campania volcanoes (modified from Peccerillo 2005).

Mount Vulture is a 0.8 to 0.1 Ma old stratovolcano rising as an isolated cone about 100 km east of Vesuvio. Although the Vulture rocks are alkaline and undersaturated in silica, they are enriched in both sodium and potassium, and show distinct composition with respect to other alkaline volcanoes in central-southern Italy. Washington (1906) propose a separate magmatic province for Mount Vulture (Apulian Province). But Peccerillo (2005) suggests to describe Mount Vulture with Campania volcanoes not only because of their geographic contiguity but also for some significant geochemical affinities.

VOLCANO	AGE	VOLCANOLOGY and PETROLOGY
Somma-Vesuvio	30 ka to 1944 AD	- Stratovolcano (Mount Somma) with multiple caldera and an intracaldera cone (Vesuvio) formed of slightly to strongly silica undersaturated trachybasalt and leucite-tephrite to trachyte and phonolite.
Campi Flegrei	About 0.2 Ma to 1538 AD. Buried volcanism 2 Ma old	- Multicentre volcanic complex with two nested calderas and several monogenetic cones and maars, formed of prevailingly pyroclastic rocks with trachybasalt to trachyte-phonolite composition.
Ischia island	150 ka to 1302 AD	- Volcano-tectonic horst formed of prevailing pyroclastic rocks with trachybasaltic to dominant trachytic composition.
Procida-Vivara islands	55 to 17 ka	- Coalescing explosive centres formed of basalt, K-trachybasalt to trachyte pyroclastics.
Pliocene buried volcanism	2 Ma	- About 1300 m thick sequence of calc-alkaline basalt to andesite underlying Campi Flegrei potassic rocks.
Ponza, Palmarola, Zannone, La Botte	4.2 to 1 Ma	- Lava flows, domes, breccias and hydrovolcanic products formed of Pliocene calc-alkaline rhyolites and Pleistocene peralkaline rhyolites and potassic trachytes.
Ventotene and Santo Stefano islands	0.8 Ma to < 130 ka	- Stratovolcano with a caldera formed of basalt, K-trachybasalt to trachyte lava flows, domes (Santo Stefano) and pyroclastics.
Vulture	0.8 to 0.13 Ma	- Stratovolcano with a summit caldera, intracaldera explosion craters and some parasitic centres formed of lavas and pyroclastics with Na-K-alkaline tephrite, foidite, melilitite, haüynophyre, and phonolite compositions. Late carbonate-rich pyroclasts.

Table 2.1 - Age and composition of volcanism in Campania province (modified from Peccerillo 2005).

The Campania Province, is located along a transect that stretches from the Tyrrhenian Sea to the Apulia foreland, across the southern Apennine chain (fig. 2.14). Southern Apennines consist of a number of thrusts, locally covered by Plio-Quaternary autochthonous shallow marine and continental sediments. Overthrusting of tectonic units occurred during Upper Oligocene to Lower Pleistocene compressional phases. These were followed by intensive extension, which generated fault systems both parallel and normal to the Apennine chain (Cello and Mazzoli 1999). Tectonic units (Sicilide, Liguride, Verbicaro-San Donato, Alburno-Cervati, Lagonegro, etc.) (Ippolito et al. 1975; Grasso 2001) consist of a wide variety of rock types (limestones,

dolostones, flysch sequences, sandstones, marls, ophiolitic rocks, etc.) ranging in age from Upper Triassic to Miocene. They mostly represent basinal sequences formed on the border of the African plate, which were delaminated and superimposed over the Apulia foreland. The latter is located east of the Apennine chain and consists of Mesozoic to Tertiary platform carbonates (e.g. Ogniben et al. 1975; Grasso 2001; Patacca and Scandone 2001; Vai and Martini 2001). The volcanic centers of the Campania Province developed inside Quaternary extensional basins along the Tyrrhenian Sea border at the intersection between NE-SW and NW-SE fault systems. The Pontine Islands form a row of volcanoes with a W-E trend, offshore the Campania Province, and along the so-called 41st Parallel Tectonic Line (Serri 1990; Bruno et al. 2000). Vulture is located at the eastern border of the Apennine compression front, in an extensional tectonic setting affecting the border of the Apulia foreland. The thickness of the lithosphere along the Pontine-Campania-Vulture transect increases from about 50 km along the Tyrrhenian Sea border to more than 110 km in the Apulia foreland (Calcagnile and Panza 1981). The depth of the Moho increases from about 20-25 km offshore the Tyrrhenian Sea coast to 40 km beneath the internal zones of the Apennines, to decrease to about 30 km beneath the Apulia foreland (e.g. Locardi and Nicolich 1988; Piromallo and Morelli 2003).

According to Beccaluva et al. (1991) the Campania volcanism has been attributed to the presence of a subducting slab beneath this region. The close compositional similarity between Campania volcanoes and Stromboli has been interpreted as an evidence for a common source and tectonic setting for these volcanoes. Stromboli is clearly related to subduction of Ionian plate, which has led to conclude that the Campania magmas have also been generated in an upper mantle contaminated by the Ionian plate (Peccerillo 2001). However, Campania volcanoes are closer to the Apulian than to the Ionian foreland, which would support that the mantle source of Campania volcanoes was contaminated by material coming from the Apulian rather than the Ionian plate. Distinct compositions would be expected for the Campania and Stromboli magmas, if contaminants with different histories modified their sources. A proposed solution to this problem is that the subducting slab was initially continuous and homogeneous from Apulia to the Ionian Sea, but that, subsequently, there was slab breakoff in the Apulian sector because of its collision with southern Apennines (De Astis et al. 2000; Peccerillo 2001). Slab break-off in Apulia caused a narrow slab to remain joined to the Ionian plate; this underwent sinking, some clockwise rotation and

rollback toward the southeast. Fluids and sediments coming from the sinking and retreating slab contaminated the upper mantle, both beneath Campania and Stromboli, leading to the similarity in the arc signatures for these volcanoes (Peccerillo 2001). The slab detachment could have occurred at about 0.8 Ma, when compression phases in the Vulture area ended and distension tectonics generated fractures along which Vulture magmas ascended to the surface (Patacca and Scandone 2001). The sketch in fig. 2.15 shows a geodynamic evolution model according to Peccerillo (2005).

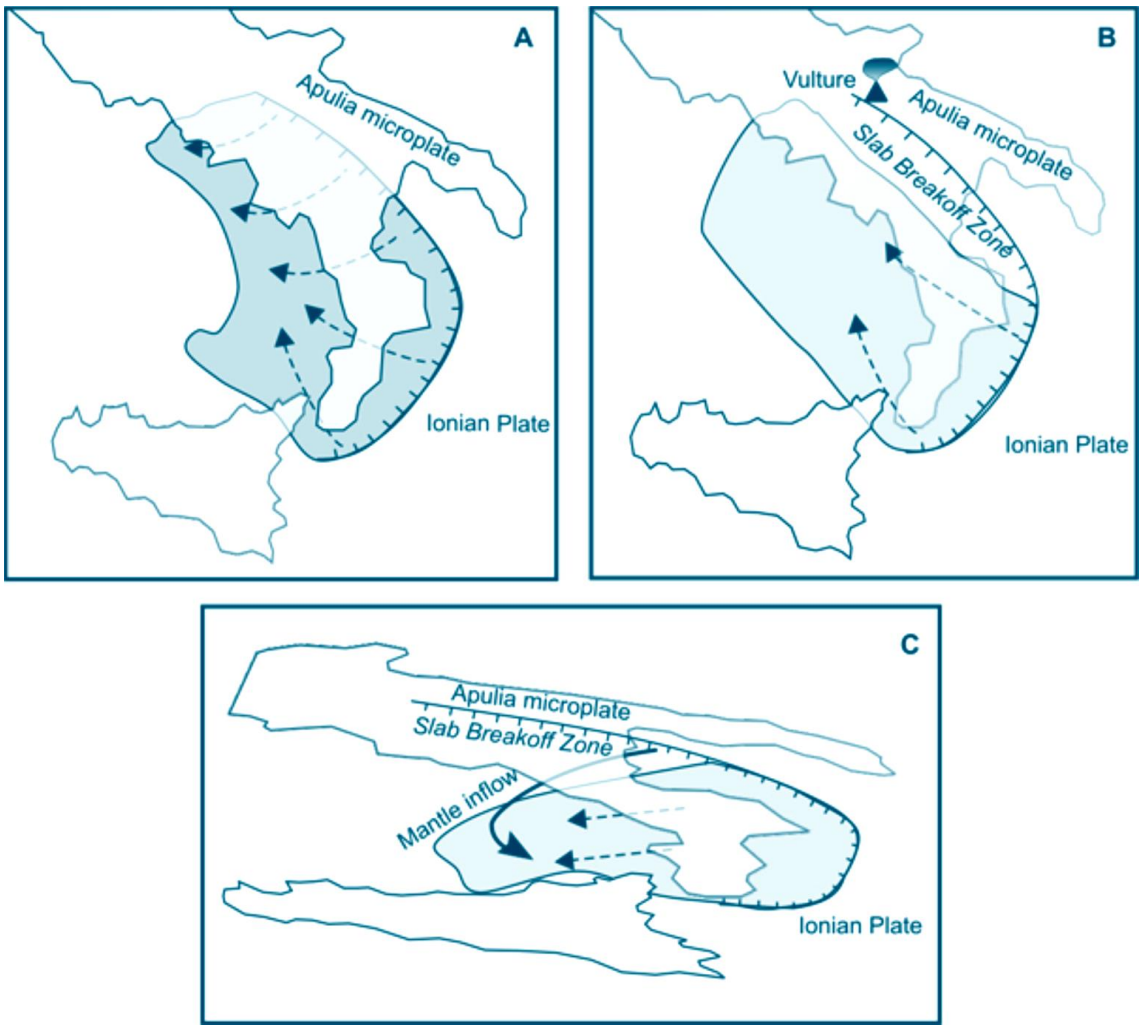

Figure 2.15 -- Geodynamic evolution model for the southern Italian Peninsula (modified from Peccerillo 2005). A) A continuous subduction zone of the Apulian-Ionian plate was active until about 0.8 Ma. B) Slab breakoff in the Apulian sector generated distension regime at the contact between Apulia and the southern Apennines; C) Sinking and rollback of the narrow Ionian slab generated suctioning of intraplate asthenosphere from the Apulia foreland; this was contaminated by sedimentary material and fluids from the subduction zone and generated a hybrid OIB-arc mantle wedge, whose melting gave the Campania volcanoes and Stromboli.

According to slab break-off model, the arc signatures of Mount Vulture would derive from melts and fluids released by the detached and sinking slab, which contaminated the mantle beneath the edge of the Apulia plate, where Mount Vulture magmas were formed. Speculatively, the OIB component in the Campania Province as well as in the Stromboli area could be related to a mantle inflow from the Apulian plate through the widow opened by slab breakoff, onto the sinking and retreating Ionian slab. According to this hypothesis, the OIB component would be allochthonous in origin. Alternative hypothesis on the origin of hybrid geochemical signatures of Campania, Pontine Islands and Vulture magmatism invokes a mantle plume rising beneath the southern Tyrrhenian Sea and contamination by subducting Ionian plate (Gasperini et al. 2002). According to this hypothesis a deep plume would have been emplaced at shallow level through a slab window formed as a consequence of differential slab retreat during the opening of the Tyrrhenian Sea. Plume material was contaminated by slab components, acquiring hybrid characteristics (Peccerillo 2005).

The Campania plain (fig. 2.16) is identified as the region of Southern Italy, bordered by Mesozoic carbonate platforms, which subsided during the Pliocene and Pleistocene with a maximum vertical extent of 5 km (Ippolito et al., 1975). Voluminous volcanic activity of Campi Flegrei, Vesuvius and the island of Procida occurred along the coast of this plain during the last 50 ka. Campi Flegrei activity spans the period from ~ 50 ka to the present (Rosi and Sbrana, 1987). Most of the explosive activity of Somma-Vesuvius occurred after 25 ka (Santacroce, 1987), whereas activity on Procida occurred between > 40 ka and 18 ka. The city of Naples lies in the middle of the plain and is bordered by the two active volcanoes of Campi Flegrei and Vesuvius (fig. 2.16) (Scandone et al., 1991).

Somma-Vesuvio, Phlegrean Fields and Ischia are the largest and best known volcanoes in this province. The composition of volcanic rocks is variable, from potassic to ultrapotassic; calc-alkaline rocks are also found by borehole drillings and among lithic ejecta. The mafic rocks with different enrichment in potassium have comparable concentrations for several incompatible elements and exhibit less extreme isotopic compositions than the equivalent rocks of the Roman Province.

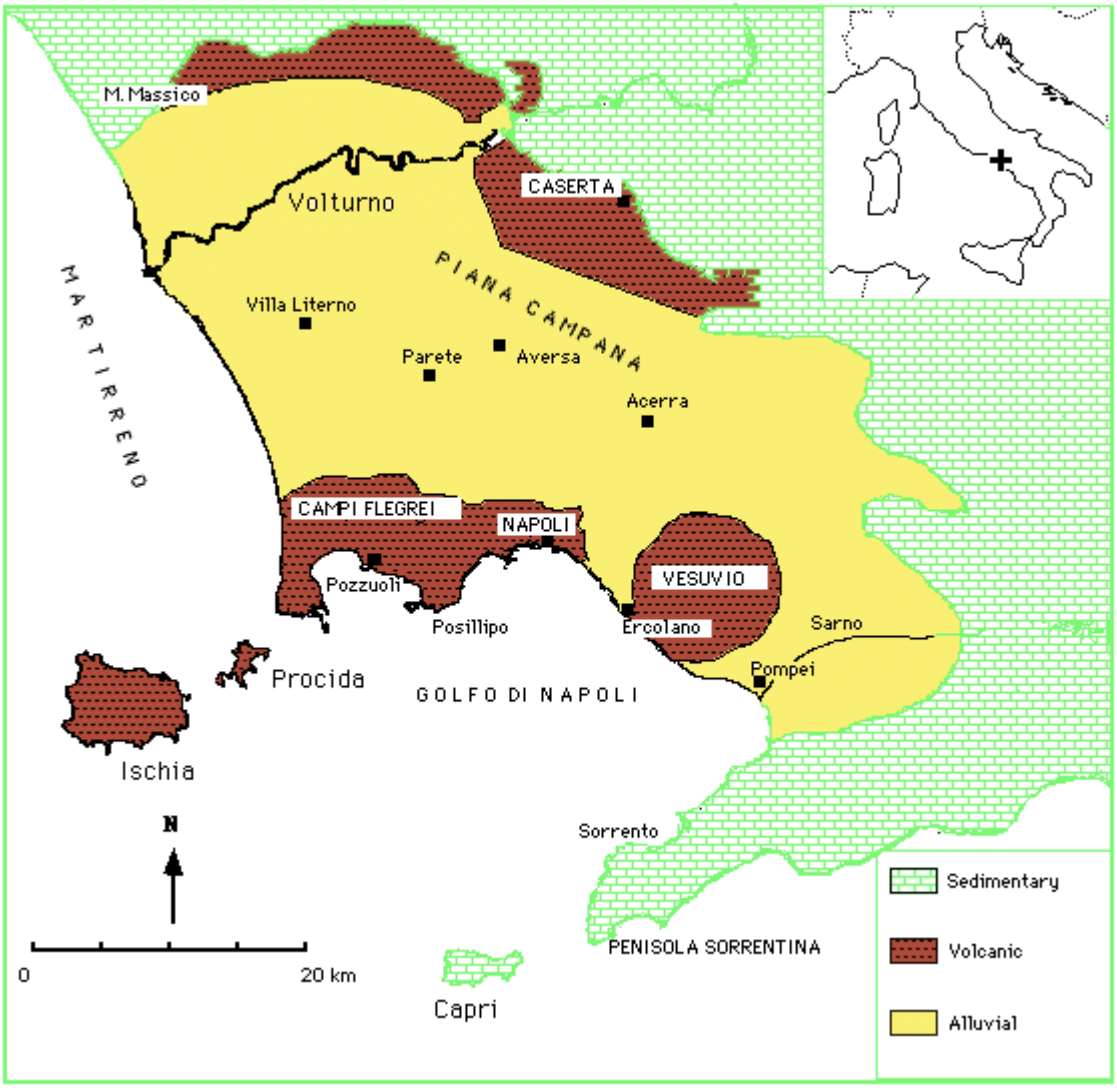

Figure 2.16 - -- Schematic geological map of the Campania Plain. The oldest volcanics of the area outcrop on lschia Island (modified from Scandone et al., 1991).

2.2.1 – Petrography and classification of Campania province source rocks -

The volcanoes in the Campania Province are composed of a wide variety of magma types. Silica undersaturated ultrapotassic volcanism is restricted to Somma-Vesuvio, whereas mildly undersaturated to oversaturated potassic rocks occur at Phlegrean fields, Ischia, Procida and Ventotene. Pliocene calc-alkaline rocks are found as rhyolites at Ponza and as basalts and basaltic andesites beneath the Campania Plain. At Vulture, volcanism is highly enriched in both Na and K, a composition that is distinct from any other volcano in the Italian peninsula. An important feature of magmatism in Campania is that the Phlegrean Fields mafic rocks are moderately potassic in composition but have very similar concentrations and ratios of several incompatible elements as the ultrapotassic rocks from Somma-Vesuvio; these, however, contain higher concentrations of K and Rb (e.g. Peccerillo 2001). The main petrological characteristics,

and in particular the variable enrichment in alkalis indicate that different proportions and amounts of K and Na-rich phases (e.g. phlogopite, amphibole) participated into the melt during generation of primary magmas (Peccerillo, 2005).

2.2.1a – PHLEGREAN FIELDS –

The Phlegrean Fields (fig. 2.17) is an active volcanic area that covers about 200 Km^2 of the coastal zone of SW Italy. The area has been active at least since 78 ka B.P., and it is structurally dominated by a caldera collapse, 8-10 km in diameter, associated with the eruption of the Neapolitan Yellow Tuff (NYT), a 30-50 Km^3 ignimbrite dated 15 ka B.P. Following the NYT event, the Phlegrean Fields were dominated by phreato-magmatic activity with occasional plinian phases and minor lava domes (Di Vito et al., 1999). The last event was the Monte Nuovo eruption in 1538 A.D. The majority of Phlegraean rocks belong to the "potassic" series. The compositional spectrum ranges from trachybasalts to latites, trachytes, alkali trachytes, and peralkaline phonolitic trachytes (fig. 2.18). The wide variability of products produces a great diversity of fragments with different composition and texture (Civetta et al., 1997).

The Phlegrean Fields volcanic complex is formed by two nested calderas and by several monogenetic cones and craters (fig. 2.17). The calderas are related to gigantic explosive eruptions which deposited the Campania Ignimbrite and Neapolitan Yellow Tuff (Orsi et al. 1995). Campania Ignimbrite eruption (39 ka) (De Vivo et al. 2001), is a phreatoplinian event that outpoured some 200 km^3 of phonolitic-trachytic pyroclastics. The Neapolitan Yellow Tuff eruption (15 ka), discharged some 40 km^3 of latite to trachyte-phonolite pyroclastics, forming an internal caldera (Orsi et al. 1995). The pyroclastic rocks of these eruptions rest over older products, some of which have been dated between about 157 ka to 205 ka (De Vivo et al. 2001). The volcanism younger than 15 ka concentrated inside the caldera and has been characterised by several explosive events. These generated a large number of craters and cones, which pockmark Phlegrean Fields caldera and represent a main morphological feature of the area (e.g. Orsi et al. 1996; Santacroce et al. 2003 and references therein). The latest eruption dates back to 1538 AD when the Monte Nuovo phonolitic cone was formed. After this eruption, Campi Flegrei has been subjected to a number of volcanic crises characterised by strong soil uplift and intense shallow seismicity, but no eruptions have occurred. The main unrest events in the past 40 years, took place in 1969-72 and 1982-84, and generated uplifts of 170 and 180 cm, respectively (e.g. Orsi et al. 1996).

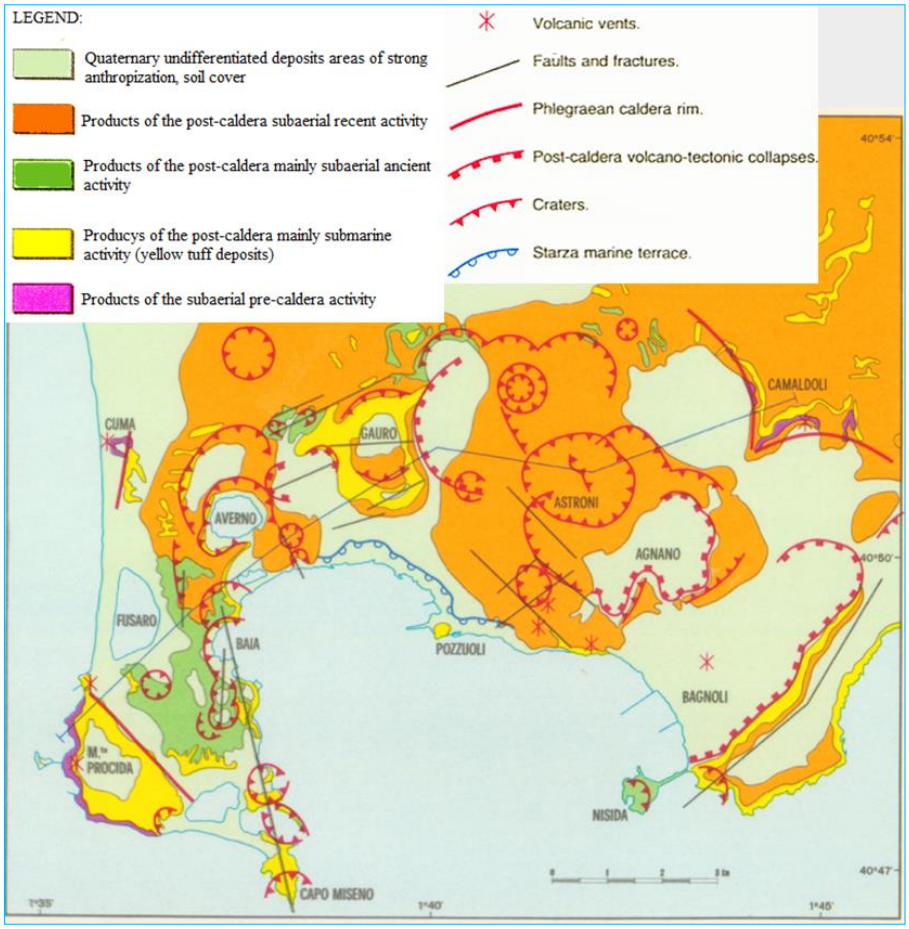

Figure 2.17 - --Geological and structural sketch map of Phlegrean fields (modified from Barberi et al., 1986).

The Campi Flegrei rocks consist of dominant pyroclastic deposits and minor lavas (Armienti et al. 1983; Rosi and Sbrana 1987). Compositions are slightly undersaturated to oversaturated in silica and range from trachybasalt to trachyte and phonolite on the TAS diagram (fig. 2.18). Some phonolites are peralkaline. Overall mafic and intermediate rocks show moderate enrichment in potassium. The rocks older than 39 ka and the Campania Ignimbrite have a composition straddling the limit between trachyte and phonolite; the Neapolitan Yellow Tuff ranges from latite to trachyte and phonolite (fig. 2.18; Pappalardo et al. 1999; Signorelli et al. 1999). Rocks younger than 12 ka have a wider compositional range, from trachybasalt-shoshonite to trachyte and phonolite (Peccerillo, 2005 and references therein).

Rock textures range from porphyritic to sub-aphyric, with phenocryst contents decreasing from trachybasalts to trachytes and phonolites (Armienti et al. 1983). The least-evolved rocks have abundant clinopyroxene and plagioclase, minor olivine and rare biotite and magnetite phenocrysts set in a groundmass formed by the same phases. Latites contain clinopyroxene, plagioclase and biotite phenocrysts, set in a

hypocrystalline groundmass made of abundant sanidine, Fe-Ti oxides and glass. Trachytes and phonolites range from holocrystalline to almost glassy, with phenocrysts of alkali-feldspar, minor clinopyroxene, biotite, plagioclase, Fe-Ti oxides and rare amphibole and sodalite-group minerals. Accessory phases include apatite, zircon and sphene (Armienti et al. 1983; Rosi and Sbrana 1987). Clinopyroxene composition ranges from diopside in the mafic rocks to ferrosilite in the felsic rocks. Single crystals often show colour and compositional zoning in thin section. Olivine (about Fo_{80}) is commonly altered to iddingsite. Plagioclase (about An_{90-35}) is generally zoned and is mantled by sanidine in the most evolved rocks (Armienti et al. 1983).

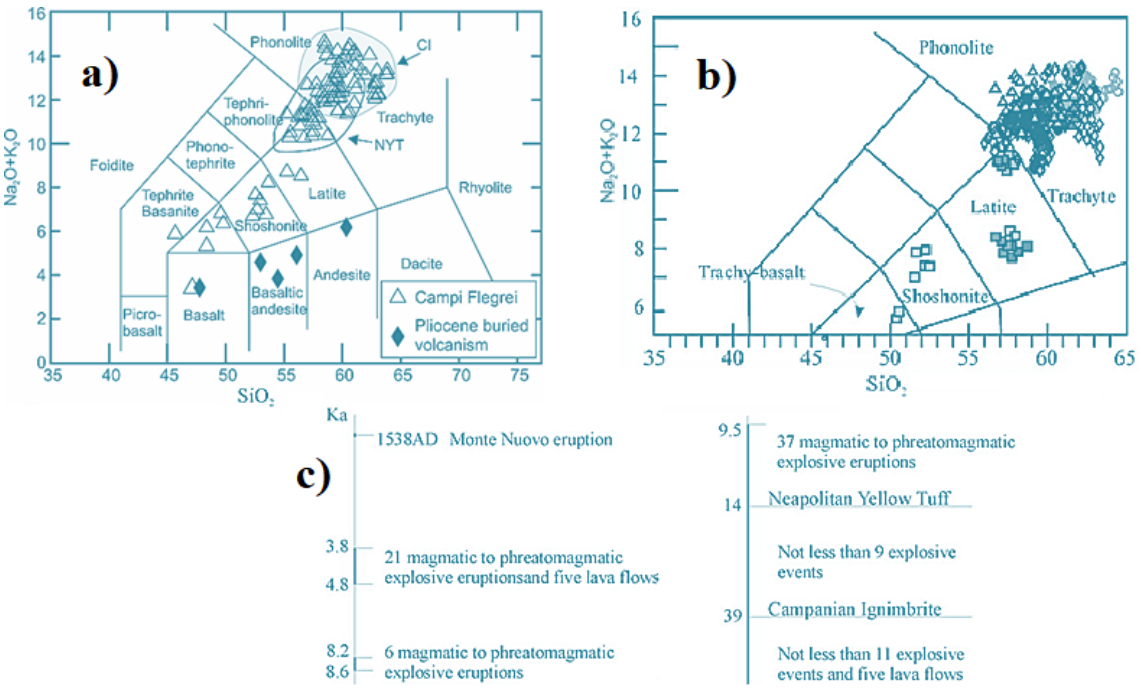

Figure 2.18 - Plot of total alkalis vs. silica for Phlegrean Fields. Data are from Peccerillo, 2005 (a) and from Pappalardo and Mastrolorenzo, 2012 (b); c) schematic chronogram of Phlegrean Fields activity as recorded by stratigraphic successions (modified from Pappalardo and Mastrolorenzo, 2012).

2.2.1b – MOUNT VESUVIUS –

Vesuvius is a 1279 m high composite volcano consisting of an older dissected cone (Somma) with a summit polyphasic asymmetrical caldera, and an intra-caldera cone (fig. 2.19). Vesuvius is younger than the 79 AD eruption that destroyed Pompeii and Herculaneum, and probably started to grow after the 472 AD eruption, inside the amphitheatre shaped depression of the Somma caldera (Santacroce 1987; Rolandi et al. 1998; Santacroce et al. 2003). The lowest exposed rocks of Somma volcano consist of alternating mafic lava flows and scoriae with a trachybasalt to potassic tephrite

composition. Starting from about 18 ka up to 79 AD, the style of volcanic activity became more explosive, and plinian eruptions took place, affecting evolved potassic magmas ranging from latite and trachyte to phonolite and tephriphonolite. Plinian activity was preceded by long periods of volcanic quiescence, and was accompanied by volcano collapses that formed the Somma caldera; emissions of lavas and pyroclastics by strombolian, vulcanian and subplinian eruptions also occurred during inter-plinian phases. After the 79 AD eruption, Vesuvio has been characterised by strombolian and effusive activity alternating with periods of 200-500 years of volcanic quiescence (e.g. 472 AD and 1631 AD), each closed by large explosive eruptions (Peccerillo, 2005).

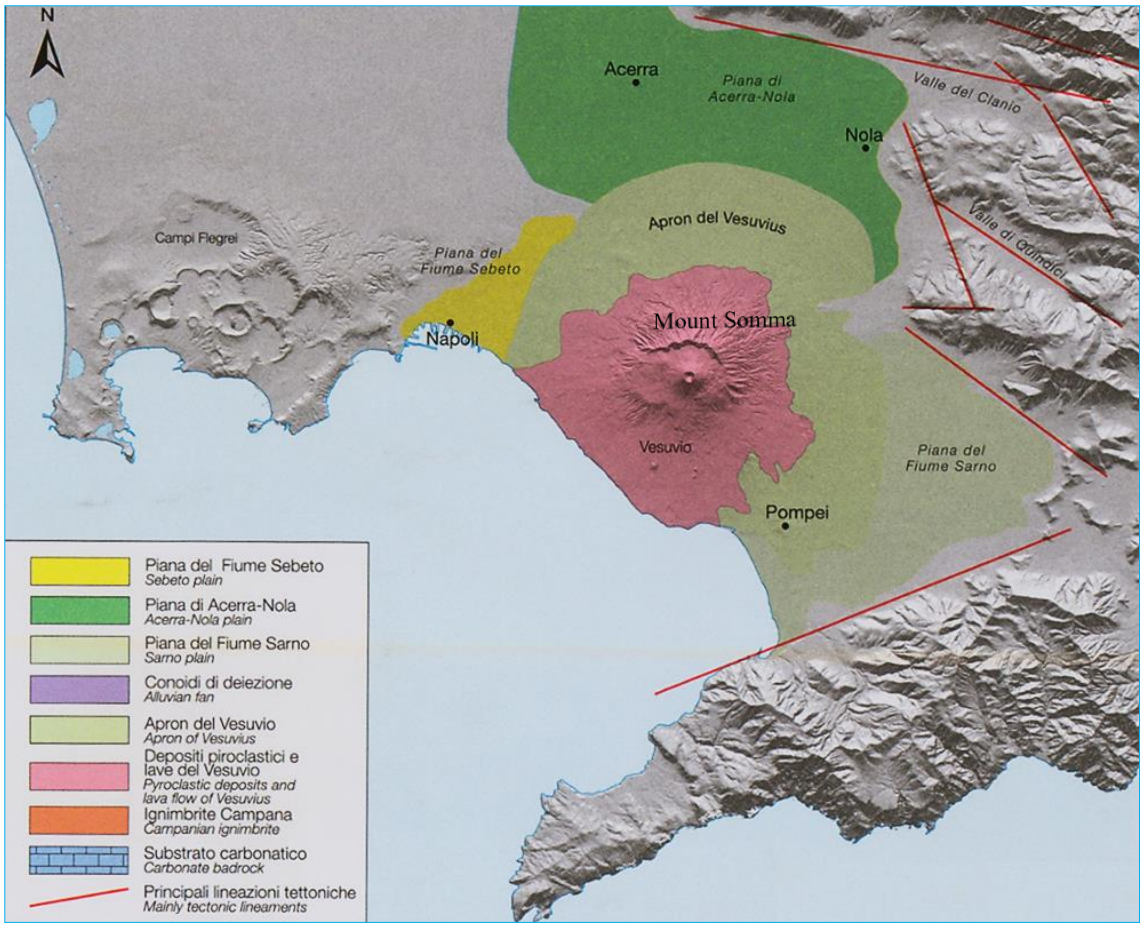

Figure 2.19 - Schematic relationship between Vesuvius units and alluvial plain deposits (modified from Santacroce et al., 2003).

According to Joron et al. (1987), the rocks of the first series (older than about 8 ka) consist of slightly silica undersaturated potassic trachybasalt to trachyte. A second series (about 8 ka to 79 AD) consists of phonotephrites, tephriphonolites and phonolites with intermediate degrees of silica undersaturation. Finally, a third series (younger than 79 AD) shows a strongly undersaturated leucite tephrite, leucitite, phonotephrite,

tephriphonolite and phonolite composition (fig. 2.20). However, trachybasalts are also found among the products of the 1906 eruption (Santacroce et al. 1993).

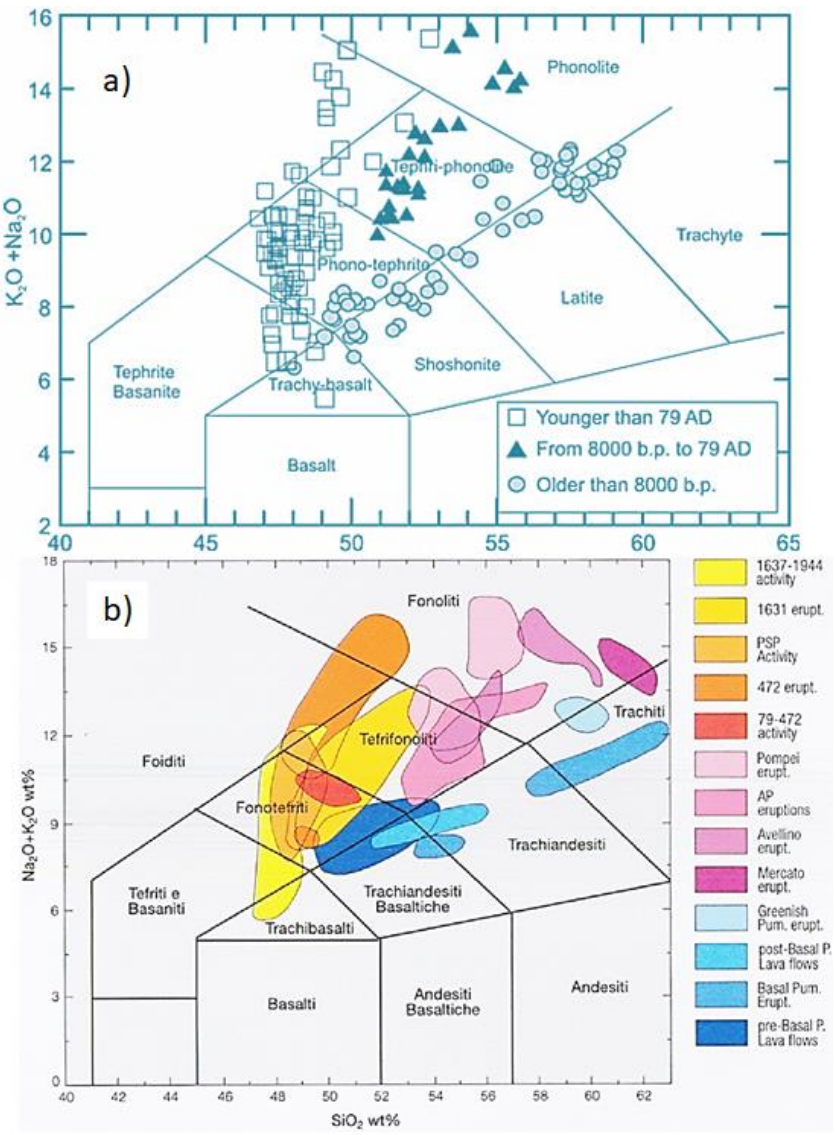

Figure 2.20 – Classification of Vesuvius volcanic products based on TAS diagram (a: modified from Peccerillo, 2005; b: modified from Santacroce et al., 2003).

The rocks belonging to the slightly undersaturated older series display moderately to poorly porphyritic textures, with decreasing phenocryst contents from mafic to felsic rocks. Plagioclase and clinopyroxene are ubiquitous phenocrysts; olivine and leucite occur in the mafic rocks, whereas biotite, K-feldspar and some amphibole are observed in the latites and trachytes. Groundmasses range from holocrystalline to hypocrystalline and contain the same phases as the phenocrysts plus Fe-Ti oxides, accessory garnet, apatite and variable amounts of glass. Trachytic pumices are strongly vesicular and range from aphyric to poorly porphyritic with a few phenocrysts of sanidine, plagioclase, green clinopyroxene and Fe-Ti oxides. Phonotephrites of the mildly

undersaturated series are strongly porphyritic with phenocrysts of plagioclase, clinopyroxene and leucite set in a groundmass formed by the same phases and glass. Tephriphonolites include lavas and pumices exhibiting variably porphyritic textures, with phenocrysts of clinopyroxene, plagioclase, leucite, alkali-feldspar, biotite and Fe-Ti oxides, set in a glassy groundmass. Melanite garnet and amphibole have been sometimes observed. Phonolites consists of pumices with a poorly porphyritic to aphyric vesicular texture; phenocrysts are represented by clinopyroxene, sanidine, some biotite and leucite set in a glassy groundmass; minor phases include garnet, olivine and calcic plagioclase; nepheline is observed in some rocks. Tephrites, leucitites and phonotephrites of the highly undersaturated younger series are more strongly porphyritic than older rocks. Phenocrysts consist of dominant clinopyroxene, and minor leucite and olivine; groundmass is holocrystalline to hypocrystalline and contains the same phases as the phenocrysts plus plagioclase, opaques and some brown mica. Tephriphonolites are strongly porphyritic with phenocrysts of leucite, clinopyroxene and plagioclase, and sporadic olivine and biotite set in holocrystalline to hypocrystalline groundmass formed by the same phases, Fe-Ti oxides and accessory apatite. Phonolites consist of vesicular porphyritic pumices made of leucite and clinopyroxene phenocrysts and of a glassy matrix containing plagioclase, sanidine, garnet, amphibole, Fe-Ti oxides and sporadic haüyne. Clinopyroxene shows mainly a diopsidic composition with common occurrence of zoned crystals showing salitic rims. Olivine is scarce and exhibits a large compositional variation both in the phenocrysts (up to about Fo_{90}) and in the groundmass (about Fo_{70-45}). Plagioclase is strongly zoned and exhibits a wide range of compositions (An_{90-50}). Sanidine is more sodic in the slightly undersaturated latites and trachytes than in the highly undersaturated tephriphonolites and phonolites. Leucite shows an almost stoichiometric composition. Mica ranges from phlogopite to biotite, the latter being confined to felsic products. Amphibole has potassic ferropargasite composition (Cioni et al., 1997). Several mafic and ultramafic xenoliths are found in the Somma-Vesuvius pyroclastics (e.g. Joron et al. 1987; Peccerillo, 2005, and references therein).

2.2.1c – VOLTURNO RIVER DRAINED SOURCE ROCKS –

This study has interested also sediments which have been drained and transported by Volturno river until the coastal stretch that regard the north portion of Campania plain which is also a part of studied areas (fig. 2.21).

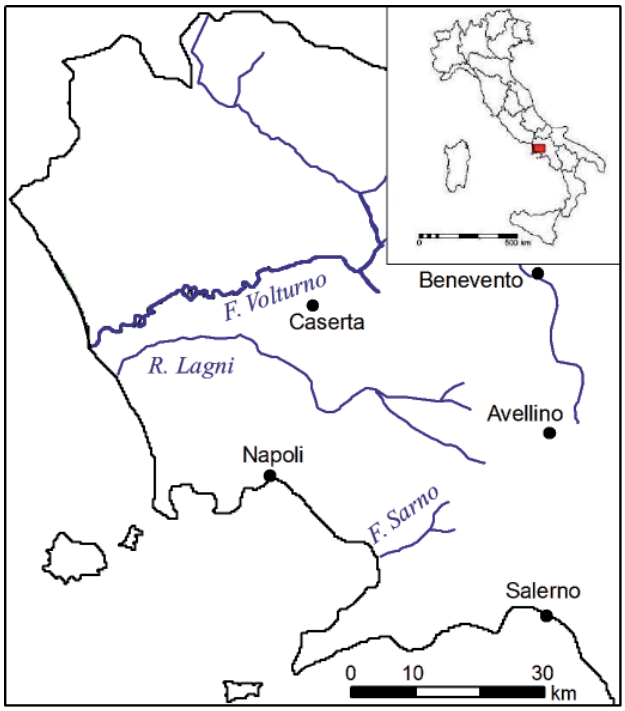

Figure 2.21 -- Location map of Volturno River (modified from Corniello, 2010).

The Campania plain extends from Mt. Massico (north) to Lattari mounts (south). It is articulated in two areas: the first is crossed by Volturno river and the second (southward) is crossed by the Sarno river (fig. 2.21). The Campania plain was part of marine environments until 130,000 years ago (Romano et al., 1964; Cinque and Romano, 2001), and corresponds to a structural depression which has been formed during the Lower Pleistocene caused by a general subsidence extending until Caserta mountains. Subsequently, the rate of tectonic subsidence decreased (almost ceased) and the area was invaded by fall-out and pyroclastic flow deriving from Phlegrean Fields and Vesuvius (figs. 2.22; 2.23). Campania Grey Tuff (Campania Ignimbrite) is widely distributed in this area, consists of a greyish ash rock (tuff) associated with black scoriae and lavas, and shows low permeability and a variable degree of diagenesis. Campania grey Tuff crops out especially on the plain margin where reach big thicknesses (40-50 m, figs. 2.22, 2.23) and become gradually thinner towards the Volturno river, which has severely eroded the tuff layers during the time. Above the Campania Ignimbrite crop out layers of loose pyroclasts directly deposited or produced by weathering of the tuff

complexes below, linked to re-sedimentation. The grain size is somewhat variable and thicknesses range from few to tens meters (fig. 2.23; Corniello, 2010).

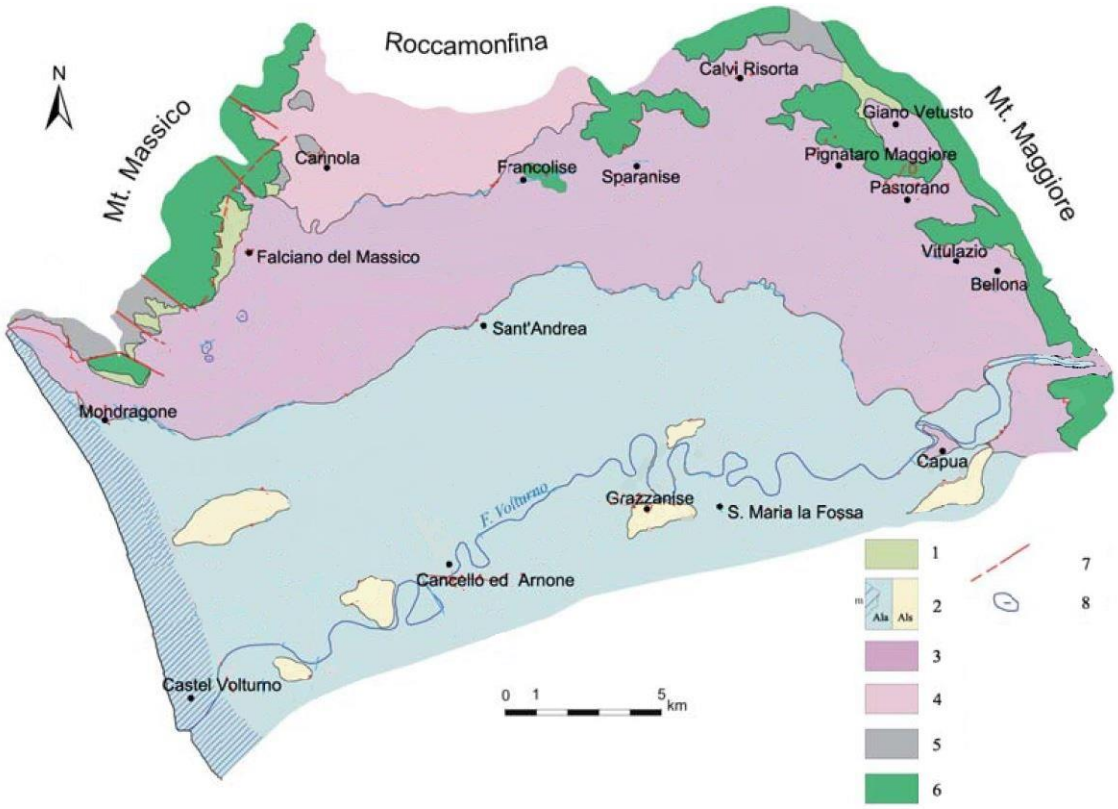

Figure 2.22 – Geological sketch map of the drained products of Volturno river. 1) Calcareous debris deposits; 2) Alluvial, lacustrine and marine clay - silt deposits or sand deposits; 3) Campania Ignimbrite, often covered by pyroclastic deposits; 4) Old tuffs; 5) Arenaceous-clayey-marly deposits; 6) Limestones and dolomite limestones; 7) Main faults; 8) Crater-shaped forms (modified from Corniello, 2010).

Pyroclasts are associated to detritus derived from the limestone slopes and dolomitic limestone, whereas, close to the river network, they are replaced by alluvial deposits linked to the Volturno fluvial enlargement and marsh phases (ancient and recent) as well as marine episodes. Below the Campania Grey Tuff, occur ancient alluvial deposits associated with pyroclastic formations (emplaced during various cycles of Phlegrean Fields and Roccamonfina volcanic activity), transitional and marine deposits, and large layers of organic matter. All these lithologies show a strong grain-size variability (Corniello, 2010).

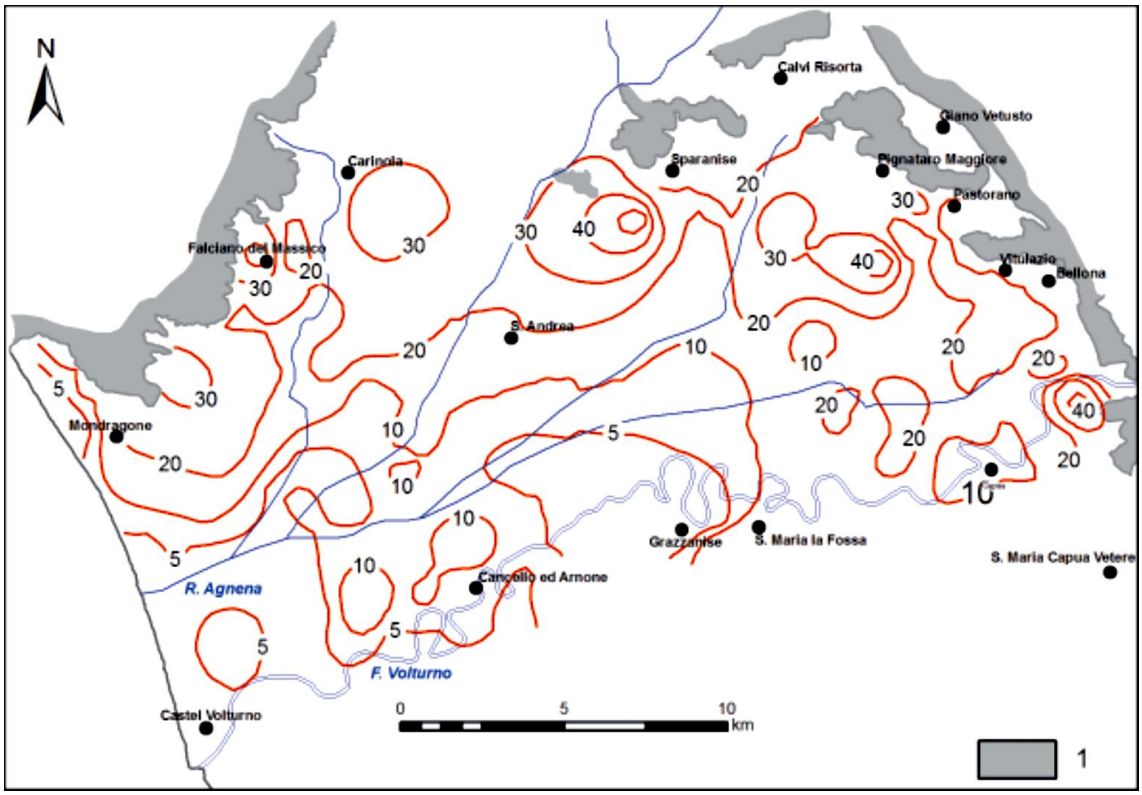

Figure 2.22 -- Campania Ignimbrite isopach map (in meters); 1: Carbonate mountains (modified from Corniello, 2010).

- Chapter 3 - Sample locations-

This chapter provides the details of sample collection, gives the longitude and latitude coordinates and a brief description of the areas where each sample was collected. These descriptions are accompanied by sample locations photographs, elevation model and map locations (figs. 3.1, 3.17). The relative grain size distribution of each sample observed after sieving is presented in chapter 4.

The approach to sample collection is straightforward; generally the samples were collected from a few centimeters below the surface from the different locations shown in figure 3.1 and 3.17 during the past three years. A plastic scoop was used to extract the sample from the ground (e.g. figs. 3.5). A plastic sieve was used to remove pebble-size and larger (> 8 mm) grains, and the remainder of each sample was then stored in separate Ziploc bags. As shown in figures 3.1 and 3.17, the sample locations cover two main areas: (1) the coastal perimeters of Aeolian Islands and (2) the Campania region coastal stretch (northern portion) in southern Tyrrhenian Sea. In total were collected 139 sand samples (mostly consist of beach sand samples and in some cases were collected also crater sand; e.g. Stromboli and Vesuvius).

3.1 – Aeolian Islands-

In this area have been collected 68 samples among all the islands. Here, sometimes, was necessary to use a little boat to circumnavigate the islands to collect samples. For this studied area, has been identified the coastal drainage basins connected with the samples location on each island (fig. 3.2 and following figures).

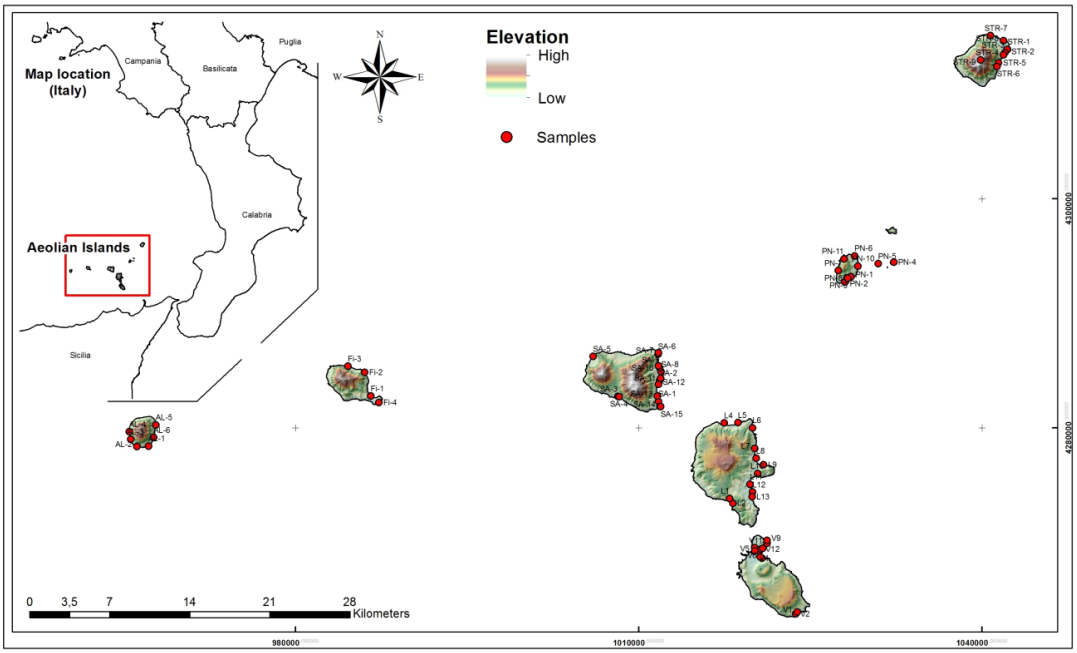

Figure 3.1 – Elevation model, map and sample location of Aeolian Islands.

3.1a - ALICUDI ISLAND -

On Alicudi island seven sand samples were collected and the relative coastal drainage basins were identified (AL-1 →AL-7, fig. 3.2a). The samples are mostly from pocket beach (fig. 3.2b), characterized by an immature texture (fig. 3.3). In fact, they consist of boulders, cobbles, pebbles and a low percentage of sand. GPS coordinates for sample location were recorded by using a GPS device (Garmin), then the coordinates (UTM) have been reported on Qgis 2.18 (tab. 3.1 and fig. 3.2a).

Sample	LONG	LAT	Environment	Localities
AL-1	443989.95	4264969.57	Shoreface	Scoglio Perciato
AL-2	443000.46	4265019.44	High-tide berm	Sciara Vigna
AL-3	442499.53	4265673.71	High-tide berm	Scarato
AL-4	442428.14	4266338.19	High-tide berm	Singa ianca
AL-5	444763.89	4266771.17	Swash zone	Sciara i Painu
AL-6	444517.94	4265698.32	Swash zone	Bazina
AL-7	443987.45	4264975.16	Swash zone	Scoglio Perciato

Table 3.1 – Table displaying name, latitude, longitude, localities and sampling environment of each sample collected on Alicudi island (UTM coordinates system).

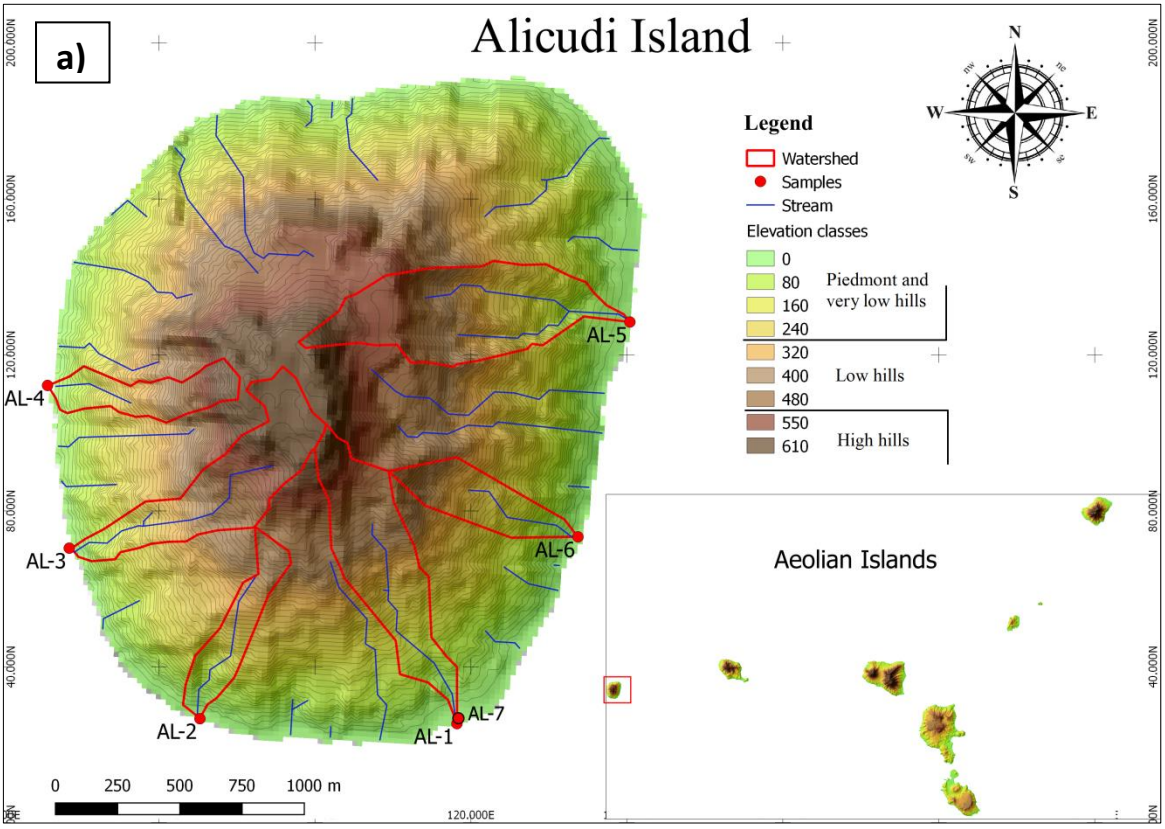

Figure 3.2 – a) Qgis image showing the elevation classes, samples location and relative drainage basins of Alicudi island; b) very poorly sorted pocket beach (AL-5).

AL-7 was sampled at the same location of AL-1, but the latest was sampled 2/3 meters below the sea level, whereas AL-7 was taken from the low-tide berms to verify (as a test) if there may be differences in texture and composition between these two different environments (as well as upper shoreface and foreshore / low-tide berm).

Figure 3.3 – Very poorly sorted beach (immature texture) ranging from gravel to sand in grain-size. Red circle shows the exact sampled point (AL-6).

3.1b - FILICUDI ISLAND -

On Filicudi island four beach sand samples were collected and the relative coastal drainage basins were identified (Fi-1→Fi-4; fig. 3.4a). Along all the coastal perimeter it was possible to take only 4 sand samples because the pocket beaches occur predominantly on the eastern portion of the island and there are no developed beaches on the western sector (as well as along all Aeolian Islands coastal perimeters; Morrone et al., 2018) (fig. 3.4a). Latitude, longitude and other data of each samples are shown in table 3.2.

Sample	LONG	LAT	Environment	Localities
Fi-1	463638.24	4268063.30	Low-tide berm	Porto
Fi-2	463241.43	4270143.87	High-tide berm	Fuocogrande
Fi-3	461813.03	4270781.22	Swash zone	Sciara cuddunedda
Fi-4	464302.22	4267461.09	Low-tide berm	Capograziano

Table 3.2 – Table displaying name, latitude, longitude, localities and sampling environment of each sample collected on Filicudi island (UTM coordinates system).

Furthermore, it has been noticed that usually those pocket beaches are developed below and in correspondence of a slope detrital cone which develops on the steep flank of the islands, especially on Alicudi and Filicudi islands (fig. 3.4b).

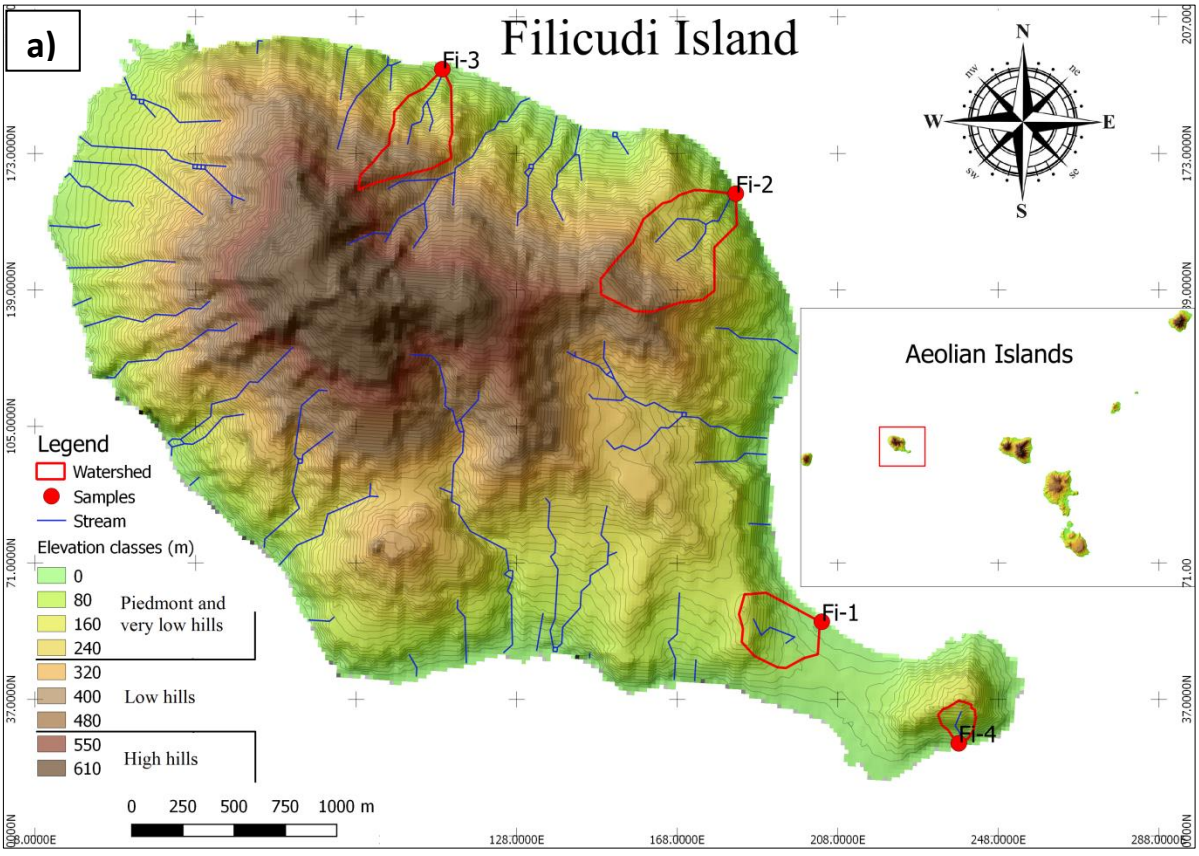

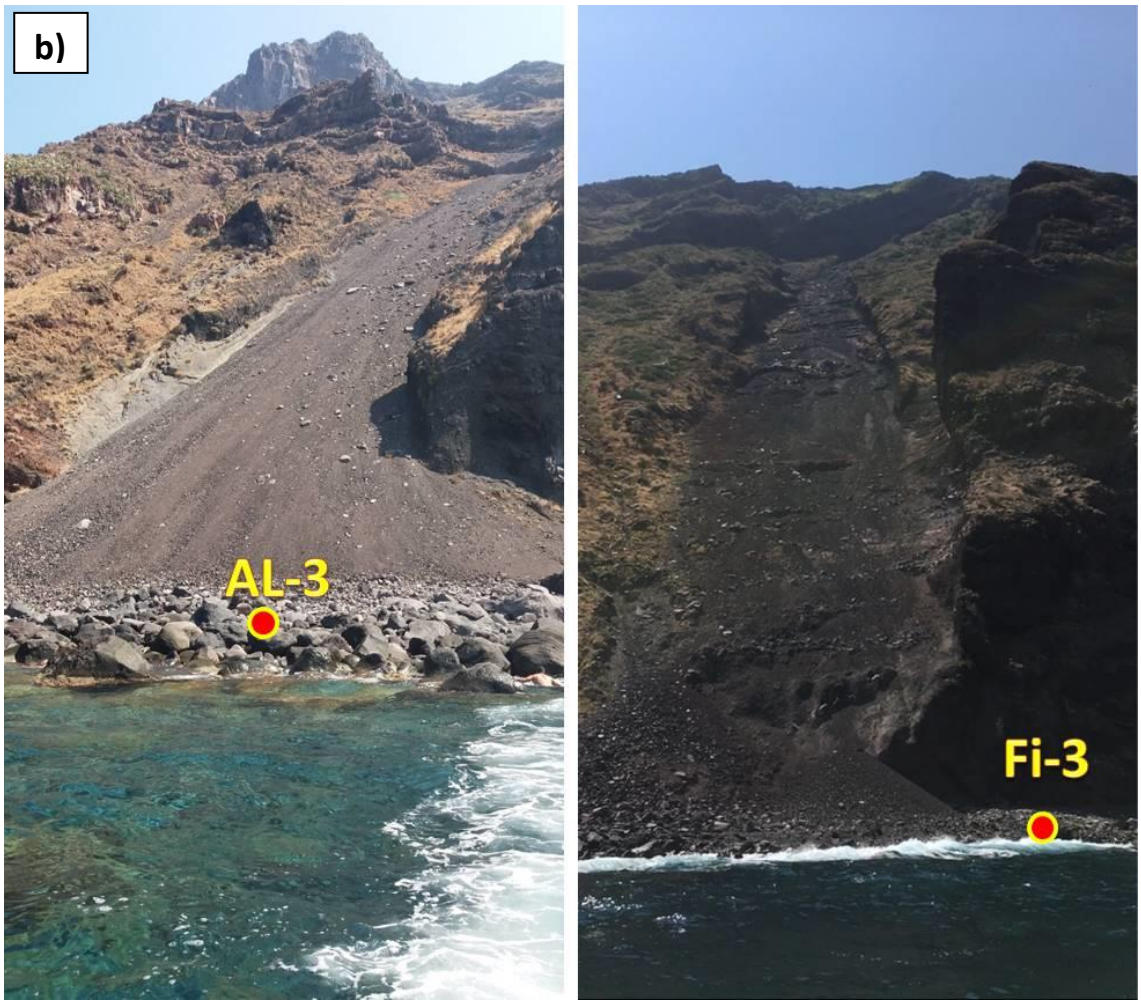

Figure 3.4 – a) Qgis image showing the elevation classes, samples location and relative drainage basins of Filicudi island; b) very poorly sorted pocket beaches with an immature texture developed in correspondence of a slope detrital cones.

Figure 3.5 - Very poorly sorted beach with immature-texture on Filicudi islands. Circle: Fi-1 sample location.

3.1c - SALINA ISLAND -

Salina (26.4 Kmq), is the largest island after Lipari. Fifteen samples have been taken (SA-1→SA-15) on Salina island from Lingua to Le Canne localities (tab. 3.3 and fig. 3.7) and the relative coastal drainage basins were identified. On Salina, as well as other Aeolian Islands, the pocket beaches occur predominantly on the eastern portion of the island. Salina beaches, have different percentage among boulders/cobbles, pebbles and sand. There are beaches ranging from very poorly to very well sorted, for instance, the beach sands from Rinella are almost totally formed by sand and they are very well sorted, whereas those from Passo di Megna localities are very poorly sorted and have more than 80 % of bounds and cobbles with only 15-20 % of sand (tab. 3.3, and figs 3.6b, c). Salina island has beaches larger than those of Alicudi and Filicudi islands.

Sample	LONG	LAT	Environment	Localities
SA-1	488614.22	4265963.77	Low-tide berm	Lingua
SA-2	488830.24	4267764.76	Swash zone	Porto S. Marina
SA-3	485112.35	4266626.94	Low-tide berm	Rinella
SA-4	485250.03	4266594.34	High-tide berm	Rinella
SA-5	483191.20	4270237.97	Swash zone	Pollara
SA-6	488861.15	4270077.23	High-tide berm	Capo Faro
SA-7	488884.27	4270178.86	Low-tide berm	Capo Faro
SA-8	489024.41	4268522.56	Low-tide berm	Rapa Nui
SA-9	488900.05	4268887.24	High-tide berm	Passo di Megna
SA-10	488810.62	4269048.26	Low-tide berm	Punta Barone
SA-11	488945.85	4267958.78	Low-tide berm	Pozzo D'Agnello
SA-12	488714.50	4267426.48	Low-tide berm	Le canne
SA-13	488547.23	4266441.00	High-tide berm	Le canne
SA-14	488728.29	4265492.01	Lacustrine	Lingua Lake
SA-15	488776.62	4265486.40	High-tide berm	Punta Lingua (Faro)

Table 3.3 – Table displaying name, latitude, longitude, localities and sampling environment of each sample collected on Filicudi island (UTM coordinates system).

Figure 3.6 – Textural-maturity differences among Salina beaches. a) Well sorted sand (medium to fine sand, SA-14); b) very well sorted beach sand (medium to fine sand SA-3); c) very poorly sorted beach (boulders-pebbles, sand, SA-9); d) poorly sorted beach ranging from gravel to fine sand in grain-size (SA-12).

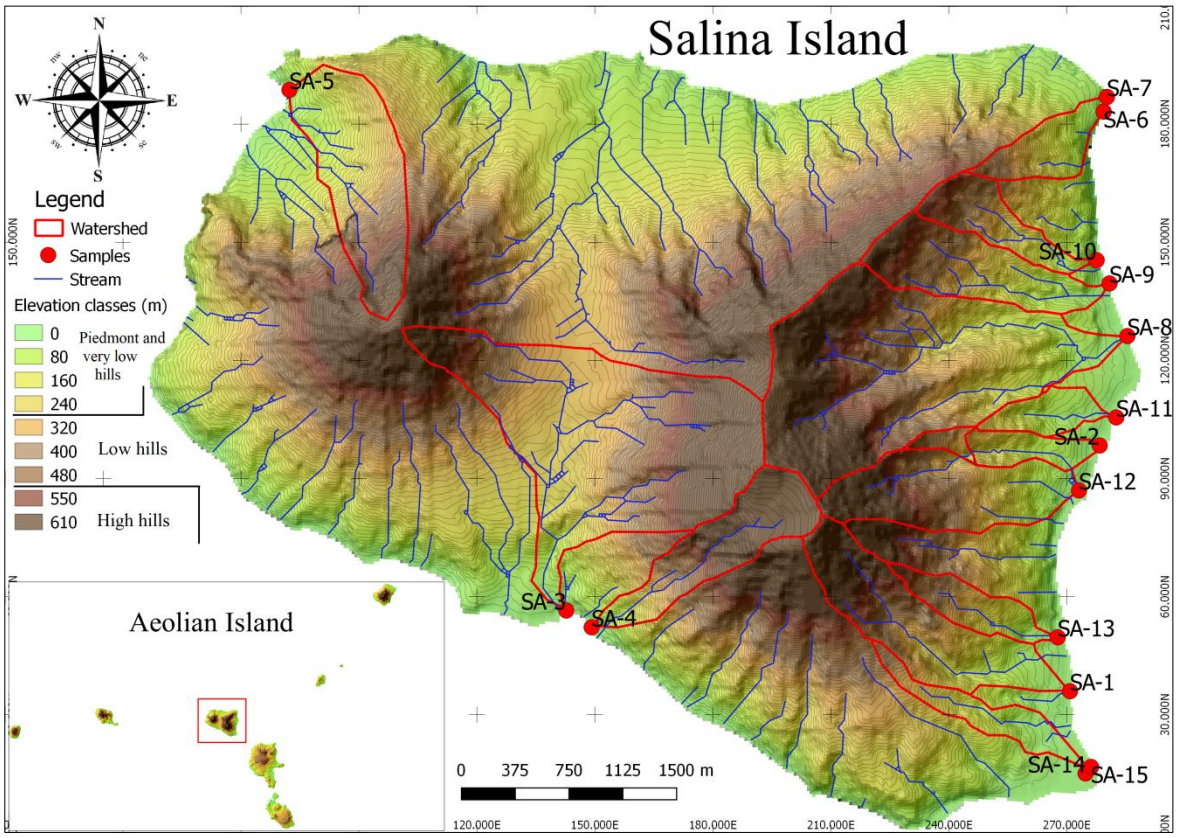

Figure 3.7 – Qgis image showing the elevation classes, samples location and relative drainage basins of Salina island.

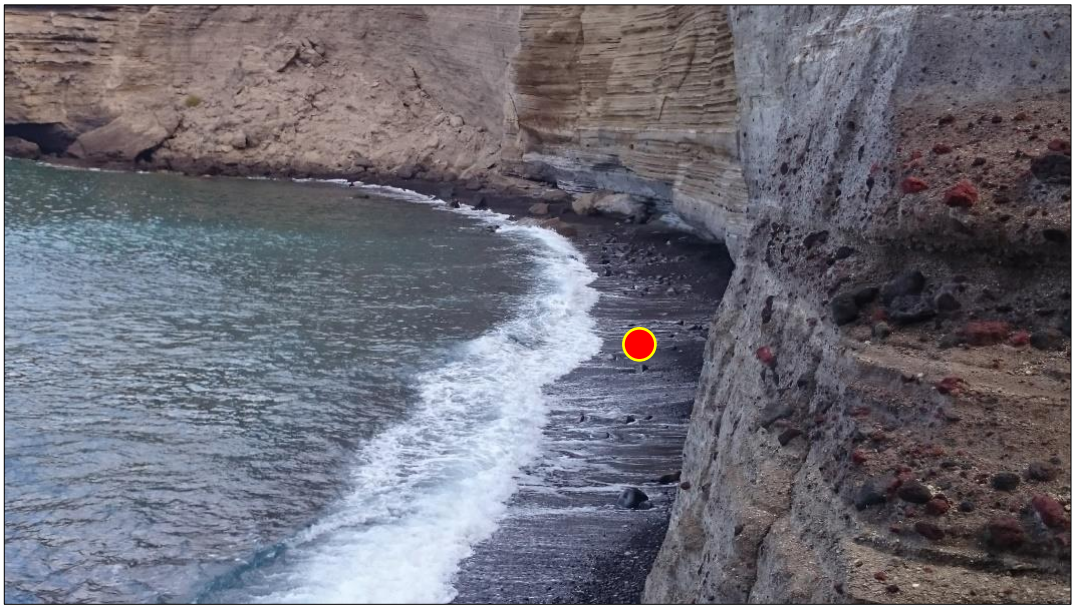

Figure 3.8 – Poorly sorted beach ranging from very coarse to medium in grain-size on Salina island (Pollara, SA-5).

3.1d - LIPARI ISLAND -

Twelve coastal drainage basins were identified and the corresponding beach sands were collected from high-tide berms spaced along Lipari's accessible coastal perimeter, from Acquacalda to Valle Muria (L1→ L13, no sand from sample site L3). The NE coast between Acquacalda and Valle Muria is formed predominantly by coarse sandy and cobbly pocket beaches, alternating with high rocky cliffs and headlands (tab. 3.4 and figs. 3.9, 3.10).

Sample	LONG	LAT	Environment	Localities
L1	494268,63	4257120,738	High-tide berm	Valle Muria
L2	494500,269	4256706,262	High-tide berm	Valle Muria
L4	494202,957	4263707,579	High-tide berm	Acquacalda
L5	495421,017	4263669,066	High-tide berm	Acquacalda
L6	496645,505	4263116,826	High-tide berm	Porticello
L7	496708,282	4261346,923	High-tide berm	Papesca
L8	496786,254	4260461,885	High-tide berm	Canneto
L9	497392,542	4259863,846	High-tide berm	Canneto
L10	496835,11	4259132,657	High-tide berm	Pietra Campana
L11	496091,527	4258247,006	High-tide berm	Marina di Portosalvo
L12	496285,331	4257546,211	High-tide berm	Marina Corta
L13	496222,438	4257142,046	High-tide berm	Portinente

Table 3.4 – Table displaying name, latitude, longitude, localities and sampling environment of each sample collected on Lipari island (UTM coordinates system).

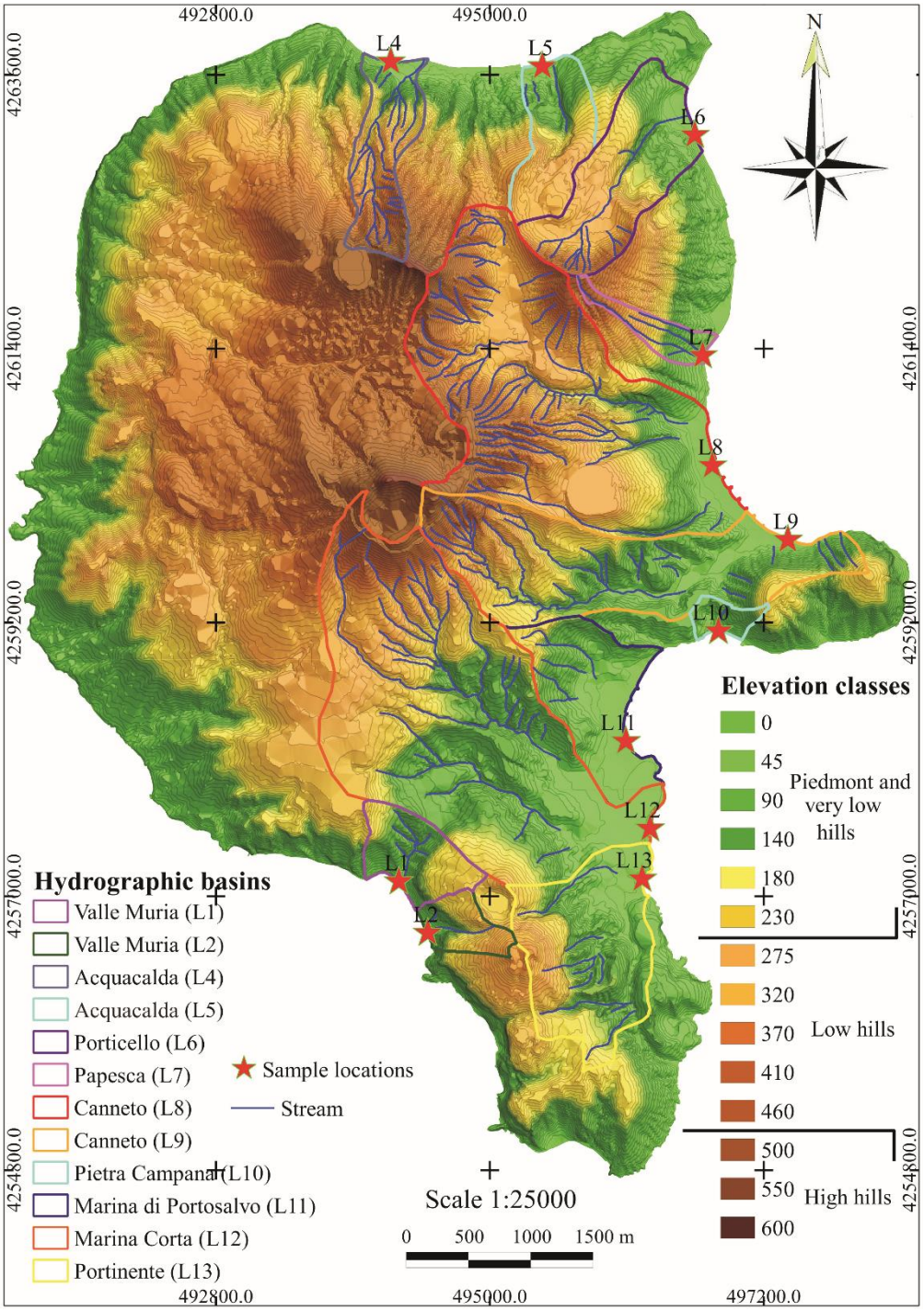

Figure 3.9 - Digital elevation map of Lipari island showing the boundaries of the drainage basins with respect to samples location (modified from Morrone et al., 2017).

No samples were taken in the NW-W coastal domain of Lipari, from Punta del Legno Nero to Punta le Grotticelle, where the coast is straight, with high rocky cliffs and headlands. In this coastal stretch, beach sedimentation is represented only by rock falls and wide beaches are not developed (figs. 3.7, 3.8; Morrone et al., 2017). In table 3.4 are shown latitude and longitude coordinates, localities and sampling environments.

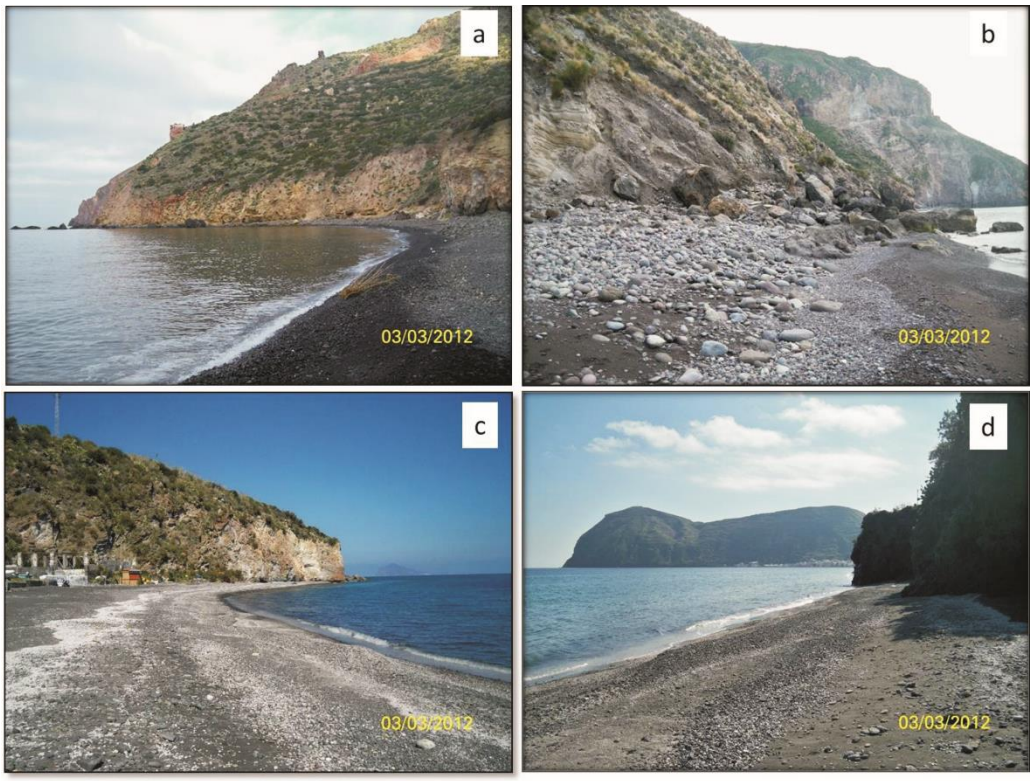

Figure 3.10 - (a) Valle Muria beach (sample L1). (b) Valle Muria beach (sample L2). (c) Acquacalda beach (sample L4). (d) Acquacalda beach (sample L5). (modified from Morrone et al., 2017).

3.1e - VULCANO ISLAND -

Eleven sand samples have been collected on Vulcano island beaches (V1 →V12, no sand from sample site V3), from Porto di Ponente to Porto di Levante to Gelso localities (the latter, was sampled in the southernmost portion of the island). Moreover, the relative coastal drainage basins were identified (fig. 3.11). In table 3.5 are shown data from each samples.

Sample	LONG	LAT	Environment	Localities
V1	499501,415	4246884,688	Low-tide berm	Gelso
V2	499355,818	4246724,347	High-tide berm	Gelso (faro)
V4	496558,141	4252406,321	Swash zone	Fumarole
V5	496137,015	4252418,301	Low-tide berm	Spiaggia Nera
V6	496169,839	4252701,469	Swash zone	Spiaggia Nera
V7	496581,179	4251905,025	Low-tide berm	Porto di Levante
V8	496718,482	4251755,741	High-tide berm	Porto di Levante
V9	497268,153	4253267,666	Low-tide berm	Valle dei Mostri
V10	497262,507	4253016,326	Swash zone	Punta Samossà
V11	496840,12	4252612,737	Low-tide berm	Vulcanello
V12	496690,837	4252542,703	Swash zone	Vulcanello

Table 3.5 – Table displaying name, latitude, longitude, localities and sampling environment of each sample collected on Vulcano island (UTM coordinates system).

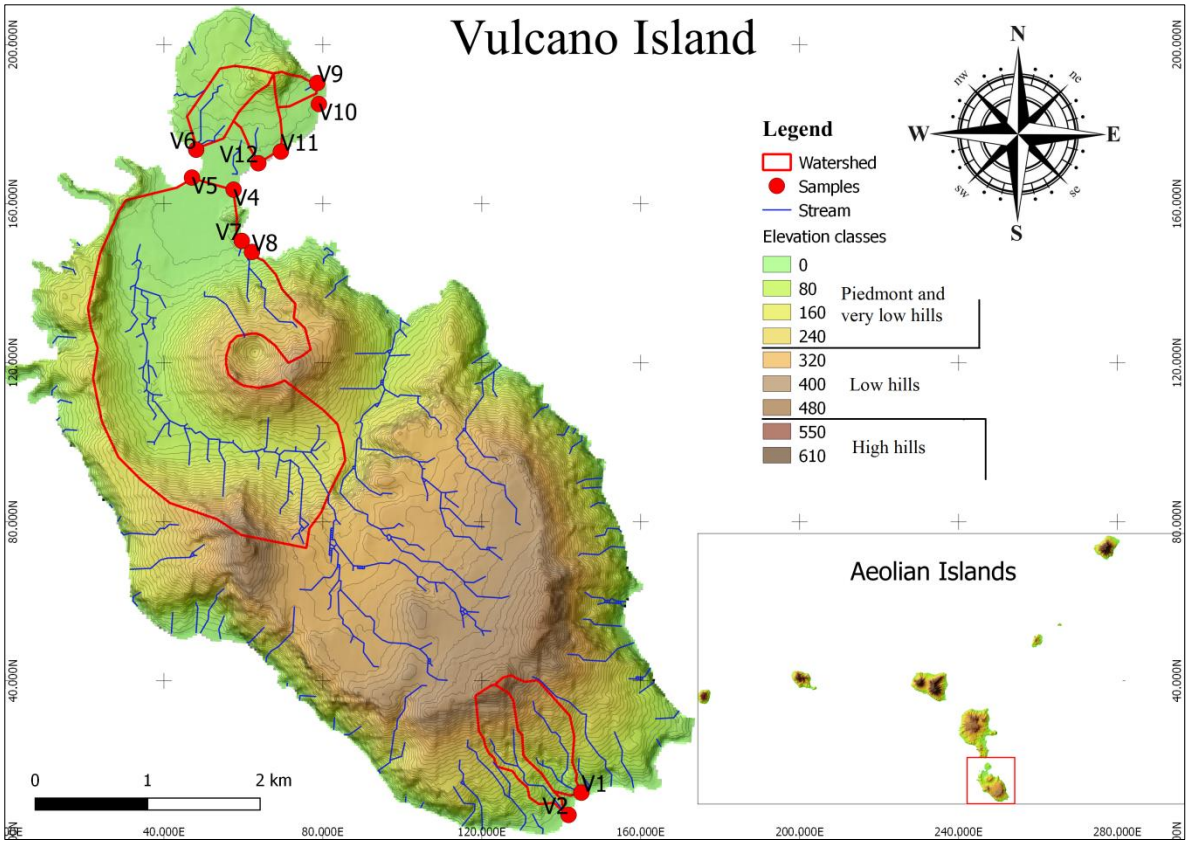

Figure 3.11 – Qgis image showing the elevation classes, samples location and relative drainage basins of Vulcano island.

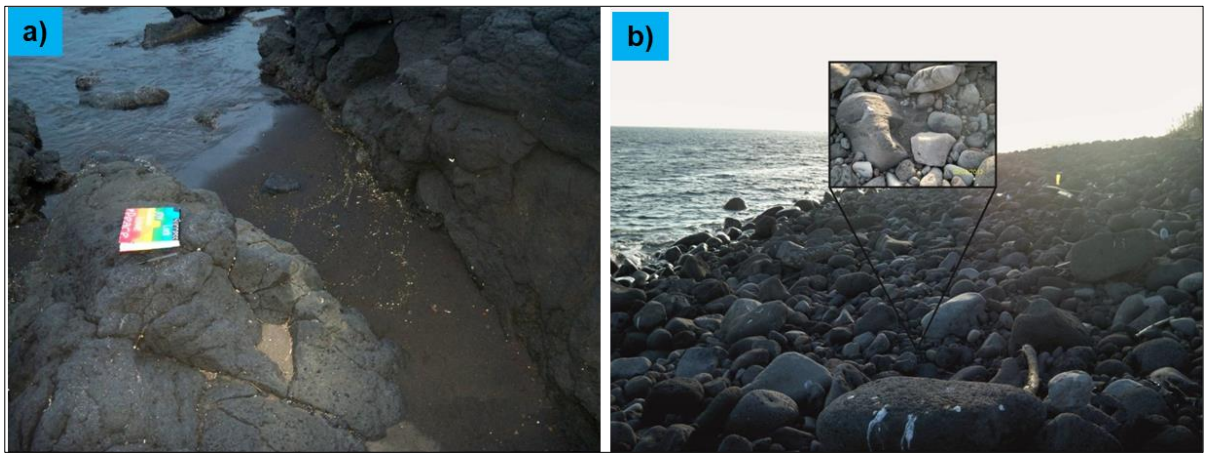

Figure 3.12 – a) Well sorted (pocket) beach sand ranging from medium to coarse in grain-size, sampled on the eastern side of Vulcanello peninsula (V12); b) close-up of very poorly sorted beach ranging from coarse to medium in grain-size, it was sampled on the southernmost portion of Vulcano island (Gelso).

3.1f - PANAREA ISLAND -

On Panarea island eleven beach sand have been sampled and the relative coastal drainage basins were identified from Baia di Drautto to Baia di Pietra Nava (PN-1→PN-11; fig. 3.13). Moreover, other sand samples were taken from two Panarea islets

(Lisca Bianca and Dattilo). Latitude, longitude and other data of each samples are shown in table 3.6. Figure 3.14 shows some Panarea beaches (sample sites) with different grain-size and sorting.

Sample	LONG	LAT	Environment	Localities
PN-1	506058.69	4275683.00	Swash zone	Baia di Drautto
PN-2	505558.11	4275301.28	Low-tide berm	Cala del Moro
PN-3	505501.51	4275235.32	Swash zone	Baia di Calajunco
PN-4	509870.56	4276699.12	Swash zone	Lisca Bianca islet
PN-5	508509.58	4276667.86	High-tide berm	Dattilo islet
PN-6	506511.21	4277480.34	High-tide berm	Calcara
PN-7	504983.83	4276295.63	Swash zone	Punta Muzza
PN-8	505709.48	4275574.53	Low-tide berm	Cala degli Zimmari
PN-9	505774.70	4275597.08	High-tide berm	Cala degli Zimmari
PN-10	506712.88	4276569.67	Swash zone	Porto
PN-11	505576.75	4277284.05	High-tide berm	Baia di Pietra Nava

Table 3.6 – Table displaying name, latitude, longitude, localities and sampling environment of each sample collected on Panarea island (UTM coordinates system).

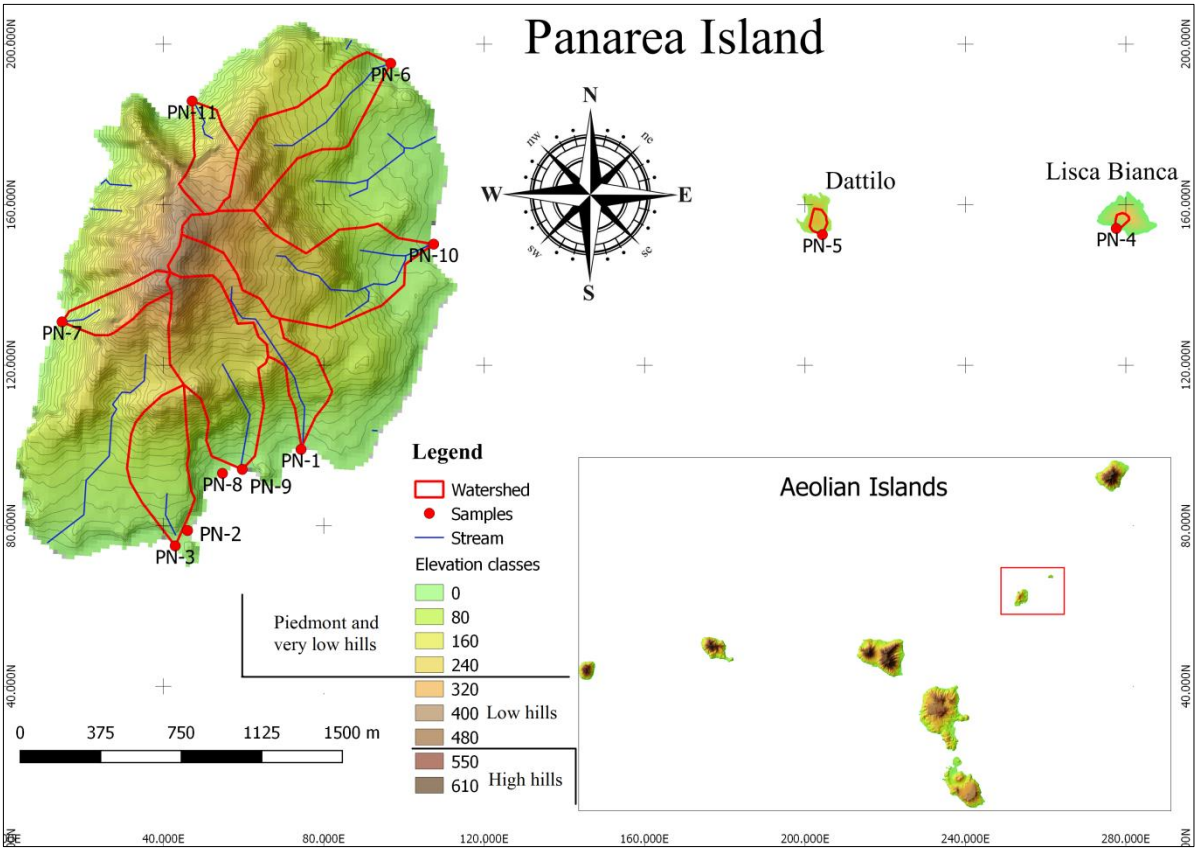

Figure 3.13 – Qgis image showing the elevation classes, samples location and relative drainage basins of Panarea island.

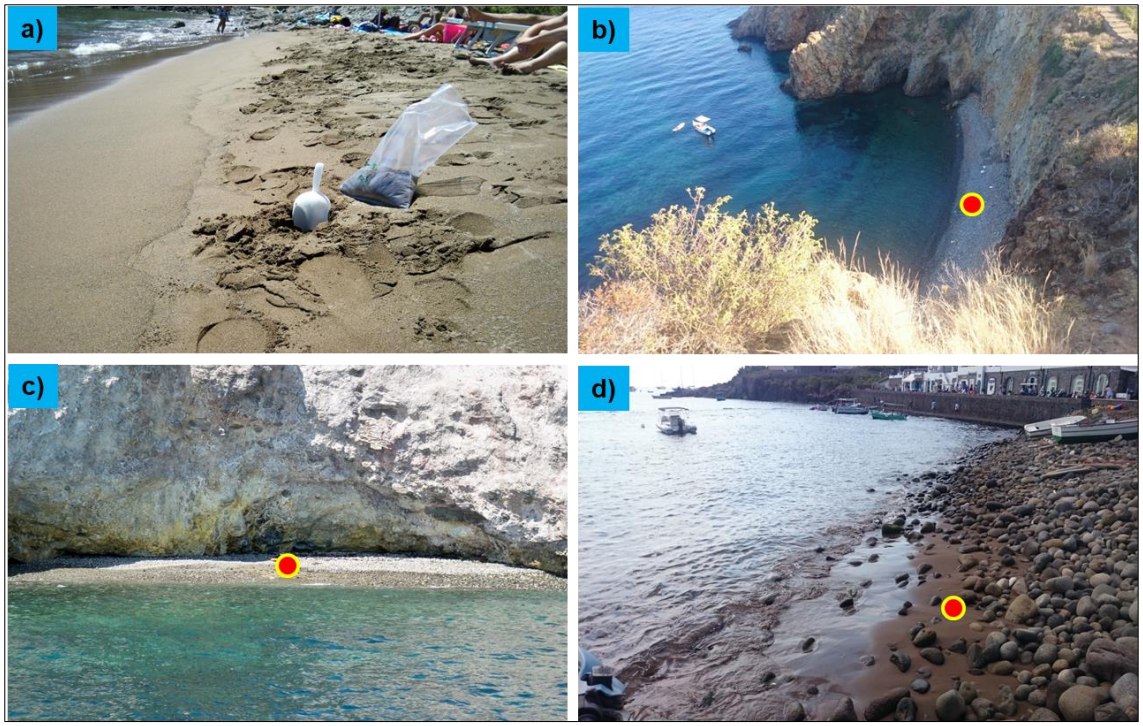

Figure 3.14 – Some sample sites and textural-maturity differences on Panarea beaches. a) Very well sorted sandy beach (PN-8); b) poorly sorted gravelly beach (PN-2), c) moderately sorted beach from Lisca Bianca islet ranging from very coarse to medium sand (PN-4); d) very poorly sorted beach consisting of cobbles and sand (PN-10).

3.1g - STROMBOLI ISLAND –

Seven coastal beach sands were collected from swash zone, high- and low-tide berm spaced along coastal perimeter from Pizzillo to Ficogrande and the corresponding drainage basins were identified. Moreover, one crater sand has been sampled from craters area on the top of Stromboli island (tab 3.7 and figs. 3.15, 3.16).

Sample	LONG	LAT	Environment	Localities
STR-1	520956.62	4294532.50	Swash zone	Pizzillo (Porto)
STR-2	520926.15	4294531.60	High-tide berm	Pizzillo (Porto)
STR-3	520738.48	4294267.35	Low-tide berm	Petrazza
STR-4	520593.84	4294085.91	Low-tide berm	Malpasso
STR-5	520109.70	4293421.94	Low-tide berm	Malpasseddu
STR-7	519551.88	4295810.52	High-tide berm	Faraglione
STR-8	520684.40	4295319.89	High-tide berm	Ficogrande
STR-9	518573.07	4293772.21	Crater	Craters

Table 3.7 – Table displaying name, latitude, longitude, localities and sampling environment of each sample collected on Stromboli island (UTM coordinates system).

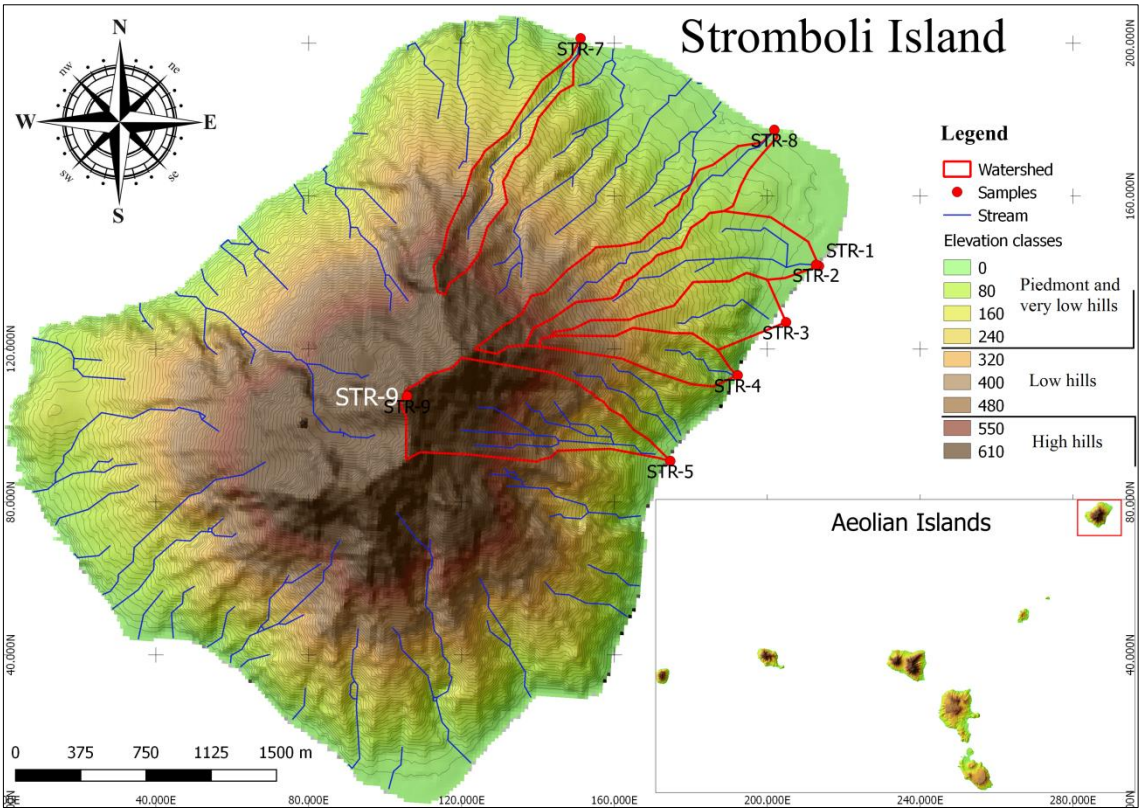

Figure 3.15 – Qgis image showing the elevation classes, samples location and relative drainage basins of Stromboli island. STR-9 is the crater sample.

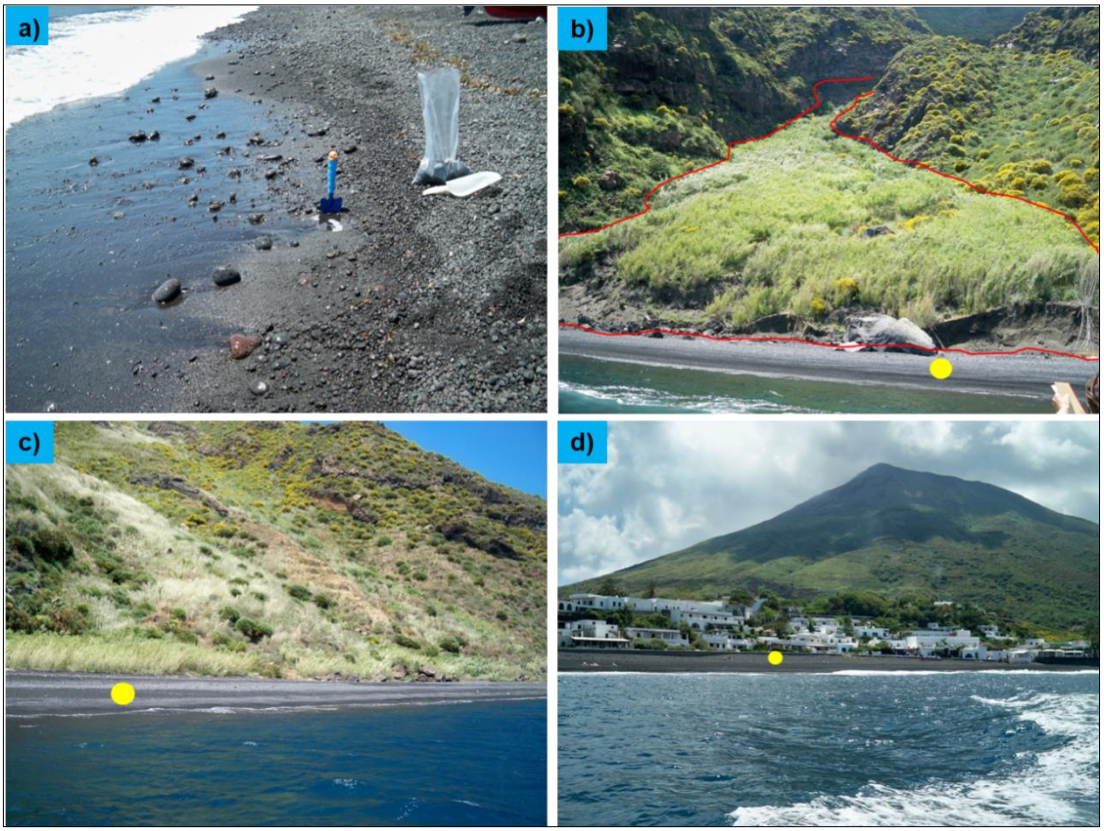

Figure 3.16 – Some sample sites on Stromboli island. a) poorly sorted gravel-sandy beach near the main port (STR-1); b) very poorly sorted beach formed at the bottom of a slope detrital cone (STR-5); c) moderately sorted beach from Malpasso (STR-4); d) moderately sorted beach ranging from coarse to medium sand in grain-size (Ficogrande beach, STR-8).

3.2 – Campanian Province -

In this area have been collected 64 sand samples along about 80 kilometers coastal stretch from Volturno river mouth to Sorrento (fig. 3.17 and tab 3.8). Moreover, we also looked to take samples from different environments around the study areas coast in order to understand if there may be any compositional and texture changes among these different environments. Thus, three Vesuvius crater sand (VE series), one from a Volturno bar sand (some hundred meters before its mouth, VO-1), one dunal sand (e.g. Li-4), one lacustrine sand (Torrefumo lake, PZ-20) and one slope detrital cone sand (PZ-18) from a steep slope behind Bacoli shoreline have been sampled (tab. 3.8 and figs. 3.18, 3.19, 3.20).

Samples name are from different localities and range from VO-1 to VO-11, from BC-1 to BC-5, from Li-1 to Li-6, from PZ-1 to PZ-20, from NA-1 to NA-6, from PO-1 to PO-3; from VE-1 to VE-3, from TG-1 to TG-3, from TA-1 to TA-2, from CA-1 to CA-3 and from SO-1 to SO-5. Moreover, CO-1, GA-1 and MC-1 belong to this samples collection (tab. 3.8).

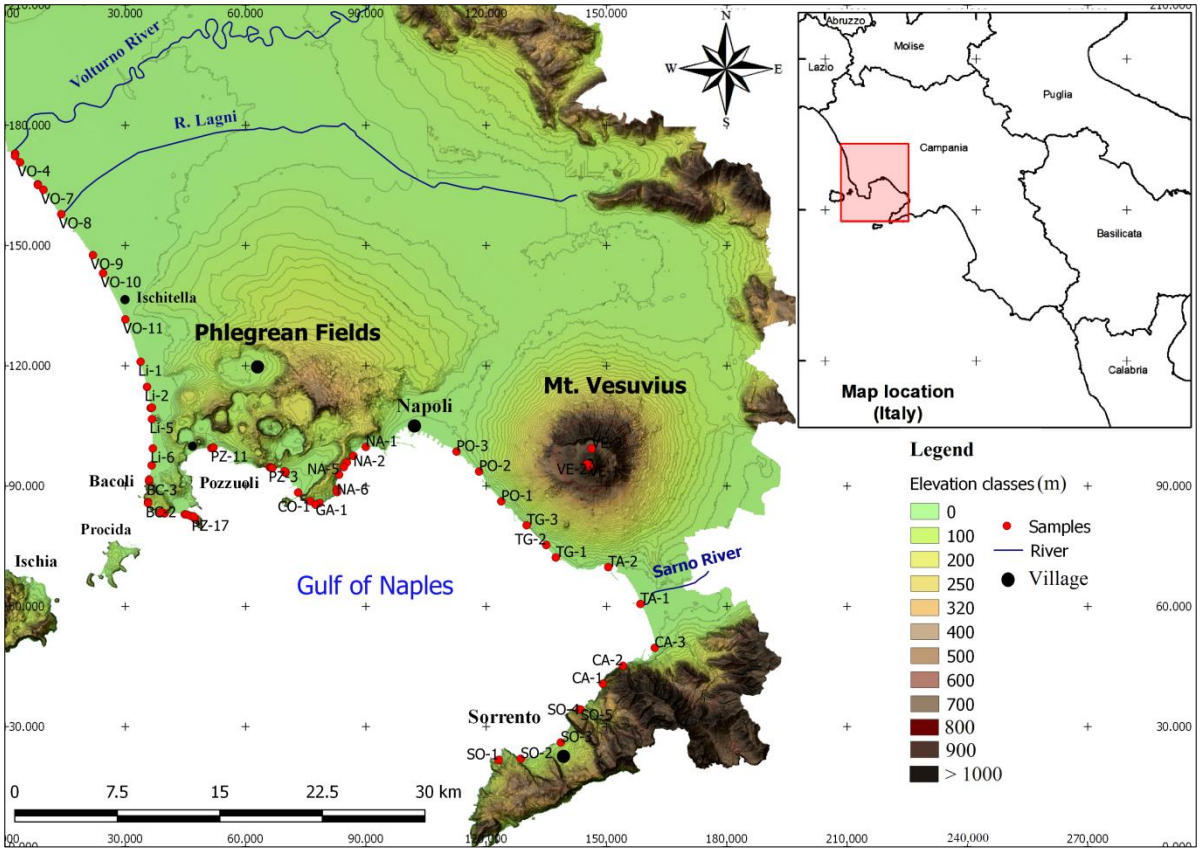

Figure 3.17 – Digital elevation map of the Campanian province showing sample locations of both Mt. Vesuvius and Phlegrean Fields areas.

Sample	LONG	LAT	Environment	Localities
VO-1	409943.97	4541873.96	Fluvial bar	Oasi dei Variconi
VO-2	409951.06	4541881.27	Fluvial bar (placer)	Oasi dei Variconi
VO-3	409933.45	4541702.30	Volturno R. mouth	Oasi dei Variconi
VO-4	410293.72	4541250.69	High-tide berm	Oasi dei Variconi
VO-5	411569.41	4539644.72	High-tide berm	Castel Volturno
VO-6	411574.31	4539585.45	High-tide berm	Castel Volturno
VO-7	411972.48	4539238.33	High-tide berm	G. Vasari (C.Volturno)
VO-8	413244.02	4537456.01	R. Lagni R. mouth	Castel Volturno
VO-9	415514.99	4534467.01	Swash zone	Pineta Mare
VO-10	416235.05	4533148.67	Swash zone	Ischitella Lido
VO-11	417815.22	4529783.47	Patria lake mouth	Lago Patria
Li-1	418893.04	4526701.73	Low-tide berm	Lido di Licola
Li-2	419340.64	4524870.50	Low-tide berm	Lido di Licola
Li-3	419592.18	4523333.80	Swash zone	Licola Mare
Li-4	419681.02	4523364.29	Dune	Licola Mare
Li-5	419671.92	4522528.02	Low-tide berm	Cuma
Li-6	419714.78	4520395.93	Low-tide berm	Bacoli
BC-5	419615.66	4519164.67	High-tide berm	Lago del fusaro
BC-4	419423.99	4518130.56	High-tide berm	Torregaveta
BC-3	419411.65	4518030.16	Swash zone	Torregaveta
BC-1	419317.79	4516514.51	High-tide berm	Porto di Acquamorta
BC-2	419325.74	4516427.46	High-tide berm	Porto di Acquamorta
PZ-20	420232.48	4515749.65	Lacustrine	Torrefumo lake
PZ-19	420386.84	4515718.38	Dune	Torrefumo lake
PZ-18	420521.32	4515668.83	Slope detrital cone	Torrefumo lake
PZ-14	421992.93	4515588.40	High-tide berm	Lido Miliscola
PZ-15	422147.41	4515568.27	High-tide berm	Miseno
PZ-16	422410.79	4515471.14	Low-tide berm	Lido Miliscola
PZ-17	422660.48	4515409.32	Dune	Miseno
PZ-13	422734.72	4515245.71	Low-tide berm	Capo Miseno
PZ-10	423977.36	4520380.45	High-tide berm	Pozzuoli
PZ-11	424109.88	4520419.79	Low-tide berm	Pozzuoli
PZ-12	424130.94	4520417.73	Low-tide berm	Pozzuoli
PZ-1	428220.50	4518948.43	High-tide berm	Lungomare v. Napoli
PZ-3	428307.23	4518905.03	High-tide berm	Lungomare v. Napoli
PZ-4	428338.12	4518901.03	High-tide berm	Lungomare v. Napoli
PZ-2	428394.07	4518872.73	High-tide berm	Lungomare v. Napoli
PZ-5	428394.07	4518872.73	Swash zone	Lungomare v. Napoli
PZ-8	429285.91	4518643.96	High-tide berm	Bagnoli

Table 3.8 – Table displaying name, latitude, longitude, localities and sampling environment of each sample collected along Campania coastal strech (UTM coordinates system). Samples are grouped from north to south.

Sample	LONG	LAT	Environment	Localities
PZ-7	429362.74	4518593.27	High-tide berm	Bagnoli
PZ-6	429362.14	4518530.36	High-tide berm	Bagnoli
PZ-9	430269.30	4517087.78	High-tide berm	Coroglio
CO-1	431152.00	4516452.00	Swash zone	Coroglio
GA-1	431553.00	4516194.00	Low-tide berm	Gaiola
MC-1	431812.00	4516314.00	Swash zone	Marechiaro
NA-7	433117.95	4517092.92	Swash zone	Marechiaro
NA-6	433080.42	4517296.79	Swash zone	Marechiaro
NA-5	433263.58	4518353.44	Swash zone	Posillipo
NA-4	433613.64	4518901.72	Low-tide berm	Posillipo
NA-3	433834.58	4519243.89	High-tide berm	Posillipo
NA-2	434318.08	4519715.10	Low-tide berm	Mergellina
NA-1	435227.06	4520355.72	Swash zone	Chiaia
PO-3	441836.58	4519964.79	Low-tide berm	Comune di Napoli
PO-2	443469.75	4518505.23	Low-tide berm	Portici
PO-1	445068.68	4516324.73	High-tide berm	Ercolano
TG-3	446906.55	4514575.82	Low-tide berm	Torre del Greco
TG-2	448322.55	4513128.20	High-tide berm	Torre del Greco
TG-1	449012.59	4512216.82	High-tide berm	Via Litoranea (Tg)
TA-2	452838.81	4511490.26	Low-tide berm	Torre Annunziata
TA-1	455165.15	4508800.49	High-tide berm	Sarno River mouth
CA-3	456194.87	4505606.54	Low-tide berm	Castellammare di Stabia
CA-2	453864.90	4504312.61	Low-tide berm	Spiaggia Calcina
CA-1	452387.72	4503021.28	Low-tide berm	Vico Equense
SO-5	450759.62	4501142.89	High-tide berm	Vico Equense
SO-4	450658.30	4501162.07	Low-tide berm	Vico Equense
SO-3	449289.35	4498762.39	High-tide berm	Marina di Cassano
SO-2	446352.21	4497600.74	Low-tide berm	Marina Grande
SO-1	444731.97	4497525.64	High-tide berm	Marina di Puolo
VE-1	451492.68	4518838.63	Crater sand	Vesuvius crater
VE-2	451353.17	4518996.81	Crater sand	Vesuvius crater
VE-3	451679.53	4520114.04	Crater sand	Vesuvius crater

Table 3.8 (continued) – Table displaying name, latitude, longitude, localities and sampling environment of each sample collected along Campania coastal strech (UTM coordinates system). Samples are grouped from north to south.

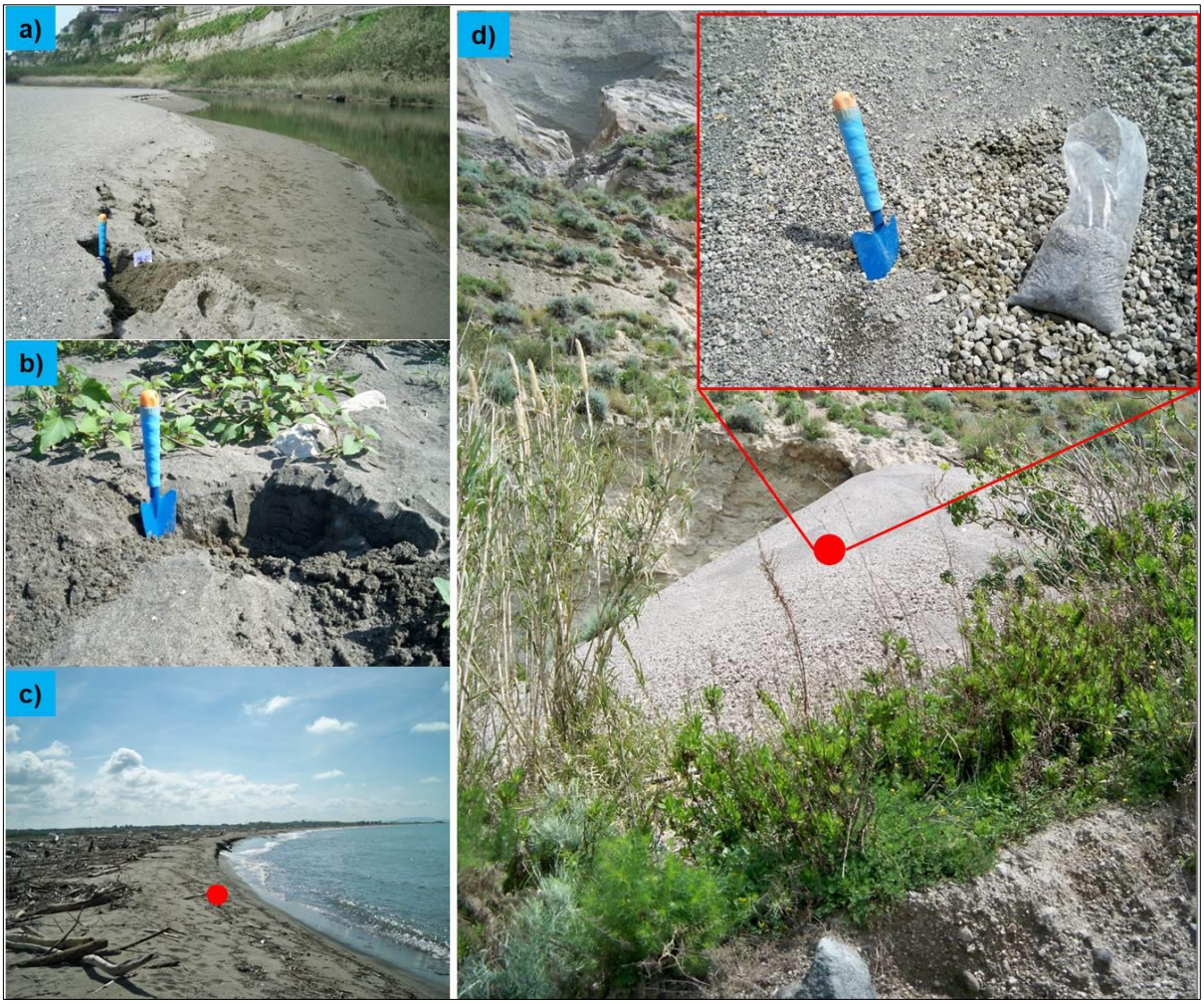

Figure 3.18 – a) Well sorted lake sand ranging from medium to very fine in grain size (PZ-20, Torrefumo); b) well sorted fluvial bar sand ranging from medium to very fine in grain-size (VO-1, Volturno river); c) very well sorted Volturno river mouth sand ranging from medium to very fine in grain-size (VO-3); d) moderately sorted slope detrital cone sand ranging from gravel to medium sand in grain-size (PZ-18).

The Campania studied area showed a very well developed beach, often very well sorted and then an higher texture-maturity degrees than Aeolian Island beaches.

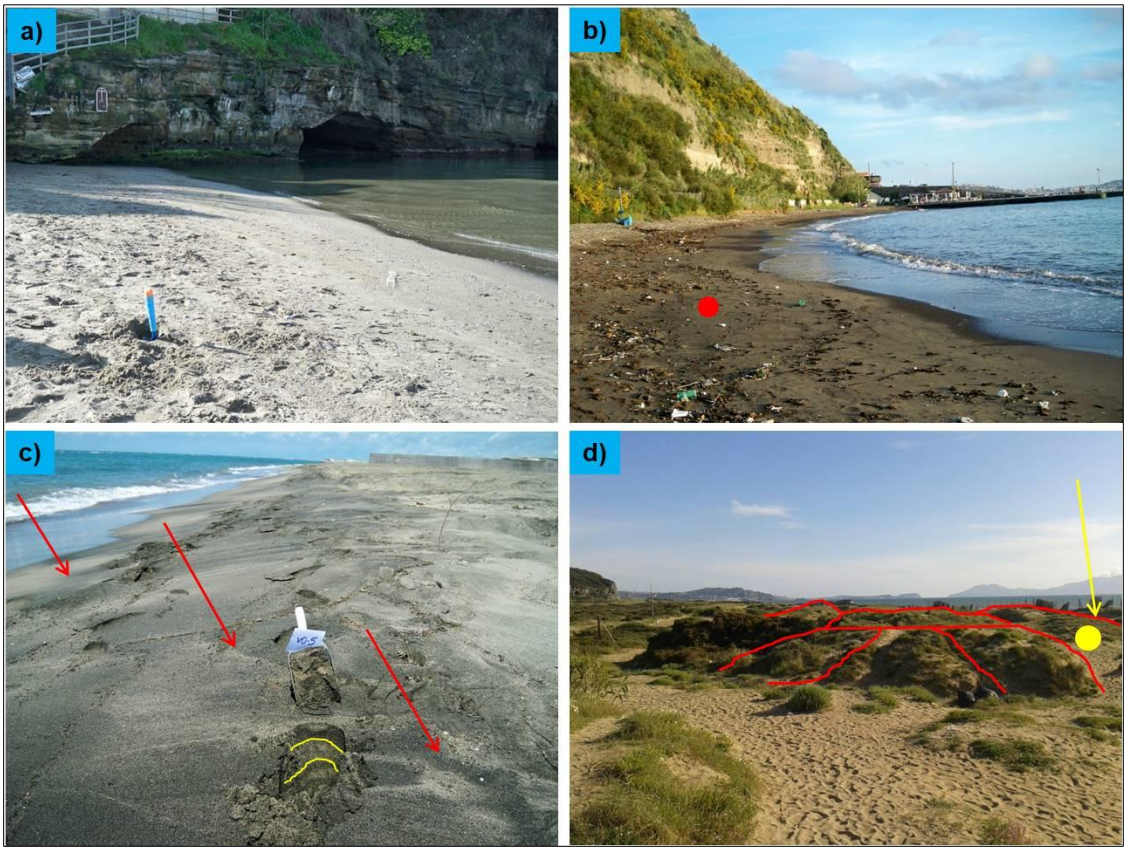

Figure 3.19 – a) Very well sorted beach sand ranging from medium to fine in grain-size (PZ-13, Capo Miseno); b) very well sorted beach sand ranging from medium to very fine in grain-size (BC-2, Acqua Morta; 2); c) very well sorted beach sand showing an heavy mineral concentrations and a "traction carpet" ranging from medium to very fine in grain-size (VO-5, Castel Volturno); d) very well sorted sand ranging from medium to very fine in grain-size, it was sampled from dunal environment (Li-4, Licola mare).

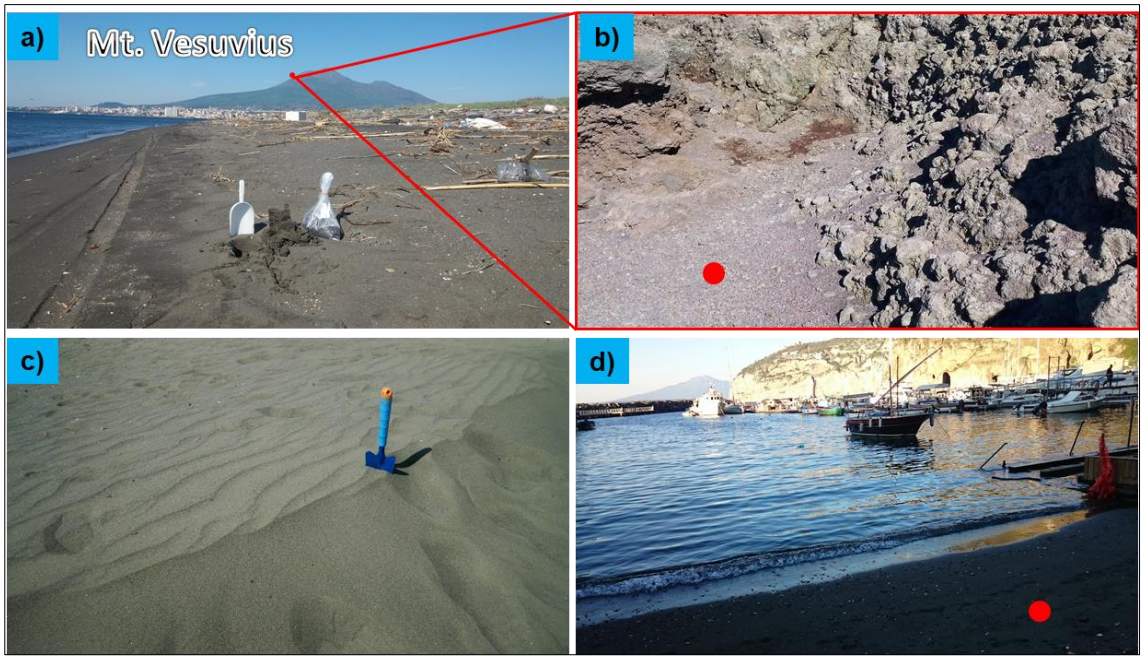

Figure 3.20 – a) moderately sorted beach sand (TA-1). In the background is shown the Mt. Vesuvius (TA-1); b) poorly sorted crater sand (VE-2); c) very well sorted beach sand sampled from a dune (PZ-17); d) moderately sorted "black" beach sand from Sorrento (SO-3).

Chapter 4 Methods and Results

This chapter will describe the methodologies used to analyze the hundred samples described in chapter 3 and successively will show the obtained results. In order to investigate on provenance, pre-burial processes, composition and texture of modern sand supplied from volcanic terrains such as those discussed in the previous chapters, different studies have been carried out through:

- Sieving analyses;
- Polarizing microscope and Electron Microprobe;
- Image analysis (roundness study);
- Geographic Information System analysis (SGI calculation).

4.1 – Sieving analysis -

Sand samples were washed using H_2O_2 (10 %) to remove organic matter, air-dried, subsampled using a splitter and mechanically sieved using 1Φ intervals (from -1 Φ to 4 Φ) in order to obtain granulometric sand distribution (fig. 4.1) and the grain-size fraction chosen to realize the thin sections (fig. 4.1g).

Figure 4.1 – Main step during sieving analyses.

4.1.1 – Aeolian Islands sieving analysis results-

4.1.1a - ALICUDI ISLAND –

Grain size distribution of Alicudi beach sediment samples is shown in table 4.1 and figure 4.2.

Grain size (%)	AL-1	AL-2	AL-3	AL-4	AL-5	AL-6	AL-7
Gravel	0	19,8	5,0	31,4	1,1	19,1	27,0
Vc Sand	0	31,4	10,9	61,5	2,9	22,6	30,6
c Sand	0,4	43,5	27,8	6,8	26,8	40,7	23,2
m Sand	25	5,0	42,4	0,2	51,3	17,1	12,7
f Sand	66	0,3	13,1	0,1	15,9	0,5	5,6
Vf Sand	8	0,1	0,7	0,0	0,7	0	0,4
Silt-Clayt	0	0	0,1	0,0	1,3	0	0,5

Table 4.1 – Grain-size distribution. Vc: Very coarse; C: Coarse; m: Medium; f: Fine; Vf: Very fine.

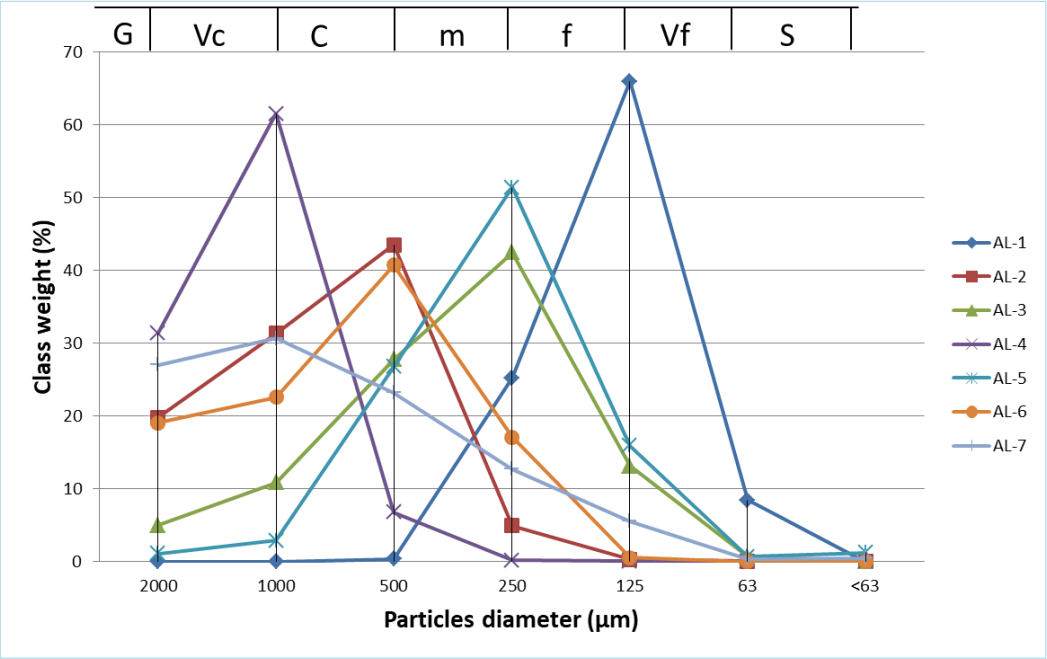

Figure 4.2 - Granulometric distribution. The particles diameter is shown on the x-axis, and the class weight on the y-axis. G: gravel; Vc: very coarse sand; C: coarse sand; m: medium sand; f: fine sand; Vf: very fine sand; S: silt.

4.1.1b - FILICUDI ISLAND –

Grain size distribution of Filicudi beach sediment samples is shown in table 4.2 and figure 4.3.

Grain size (%)	Fi-1	Fi-2	Fi-3	Fi-4
Gravel	39,0	41,4	16,2	52,7
Vc Sand	25,2	20,2	9,4	16,3
C Sand	12,9	18,9	19,5	6,4
m Sand	13,5	17,6	24,9	12,9
f Sand	8,9	1,5	22,2	11,1
Vf Sand	0,2	0,3	6,3	0,6
Silt-Clay	0,3	0,2	1,5	0,0

Table 4.2 – Granulometric distribution. Vc: Very coarse; C: Coarse; m: Medium; f: Fine; Vf: Very fine.

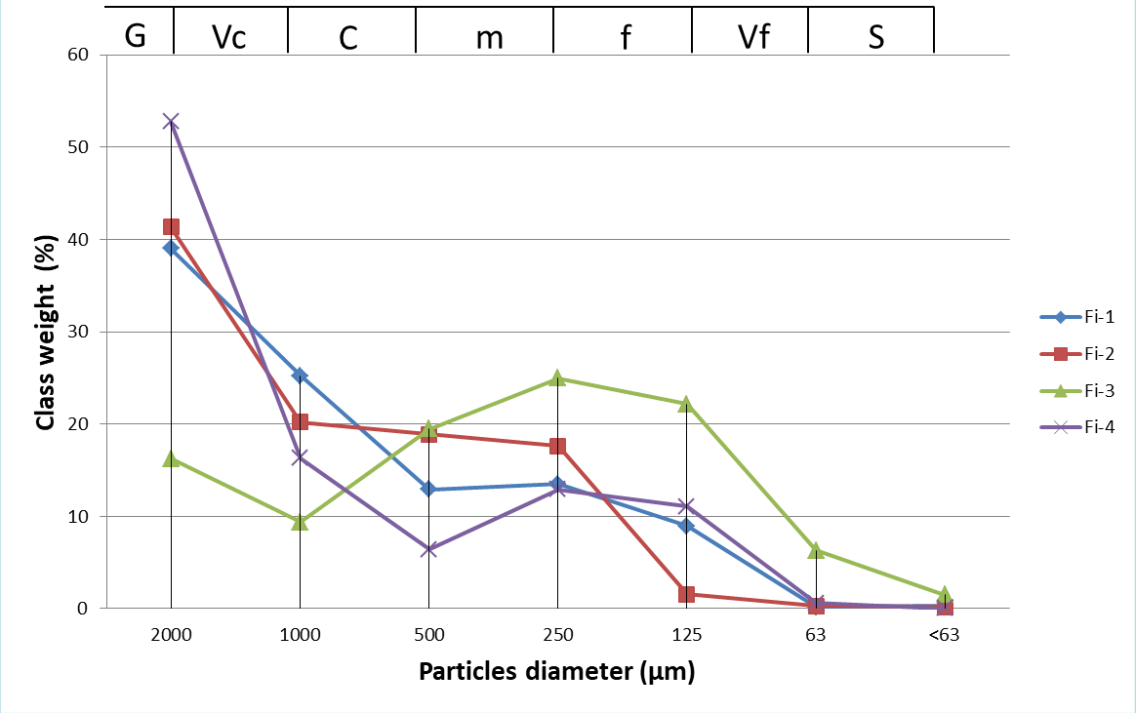

Figure 4.3 - Granulometric distribution. The particles diameter is shown on the x-axis, and the class weight on the y-axis. G: gravel; Vc: very coarse sand; C: coarse sand; m: medium sand; f: fine sand; Vf: very fine sand; S: silt.

4.1.1c - SALINA ISLAND –

Grain size distribution of Salina beach sediment samples is shown in table 4.3 and figure 4.4.

Grain size (%)	SA-1	SA-2	SA-3	SA-4	SA-5	SA-6	SA-7	SA-8
Gravel	33,7	6,4	0,5	53,4	50,2	16,8	14,3	39,5
Vc Sand	14,1	10,7	1,4	20,8	43,6	30,8	15,5	25,3
C Sand	13,6	20,9	21,5	13,8	5,9	28,8	26,2	19,0
m Sand	26,8	53,1	60,7	9,0	0,3	13,1	22,7	13,4
f Sand	11,6	8,7	15,4	3,0	0,1	5,6	15,5	2,7
Vf Sand	0,3	0,1	0,2	0,1	0,0	2,6	4,4	0,0
Silt-Clay	0,0	0,0	0,1	0,0	0,0	2,2	1,4	0,0

Grain size (%)	SA-9	SA-10	SA-11	SA-12	SA-13	SA-14	SA-15
Gravel	20,0	6,8	17,7	1,4	27,0	0,2	0,0
Vc Sand	7,4	17,1	10,2	4,3	30,6	27,0	0,0
C Sand	11,8	41,1	17,9	18,8	23,2	63,9	0,3
m Sand	48,7	21,8	30,6	49,3	12,7	8,4	20,7
f sand	11,9	7,9	18,8	25,7	5,6	0,3	73,1
Vf Sand	0,1	2,5	2,9	0,6	0,4	0,1	4,9
Silt-Clay	0,1	2,8	1,9	0,0	0,5	0,2	0,9

Table 4.3 – Granulometric distribution. Vc: Very coarse; C: Coarse; m: Medium; f: Fine; Vf: Very fine.

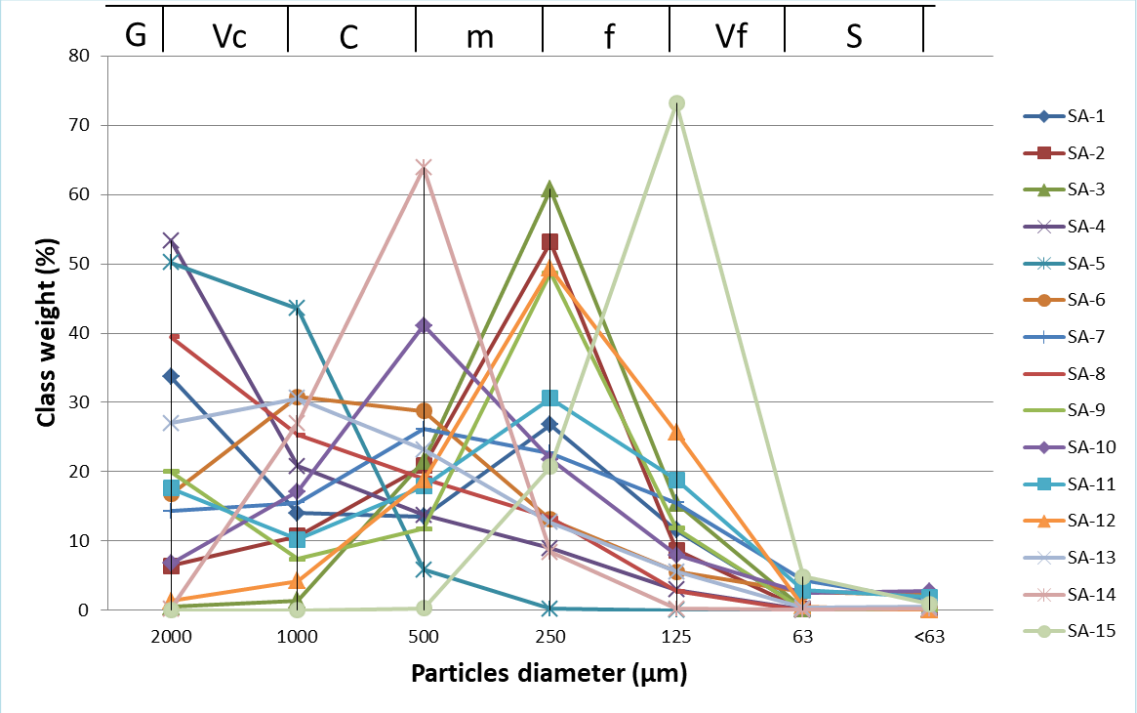

Figure 4.4 - Granulometric distribution. The particles diameter is shown on the x-axis, and the class weight on the y-axis. G: gravel; Vc: very coarse sand; C: coarse sand; m: medium sand; f: fine sand; Vf: very fine sand; S: silt.

4.1.1d – LIPARI ISLAND –

Grain size distribution of Lipari beach sediment samples is shown in table 4.4 and figure 4.5.

Grain size (%)	L1	L2	L4	L5	L6	L7
Gravel	1,3	0,1	72,3	1,7	4,2	0,0
Vc Sand	34,2	4,9	19,5	4,5	12,4	0,7
c Sand	51,5	31,2	6,3	36,4	50,5	36,9
m Sand	13,0	52,6	1,4	55,7	32,2	60,6
f Sand	0,1	11,0	0,7	1,6	0,5	1,5
Vf Sand	0,0	0,1	0,2	0,0	0,0	0,2
Silt-Clay	0,0	0,0	0,3	0,0	0,1	0,0

L8	L9	L10	L11	L12	L13
4,4	68,5	0,0	0,0	7,0	51,5
15,9	16,4	0,0	0,8	15,6	33,4
37,1	6,1	1,7	20,1	44,8	3,1
18,1	7,0	52,7	64,8	29,7	11,7
9,6	1,8	45,4	14,1	2,9	0,4
9,2	0,1	0,7	0,1	0,0	0,0
5,5	0,0	0,1	0,0	0,0	0,0

Table 4.4 – Granulometric distribution. Vc: Very coarse; C: Coarse; m: Medium; f: Fine; Vf: Very fine (data are from Morrone et al., 2017).

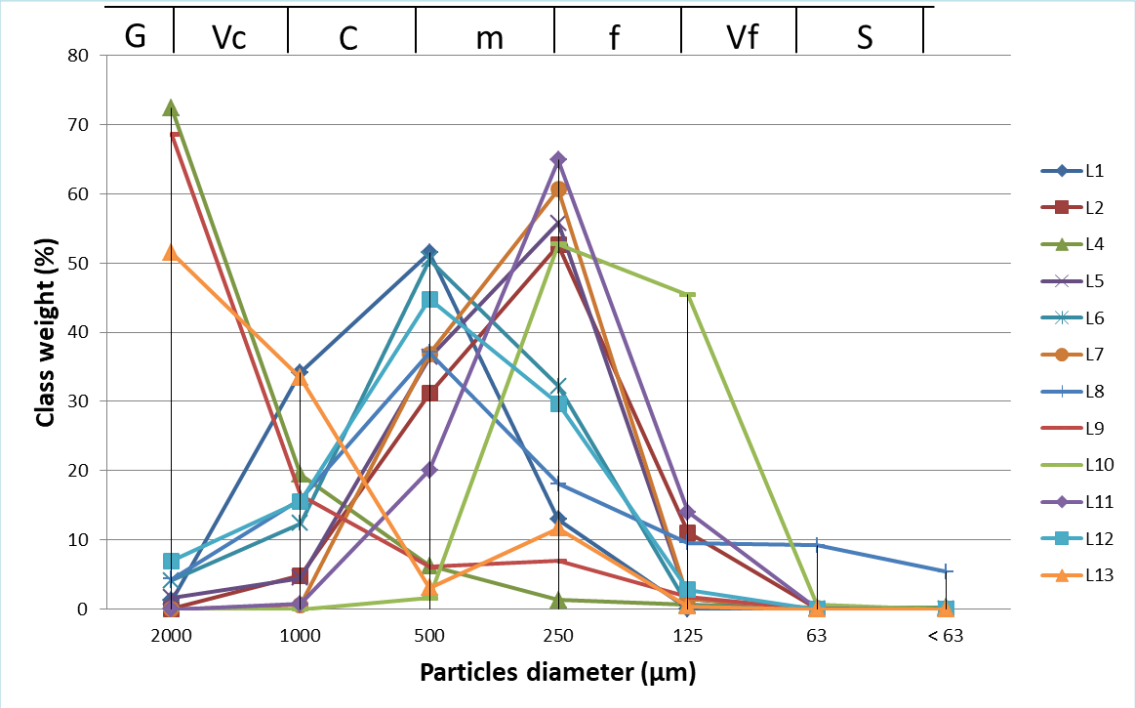

Figure 4.5 - Granulometric distribution. The particles diameter is shown on the x-axis, and the class weight on the y-axis. G: gravel; Vc: very coarse sand; C: coarse sand; m: medium sand; f: fine sand; Vf: very fine sand; S: silt (data are from Morrone et al., 2017).

4.1.1e – VULCANO ISLAND –

Grain size distribution of Vulcano beach sediment samples is shown in table 4.5 and figure 4.6.

Grain size (%)	V1	V2	V4	V5	V6	V7
Gravel	0	3,4	0,9	0,7	0	1,2
Vc Sand	0	12,9	26,9	20,6	0	13,4
c Sand	16,4	38,7	33,5	41,3	2,8	43,5
m Sand	71,1	40,8	32,4	28,2	46,0	38,8
f Sand	12,5	4,2	6,1	9,2	49,3	3,1
Vf Sand	0,0	0,1	0,2	0,1	1,7	0
Silt-Clay	0	0,0	0,1	0,0	0,3	0

V8	V9	V10	V11	V12
6,2	5,5	0,3	0	0
56,8	49,3	27,6	0	0
28,4	24,6	23,8	6,7	6,1
8,2	16,8	45,2	78,2	70,9
0,2	3,4	3,1	15,0	22,9
0,1	0,2	0,1	0,1	0,1
0,1	0,1	0,0	0,0	0,0

Table 4.5 – Granulometric distribution. Vc: Very coarse; C: Coarse; m: Medium; f: Fine; Vf: Very fine.

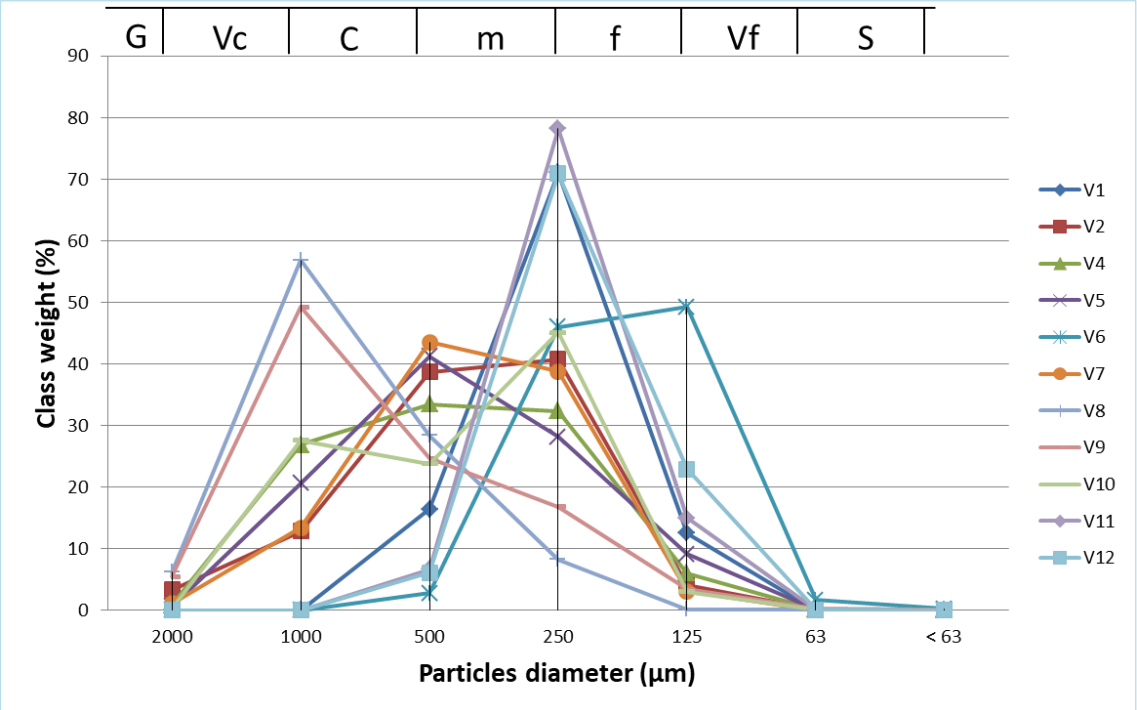

Figure 4.6 - Granulometric distribution. The particles diameter is shown on the x-axis, and the class weight on the y-axis. G: gravel; Vc: very coarse sand; C: coarse sand; m: medium sand; f: fine sand; Vf: very fine sand; S: silt.

4.1.1f – Panarea island –

Grain size distribution of Panarea beach sediment samples is shown in table 4.6 and figure 4.7.

Grain size (%)	PN-1	PN-2	PN-3	PN-4	PN-5	PN-6
Gravel	15,2	0,1	0,0	25,1	38,9	16,8
Vc Sand	18,7	0,2	0,1	11,4	24,3	20,4
c Sand	36,7	0,5	1,2	41,4	16,2	16,6
m Sand	26,1	6,9	41,7	21,7	9,6	11,4
f Sand	3,2	77,2	53,4	0,3	5,5	10,5
Vf Sand	0,1	14,8	3,4	0,1	2,9	12,7
Silt-Clay	0,1	0,3	0,2	0,0	2,6	11,5

Grain size (%)	PN-7	PN-8	PN-9	PN-10	PN-11
Gravel	0,4	0,0	0,0	8,6	33,6
Vc Sand	8,2	0,1	0,0	6,2	21,3
c Sand	16,9	4,8	1,4	7,2	16,0
m Sand	65,8	75,9	43,5	33,6	11,9
f Sand	8,5	19,2	54,1	36,1	8,3
Vf Sand	0,2	0,0	1,0	7,1	5,0
Silt-Clay	0,0	0,0	0,0	1,3	3,9

Table 4.6 – Granulometric distribution. Vc: Very coarse; C: Coarse; m: Medium; f: Fine; Vf: Very fine.

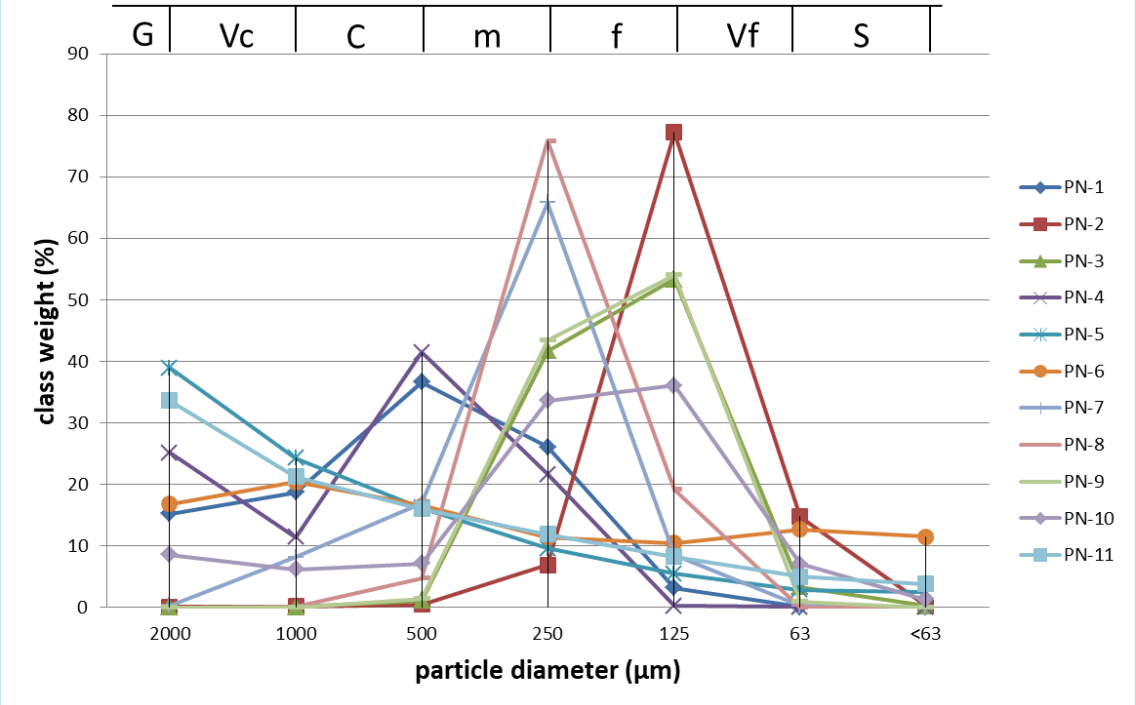

Figure 4.7 - Granulometric distribution. The particles diameter is shown on the x-axis, and the class weight on the y-axis. G: gravel; Vc: very coarse sand; C: coarse sand; m: medium sand; f: fine sand; Vf: very fine sand; S: silt.

4.1.1g – STROMBOLI ISLAND –

Grain size distribution of Stromboli beach sediment samples is shown in table 4.7 and figure 4.8.

Grain size (%)	STR-1	STR-2	STR-3	STR-4	STR-5	STR-7	STR-8	STR-9
Gravel	37,4	0,3	29,1	33,9	19,9	0,1	5,7	6,4
Vc Sand	9,6	0,2	10,4	8,4	4,8	2,9	11,0	1,7
c Sand	30,0	25,1	41,1	28,8	30,1	55,7	46,6	15,3
m Sand	18,3	70,9	14,8	26,4	38,2	37,0	33,4	46,4
f Sand	4,4	3,5	4,3	2,4	6,8	4,1	3,3	24,3
Vf Sand	0,2	0,0	0,3	0,1	0,1	0,3	0,1	4,5
Silt-Clay	0,0	0,0	0,0	0,0	0,0	0,0	0,0	1,3

Table 4.7 – Granulometric distribution. Vc: Very coarse; C: Coarse; m: Medium; f: Fine; Vf: Very fine.

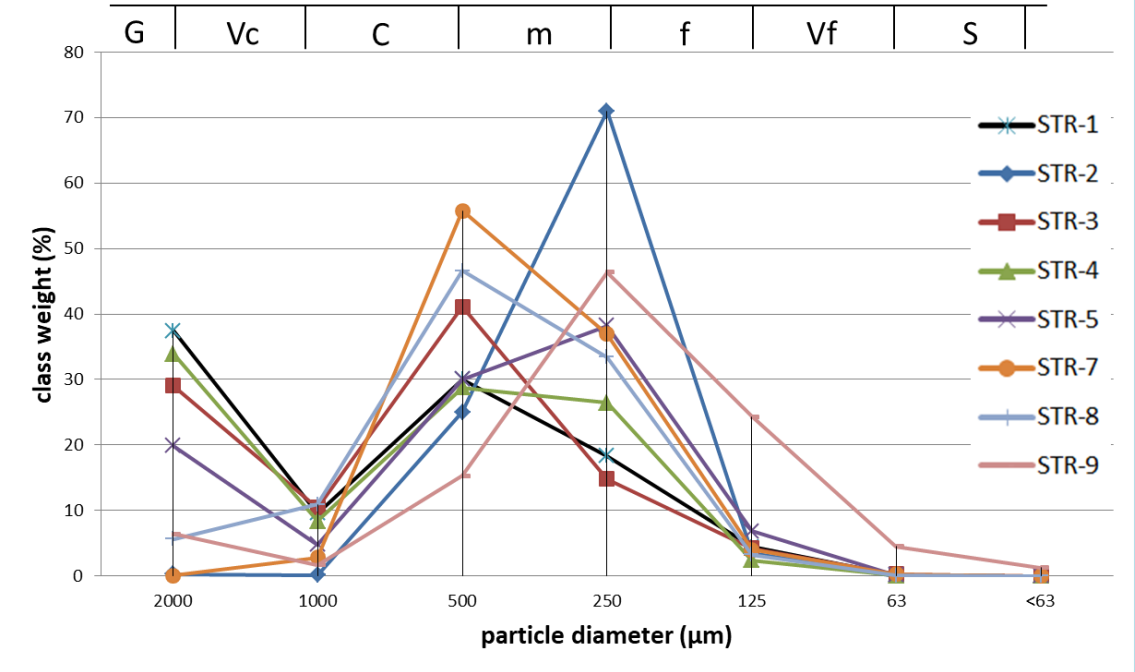

Figure 4.8 - Granulometric distribution. The particles diameter is shown on the x-axis, and the class weight on the y-axis. G: gravel; Vc: very coarse sand; C: coarse sand; m: medium sand; f: fine sand; Vf: very fine sand; S: silt.

Among the seven Alicudi beach sand, one is dominated by very coarse fraction (AL-4), two are dominated by coarse fraction (AL-2; AL-6), one is dominated by medium fraction (AL-5), one is dominated by fine fraction (AL-1), AL-7 shows a growing distribution among the five sand fraction, from Vf to Vc sand, whereas AL-3 has an homogeneous sandy grain-size distribution, in fact it was chosen as a test to realize thin sections on the five sand fractions (tab.4.1; fig. 4.2; appendix A, B, C).

Filicudi sand samples are dominated by gravel except Fi-3 which has an homogeneous sand distribution with the higher amount in the medium fraction, in fact it was chosen as a test to realize thin sections for the five sand fractions (tab.4.2; fig. 4.3; appendix A, B, C).

Among Salina sand samples, SA-4, SA-5, SA-8 are dominated by gravel with lesser amount of sand, SA-6, SA-13 are dominated by very coarse fraction, SA-7, SA-10, SA-14 are dominated by coarse fraction, SA-2, SA-3, SA-9, SA-11, SA-12, SA-15 is dominated by fine sand, whereas SA-1 has an homogeneous sandy grain-size distribution, in fact it was chosen as a test to realize thin sections for the five sand fractions (tab.4.3; fig. 4.4; appendix A, B, C).

All beach sediment samples on Lipari island are dominated by sand fraction (table 4.4; fig. 4.5). Most are medium (L2, L5, L7, L10, L11), or coarse (L12, L6, L8, L1) sand, while a few are very coarse sand (L4, L9, L13; Morrone et al., 2017).

As shown in table 4.5 and figure 4.6, it is possible to deduce that the Vulcano samples show that V8 and V9 are dominated by very coarse sand fraction, V4, V5 and V7 are dominated by coarse sand fraction, V1, V2, V10, V11 and V12 are dominated by medium sand fraction whereas only V6 is dominated by fine sand fraction.

Among Panarea island sediment samples, PN-5, PN-11 are gravel dominated, PN-6 is dominated by very coarse sand fraction, PN-4 is dominated by coarse sand fraction, PN-7 and PN-8 are dominated by medium sand fraction, PN-2, PN-3, PN-9 and PN-10 are dominated by fine sand fraction, whereas PN-1 exhibit an homogeneous sandy grain-size distribution, in fact it was chosen as a test to realize thin sections for the five sand fractions (tab.4.6; fig. 4.7; appendix A, B, C).

Two beach samples are dominated by gravel on Stromboli island (STR-1, STR-4), whereas STR-3, STR-7 and STR-8 are dominated by coarse sand fraction, STR-2, STR-5 and STR-9 are dominated by medium sand fraction. Moreover, STR-1 and STR-9 (crater sand) have been chosen as a test to realize thin sections for the five sand fractions (tab.4.6; fig. 4.7; appendix A, B, C).

4.1.2 – Campania province sieving analysis results-

Campania province has been subdivided into three different coastal stretch: 1) from Volturno river mouth to the southernmost Licola sample; 2) from Bacoli to Naples localities (southernmost Naples sample); 3) from Portici to the southernmost Sorrento sample (see fig. 3.17; Tab. 3.8).

4.1.2a – VOLTURNO-LICOLA COASTAL STRETCH –

Grain size distribution of beach sediment samples going to Volturno river mouth to Licola is shown in table 4.8 and figure 4.9.

Grain size (%)	VO-1	VO-2	VO-3	VO-4	VO-5	VO-6
Gravel	0,1	0,0	0,0	0,0	0,0	0,0
Vc Sand	0,1	0,0	0,2	0,1	0,0	0,0
c Sand	1,4	0,2	29,7	22,3	5,8	0,7
m Sand	53,6	23,7	66,0	68,8	82,6	44,4
f Sand	43,2	74,5	3,8	8,7	11,4	53,2
Vf Sand	1,5	1,6	0,2	0,2	0,1	1,6
Silt-Clay	0,1	0,0	0,1	0,0	0,1	0,0

Grain size (%)	VO-7	VO-8	VO-9	VO-10	VO-11
Gravel	0,0	0,0	0,0	0,0	0,0
Vc Sand	0,0	0,0	0,2	0,0	0,0
c Sand	9,0	3,6	4,7	0,0	18,5
m Sand	84,0	89,5	59,2	15,5	71,2
f Sand	6,9	6,8	35,1	82,1	9,9
Vf Sand	0,0	0,0	0,8	2,4	0,3
Silt-Clay	0,0	0,0	0,0	0,0	0,1

Grain size (%)	Li-1	Li-2	Li-3	Li-4	Li-5	Li-6
Gravel	0,0	0,0	0,0	0,0	0,0	0,0
Vc Sand	0,0	0,0	0,0	0,0	0,0	0,0
c Sand	0,2	0,0	0,0	0,0	0,0	0,0
m Sand	30,0	10,9	10,9	8,5	8,2	5,6
f Sand	69,1	88,2	88,5	90,0	91,3	93,8
Vf Sand	0,6	0,8	0,6	1,4	0,4	0,6
Silt-Clay	0,2	0,0	0,0	0,1	0,0	0,0

Table 4.8 – Granulometric distribution. Vc: Very coarse; C: Coarse; m: Medium; f: Fine; Vf: Very fine.

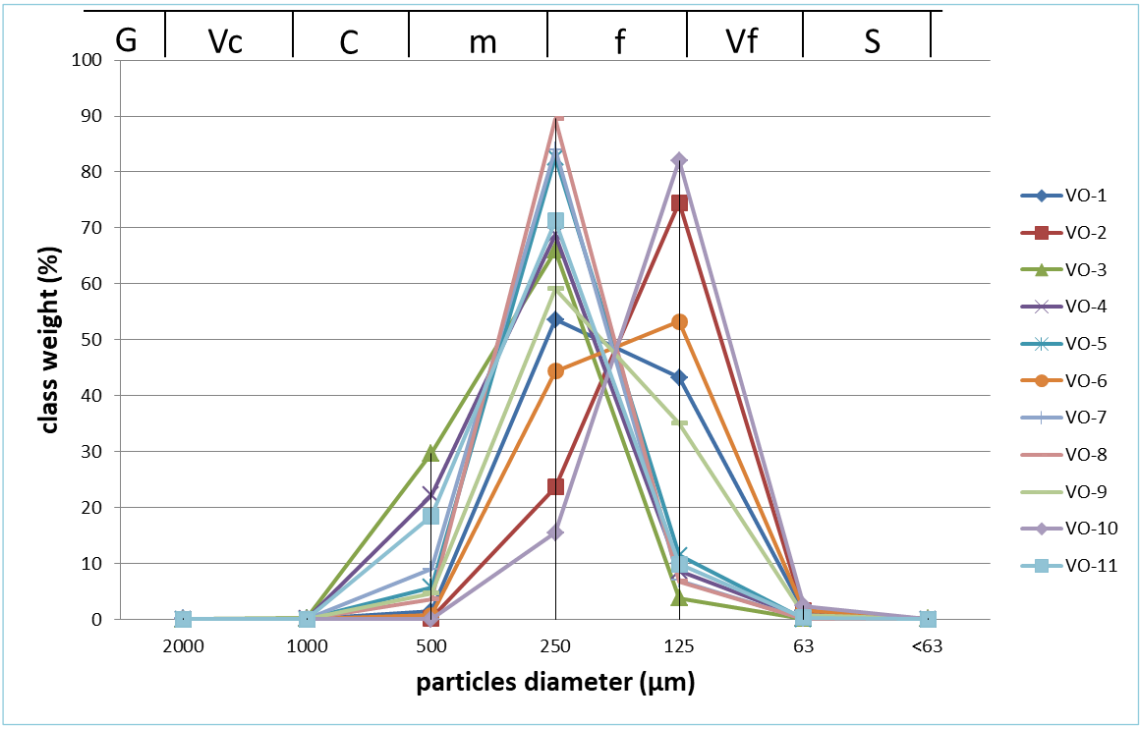

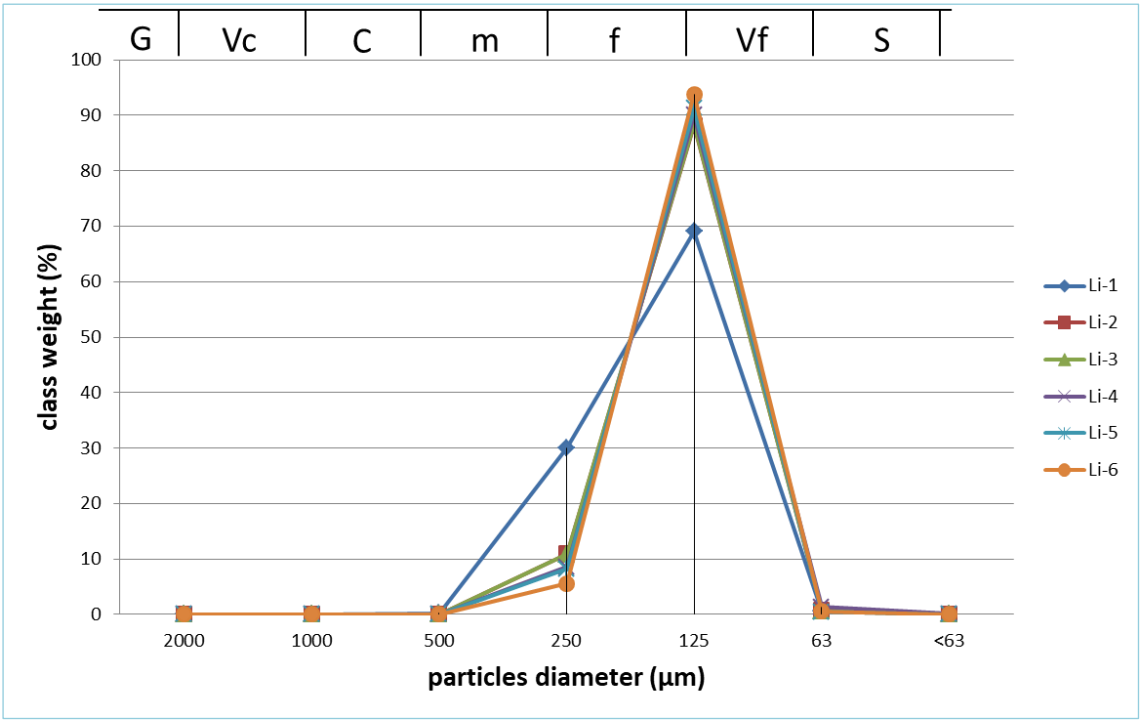

Figure 4.9 – Grain-size distribution. The particles diameter is shown on the x-axis, and the class weight on the y-axis. G: gravel; Vc: very coarse sand; C: coarse sand; m: medium sand; f: fine sand; Vf: very fine sand; S: silt.

4.1.2b – BACOLI-NAPLES COASTAL STRETCH –

Grain size distribution of beach sediment samples going to Bacoli to Naples is shown in table 4.9 and figure 4.10.

Grain size (%)	BC-1	BC-2	BC-3	BC-4	BC-5
Gravel	0,3	1,2	0,1	0,0	0,0
Vc Sand	17,0	1,3	0,3	0,1	0,0
c Sand	18,2	8,9	0,9	0,2	0,1
m Sand	19,1	27,8	8,0	7,3	3,4
f Sand	44,9	59,8	90,1	91,6	95,3
Vf Sand	0,5	0,8	0,7	0,7	1,2
Silt-Clay	0,1	0,2	0,0	0,0	0,0

Grain size (%)	PZ-1	PZ-2	PZ-3	PZ-4	PZ-5	PZ-6	PZ-7	PZ-8	PZ-9	PZ-10
Gravel	6,0	0,0	0,0	14,7	0,0	1,6	0,0	3,6	0,0	0,6
Vc Sand	26,5	0,0	0,7	10,5	0,2	0,0	0,1	23,2	0,1	3,6
c Sand	21,3	0,7	12,1	32,5	6,0	5,1	3,5	35,4	2,7	17,1
m Sand	36,3	54,1	64,9	35,4	65,2	52,8	46,9	30,3	36,4	47,3
f Sand	9,7	45,0	22,1	6,8	28,3	39,3	48,4	7,3	59,0	30,4
Vf Sand	0,2	0,2	0,2	0,2	0,2	1,1	1,1	0,2	1,8	0,9
Silt-Clay	0,1	0,0	0,0	0,0	0,0	0,0	0,0	0,1	0,0	0,1

Grain size (%)	PZ-11	PZ-12	PZ-13	PZ-14	PZ-15	PZ-16	PZ-17	PZ-18	PZ-19	PZ-20
Gravel	0,2	0,1	1,0	0,5	0,1	0,0	0,0	56,0	1,0	16,6
Vc Sand	0,7	0,3	0,5	1,8	0,3	0,3	0,0	37,8	1,1	12,7
c Sand	11,6	0,8	3,4	13,5	6,1	4,6	0,6	3,1	2,4	17,4
m Sand	52,9	20,8	18,4	40,9	32,5	45,5	17,8	0,3	13,2	18,8
f Sand	33,6	71,8	75,2	42,4	59,5	49,0	78,8	0,3	75,4	27,0
Vf Sand	0,9	6,2	1,4	0,9	1,5	0,5	2,8	0,5	6,7	6,7
Silt-Clay	0,1	0,0	0,0	0,0	0,0	0,0	0,0	2,1	0,1	0,8

Grain size (%)	CO-1	GA-1	MC-1	NA-1	NA-2	NA-3	NA-4	NA-5	NA-6	NA-7
Gravel	8,9	3,3	4,1	1,0	0,6	0,4	1,4	2,8	0,0	2,9
Vc Sand	15,3	8,9	1,4	2,3	2,4	3,5	4,9	34,4	0,3	4,9
c Sand	31,4	54,8	29,5	11,4	9,2	25,7	14,1	56,8	2,5	12,1
m Sand	42,3	30,8	63,5	44,9	36,1	58,0	36,5	5,9	51,4	36,9
f Sand	2,0	2,1	1,4	38,4	45,7	12,4	40,5	0,2	44,8	38,5
Vf Sand	0,1	0,1	0,0	1,9	5,9	0,1	2,5	0,0	1,0	4,7
Silt-Clay	0,0	0,0	0,0	0,1	0,1	0,0	0,1	0,0	0,0	0,1

Table 4.9 – Grain-size distribution. Vc: Very coarse; C: Coarse; m: Medium; f: Fine; Vf: Very fine.

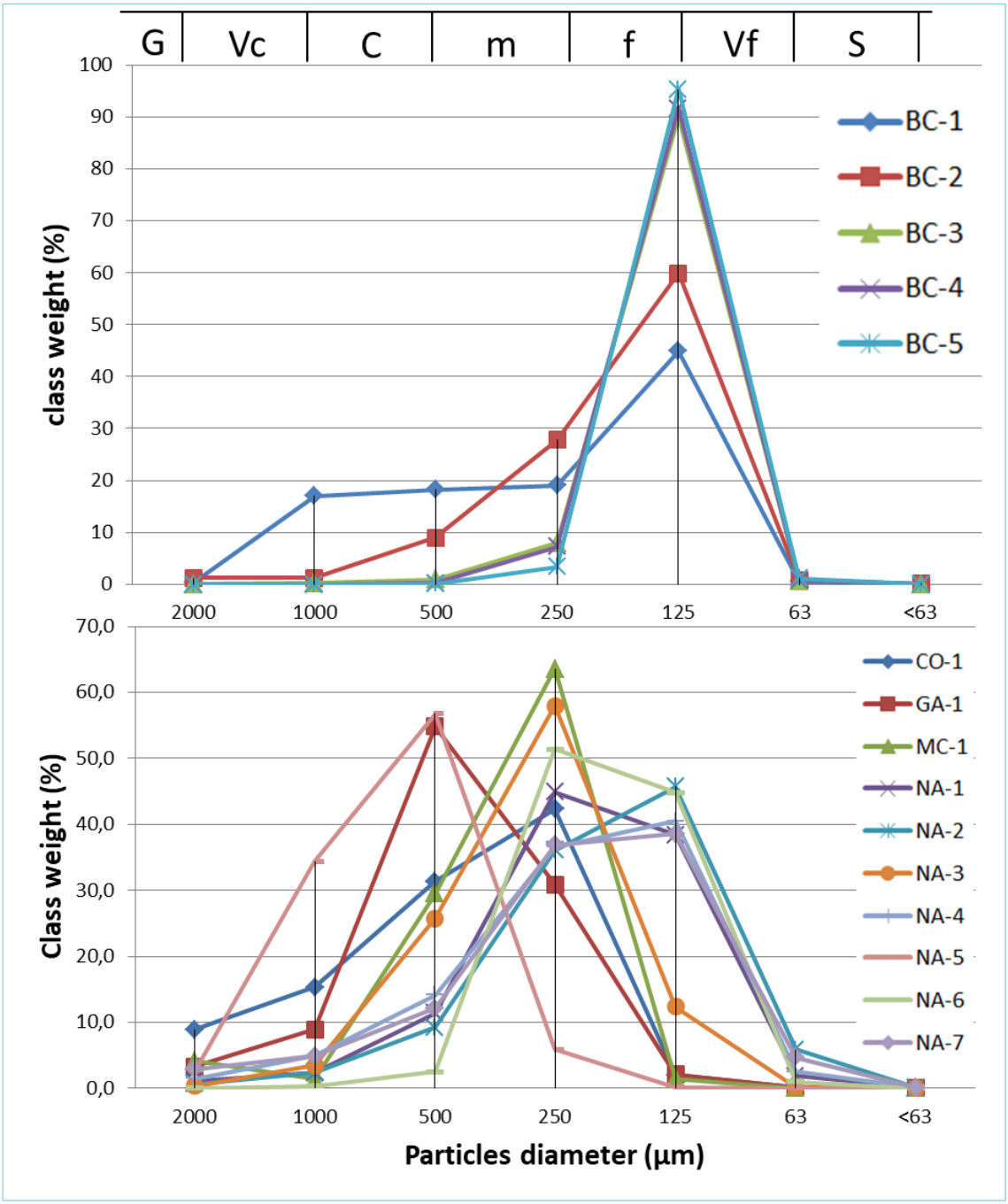

Figure 4.10 – Grain-size distribution. The particles diameter is shown on the x-axis, and the class weight on the y-axis. G: gravel; Vc: very coarse sand; C: coarse sand; m: medium sand; f: fine sand; Vf: very fine sand; S: silt.

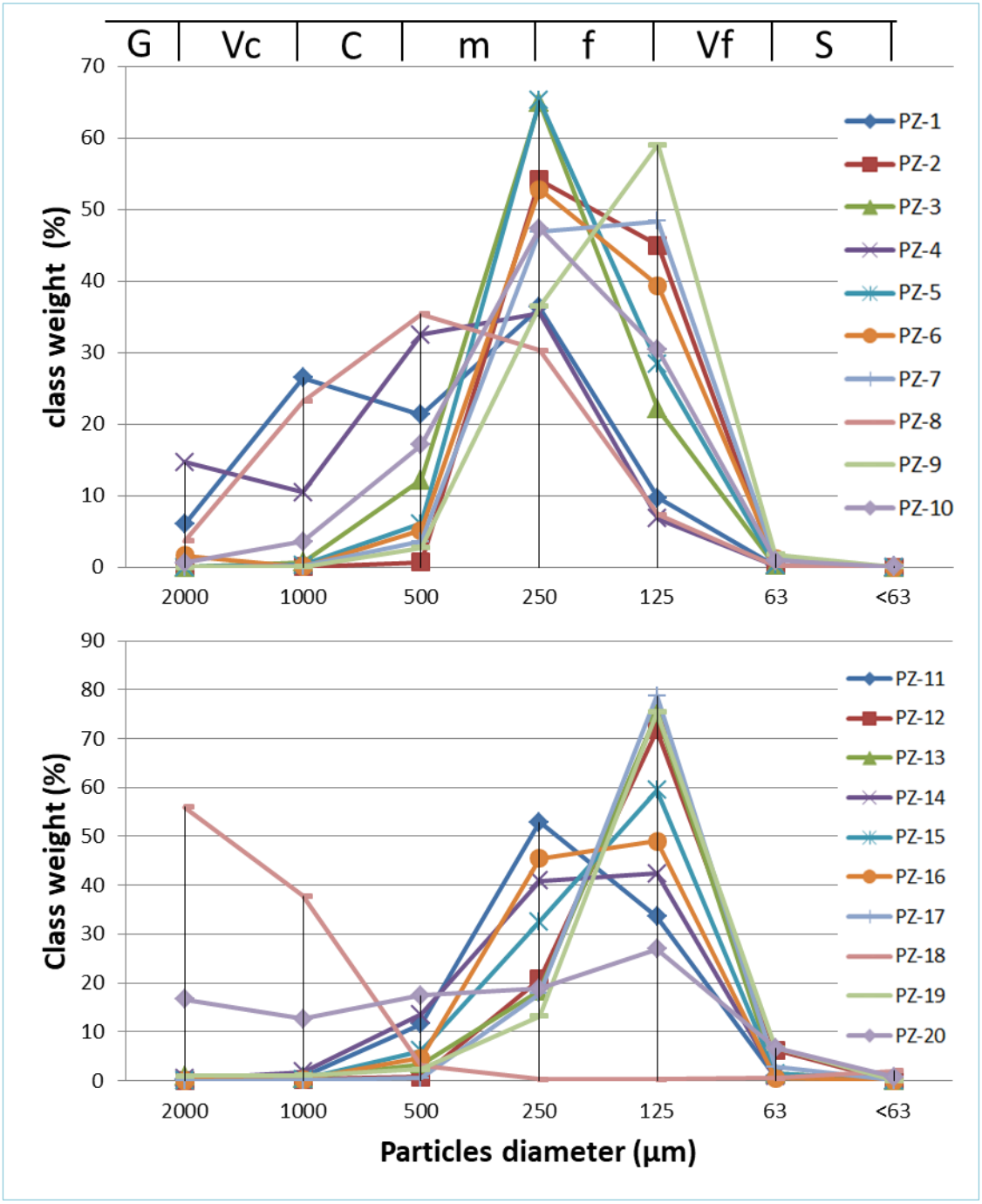

Figure 4.10 - (continued) – Grain-size distribution. The particles diameter is shown on the x-axis, and the class weight on the y-axis. G: gravel; Vc: very coarse sand; C: coarse sand; m: medium sand; f: fine sand; Vf: very fine sand; S: silt.

4.1.2c – PORTICI-SORRENTO COASTAL STRETCH –

Grain-size distribution of beach sediment samples going to Portici to Sorrento is shown in table 4.10 and figure 4.11.

Grain size (%)	PO-1	PO-2	PO-3	TG-1	TG-2	TG-3	TA-1	TA-2	VE-1	VE-2	VE-3
Gravel	0,2	3,5	0,1	0,3	0,2	41,0	0,1	0,0	25,1	16,9	44,4
Vc Sand	2,0	21,8	1,0	7,2	2,2	17,1	1,5	0,0	29,6	36,1	29,9
c Sand	33,0	41,0	9,2	49,3	14,0	16,2	3,3	1,8	23,5	35,2	17,2
m Sand	63,5	30,6	74,2	36,1	67,2	12,6	30,4	49,5	13,1	9,1	4,5
f Sand	1,2	3,0	15,4	6,5	16,2	9,8	63,2	48,2	5,9	1,8	2,8
Vf Sand	0,0	0,0	0,1	0,4	0,1	2,2	1,4	0,5	1,9	0,4	0,9
Silt-Clay	0,0	0,0	0,0	0,2	0,0	1,1	0,0	0,0	1,0	0,4	0,2

Grain size (%)	CA-1	CA-2	CA-2B	CA-3	SO-1	SO-2	SO-3	SO-4	SO-5
Gravel	37,9	14,4	1,0	0,4	14,2	0,2	1,2	56,3	1,4
Vc Sand	4,5	10,4	1,7	0,8	4,4	0,9	0,8	13,9	17,3
c Sand	2,7	35,8	16,7	3,8	9,4	8,9	8,9	19,9	67,2
m Sand	23,7	31,5	73,6	30,5	35,0	42,2	46,2	7,4	13,1
f Sand	30,9	7,7	6,9	60,3	35,3	44,7	41,5	2,4	0,6
Vf Sand	0,3	0,1	0,1	4,1	1,5	3,0	1,4	0,1	0,4
Silt-Clay	0,0	0,1	0,0	0,1	0,0	0,1	0,1	0,0	0,0

Table 4.10 – Grain-size distribution. Vc: Very coarse; C: Coarse; m: Medium; f: Fine; Vf: Very fine.

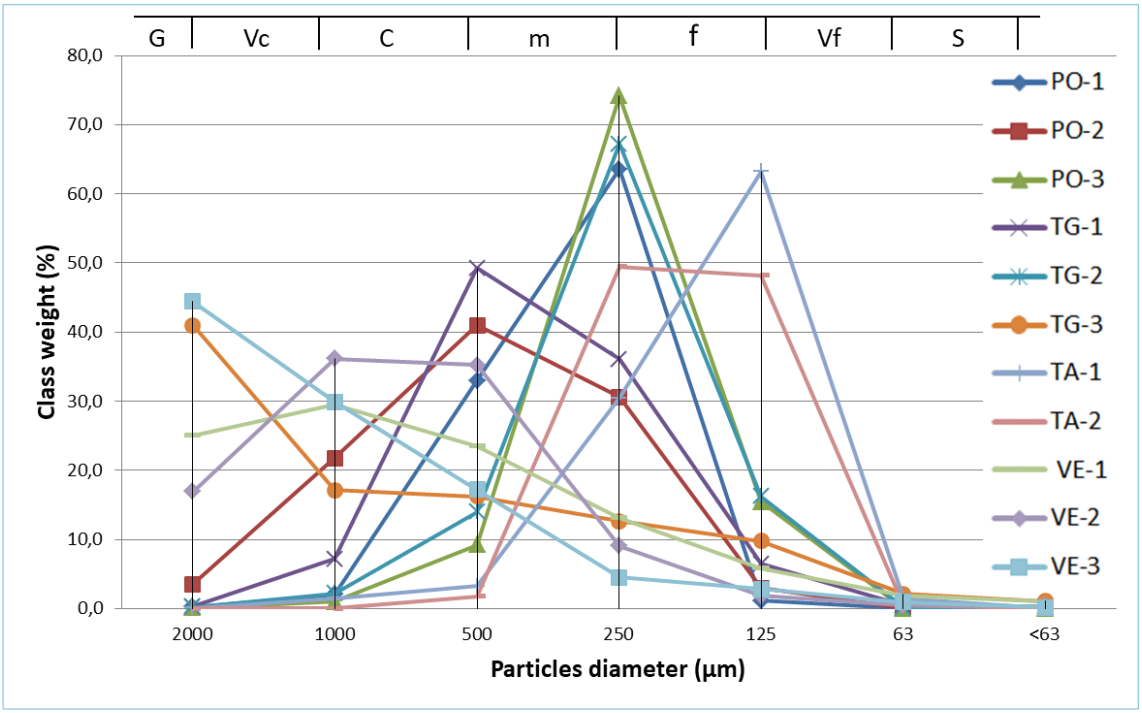

Figure 4.11 – Grain-size distribution. The particles diameter is shown on the x-axis, and the class weight on the y-axis. G: gravel; Vc: very coarse sand; C: coarse sand; m: medium sand; f: fine sand; Vf: very fine sand; S: silt.

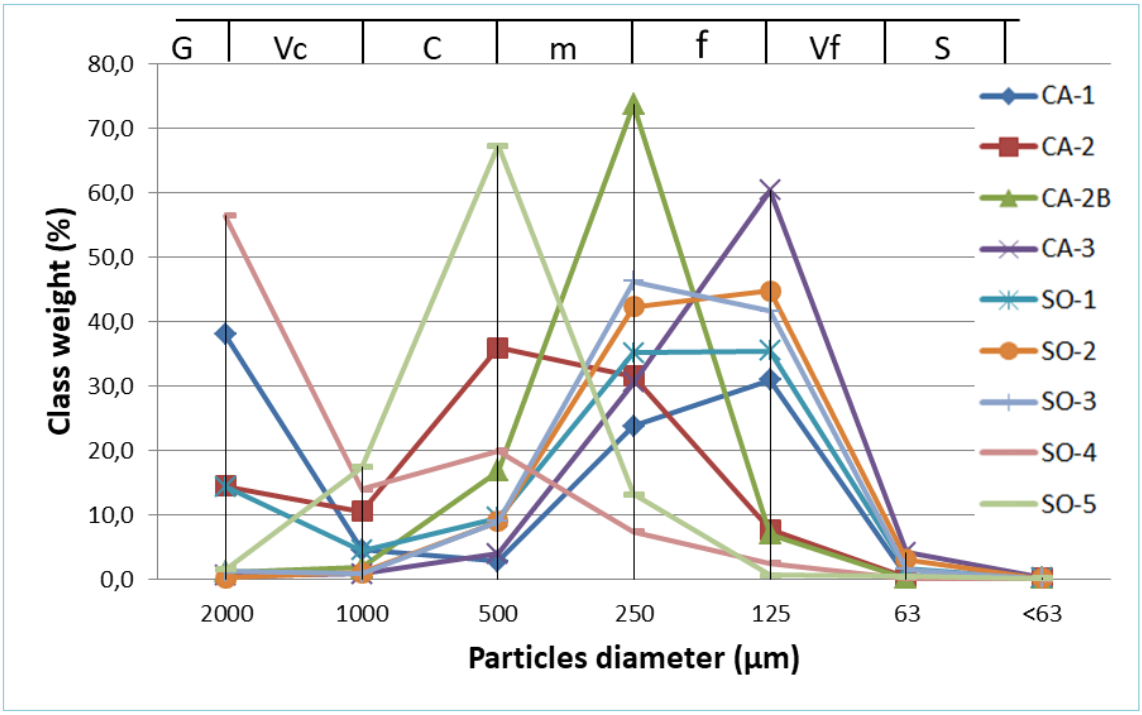

Figure 4.11 - (continued) – Grain-size distribution. The particles diameter is shown on the x-axis, and the class weight on the y-axis. G: gravel; Vc: very coarse sand; C: coarse sand; m: medium sand; f: fine sand; Vf: very fine sand; S: silt.

The samples which are from Volturno-Licola coastal stretch, show two mean sand fraction peak (fig. 4.9), they are represented by medium and fine sand. Among the 17 samples, nine are dominated by fine sand, eight are dominated by medium sand (tab. 4.8). Among the 35 sand samples from the Bacoli-Naples coastal stretch, BC series is dominated by fine sand fraction (125-250 µm). PZ series is dominated by medium sand (PZ-1, PZ-2, PZ-3, PZ-4, PZ-5, PZ-6, PZ-7, PZ-10, PZ-11) and fine sand (PZ-12, PZ-13, PZ-14, PZ-15, PZ-16, PZ-17, PZ-19, PZ-20). Only PZ-18 is dominated by the gravelly fraction. Also CO-1, MC-1, NA-1, NA-3, NA-6 are dominated by medium sand, whereas NA-2, NA-4, NA-7 are represented by fine sand, GA-1 and NA-5 are dominated by coarse sand (tab 4.9; fig. 4.10). Vesuvius crater (zero-order) sand are dominated by gravel and very coarse fraction (VE-1, VE-2, VE-3) (table 4.10 and figure 4.11). Along the Portici-Sorrento coastal stretch, among the 17 samples, three of them are dominated by gravelly fraction (TG-3, CA-1, SO-4), four are dominated by coarse sand (PO-2, TG-1; CA-2, SO-5), six are dominate by medium sand fraction (PO-1, PO-3, TG-2, TA-2, CA-2B, SO-3), four are dominated by fine sand fraction (TA-1, CA-3, SO-1, SO-2). Some samples have been chosen as a test to realize thin sections for the five sand fractions (BC-1, PZ-8; PZ-14). This method has been used in order to

differentiate among each sandy grains-size the composition and to test the effect of grain-size composition on sand detrital modes (e.g., Ingersoll et al., 1984).

In summary, among 68 Aeolian coastal samples, the 20,6% is represented by gravel (< 2,00 mm), the 10,3% is represented by very coarse sand, the 26,5% is represented by coarse sand, the 32,4% is represented by medium sand, the 10,3% is represented by fine sand; whereas among 72 Campania coastal samples, the 5,8% is represented by gravel, the 10,1% is represented by coarse sand, the 39,1% is represented by medium sand, the 44,9% is represented by fine sand (fig. 4.12).

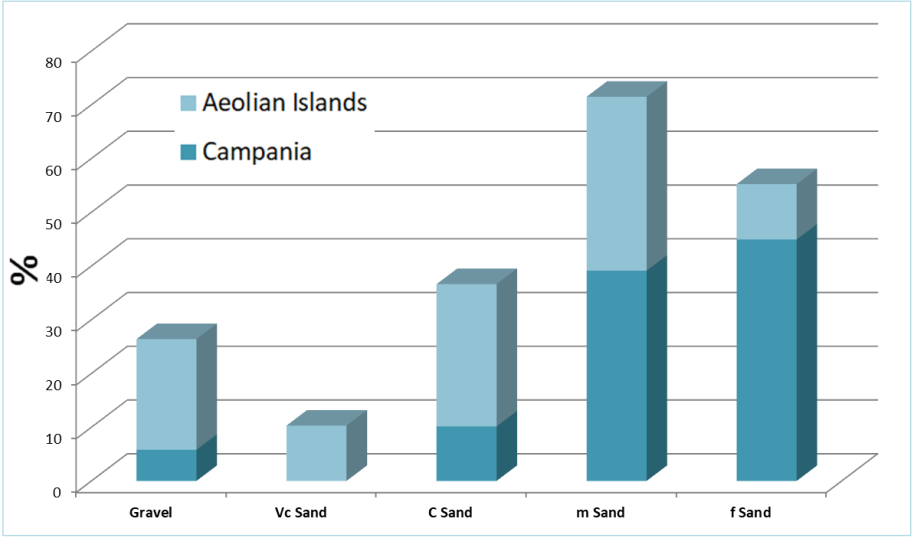

Figure 4.12 – Most representative grain-size distributions from the two study areas. Campania province is dominated by medium and fine sand. The Aeolian Islands beaches sediments are mainly dominated by coarser fractions with respect to the Campania province beaches. Vc: very coarse; C: coarse; m: medium; f: fine.

The most representative sampling environment were the berms (high-tide and low –tide berm), followed by the swash zone and others (see tab. 4.11). The most representative fraction among all samples from the two studied areas is the medium sand fraction, immediately followed by the fine and then coarse fractions, which were sampled mainly from high-tide berm, low-tide berm and swash zone (tab. 4.11).

	HtB	LtB	Dn	FB	RM	SDC	SwZ	Cr	Lc	LM	ShF	Tot
Gravel	6	8	-	-	-	1	2	1	-	-	-	18
Vc Sand	5	1	-	-	-	-	1	2	-	-	-	9
c Sand	10	9	-	-	-	-	5	-	1	-	-	25
m Sand	23	10	-	1	2	-	12	1	-	1	-	50
f Sand	13	11	3	1	-	-	8	-	1	-	1	38
Vf Sand	-	-	-	-	-	-	-	-	-	-	-	0
Silt	-	-	-	-	-	-	-	-	-	-	-	0
Tot	57	39	3	2	2	1	28	4	2	1	1	140

Table 4.11 - Grain-size vs. sampling environments. HtB: high-tide berm; LtB: low-tide berm; Dn: dune; FB: fluvial bar; RM: river mouth; SDC: slope detrital cone; SwZ: swash zone; Cr: crater; Lc: lacustrine; LM: lake mouth; ShF: shoreface; Tot: total.

4.2 - Polarizing microscope and Electron Microprobe analyses –

Detrital modes were defined for the medium-sand fraction (250 – 500 μm) of each sample, moreover some samples among the two studied areas, were selected for more detailed analysis to detect potential grain-size dependence of composition through petrographic analysis of very coarse (1000 – 2000 μm) , coarse (500 – 1000 μm), fine (125 – 250 μm) and very fine (63 – 125 μm) grain size fractions (appendix A).

The medium size fraction was chosen because monocrystalline, polycrystalline and lithic grains generally, are all occurring within this grain-size fraction (250 – 500 μm); moreover, these grain components are better distributed in the medium fraction rather than others sand fractions (e.g., van der Plas and Tobi, 1965). Especially for the Aeolian Islands, the medium sand fraction is the most likely to be transported into adjacent marine basins, the settings where most workers on island arc sediments have concentrated their efforts (e.g. Marsaglia, 1993; Garzanti and Andò, 2007).

Some thin sections (VO-, Li-, BC-, Pz- series for Campanian province, L- and V-series for Aeolian islands) were subsequently stained for both calcium-rich and potassium-rich feldspar grains according to the method outlined in Marsaglia & Tazaki (1992) (e.g. plate $III_{(e)}$, $X_{(a,b)}$).

Point count data were collected using a petrographic microscope with an automated point-counting stepper stage (fig. 4.13). Four hundred points were counted on each thin section using the *Gazzi–Dickinson* method (Ingersoll *et al.* 1984; Zuffa, 1985) in order to determine the mean modal composition of the analyzed fractions. Counted grains were assigned to the monomineralic and polymineralic compositional categories listed in table 4.12 The mineralogy and texture classification of volcanic fragments in the sand samples were determined according to the classification scheme of Marsaglia (1992, 1993), Critelli et al. (2002), Dickinson (1970). Raw data and recalculated petrographic parameters are shown in appendix A, B and C.

Changes in grain roundness were assessed to evaluate grain durability during transport. Variations in mean roundness were determined on medium-sand sized and in some cases on all the five sand fractions of monocrystalline grains of plagioclase (Plag), pyroxene (Py), olivine (Ol), hornblende (Hb), opaque (Op), K-feld (K), quartz (Qm), calcite (Ca), and of volcanic and sedimentary lithic fragments such as *Lvl* (volcanic lithic fragments with lathwork texture), *Lvmi* (volcanic lithic fragments with microlitic texture), Lvv (volcanic lithic fragments with vitric texture), Lvf (volcanic lithic fragments with felsitic texture), Lss (sedimentary lithic fragments with siliciclastic

composition), Lsc(xx) (sedimentary lithic fragments with crystalline carbonate composition) and Lsc(micr) (sedimentary lithic fragments with micritic carbonate composition).

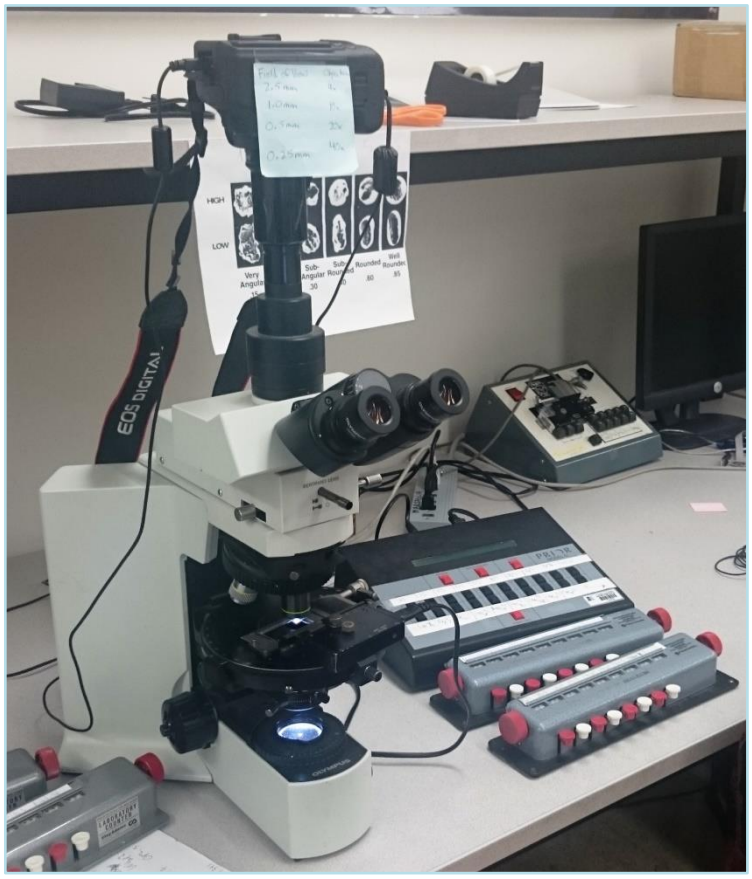

Figure 4.13 – Polarizing microscope connected to a point counter with automated stepper-stage.

Grain projections can be compared with a visual comparator such as that developed by Powers (1953). The Powers classification has two classes of sphericity combined with six classes of grain roundness (fig. 4.14).

Wadell (1933) proposed a measure of degree of roundness, P_d:

$$P_d = \frac{\sum(r/R)}{N};$$

where r is the curvature radius of individual grain corners, N the number of grain corners including corners whose radii are zero and R the radius of the maximum inscribed circle.

Because measurements of this type are time consuming, most workers have estimated roundness by reference to the Powers or some other visual comparator. Numerical values are assigned to each Powers roundness class using Wadell's formula (tab. 4.13).

Qm	**Monocrystalline quartz**
Qp	**Polycrystalline quartz**
	tf = tectonic fabric
Ch	**Chert**
K	**K-feldspar**
K alt	**Altered k-feldspar**
San	**Sanidine**
Ort	**Orthoclase**
Micr	**Microcline**
P	**Plagioclase feldspar**
P alt	**Altered plagioclase**
Ca	**Calcite**
Ca alt	**Altered calcite**
CC	**Calcite cement**
Py	**Pyroxene**
Py alt	**Altered Pyroxene**
Ol	**Olivine**
Ol alt	**Altered olivine**
Hb	**Hornblende**
Hb alt	**Altered hornblende**
Gr	**Garnet**
	br= *brown*
Le	*Leucite*
Ne	**Nepheline**
Bt	**Biotite**
Mu	**Muscovite**
D(op)	**Opaque dense**
Ti	**Titanite**
Tourm	**Tourmaline**
Ru	**Rutile**
Zeo/Dev	**Zeolite and/or devetrification**
Lvf:	**Volcanic lithic with felsitic texture**
Lvv:	**Vitric volcanic lithic**
	brgl= brown glass
	orgl = orange glass
	blgl = black glass
	algl = altered glass
	grgl = grey glass
	clgl = colourless glass

Lvmi:	**Volcanic lithic with microlitic texture**
	brgl= brown glass
	orgl= orange glass
	blgl = black glass
	algl = altered glass
	grgl = grey glass
	clgl = colourless glass
Lvl:	**Volcanic lithic with lathwork texture**
	brgl = brown glass
	orgl = orange glass
	blgl = black glass
	algl = altered glass
	grgl = dark grey glass
Lvo	*Holocrystalline volcanic lithic*
Lv alt	**Altered volcanic lithic**
Pm	**Pumice**
	br *= brown (aphyric)*
	cl = colourless (aphyric)
	xx = porphyric
Pm alt	*Altered pumice*
Lss	**Siliciclastic sedimentary lithic**
Lsc(micr)	**carbonate micrite**
Lsc(xx)	**carbonate crystalline**
Lp	**Plutonic lithic**
Lmt	**Metamorphic lithic**
Rp	**Plutonic rock fragment**
Rm	**Metamorphic rock fragment**
Rs	**Sedimentary rock fragment**
Ar	**Arenite**
Bio	**Bioclast**
BioM	**Biomicrite**
Xe	**Variuos xenolithes**
Unk	**Uncertain clast**

Table 4.12 - Key to counted parameters (modified from Marsaglia, 1992, 1993, Critelli et al., 2002; Dickinson, 1970).

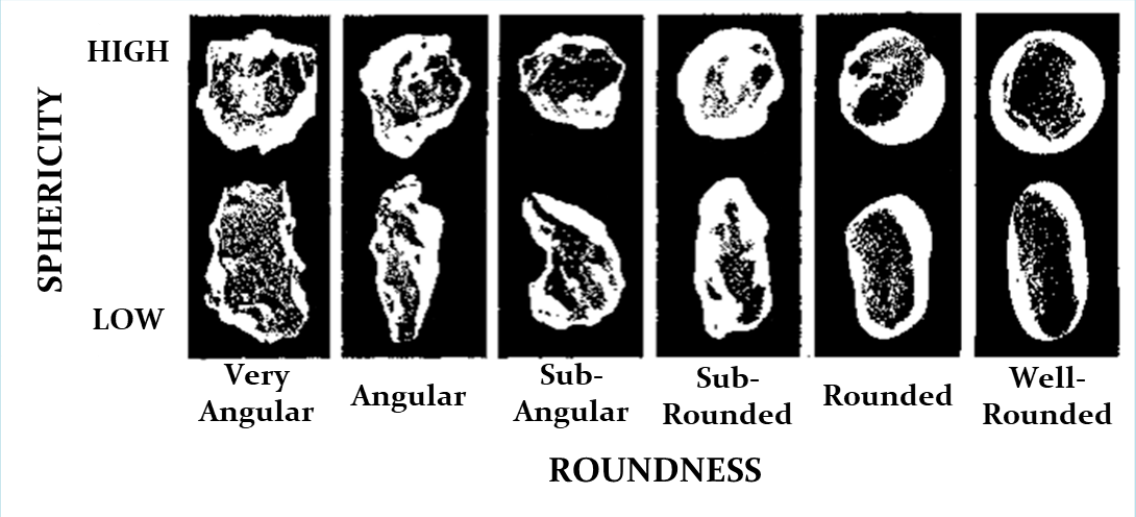

Figure 4.14 - Grain roundness and sphericity classes used as visual comparator during point counting (modified from Powers 1953).

Powers roundness class name	Corresponding Wadell (1933) class intervals	Corresponding values of Folk's rho scale (1955)
very angular	0,12 - 0,17	0,0 - 1,0
angular	0,17 - 0,25	1,0 - 2,0
sub-angular	0,25 - 0,35	2,0 - 3,0
sub-rounded	0,35 - 0,49	3,0 - 4,0
rounded	0,49 - 0,70	4,0 - 5,0
well rounded	0,70 - 1,00	5,0 - 6,0

Table 4 .13 – Degree of roundness class terminology and numerical indices. For this study was used the Folk's scale.

A numerical value was assigned to very angular (1), angular (2), sub-angular (3), sub-rounded (4), rounded (5), well-rounded (6) by following the Folk (1955) numerical indices related to degree of roundness classes (tab. 4.13, fig. 4.47). The mean roundness was calculated by using the modified McBride and Picard (1987) technique, for all grains, encountered at the cross-hair, during point-counting and not only for the firsts 30 (appendix A, C).

4.2.1 – Grain types and modal composition -

The major components of Aeolian islands and Campanian beach sands are monomineralic grains, sedimentary and volcanic lithic fragments with minor amounts of calcareous bioclasts (appendix A). Monomineralic grains in Aeolian islands beach samples are predominantly pyroxene, plagioclase, with minor olivine, hornblende,

opaque minerals, K-feldspar and quartz. Volcanic lithic fragments range in texture from lathwork to microlitic to vitric and felsitic varieties, whereas holocrystalline lithic volcanic grains are minor constituents (appendix A, from plate I to plate XIX).

Monomineralic components in Campania beaches sand samples are mostly plagioclase, pyroxene, k-feldspar with minor amount of leucite, nepheline, garnet, hornblende, opaque minerals and biotite (appendix A, from plate I to plate XIX). In the Bacoli-Volturno coastal stretch they consist mostly of quartz, plagioclase, calcite and k-feldspar, with except of some placer (e.g. BC-2. VO-2, VO-6) constitute mainly of pyroxene, opaque minerals and lesser garnet, olivine (paragraph 4.2.1.2). Lithics are subdivided in two main categories: volcanic lithic fragments, which range in texture from lathwork to microlitic to vitric and felsitic varieties, and sedimentary lithics which are Lss (with siliciclastic composition), and sedimentary lithic fragments with crystalline ($Lsc_{(xx)}$) and micritic ($Lsc_{(micr)}$) carbonate composition (appendix A, from plate I to plate XIX).

4.2.1A - VOLCANIC LITHIC FRAGMENTS -

Varieties of volcanic lithic fragments in both studied beach sand include, in order of decreasing abundance, lathwork, microlitic, vitric, felsitic and holocrystalline categories. In addition, the first three categories were divided according to glass color and texture of their glassy groundmass as observed in plane-polarized light and in some cases observed also through electron microprobe. Glassy groundmass of the lithic fragments was divided into black, brown, orange, grey, colorless and altered varieties (appendix A, from plate I to plate XIX). These subdivisions of detrital volcanic glass provide a direct means of assessing magmatic affinities of the source terrane (e.g., Cawood, 1991) and also because glass color is thought to be a function of composition and cooling rate (e.g., Schmincke, 1981; Marsaglia, 1992; 1993).

Lathwork [Lvl] volcanic lithic fragments are glassy fragments that contain variable amounts of plagioclase, pyroxene, olivine, opaque minerals, k-feldspar, leucite and nepheline as sand-sized microlites/phenocrysts (appendix A, from plate I to plate XIX).

Microlitic [Lvmi] volcanic lithic fragments contain variable amounts of microlites of feldspar and ferromagnesian minerals visible at high magnification. These microlites are primarily silt-sized plagioclase, pyroxene, olivine, k-feldspar and leucite crystals (appendix A, from plate I to plate XIX).

Vitric [Lvv] lithic fragments are characterized by their lack of microlites. They

exhibit variable morphologies and different glass colors from brown [Lvvbrgl], to black [Lvvblgl], to orange [Lvvorgl], to grey/dark grey [Lvvgrgl], to colorless [Lvvclgl]. Moreover, pumice grains have been found in some sand samples (especially in the Phlegrean fields area) (appendix A, from plate I to plate XIX).

Felsitic [Lvf] volcanic lithic fragments contain dominantly feldspars and quartz and include two types: granular felsitic and seriate felsitic (appendix A, plate II $_{(c, d)}$).

Clasts in the "other volcanic lithic category" [Lvo, (appendix A)], as in other arc systems (e.g., Marsaglia, 1993), constitute only a few percent of the grains in the sand of Aeolian islands beaches. They include holocrystalline aggregates of: (1) plagioclase and opaque minerals, (2) opaque minerals and pyroxene, (3) pyroxene and plagioclase, and (4) pyroxene, plagioclase and opaque minerals.

4.2.1B - MINOR CONSTITUENTS -

Minor constituent grains (table 4.12) found in some samples include: (1) some micritic beachrock calcite cement; (2) metamorphic lithic fragments which have an higher amount in Volturno-Licola coastal stretch; (3) plutonic lithic fragments; (4) various xenoliths; (5) muscovite; (6) grains of zeolite that could be hydrothermal alteration phases (e.g., those associated with the Mount Guardia eruption; De Rosa & Sheridan, 1983); and (7) grains of titanite, rutile and tourmaline.

4.2.1.1 – Aeolian Islands –

4.2.1.1A - MONOMINERALIC COMPONENTS -

Quartz, k-feldspar and especially plagioclase are much more abundant in the fine sand fractions than in the medium sand fractions (appendix A, B). Quartz and K-feldspar occur mainly as sand-sized phenocrysts set in lithic grains exhibiting felsitic textures (e.g. plate II $_{(c, d)}$), plate IV $_{(a, b)}$). However, they occur, to a lesser extent, as monocrystalline quartz, and individual monocrystalline grains of angular to sub-rounded sanidine (appendix A).

Plagioclase grains range from unaltered to slightly altered to sericite, and very few grains show argillification processes such as grain coatings (James *et al.* 1981). Individual monocrystalline plagioclase grains are poorly or not rounded (see paragraphs below), and commonly they are euhedral and zoned suggesting a provenance from a specific volcanic lithotype or source rock (e.g., Pittman, 1970; Dickinson, 1970; Zuffa, 1987). Albite twinning is more evident in very coarse, coarse and medium sand grains, whereas in finer plagioclase grains these features are lost probably because of

mechanical breakage along cleavage or twin planes (Pittman, 1969; Garzanti, 1986; Caracciolo et al. 2012).

Monomineralic pyroxene grains, and/or sand-sized pyroxene crystals in volcanic lithic grains, are generally preserved unaltered in the sandy detritus (e.g. plate $I_{(a, b)}$). Despite their occurrence as detrital grains, the individual monocrystalline grains of pyroxene and olivine retain a crystalline morphology, or habit, inherited from the volcanic source rock. Opaque minerals grains occur as local concentrations in some beach samples and generally increasing from medium to very fine sand fraction. Opaque dense minerals were grouped into one category (appendix A) because reflected light microscopy is not sufficient to discriminate among magnetite, ilmenite, pyrite and hematite, and among their intergrown phases and textures. Electron microprobe analysis aimed at geochemical discrimination (i.e., Basu and Molinaroli, 1989; 1991; Andò and Garzanti, 2012) have been used for the Campanian province where deposits of placer occur with a greater frequency (see paragraphs below).

4.2.1B – MODAL COMPOSITION –

On the basis of the data presented in appendix A, and the compositional parameters showed in Table 4.12, Qt:F:L, single-crystals vs. lithics, Lvl:Lvmi:Lvv, Lvf:Lvmi:Lvl, Lvvclgl:Lvvblgl:Lvvbrgl, and VFR:ACC:PLG percentages were calculated for all the analyzed samples (appendix A, B). Besides differences in the source rocks, modal analysis of studied beach sands shows a uniform composition characterized by trace amounts of quartz, moderate to low feldspar, mainly plagioclase, and dominant volcanic rock fragments, as emphasized on a Qt:F:L plot (fig. 4.15). In particular, all the Aeolian Islands beach sand samples plot along the L–F tie, toward the L apex, although the *Gazzi–Dickinson* method of point counting was used in this study to minimize the effects of grain-size, the diagram shows an inherent relationship between grain-size and the considered detrital modes (figs. 4.15, 4.16, 4.17, 4.18, 4.21, 4.22, 4.28e, 4.29).

The coarser sand samples are more lithic-rich than the finer sand samples, and there is a shift toward more feldspathic compositions with decreasing grain-size (fig. 4.15).

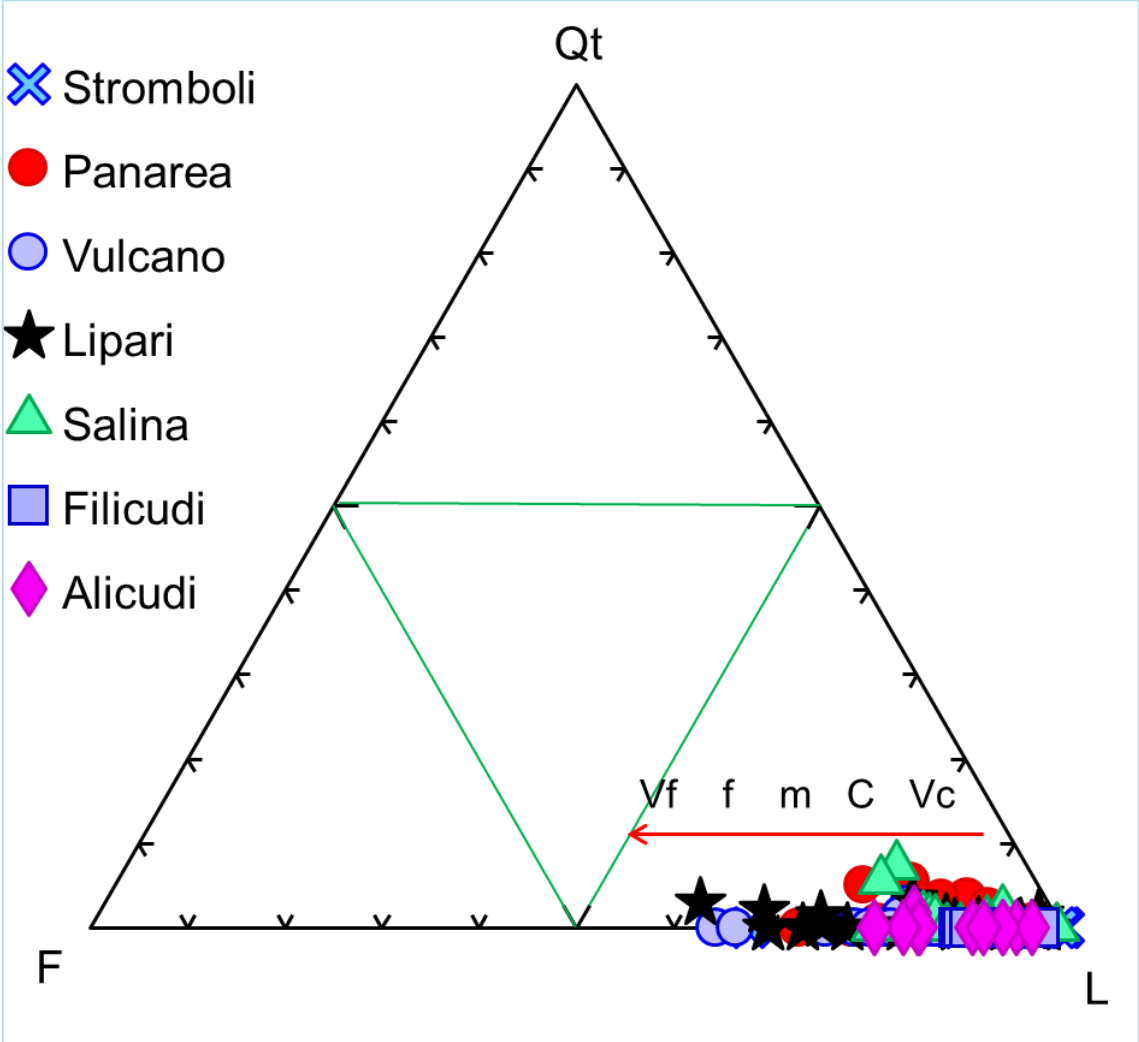

Figure 4.15 - Qt:F:L diagram. Qt: total quartz (monocrystalline + polycrystalline quartz); F: feldspars; L: all lithics.

Figures 4.16 and 4.17 show that all medium sand samples are lithic-rich (with only three exceptions, STR-2 [placer], L7, V12 samples). Composite lithic grains are 1,0 (V1) to 32 times (L13) more abundant than grains occurring as monocrystals. This lower monocrystal content in respect to the higher polycrystalline lithic grains in the medium sand of Aeolian Islands suggests that abrasion instead of mechanical breakdown played a main role in the comminution of grains. Textural immaturity of sandy detritus is consistent with such an active volcanic arc (Favalli et al., 2005). Whereas, in the finer sand (fig. 4.17 b, d) there is a slight trend which evidences a single-crystals increasing. In this regard we investigated more thoroughly among the five sand fractions doing a test on six samples (fig. 4.18). Within all the beach sands, there is always an increasing of single crystals and a decreasing of lithic grains from very coarse to very fine sand fraction (fig. 4.18).

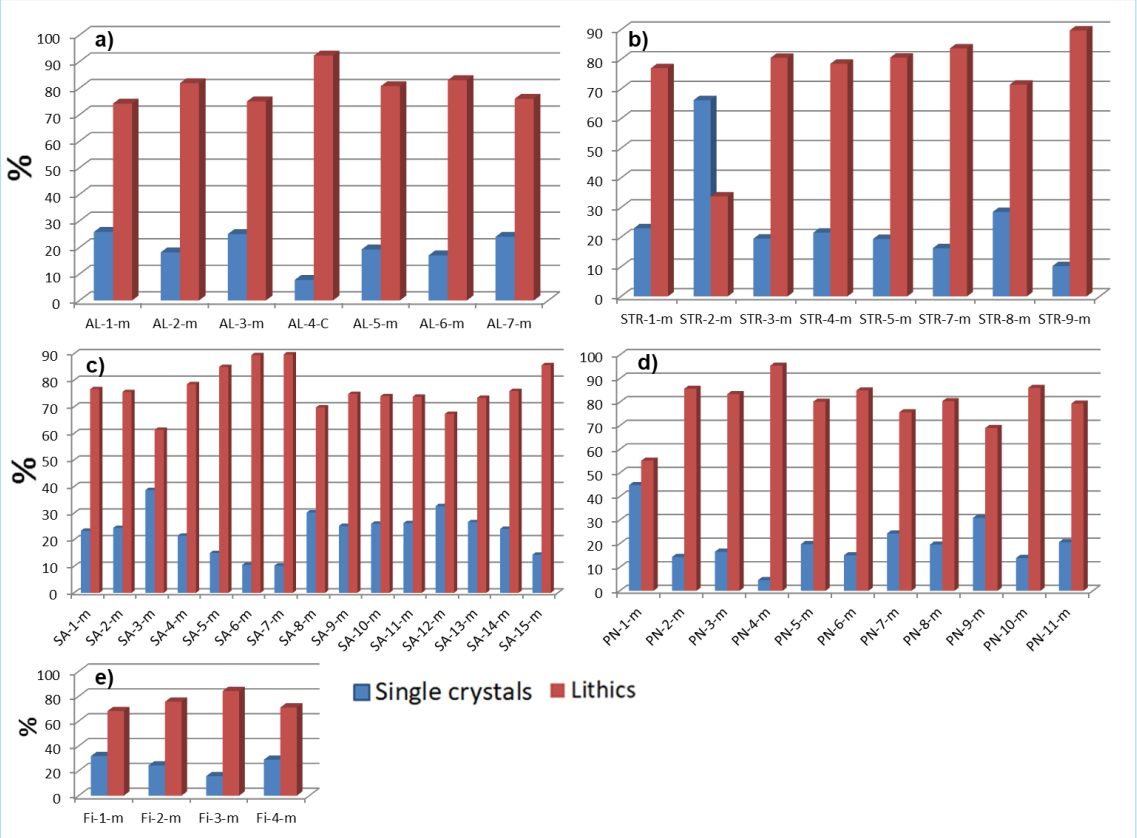

Figure 4.16 – Single crystals vs. volcanic lithic grains in the medium sand fraction. a) Alicudi, (b) Stromboli, (c) Salina, (d) Panarea, (e) Filicudi islands sand samples. m= medium.

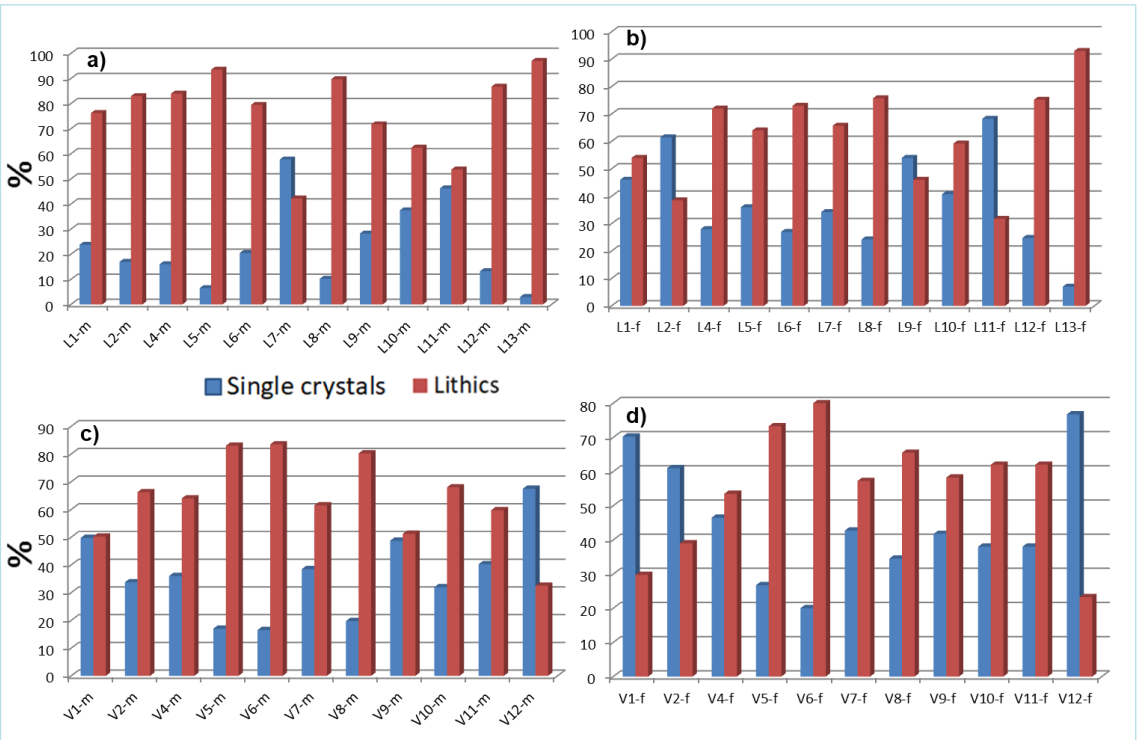

Figure 4.17 – Single crystals vs. lithic grains in the medium (a, c) and fine sand fractions (b, d). Lipari (a, b) and (b, c) Vulcano islands sand samples. m= medium; f= fine. Lipari data are from Morrone et al., 2018.

In PN-1 sample (fig. 4.18a) single-crystals range from 14% to 52% from very coarse to very fine sand fraction respectively, whereas lithics range from 86% to 48% from very coarse to very fine sand fraction respectively. In SA-1 this trend is even more pronounced (fig. 4.18b), in fact single-crystals range from 0% to 68% from very coarse to very fine sand fraction respectively, whereas lithics range from 100% to 32% from very coarse to very fine sand fraction respectively. In Alicudi and especially in Filicudi sand sample this trend is lesser evident (fig. 4.18 c, d).

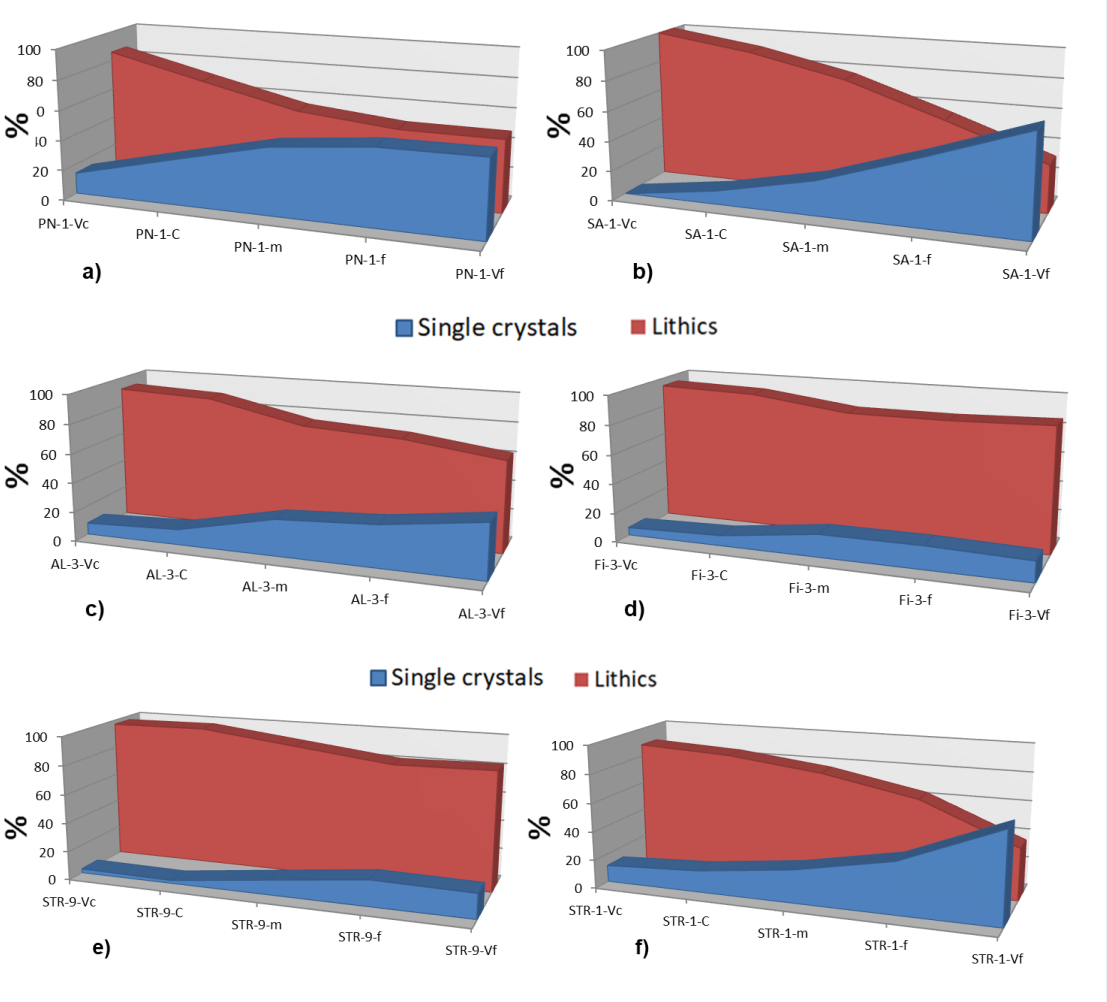

Figure 4.18 – Single crystals vs. lithic grains among the five sand fractions. a) Panarea; b) Salina; c) Alicudi; d) Filicudi; e) Stromboli crater sand; f) Stromboli beach sand.

An interesting information could be caught from Stromboli samples, collected along a transect from crater (STR-9) to beach sand (STR-1). In figure 4.18 (e, f) is shown the same trend of the others samples (fig. 4.18,a,b,c,d,) but is more pronounced. In the crater sand the single-crystals trend goes from 3% to 17% from very coarse to very fine sand, for lithics it goes from 97% to 83%, whereas in the beach sand there is a strong

single-crystals increasing (from 12% to 64%) and a strong lithics decreasing (from 88% to 36%) from very coarse to very fine sand fraction respectively. These high percentages change are probably related to mechanical breakage due to high transport energy (by stream) despite the short distance from crater to the beach. "Immature" grains (polycrystalline grains) such as lithics become single-crystals grains through mechanical breakage after transportation. The maximum length of stream transportation on Stromboli island is fairly short (3-3.5 km, fig. 4.19).

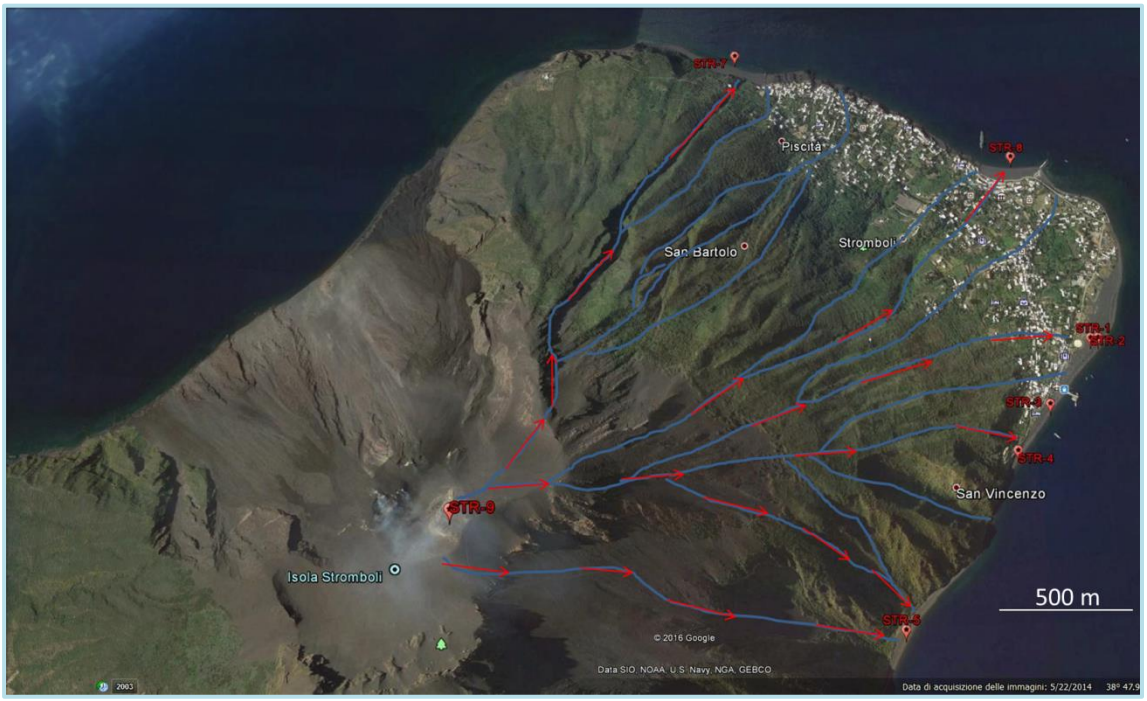

Figure 4.19 – Main Stromboli streams from craters to beaches (torrential transport). High relief, it goes from 924 to 0 m.a.s.l. in short distances (about < 1.7 km minimum and < 3,5 km maximum).

Figure 4.20 shows the relative proportion of main lithic types such as metamorphic, sedimentary and volcanic lithics (*Lm:Ls:Lv)* among all the Aeolian islands sand samples. All samples have a *Lv* percentage above 90% with exception of L13 which has 73% of *Lv*. According to Marsaglia and Ingersoll (1992) Aeolian samples are classified as "remnant, intra-oceanic and continental arc".

In the following section, modal composition results have been analyzed in terms of lithic textures (e.g. Marsaglia 1992; 1993; Critelli et al., 2002) through the ternary of figure 4.21a. showing the relative proportion of volcanic lithic with lathwork, microlitic and vitric textures (*Lvl:Lvmi:Lvv*) in the medium sand fraction. Almost all samples are dominated by the following trend: Lvl>Lvmi>Lvv with few exceptions regarding Lipari and Panarea samples.

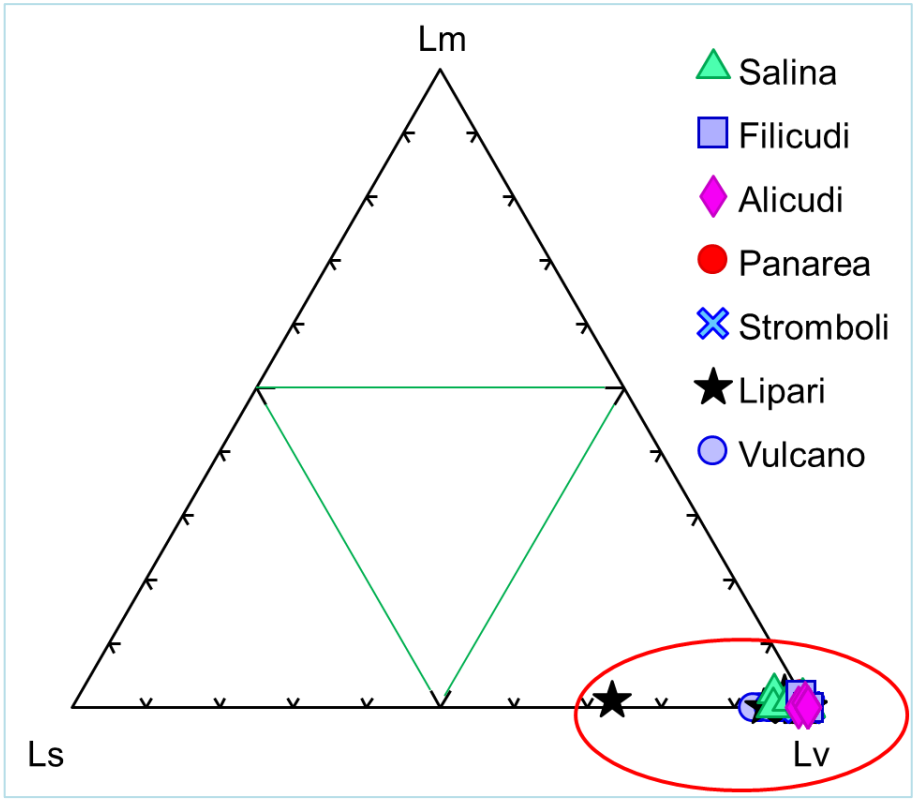

Figure 4.20 – Ternary plot of relative proportions of Lm:Ls:Lv. Lm: metamorphic lithics; Ls: sedimentary lithics; Lv: volcanic lithics (modified from Marsaglia and Ingersoll, 1992).

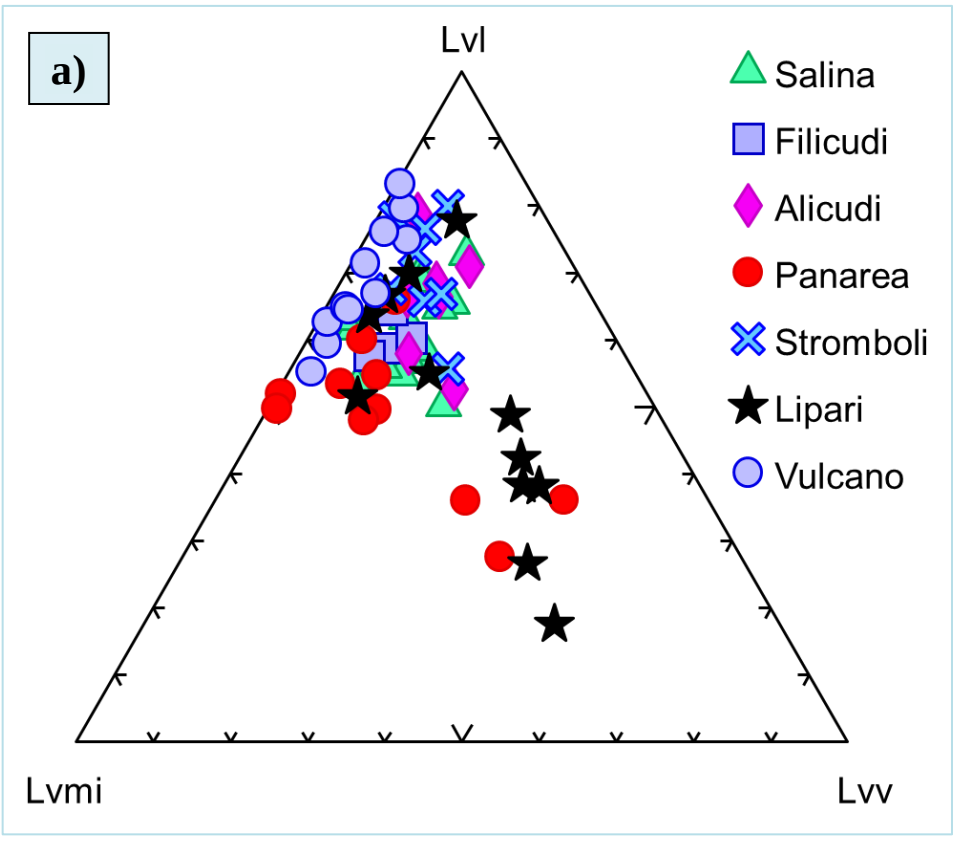

Figure 4.21a – Ternary plot of relative proportions of Lvl:Lvmi:Lvv. Lvl: lathwork texture; Lvmi: microlitic texture; Lvv: vitric texture. Lipari data are from Morrone et al., 2017.

This behavior can be explained considering the greater amount of "evolved" source rocks which range in composition from dacite to rhyolite occurring in both islands supplying an higher amount of volcanic lithic with vitric composition (e.g. Marsaglia and Ingersoll, 1992; Critelli et al., 2002; Morrone et al., 2017). In the medium sands Lvl is the dominant widespread texture, whereas (if we look at figure 4.21b which shows the relative proportion of Lvl:Lvmi:Lvv regarding five test samples on the five sand fractions) Lvl decreases from very coarse sand to very fine sand. This suggests that the Lvl strongly depend of the grain size. There is an interesting "breakage" trend that shows the increase of Lvl grains from very fine to very coarse sand fractions.

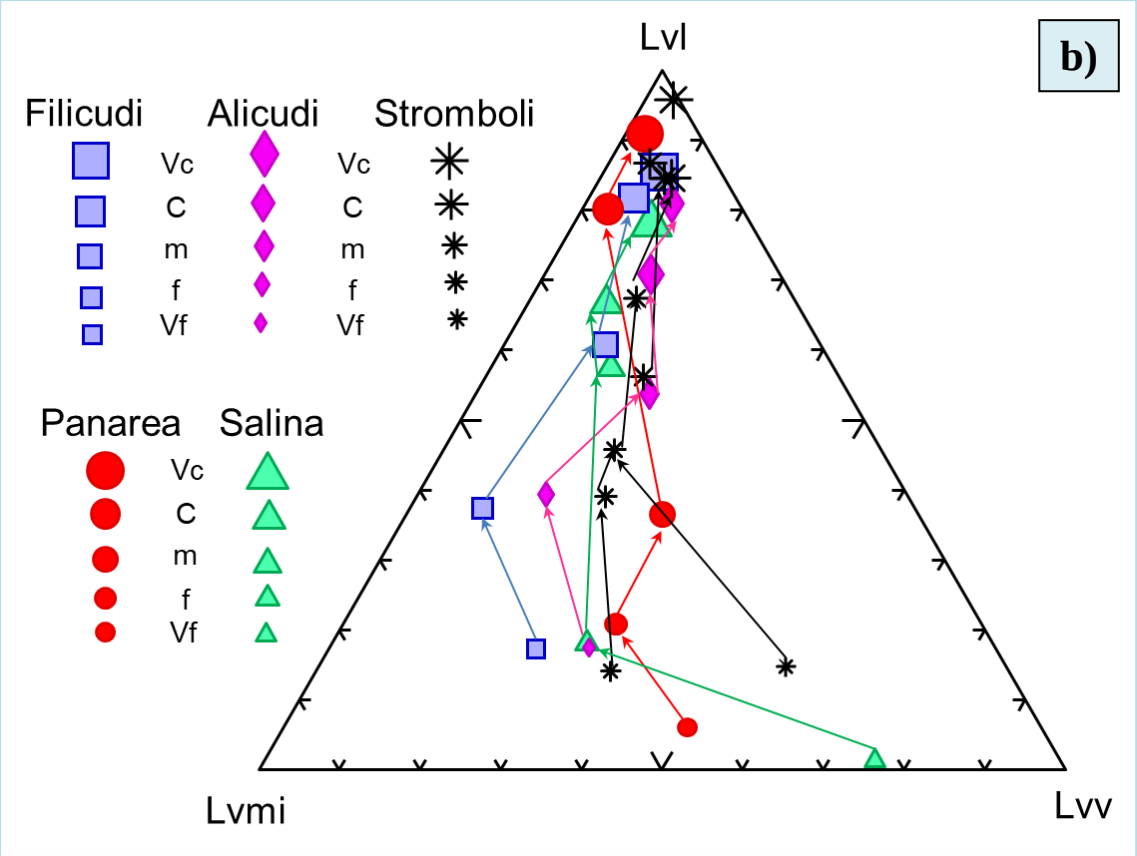

Figure 4.21b – Grain-size vs. volcanic lithic texture. Vc: very coarse sand; C: coarse sand; m: medium sand; f: fine sand; Vf: very fine sand.

The Filicudi, Alicudi, Stromboli, Salina and Vulcano samples lie on Lvl-Lvmi side, whereas Lipari and Panarea samples fall in a different field because of their higher felsitic fragment (Lvf) content recording a provenance from a more evolved lavas (fig. 4.22). Finer sands are shifted from Lvl towards Lvmi apex, this confirm that sand composition is strongly influenced by grain-size (despite Gazzi-Dickinson method was used) both in terms of lithics (among different textures) and single-crystals vs. lithics (figs. 4.16, 4.17, 4.18, 4.21, 4.22) contents.

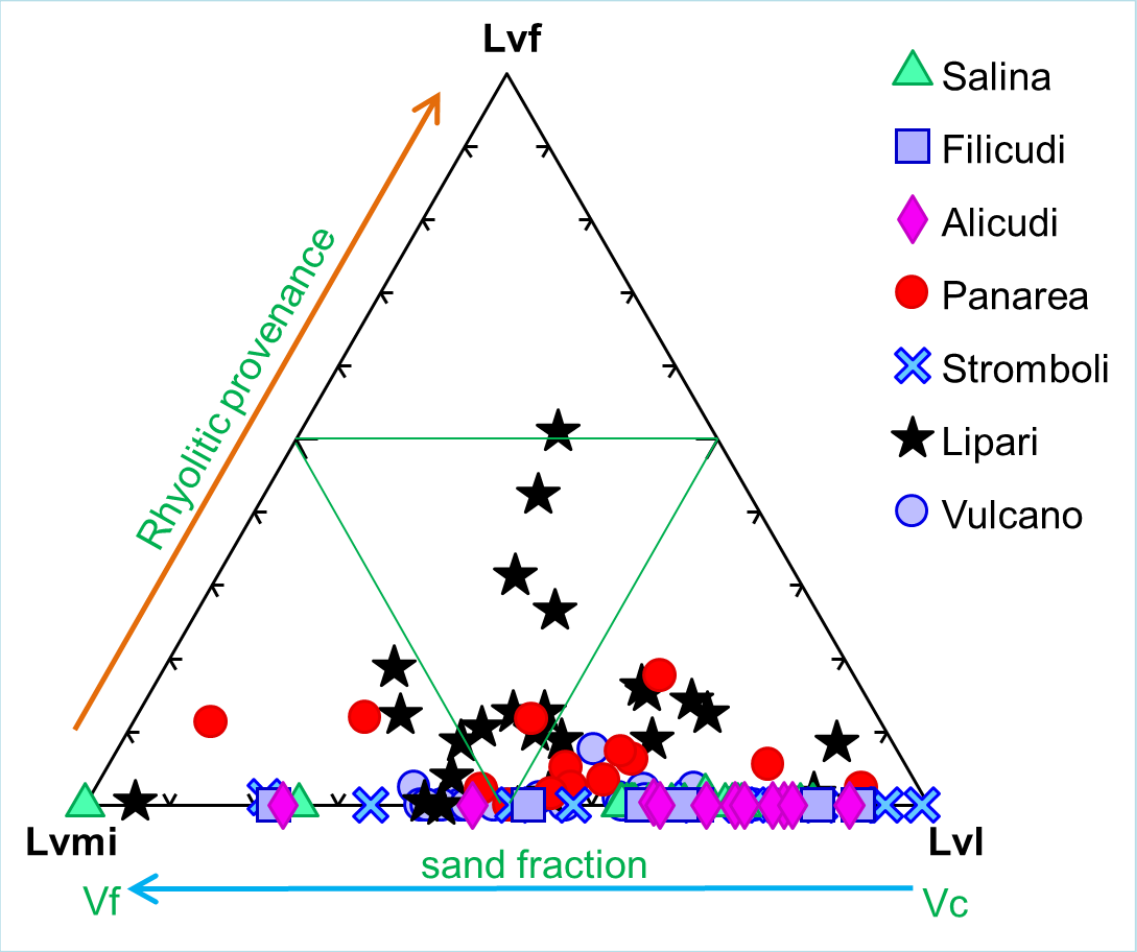

Figure 4.22 – Ternary plot of relative proportions of Lvf:Lvmi:Lvl. Lvf: volcanic lithic with felsitic texture; Lvmi: microlitic texture; Lvl: lathwork texture; Lipari data are from Morrone et al., 2017.

Figure 4.23 shows the relative proportion vitric texture fragments (*Lvv*) of different color (black, brown, colorless) occurring in the medium sand fraction. Only for Lipari and Vulcano islands also the fine sand fraction has been considered. All the five sand fractions were used for selected samples among all islands (Appendix A, B). We observe that Alicudi and Filicudi samples are equally distributed between Lvvblgl and Lvvbrgl apexes. Vulcano and Stromboli sands are constitute mainly by black glass (*Lvvblgl*) and lesser amount of brown glass (*Lvvbrgl*) with almost zero percentage of colorless glass (*Lvvclgl*). Salina sand samples show an intermediate percentage between *Lvvblgl* and *Lvvbrgl* with several samples shifted towards *Lvvclgl* apex.

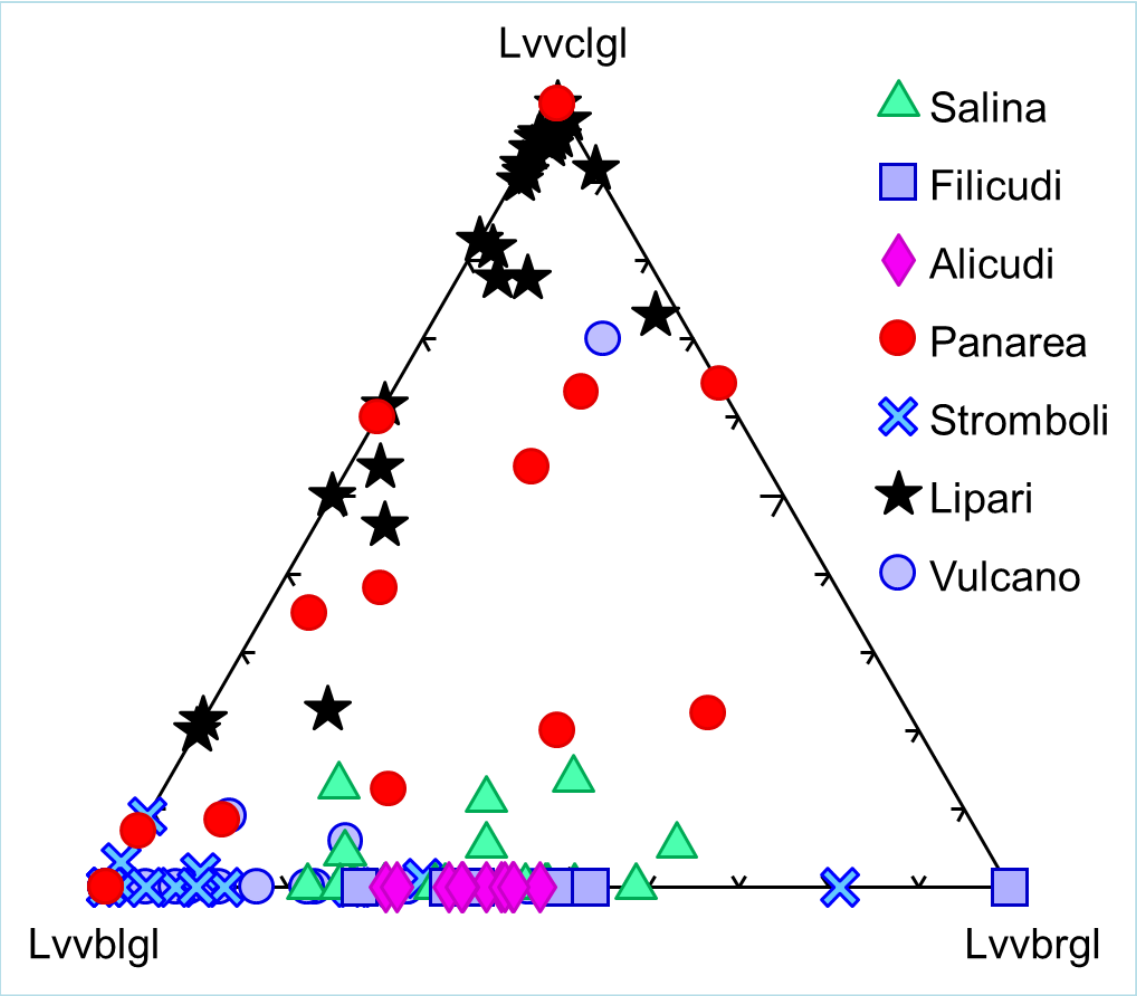

Figure 4.23 – Ternary plot of relative proportions of Lvvclgl:Lvvblgl:Lvvbrgl. Lvvclgl: vitric texture with colorless glass; Lvvblgl: vitric texture with black glass; Lvvbrgl: vitric texture with brown glass; Lipari data are from Morrone et al., 2017.

Panarea samples almost cover the inter ternary plot diagram showing an high percentage of *Lvvblgl* and *Lvvclgl* with lesser amount of *Lvvbrgl*. Lipari lacks or has very few brown glassy fragments, and contains a larger proportion of colorless and black glassy fragments (Morrone et al., 2017).

From literature data, lithics with lathwork texture (*Lvl*) are associated with basalts and basaltic andesites source rocks, volcanic lithics with microlitic texture (*Lvmi*) are associated to andesites and basaltic andesites, whereas those with vitric and felsitic texture (*Lvv*, *Lvf*) are linked to dacites and rhyolites source rocks (Dickinson, 1970; Marsaglia, 1992; 1993; Marsaglia and Ingersoll, 1992; Critelli et al., 2002; Morrone et al., 2017).

Moreover, we introduced new classification diagrams discriminating lithic fragments (lathwork and microlitic textures) by their groundmass color (fig. 4.24). This ternary plot better shows the differences between the source rocks feeding the Aeolian islands

beach sands. The proposed diagrams allow to distinguish among different volcanic products using only the optical microscope by studying in details the volcanic lithic fragments and then allow to determine the provenance.

We distinguished a new lithic grain type among Aeolian Islands which dominate in the Panarea beach sands (and in lesser amount in Lipari). We introduced the *Lvlgrgl+Lvmigrgl+Lvvgrgl* (tab 4.12, fig. 4.26, e.g. plate VIII (b, d)), for the dacitic *"signature"* provenance that was so far associated to *Lvf* texture.

The *Lvlgrgl+Lvmigrgl+Lvvgrgl* grain types were also investigated by electron microprobe in order to determine their geochemical compositions (figs. 4.26, 4.27). These grains are defined by crystals of feldspar, quartz, orthopyroxene and clinopyroxene settled in a glassy grey-colored groundmass (porphyric texture) and/or only aphyric glassy grey-coloured glassy fragment (Lvvgrgl → vitric texture) (figs. 4.26, 4.27).

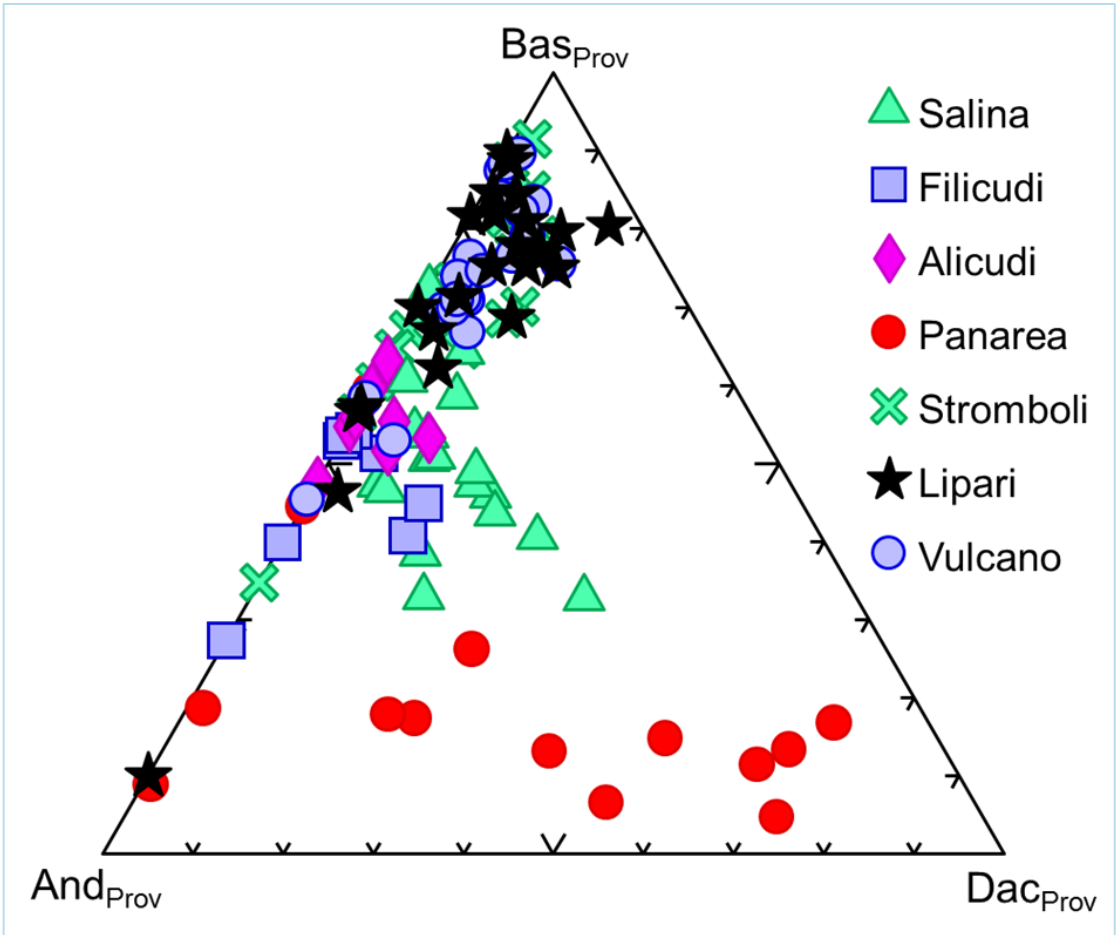

Figure 4.24 – Ternary plot of relative proportions of Bas_{Prov}:And_{Prov}:Dac_{Prov}. Bas_{Prov}= Lvlblgl+Lvmiblgl; And_{Prov}= Lvlbrgl+Lvmibrgl; Dac_{Prov}= Lvlgrgl+Lvmigrgl.

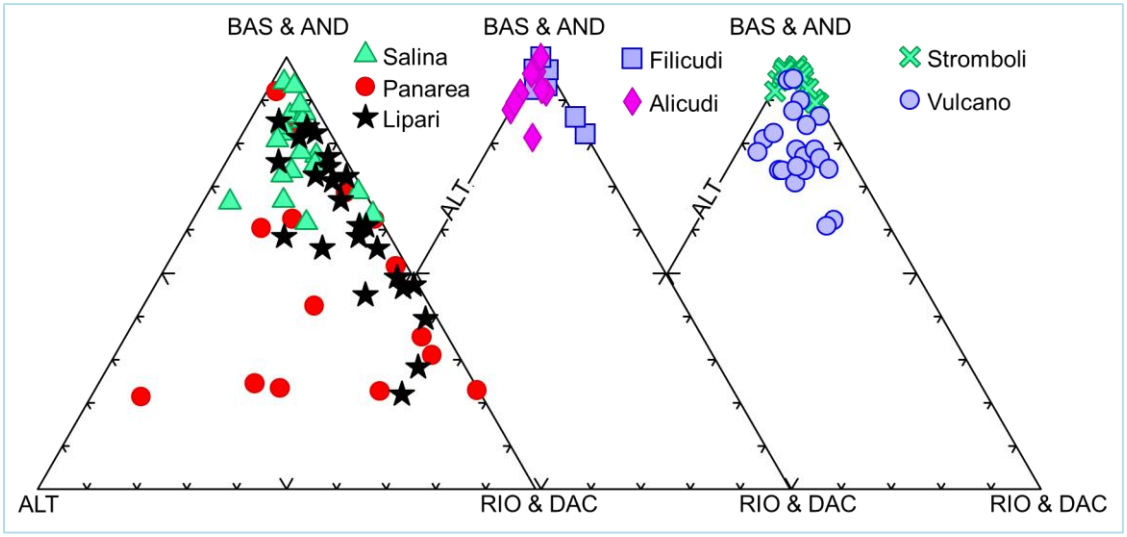

Figure 4.25 – Ternary plot of relative proportions of BAS & AND:ALT/SUB:RIO & DAC. BAS & AND= Lvlblgl + Lvmiblgl + Lvvbl + Lvlbrgl + Lvmibrgl + Lvvbrgl; ALT/SUB= Lvlorgl + Lvmiorgl + Lvvorgl +Lvlalgl + Lvmialgl + Lvvalgl; RIO & DAC = Lvlgrgl + Lvmigrgl + Lvvgrgl + Lvlclgl + Lvmiclgl + Lvvclgl. al: altered glass in clay minerals and/or palagonite.

Stromboli, Alicudi and Filicudi sands are lithic-rich with detrital grains having a dual basaltic and andesitic siliciclastic supply from effusive source rocks (figures 4.24 and 4.25). Panarea, Lipari and Salina sands are lithic-rich too, but they have a wider range of composition "*signatures*", namely from basalt (lesser amount), to → andesite → dacite → rhyolite. Moreover, figure 4.25 also shown the degree of alteration of the volcanic lithic grains. Panarea, Lipari, Salina and Vulcano samples result more altered than Stromboli, Alicudi and Filicudi samples most likely because of the higher hydrothermal activity occurring on these islands.

Figure 4.28a shows that the groundmass color of the lithic fragments (lathwork and microlitic textures) can be useful to discriminated between Panarea and Stromboli provenance. Stromboli sands are lithic-rich with detrital grains having a dual basaltic and andesitic siliciclastic supply from effusive source rocks. Panarea sands are lithic-rich but have a wider range of composition "signatures" with respect to Stromboli sands, and namely from basalt (lesser amount), and andesites to dacitic.

Figure 4.28b shows the detritus composition vs. age of source rocks of Panarea island. The S. Nave→ P. Muzza→ Lisca bianca→ Dattilo→ Drautto and Calcara→ Porto→ Zimmari →Drautto trends, show that the older products are more evolved (e.g dacites→ Lvlgrlgl+Lvmigrlgl+Lvvgrgl) and became more basic with time. PN-1 sample shows that there is no relation between grain-size and colour ground mass.

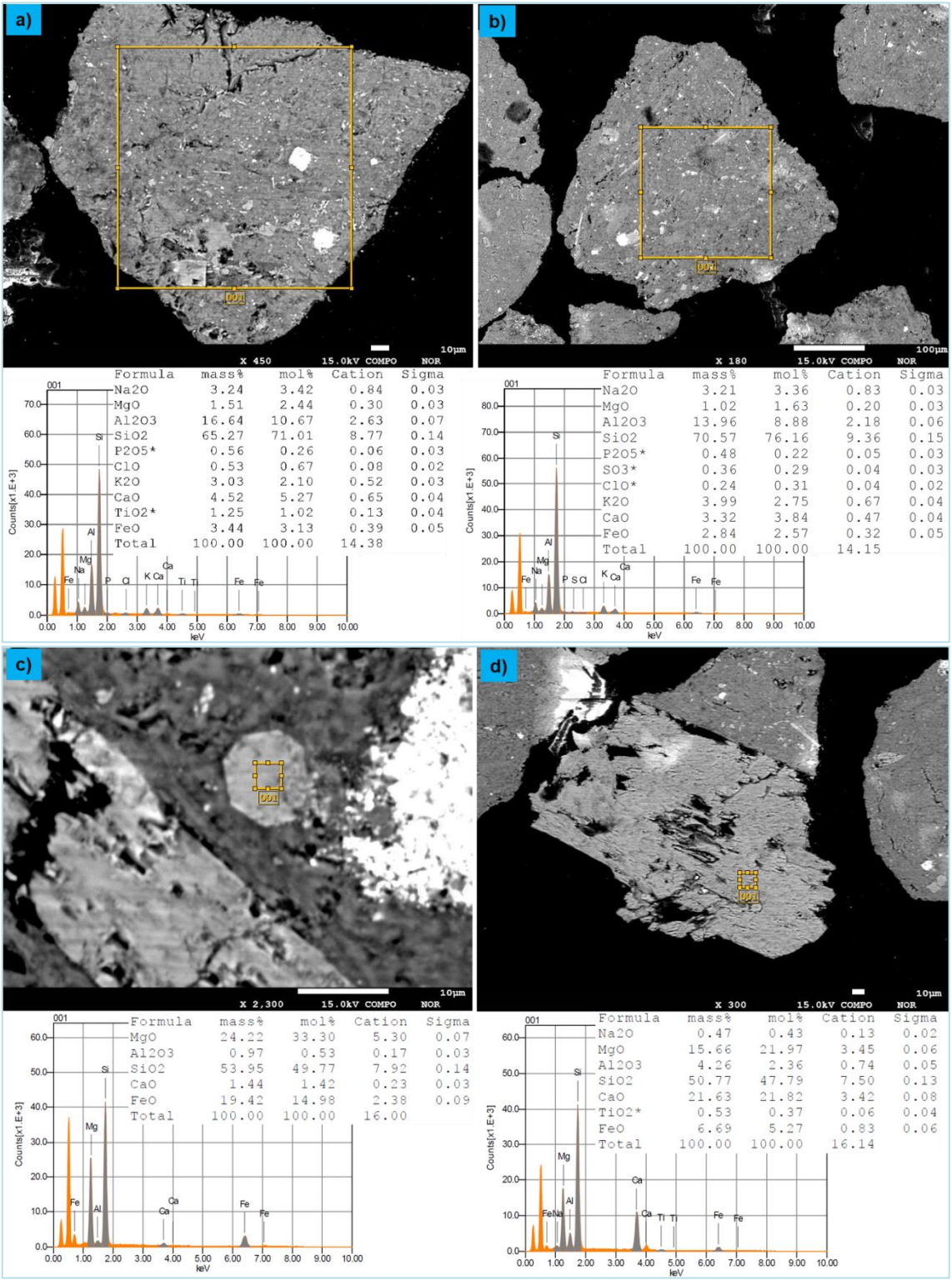

Figure 4.26 – Electron microprobe analyses of some grains found among Aeolian Islands beach sands. a) volcanic lithic grain having dacitic composition (SiO_2= 65.27; Na_2O+K_2O= 6.27) corresponding to a Lvmigrgl texture; b) volcanic lithic grain having dacitic composition (SiO_2= 70.57; Na_2O+K_2O= 7.20) corresponding to a Lvlgrgl texture; c) Enstatite basal section immersed in a glassy groundmass; d) Diopside single crystal in PN-2 sand sample.

In figure 4.28d, Stromboli samples show that the zero order sand (crater sand) is richer in brown groundmass fragments than the black one, with respect to other samples. It seems

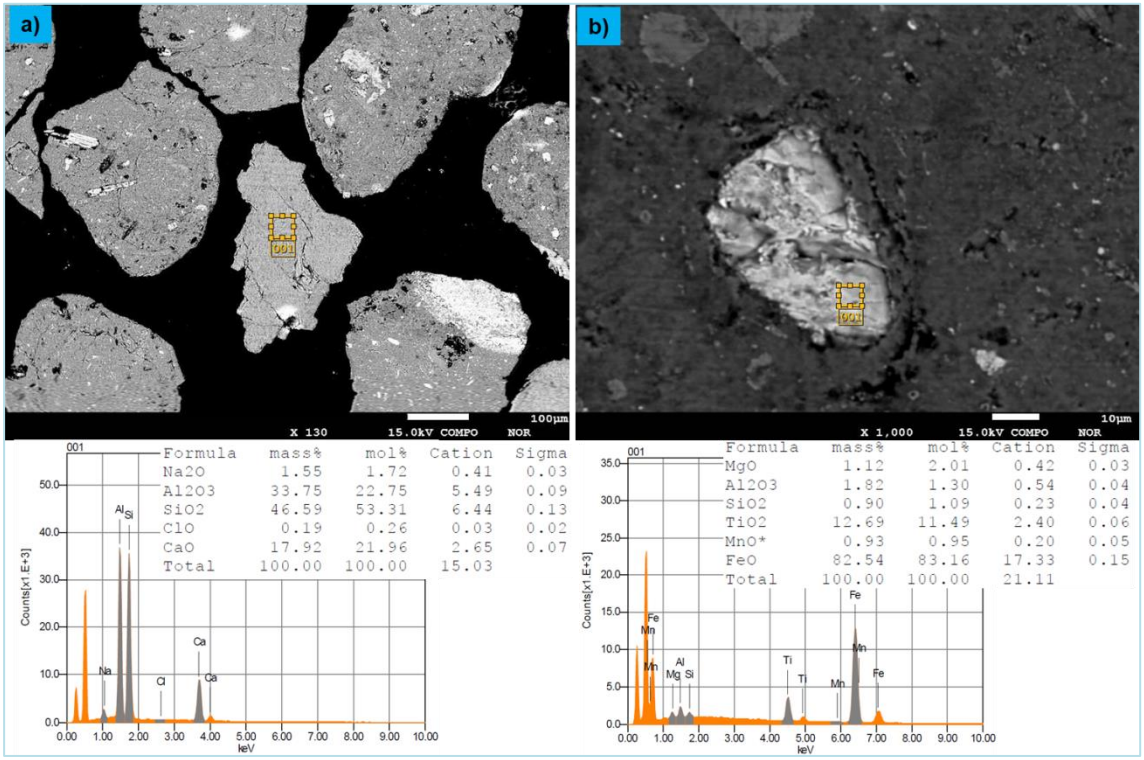

Figure 4.27 – Electron microprobe analyses of some grains found among Aeolian Islands beach sands. a) Bytownite/anortite single crystal diagnostic of calc-alkaline magmas; b) Fe-Ti oxide (ilmenite) immersed in a glassy groundmass.

that the crater sand (more recent) are slightly more evolved than the beach sand. Also in Stromboli samples the grain-size does not affect the groundmass composition (STR-1 and STR-9 trends).

In figure 4.29c Stromboli and Panarea islands are well discriminated according to the textures of vitric fragments (Lvvblgl, Lvvbrgl, Lvvorgl, Lvvalgl). Stromboli samples reflect their "basic nature" and are not altered, on the contrary Panarea samples are more evolved in composition and more altered. Dattilo (islet sample), Lisca Bianca (islet sample) and Calcara samples are much more altered due to their hydrothermal activity and sea water alteration.

The ternary plot in figure 4.29e refers to heavy mineral placer (light and opaque) represented by some Stromboli samples. It is clearly that STR-2 it is a rich dense minerals sample and STR-1-Vf is also rich in those minerals because of grain-size dependence (composition depends of grain-size); whereas STR-9 sample (crater sand) is lithic rich also in the very fine sand fraction because it does not suffered any transportation and/or mechanical breakage ("less mature detritus").

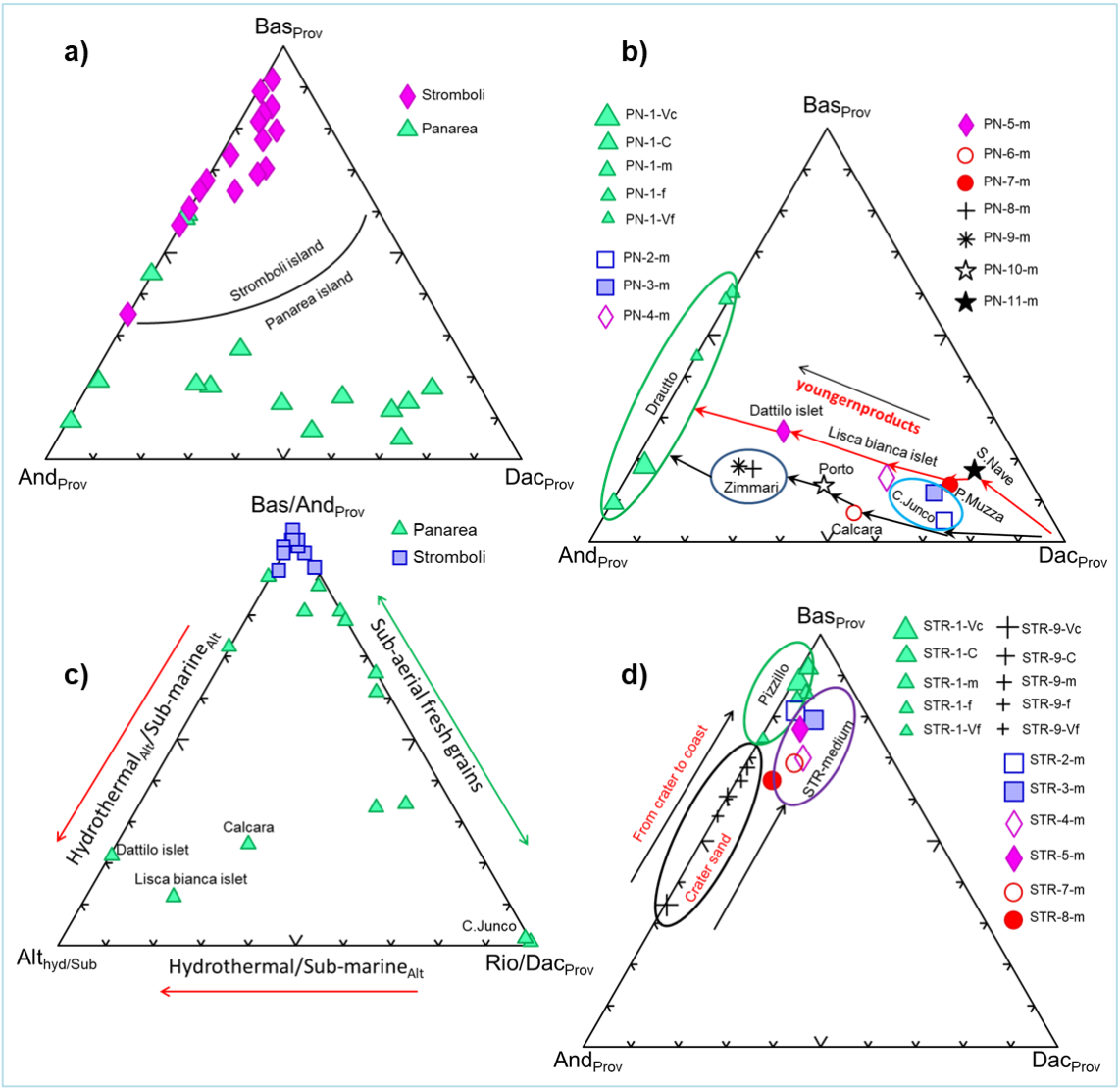

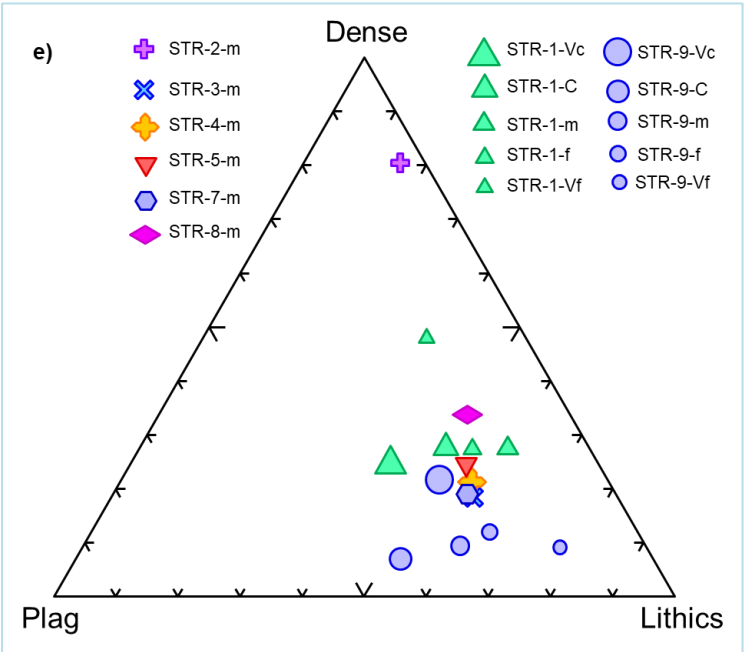

Figure 4.28 – a,b,d) ternary plot of relative proportions of BasProv:AndProv:DacProv. BasProv= Lvlblgl + Lvmiblgl; AndProv= Lvlbrgl + Lvmibrgl; DacProv= Lvlgrgl + Lvmigrgl. a) Panarea and Stronmboli samples are discriminated by islands. b) Panarea samples are discriminated by each other; d) Stromboli samples are discriminated by each other.; c) ternary plot of relative proportions of Bas/AndProv:Althyd/Sub: Rio/DacProv using only vitric textures. Bas/AndProv= Lvvblgl + Lvvbrgl; Althyd/Sub= Lvvalt + Lvvorgl; Rio/DacProv= Lvvclgl + Lvvgrgl. e) Ternary plot of relative proportions of Dense:Plag:Lithics. Dense= pyroxene, olivine, opaque and hornblende single grains; Plag= plagioclase single grains; Lithics= total volcanic lithics.

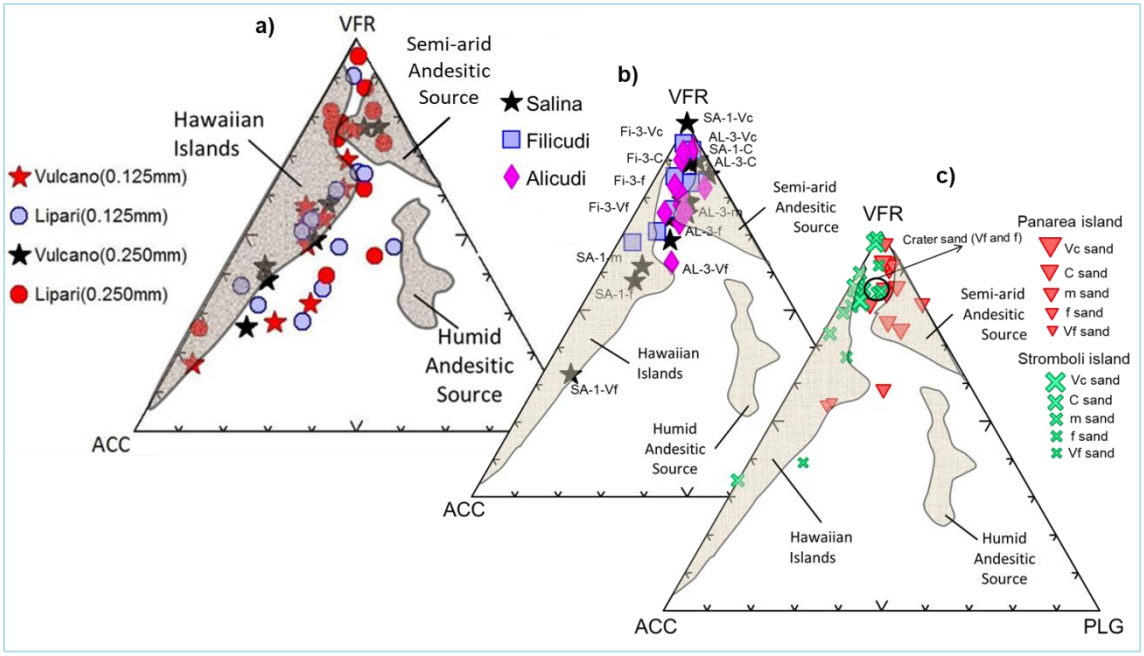

Figure 4.29 – Ternary plot of relative proportions of volcanic rock fragments with all texture typologies (VFR), accessory minerals (ACC – single grains of olivine, pyroxene, opaque) and plagioclase (PLG). Shadow areas for andesitic source are from Mack & Jerzykiewicz (1989); shadow areas from Hawaiian Islands are from Marsaglia (1993). Lipari data are from Morrone et al., 2017. a) Lipari and Vulcano islands beach sand samples (medium and fine sand fraction); b) Salina, Filicudi and Alicudi islands medium sand fraction (for SA-1, Fi-3, AL-3 samples were plotted the 5 sand fractions); c) Panarea and Stromboli islands sand samples.

On the whole, Lipari and Vulcano show an highly dispersed sand composition in a temperate Mediterranean climate. Monocrystalline grains are indicative of hydrodynamic sorting in beach environment (placers). Among Aeolian Islands, Stromboli is the island which is closer to the Hawaiian islands, whereas Panarea island is closer to andesitic source. Also in the ternary plot from Mack and Jerzykiewicz (1989), we can observe the grain-size dependence of the composition.

4.2.1.2 – Campanian province -

4.2.1.2A - MONOMINERALIC COMPONENTS AND LITHIC FRAGMENTS -

Quartz and feldspars are much more abundant in the finer sand fractions than in the coarser sand fractions (appendix A B; fig. 4.30). Quartz occurs as sand-sized phenocryst and set in sedimentary rock fragments (tab. 4.12, Q in Rs, Q in Ar) and lithic grains exhibiting felsitic and *Lvlgrgl* textures (plate II $_{(c, d)}$, plate II $_{(a, b, c, d)}$). It occurs mainly as monocrystalline and polycrystalline quartz increasing towards Volturno river mouth (appendix A; fig. 4.30; plate XI $_{(c, d, e, f)}$, plate XII $_{(a, b, e, f)}$, plate XV $_{(a, b)}$).

K-feldspar occurs mainly as monocrystalline grain of sanidine and lesser amount of orthoclase and microcline. It is lesser extent as phenocryst set in volcanic lithic texture and in sedimentary rock fragments (tab. 4.12; appendix A; fig. plate X (a, b), XIV (c, d),).

Plagioclase occurs as sand-sized phenocryst set in volcanic lithic fragments and as monocrystalline grain. It occurs as a fresh unaltered euhedral grain and sometimes is altered to sericite (appendix A; plate I (e, f), plate II (a, b), plate III (a, b), plate IV (a, b, e, f), plate V (c, d), VI (e, f), VIII (c, d), XVI (a, b)).

Pyroxene occurs often as a single grain but it occurs also as a sand-sized pyroxene crystals in volcanic lithic grains. They show sometime a glassy rim or intra-crystalline glass indicating their volcanic provenance (appendix A; plate I (a, b), plate II (e, f), plate VI (a, b, c, d, e, f), plate VIII (c, d), plate XVII (c, d, e, f), plate XIX (a, b)).

Leucite minerals are generally included in a volcanic lithic fragments and often occur as a preserved grain with its hexagonal habit (euhedral) and it is pseudo isotropic (appendix A; plate XII (c, d), plate XVI (e, f), plate XVIII (c, d), plate XIX (a, b)).

Among lithic fragments the most common are volcanic and sedimentary lithichs. The volcanic lithic fragments have been already explained in a previous paragraphs (4.2.1a). Sedimentary lithic fragments occur as a grains having crystalline carbonate composition ($Lsc_{(xx)}$), micritic carbonte composition ($Lsc_{(micr)}$) and siliciclastic composition (Lss) (tab. 4.12; appendix A; plate IX (c, d, e, f), plate XIII (c, d), plate XIV (c, d), plate XV (c, d)), plate XIV (e, f)).

Garnet mineral was found in two color varieties such as colourless and brown garnet. It occurs as a single grain and sometimes as phenocryst set in a lithic grains (plate XIV (e, f), plate XVII (c, d), plate XVIII (e, f)).

In this studied area we have better investigated on heavy minerals grains because many placer have been found. Thus, we investigated in the fine sand of some samples where there is a greater heavy minerals concentration including opaque minerals, pyroxenes, amphiboles, garnets, rutiles and tourmalines (see paragraph below).

4.2.1.2b – MODAL COMPOSITION -

By raw data processing showed in appendix A and B, we created several diagrams which allowed to define the modal composition of Campanian sand samples. Thus, were calculated the following relative proportions: Qt:F:L, single-crystals vs. lithics, Lm:Ls:Lv; Lvl:Lvmi:Lvv, Lvf:Lvmi:Lvl, Lvvclgl:Lvvblgl:Lvvbrgl, Bas_{Prov}:And_{Prov}:Dac_{Prov}, $Bas_{/}And_{Prov}$:$Alt_{hyd/Sub}$, Pm:Lvl:Lvmi and VFR:ACC:PLG, for medium sand and in some cases for the five sand fractions (appendix A, B). Modal

analysis of Campanian sand samples shows two main samples populations: Phlegrean Fields and Portici-Sorrento coastal stretch which is characterized by high lithic fragments percentage and moderate feldspars percentage (except SO-1 samples which shows an higher quartz percentage); PZ-8, PZ-14 and BC-1 samples have been analyzed among the five sand fractions, it is evident the grain-size dependence of the composition (single grains shifted towards quartz and feldspars apexes, fig. 4.30); other samples population regards the coastal stretch from Bacoli to Volturno river mouth (passing from Licola localities), which show a strong increasing in quartz (Qt) percentage (fig. 4.30).

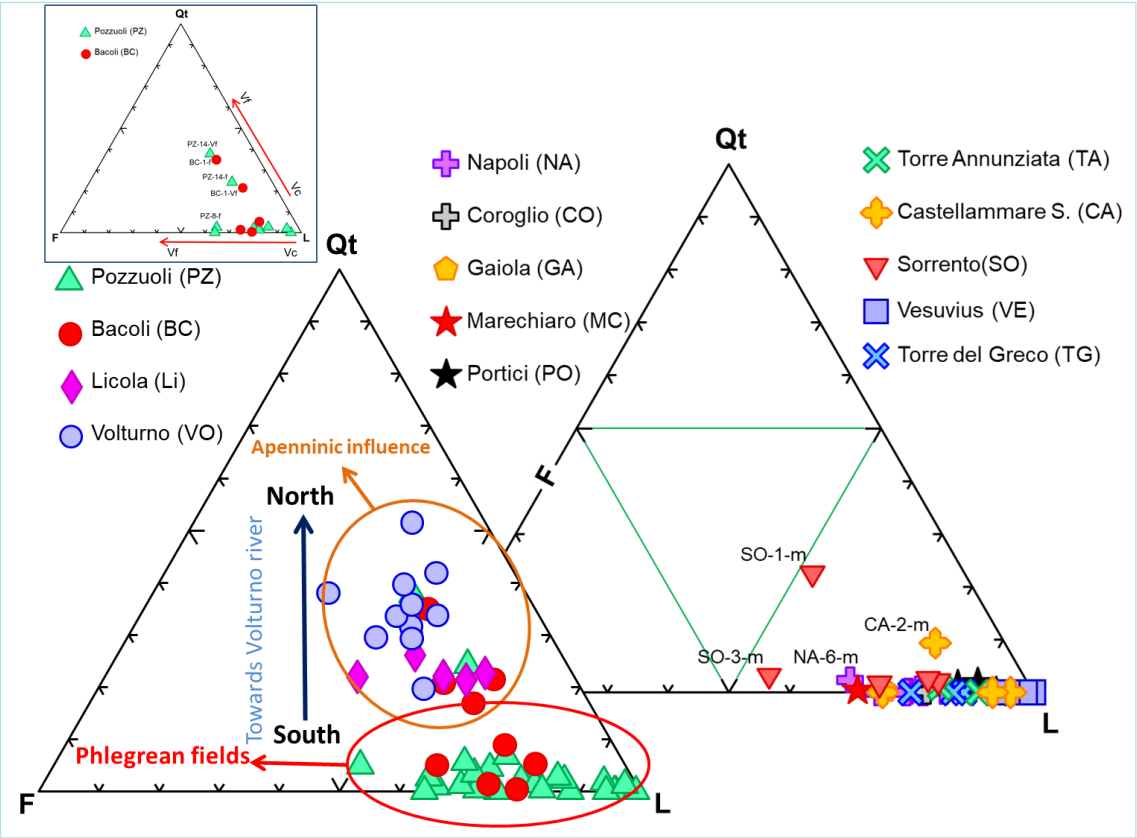

Figure 4.30 - Qt:F:L diagram (e.g. Dickinson, 1970). Qt: total quartz (monocrystalline + polycrystalline quartz); F: feldspars; L: all lithic fragments.

By comparing single crystals and lithic fragments, it was found out a significant trend which allow us to understand that the sand samples along Volturno-Bacoli coastal stretch are "mature" sands, they are constitute mainly by single crystal grains with lower percentage of lithic fragments (total lithic fragments). Going southward to Phlegrean Fields area, there is a single crystal grains decreasing and a lithic fragments increasing (mainly volcanic lithic fragments). Likewise by going away from Phlegrean Fields area towards Portici-Sorrento coastal stretch (southward), again there is to a

lesser extent, a lithic fragments decreasing and a single crystal grains increasing (fig. 4.31). All these probably means that being in the vicinity to the Volturno river mouth and in a wide open beaches, the strong reworking (wave and river high-energy) play a fundamental role in the mechanical breakage processes from coarser sediment (mainly lithic fragments) to finer sediment (mainly single crystals grain), even if this trend occurs also in the medium sand fraction along that coastal stretch. Whereas Pozzuoli bay is a more protected area with a lower-wave energy, in fact Pozzuoli samples show also an higher percentage of coarser sand with respect Volturno-Bacoli coastal stretch (see previous paragraphs) and going toward Sorrento there are again wider open beaches.

The histogram in figure 4.31h shows the zero order crater sands from Vesuvius volcano, which are obviously immature and lithic-rich and display an angular texture grains (see paragraphs below). Moreover, among the three crater samples, VE-3 which have been sampled few kilometers below (about 2 km) from the main crater, shows a slightly lithic fragments decreasing and a slightly single crystals increasing despite the short distance transport.

Along the trend (fig. 4.31, single crystals vs. lithichs) which goes from Volturno river mouth to Phlegrean fields area, there are few exception, namely VO-2, VO-6, BC-2, PZ-2, PZ-7, PZ-12 sand samples, because they resulted to be heavy minerals placer (see paragraph below 4.2.1.2c).

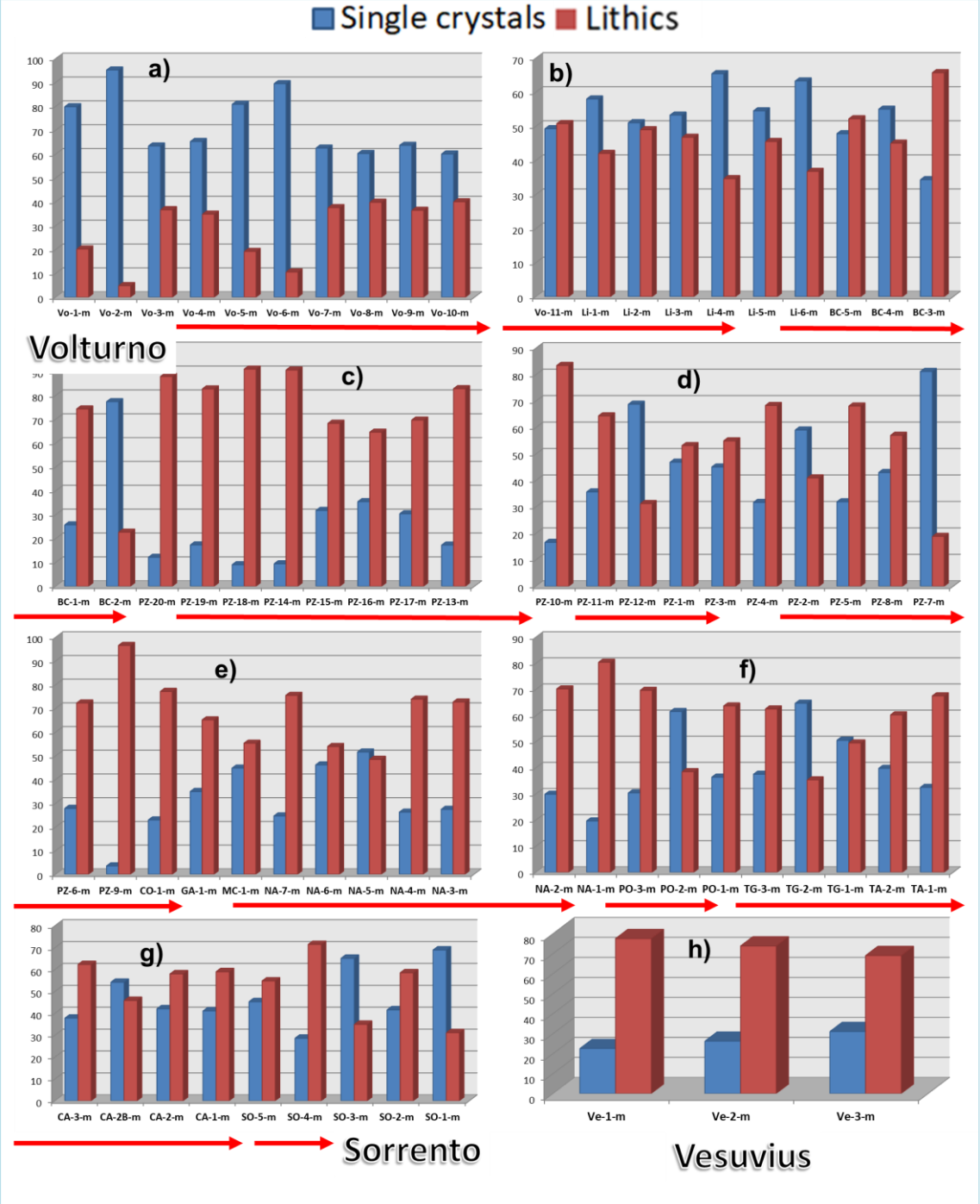

Figure 4.31 - Single crystals vs. lithic grains (% on y axis) in the medium sand fraction. The samples have been ordered from north (Volturno river mouth) to south (Sorrento) along Campania coastal stretch. a) from VO-1 to VO-10; b) from VO-11 to BC-3; c) from BC-1 to PZ-13; d) from PZ-10 to PZ-7; e) from PZ-6 to NA-3; f) from NA-2 to TA-1; g) from CA-3 to SO-1; h) Vesuvius craters samples.

In Campania beach sands as well as Aeolian beach sands, breakage trend occurs from very coarse to very fine sand fraction, there is a single crystals increasing and a lithic grains decreasing from very coarse to very fine sand fraction (fig. 4.32).

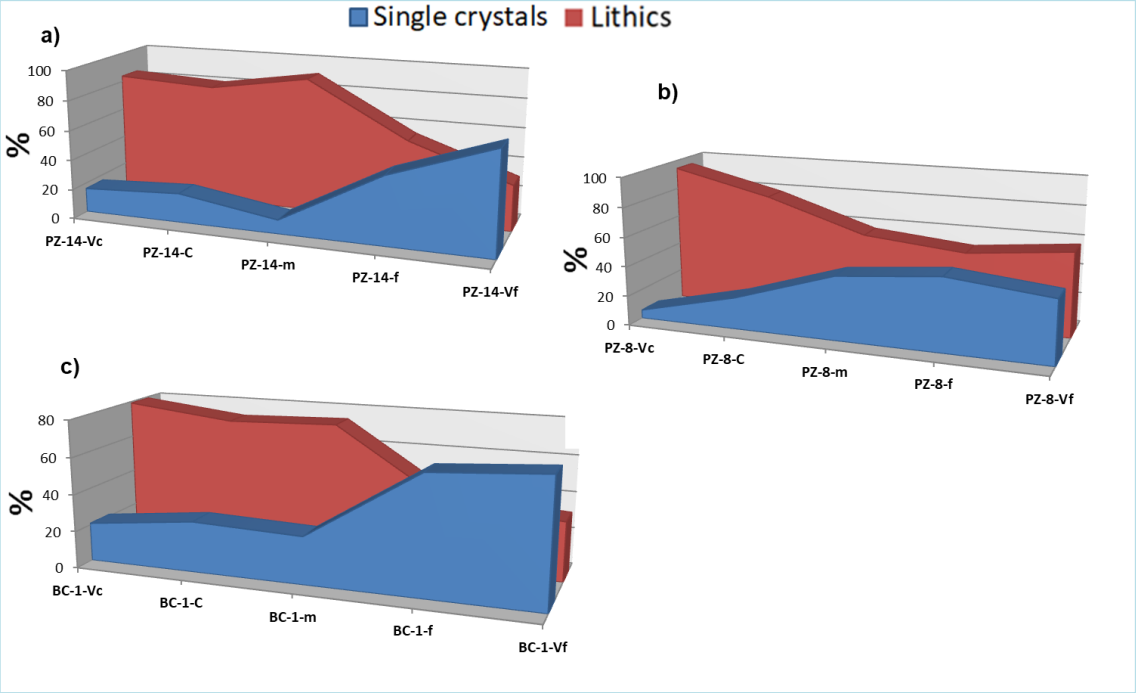

Figure 4.32 – Single crystals vs. lithic grains among the five sand fractions. a) PZ-14 sand sample; b) PZ-8- sand sample; c) BC-1 sand sample.

Figure 4.33 shows the relative proportion of main lithic types such as metamorphic, sedimentary and volcanic lithic fragments (*Lm:Ls:Lv)* among Campania sand samples, from Volturno river mouth to Sorrento village. Samples which are from Volturno (VO-series), Licola (Li-series) and some from Bacoli (toward north) are shifted toward sedimentary lithic apex (Ls) having more than 50% in Ls, and some VO- series samples have also until 14% of metamorphic lithic fragments (Lm); whereas going closer to Phlegrean fields area there is a string volcanic lithic fragments increasing. Thus, samples from northern coastal stretch with respect to Pozzuoli (toward Volturno river mouth), show a lower percentage of volcanic lithic fragment, and an increasing in sedimentary lithic fragment toward Volturno river mouth, as a result from clastic supply from Apennines sedimentary source rocks (figs.4.33, 4.34); whereas going from Portici to Sorrento we mainly found volcanic lithic fragments with exception of Castellammare di Stabia (CA-1, CA-2, CA-2B) and SO-1 (the southernmost sand sample of this study) which show a "*Ls"* percentage higher than 50%. Thus, by only analyzing the three typologies of lithic fragments we can affirm that these sand samples have a mixed (dual main source rock) provenance source rocks: sedimentary source rocks and volcanic source rooks; probably from northern and southern part the volcanic "signal" is influenced by Apennines (figs. 4.33, 4.34).

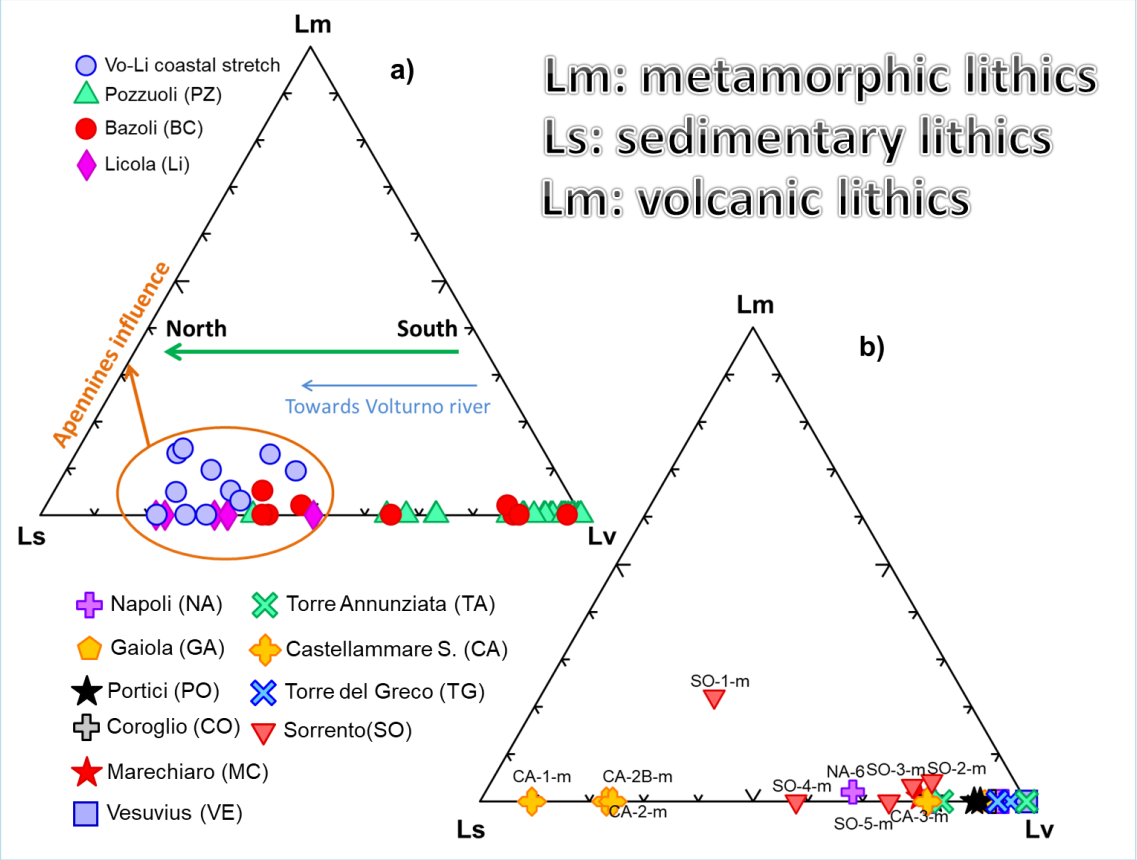

Figure 4.33 – Ternary plot of relative proportions of Lm:Ls:Lv. Lm: metamorphic lithics; Ls: sedimentary lithics; Lv: volcanic lithics (modified from Marsaglia and Ingersoll, 1992). a) samples are from Volturno river mouth to Pozzuoli; b) samples are from Pozzuoli to Sorrento coastal stretch.

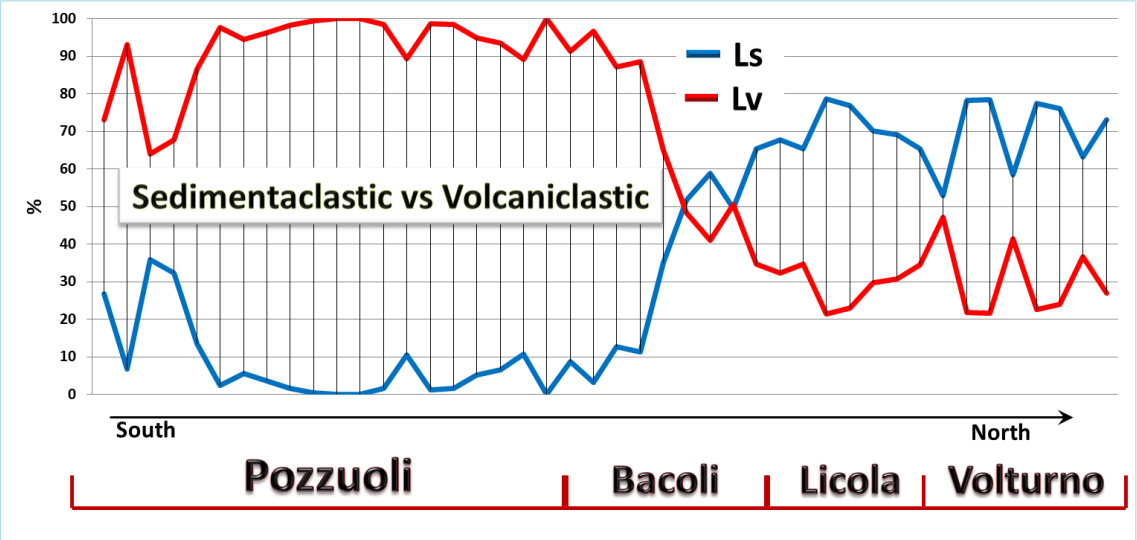

Figure 4.34 – Sedimentaclastic vs. volcaniclastic "SIGNAL" from Phlegran Fields to Volturno river mouth (from south to north). It is clearly evident how the volcaniclastic signal strongly decreases after Bacoli which probably marks the transition between volcanic and sedimentary petrofacies along the north Campania coastal stretch.

Ternary plots displayed in figure 4.34 show the relative proportion of volcanic lithic with lathwork, microlitic and vitric textures (*Lvl:Lvmi:Lvv*) in the medium sand fraction. Samples from Phlegrean Fields (PZ-, NA- and some BC- series) display a slightly shifted distribution toward Lvv apex, but generally have an equally distributed percentage among Lvl:Lvmi:Lvv with few exceptions (e.g. PZ-9). "Lvv shift" usually happen when the detritus has a more evolved volcanic source rock provenance.

Volturno samples has few volcanic lithic fragments, and they are mainly constitute by Lvl texture, this explain why almost all VO- series samples are strongly shifted toward Lvl apex, VO-2 sample has very few lithic in its sandy composition because it is a placer constitute almost totally of single crystal grain (fig. 4.35).

Portici-Sorrento coastal stretch samples have a Lvl percentage higher than 50% with few exceptions (CA-3, TA-1, SO-4). CA-1 samples has very few volcanic lithic fragments in its sandy composition and they are Lvl, on the contrary has predominately sedimentary lithic fragments, this explain its 100% of Lvl (fig. 4.35).

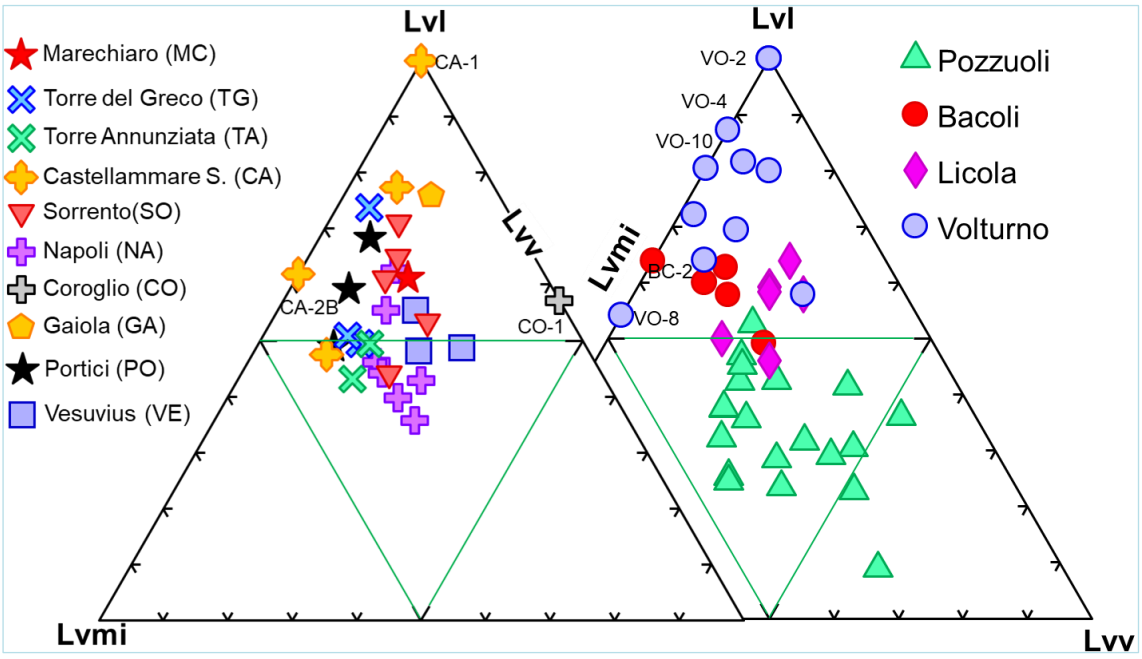

Figure 4.35 – Ternary plot of relative proportions of Lvl:Lvmi:Lvv. Lvl: lathwork texture; Lvmi: microlitic texture; Lvv: vitric texture. Samples goes from Volturno river-mouth to Sorrento village.

It was carried out a test for the five sand fractions for three samples (PZ-8, PZ-14, BC-1). Despite in Campania there are more mature beach sand than Aeolia Islands, where in general in the medium sand fraction there is a Lvl:Lvmi:Lvv equally distributed percentage, the result is that also in Campania the lithic compositions are differentiated by grain-size. There is breakage trend that shows the increase of *Lvl*

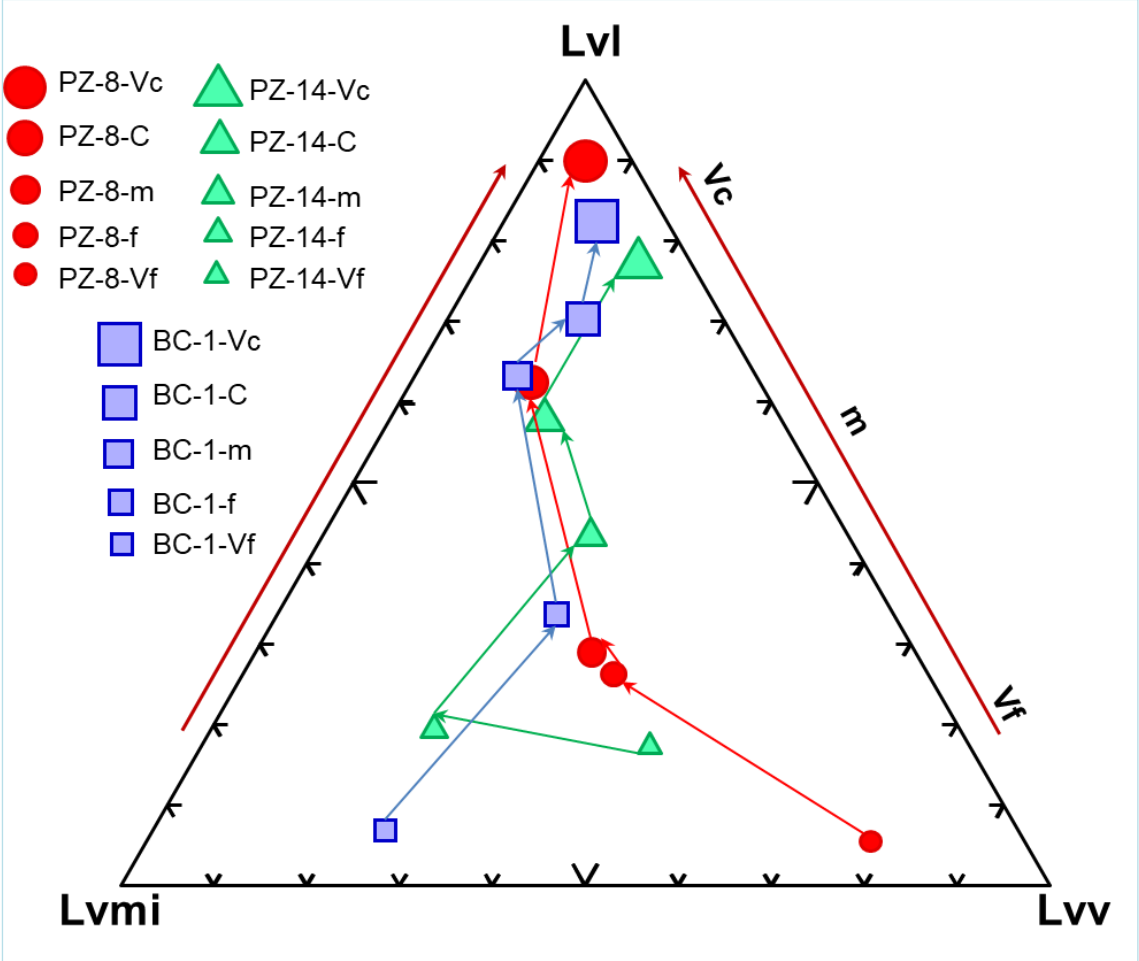

Figure 4.36 – Grain-size vs. volcanic lithic texture. Vc: very coarse sand; C: coarse sand; m: medium sand; f: fine sand; Vf: very fine sand.

grains from very fine to very coarse sand fractions (fig. 4.36). Even if it is more difficult especially along Bacoli-Volturno river-mouth to find sands coarser than medium sand (see paragraph 4.1.2).

In figure 4.37 are shown the relative proportion of Lvf:Lvmi:Lvl. Phlegrean fields are (PZ-, BC-, series) has an high Lvf percentage but always lesser then 50%. Only Li-4 has 13% of Lvf texture among Licola samples which is a dunal sand sampled in front of a rhyolitic dome. Among VO- series samples (toward Volturno river-mouth), all samples have almost zero Lvf percentage with few exceptions (VO-5, VO-8, VO-9) which have lesser then 20% Lvf textures. Whereas the totality of Portici-Sorrento coastal stretch lie on Lvl-Lvmi side which are equally distributed.

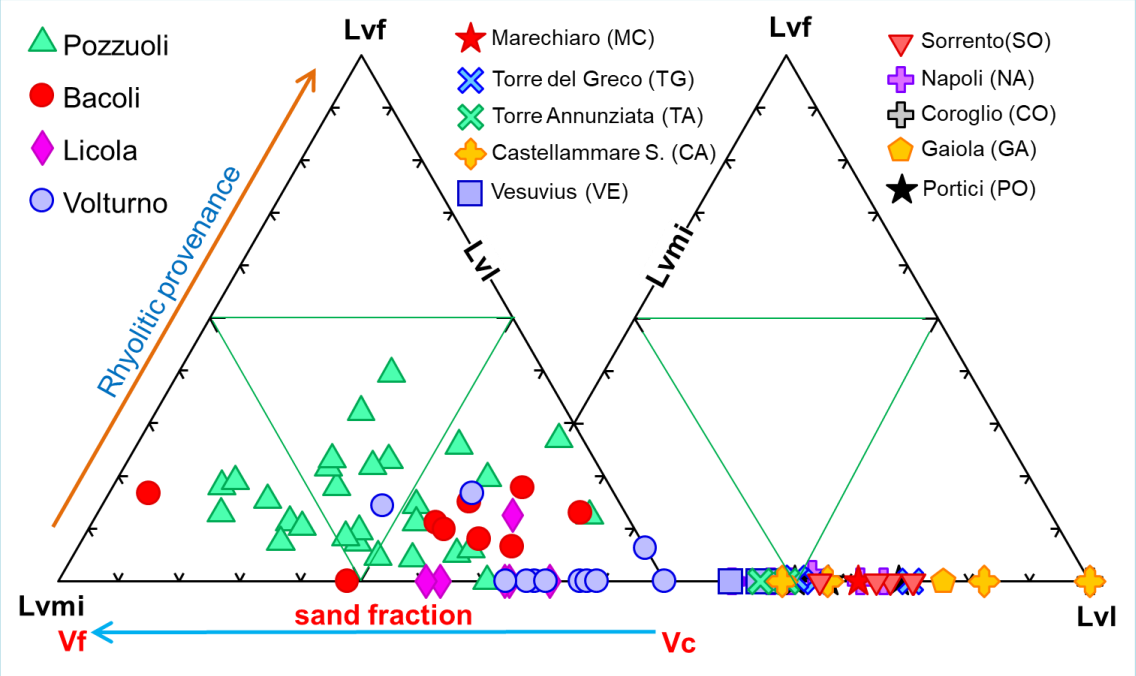

Figure 4.37 – Ternary plot of relative proportions of Lvf:Lvmi:Lvl. Lvf: volcanic lithic with felsitic texture; Lvmi: microlitic texture; Lvl: lathwork texture.

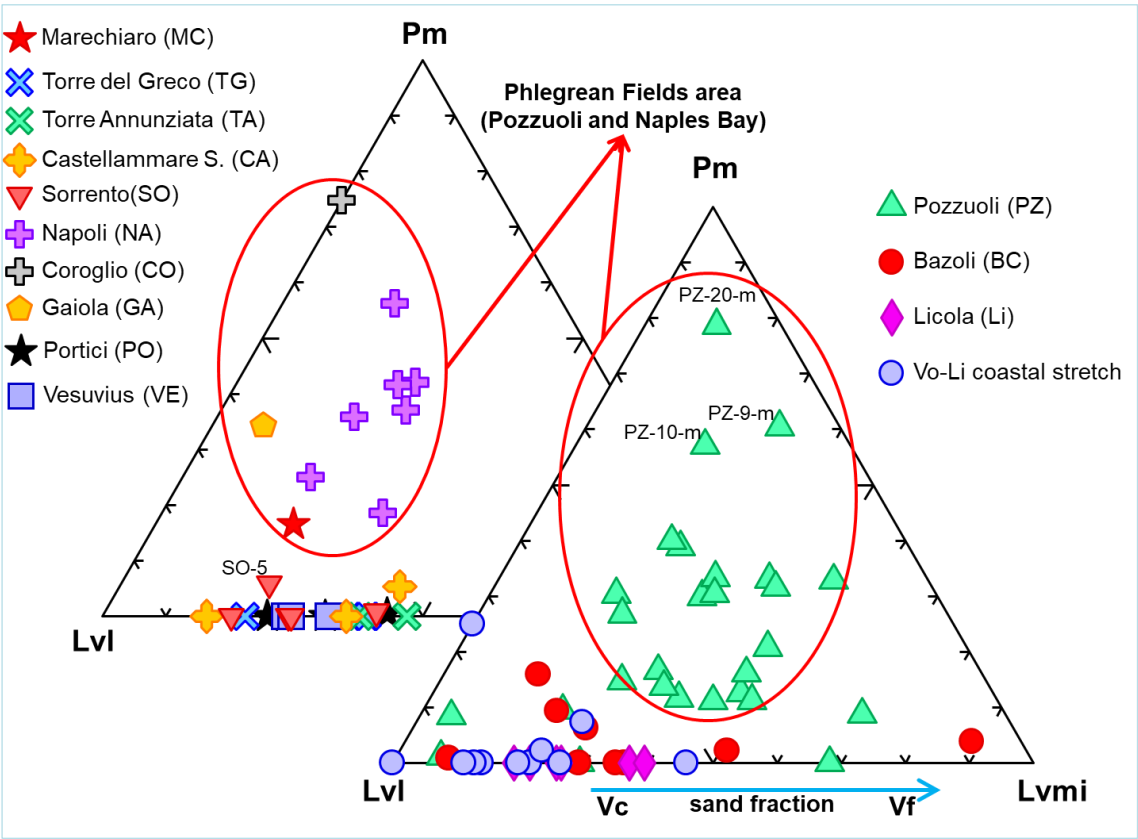

Figure 4.38 – Ternary plot of relative proportions of Pm:Lvl:Lvmi. Pm: pumice grains; Lvl: lathwork texture; Lvmi: microlitic texture.

All these probably means that according to the source rocks, the dacitic –rhyolitic "signal" eroded from lavas, which produce Lvl-Lvmi-Lvv (higher amount of Lvv) with colorless and grey groundmass, goes lost in the sandy detritus as well as those eroded from pyroclastic rocks (which produce pumice) after strong reworking and recycle in high-energy environment (wide open beach-environment) such as Licola-Volturno and Portici-Sorrento coastal stretch, whereas in more protected and quite beach-environment such as Pozzuoli bay, this type of volcanic lithic texture (Lvf, pumice, which are associated to more evolved [acid] volcanism and then explosive volcanism) are more preserved (fig. 3.17). This is hypothesis is confirmed by looking figures 4.37 and 4.38 which shows that all samples collected along Phlegrean Fields area, located in Pozzuoli and Naples bay, have an higher Lvf and pumice percentage, whereas along Volturno-Bacoli and Portici-Sorrento coastal stretch Lvf and pumice percentage drop down around zero except SO-5 sample which coincidentally it was taken from a little bay protected by a promontory beneath Sorrento Village (fig. 3.17). Moreover, CO-1 sample location is even more protected, in fact has a really high pumice percentage (75%), whereas PZ-20 was sampled in lacustrine environment (Torrefumo lake, tab. 3.8) and shows the highest pumice percentage among all samples (fig. 4.38).

In figure 4.39 have been compared the relative proportion of volcanic lithic fragments with vitric texture (Lvv) discriminated by color (black, brown, colorless). It was built by using the medium sand fraction and for some samples the five sand fractions were used (PZ-8, PZ14, BC-1). There is no relation between vitric color texture and grains-size. Portici-Sorrento samples are equally distributed between Lvvblgl and Lvvbr apexes with a slight shift toward Lvvblgl; whereas Phlegrean Fields samples (PZ-, BC-, NA- series) almost cover the inter ternary plot diagram having high percentages of Lvvblgl and Lvvclgl with lesser amount of Lvvbrgl. Volturno-Licola sand samples are not plotted on this diagram because they have the three components (*Lvvclgl:Lvvblgl:Lvvbrgl*) percentage close to the zero.

Sandy detritus from Portici-Sorrento coastal stretch is enriched in lithic fragments with basaltic "*signature*" having more than 50% in all samples with lesser amount of lithic with andesitic "*signature"* and very low "Dac_{Prov}" percentages (fig. 4.40); whereas Phlegrean Fields samples have an higher percentage of lithic fragments with dacitic *"signatures"* and three samples exceed 50% preserving dacitic provenance.

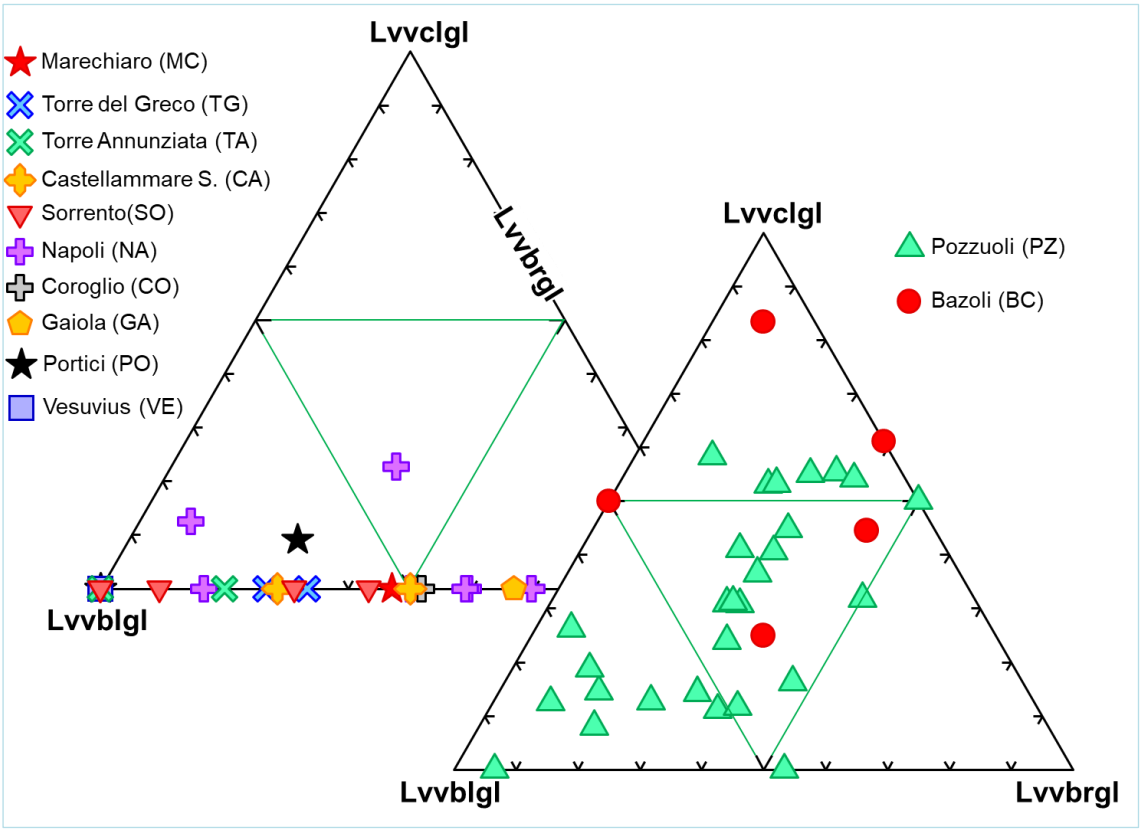

Figure 4.39 – Ternary plot of relative proportions of Lvvclgl:Lvvblgl:Lvvbrgl. Lvvclgl: vitric texture with colorless glass; Lvvblgl: vitric texture with black glass; Lvvbrgl: vitric texture with brown glass. Data are referred to entire Volturno-Sorrento coastal stretch.

Toward Volturno rive-mouth sandy detritus enriching in lithic fragments with basaltic and to a lesser extend in andesitic "*signature*" (fig. 4.40).

Moreover, in figure 4.41 is shown also the altered degree of the volcanic lithic grains which composing Campania beach sands. Portici-Sorrento samples have low lithic altered percentages, whereas Licola-Volturno samples result more altered than Portici-Sorrento samples. Phlegrean Fields samples (NA-, PZ-, BC- series) have few samples containing altered lithic fragments and show an higher percentage of lithic fragments with "*RIO & DAC*" provenance (figs. 4.40, 4.41).

By looking at figures 4.40 and 4.41 we see that volcanic lithic with felsitic, colorless and grey groundmass are more preserved in the detritus in more protected and quite beach-environment such as Pozzuoli and Naples bay probably because glassy-rich fragments tend to alter more quickly during sedimentation processes, then during the time it will find basaltic-andesitic-rich sandy detritus overestimating mafic source rocks and underestimating more acid source rocks.

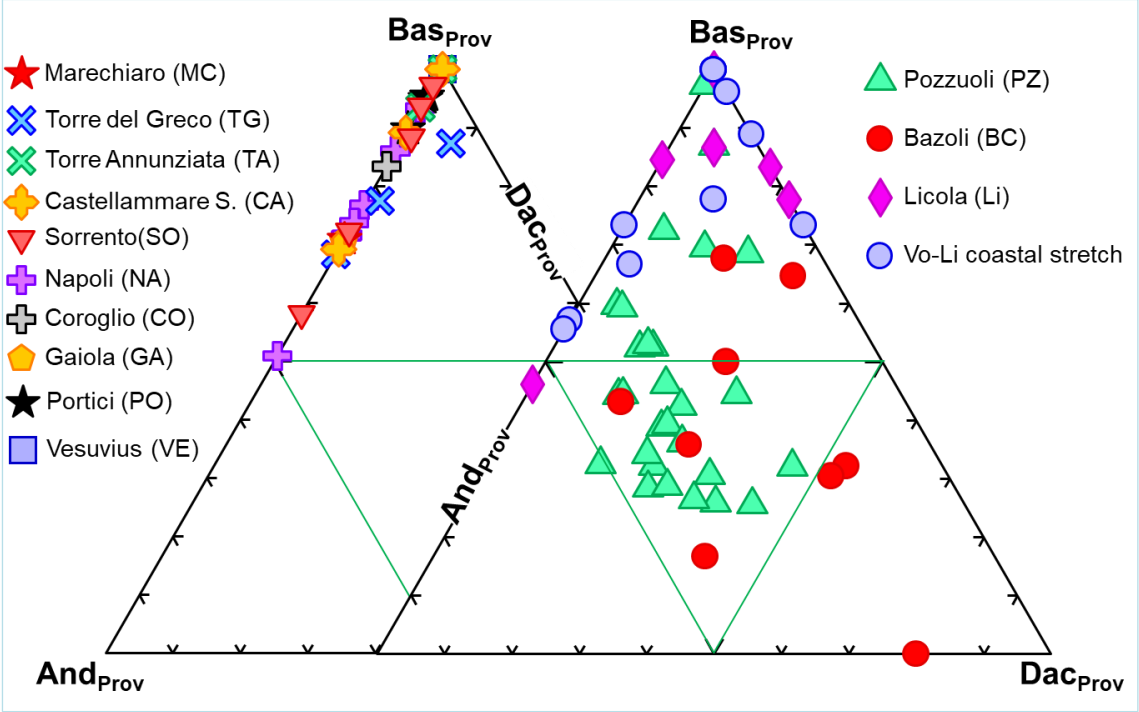

Figure 4.40 – Ternary plot of relative proportions of Bas_{Prov}:And_{Prov}:Dac_{Prov}. Bas_{Prov}= Lvlblgl+Lvmiblgl; And_{Prov}= Lvlbrgl+Lvmibrgl; Dac_{Prov}= Lvlgrgl+Lvmigrgl.

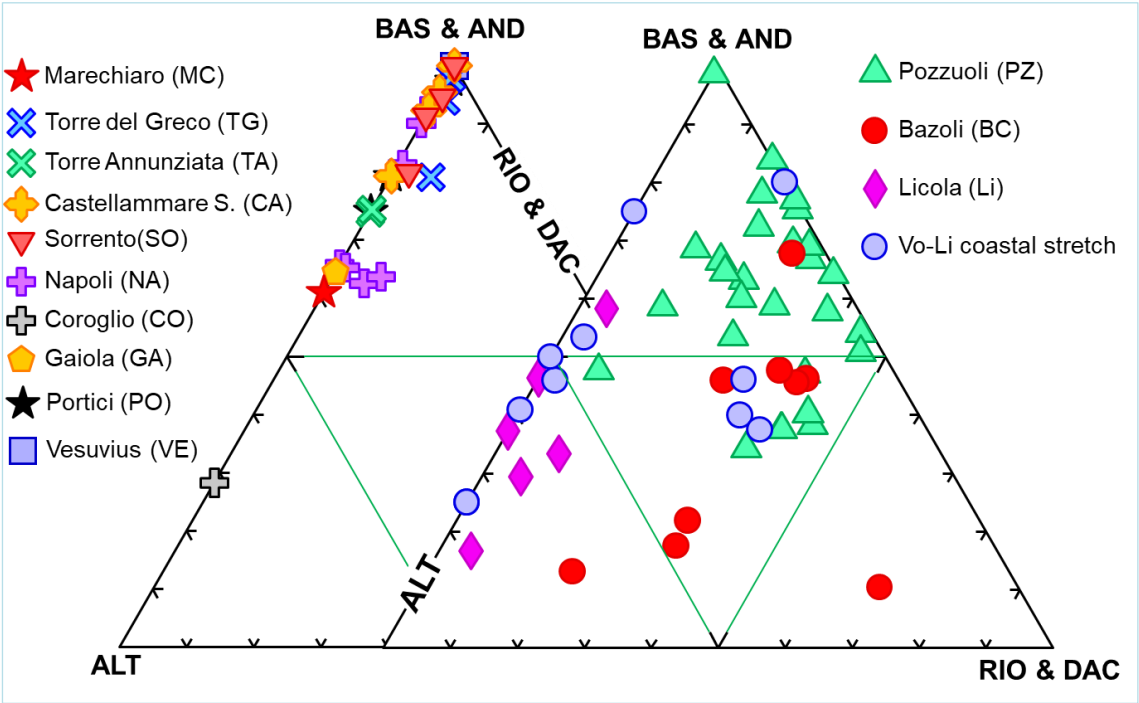

Figure 4.41 – Ternary plot of relative proportions of BAS & AND:ALT:RIO & DAC. BAS & AND= Lvlblgl + Lvmiblgl + Lvvbl + Lvlbrgl + Lvmibrgl + Lvvbrgl; ALT= Lvlorgl + Lvmiorgl + Lvvorgl +Lvlalgl + Lvmialgl + Lvvalgl; RIO & DAC = Lvlgrgl + Lvmigrgl + Lvvgrgl + Lvlclgl + Lvmiclgl + Lvvclgl + Lvf. al: altered glass in clay minerals and/or palagonite.

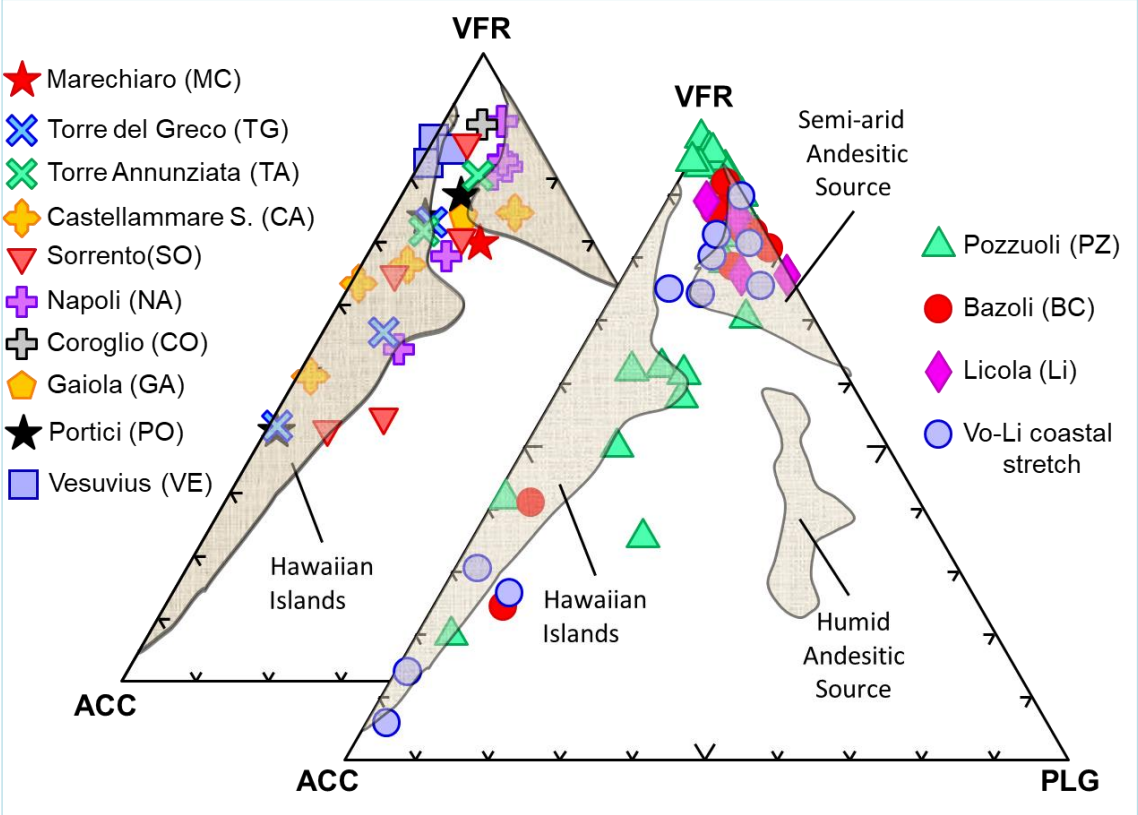

Figure 4.42 – Ternary plot of relative proportions of volcanic rock fragments with all texture typologies (VFR), accessory minerals (ACC – single grains of olivine, pyroxene, opaque) and plagioclase (PLG). Shadow areas for andesitic source are from Mack & Jerzykiewicz (1989); shadow areas from Hawaiian Islands are from Marsaglia (1993).

By plotting our data on Mack and Jerzykiewicz (1989) diagram, Portici-Sorrento samples comprising Vesuvius crater sands overlap shadow area from Hawaiian Islands, whereas Phlegran fields and Licola-Volturno samples principally overlap semi-arid andesitic source, only few samples are shifted toward ACC apex because they are heavy minerals placer (fig. 4.42, see paragraph below).

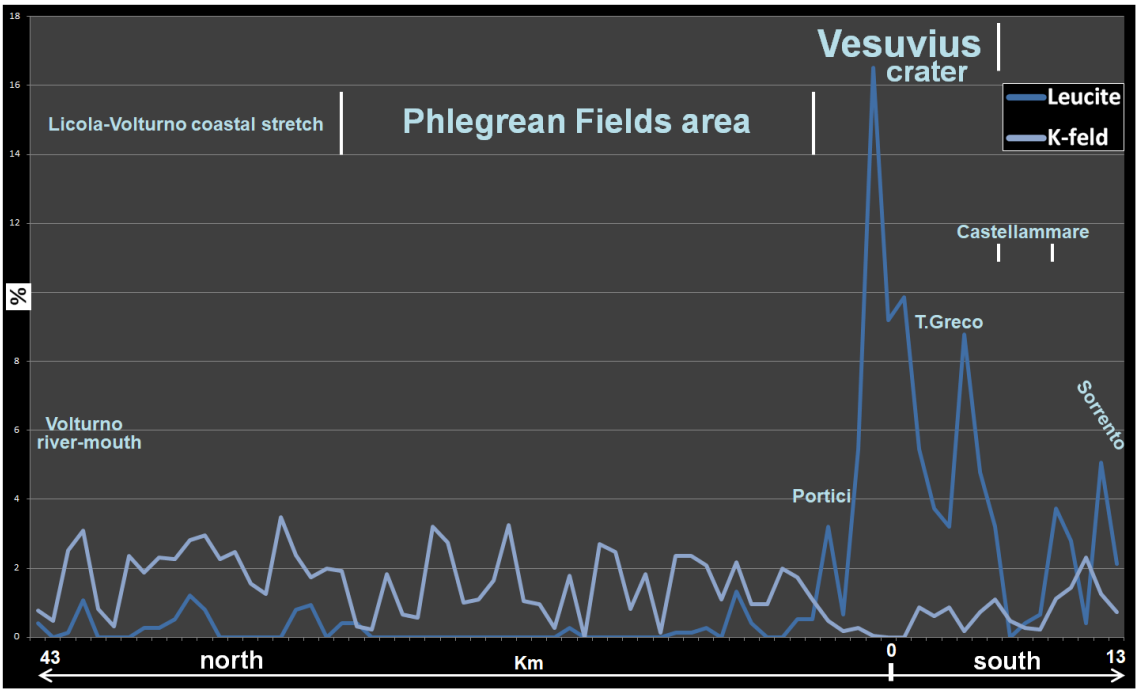

Figure 4.43 – Leucite and K-feldspar proportion vs. distance from Vesuvius volcanic edifice along Volturno river-mouth (north) to Sorrento village (south) coastal stretch.

According to Vesuvius volcanism we know that the main products contain leucite minerals which it has been found into sandy detritus both as phenocryst in lithic fragments and as single crystals, whereas k-feldspar (mainly sanidine) is typically from Phlegrean Fields products even if it is also among the Vesuvius products (in lesser amount). Figure 4.43 allows to understand where Vesuvius products start, and where they finish by looking leucite increasing and decreasing along the studied coastal stretch. The little peaks in the Volturno river-mouth vicinity are probably due to some drained Roccamonfina volcano products (Latium province). Licola (to the north) and Naples bay (to the south) delimit Phlegrean fields products (based on sandy detritus modal composition / petrography). The diagram shows a strong leucite increase starting from Portici until Castellammare di Stabia where a strong leucite decreasing occurs, probably because in those areas an Apennine clastic supply take place (sedimentary source rocks), but leucite "signal" increase again around Sorrento village until the southernmost promontory immediately after Sorrento village where another strong decrease is recorded.

4.2.1.2C – HEAVY MINERALS STUDY –

Campania region, in southern Italy, is an excellent area to determine the effects of multiple source lithology (volcanic+sedimentary), climate, weathering, transport and depositional environment on heavy minerals enrichments in the sandy beaches of the coastline between Pozzuoli and Bacoli, and at the Volturno river-mouth. The heavy mineral assemblage should reflect the clastic supply from the potassic to ultrapotassic lavas and pyroclastic rocks of the Campania Magmatic Province and of the Roman Magmatic Province (Campi Flegrei, Roccamonfina volcano) and from the recycling of sedimentary – both carbonate and siliciclastic - terranes of the Apennine thrust belt. Opaque oxides, pyroxene and amphibole assemblage dominates in the beach placers of the Campania shoreline - from Bacoli to Pozzuoli - as well as in the Volturno river mouth sands to the north. Modern heavy minerals assemblages reflect clastic contribution from magmatic source rocks whereas contribution from sedimentary terranes - exposed extensively in the Volturno river drainage - provide no recycled heavy minerals to the river-mouth sand. Thus, heavy minerals linked to a provenance from the Apennine thrust belt source rocks result diluted and/or unrecognizable using the only HM (Heavy Minerals) approach with respect to the minerals provenance sourced by the potassic volcanic fields of Latium and Campania. The diverse detrital heavy minerals have been characterized describing major stages of progressive chemical weathering, from unweathered to corroded to etched morphologies, a process – in this case-history - playing a minor role in reducing HM diversity through dissolution of moderately stable mineral species (Le Pera and Morrone 2018).

Six beach samples of “black sands” (e.g., Peterson et al., 1985) were collected to examine placers deposits in detail. After sieving, the heavy mineral assemblage has been obtained from the 125-250 μm size-fraction. Polished thin sections of the concentrates were used for petrographic and electron microprobe analysis, the characteristic of a sample has been obtained from combining the modal data with the chemical compositions of many grains of different mineral phases in a sample, such as opaque oxides and pyroxene grains. Four beach sand samples from high and low-tide berms were collected spaced over the coast from Pozzuoli to Bacoli and two sand samples have been taken in the vicinity of the Volturno river mouth (fig. 4.44). We refer to the rocks that are decomposed to produce heavy minerals in the sand as provenance lithotypes (e.g., Heins and Kairo, 2007). Hence hinterland territories contribute such

aliquot of grains - with respect to the bulk sandy detritus - to the studied coastal stretch include (fig. 4.44):

1. *volcanic provenance lithotypes* (*sensu* Heins and Kairo, 2007), of the *Campania Magmatic Province* (i.e., Phlegrean Fields) behind the coast of the Napoli Gulf, influencing sedimentation between Pozzuoli and Bacoli sand;

2. *mixed sedimentary* (i.e. Apennine thrust belt) + *volcanic provenance lithotypes* (i.e., Phlegrean Fields and Roccamonfina edifice), governing sand generation and sedimentation at Volturno river-mouth (Le Pera and Morrone 2018).

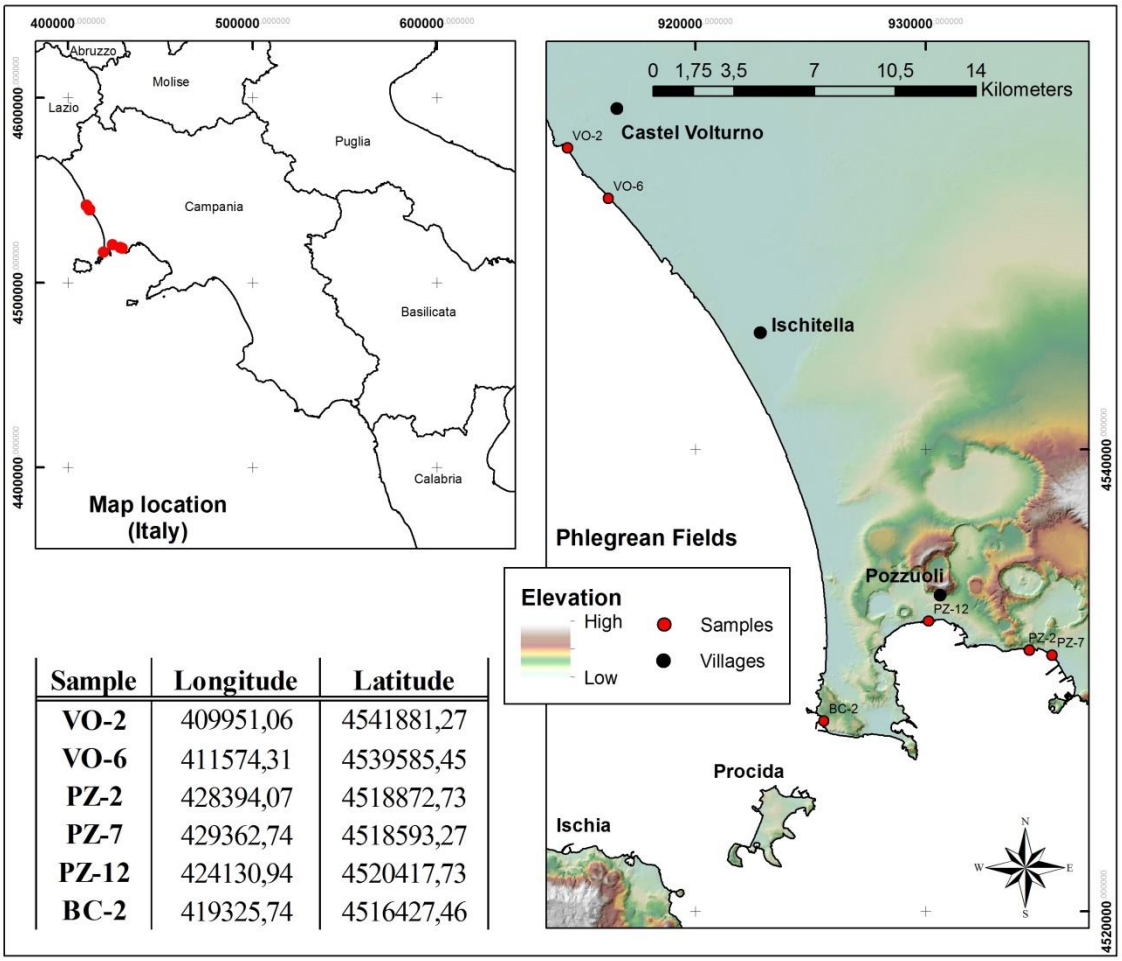

Sample	Longitude	Latitude
VO-2	409951,06	4541881,27
VO-6	411574,31	4539585,45
PZ-2	428394,07	4518872,73
PZ-7	429362,74	4518593,27
PZ-12	424130,94	4520417,73
BC-2	419325,74	4516427,46

Figure 4.44 – Heavy minerals samples location. Pozzuoli beaches: PZ-7, PZ-2 e PZ-12; Bacoli beache: BC-2; Volturno river-mouth area: VO-2 e VO-6. (modified from Le Pera and Morrone, 2018).

Definition of weathering stages

The description of the weathering morphologies has been carried out according to Andò et al. (2012) who documented the morphology of weathered heavy minerals in modern sands of equatorial Africa and classified as follow:

1. *Unweathered stage (U)* The surface of the grain is uncorroded, with continuous outline without etch pits or re-entrants;
2. *Corroded stage (C)* The original surface of the grain is recognized, but corrosion pits and re-entrants characterize the entire outline, and become progressively deeper with increasing degree of corrosion;
3. *Etched stage (E)* The original grain surface can still be recognized, but hacksaw terminations appear, initially at the extremity of prismatic crystals along preferential crystallographic directions (e.g., c-axis in amphiboles and pyroxenes). The studied sandy grains are lacking in the *deeply etched (D)* and *skeletal (K)* weathering categories proposed by Andò et al. (2012) which are produced by intense chemical dissolution in tropical regions (Le Pera and Morrone 2018).

Sample	Opaque (Op)	Pyroxene (Py)	Amphibole (Anf)	Biotite (Bt)	Garnet (Gr)	Rutile (Ru)	Tourmaline (To)	TOT
PZ-2								300
Unweathered (U)	161	26	10	0	3	0	0	200
Corroded (C)	91	3	0	0	0	0	0	94
Etched (E)	6	0	0	0	0	0	0	6
%	**86**	**9,6**	**3,3**	**0**	**1,1**	**0**	**0**	**100**
PZ-7								300
Unweathered (U)	120	45	20	0	0	0	0	185
Corroded (C)	87	20	3	0	0	0	0	110
Etched (E)	0	5	0	0	0	0	0	5
%	**69**	**23,3**	**7,7**	**0**	**0**	**0**	**0**	**100**
PZ-12								300
Unweathered (U)	31	129	92	1	0	0	1	254
Corroded (C)	8	19	11	1	0	1	0	40
Etched (E)	0	4	2	0	0	0	0	6
%	**13**	**50,6**	**35**	**0,6**	**0**	**0,4**	**0,4**	**100**
VO-2								300
Unweathered (U)	111	47	50	0	0	0	0	208
Corroded (C)	57	20	8	0	0	0	0	85
Etched (E)	1	5	1	0	0	0	0	7
%	**56,3**	**24**	**19,7**	**0**	**0**	**0**	**0**	**100**
VO-6								300
Unweathered (U)	91	79	60	1	2	0	0	233
Corroded (C)	28	11	16	1	0	0	0	56
Etched (E)	0	6	5	0	0	0	0	11
%	**39,6**	**32**	**27**	**0,7**	**0,7**	**0**	**0**	**100**
BC-2								300
Unweathered (U)	122	30	17	0	0	0	0	169
Corroded (C)	110	15	1	0	0	0	0	126
Etched (E)	5	0	0	0	0	0	0	5
%	**79**	**15**	**6**	**0**	**0**	**0**	**0**	**100**

Table 4.14 – Point-counting of heavy mineral analyses of 125 μm sand fraction (300 points) and grain percentages for each sample (data are from Le Pera and Morrone, 217).

- PETROGRAPHY-

To determine the relative abundance of heavy minerals in the fine sand (125 μm) the Ribbon counting method has been used (e.g., Galehouse, 1971) using standard polarizing microscope and by counting 300 grains in each thin section. Transparent heavy mineral species and weathering stage were recognized during modal analysis (tab. 4.14).

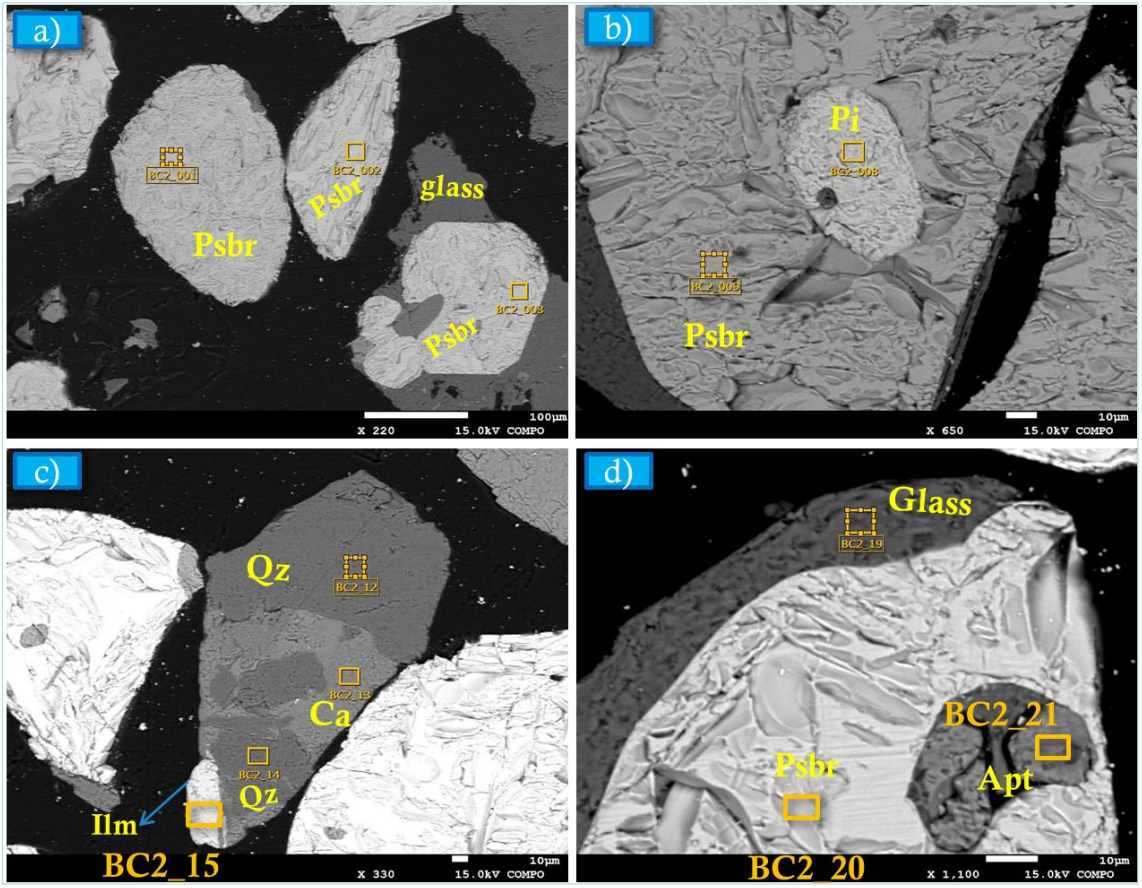

Figure 4.45 – Microprobe analysis of monomineralic and polymineralic grains. a) Spots 001, 002 and 003 show an opaque oxide with pseudobrookite composition [Fe_2TiO_5]. Spots 001 and 002 display pseudobrookite in monomineralic grain whereas spot 003 display pseudobrookite in volcanic lithic fragment [Op in Lvv]; b) Spots 008 shows an opaque oxide with pyrite composition [FeS_2] and spot 009 displays pseudobrookite in volcanic lithic fragment; c) Weathered volcanic lithic fragment or siliciclastic sedimentary polymineralic grain containing oxide opaque such as ilmenite [Fe_2+TiO_3]. d) Apatite and pseudobrookite in volcanic lithic fragment. Psbr = pseudobrookite, Pi = pyrite, Ilm = ilmenite, Qz = quartz, Ca = calcite, Apt = apatite.

Opaque dense minerals were grouped into one category rather than subdivided, because reflected light microscopy is not sufficient to discriminate among magnetite, ilmenite, pyrite and hematite, and among their inter-grown phases and textures (e.g., Morrone et al., 2017). Then, microprobe analysis technique, aimed at geochemical discrimination among opaques (e.g., Basu & Molinaroli, 1989, 1991) has been used to

identify these problematic grains (e.g., Morton and Johnsson, 1993). Identified opaque constituents – have proved to be extremely useful in this study on modern sands – or in other geological settings to discern their discriminating power with regard to provenance (e.g., Schneiderman, 1995) as well as in providing clues for reconstruction of the geochemical history of a given succession of the stratigraphic record (e.g., Rikke & Friis, 2007).

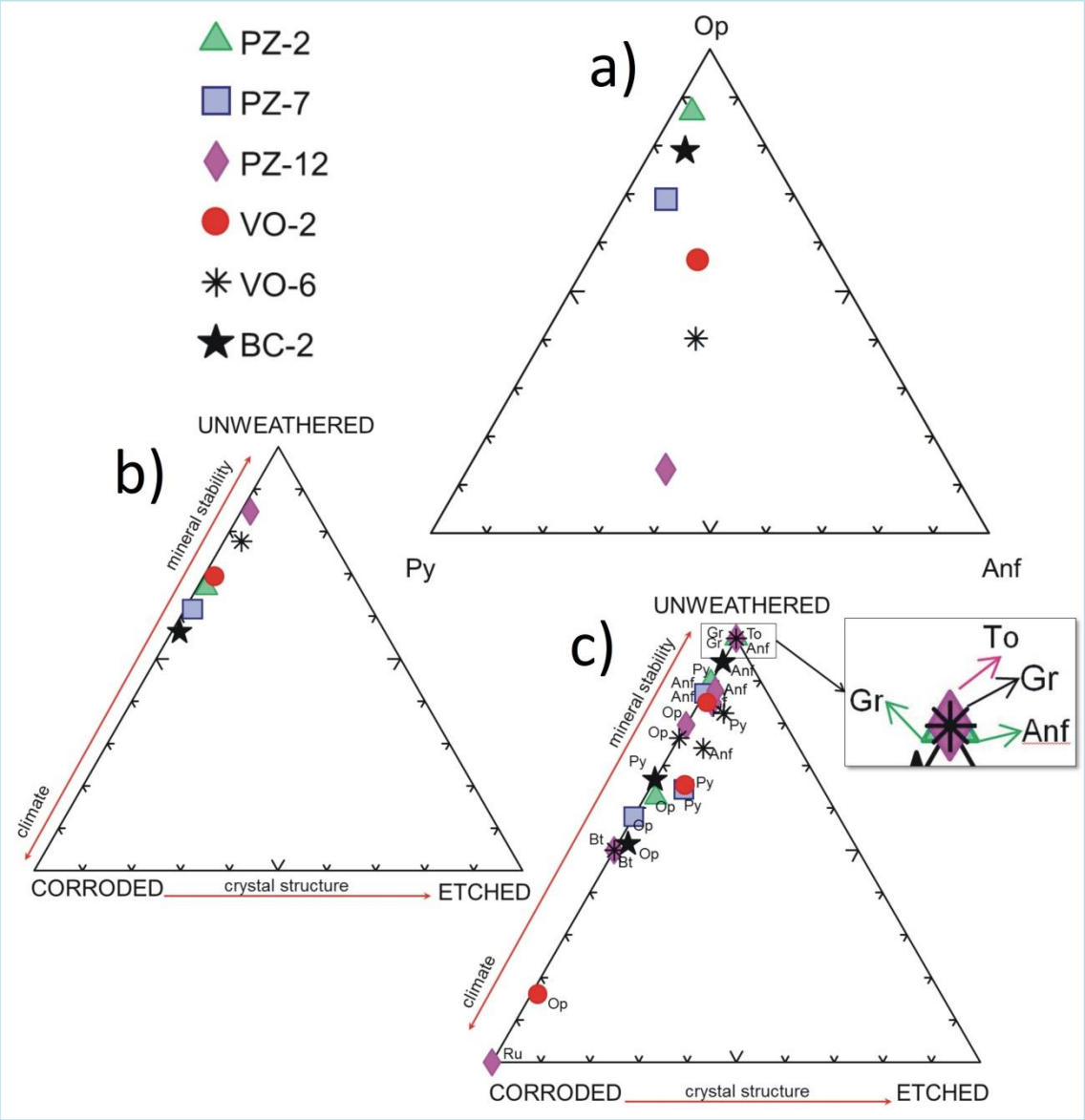

Figure 4.46 – a) Relative abundances of opaques, pyroxene and amphibole in samples from Pozzuoli and Bacoli pocket beaches and of the Volturno river-mouth illustrating the difference between sedimentary provinces and the homogenization of the mineral association at delta environment. b) Different response to weathering of heavy minerals from Campania beach sands. c) Op= Opaques; To= Tourmaline; Py= Clinopyroxene; Anf= Amphibole; Bt= Biotite; Ru=Rutile; Gr= Garnet. Frequency and type of etched surface depends on crystal structure (etched morphology developed on cleavable pyroxenes and amphiboles, but less easily on other minerals) (modified from Le Pera and Morrone, 2017).

The dominant heavy minerals in the fine sand samples are opaques, pyroxenes and amphiboles. They contain also sporadic occurrence of biotite, garnet, rutile and tourmaline (fig. 4.45 and tab. 4.14). With the exception of only one beach sample (PZ-12), the pocket beaches of the Gulf of Napoli and Volturno river-mouth samples have a mineral suite dominated by opaques - forming a volumetrically significant phase (86% to 13%; tab. 4.14) – with variable clinopyroxene (range 50.6% - 9.6%) and amphibole (range 35% - 3,0%) (fig. 4.46a). Half of identified minerals are unweathered: some clinopyroxene are corroded and etched and amphibole is less etched than clinopyroxene (tab. 4.14; fig. 4.46b, c). Informations through polarizing microscope have been integrated with electron microprobe analysis. Some analyses are of homogeneous monomineralic opaque grains, but other analyzed grains are embedded in polymineralic grains (fig. 4.45). The mineral chemical data of the opaque grains population indicate that they include pseudobrookite, pyrite and ilmenite (fig. 4.45). Pseudobrookite occurs frequently as primary mineral in subaerially extruded basalts and in alkaline complex or as a secondary oxidation product of ilmenite and titanomagnetite, though both primary and secondary phases are similar in chemical composition (e.g., Staehle and Koch, 2003). Pyrite – if volcanic in origin – is associated to hydrothermally-altered rhyolitic/dacitic volcanics (e.g., Sanchez-Espana and Roldano, 2000) and ilmenite can occur as xenocrysts in ultrapotassic lavas (e.g., Barton, 1987).

4.2.2 - Roundness study (optical microscope) –

Changes in grain roundness, calculated for both studied areas, were assessed to evaluate grain resistance to transport (stream and marine mechanical transport processes). Variations in mean roundness were determined on medium-sand sized and some test on the five sand fractions were carried out (AL-3, Fi-3, SA-1, STR-1, STR-9, PN-1, PZ-8, PZ-14, BC-1) of monocrystalline grains of plagioclase (P), k-feldspar (K), pyroxene (Py), olivine (Ol), hornblende (Hb), Leucite (Le), opaques (Op), qartz (Qm), calcite (Ca), and of volcanic lithic fragments such as Lvl (volcanic lithic fragments with lathwork texture), Lvmi (volcanic lithic fragments with microlitic texture), Lvv (volcanic lithic fragments with vitric, Lvf (volcanic lithic fragments with felsitic texture), pumice (Pm), and of sedimentary lithic fragment such as Lss (with siliciclastic composition), and sedimentary lithic fragments with crystalline ($Lsc_{(xx)}$) and micritic ($Lsc_{(micr)}$) carbonate composition (appendix A, C).

4.2.2.1 – AEOLIAN ISLANDS -

The most common roundness category among all grain types from Panarea and Stromboli islands is 2 (angular), followed by 3 (sub-angular), 1 (very angular), 4 (sub-rounded), and then with a very low occurrence of 5 (rounded), and no 6 (well rounded) grains categories whereas, the samples from Alicudi, Filicudi, Salina, Vulcano and Lipari islands show an higher percentage of sub-rounded category (3). The Aeolian Islands central sector (Salina, Lipari, Vulcano) have the most rounded grains and Vulcano has the highest well rounded percentage among all the Aeolian islands (fig. 4.47, 4.48). This trend is probably attributable to the continuous clastic supply from steep slopes, consistent with a weathering-limited erosion regime of the volcanic edifices (e.g., Morrone et al., 2017).

By comparing grain roundness degree and sand composition it was possible to link the transport distance (Km) from crater to the coast on Stromboli island (fig. 4.49a, 4.50). The maximum length of stream transportation on the Aeolian Islands is fairly short, especially on Stromboli islands (3-3.5 km). After only 3 km of transportation from the stream setting to the beach (from the crater to the coast), the mean roundness change from 2 (angular) to 3.5 (sub-angular/sub-rounded) (fig. 4.49a, 4.50). Moreover it is possible to notice that among the volcanic lithic grains, vitric fragments (Lvv) are often more angular than lathwork (Lvl) and microlitic one (Lvmi). Single crystal grains (pyroxene, olivine, plagioclase) have the same behavior.

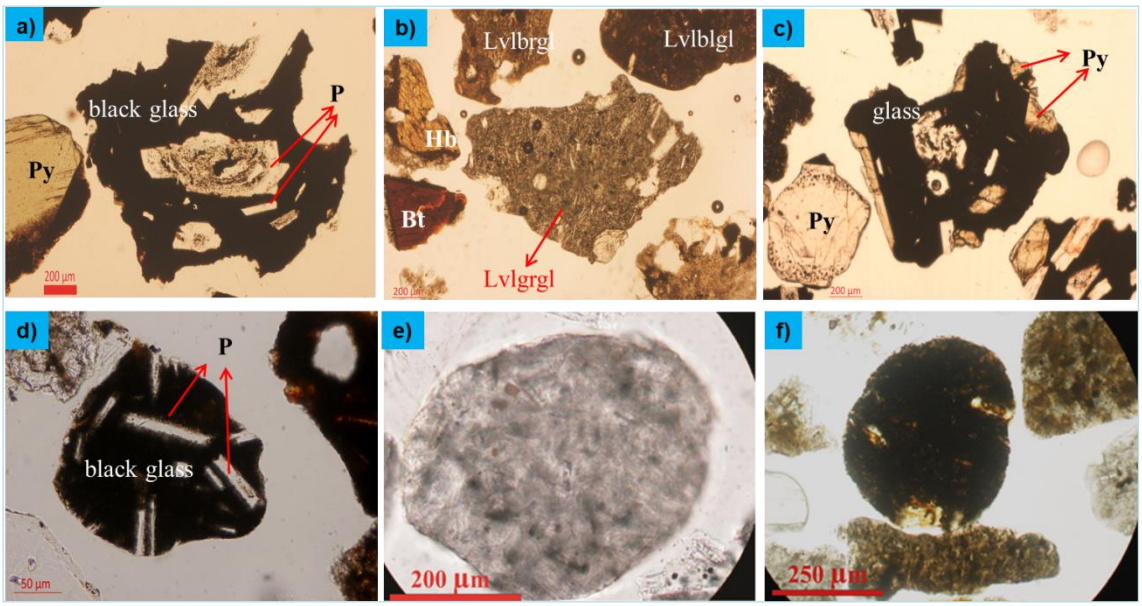

Figure 4.47 – Microphotographs showing the different roundness category. a) Very angular grain (1); b) angular grain (2); c) sub-angular grain (3); d) sub-rounded grain (4); e) rounded grain (5); f) well rounded grain (6).

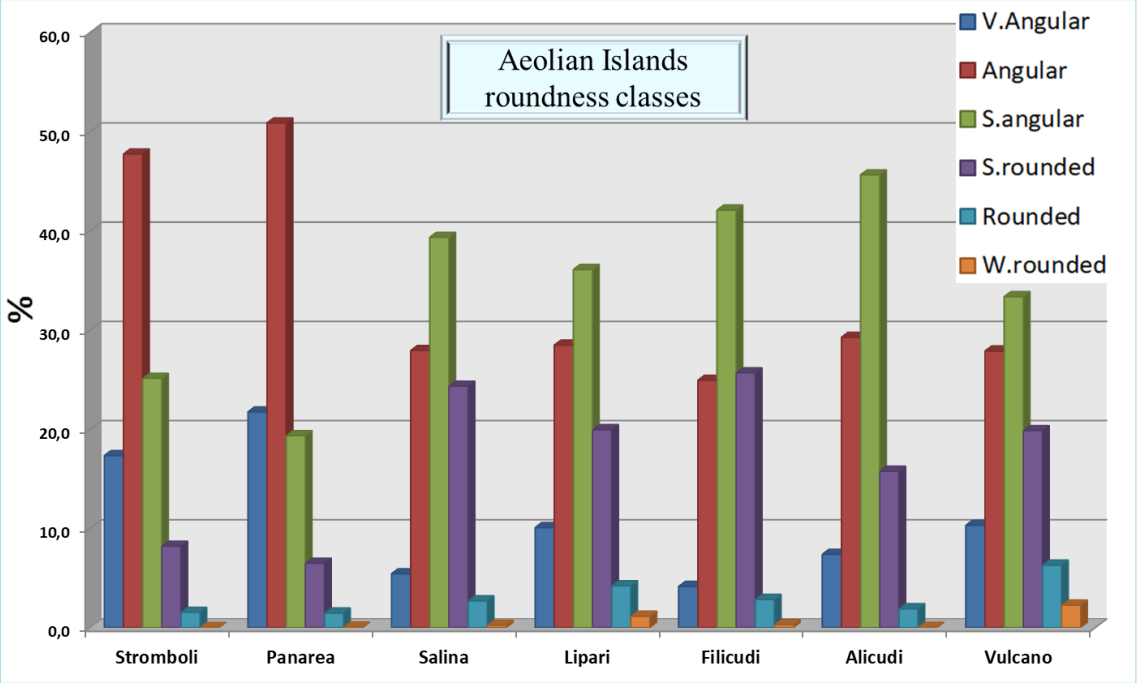

Figure 4.48 – Mean roundness percentage of all grain typologies among Aeolian Islands.

Moreover, it has been compared the roundness degree discriminated by sand composition and beach area of the each sample site related to the samples (m^2) which have been calculated using ACME Planimeter (fig.4.49b, https://acme.com/planimeter) for all Aeolian islands.

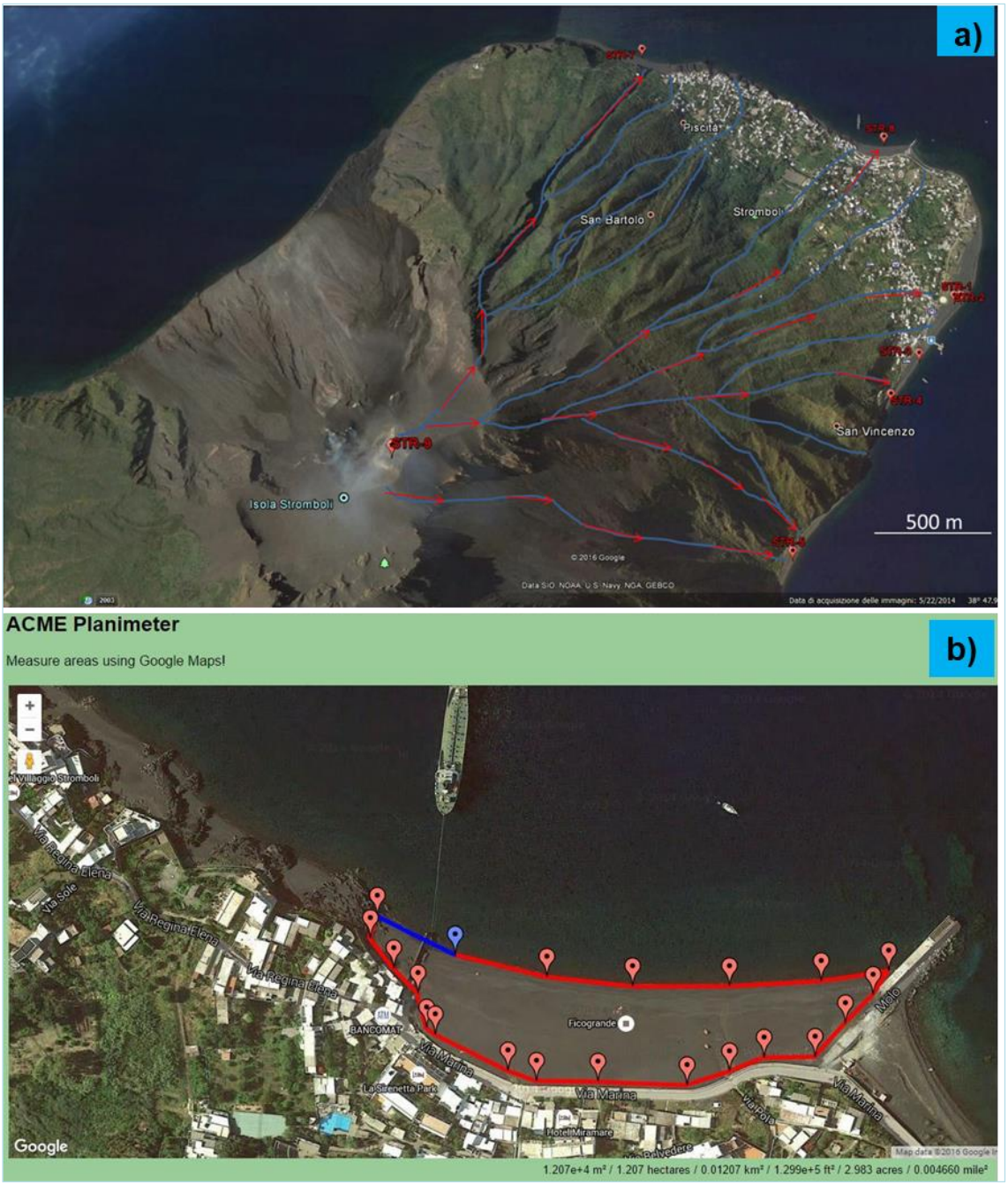

Figure 4.49 – a) Torrential-type transport on Stromboli island; b) example of beach area calculation for STR-8 sample site on Stromboli island.

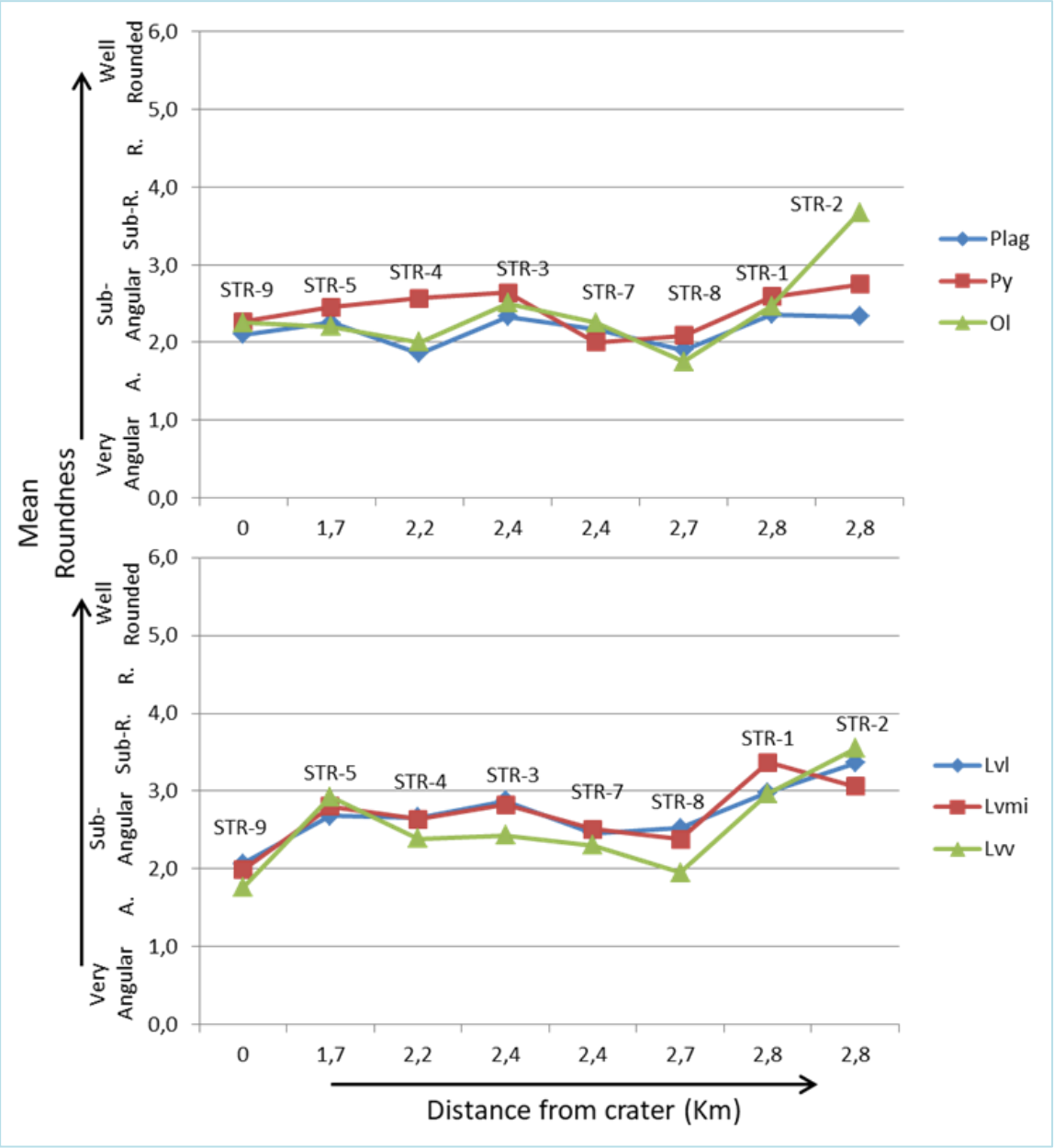

Figure 4.50 - Roundness degree among different grain types (single crystal grains and volcanic lithic fragments) vs. transport-distance on Stromboli island.

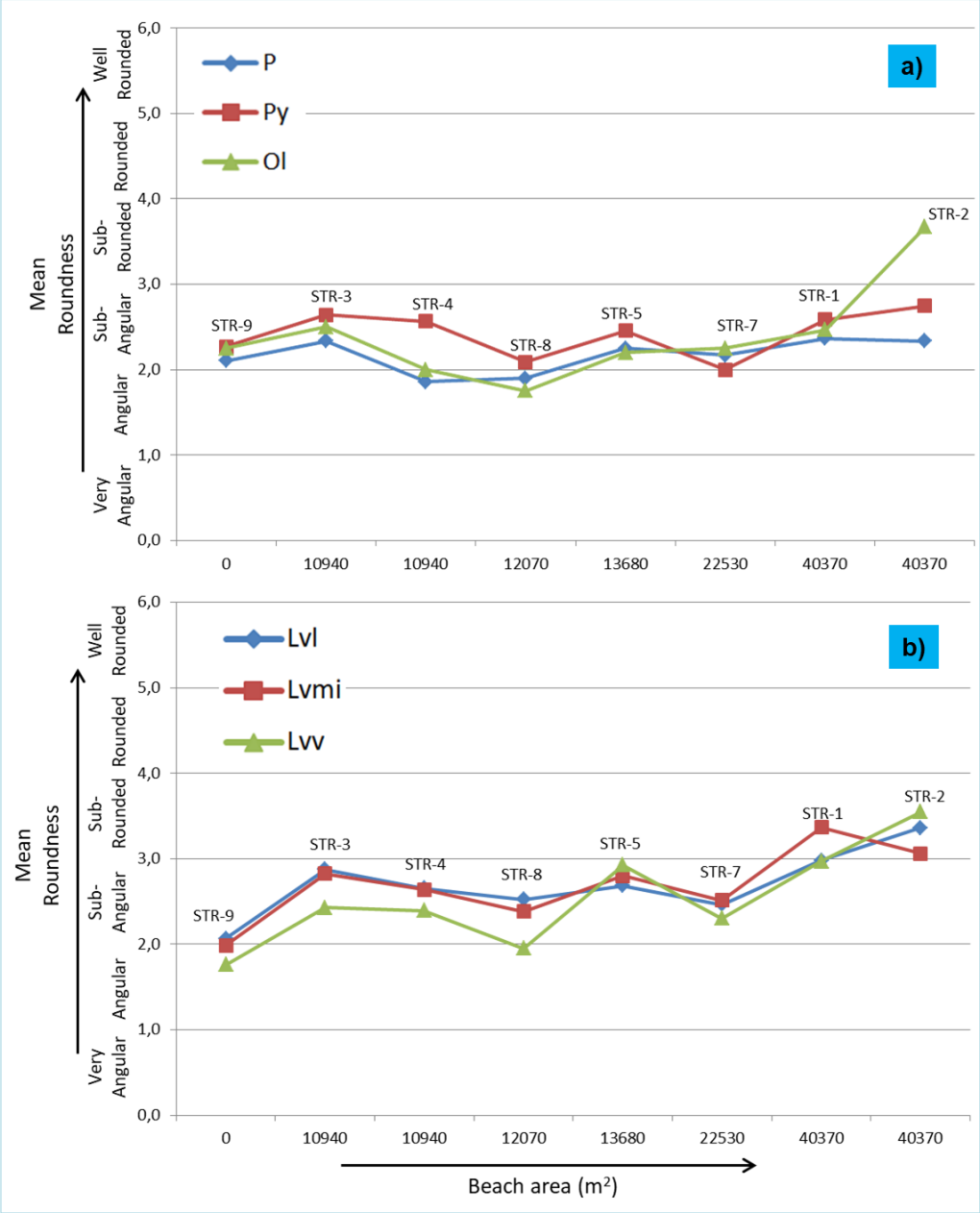

Figure 4.51 – Roundness degree vs. beach areas for Stromboli island beach sand (medium sand fraction). a) Single crystal grains roundness degree; b) Volcanic lithic fragments roundness degree.

Figure 4.51 shows the mean roundness compared with beach area (m^2) for Stromboli island. Pyroxene is more rounded than olivine and plagioclase which show a similar trend among all samples with except of STR-2 where olivine results much more rounded. Lithic fragments show a roundness degree increasing and the Lvv texture results more angular than Lvl and Lvmi in all samples with only two exception (STR-5, STR-2).

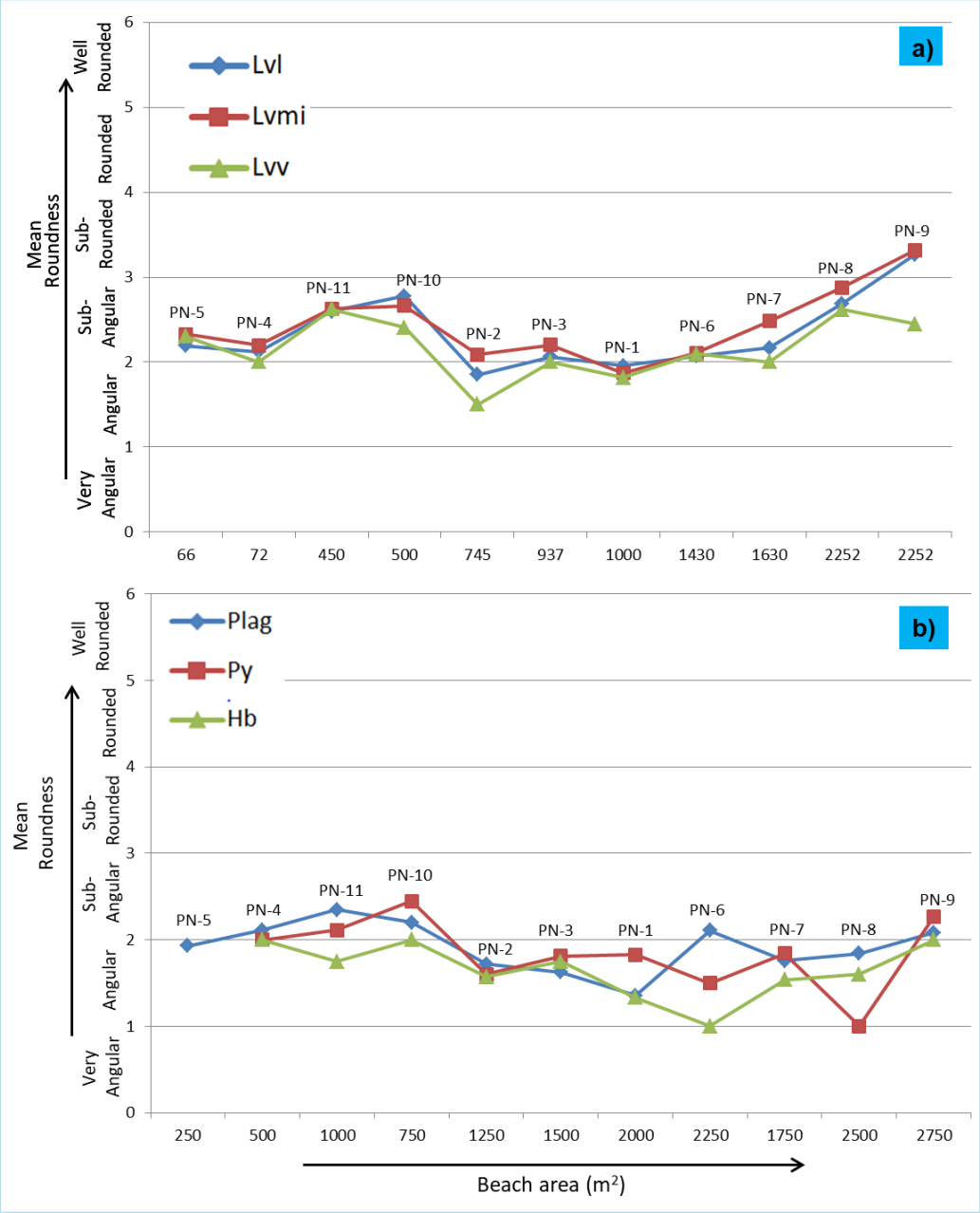

Figure 4.52 – Roundness degree vs. beach areas for Panarea island beach sand (medium sand fraction). a) Volcanic lithic fragments roundness degree; b) single crystal grains roundness degree.

Figure 4.52(a) shows a slight positive trend for lithic fragments, whereas for the single crystal grains there is no correlation between grain roundness and beach area (fig. 4.52b). Lithic fragments with vitric texture (Lvv) are more angular than *Lvl* and *Lvmi* among all samples whereas Lvmi fragments are more rounded in almost all samples. Among single crystal grains hornblende is more angular than plagioclase and pyroxene.

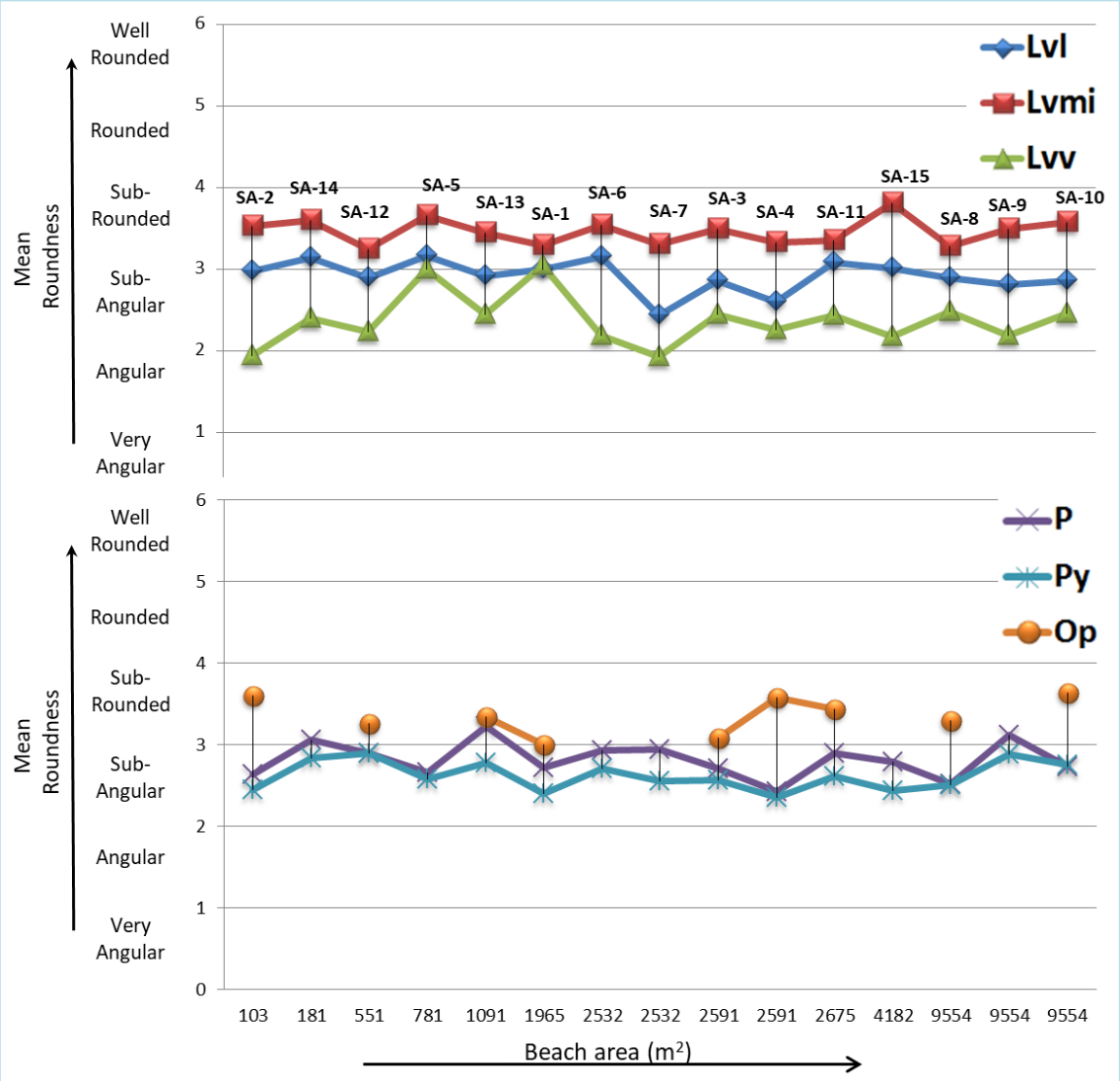

Figure 4.53 - Mean roundness vs. size of beaches area on Salina island (medium sand fraction).

Figure 4.53 shows that there is no correlation between beach area and roundness degree for both single crystal grains and volcanic lithic fragments on Salina island sand samples. Among single crystal grains opaque minerals result always the most rounded grain in all samples followed by plagioclase and then by pyroxene. Among volcanic lithic fragments Lvmi texture is always the most rounded grain in all samples, whereas Lvv texture is always the most angular in all sand samples, Lvl texture shows an intermediate roundness degree between Lvmi and Lvv textures.

Lipari roundness analyses (fig. from 4.54b to 4.54e) indicate that mechanical preservation potential for this sedimentary environment is Lvv>Lvf>Lvl>Lvmi regardless of both size of drainage basin (fig. 4.54b) and aerial extend of the beach (fig. 4.54d). Plagioclase and pyroxene single crystal grains exhibit quite similar mean roundness trends with drainage basins size (fig. 4.54c) and beach area (fig. 4.54e)

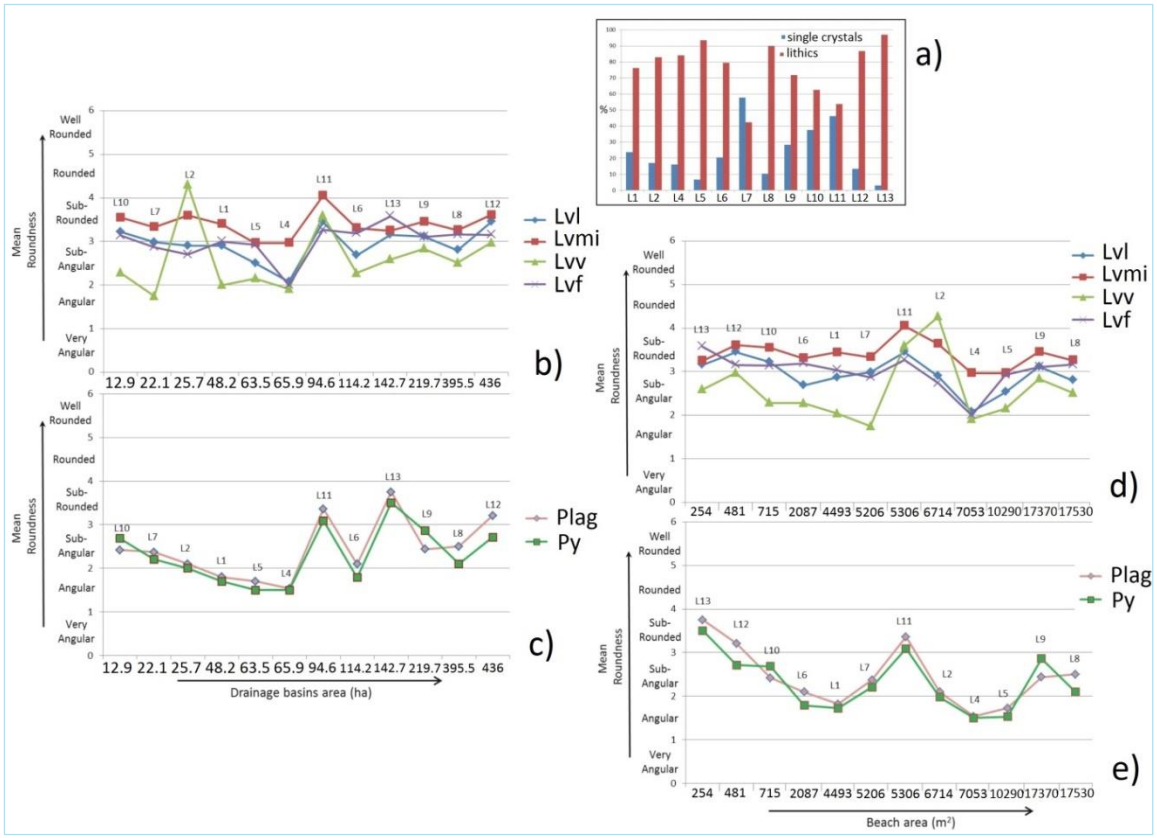

Figure 4.54 – a) Single crystals Vs lithic grains; b,c) mean roundness vs. size of drainage basins (drainage basins area are from Morrone et al., 2017); d,e) mean roundness vs. size of beaches area (modified from Morrone et al., 2018).

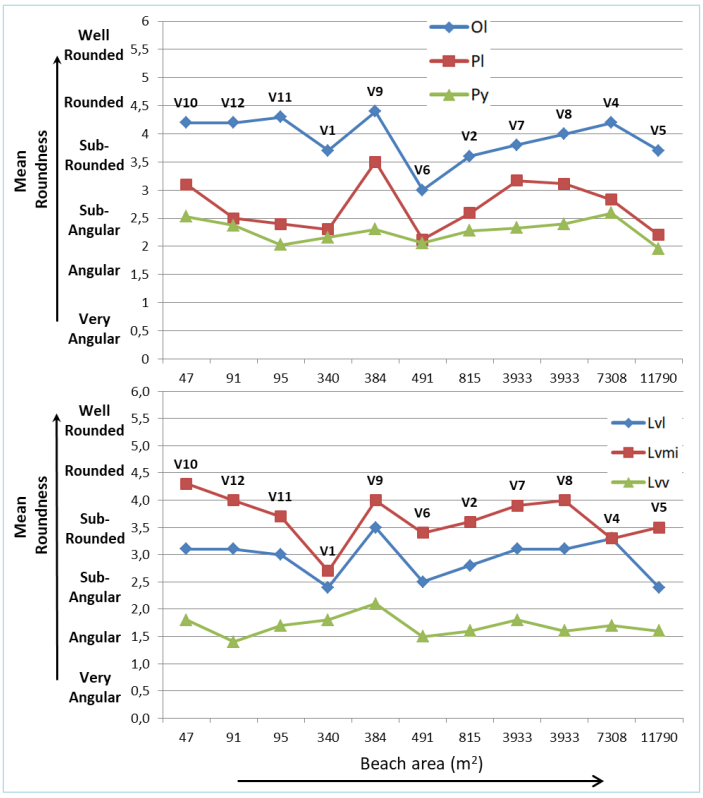

Figure 4.55 - Mean roundness Vs size of beaches area on Vulcano island (medium sand fraction).

although the abrasion process seems to be slightly prevailing at the expense of plagioclase if compared to pyroxene (Morrone et al 2018).

Also figure 4.55 shows that there is no correlation between beach area and roundness degree for both single crystal grains and volcanic lithic fragments on Vulcano island sand samples. Among single crystal grains olivine results always the most rounded grain in all samples followed by plagioclase and then by pyroxene. Among volcanic lithic fragments Lvmi texture is always the most rounded grain in all samples, whereas Lvv texture is always the most angular in all sand samples, Lvl texture shows an intermediate roundness degree between Lvmi and Lvv textures.

On Filicudi sand samples opaque minerals show the highest roundness degree regardless beach area, they are followed by plagioclase and pyroxene single grains; whereas on Alicudi sand samples olivine grains result the most rounded followed by plagioclase and pyroxene single grains, even if in both islands plagioclase and pyroxene monocrystals exhibit quite similar mean roundness trends (fig. 4.56). Lvmi texture is always much more rounded than Lvl and Lvv textures in all sand samples among volcanic lithic fragments of both Filicudi and Alicudi islands regardless beach area.

In addition have been carried out six test among Aeolian Islands beach sand by comparing roundness degree, grain textures and grain-size (fig. 4.57, 4.58) among the five sand fraction (Vc, C, m, f, Vf) for AL-3, Fi-3, SA-1, PN-1, STR-1, STR-9. By looking at figures 4.56a which relates mean roundness degree among both single crystal grains and lithic fragments it is possible to see a roundness degree increasing from very coarse to fine sand fraction for the Alicudi sample test (fig. 4.57a AL-3), whereas Filicudi test sample shows a roundness degree increasing from very coarse to medium sand fraction and a decreasing in the finer fractions (fig. 57 a Fi-3). By looking at the different grain textures trend (e.g. single crystal grains and lithic fragments) it is evident that also in the different sand fractions Lvv fragments are always the most angular grains among volcanic lithic fragments (fig. 4.57b, AL-3, Fi-3) especially in the very coarse sand fraction, whereas Lvv are more rounded in the very fine sand fraction (AL-3, Fi-3). On the contrary Lvmi texture is always the most rounded among the five sand fraction (fig. 4.57b, AL-3, Fi-3) and Lvl texture shows an intermediate roundness degree between Lvmi and Lvv among the five sand fractions. For both single crystal grains and lithic fragments very coarse sand fraction is the most angular (fig. 4.57 AL-3, Fi-3). In AL-3

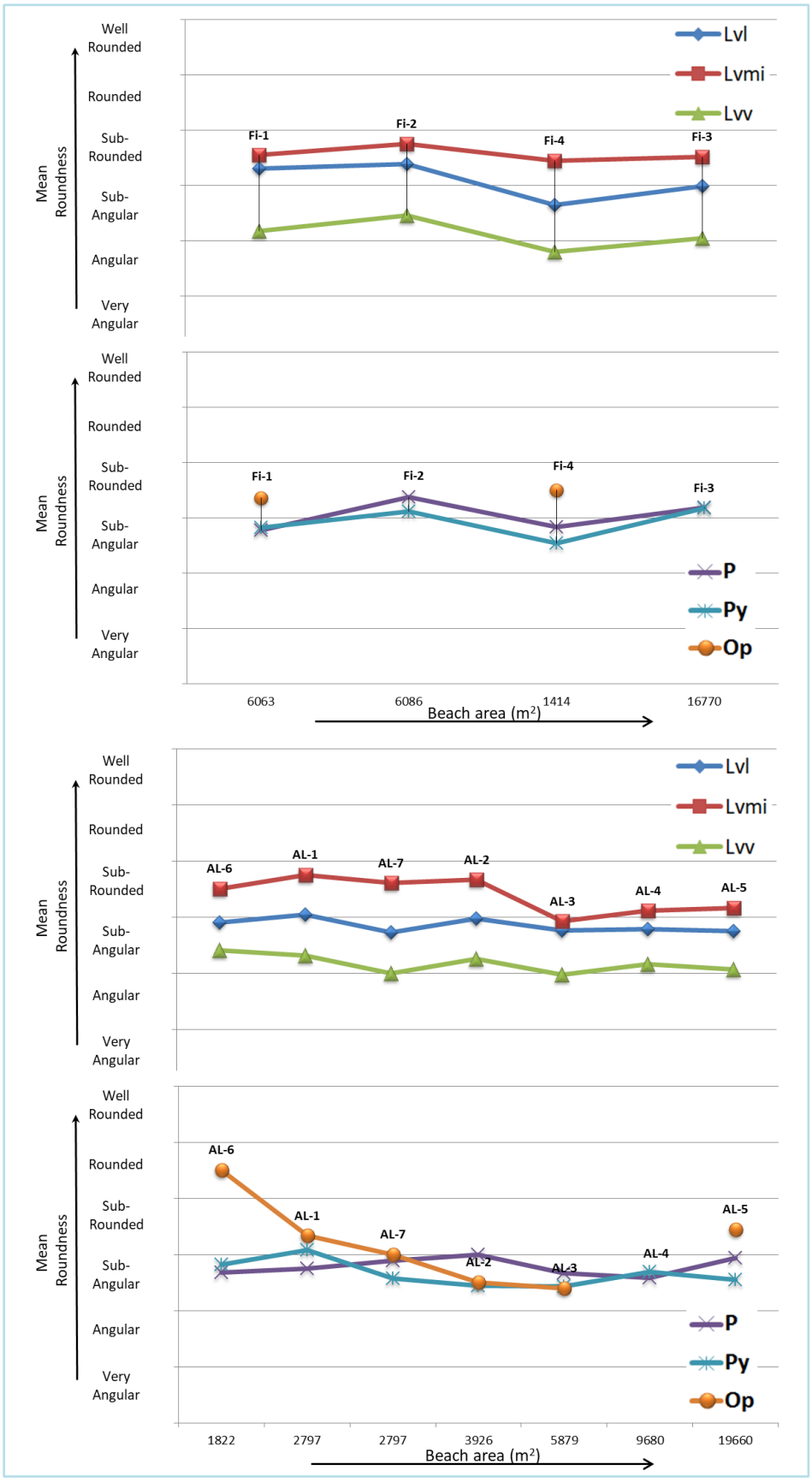

Figure 4.56 - Mean roundness vs. beaches area on Filicudi (upper) and Alicudi islands (lower).

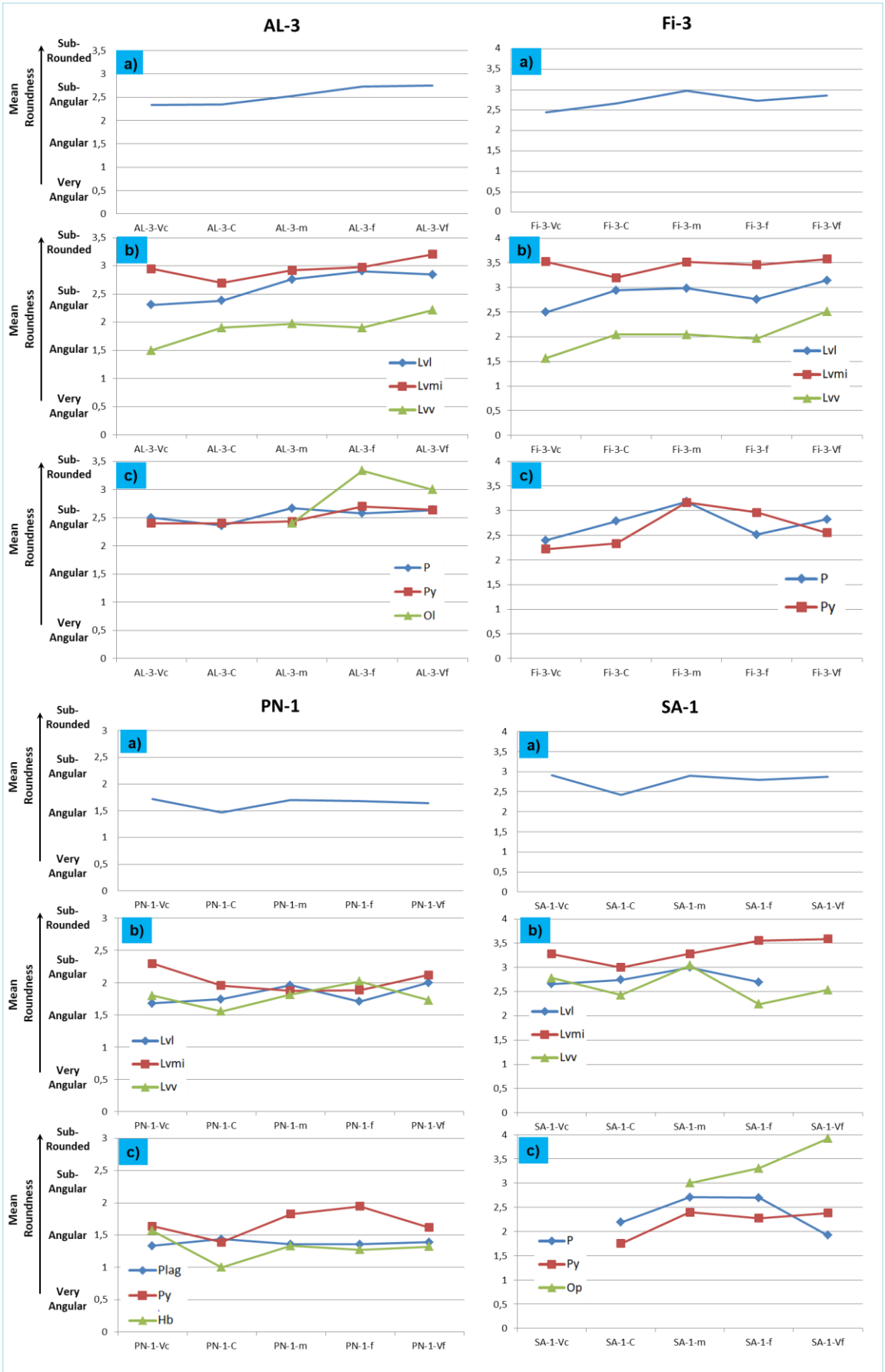

Figure 4.57 - Mean roundness vs. grain-size for Alicudi (upper left), Filicudi (upper right), Panarea (lower left) and Salina islands (lower right). a) mean roundness degree among all grain types.

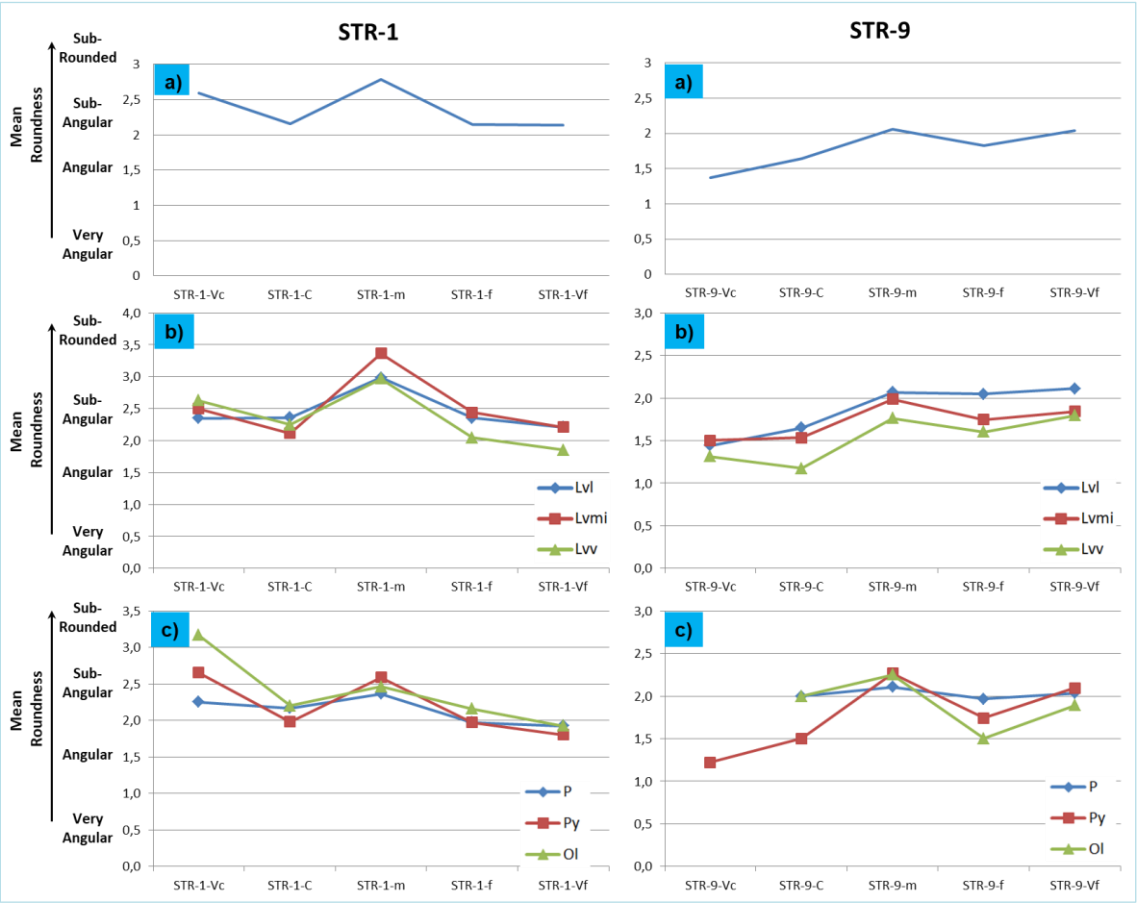

Figure 4.58 -- Mean roundness vs. grain-size for Stromboli beach sand (STR-1) and Stromboli crater sand (STR-9). a) mean roundness degree among all grain types; b) grain–size vs. mean roundness discriminated among the different volcanic lithic fragments; c) grain–size vs. mean roundness discriminated among single crystal grains.

sample olivine grains are more rounded in the fine sand and are not present in very coarse and coarse sand fractions, whereas in Fi-3 sample plagioclase and pyroxene are more rounded in the medium sand fraction.

Panarea sample test is more rounded than Salina sample test (fig. 4.57 PN-1a, SA-1a). There is a roundness degree decreasing trend from very coarse to coarse sand fraction and a roundness degree increasing from coarse to finer sand fractions in both samples.

Stromboli crater sand is more angular than Stromboli beach sand test samples (fig. 4.58). There is a slight positive trend from very coarse to very fine sand fraction in the crater sand sample among all grain types.

Volcanic lithic with lathwork texture (Lvl) is resulted more rounded in the medium sand fraction in five of the six tested samples, Lvv texture is resulted more rounded in the medium sand fraction in three of the six tested samples, Lvmi texture does not show any relation between roundness degree and grain-size. Pyroxene single grains are more

rounded in the medium sand fraction in four of the six tested samples, whereas plagioclase single grains are more rounded in the medium sand fraction in five of the six tested samples (fig. 4.57, 4.58).

Moreover, on the basis of geographic location beach samples have been grouped (fig.4.59). Major (e.g. western slopes) or minor (e.g. eastern slopes) escarpments (fig. 60, 61, 62, 63, 64, 65), responsible for mass-wasting, collapse and dissection of the volcanoes, seem to control the degree of evolution of beach and near-shore volcaniclastic sedimentation as the majority of beaches occur on the eastern side of the islands. The north-western side of the islands has the highest energy (wave energy) owing to predominant winds, whereas the eastern part of the islands is the most protected (C.N.R., 1985).

Thus, wave energy, in general, decreases from west to east. The mean roundness of all the grain types analyzed is considerably greater in the east than the west, and most increase progressively from north-west to east (fig. 60, 61, 62, 63,64,65).

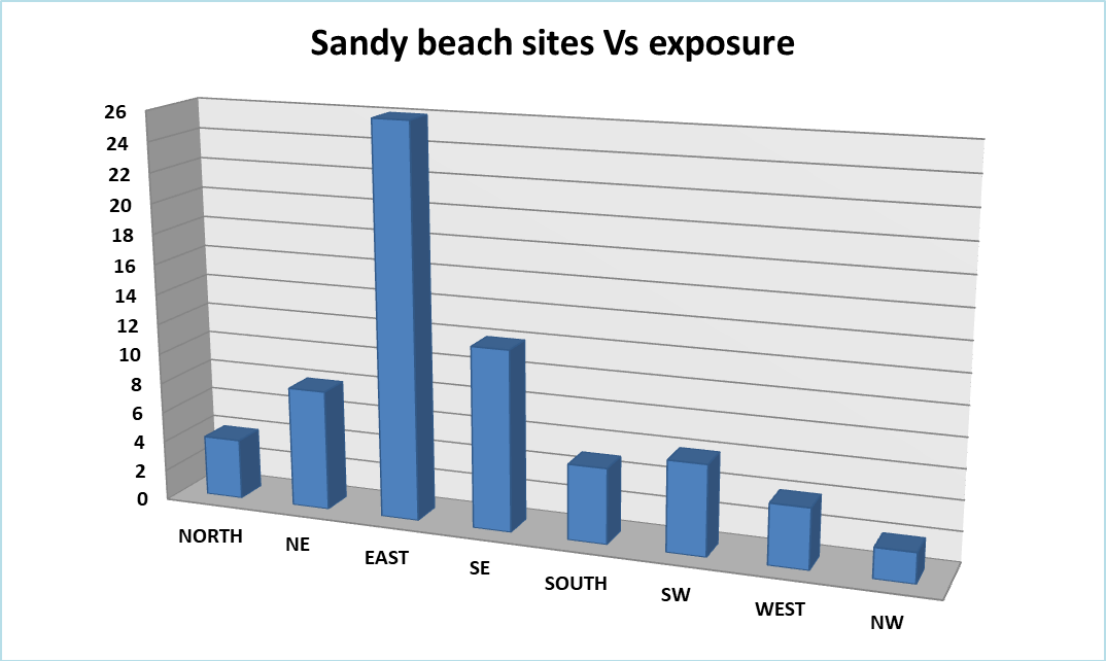

Figure 4.59 – Geographic exposure of the developed sandy beaches among all the Aeolian Islands coastal perimeters. On the y axis is shown the sampled sandy beaches total number; on the x axis is shown the geographic exposure (NE = north-east, SE= south-east, SW = south-west, NW = north-west).

Hence have been created Aeolian Islands thematic maps referred to the mean roundness among all grain types by comparing the geographic exposure of the sampled beaches (table 4.15 and figures from 4.60 to 4.64), which show roundness degree changing from western to eastern side of the Aeolian Islands.

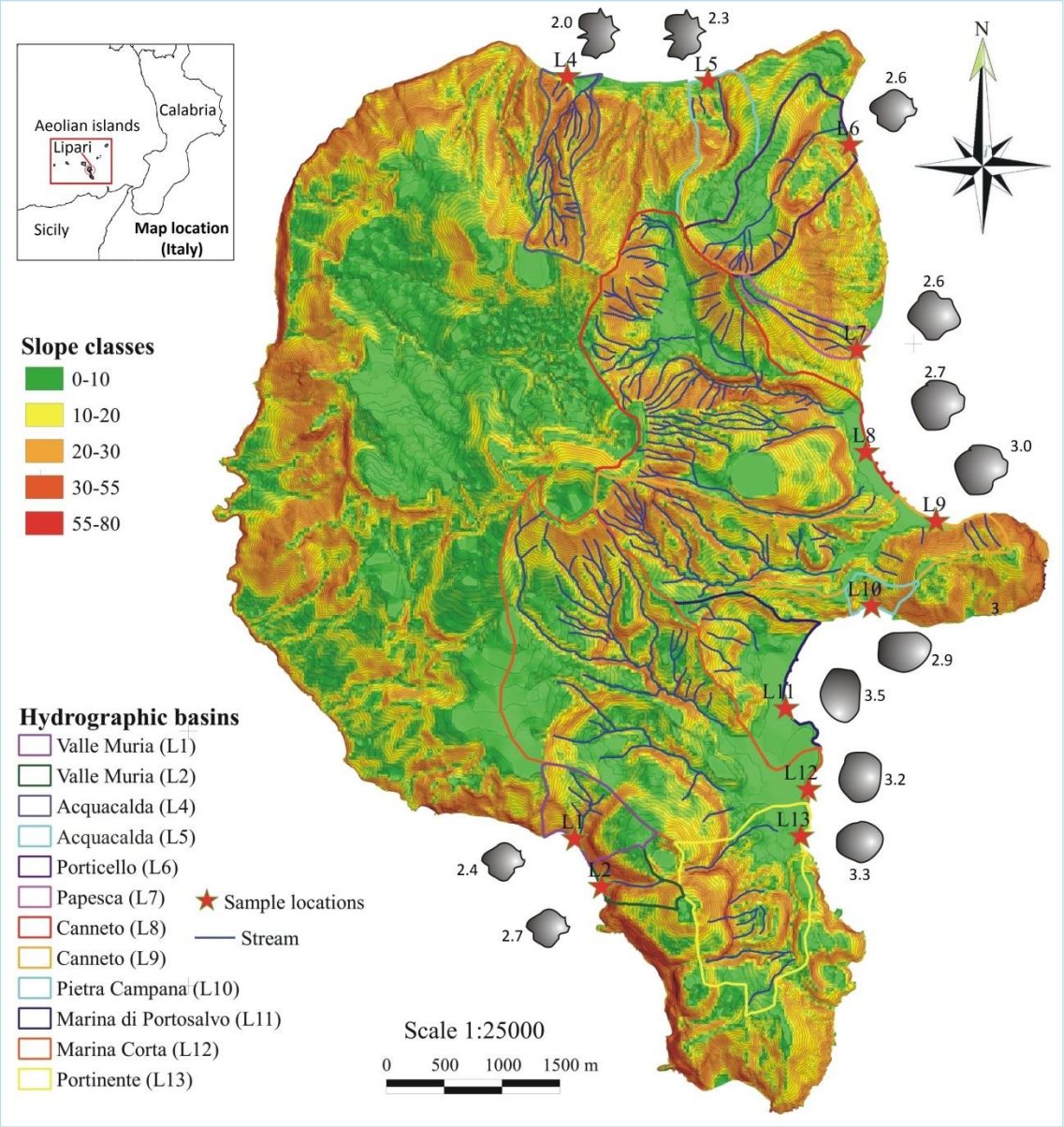

Figure 4.60 – Digital elevation map of Lipari island showing the different classes of slope, samples location and mean rounding of the analyzed sandy grain types (slope classes and hydrographic basins from Morrone et al. 2017 and mean roundness data are from Morrone et al., 2018).

Then by looking at these thematic maps is evident that the western sides of the all islands is often constituted by coastal steep-slope and by greater grain mean roundness values.

Sample	TOT MR	GE	Sample	TOT MR	GE	Sample	TOT MR	GE	Sample	TOT MR	GE
SA-1-m	2,9	E	L1-m	2,4	W	V1-m	2,5	SE	PN-1-m	1,7	SE
SA-2-m	2,9	E	L2-m	2,7	W	V2-m	2,8	SE	PN-2-m	1,7	SE
SA-3-m	2,9	SW	L4-m	2	NE	V4-m	3,0	E	PN-3-m	1,9	SE
SA-4-m	2,8	SW	L5-m	2,3	NE	V5-m	2,6	W	PN-4-m	2,1	SE
SA-5-m	2,8	NW	L6-m	2,6	NE	V6-m	2,4	W	PN-5-m	2,0	SE
SA-6-m	2,9	NE	L7-m	2,6	E	V7-m	3,0	E	PN-6-m	1,4	N
SA-7-m	2,6	NE	L8-m	2,7	E	V8-m	3,0	E	PN-7-m	1,3	W
SA-8-m	2,8	E	L9-m	3,0	E	V9-m	3,3	NE	PN-8-m	1,7	E
SA-9-m	2,9	E	L10-m	2,9	E	V10-m	3,2	E	PN-9-m	1,7	E
SA-10-m	3,0	E	L11-m	3,5	E	V11-m	2,8	E	PN-10-m	1,6	E
SA-11-m	3,0	E	L12-m	3,2	SE	V12-m	2,9	E	PN-11-m	1,5	NW
SA-12-m	2,9	E	L13-m	3,3	SE						
SA-13-m	3,0	E									
SA-14-m	3,0	SE									
SA-15-m	2,8	SE									
Sample	**TOT MR**	**GE**	**Sample**	**TOT MR**	**GE**	**Sample**	**TOT MR**	**GE**			
STR-1-m	2,7	E	AL-1-m	3,0	SE	Fi-1-m	3,0	NE			
STR-2-m	3,3	E	AL-2-m	2,8	SW	Fi-2-m	3,2	E			
STR-3-m	2,7	E	AL-3-m	2,5	W	Fi-3-m	3,0	NE			
STR-4-m	2,4	E	AL-4-C	2,7	W	Fi-4-m	2,8	S			
STR-5-m	2,6	E	AL-5-m	2,8	NE						
STR-7-m	2,3	N	AL-6-m	3,1	E						
STR-8-m	2,1	NE	AL-7-m	2,8	SE						
STR-9-m	2,0	CRATER									

Table 4.15 – Total mean roundness value of both volcanic lithic fragments and single crystal grains (TOT MR). GE = geographic exposure. SA = Salina island; L = Lipari island; V = Vulcano island; PN = Panarea island; STR = Stromboli island; AL = Alicudi island; Fi = Filicudi island.

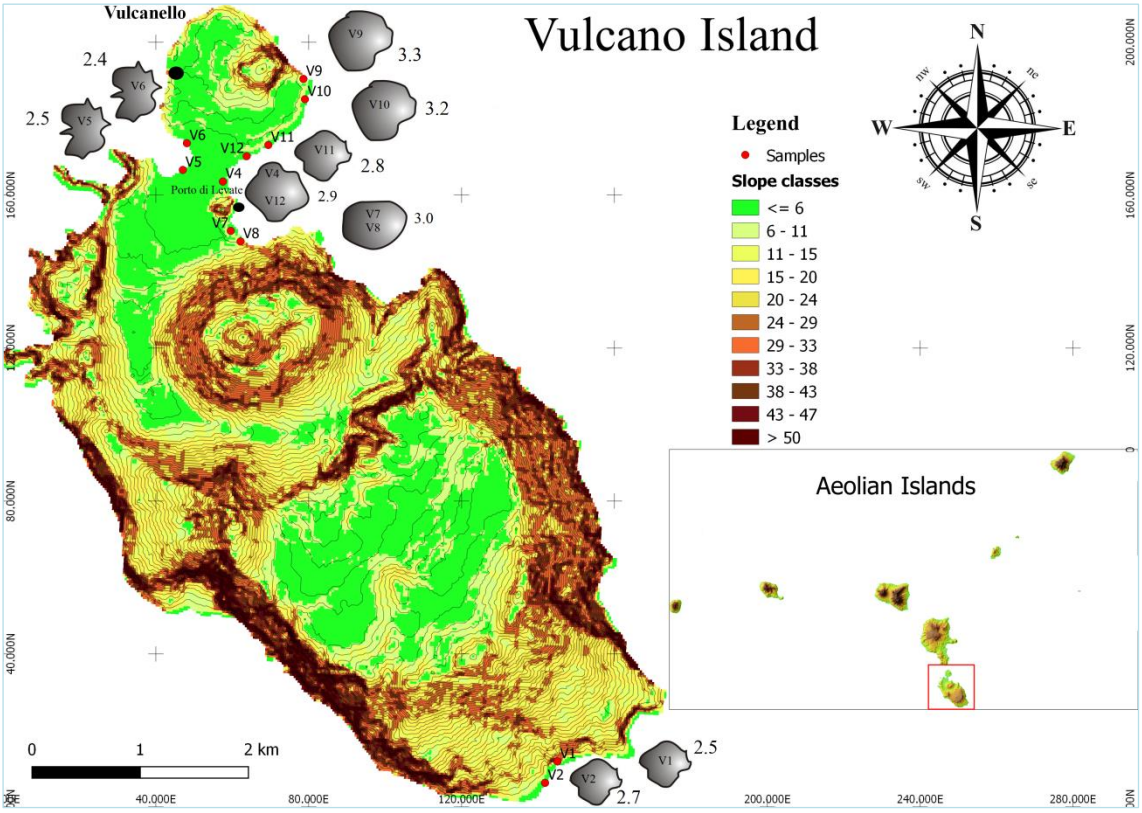

Figure 4.61 – Digital elevation map of Vulcano island showing the different classes of slope, samples location and mean rounding of the analyzed sandy grain types.

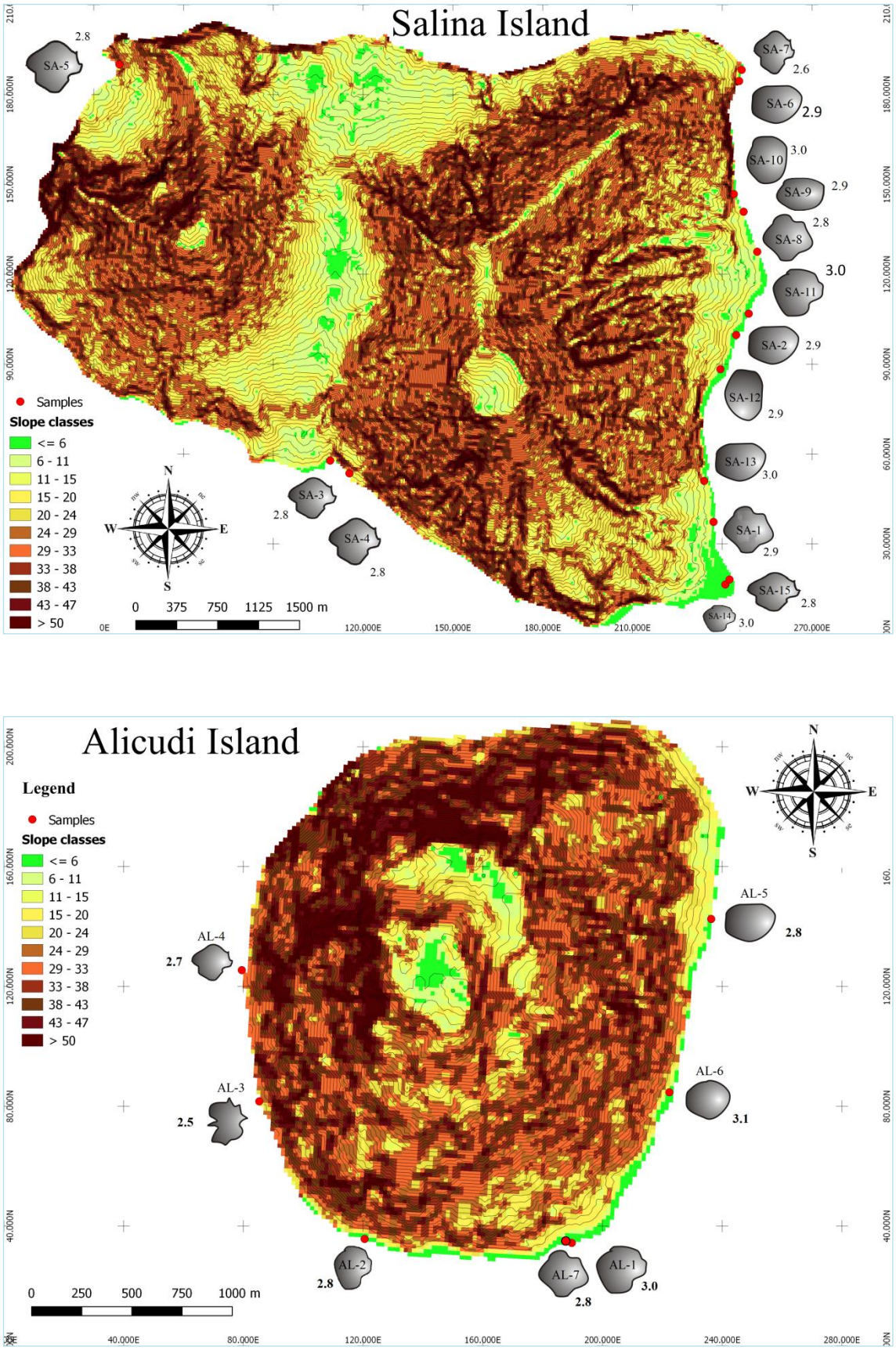

Figure 4.62 – Digital elevation map of Salina (upper) and Alicudi island (lower) showing the different classes of slope, samples location and mean rounding of the analyzed sandy grain types.

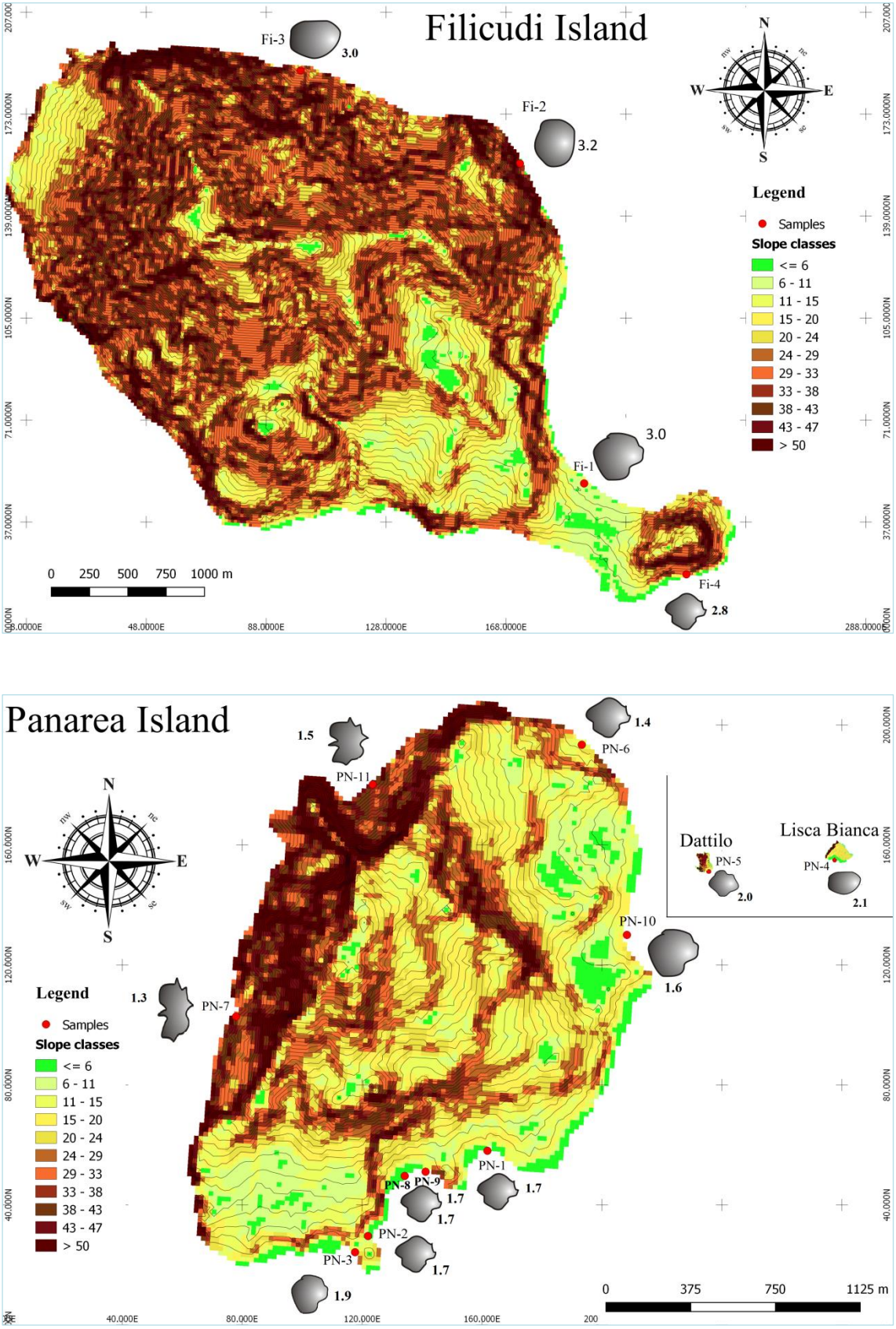

Figure 4.63 – Digital elevation map of Filicudi (upper) and Panarea island showing the different classes of slope, samples location and mean rounding of the analyzed sandy grain types.

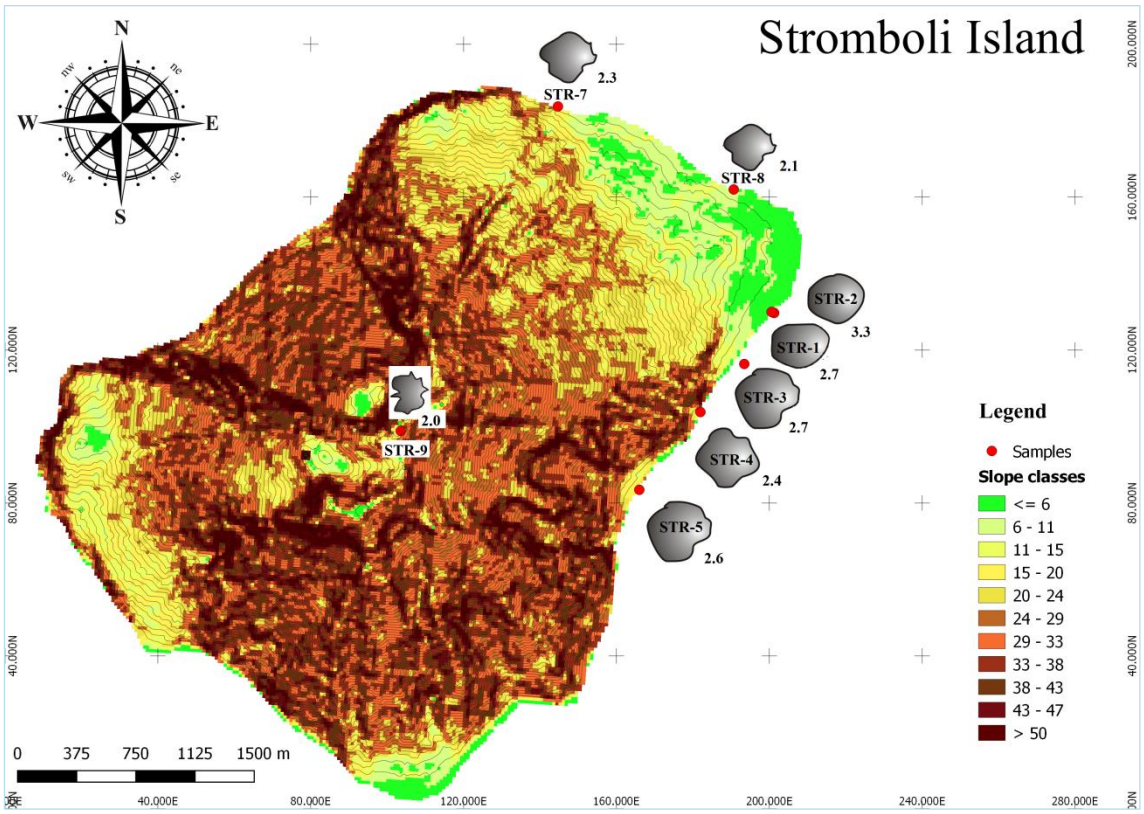

Figure 4.64 – Digital elevation map of Stromboli island showing the different classes of slope, samples location and mean rounding of the analyzed sandy grain types.

4.2.2.2 – CAMPANIA PROVINCE -

Phlegrean fields samples have an higher percentage of very angular (1) and angular (2) grains and lower percentage of sub-rounded (4) and rounded (5) grains with respect Licola-Volturno coastal stretch (fig. 4.61). The most common roundness category along Volturno-Naples coastal stretch is sub-angular (3), whereas along Portici-Sorrento coastal stretch the sub-sounded (4) followed by rounded (5) and sub-angular (3) with a very low occurrence of very angular (1), there is a mean roundness degree increasing from Portici to Sorrento coastal stretch. Vesuvius crater sands show an immature texture with higher very angular (1) category percentage (fig. 4.65).

It is very clear that the northernmost samples, towards the Volturno-river mouth, are more rounded than those toward Phlegrean Fields samples with only one peak corresponding to Gaiola sand sample (fig. 4.66), then samples become more angular around volcanic area which became again more rounded toward Portici. Among Licola sample series Li-4 sample is the most rounded. Along Portici - Torre Annunziata (Vesuvius volcanic area) coastline there is again a mean roundness decreasing and then there is a strong roundness degree increasing around Castellammare di Stabia area

(where samples are influenced by sedimentary source rocks). From Castellammare di Stabia to firsts Sorrento samples there is again a roundness degree decreasing (where samples resulted to be richer in volcanic lithic) then finally become more rounded toward the southernmost Sorrento sample (SO-1, fig. 4.66).

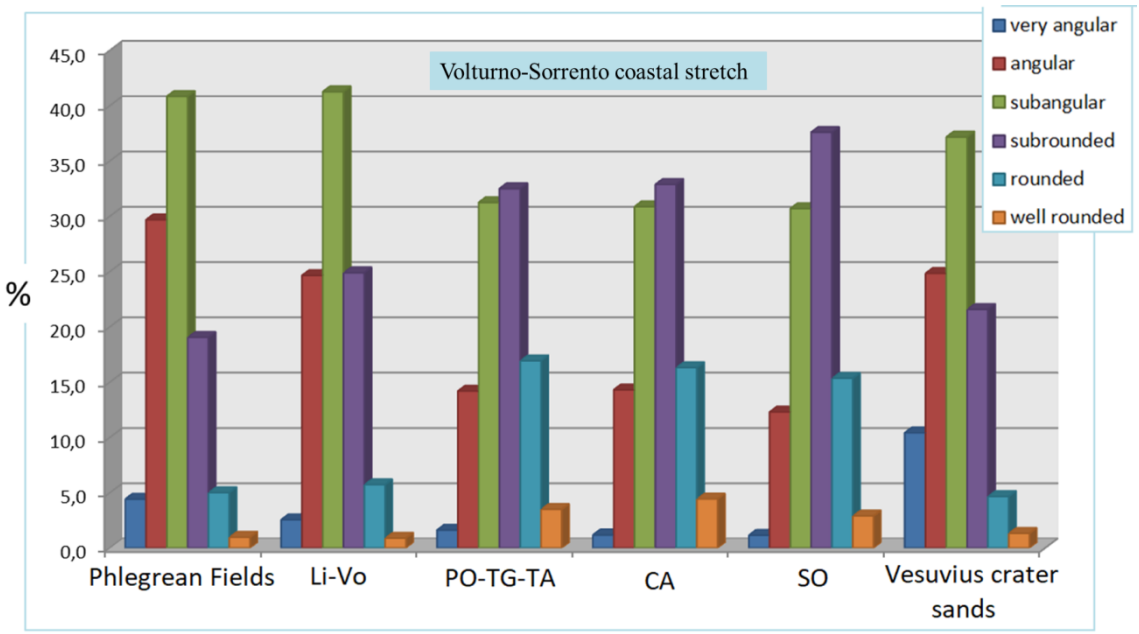

Figure 4.65 – Mean roundness percentage of all grain typologies along Volturno-Sorrento coastal stretch.

By comparing grain roundness degree and transport distance (km), from Vesuvius crater to the coast (Portici, Torre del Greco, Torre Annunziata, Castellammare di Stabia along about 15 km distance). After 15 km of transportation from the stream setting to the beach, the mean roundness change from 3 (sub-angular) to 4 (sub-rounded) (fig. 4.67), but this category jump it can be also attributed to the coastal reworking.

Moreover, it has been compared the roundness degree discriminated by sand composition (investigating in detail lithic fragments) and coastal stretch distance along Volturno-Sorrento coastal stretch (fig. 4.68, 4.69). Among the sedimentary lithic grains ($Lsc_{(xx)}$, $Lsc_{(micr)}$, Lss) those with micrite carbonate composition ($Lsc_{(micr)}$) are often more rounded than crystalline carbonate ($Lsc_{(xx)}$) and siliciclastic (Lss) composition. Between Bacoli and Nisida-Pozzuoli-bay volcanic lithic with microlitic texture (Lvmi) are always more rounded then lathwork (Lvl), vitric (Lvv) and felsitic (Lvf) textures with few exceptions (BC-2, PZ-14, PZ-2). Moreover, along this more protected coastal stretch (in depositional environment energy terms) pumice have been found in the sand fraction, they are always well preserved and show a very angular, angular and in a few cases sub-angular roundness category.

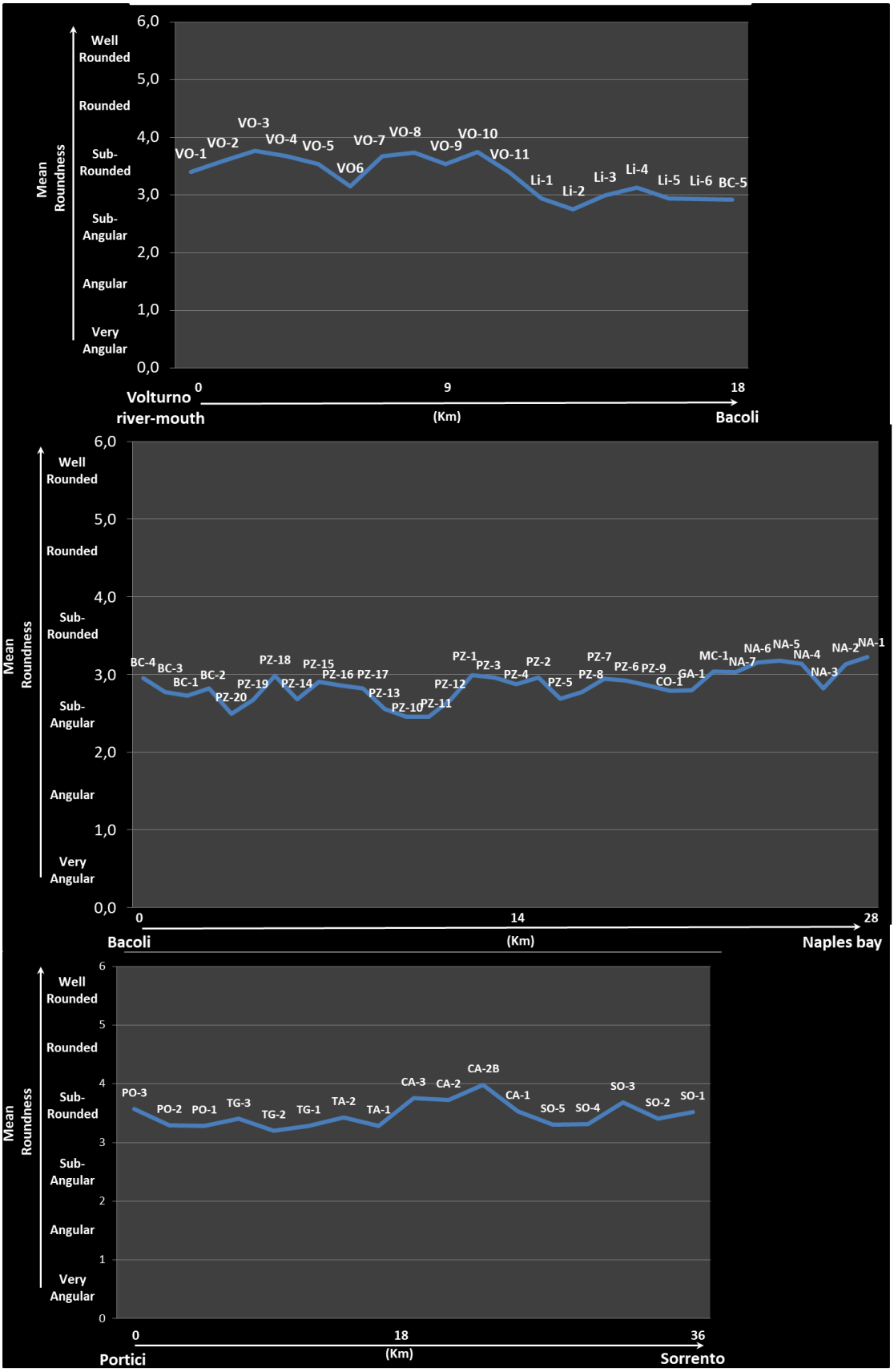

Figure 4.66 – Mean roundness variation along Volturno-Sorrento coastal stretch (about 80 km from north to south Campania coastline).

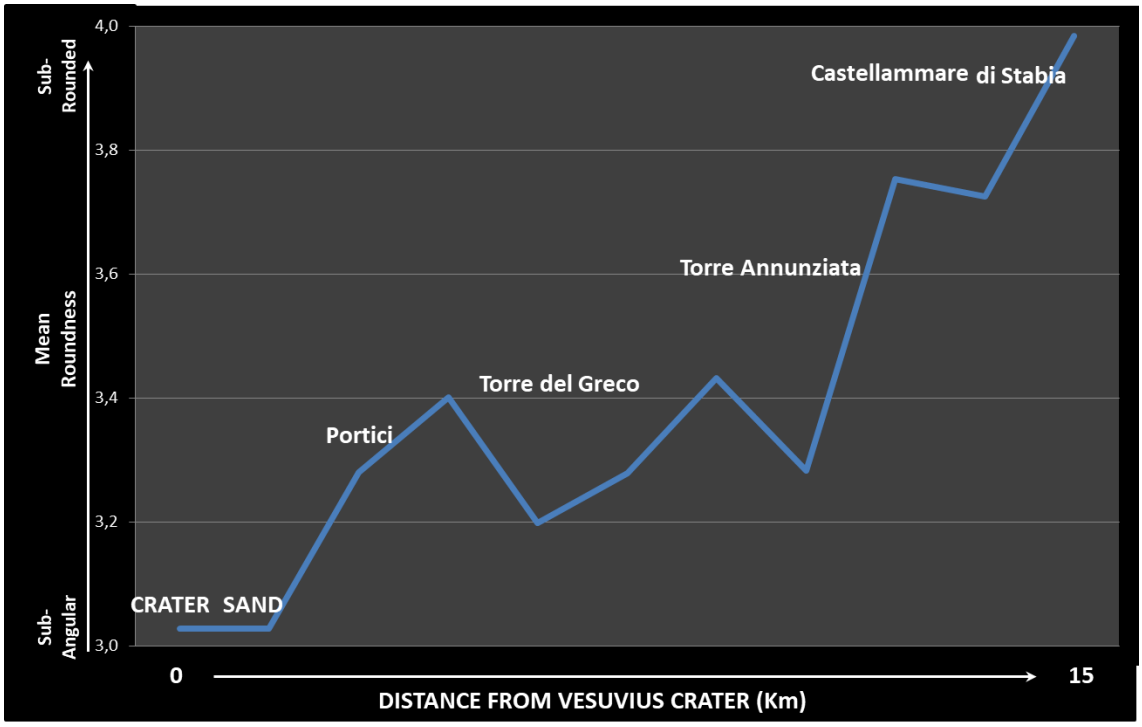

Figure 4.67 – Mean roundness variation from Vesuvius crater to Portici, Torre del Greco, Torre Annunziata, Castellammare di Stabia (along about 15 km distance).

Whereas along Coroglio-Naples-bay coastline, volcanic lithic with vitric texture (Lvv) resulted to be always more angular than lathwork (Lvl) and microlitic (Lvmi) textures among volcanic lithic fragments (fig. 4.68). Pumice are more rounded with respect previous coastal stretch (Bacoli-Pozzuoli-bay)

Along Portici-Sorrento coastal stretch is confirmed the following roundness degree ranking among volcanic lithic fragments :Lvmi > Lvl > Lvv, namely, microlitic texture is always more rounded in all sand samples analyzed in this coastal stretch (fig. 4.69a).

In Castellammare di Stabia area it is evident that the sedimentary lithic fragments ($Lsc_{(micr)}$, $Lsc_{(xx)}$) are always more rounded than volcanic lithic fragments (Lvl, Lvmi, Lvv), whereas among volcanic lithic fragments Lvmi are always more rounded than Lvl and among sedimentary lithic fragments $Lsc_{(micr)}$ are more rounded then $Lsc_{(xx)}$ (fig. 4.69b). There is a roundness category jump from 3.5 to 4.5 value for both sedimentary and lithic fragments (fig. 4.69b).

In figure 4.69c is shown the roundness degree of the Vesuvius zero order crater sands, Lvv texture are always more angular than Lvl and Lvmi textures but obviously the general roundness degree of all grains is lower than other Campania samples because of its immature texture (zero order sand).

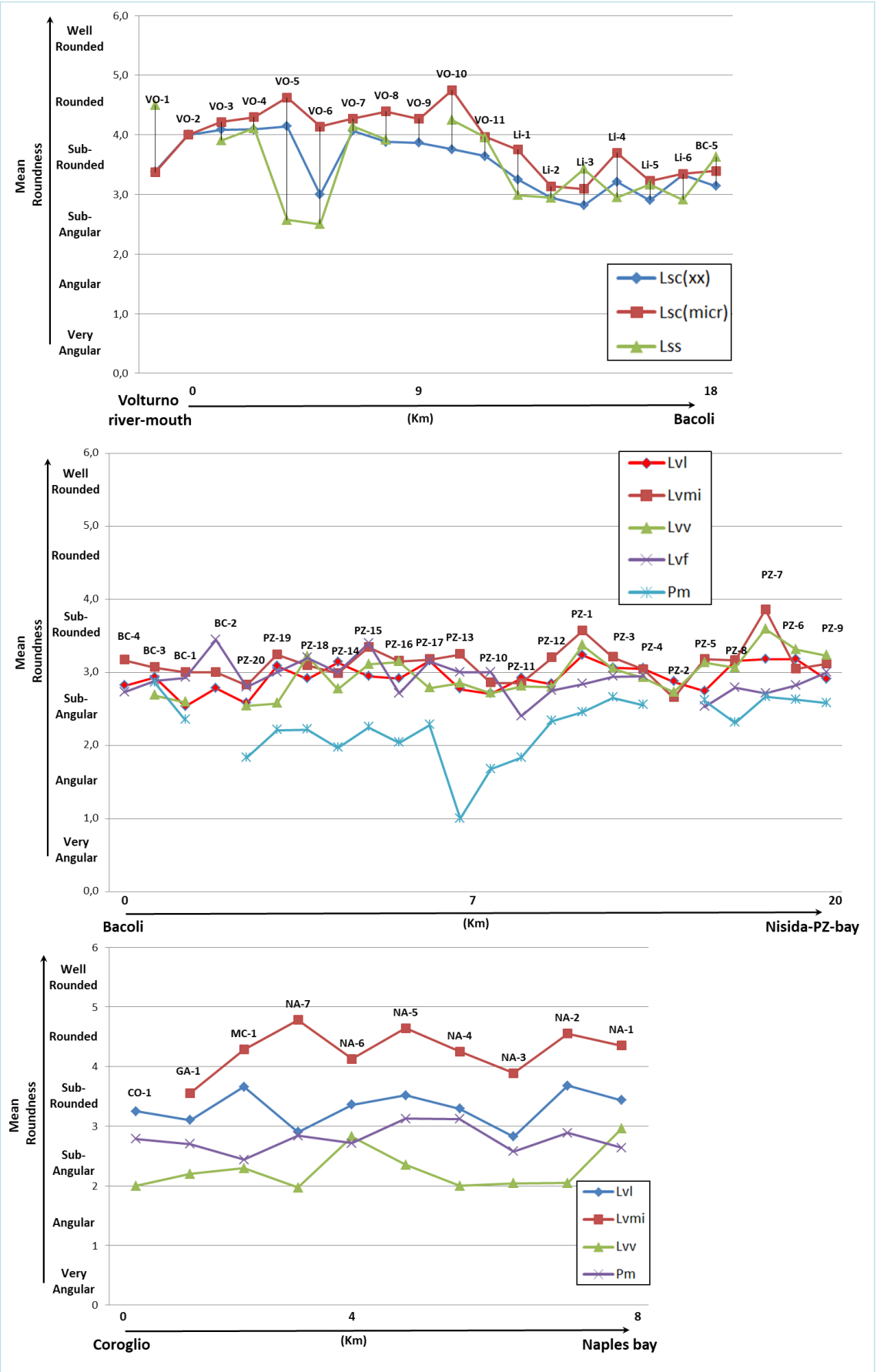

Figure 4.68 – Mean roundness vs. lithic fragments sand composition and their roundness variation along Volturno-Naples coastal stretch (about 46 km from north to south Campania coastline).

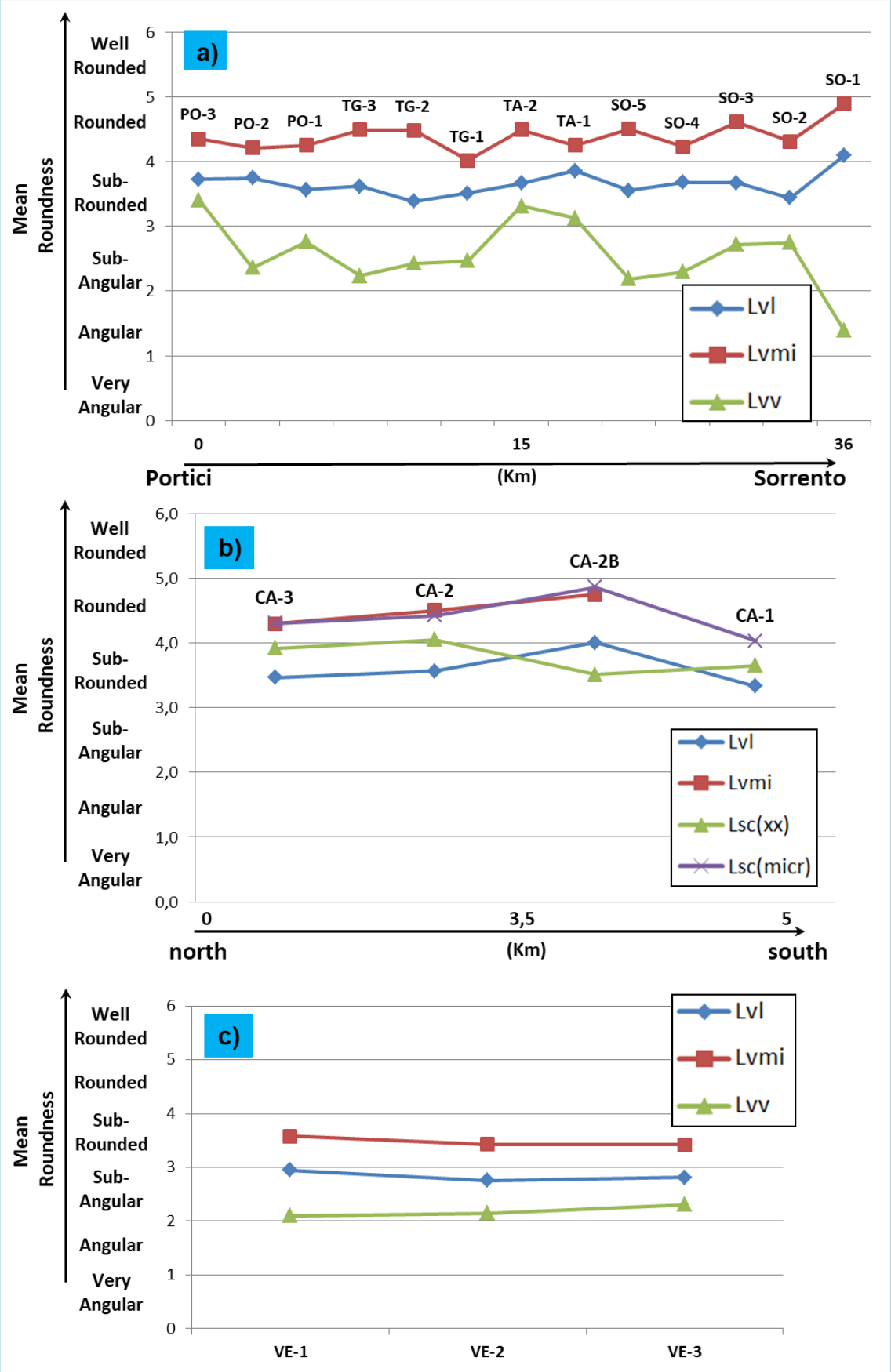

Figure 4.69 – Mean roundness vs. lithic fragments sand composition and their roundness variation along Portici-Sorrento coastal stretch (a), Castellammare di Stabia area (b) and Vesuvius crater sands (c).

In figure 4.70 and 4.71 have been compared the mean roundness among single crystal grains along Volturno-Sorrento coastal stretch. Among k-feldspar (K), monocrystalline quartz (Qm) and calcite (Ca), the latter is always more rounded than Qm and K with few exceptions (Li-1, Li-2, Li-4), whereas Qm and K have similar roundness trend (fig. 4.70).

Between Bacoli and Nisida-Pozzuoli-bay coastline, plagioclase single grain (P) is more rounded than K-feldspar (K) with few exceptions (BC-3, PZ-3,PZ-4,PZ-7) (Fi. 4.70).

Between Coroglio and Naples-bay coastline, pyroxene (Py), plagioclase (P) and K-feldspar (K) single crystal grains have a similar roundness trend showing a roundness value around 3 (sub-angular, fig. 4.70).

Along Portici-Sorrento coastal stretch among Leucite (Le), pyroxene (Py), K-feldspar (K) and plagioclase single crystal grains, the Le is always the most rounded grain type in all sand samples, Py, P and K have a similar roundness trend even if the K grain type seem to be slightly more rounded than other two (fig. 4.71a).

In Castellammare di Stabia sand samples opaque minerals are always more rounded than plagioclase (P) and pyroxene (Py) single crystal grains, whereas P and Py have a very similar roundness trend (fig. 4.71b).

In figure 4.71c is shown the roundness degree of the Vesuvius zero order crater sands, even if are zero order crater sands is clearly that leucite (Le) and olivine (Ol) single crystal grains are always more rounded than other single crystal grain and in this case more rounded than pyroxene (Py).

In addition have been carried out three test among Campania beach sand by comparing roundness degree and grain-size (fig. 4.72) among the five sand fraction (Vc, C, m, f, Vf) for PZ-8, PZ-14 BC-1. There is a roundness degree decreasing from very coarse to medium sand fraction among the three sample test (fig. 4.72) and there is a trend reversal from medium to fine for PZ-8 and from medium to very fine sand fraction for PZ-14 and BC-1 samples. Thus, there is a general trend which shows that the more rounded grain are in the very coarse sand fraction.

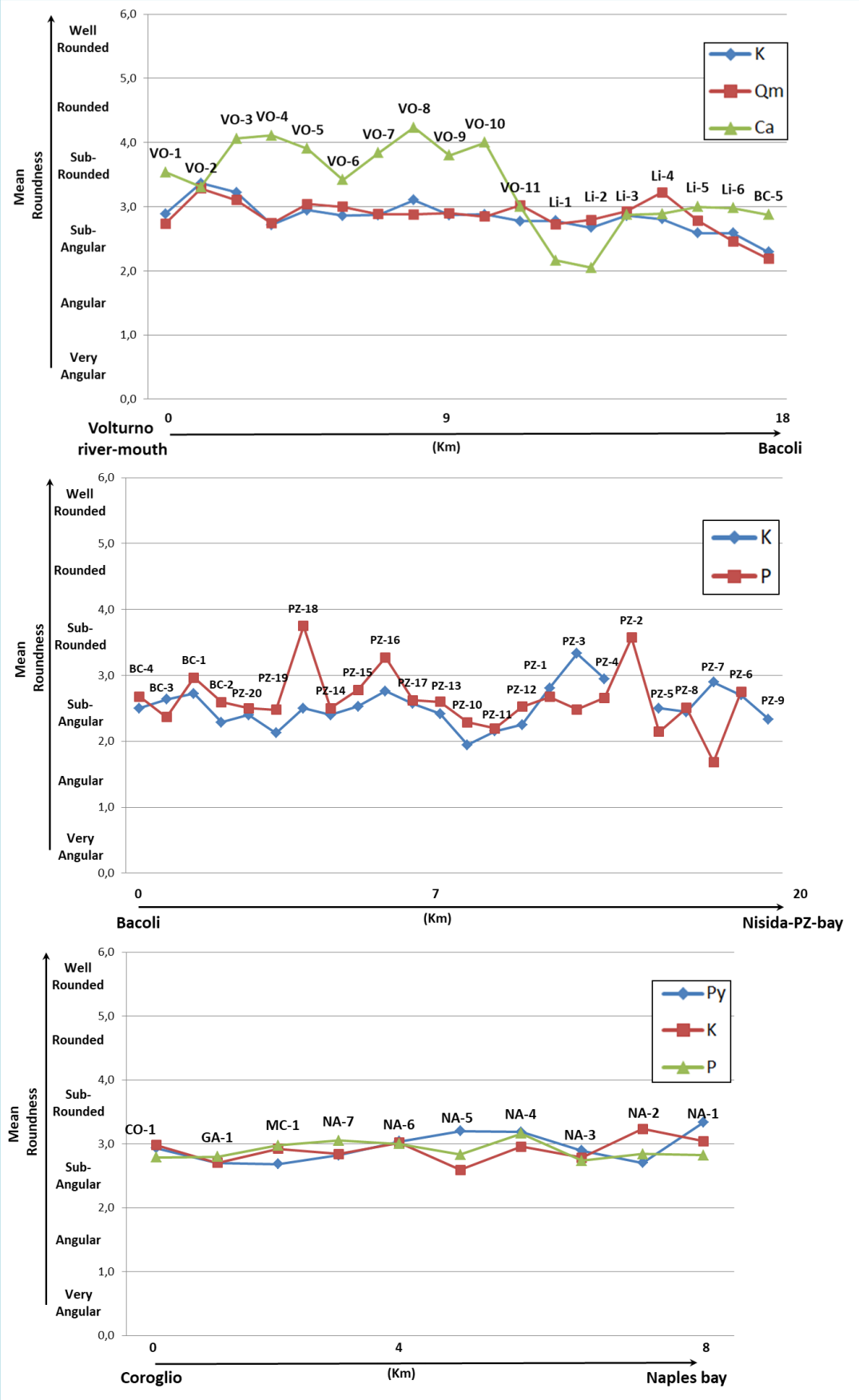

Figure 4.70 – Mean roundness vs. single crystal grains sand composition and their roundness variation along Volturno-Naples coastal stretch (about 46 km from north to south Campania coastline).

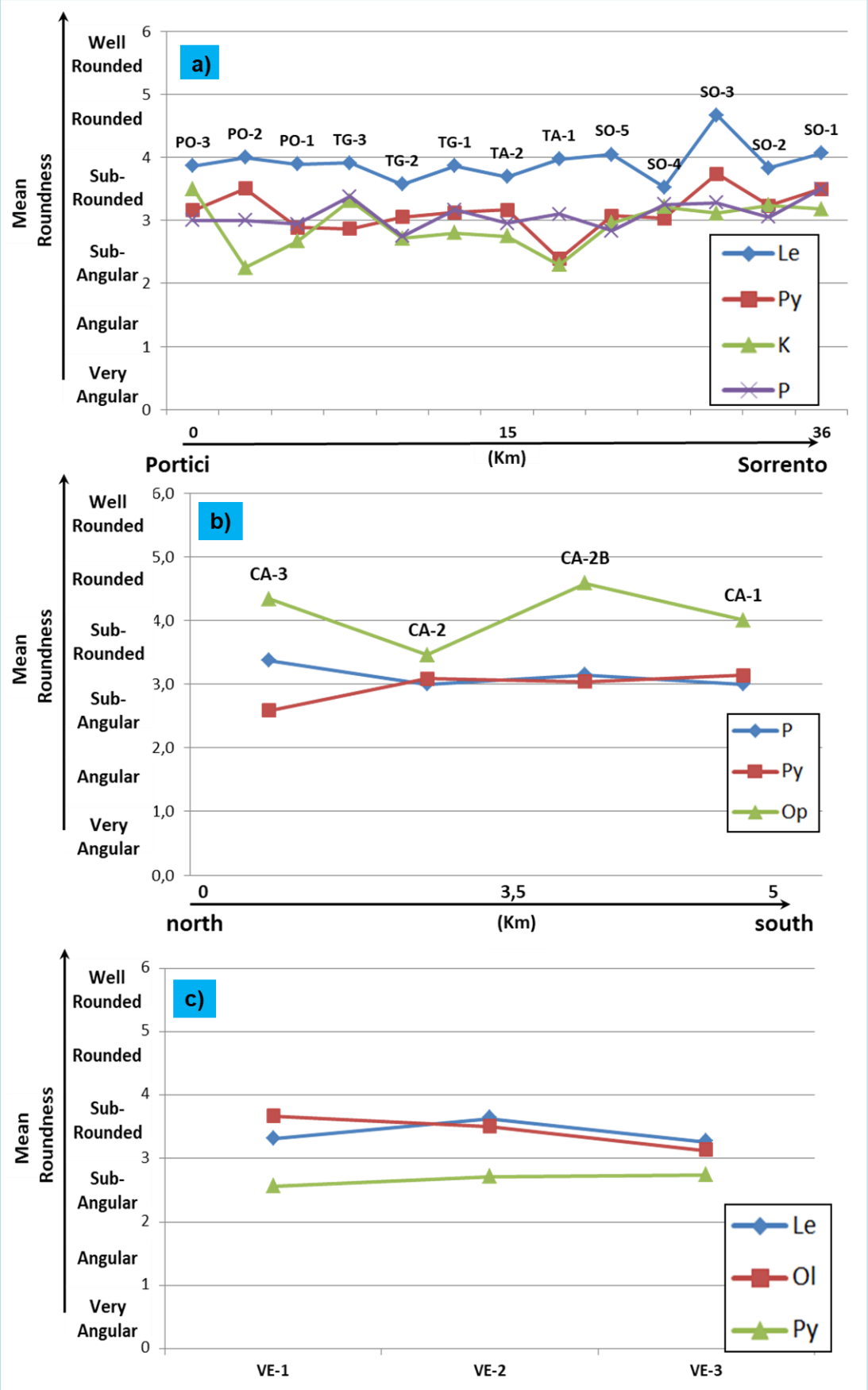

Figure 4.71 – Mean roundness vs. single crystal grains sand composition and their roundness variation along Portici-Sorrento coastal stretch (a), Castellammare di Stabia area (b) and Vesuvius crater sands (c).

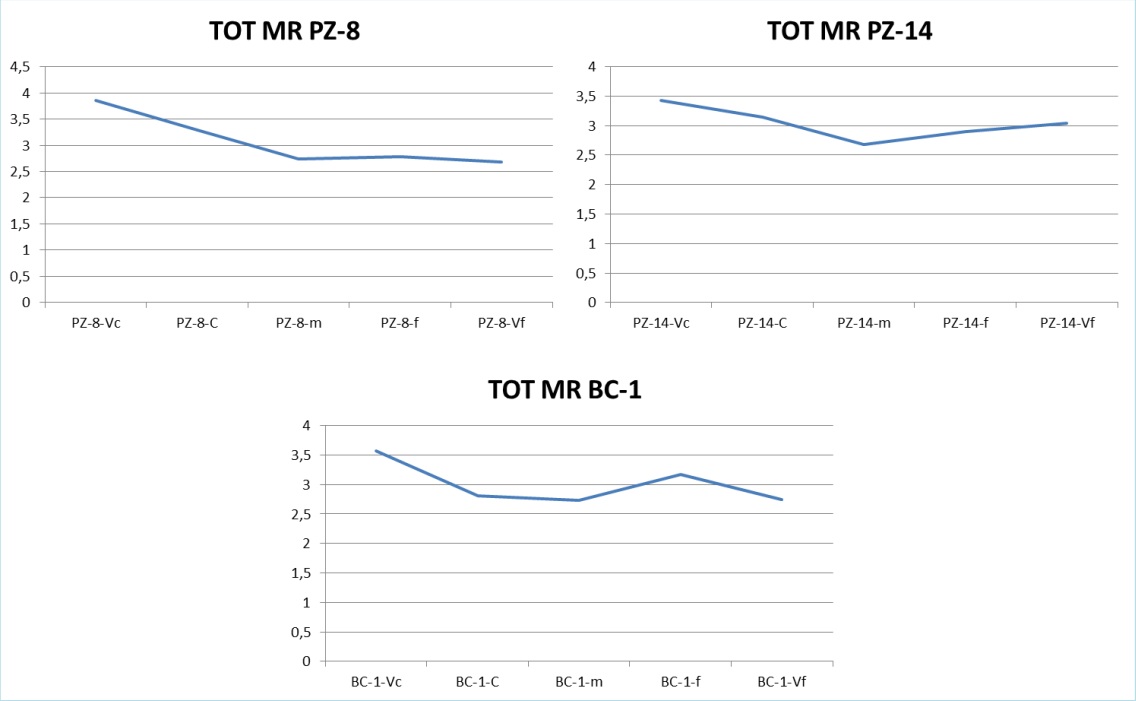

Figure 4.72 - Mean roundness degree vs. grain-size among all grain types. MR = mean roundness.

4.3 – ROUNDNESS STUDY- (IMAGE ANALYSIS) -

Image Analysis is a technique that allows to obtain measurements and information from digital images using appropriate software. Through this technique, it is possible to recognize and then isolate interested objects within a digital image and through appropriate processing, obtain various information types (for example brightness, color, size, shape, texture, spatial orientation, etc.) related to such objects.

Several studies have been carried out using image analysis as a supplemental process to normal laboratory analysis, or as an independent process (e.g. Protz and Vandenbygaart, 1998; Miriello and Crisci, 2006; Marcelino et al., 2007; Jangorzo et al. 2013, Bryk et al., 2014).

Although considerable progress has been made in recent decades, currently there isn't a universal method for micromorphological studies by image analysis; this is due to several factors such as the specific purpose of work, different samples, operator subjectivity although software procedures are largely automatic, but the operator's skills are really important to direct the software behavior then operator will check that the obtained results are plausible.

For this study it has been used the Miriello and Crisci (2006) modified technique, they study porosity in grout samples by scanning thin sections through a system consisting of a plane scanner for slides and two polarizing sheets. Thus, they acquire congruent digital images in transmitted natural light and cross-polarizers.

We wanted better to investigate grains rounding degree trough image analyses by carrying out tests on 42 sand samples of both thin section and bulk sample (fig. 4.73). Hence, mean roundness was calculated by scanning thin section in transmitted light and bulk granular sample with classic scansion using a V550 Epson scanner (fig. 4.73). The values between these different techniques have been compared for all sample grains without grain-type distinction to evaluate the general mean roundness of the samples and to test this technique by comparing mean roundness analyses trough optical microscope.

Data were processed using *ImageJ* software, in particular were used the *roundness* and *circularity* parameters to calculate the grains rounding. The *roundness* parameter is expressed by the formula (4.1):

$$Roundness = 4\ \frac{[\text{Area}]}{\pi[Major\ axis]^2} \qquad (4.1)$$

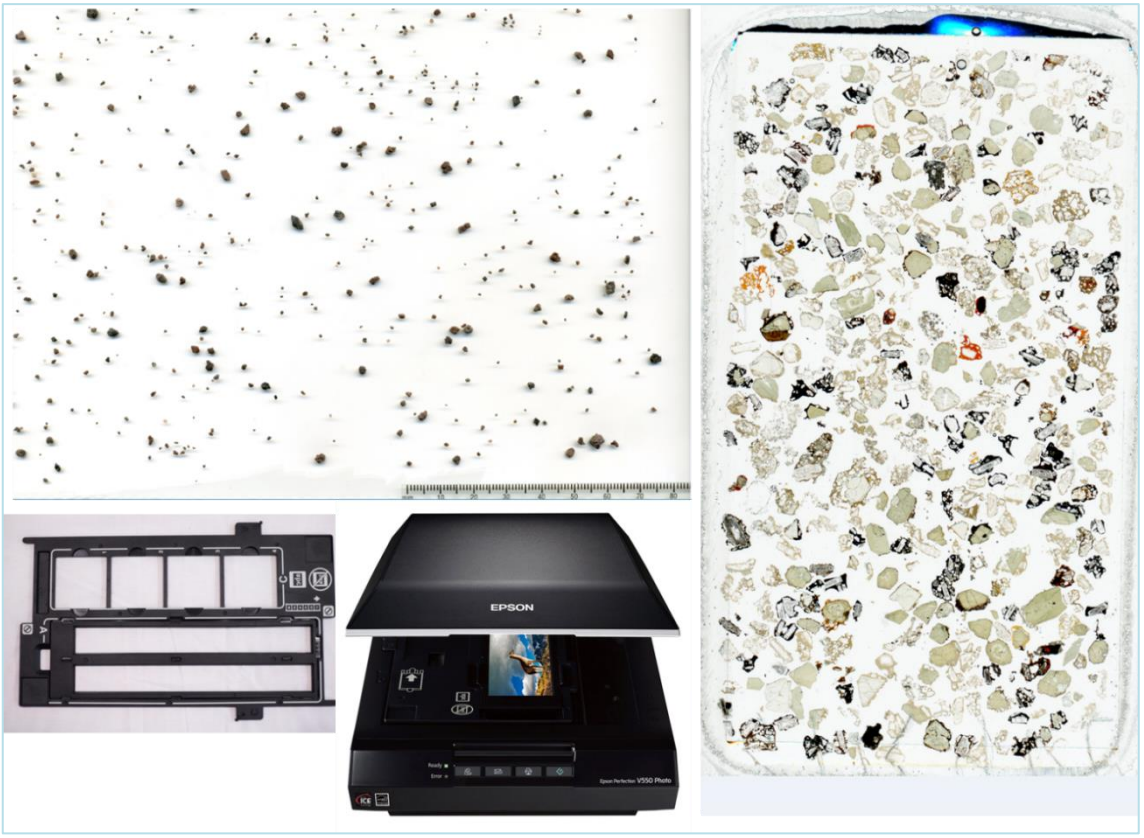

Figure- 4.73 - Thin section (upper right) and bulk sample (upper left, lower) scanning method.

Roundness parameter ranges from 0,0 to 1, from equal dimensional (1,0) to progressively elongated shape (0,0). This parameter refers to the ellipse major axis which approximates the shape, regardless shape edges, whereas circularity refers to the perimeter.

The *circularity* parameter is expressed by the formula (4.2):

$$Circularity = 4\pi \frac{[\text{Area}]}{[Perimeter]^2} \qquad (4.2)$$

Particles with size circularity values outside the range specified in this field are also ignored. It ranges from 0,0 (infinitely elongated polygon) to 1,0 (perfect circle). As the value approaches 0,0 it indicates an increasingly elongated shape. Values may not be valid for very small particles.

It has been calibrated a roundness scale with values ranges from = 0,0 to 1,0 from very angular to well rounded (fig. 4.74) after several test by analyzing specially created geometric figures and several sample grains.

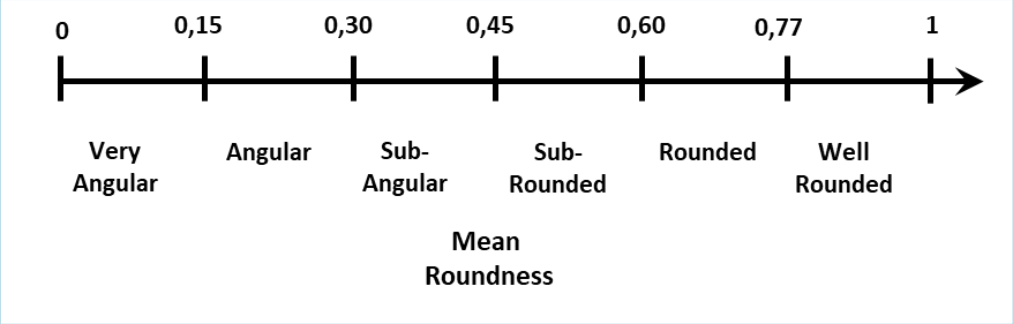

Figure 4.74 – Calibrated scale used to determine grains roundness class.

4.3.1 – THIN SECTION IMAGE ANALYSIS RESULTS-

For each analyzed sample it has been obtained a known analyzed grains number (fig. 4.75) and for each grain it is possible to know roundness and circularity values (4.75) then it has been calculated a roundness and circularity mean value for each analyzed sample, these values have been successively plotted on the calibrated roundness scale (fig. 4.76) to understand which of both parameters better reflect the real grains roundness category of the analyzed samples by also comparing these three results such as scanned thin section, scanned bulk granular samples and microscope technique results (see also discussion chapter). Figure 4.75 shows that it is also possible to recognize in detail to recognize in detail the values of each grain which

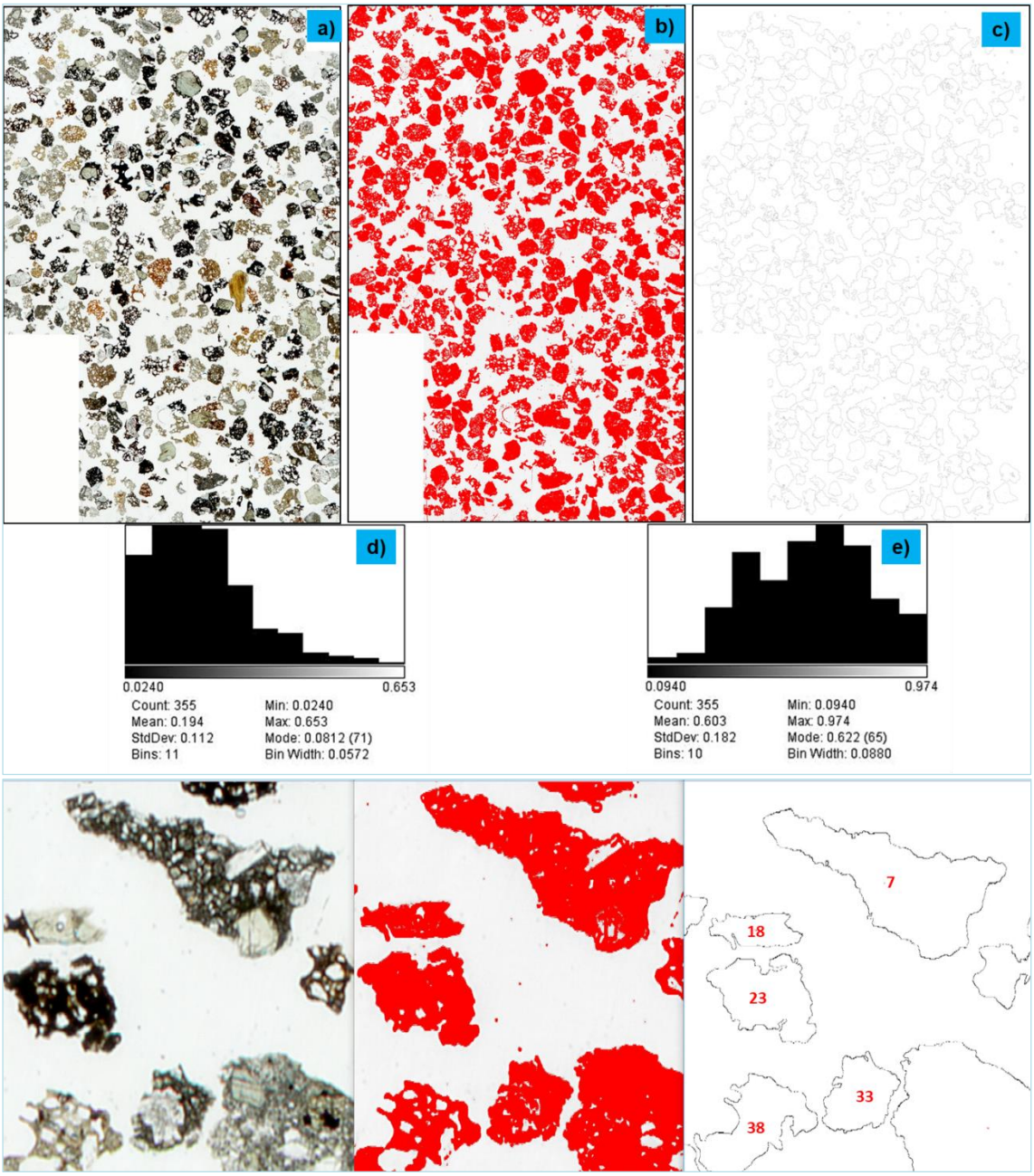

Figure 4.75 – AL-3-Vc thin section sample. a) Transmitted natural light scanned image; b) selected grains to analyzing; c) drawn grain boundaries by the software processing; d) circularity distribution values; e) roundness distribution values. Lower figure shows a close-up of the image processing steps.

have been identified by the software with a number. AL-3-Vc sample displays a 0,194 circularity mean value and a 0,603 roundness mean value among 355 analyzed grains (fig. 4.75d, e, 4.76). Based on circularity mean value AL-3-Vc sand sample falls in the angular category and based on roundness parameter it falls in the rounded category, whereas according to optical microscope results (mean roundness) it falls in sub-angular category (2,33) among 246 analyzed grains (fig. 4.76).

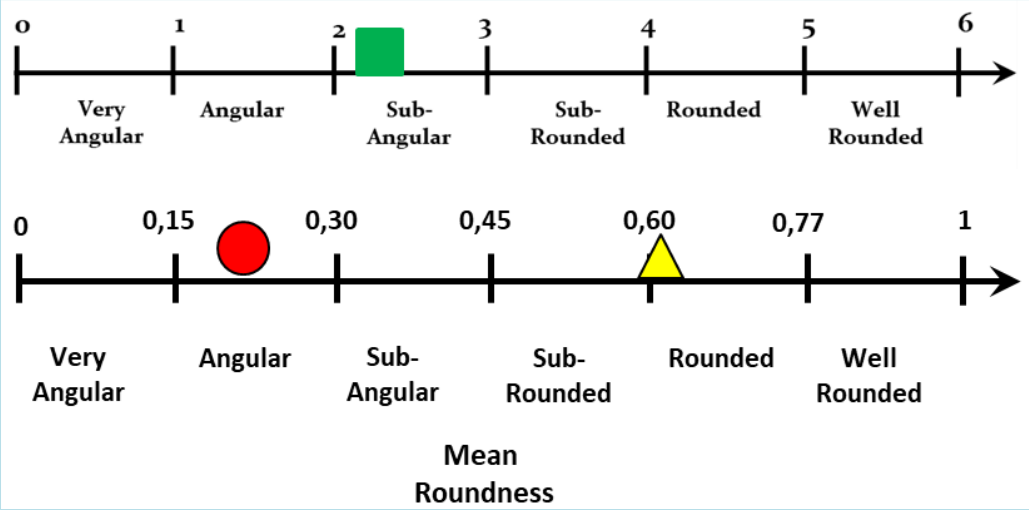

Figure 4.76 – AL-3-Vc sample. Red circle = circularity mean value; yellow triangle = roundness mean value; green square = optical microscope results plotted on Folk scale (upper).

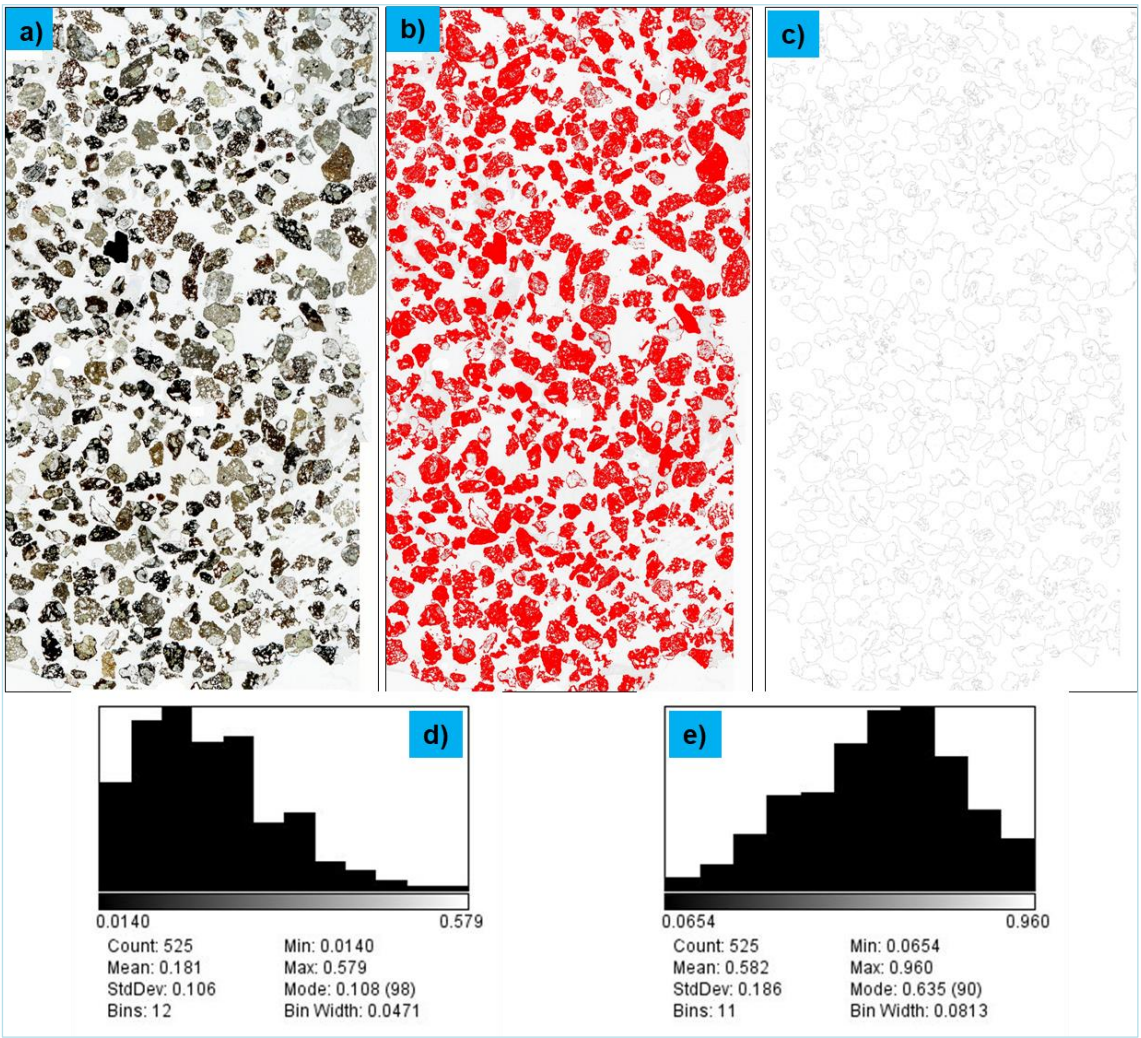

Figure 4.77 – Fi--3-Vc thin section sample. a) Transmitted natural light scanned image; b) selected grains to analyzing; c) drawn grain boundaries by the software processing; d) circularity distribution values; e) roundness distribution values.

Fi-3-Vc sand sample displays a 0,181 circularity mean value and a 0,582 roundness mean value among 525 analyzed grains (fig. 4.77d, e,). Based on circularity mean value Fi-3-Vc sample falls in the angular category and based on roundness parameter it falls in the sub-rounded category, whereas according to optical microscope results (mean roundness) it falls in sub-angular category (2,44) among 259 analyzed grains (fig. 4.78).

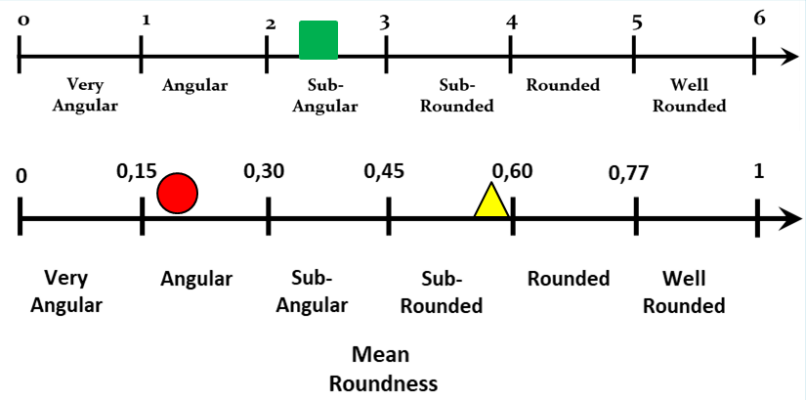

Figure 4.78 – Fi-3-Vc sample. Red circle = circularity mean value; yellow triangle = roundness mean value; green square = optical microscope results plotted on Folk scale (upper).

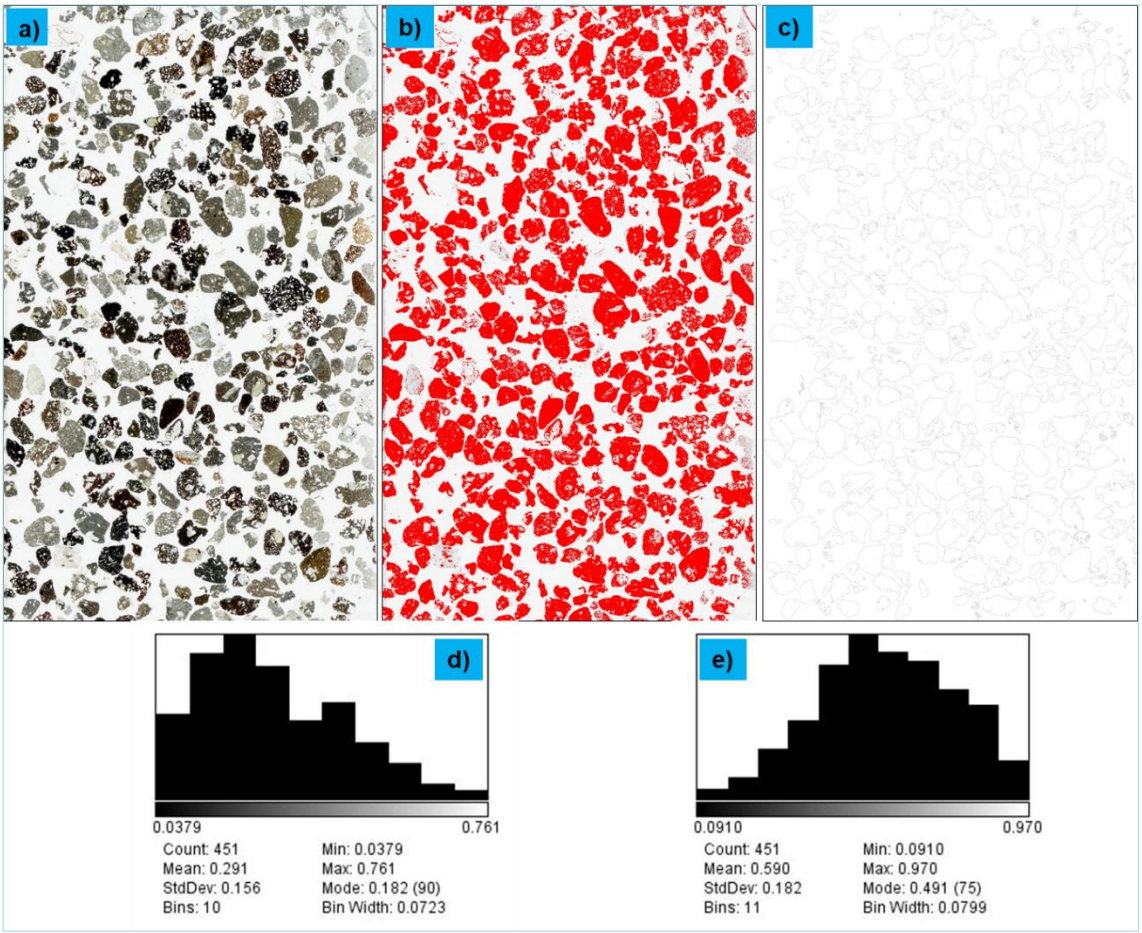

Figure 4.79 – SA-1-Vc thin section sample. a) Transmitted natural light scanned image; b) selected grains to analyzing; c) drawn grain boundaries by the software processing; d) circularity distribution values; e) roundness distribution values.

SA-1-Vc sand sample displays a 0,291 circularity mean value and a 0,590 roundness mean value among 451 analyzed grains (fig. 4.79d, e,). Based on circularity mean value SA-1-Vc sample falls in the angular category and based on roundness parameter it falls in the sub-rounded category, whereas according to optical microscope results (mean roundness) it falls in sub-angular category (2,91) calculated among 346 analyzed grains (fig. 4.80).

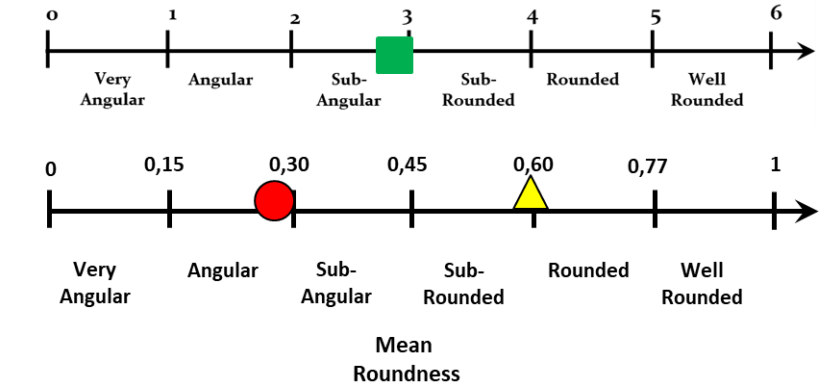

Figure 4.80 – SA-1-Vc sample. Red circle = circularity mean value; yellow triangle = roundness mean value; green square = optical microscope results plotted on Folk scale (upper).

L2-m sand sample displays a 0,40 circularity mean value and a 0,603 roundness mean value among 489 analyzed grains (fig. 4.81d, e,). Based on circularity mean value L2-m sample falls in the sub-angular category and based on roundness parameter it falls in the rounded category, whereas according to optical microscope results (mean roundness) it falls in sub-angular category (2,93) (as well as circularity results) calculated among 395 analyzed grains (fig. 4.81).

V5-m sand sample displays a 0,344 circularity mean value and a 0,594 roundness mean value among 901 analyzed grains (fig. 4.82d, e,). Based on circularity mean value V5-m sample falls in the sub-angular category and based on roundness parameter it falls in the sub-rounded category, whereas according to optical microscope results (mean roundness) it falls in sub-angular category (2,55) (as well as circularity results) calculated among 394 analyzed grains (fig. 4.81).

PN-1-Vc sand sample displays a 0,165 circularity mean value and a 0,558 roundness mean value among 901 analyzed grains (fig. 4.84d, e,). Based on circularity mean value PN-1-Vc sample falls in the angular category and based on roundness parameter it falls in the sub-rounded category, whereas according to optical microscope results (mean

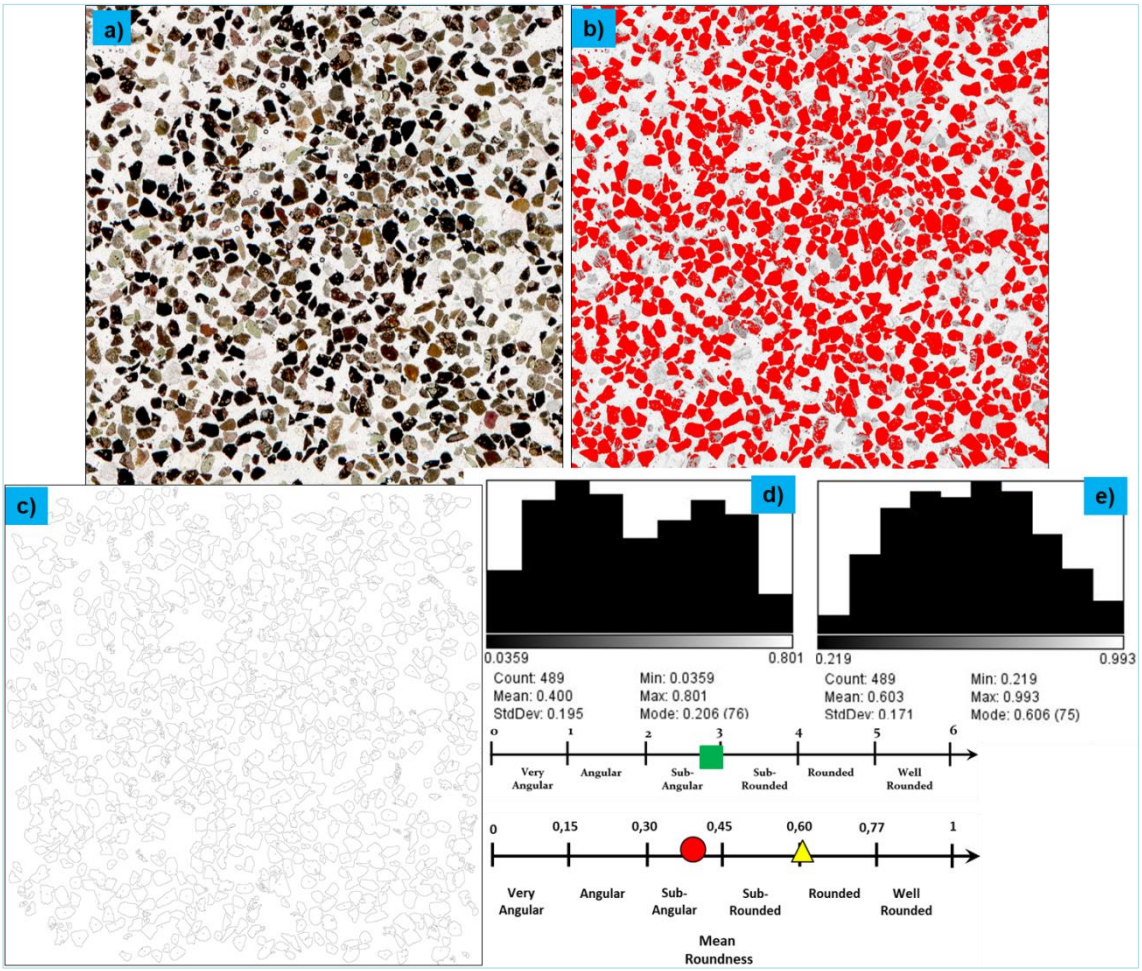

Figure 4.81 – L2-m thin section sample. a) Transmitted natural light scanned image; b) selected grains to analyzing; c) drawn grain boundaries by the software processing; d) circularity distribution values; e) roundness distribution values. Red circle = circularity mean value; yellow triangle = roundness mean value; green square = optical microscope results plotted on Folk scale.

roundness) it falls in angular category (1,72) (as well as circularity results) calculated among 392 analyzed grains (fig. 4.85).

STR-1-Vc sand sample displays a 0,237 circularity mean value and a 0,543 roundness mean value among 592 analyzed grains (fig. 4.86d, e,). Based on circularity mean value STR-Vc sample falls in the angular category and based on roundness parameter it falls in the sub-rounded category, whereas according to optical microscope results (mean roundness) it falls in sub-angular category (2,59) calculated among 286 analyzed grains (fig. 4.87).

STR-9-Vc sand sample displays a 0,105 circularity mean value and a 0,549 roundness mean value among 516 analyzed grains (fig. 4.88d, e,). Based on circularity mean value STR-9-Vc sample falls in the very-angular category and based on roundness parameter it falls in the sub-rounded category, whereas according to optical microscope results (mean roundness) it falls in angular category (1,37) calculated among 200 analyzed grains (fig. 4.89).

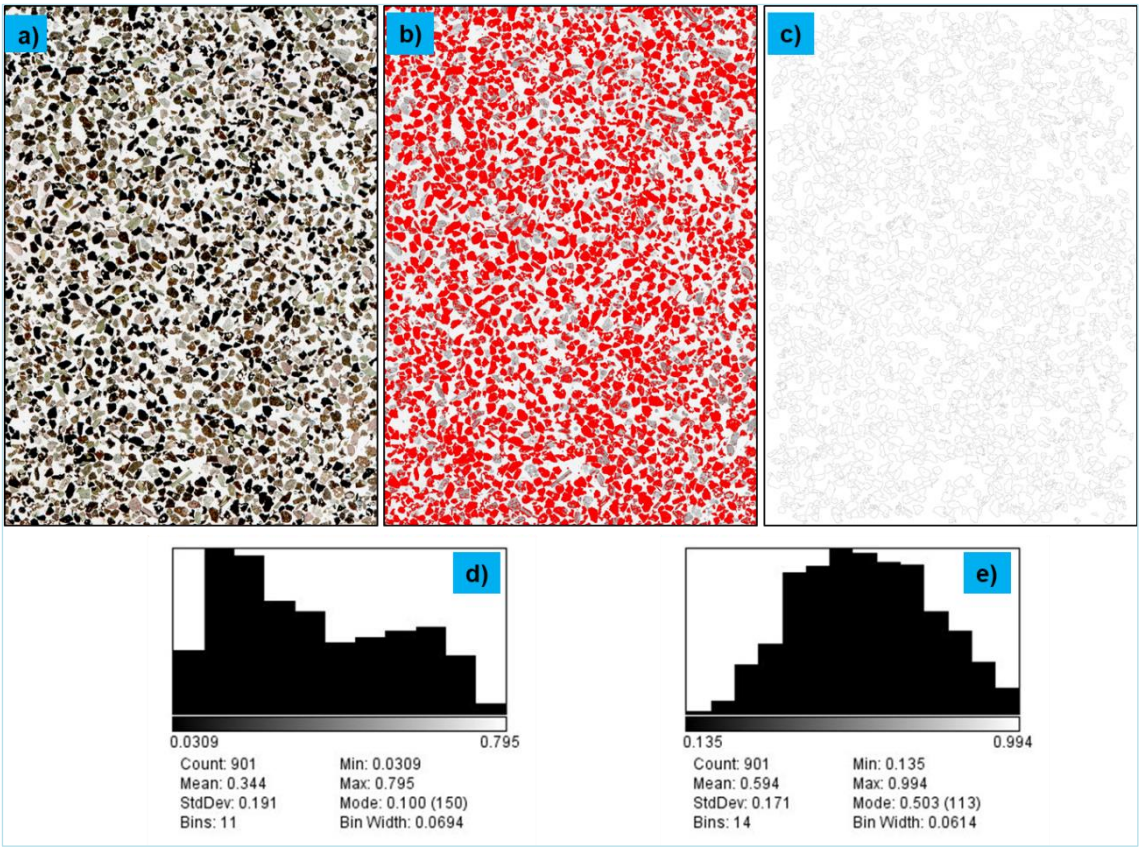

Figure 4.82 – V5-m thin section sample. a) Transmitted natural light scanned image; b) selected grains to analyzing; c) drawn grain boundaries by the software processing; d) circularity distribution values; e) roundness distribution values.

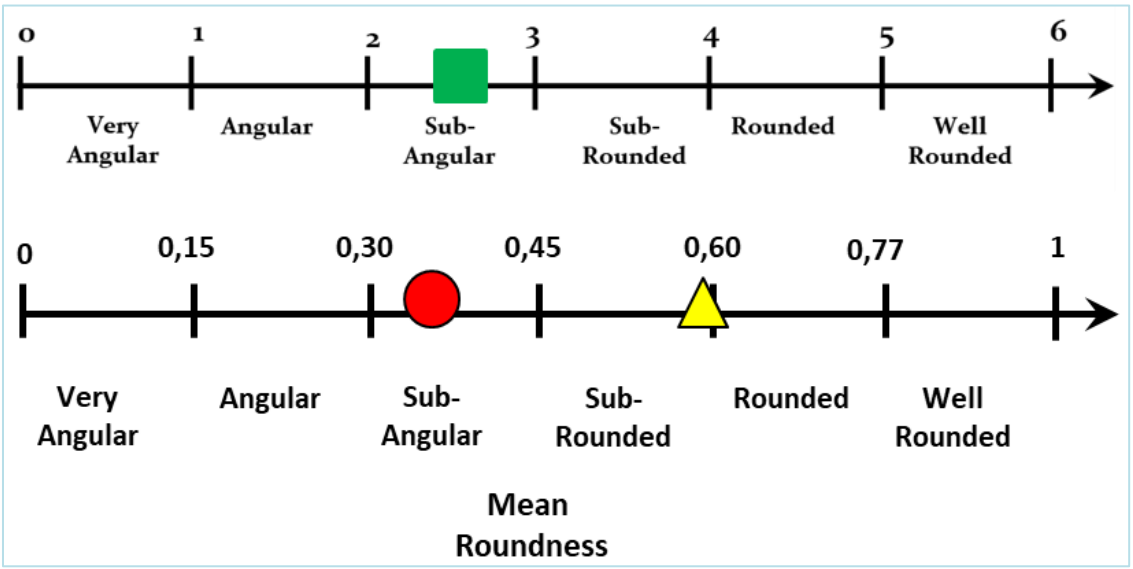

Figure 4.83 – V5-m sample. Red circle = circularity mean value; yellow triangle = roundness mean value; green square = optical microscope results plotted on Folk scale (upper).

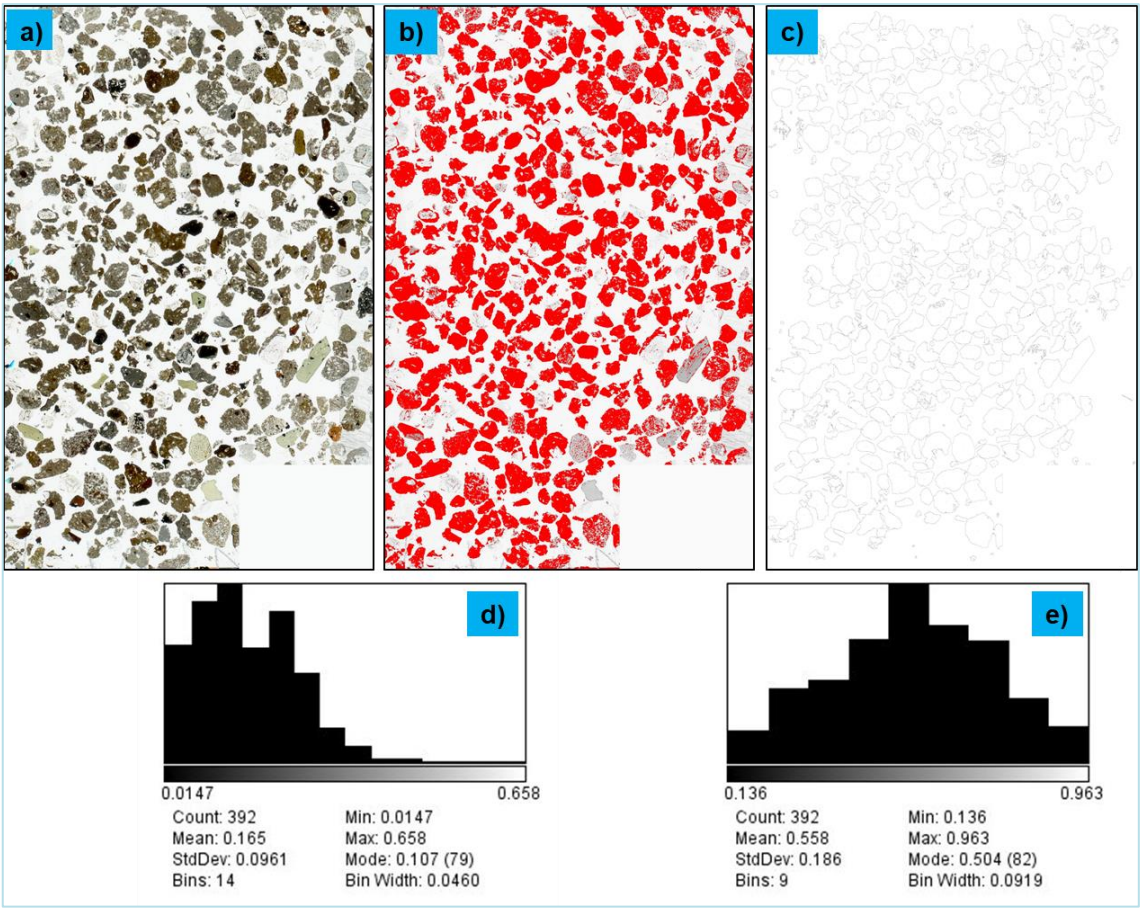

Figure 4.84 – PN-1-Vc thin section sample. a) Transmitted natural light scanned image; b) selected grains to analyzing; c) drawn grain boundaries by the software processing; d) circularity distribution values; e) roundness distribution values.

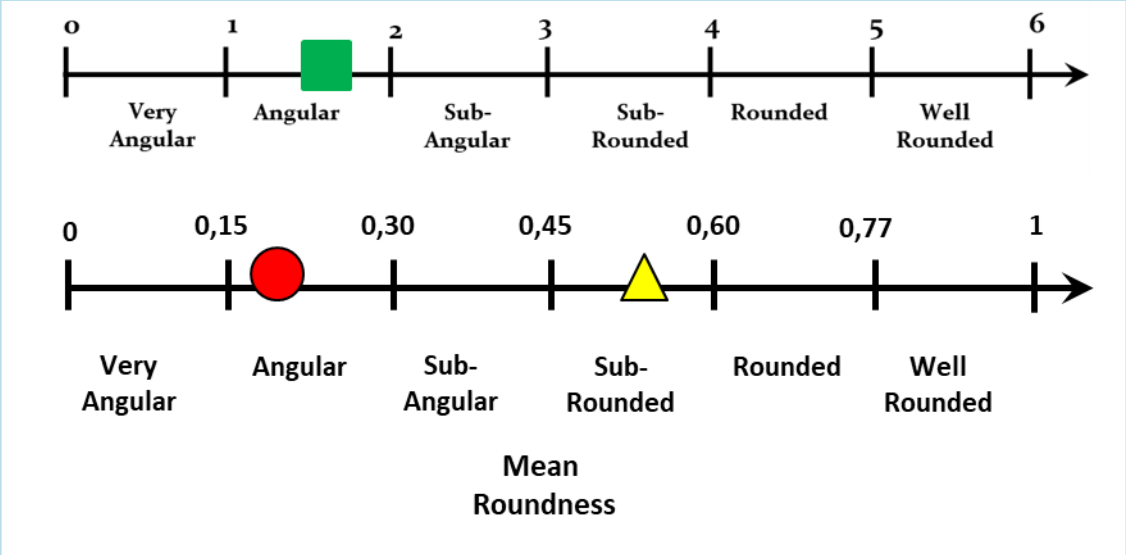

Figure 4.85 – PN-1-Vc sample. Red circle = circularity mean value; yellow triangle = roundness mean value; green square = optical microscope results plotted on Folk scale (upper).

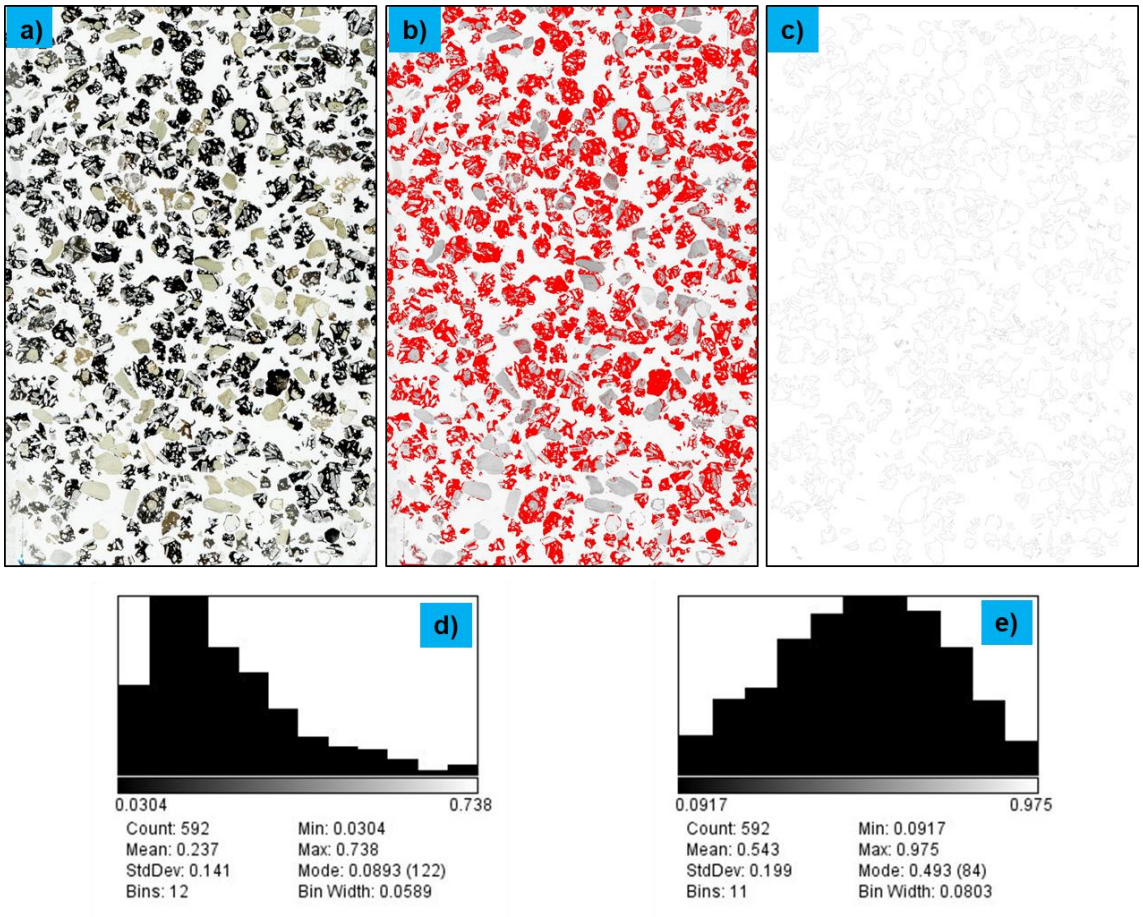

Figure 4.86 – STR-1-Vc thin section sample. a) Transmitted natural light scanned image; b) selected grains to analyzing; c) drawn grain boundaries by the software processing; d) circularity distribution values; e) roundness distribution values.

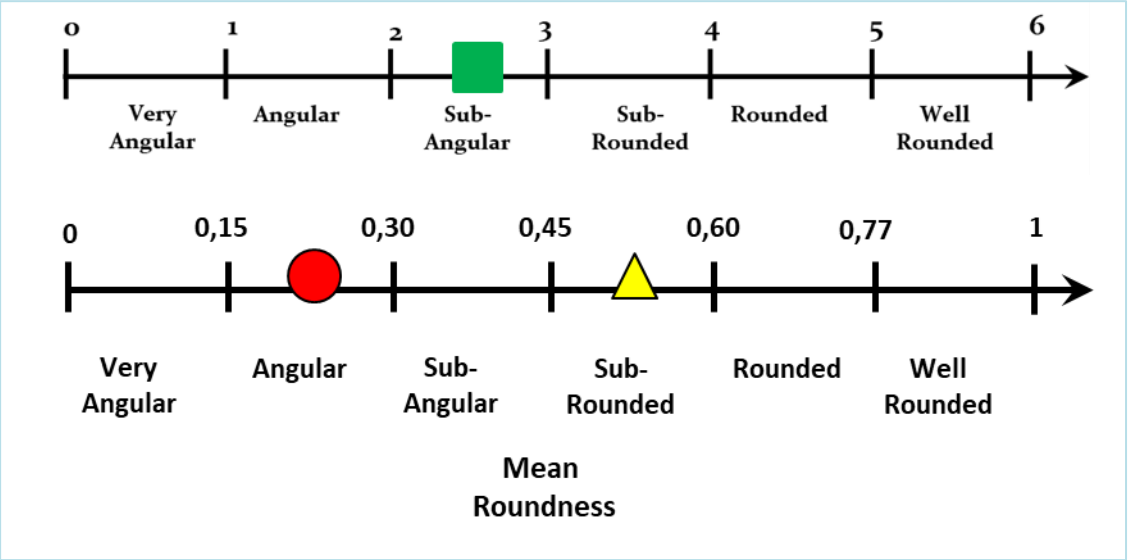

Figure 4.87 – STR-1-Vc sample. Red circle = circularity mean value; yellow triangle = roundness mean value; green square = optical microscope results plotted on Folk scale (upper).

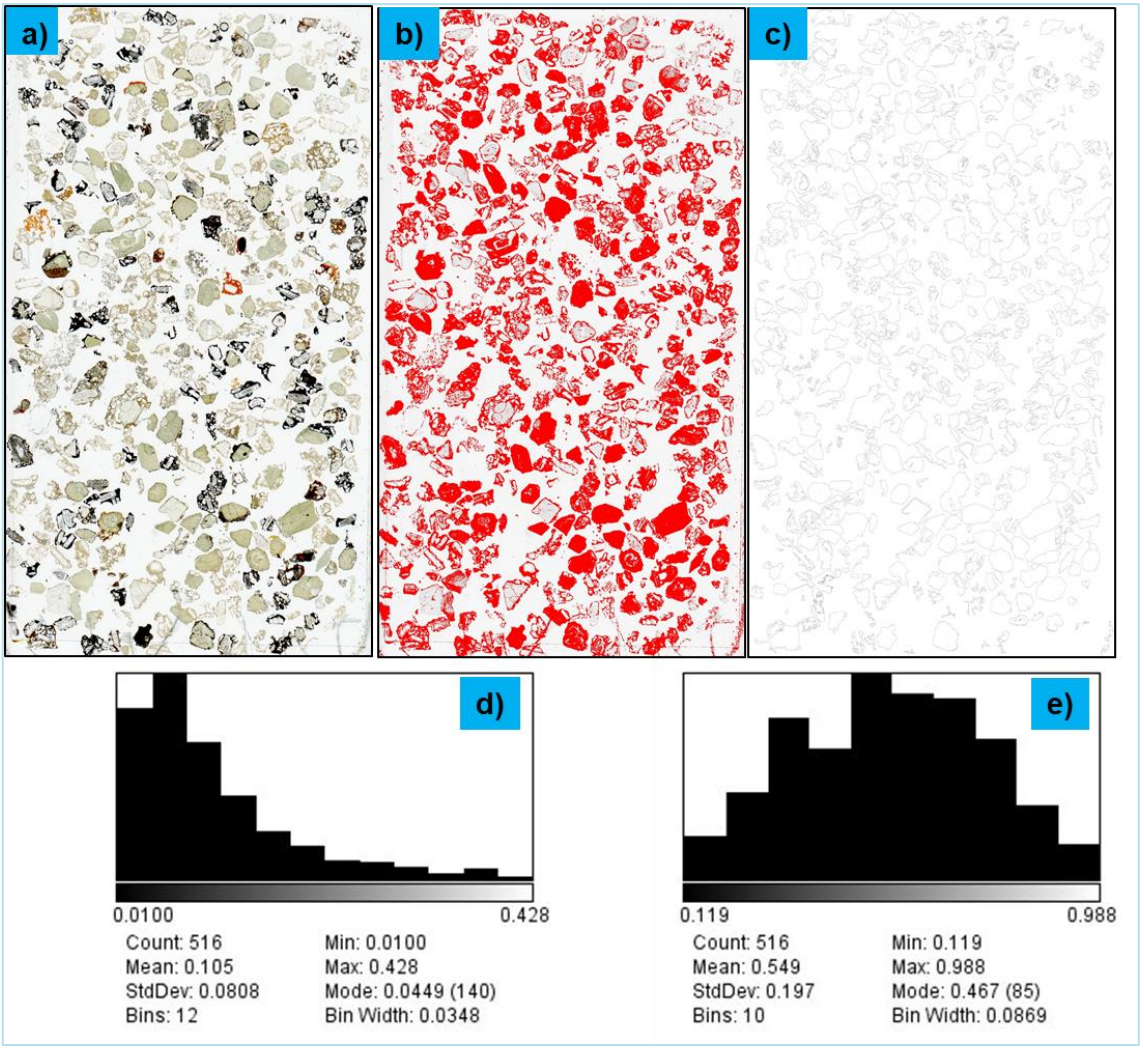

Figure 4.88 – STR-9-Vc thin section sample. a) Transmitted natural light scanned image; b) selected grains to analyzing; c) drawn grain boundaries by the software processing; d) circularity distribution values; e) roundness distribution values.

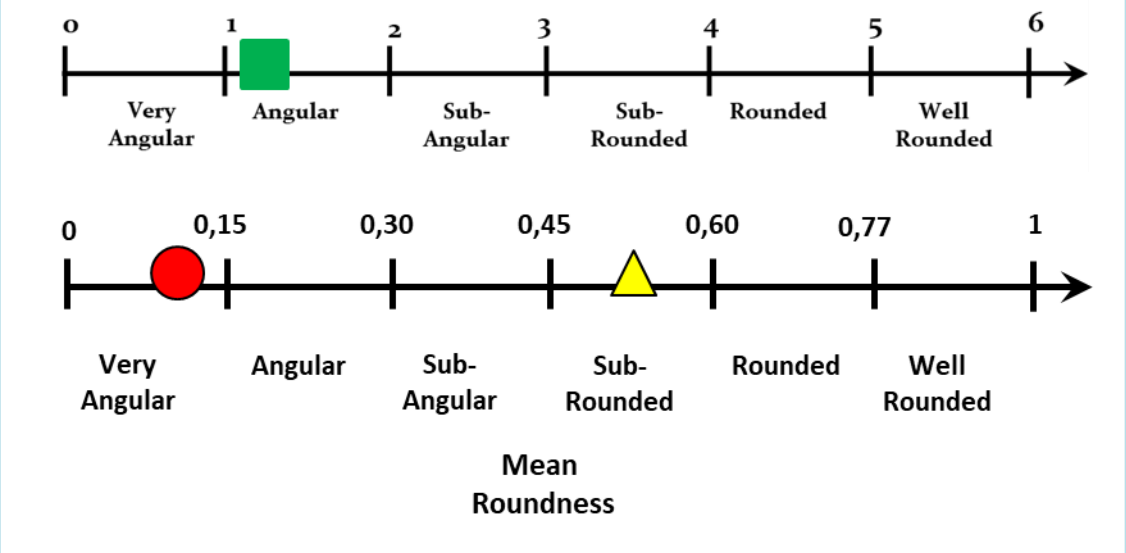

Figure 4.89 – STR-9-Vc sample. Red circle = circularity mean value; yellow triangle = roundness mean value; green square = optical microscope results plotted on Folk scale (upper).

For Campania samples were utilized the same calculation procedure. Following here will be described Campania data results. 13 thin sections were processed among Campania samples: VO-3-m, Li-1-m, BC-1-Vc, PZ-8-Vc, PZ-14-Vc, GA-1-m, NA-1-m, PO-1-m, TG-1-m, TA-1-m, VE-1-m, CA-1-m, SO-1-m.

VO-3-m sand sample displays a 0,197 circularity mean value and a 0,587 roundness mean value among 1962 analyzed grains (fig. 4.90a). Based on circularity mean value VO-3-m sample falls in the angular category and based on roundness parameter it falls in the sub-rounded category, whereas according to optical microscope results (mean roundness) it falls in sub-rounded category (3,76) (as well as roundness results) calculated among 240 analyzed grains (fig. 4.90a).

Li-1-m sand sample displays a 0,201 circularity mean value and a 0,580 roundness mean value among 2369 analyzed grains (fig. 4.90b). Based on circularity mean value Li-1-m sample falls in the angular category and based on roundness parameter it falls in the sub-rounded category, whereas according to optical microscope results (mean roundness) it falls in sub-angular category (2,94) calculated among 286 analyzed grains (fig. 4.90b).

BC-1-Vc sand sample displays a 0,196 circularity mean value and a 0,589 roundness mean value among 343 analyzed grains (fig. 4.90c). Based on circularity mean value BC-1-Vc sample falls in the angular category and based on roundness parameter it falls in the sub-rounded category, whereas according to optical microscope results (mean roundness) it falls in sub-rounded category (3,57) (as well as roundness results) calculated among 341 analyzed grains (fig. 4.90c).

PZ-8-Vc sand sample displays a 0,176 circularity mean value and a 0,570 roundness mean value among 315 analyzed grains (fig. 4.90d). Based on circularity mean value PZ-8-Vc sample falls in the angular category and based on roundness parameter it falls in the sub-rounded category, whereas according to optical microscope results (mean roundness) it falls in sub-rounded category (3,86) (as well as roundness results) calculated among 296 analyzed grains (fig. 4.90d).

PZ-14-Vc sand sample displays a 0,269 circularity mean value and a 0,592 roundness mean value among 170 analyzed grains (fig. 4.90e). Based on circularity mean value PZ-14-Vc sample falls in the angular category and based on roundness parameter it falls in the sub-rounded category, whereas according to optical microscope results (mean roundness) it falls in sub-rounded category (3,43) (as well as roundness results) calculated among 133 analyzed grains (fig. 4.90e).

GA-1-m sand sample displays a 0,184 circularity mean value and a 0,613 roundness mean value among 411 analyzed grains (fig. 4.90f). Based on circularity mean value GA-1-m sample falls in the angular category and based on roundness parameter it falls in the rounded category, whereas according to optical microscope results (mean roundness) it falls in sub-angular category (2,84) calculated among 301 analyzed grains (fig. 4.90f).

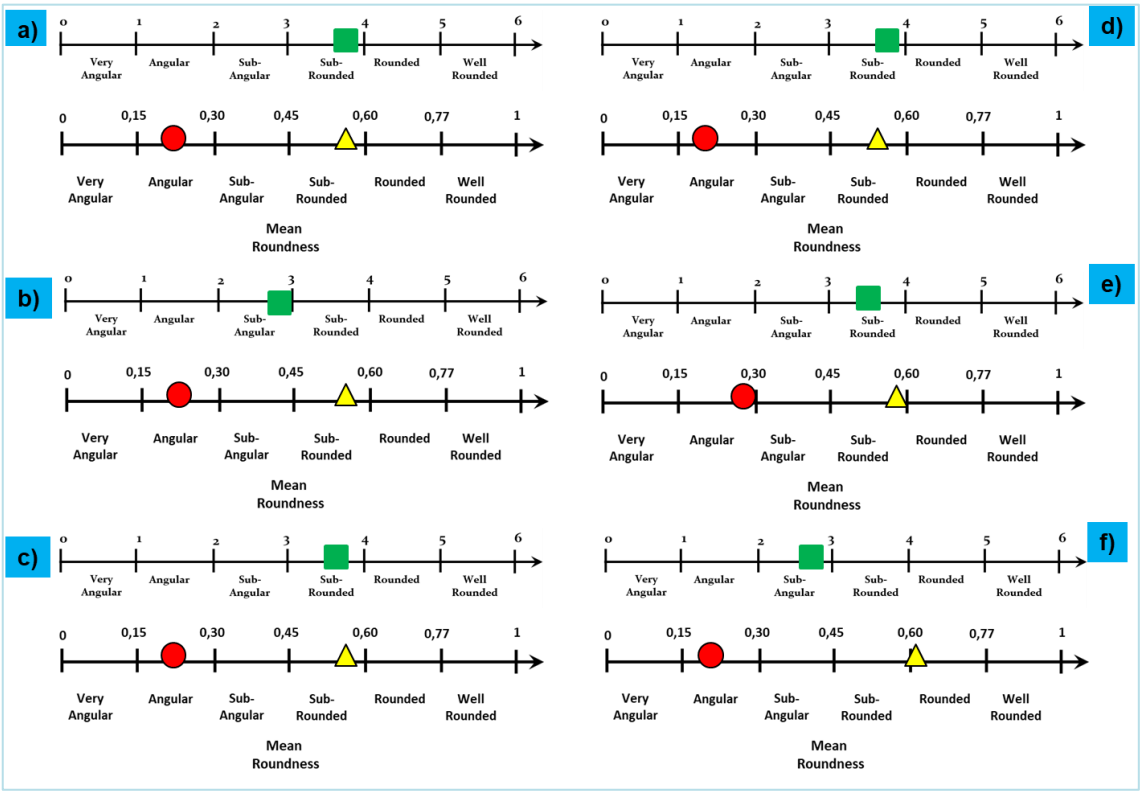

Figure 4.90 – a) VO-3-m sample; b) Li-1-m sample; c) BC-1-Vc sample; d) PZ-8-Vc sample; e) PZ-14-Vc sample; f) GA-1-m sample. Red circle = circularity mean value; yellow triangle = roundness mean value; green square = optical microscope results plotted on Folk scale.

NA-1-m sand sample displays a 0,157 circularity mean value and a 0,585 roundness mean value among 875 analyzed grains (fig. 4.91a). Based on circularity mean value NA-1-m sample falls in the angular/very-angular category and based on roundness parameter it falls in the sub-rounded category, whereas according to optical microscope results (mean roundness) it falls in sub-rounded category (3,22) (as well as roundness results) calculated among 293 analyzed grains (fig. 4.91a).

PO-1-m sand sample displays a 0,155 circularity mean value and a 0,551 roundness mean value among 1492 analyzed grains (fig. 4.91b). Based on circularity mean value PO-1-m sample falls in the angular/very-angular category and based on roundness parameter it falls in the sub-rounded category, whereas according to optical microscope

results (mean roundness) it falls in sub-rounded category (3,28) (as well as roundness results) calculated among 339 analyzed grains (fig. 4.91b).

TG-1-m sand sample displays a 0,195 circularity mean value and a 0,574 roundness mean value among 302 analyzed grains (fig. 4.91c). Based on circularity mean value TG-1-m sample falls in the angular category and based on roundness parameter it falls in the sub-rounded category, whereas according to optical microscope results (mean roundness) it falls in sub-rounded category (3,28) (as well as roundness results) calculated among 372 analyzed grains (fig. 4.91c).

TA-1-m sand sample displays a 0,195 circularity mean value and a 0,569 roundness mean value among 113 analyzed grains (fig. 4.91d). Based on circularity mean value TA-1-m sample falls in the angular category and based on roundness parameter it falls in the sub-rounded category, whereas according to optical microscope results (mean roundness) it falls in sub-rounded category (3,28) (as well as roundness results) calculated among 316 analyzed grains (fig. 4.91d).

VE-1-m sand sample displays a 0,183 circularity mean value and a 0,519 roundness mean value among 152 analyzed grains (fig. 4.91e). Based on circularity mean value VE-1-m sample falls in the angular category and based on roundness parameter it falls in the sub-rounded category, whereas according to optical microscope results (mean roundness) it falls in sub-angular category (3,00) calculated among 398 analyzed grains (fig. 4.91e).

CA-1-m sand sample displays a 0,371 circularity mean value and a 0,543 roundness mean value among 96 analyzed grains (fig. 4.91f). Based on circularity mean value CA-1-m sample falls in the sub-angular category and based on roundness parameter it falls in the sub-rounded category, whereas according to optical microscope results (mean roundness) it falls in sub-rounded category (3,52) (as well as roundness results) calculated among 339 analyzed grains (fig. 4.91f).

SO-1-m sand sample displays a 0,217 circularity mean value and a 0,543 roundness mean value among 740 analyzed grains (fig. 4.91g). Based on circularity mean value SO-1-m sample falls in the angular category and based on roundness parameter it falls in the sub-rounded category, whereas according to optical microscope results (mean roundness) it falls in sub-rounded category (3,51) (as well as roundness results) calculated among 246 analyzed grains (fig. 4.91g).

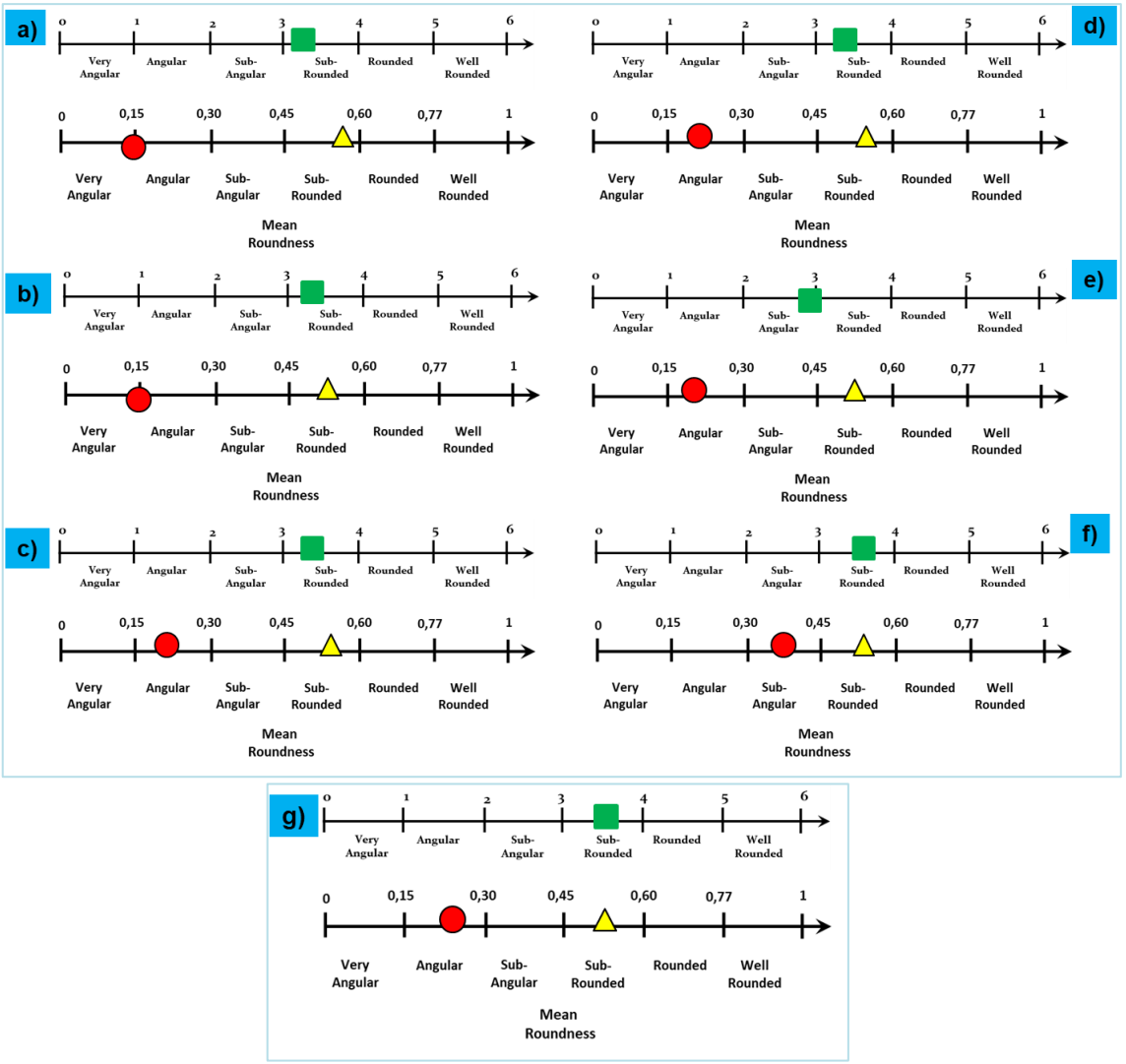

Figure 4.91 – a) NA-1-m sample; b) PO-1-m sample; c) TG-1-m sample; d) TA-1-m sample; e) VE-1-m sample; f) CA-1-m sample; g) SO-1-m sample. Red circle = circularity mean value; yellow triangle = roundness mean value; green square = optical microscope results plotted on Folk scale.

4.3.2 – BULK GRANULAR SAMPLE RESULTS-

About 1 gr of bulk granular sample have been used for this analysis type by placing the sample on a transparent film (fig. 4.73). A total of 21 samples have been analyzed among the two studied areas. Also in this case for each analyzed sample it has been obtained a known analyzed grains number (fig. 4.92, 4.93) and for each grain it is possible to know roundness and circularity values (fig. 4.92), then it has been calculated a roundness and circularity mean value for each analyzed sample. These values have been successively plotted on the calibrated roundness scale (fig. 4.74) to understand which of both parameters better reflect the real grains roundness category of the analyzed samples. During this analysis is really important to place the grains spaced apart from each other for the analysis success (fig. 4.73, 4.92, 4.93).

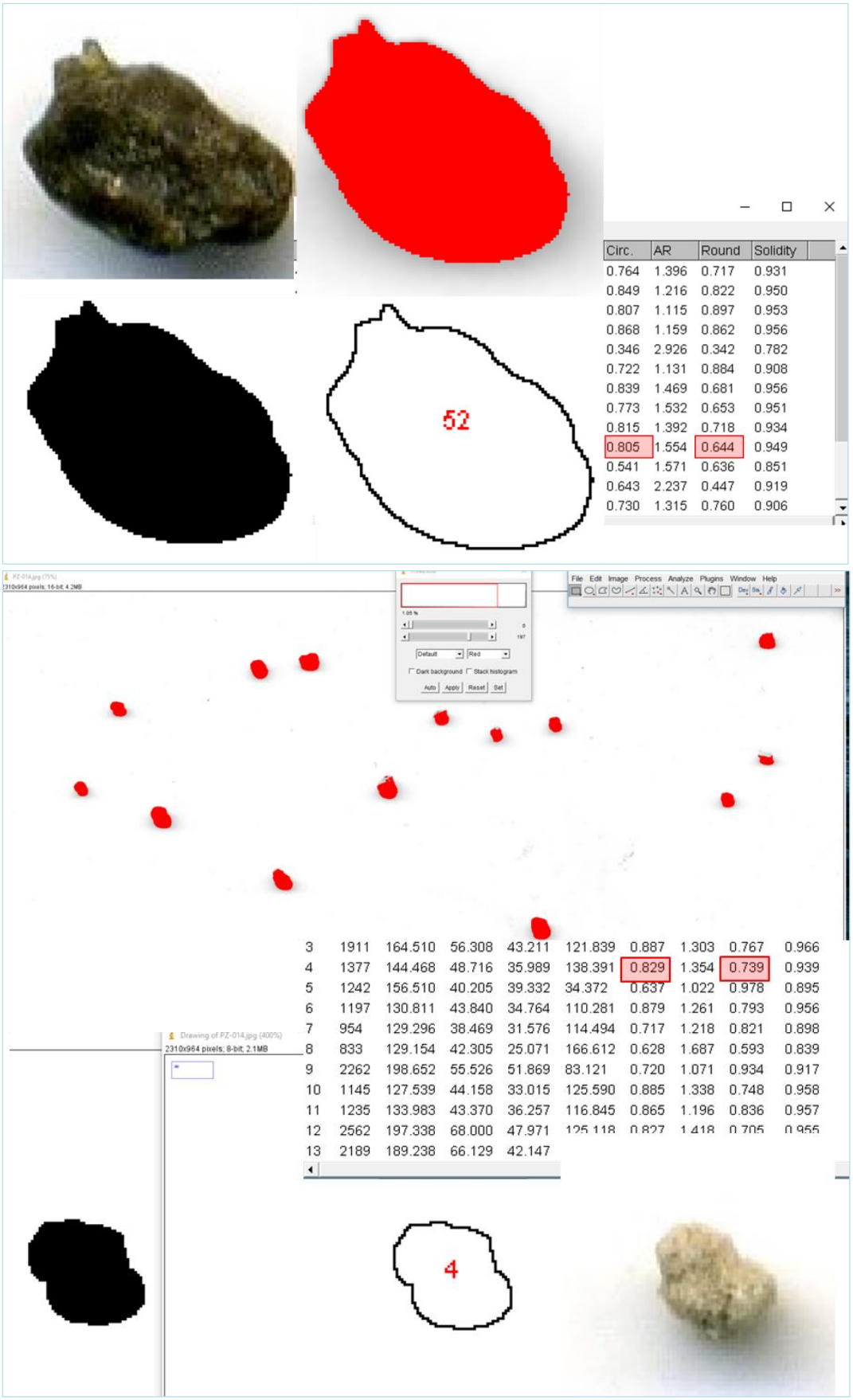

Figure 4.92 – Scanning method of a granular bulk sample. Image processing steps through ImageJ software. Real grains are on the upper left (pyroxene) and lower right (pumice).

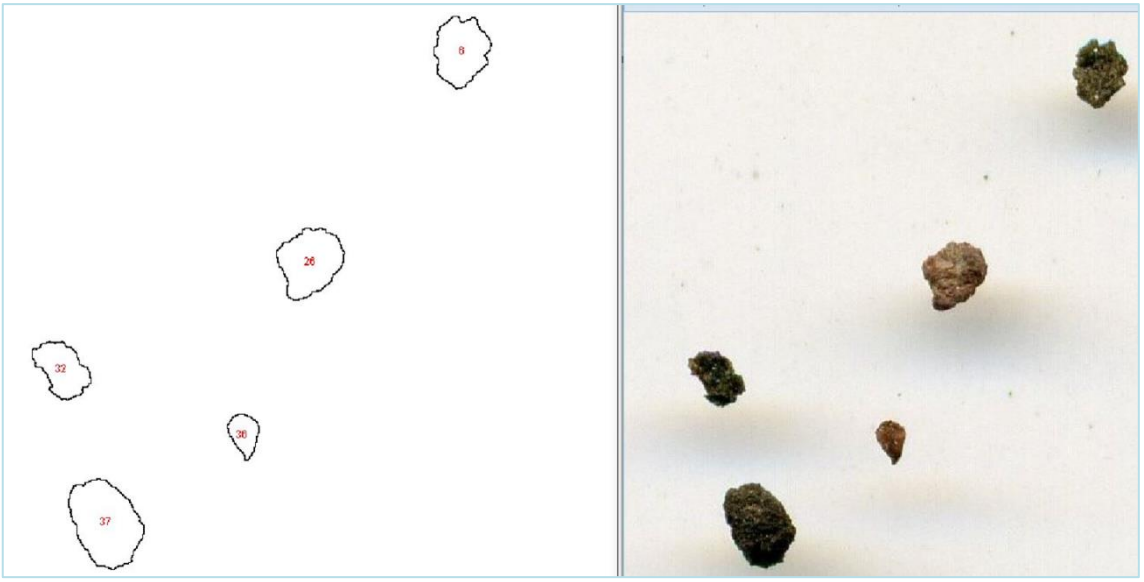

Figure 4.93 –Example of a processed image (left) and scanned granular bulk sample (right).

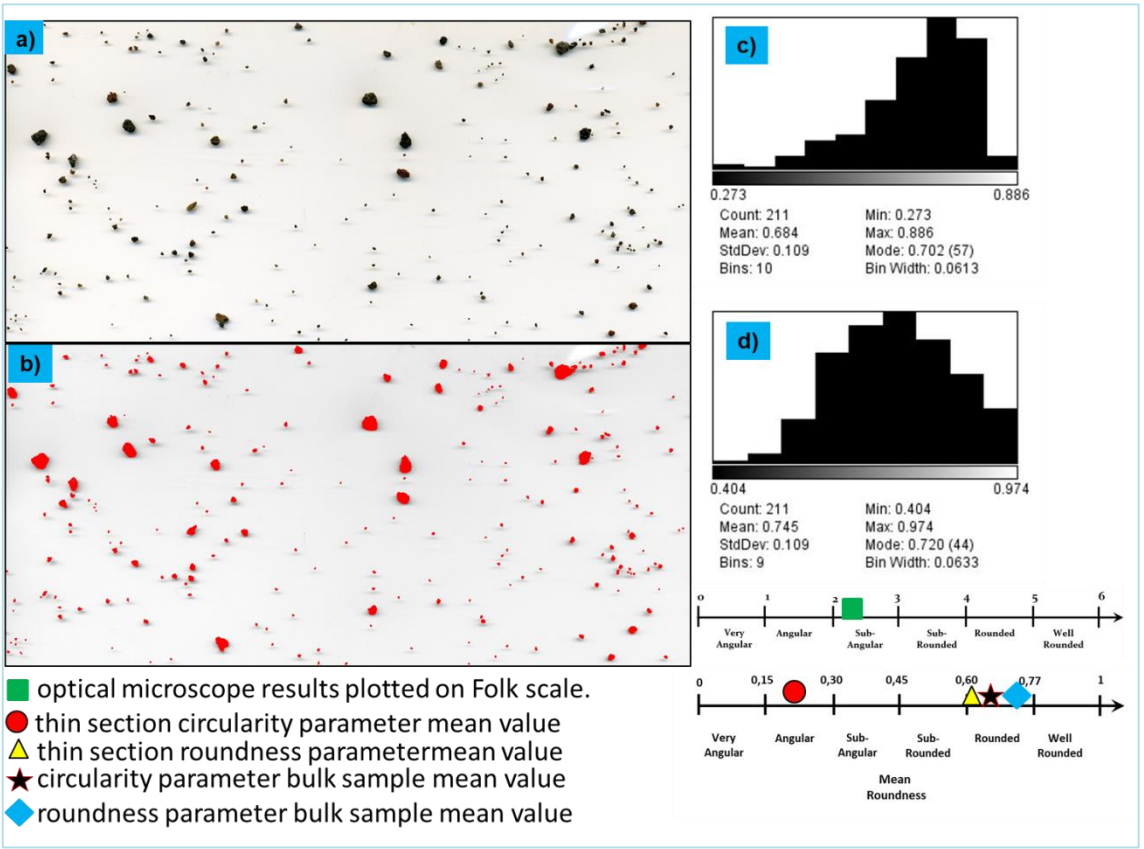

Figure 4.94 –AL-3 sample image analyses results. a) Transmitted natural light scanned image; b) selected grains to analyzing; c) circularity distribution values; d) roundness distribution values.

AL-3 bulk sample displays a 0,684 circularity mean value and a 0,745 roundness mean value among 211 analyzed grains. Based on circularity and roundness mean values AL-3 bulk sample falls in the rounded category (fig. 4.94).

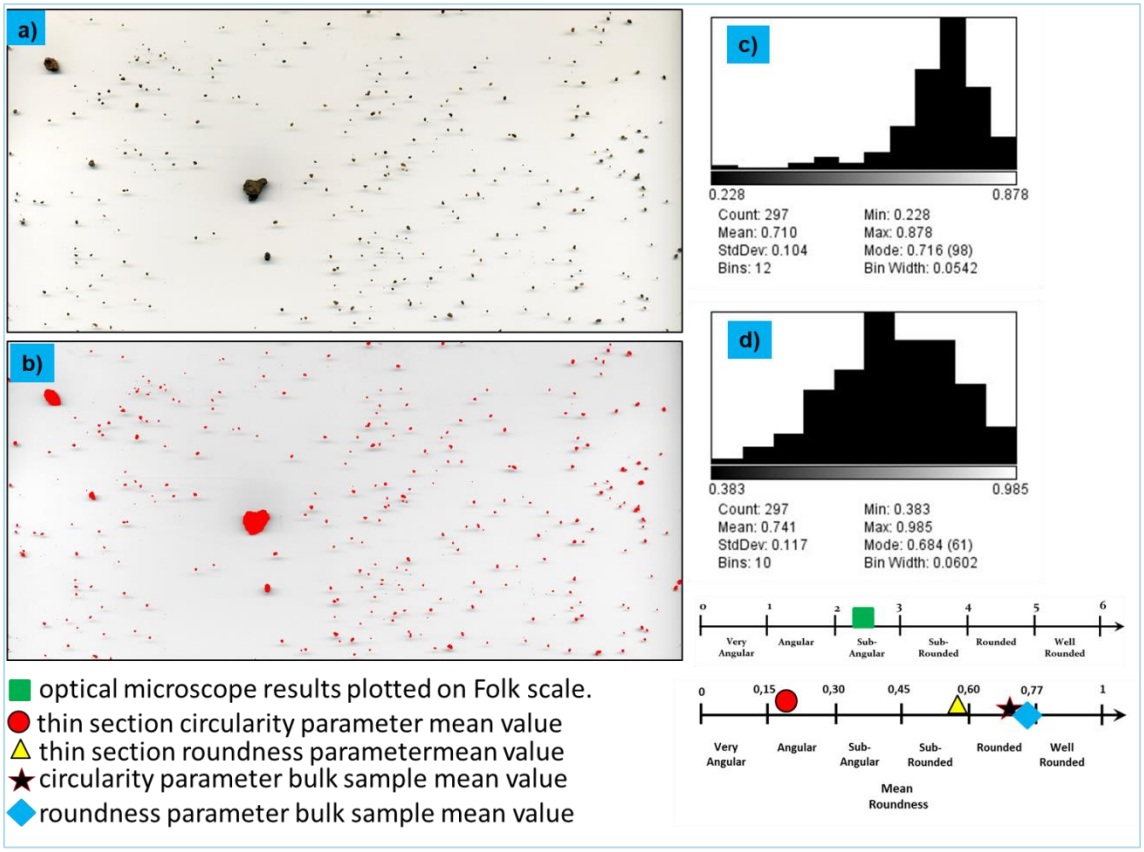

Figure 4.95 –Fi-3 sample image analyses results. a) Transmitted natural light scanned image; b) selected grains to analyzing; c) circularity distribution values; d) roundness distribution values.

Fi-3 bulk sample displays a 0,710 circularity mean value and a 0,741 roundness mean value among 297 analyzed grains. Based on circularity and roundness mean values Fi-3 bulk sample falls in the rounded category (fig. 4.95).

SA-1 bulk sample displays a 0,654 circularity mean value and a 0,751 roundness mean value among 358 analyzed grains. Based on circularity and roundness mean values SA-1 bulk sample falls in the rounded category (fig. 4.96).

L2 bulk sample displays a 0,749 circularity mean value and a 0,704 roundness mean value among 101 analyzed grains. Based on circularity and roundness mean values L2 bulk sample falls in the rounded category (fig. 4.97).

V5 bulk sample displays a 0,636 circularity mean value and a 0,753 roundness mean value among 268 analyzed grains. Based on circularity and roundness mean values V5 bulk sample falls in the rounded category (fig. 4.98).

PN-1 bulk sample displays a 0,550 circularity mean value and a 0,704 roundness mean value among 343 analyzed grains. Based on circularity mean value PN-1 bulk sample falls in the sub-rounded category and based on roundness parameter it falls in the rounded category (fig. 4.99).

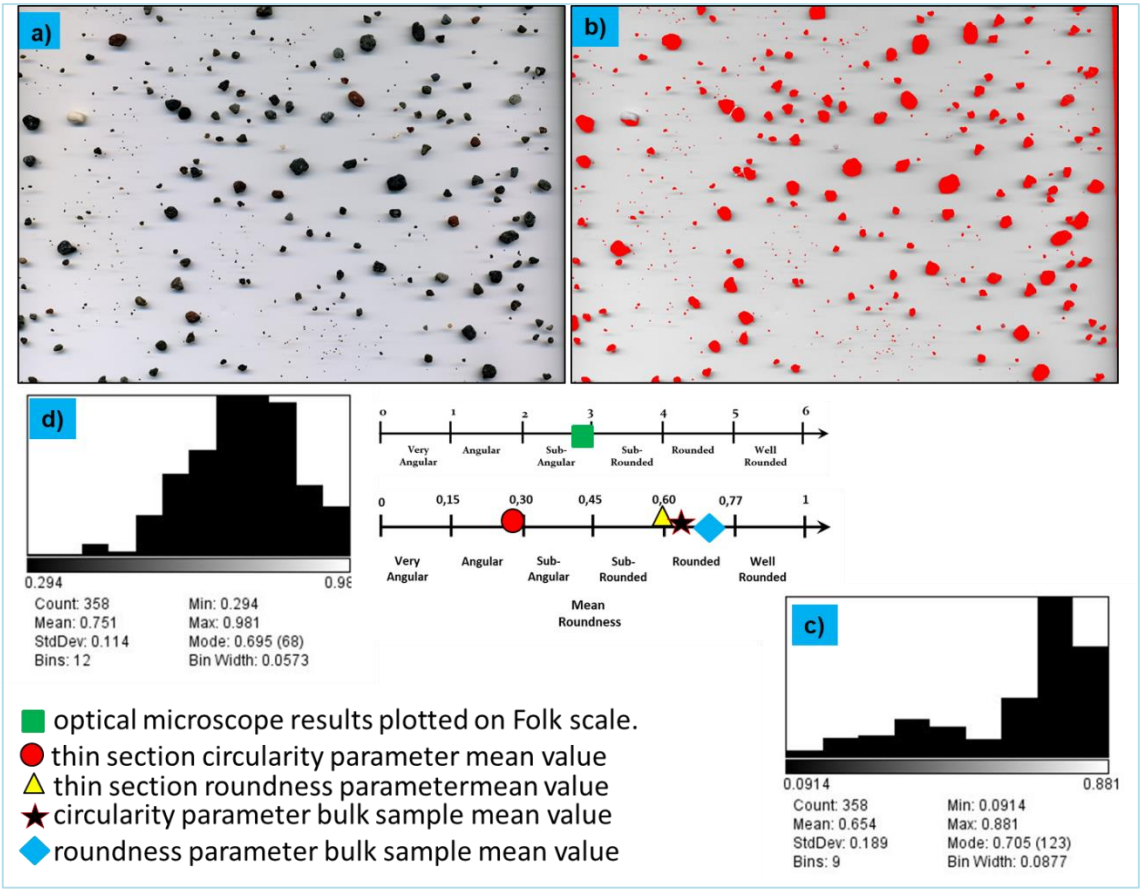

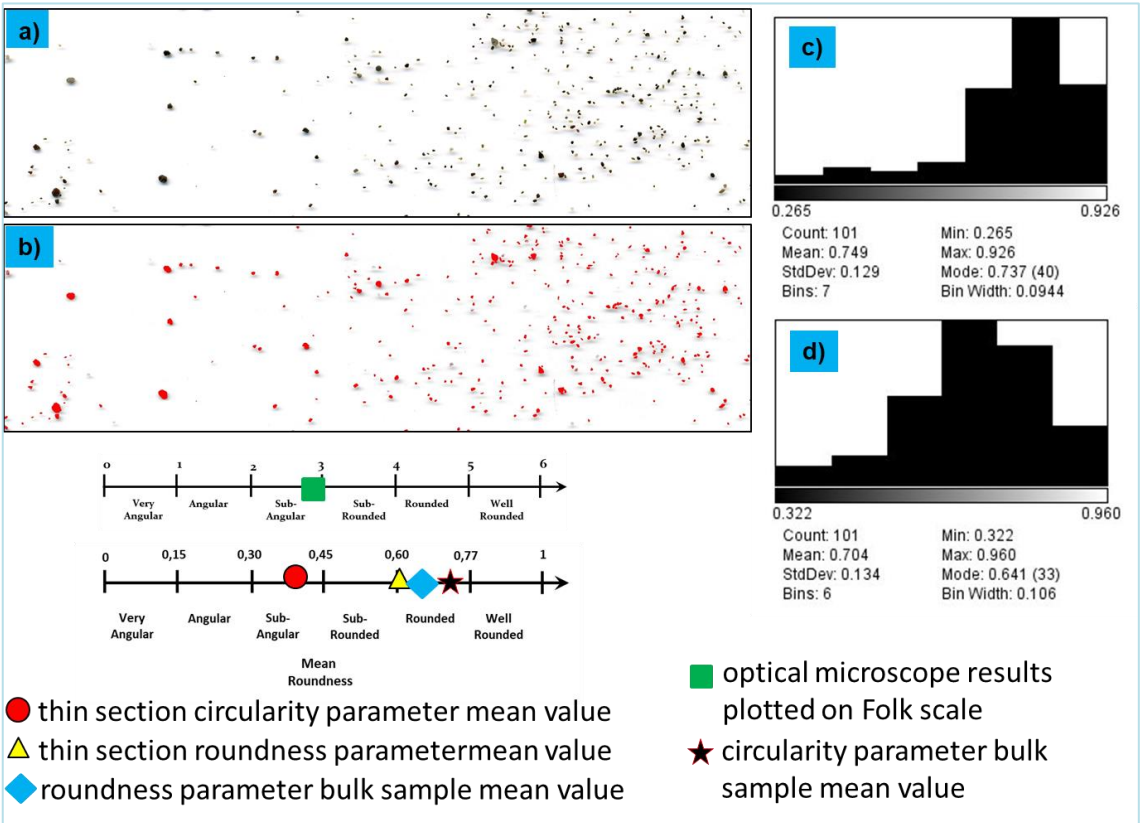

Figure 4.96 (upper) - SA-1 sample image analyses results. Figure 4.97 (lower) L2 sample image analyses results. a) Transmitted natural light scanned image; b) selected grains to analyzing; c) circularity distribution values; d) roundness distribution values.

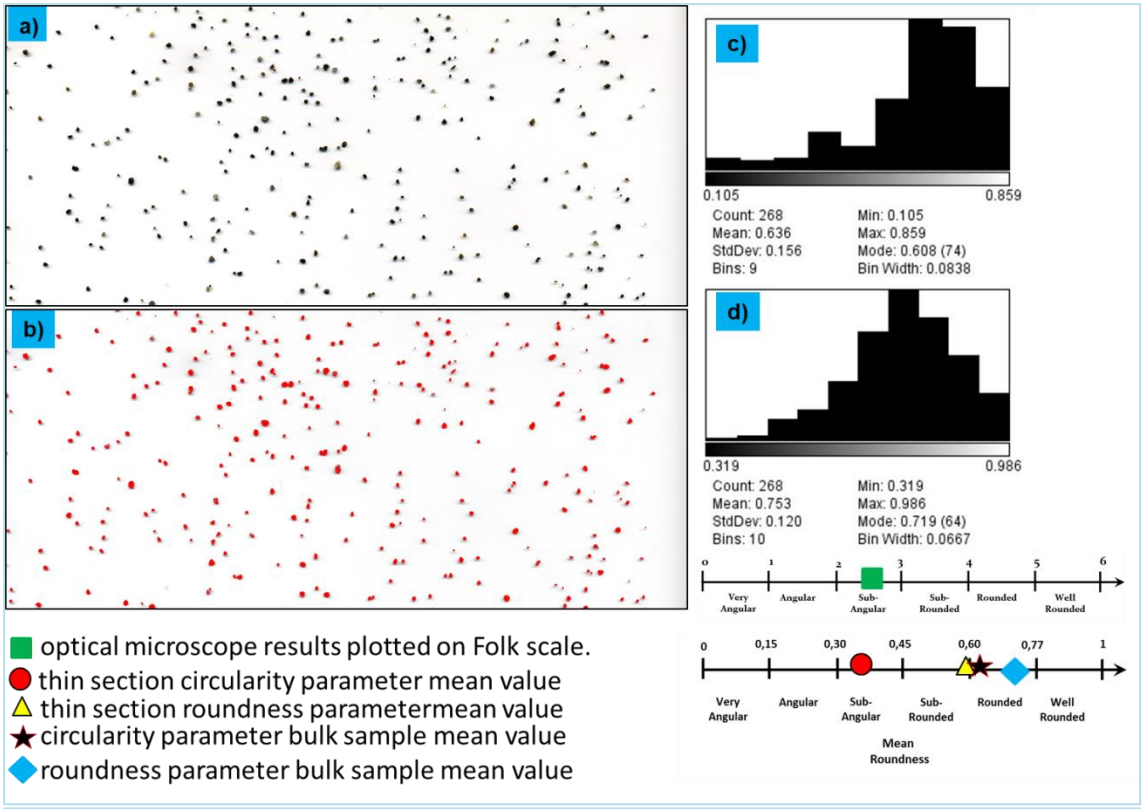

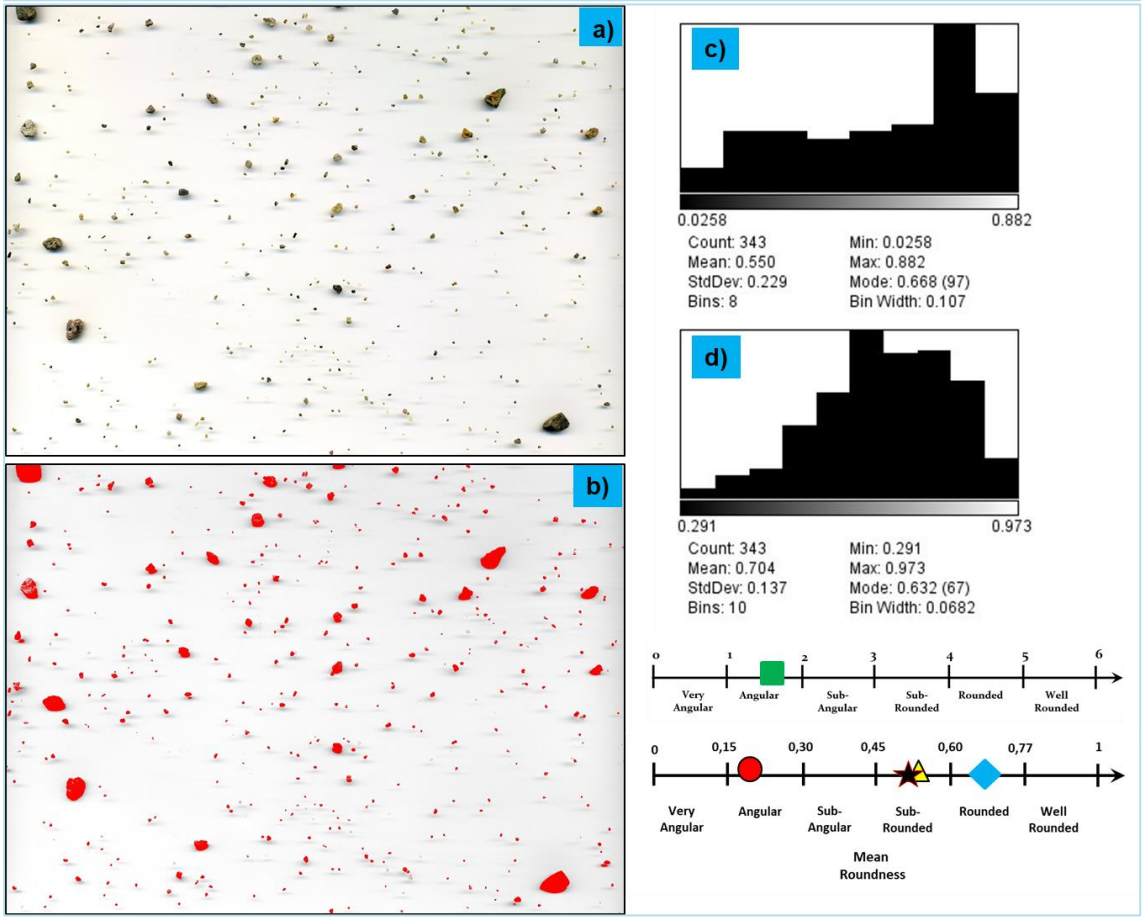

Figure 4.98 (upper) –V5 sample image analyses results. Figure 4.99 (lower) PN-1 sample image analyses results. a) Transmitted natural light scanned image; b) selected grains to analyzing; c) circularity distribution values; d) roundness distribution values.

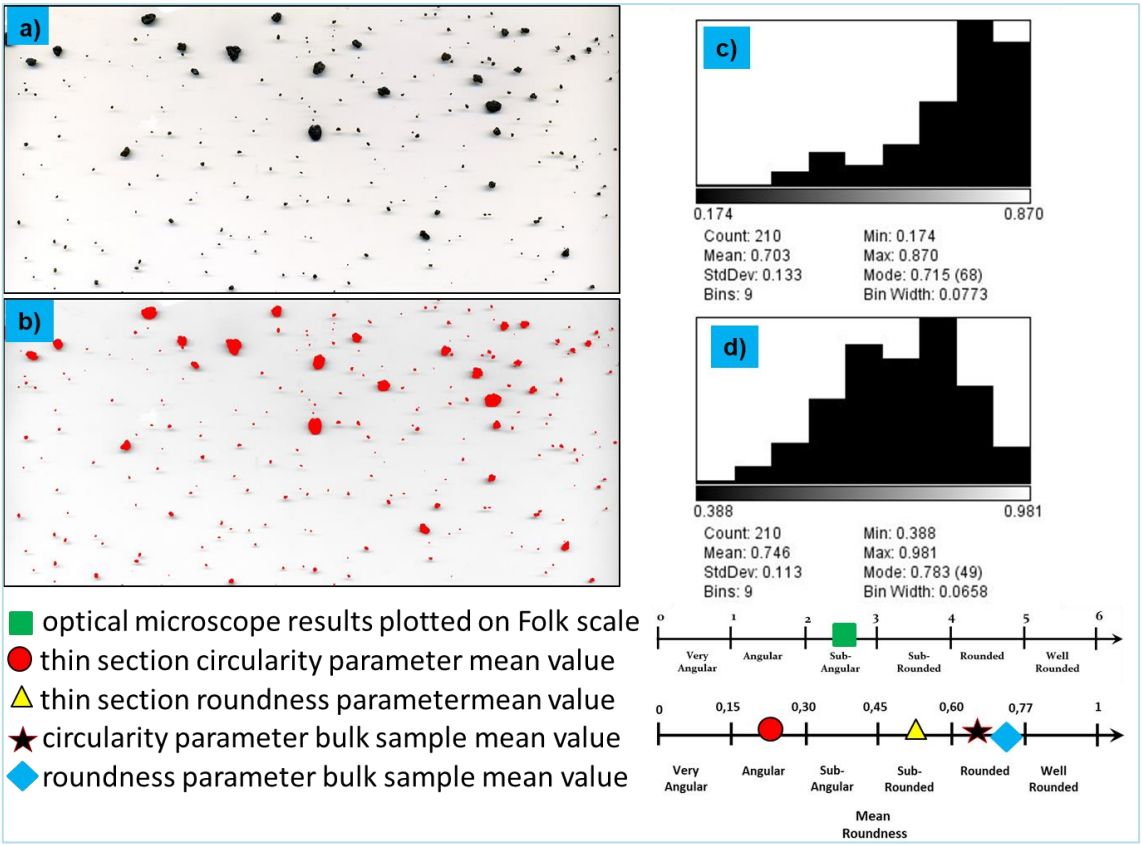

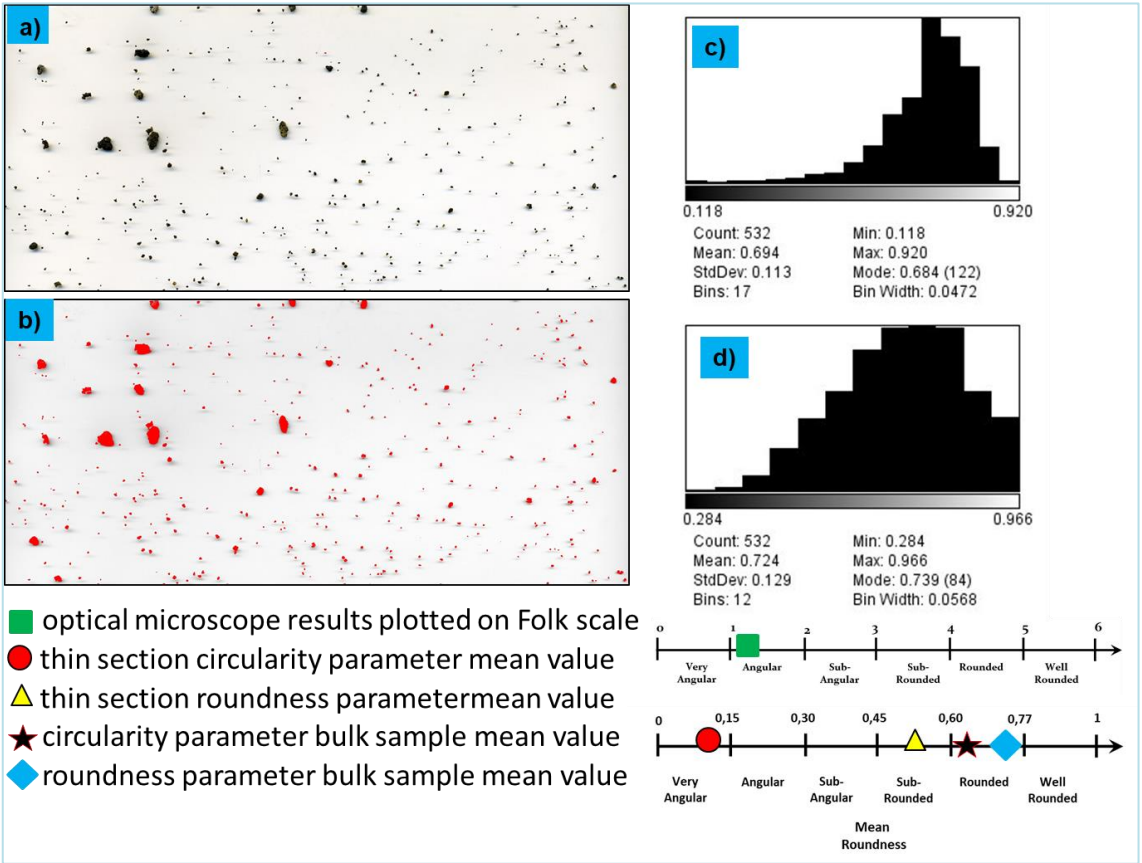

Figure 4.100 (upper) –STR-1 sample image analyses results. Figure 4.101 (lower) STR-9 sample image analyses results. a) Transmitted natural light scanned image; b) selected grains to analyzing; c) circularity distribution values; d) roundness distribution values.

STR-1 bulk sample displays a 0,703 circularity mean value and a 0,746 roundness mean value among 210 analyzed grains. Based on circularity and roundness mean values STR-1 bulk sample falls in the rounded category (fig. 4.100).

STR-9 bulk sample displays a 0,694 circularity mean value and a 0,724 roundness mean value among 532 analyzed grains. Based on circularity and roundness mean values STR-9 bulk sample falls in the rounded category (fig. 4.101).

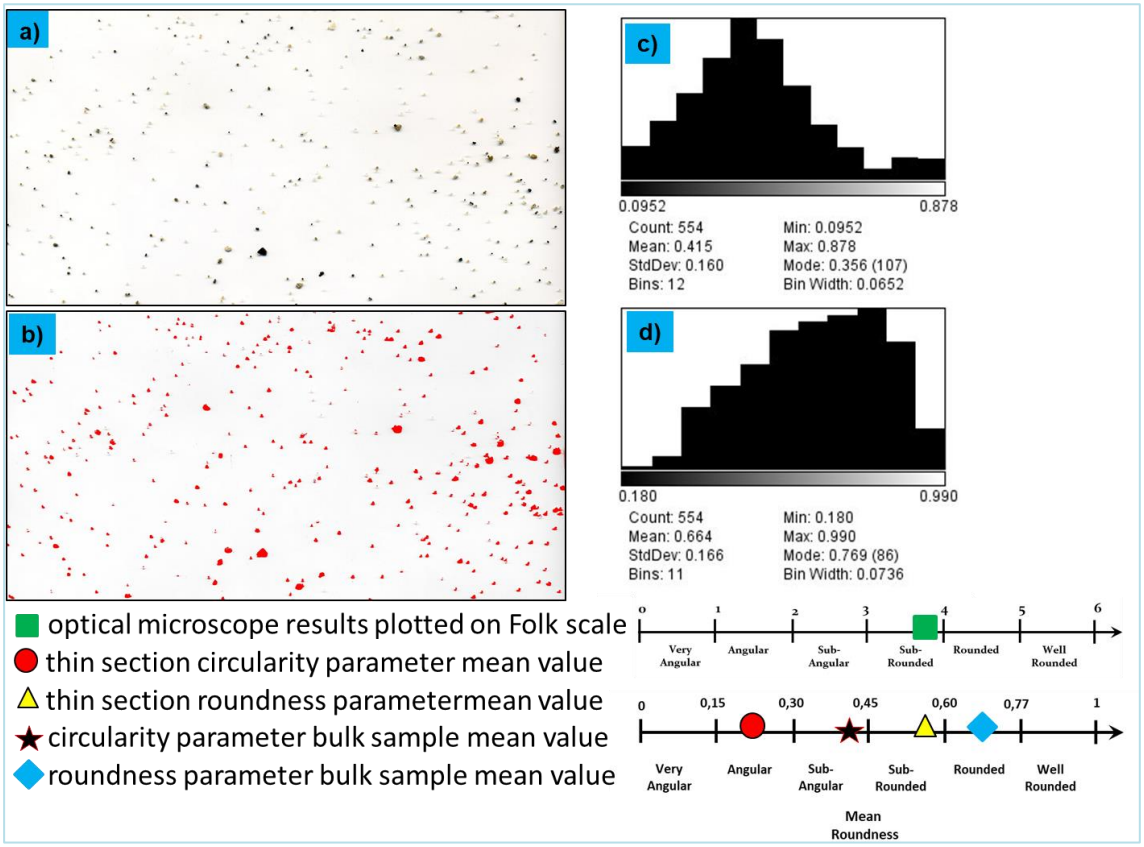

Figure 4.102 – VO-3 sample image analyses results. a) Transmitted natural light scanned image; b) selected grains to analyzing; c) circularity distribution values; d) roundness distribution values.

VO-3 bulk sample displays a 0,415 circularity mean value and a 0,664 roundness mean value among 554 analyzed grains. Based on circularity value VO-3 falls in the sub-angular category, whereas based on roundness mean value it falls in the rounded category (fig. 4.102).

Li-1 bulk sample displays a 0,486 circularity mean value and a 0,690 roundness mean value among 240 analyzed grains. Based on circularity value Li-1 falls in the sub-rounded category, whereas based on roundness mean value it falls in the rounded category (fig. 4.103).

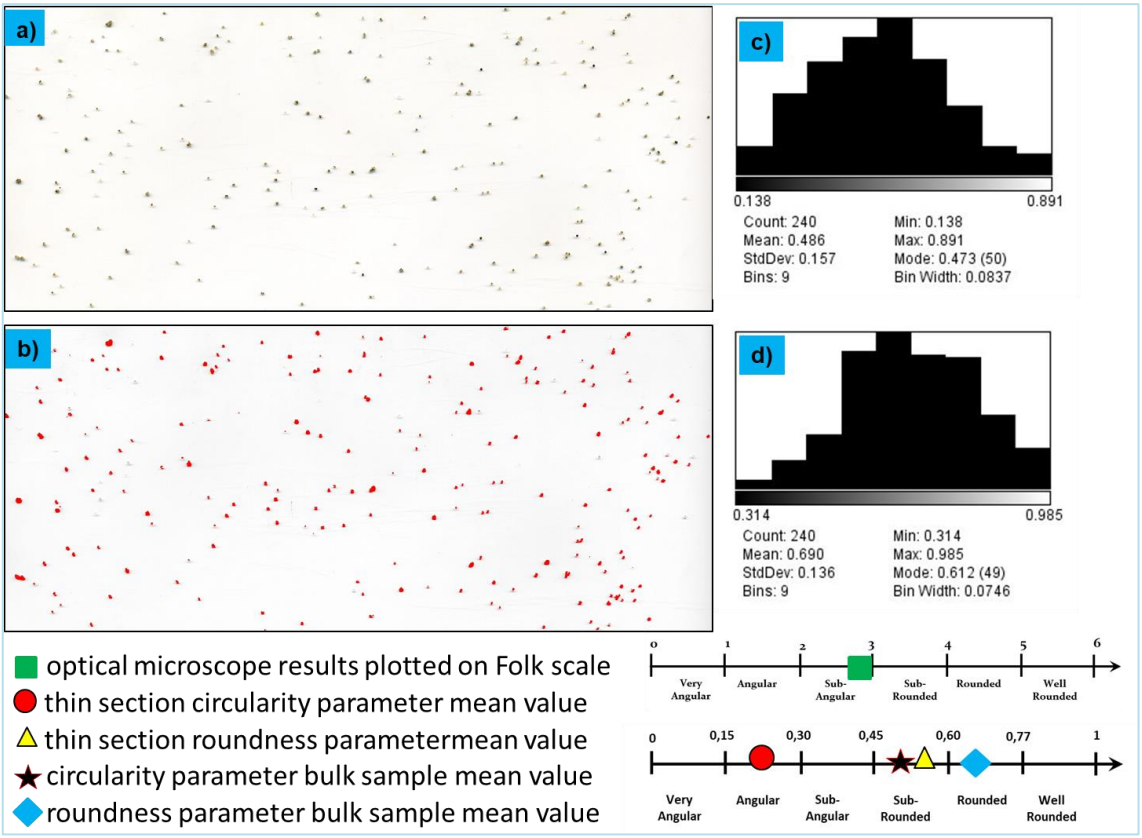

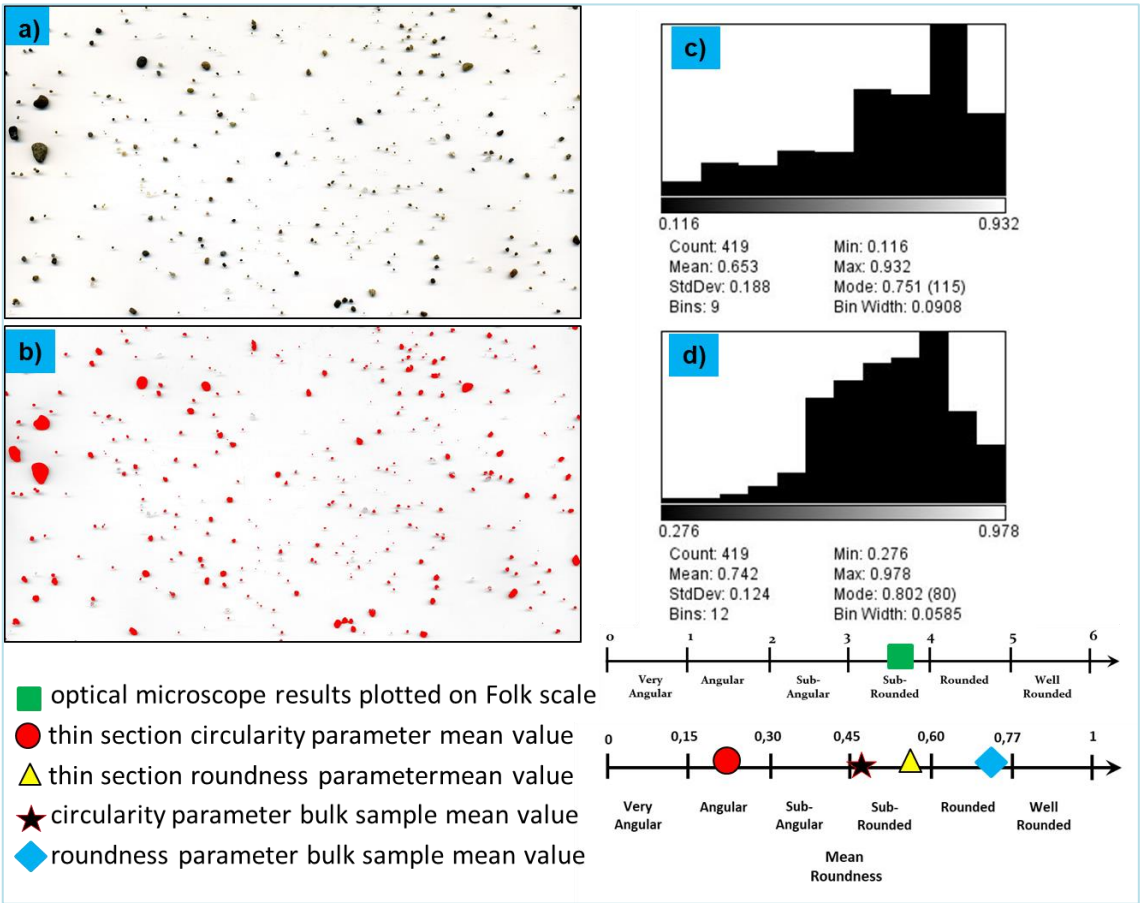

Figure 4.103 (upper) – Li-1 sample image analyses results. Figure 4.104 (lower) – PZ-8 sample image analyses results. a) Transmitted natural light scanned image; b) selected grains to analyzing; c) circularity distribution values; d) roundness distribution values.

PZ-8 bulk sample displays a 0,653 circularity mean value and a 0,742 roundness mean value among 419 analyzed grains. Based on circularity value PZ-8 falls in the sub-rounded category, whereas based on roundness mean value it falls in the rounded category (fig. 4.104).

PZ-14 bulk sample displays a 0,561 circularity mean value and a 0,713 roundness mean value among 425 analyzed grains. Based on circularity value PZ-14 falls in the sub-rounded category, whereas based on roundness mean value it falls in the rounded category (fig. 4.105).

GA-1 bulk sample displays a 0,672 circularity mean value and a 0,723 roundness mean value among 301 analyzed grains. Based on circularity and roundness values GA-1 falls in the rounded category (fig. 4.106).

NA-1 bulk sample displays a 0,703 circularity mean value and a 0,682 roundness mean value among 500 analyzed grains. Based on circularity and roundness values NA-1 falls in the rounded category (fig. 4.107).

PO-1 bulk sample displays a 0,697 circularity mean value and a 0,732 roundness mean value among 441 analyzed grains. Based on circularity and roundness values PO-1 falls in the rounded category (fig. 4.108).

TG-1 bulk sample displays a 0,702 circularity mean value and a 0,723 roundness mean value among 348 analyzed grains. Based on circularity and roundness values TG-1 falls in the rounded category (fig. 4.109).

TA-1 bulk sample displays a 0,763 circularity mean value and a 0,768 roundness mean value among 496 analyzed grains. Based on circularity and roundness values TA-1 falls in the rounded category (fig. 4.110).

VE-1 bulk sample displays a 0,598 circularity mean value and a 0,717 roundness mean value among 357 analyzed grains. Based on circularity value VE-1 falls in the sub-rounded category, whereas based on roundness parameter it falls in the rounded (fig. 4.111).

CA-1 bulk sample displays a 0,703 circularity mean value and a 0,681 roundness mean value among 705 analyzed grains. Based on circularity and roundness values CA-1 falls in the rounded category (fig. 4.112).

SO-1 bulk sample displays a 0,728 circularity mean value and a 0,652 roundness mean value among 427 analyzed grains. Based on circularity and roundness values SO-1 falls in the rounded category (fig. 4.113).

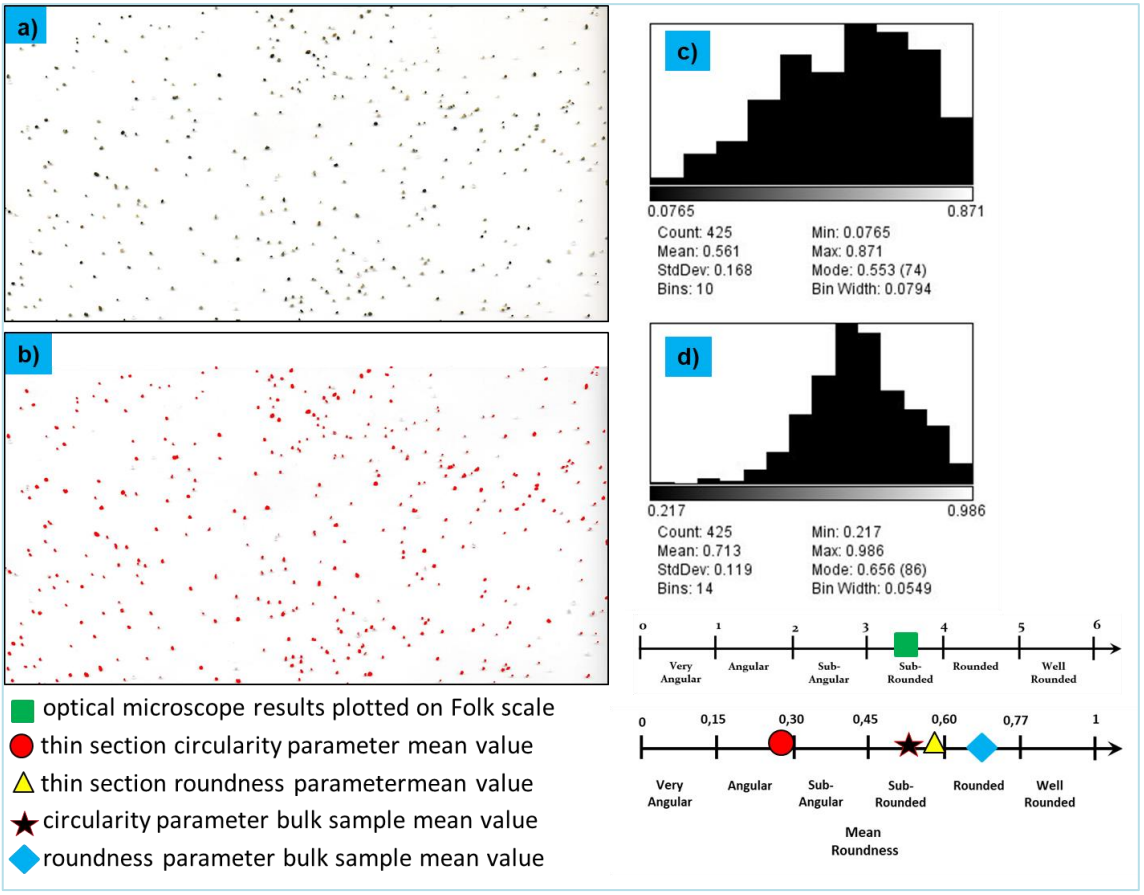

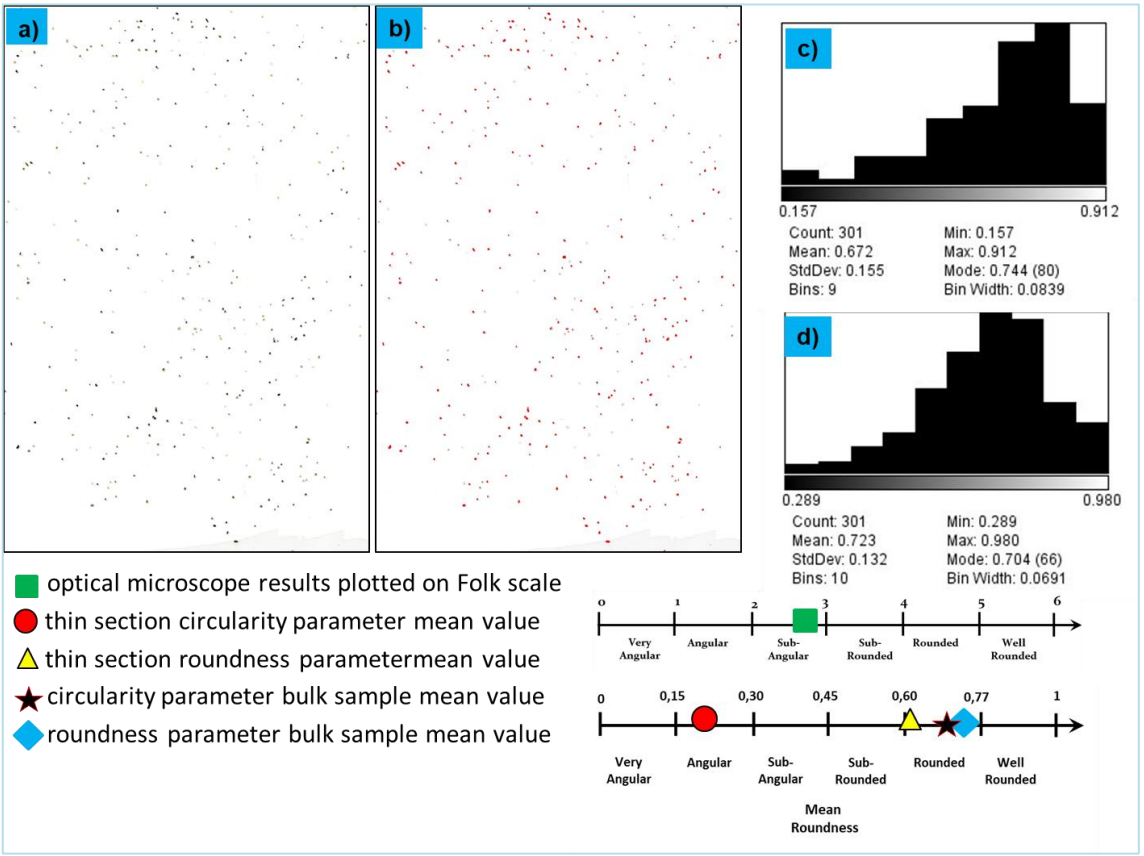

Figure 4.105 (upper) – PZ-14 sample image analyses results. Figure 4.106 (lower) – GA-1 sample image analyses results. a) Transmitted natural light scanned image; b) selected grains to analyzing; c) circularity distribution values; d) roundness distribution values.

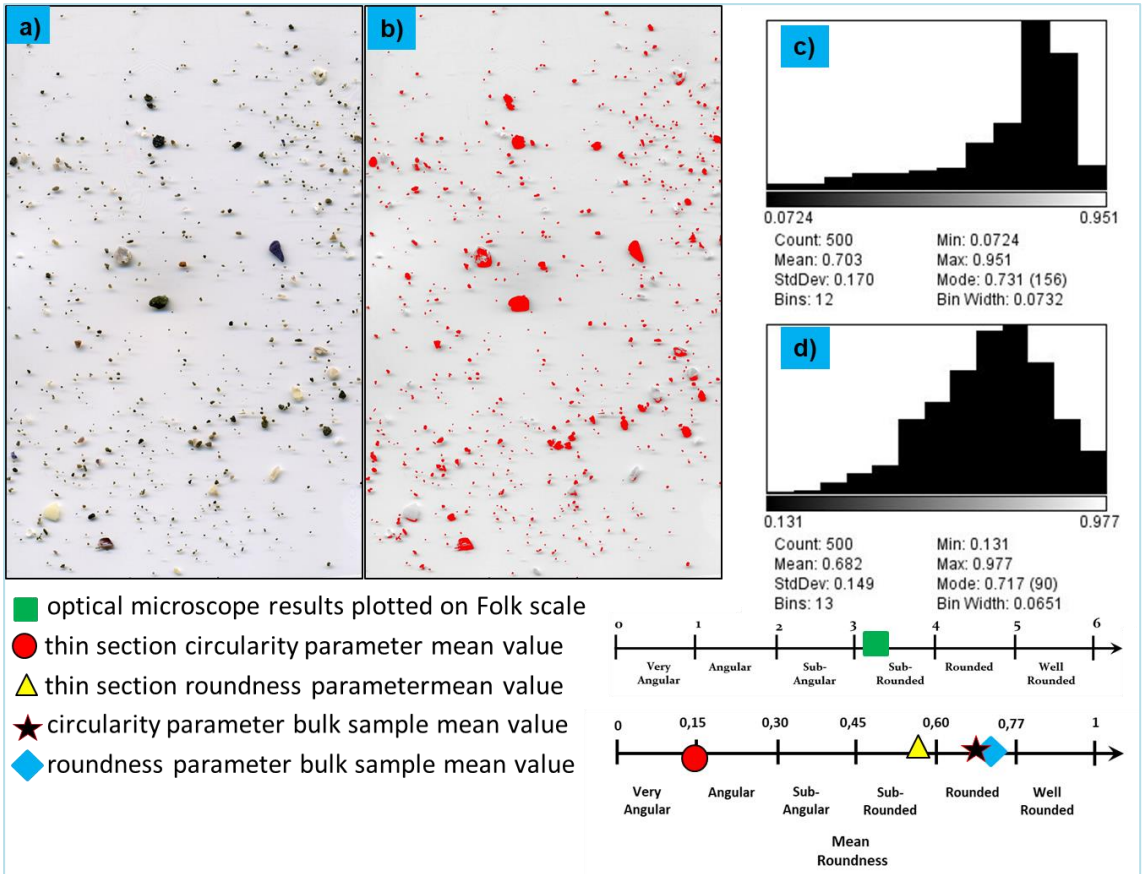

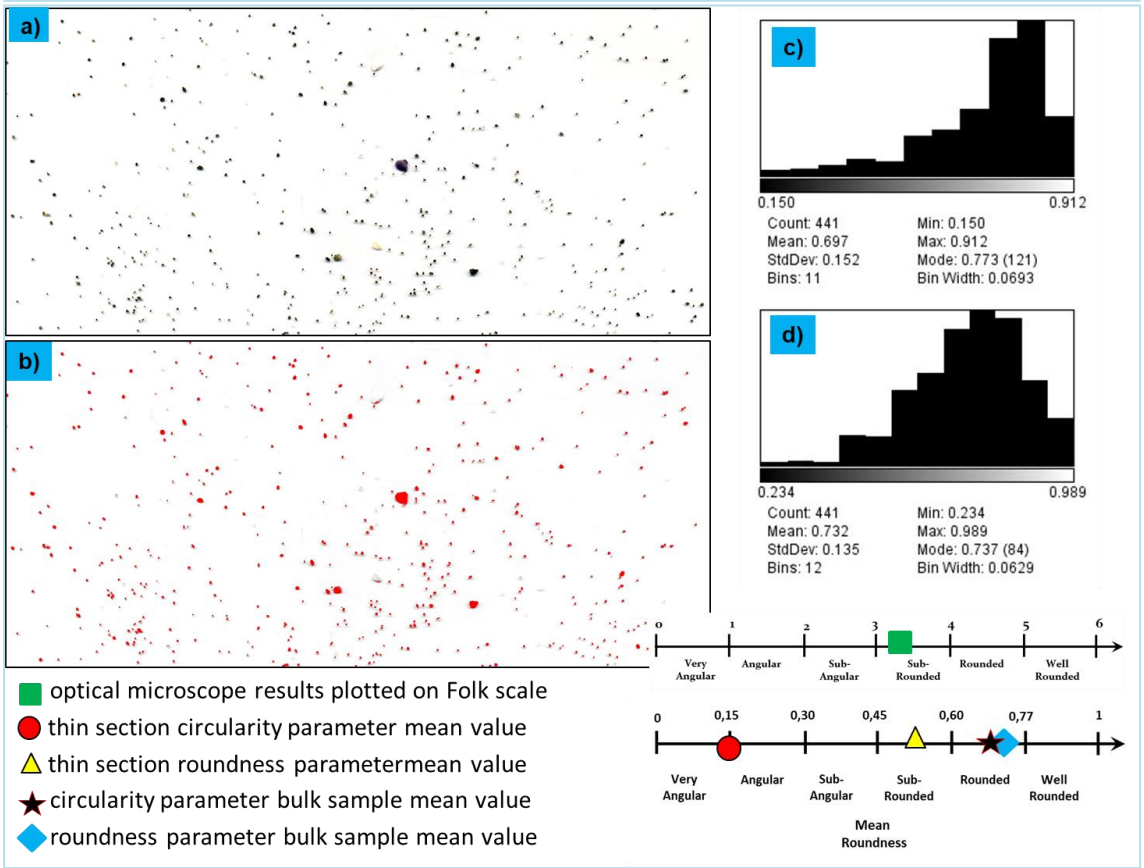

Figure 4.107 (upper) – NA-1 sample image analyses results. Figure 4.108 (lower) – PO-1 sample image analyses results. a) Transmitted natural light scanned image; b) selected grains to analyzing; c) circularity distribution values; d) roundness distribution values.

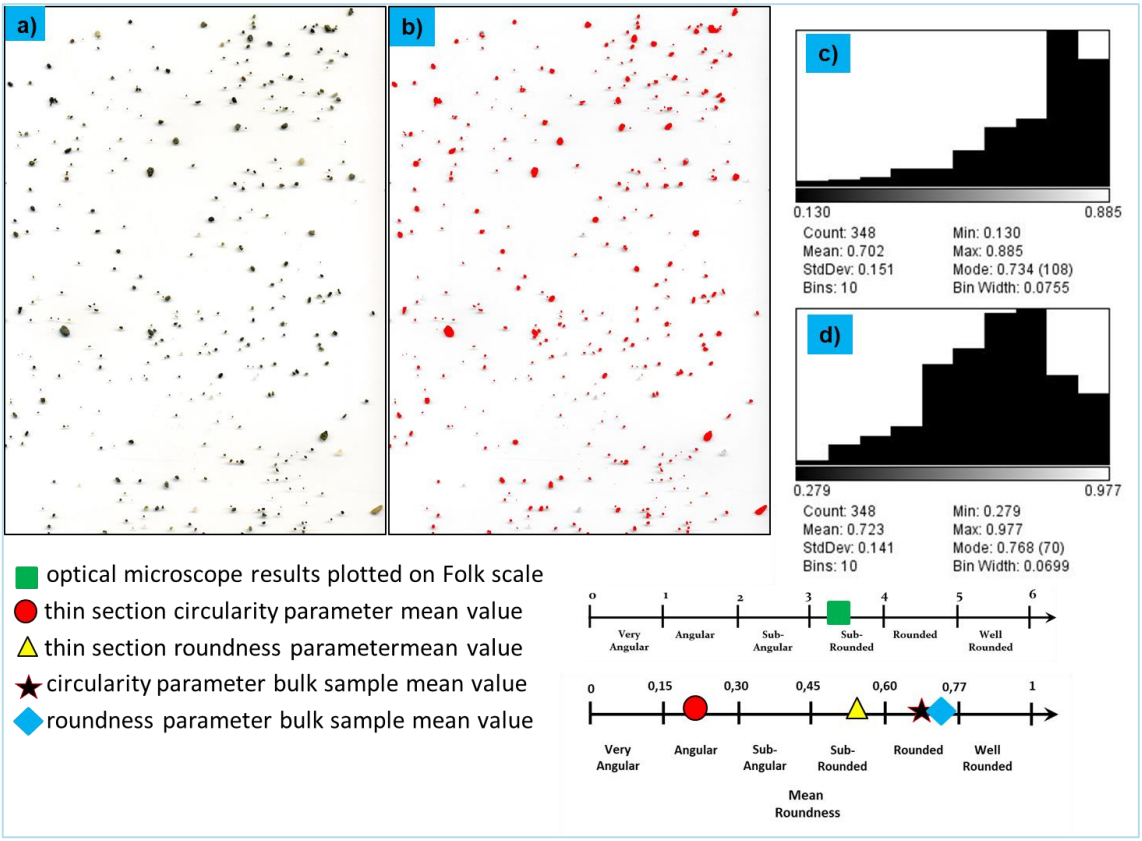

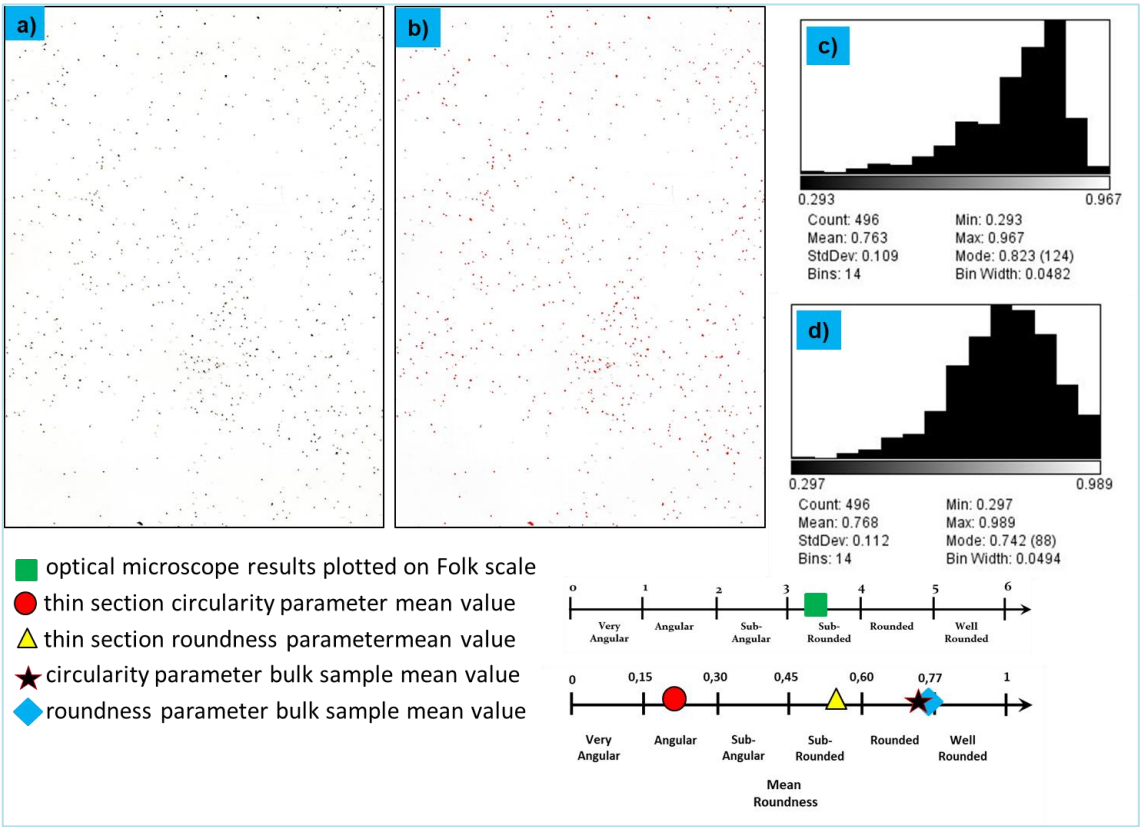

Figure 4.109 (upper) – TG-1 sample image analyses results. Figure 4.110 (lower) – TA-1 sample image analyses results. a) Transmitted natural light scanned image; b) selected grains to analyzing; c) circularity distribution values; d) roundness distribution values.

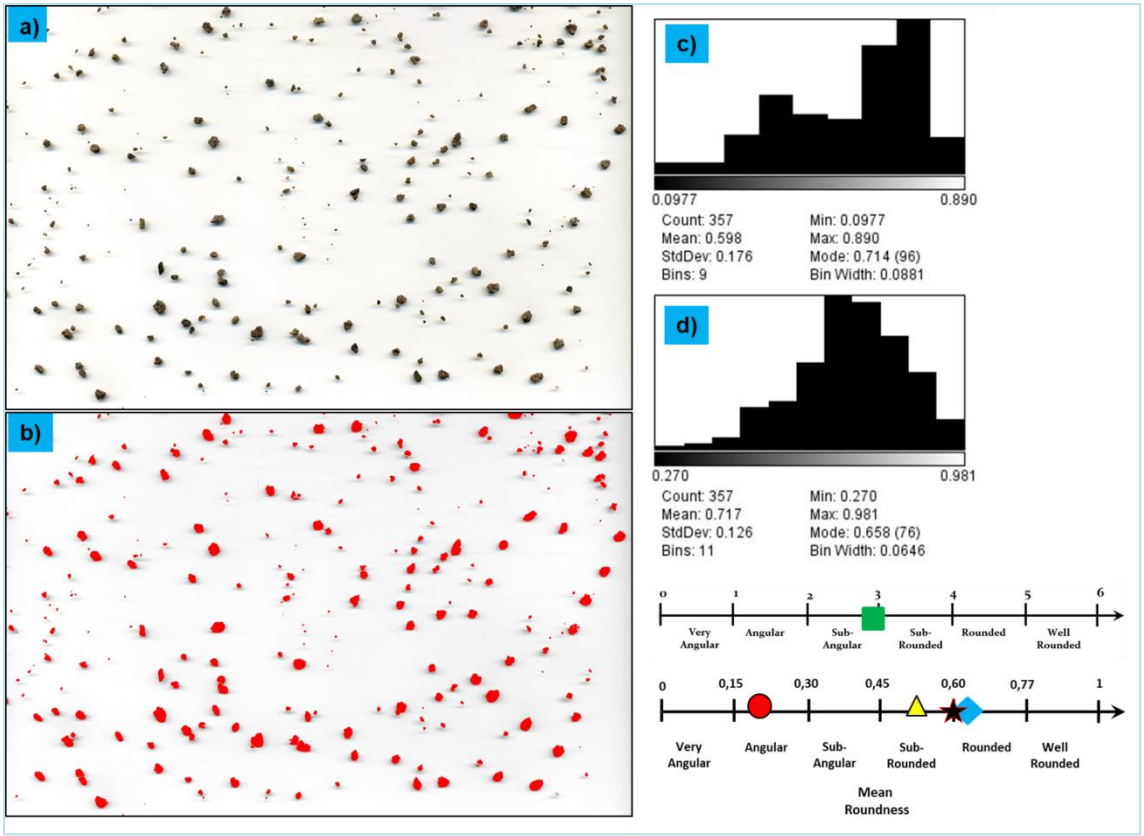

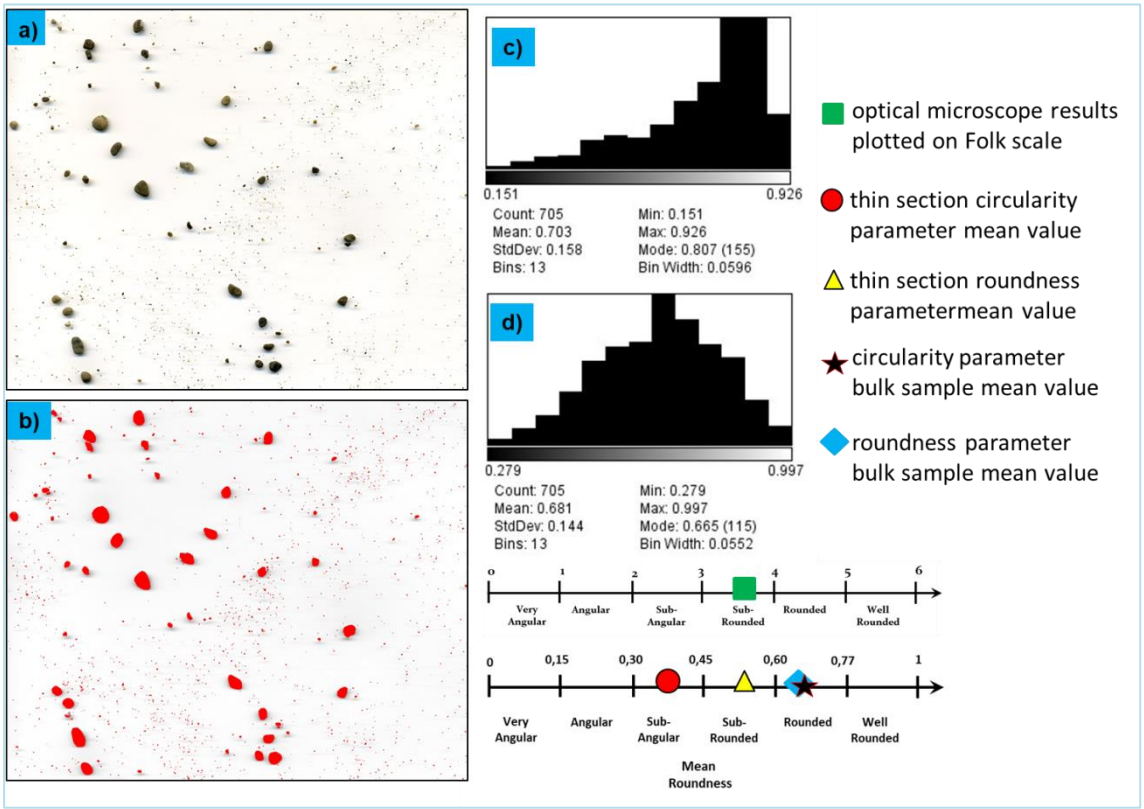

Figure 4.111 (upper) – VE-1 sample image analyses results. Figure 4.112 (lower) – CA-1 sample image analyses results. a) Transmitted natural light scanned image; b) selected grains to analyzing; c) circularity distribution values; d) roundness distribution values.

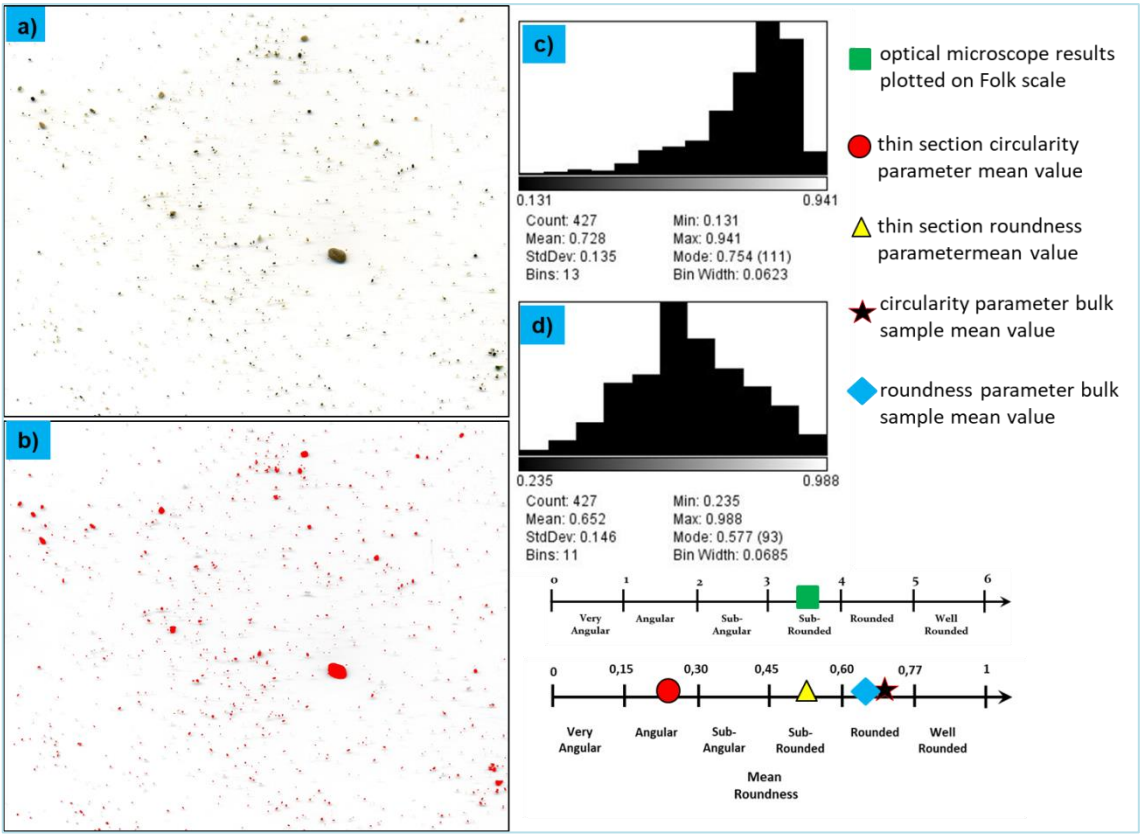

Figure 4.113 (lower) – SO-1 sample image analyses results. a) Transmitted natural light scanned image; b) selected grains to analyzing; c) circularity distribution values; d) roundness distribution values.

4.4 – Aeolian Islands GIS analysis (SGI calculation) -

It has been carried out a furthermore study for the Aeolian Islands regarding the sandy detritus production from volcanic rocks calculating a sand generation index (SGI) by following a modified Palomares and Arribas (1993) technique.

For each drainage basin (connected to sample) the percentage of the type of source rock were assessed using Geographic information system. GIS analysis and its cartographic output were produced by Quantum GIS extracting data from Tranne et al. (2002), Lucchi et al. (2013) geological maps. This enabled the quantification of the area occupied by each type of lithology in the drainage basin, together with the topography.

GIS regional mapping shows that based upon topography, Aeolian Islands are characterized by three major landforms: piedmonts and very low hills (0 - 240 m above sea level), low hills (240 – 480 m a.s.l.), and high hills (>500 m a.s.l.) (figs 3.2a, 3.4a, 3.7, 3.9, 3.11, 3.13, 3.15). Geomorphologic mapping followed the approach where drainage basins are considered as discrete units with differentiated source rocks (from tables 4.16 to 4.29) supplying clastic detritus to the beach environment through stream erosion and mass-failure processes. Each drainage basin can be subdivided into three

parts (upstream, downstream and alluvial system), each part having distinctive morphological characteristics (figs 3.2a, 3.4a, 3.7, 3.9, 3.11, 3.13, 3.15 and from fig. 4.60 to fog 4.64). The uppermost parts of the watersheds, corresponding to the 'high hills', are steeply sloping, and the morphology is rugged and controlled by high-rate mass-wasting processes (Favalli et al. 2005). The mid-courses of the watersheds, corresponding to the 'low hills', are gently sloping. A sharp decrease in overall topographic slope marks the transition from the 'low hills' to the piedmont and very low hills area. In these lower reaches the drainage system presents a wide alluvial plain, and sedimentation, in the form of gravelly sand, is widespread throughout the coastal plain.

Hence, the concept of Sand Generation Index (i.e. SGI of Palomares & Arribas, 1993) is introduced (from tab. 4.16 to tab. 4.29) this is a relative measure of the capacity of one bedrock type to generate sand with respect to another in a compound source area. It is referred to the SGI of the lavas and of the pyroclastic source rocks. Thus,

$$SGI_{L(L+P)} = \frac{S_L + S_P}{S_L}; \quad SGI_{P(P+L)} = \frac{S_P + S_L}{S_P};$$

where $SGI_{L(L+P)}$ indicates the SGI of the lavas referred to a dual source constituted by the association lavas + pyroclastic rocks ($S_L + S_P$); and $SGI_{P(P+L)}$ denotes the SGI of the pyroclastic rocks. S_L is the percentage of lava (source rock) outcropping in the basin; S_P is the percentage of pyroclastic rock (source rock) outcropping in the basin.

4.4.1 – ALICUDI ISLAND DRAINAGE BASINS CHARACTERISTICS -

Six coastal drainage basins were identified and the corresponding beach sands were collected spaced along Alicudi coastal perimeter (figs 3.2a, 4.114). In order to evaluate the relationships among source rocks, areal distribution and type of volcanic detritus, source rocks have been described (see 2.1.1a section in chapter 2) and volcanic detritus have been analyzed (see 4.2.1 section in chapter 4). Alicudi drainage basins are predominately constituted by basalts and basaltic andesites products (lavas and lesser amount of pyroclastic rocks, fig. 4.114 and tab. 4.16, 4.17). According to bedrock lithology at the source, relative proportions have been quantified (fig. 4.114, tab. 4.16, 4.17).

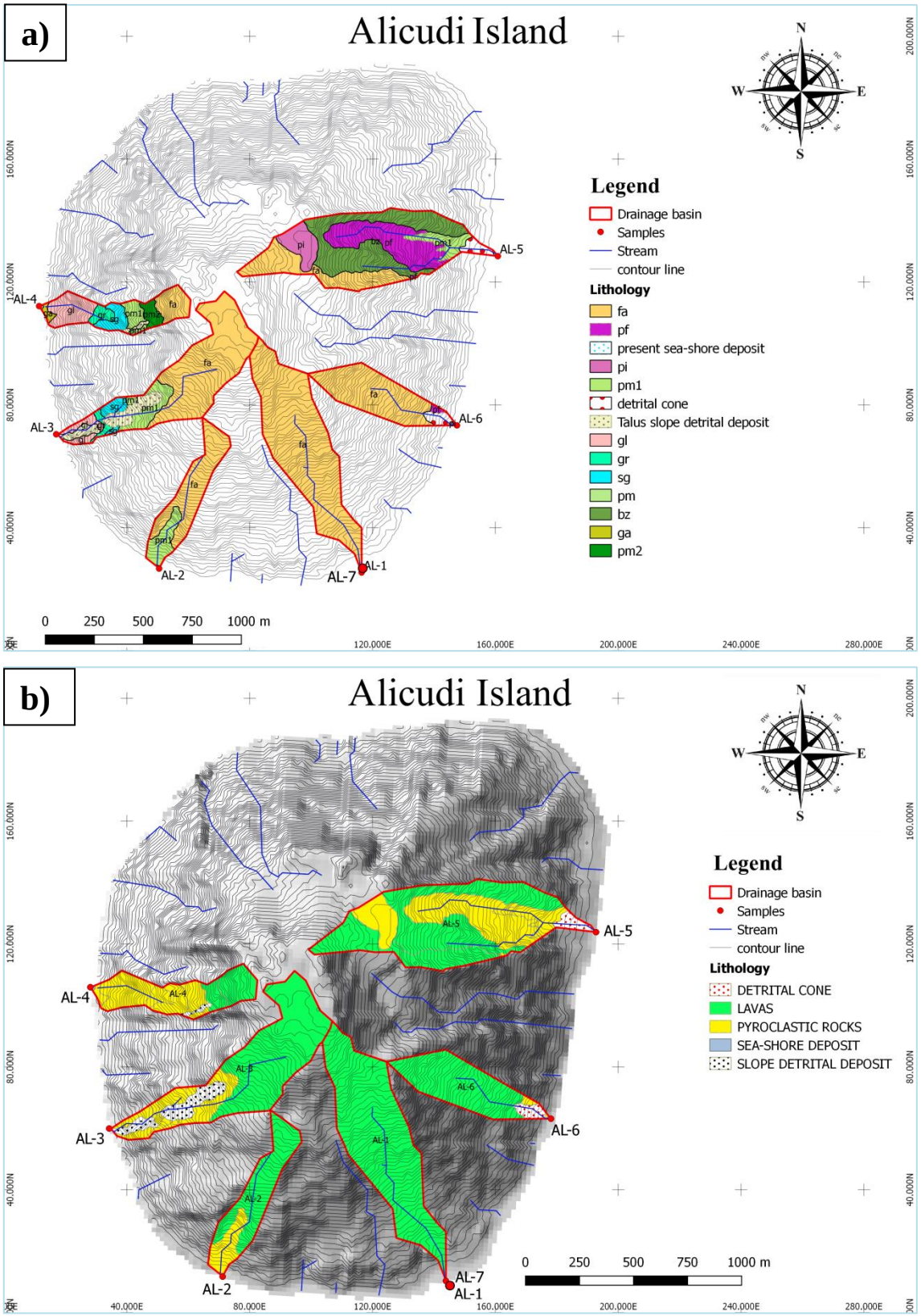

Figure 4.114 – Identified drainage basin (a,b), source rock lithologies (a) and grouped lithologies in lavas and pyroclastic rocks (b).

Drainage Basin	Basin area (ha)	Geological map symble	Outcrop area (ha)	Source rock	Lithology composition
AL-1 / AL-7	25,21	fa	25,21	Lava	High-k Andesite
AL-2	10	fa	7,6	Lava	High-k Andesite
		pm1	2,4	Pyroclastics	CA basalts to basaltic-andesites
AL-3	24,73	fa	16,7	Lava	High-k Andesite
		pm1	2,31	Pyroclastics	CA basalts to basaltic-andesites
		sg	1,02	Pyroclastics	CA basalts to basaltic-andesites
		gr	0,51	Pyroclastics	CA basalts to basaltic-andesites
		gl	1,23	Pyroclastics	CA basalts to basaltic-andesites
		slope detrital deposit	2,96	/	/
AL-4	10,7	ga	0,32	Pyroclastics	CA basalts
		gl	3,11	Pyroclastics	CA basalts to basaltic-andesites
		gr	0,81	Pyroclastics	CA basalts to basaltic-andesites
		sg	1,37	Pyroclastics	CA basalts to basaltic-andesites
		pm1	1,33	Pyroclastics	CA basalts to basaltic-andesites
		pm2	1	Lava	CA andesites
		fa	2,46	Lava	High-k Andesite
		slope detrital deposit	0,24	/	/
AL-5	33,08	pm1	2	Pyroclastics	CA basalts to basaltic-andesites
		bz	11,97	Lava	Ca to high-K andesites
		pf	8,3	Pyroclastics	Ca to high-K andesites
		fa	7,05	Lava	Highk Andesite
		pi	2,87	Pyroclastics	Trachy-andesite
		detrital slope	0,89	/	/
AL-6	11,61	fa	10,59	Lava	High-k Andesite
		pf	0,2	Pyroclastics	Ca to high-K andesites
		pi	0,02	Pyroclastics	Trachy-andesite
		detrital cone	0,8	/	/

Table 4.16 – Outcropping source rocks in the different drainage basins (geological map symbols are from Lucchi et al., 2013); ha = hectares

Drainage basin	L + P area (ha)	Lavas (ha)	Pyroclasts (ha)	% LAVAS	% PYROCLASTICS	%TOT	SGI (L)	SGI (P)	SGI Ratio
AL-1 / AL-7	25,2	25,2	0	100	0	100	1	0	0
AL-2	10	7,6	2,4	76	24	100	1,32	4,17	0,32
AL-3	21,8	16,7	5,1	76,7	23,3	100	1,30	4,29	0,30
AL-4	10,4	3,5	6,9	33,3	66,7	100	3,01	1,50	2,01
AL-5	32,2	19,0	13,2	59,1	40,9	100	1,69	2,44	0,69
AL-6	10,8	10,6	0,2	98,0	2,0	100	1,02	49,14	0,02
				TOT %	TOT %				
				73,84	26,16	100			

Table 4.17 – Lavas and pyroclastic rocks percentage calculated for each drainage basin and relative SGI values (e.g. Palomares and Arribas, 1993). L = lavas; P = Pyroclastic rocks; ha = hectares.

4.4.2 – FILICUDI ISLAND DRAINAGE BASINS CHARACTERISTICS -

Four coastal drainage basins were identified and the corresponding beach sands were collected spaced along Filicudi coastal perimeter (figs 3.4a, 4.115). In order to evaluate the relationships among source rocks, areal distribution and type of volcanic detritus, source rocks have been described (see 2.1.1b section in chapter 2) and volcanic detritus have been analyzed (see 4.2.1 section in chapter 4). Filicudi drainage basins are predominately constituted by basalts and andesites products, only Fi-4 drainage basin is constituted by andesite to dacite lava outcrops (fig. 4.115 and tab. 4.18, 4.19). According to bedrock lithology at the source, relative proportions have been quantified (fig. 4.114, tab. 4.16, 4.17).

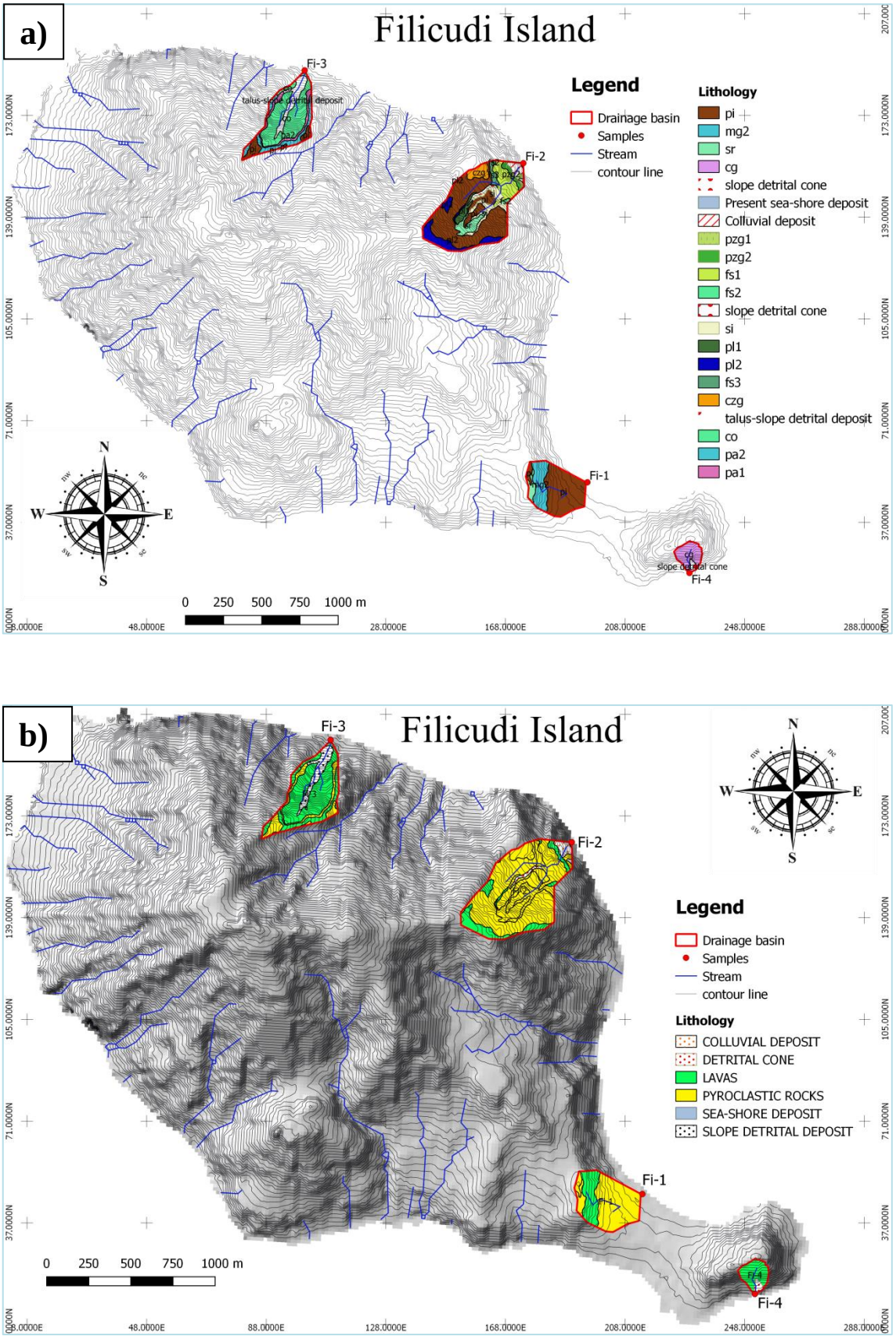

Figure 4.115 – Identified drainage basin (a,b), source rock lithologies (a) and grouped lithologies in lavas and pyroclastic rocks (b).

Drainage Basin	Basin area (ha)	Geological map symble	Outcrop area (ha)	Source rock	Lithology composition
Fi-1	10,15	pi	7,15	Pyroclastics	Trachy-andesites
		mg2	2,38	Lava	basalts and basaltic andesites
		sr	0,62	Pyroclastics	basalts and basaltic andesites
Fi-2	24,16	pzg1	0,26	Pyroclastics	Andesites
		pzg2	0,52	Lava	Basaltic andesites to andesites
		fs1	2,47	Pyroclastics	Basaltic andesites
		fs2	0,17	Lava	Basaltic andesites
		fs3	0,41	Pyroclastics	Basaltic andesites
		si	1,93	Pyroclastics	/
		sr	1,22	Pyroclastics	Basalts and basaltic andesites
		czg	1,06	Pyroclastics	Andesites to high-K andesites
		pi	12,44	Pyroclastics	Trachy-andesites
		pl1	0,72	Pyroclastics	Basalts to basaltic andesites
		pl2	2,83	Lava	Basaltic andesites
		colluvial deposit	0,13		/
Fi-3	13,2	co	6,75	Lava	Basaltic andesites
		slope detrital deposit	1,86	/	/
		pa1	1,34	Pyroclastics	Basalts
		pa2	2,04	Lava	Basalt and basaltic andesites
		pi	1,18	Pyroclastics	Trachy-andesites
		present sea-shore deposit	0,03	/	/
Fi-4	2,49	cg	2,17	Lava	High-K andesite to dacite
		slope detrital cone	0,32	/	/

Table 4.18 – Outcropping source rocks in the different drainage basins (geological map symbols are from Lucchi et al., 2013); ha = hectares.

Drainage basin	L + P area (ha)	Lavas (ha)	Pyroclasts (ha)	% LAVAS	% PYROCLASTICS	%TOT	SGI (L)	SGI (P)	SGI Ratio
Fi-1	10,2	2,4	7,8	23,4	76,6	100	4,26	1,31	3,26
Fi-2	24,0	3,5	20,5	14,6	85,4	100	6,83	1,17	5,83
Fi-3	11,3	8,8	2,5	77,7	22,3	100	1,29	4,49	0,29
Fi-4	2,2	2,2	0	100	0	100	1	0	0
				TOT %	TOT %				
				53,95	46,05	100			

Table 4.19 – Lavas and pyroclastic rocks percentage calculated for each drainage basin and relative SGI values (e.g. Palomares and Arribas, 1993). L = lavas; P = Pyroclastic rocks.; ha = hectares.

4.4.3 – SALINA ISLAND DRAINAGE BASINS CHARACTERISTICS -

Fourteen coastal drainage basins were identified and the corresponding beach sands were collected spaced along Salina coastal perimeter (figs 3.7, 4.116). In order to evaluate the relationships among source rocks, areal distribution and type of volcanic detritus, source rocks have been described (see 2.1.1c section in chapter 2) and volcanic detritus have been analyzed (see 4.2.1 section in chapter 4). Salina drainage basins are predominately constituted by basalts, basaltic andesites and andesites products, with exception of SA-5 drainage basin where there is a dacite to rhyolite pyroclastic outcrop (tab 4.20). Among Salina drainage basin outcrops more than 80 % is constituted by pyroclastic rocks (tab 4.20, 4.21, fig. 4.116a,b). According to bedrock lithology at the source, relative proportions have been quantified (fig. 4.116, tab. 4.20 4.21).

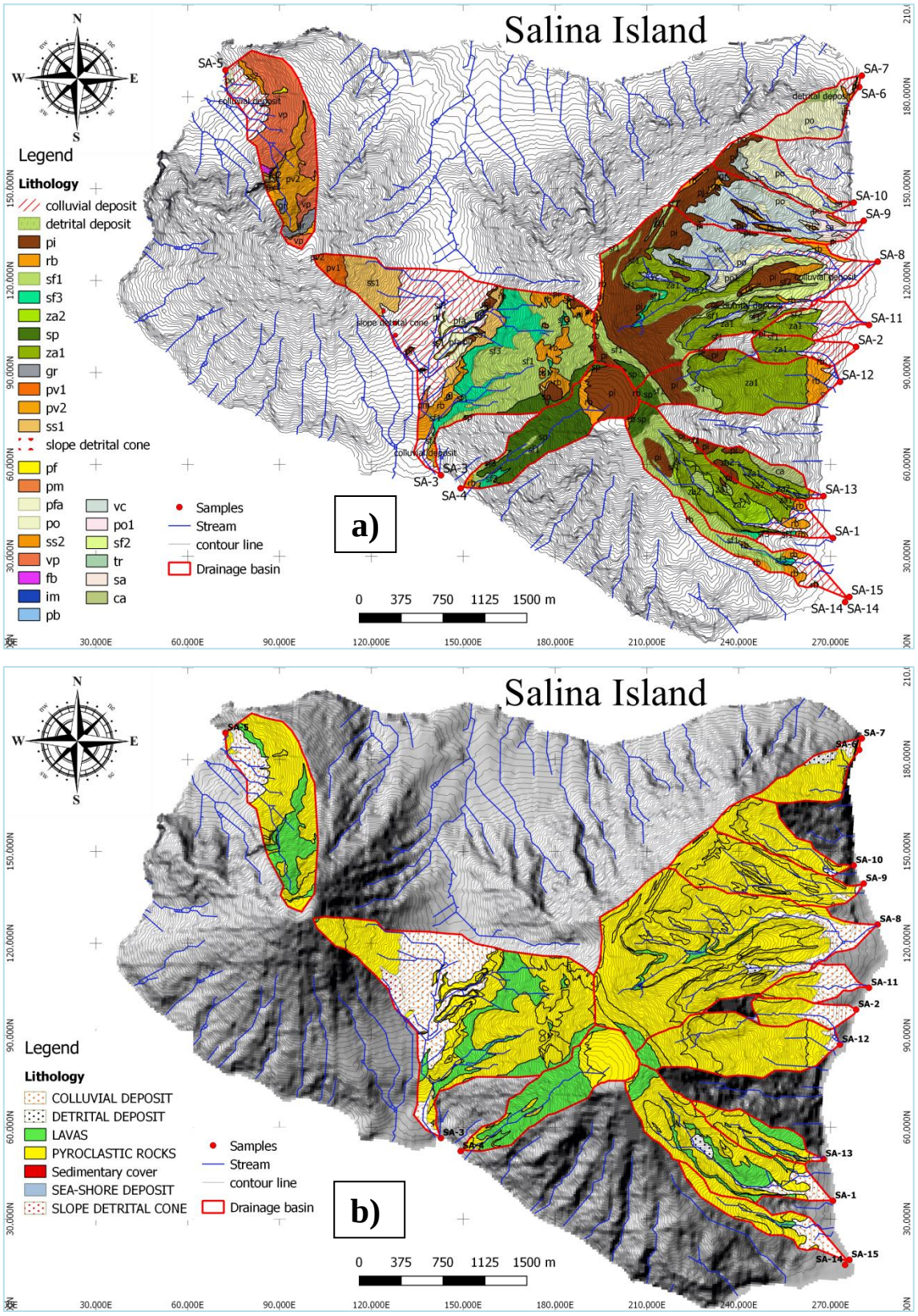

Figure 4.116 – Identified drainage basin (a,b), source rock lithologies (a) and grouped lithologies in lavas and pyroclastic rocks (b).

Drainage Basin	Basin area (ha)	Geological map symble	Outcrop area (ha)	Source rock	Lithology composition
SA-1	80,42	Colluvial deposit	6,74	/	/
		rb	3,82	Pyroclastics	Basalts and basaltic andesites
		sf3	1,33	Lava	CA andesites
		za1	24,55	Pyroclastics	CA basalts
		sf1	17,81	Pyroclastics	CA andesites
		za2	12,51	Lava	Basalts
		detrital deposit	2,26	/	/
		pi	7,04	Pyroclastics	Trachy-andesite
		sp	4,36	Lava	CA basaltic andesites
SA-2	17,96	Colluvial deposit	6,82	/	/
		rb	0,21	Pyroclastics	Basalts and basaltic andesites
		za1	9,89	Pyroclastics	CA basalts
		sf1	1,00	Pyroclastics	CA andesites
		pi	0,04	Pyroclastics	Trachy-andesite
SA-3	224	Colluvial deposit	59,13	/	/
		Slope detrital cone deposit	4,54	/	/
		sf1	55,24	Pyroclastics	CA andesites
		rb	23,01	Pyroclastics	Basalts and basaltic andesites
		sf3	28,12	Lava	CA andesites
		pm	4,46	Lava	CA basaltic andesites
		ss1	28,46	Pyroclastics	CA basaltic andesites
		pi	6,32	Pyroclastics	Trachy-andesite
		pf	1,95	Pyroclastics	Basaltic andesites
		pv1	5,32	Pyroclastics	CA basaltic andesites
		pv2	0,54	Lava	CA to high-K andesites
		gr	0,28	Pyroclastics	trachy-andesites
		pfa	6,73	Pyroclastics	Basaltic andesites

Table 4.20 – Outcropping source rocks in the different drainage basins (geological map symbols are from Lucchi et al., 2013); ha = hectares -(continued)-

Drainage Basin	Basin area (ha)	Geological map symble	Outcrop area (ha)	Source rock	Lithology composition
SA-4	58	rb	4,93	Pyroclastics	Basalts and basaltic andesites
		sf1	2,85	Pyroclastics	CA andesites
		detrital deposit	0,06	/	/
		sf3	1,67	Lava	CA andesites
		sp	31,6	Lava	CA basaltic andesites
		pi	16,88	Pyroclastics	Trachy-andesite
SA-5	84,4	Colluvial deposit	12,77	/	/
		po	1,2	Pyroclastics	/
		ss2	3,17	Lava	CA basaltic andesites
		pf	0,35	Pyroclastics	Basaltic andesites
		vp	43,62	Pyroclastics	High-k dacite to rhyolite
		pv2	17,73	Lava	CA to high-K andesites
		ss1	0,53	Pyroclastics	CA basaltic andesites
		rb	0,16	Pyroclastics	Basalts and basaltic andesites
		fb	0,6	Pyroclastics	CA basalts
		pv1	0,39	Pyroclastics	CA basaltic andesites
		gr	3,88	Pyroclastics	trachy-andesites
SA-6-7	26,85	po	22,15	Pyroclastics	CA basalts
		pb	0,09	sedimentary cover	/
		im	0,05	sedimentary cover	/
		rb	1,03	Pyroclastics	Basalts and basaltic andesites
		pi	0,08	Pyroclastics	Trachy-andesite
		Colluvial deposit	1,47	/	/
		Detrital deposit	1,98	/	/
SA-8	213,76	Colluvial deposit	15,03	/	/
		rb	7,07	Pyroclastics	Basalts and basaltic andesites
		sf2	14,10	Pyroclastics	CA andesites
		vc	30,89	Pyroclastics	CA basalts
		sf1	20,63	Pyroclastics	CA andesites
		pi	67,23	Pyroclastics	Trachy-andesite
		tr	0,53	Pyroclastics	CA to high-K dacites
		za1	44,42	Pyroclastics	CA basalts
		sp	3,09	Lava	CA basaltic andesites
		po	8,88	Pyroclastics	CA basalts
		po1	0,91	Lava	CA basalts
		Detrital deposit	1,00	/	/
SA-9	59,96	rb	4,50	Pyroclastics	Basalts and basaltic andesites
		pi	12,52	Pyroclastics	Trachy-andesite
		vc	31,59	Pyroclastics	CA basalts
		po	2,65	Pyroclastics	CA basalts
		sf1	0,29	Pyroclastics	CA andesites
		gr	0,58	Pyroclastics	trachy-andesites
		sa	6,93	Pyroclastics	reworked
		colluvial deposit	0,90	/	/
SA-10	31,14	detrital deposit	0,57	/	/
		po	21,40	Pyroclastics	CA basalts
		vc	3,90	Pyroclastics	CA basalts
		pi	5,28	Pyroclastics	Trachy-andesite
SA-11	18,87	sf2	1,31	Pyroclastics	CA andesites
		pi	0,04	Pyroclastics	Trachy-andesite
		sf1	0,38	Pyroclastics	CA andesites
		za1	7,40	Pyroclastics	CA basalts
		colluvial deposit	9,74	/	/
SA-12	73,98	sp	3,19	Lava	CA basaltic andesites
		rb	6,46	Pyroclastics	Basalts and basaltic andesites
		sf1	8,25	Pyroclastics	CA andesites
		pi	10,28	Pyroclastics	Trachy-andesite
		za1	44,01	Pyroclastics	CA basalts
		colluvial deposit	1,79	/	/

Table 4.20 – Outcropping source rocks in the different drainage basins (geological map symbols are from Lucchi et al., 2013); ha = hectares -(continued)-

Drainage Basin	Basin area (ha)	Geological map symble	Outcrop area (ha)	Source rock	Lithology composition
SA-13	25,29	za2	2,03	Lava	Basalts
		rb	0,78	Pyroclastics	Basalts and basaltic andesites
		pi	4,03	Pyroclastics	Basalts and basaltic andesites
		sf1	0,16	Pyroclastics	CA andesites
		za1	12,81	Pyroclastics	CA basalts
		ca	5,14	Lava	CA basalts
		colluvial deposit	0,34	/	/
SA-14-15	26,32	rb	5,03	Pyroclastics	Basalts and basaltic andesites
		present sea-shore deposit	0,04	/	/
		colluvial deposit	6,94	/	/
		sf3	1,01	Lava	CA andesites
		sf1	13,31	Pyroclastics	CA andesites

Table 4.20 – Outcropping source rocks in the different drainage basins (geological map symbols are from Lucchi et al., 2013); ha = hectares.

Drainage basin	L + P area (ha)	Lavas (ha)	Pyroclasts (ha)	% LAVAS	% PYROCLASTICS	%TOT	SGI (L)	SGI (P)	SGI Ratio
SA-1	71,4	18,2	53,2	25,5	74,5	100	3,92	1,34	2,92
SA-2	11,1	0,0	11,1	0,0	100,0	100	0,00	1,00	0,00
SA-3	160,4	33,1	127,3	20,6	79,4	100	4,84	1,26	3,84
SA-4	57,9	33,3	24,7	57,4	42,6	100	1,74	2,35	0,74
SA-5	71,6	20,9	50,7	29,2	70,8	100	3,43	1,41	2,43
SA-6-7	23,3	0,0	23,3	0,0	100,0	100	0,00	1,00	0,00
SA-8	197,7	4,0	193,7	2,0	98,0	100	49,41	1,02	48,41
SA-9	59,1	0,0	59,1	0,0	100,0	100	0,00	1,00	0,00
SA-10	30,6	0,0	30,6	0,0	100,0	100	0,00	1,00	0,00
SA-11	9,1	0,0	9,1	0,0	100,0	100	0,00	1,00	0,00
SA-12	72,2	3,2	69,0	4,4	95,6	100	22,62	1,05	21,62
SA-13	25,0	7,2	17,8	28,7	71,3	100	3,48	1,40	2,48
SA-14-15	19,3	1,0	18,3	5,2	94,8	100	19,19	1,05	18,19
				TOT %	TOT %				
				13,3	86,7	100			

Table 4.21 – Lavas and pyroclastic rocks percentage calculated for each drainage basin and relative SGI values (e.g. Palomares and Arribas, 1993). L = lavas; P = Pyroclastic rocks.; ha = hectares.

4.4.4 – LIPARI ISLAND DRAINAGE BASINS CHARACTERISTICS -

Twelve coastal drainage basins were identified and the corresponding beach sands were collected spaced along Lipari coastal perimeter (figs 3.9, 4.117). In order to evaluate the relationships among source rocks, areal distribution and type of volcanic detritus, source rocks have been described (see 2.1.1d section in chapter 2) and volcanic detritus have been analyzed (see 4.2.1 section in chapter 4). Lipari drainage basins are constituted by a wider range of volcanic products ranging from basalts to rhyolite, then according to bedrock lithology at the source, relative proportions have been quantified (Morrone et al., 2017; tab 4.22, 4.23).

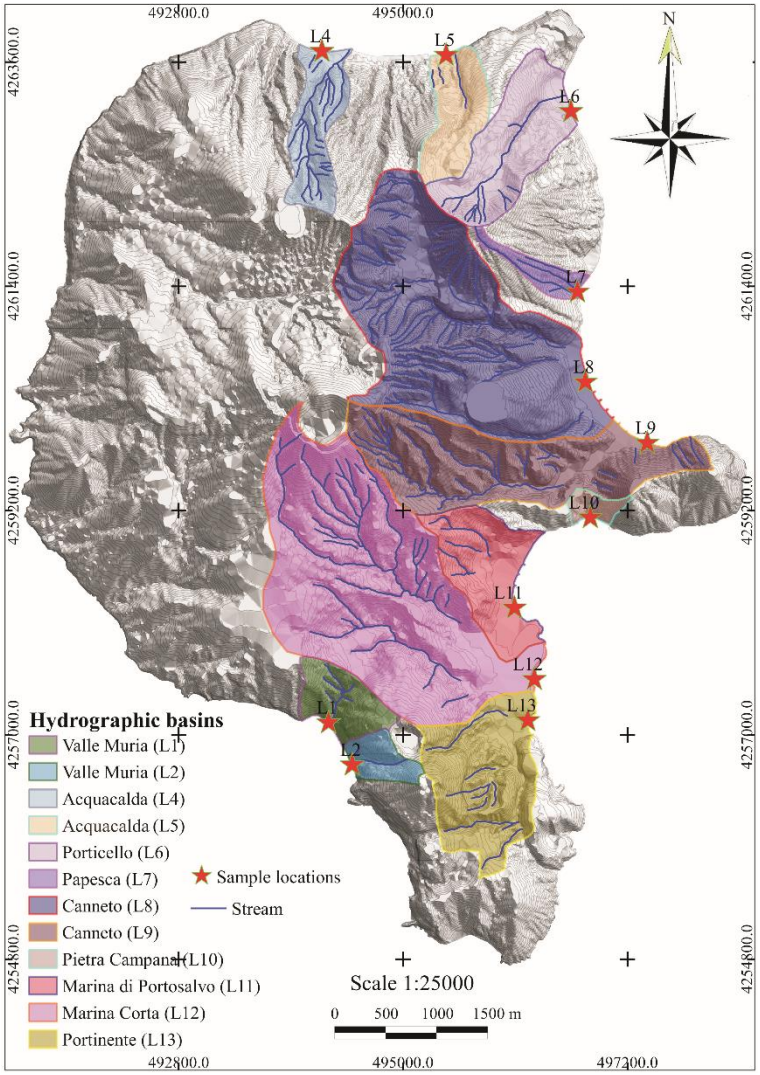

Figure 4.117 - TIN (triangular irregular network) of Lipari island showing the boundaries of the drainage basins with respect to samples (watershed) (modified from Morrone et al., 2017).

Drainage basins source rocks/ Sample number	Lavas (%)			Pyroclastic Rocks (%)					TOT(%)
	Rhyolitic	Bas-And	And	Bas-And Tuffs	Rhyol Tuffs	Pumices	Rhyol Breccia	And Breccia	
L1	0	0	0	8.1	38.9	45.5	7.5	0	100
L2	52.2	0	0	27.2	19.6	1.0	0	0	100
L4	0	10.9	0	31.2	0	57.9	0	0	100
L5	46.7	0	0	0	0	38.2	15.1	0	100
L6	36.8	0	0	0	0	42.4	20.8	0	100
L7	27.6	0	0	0	0	66.5	5.9	0	100
L8	18.6	0.6	0.7	2.2	0	71.4	6.5	0	100
L9	1.4	2.2	3.8	42.7	15.3	19.9	7.3	7.4	100
L10	0	0	0	74.9	3.5	2.6	2.3	16.7	100
L11	5.9	3.4	2.3	76.7	4.1	7.7	0	0	100
L12	5.1	0.7	3.0	20.6	46.6	18.2	0	5.8	100
L13	27.6	0	0	1.1	36.6	34.7	0	0	100
Average source rocks of the studied drainage basins	18.5	1.5	0.8	23.7	13.7	33.8	5.4	2.6	100

Table 4.22 - Outcrop areas of each source rock concerning drainage systems. Bas-And: Basaltic Andesitic; And: Andesitic; Rhyol: Rhyolitic (modified from Morrone et al., 2017).

Basin	Basin Area (ha)	Lavas (%)	Pyroclastic rocks (%)	SGI (L) SGI (P)	SGI Ratio
L1	48,2	0.0	100	0.0 1.0	0.0
L2	25,7	52.2	47.8	1.9 2.1	0.9
L4	65,9	10.9	89.1	9.2 1.1	8.4
L5	63,5	46.7	53.3	2.1 1.9	1.1
L6	114,2	36.8	63.2	2.7 1.6	1.7
L7	22,1	27.6	72.4	3.6 1.4	2.6
L8	395,5	19.9	77.9	5.0 1.3	3.8
L9	219,7	7.4	92.6	13.5 1.1	12.3
L10	12,9	0.0	100	0.0 1.0	0.0
L11	94,6	11.6	88.4	8.6 1.1	7.8
L12	436	8.8	91.2	11.3 1.1	10.3
L13	142,7	27.6	72.4	3.6 1.4	2.6

Table 4.23 - Basin areas, bedrock associations and Sand Generation Index for Lavas and Pyroclastic rocks. SGI: Sand Generation Index (e.g., Palomares & Arribas 1993); L: Lavas; P: Pyroclastic rocks; ha: hectares (modified from Morrone et al., 2017).

4.4.5 – VULCANO ISLAND DRAINAGE BASINS CHARACTERISTICS -

Six coastal drainage basins were identified and the corresponding beach sands were collected spaced along Vulcano coastal perimeter (figs 3.11, 4.118). Some samples have been grouped in the same drainage basin (fig. 4.18). In order to evaluate the relationships among source rocks, areal distribution and type of volcanic detritus, source rocks have been described (see 2.1.1e section in chapter 2) and volcanic detritus have been analyzed (see 4.2.1 section in chapter 4).

Vulcano drainage basins are constituted by volcanic products ranging from basalt to rhyolite and also high-k products such as shoshonite (tab. 4.24). Among Vulcano drainage basins, pyroclastic rocks and lavas have a similar areal distribution percentage (tab 4.24, 4.25, fig. 4.118a,b).

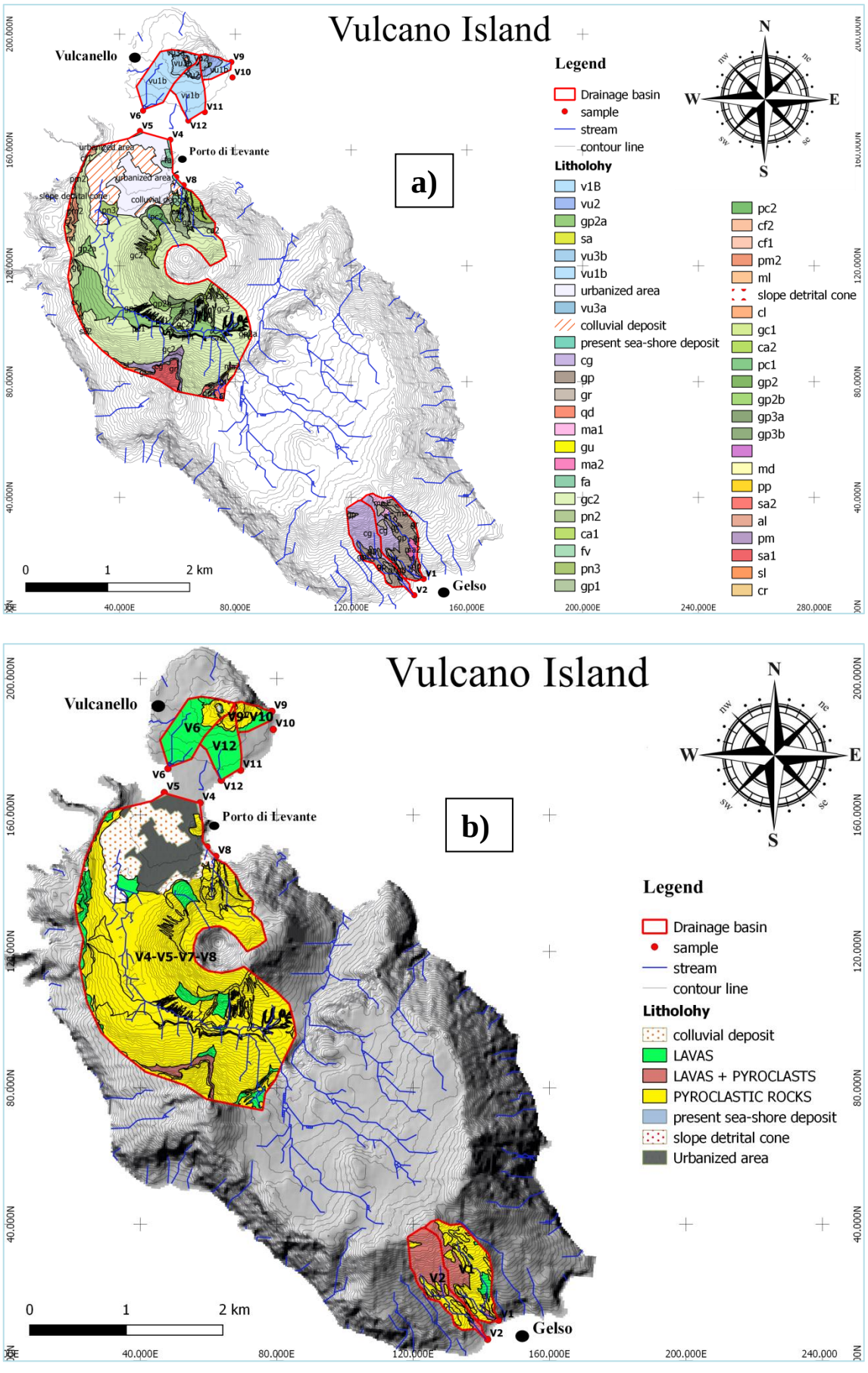

Figure 4.118 – Identified drainage basin (a,b), source rock lithologies (a) and grouped lithologies in lavas and pyroclastic rocks (b).

Drainage Basin	Basin area (ha)	Geological map symble	Outcrop area (ha)	Source rock	Lithology composition
V1	40,08	gu	0,04	Pyroclasts	Rhyolite
		present sea-shore deposit	0,1	/	/
		gr	4,97	Pyroclasts	High-k andesites to dacites
		cg	10,36	L/P	basalts to high-k basaltic andesites
		qd	0,37	Pyroclasts	Shoshoniti
		gp	18,11	Pyroclasts	Shoshoniti
		ma1	3,57	Pyroclasts	Shoshoniti
		ma2	2,56	Lava	Shoshoniti
V2	30,83	present sea-shore deposit	0,07	/	/
		cg	20,83	L/P	basalts to high-k basaltic andesites
		gp	7,23	Pyroclasts	Shoshoniti
		qd	0,51	Pyroclasts	Shoshoniti
		gr	2,19	Pyroclasts	High-k andesites to dacites
V4-V5-V7-V8	472,42	ma2	0,36	Lava	Shoshoniti
		sa1	7,89	Pyroclasts	Shoshoniti
		md	1,32	Pyroclasts	Shoshoniti
		fa	1,97	Pyroclasts	/
		sl	2,14	Pyroclasts	Shoshonitic basalts to shoshoniti
		pp	0,32	Lava	Basalts
		al	0,24	Pyroclasts	/
		ca1	0,16	Pyroclasts	/
		ca2	20,31	Pyroclasts	/
		gp3a	1,34	Pyroclasts	Trachyte
		pm	1,07	Lava	High-k basaltic andesites
		cg	5,22	L/P	basalts to high-k basaltic andesites
		pc1	5,36	Pyroclasts	Trachy-rhyolite
		pc2	4,35	Lava	Rhyolite
		gp1	13,36	Pyroclasts	Shoshoniti
		gp2	0,29	Pyroclasts	Trachy-rhyolite
		gp2a	41,69	Pyroclasts	Trachy-rhyolite
		gp2b	3,16	Lava	Rhyolite
		gp3b	3,13	Lava	Trachyte
		pn3	3,89	Lava	Trachyte
		pn2	1,09	Pyroclasts	Latites and trachytes
		fv	2,03	Pyroclasts	Altered
		sa2	3,36	Lava	Shoshoniti and basaltic andesites
		ml	4,7	Lava	Rhyolite
		gr	2,9	Pyroclasts	High-k andesites to dacites
		pm2	2,51	Lava	Trachy-rhyolite
		gc2	245,82	Pyroclasts	Latite to rhyolite
		gc1	1,19	Pyroclasts	Trachy-rhyolite
		cf1	0,05	Pyroclasts	Trachy-rhyolite
		cf2	0,81	Lava	Trachy-rhyolite
		cl	0,76	Lava	Trachyte
		cr	1,31	Lava	Rhyolite
		slope detrital cone	0,23	/	/
		present sea-shore deposit	1,43	/	/
		urbanized area	42,07	/	/
		colluvial deposit	44,59	/	/
V6		vu1b	20,97	Lava	Shoshoniti
		vu3a	1,11	Lava	Latite
		vu2	0,49	Pyroclasts	Shoshoniti
		vu3b	5,28	Pyroclasts	Shoshoniti
		colluvial deposit	0,2	/	/
		urbanized area	0,2	/	/
V9-V10	8,43	gp2a	0,14	Pyroclasts	Trachy-rhyolite
		sa	0,01	Pyroclasts	Shoshoniti
		vu1b	3,63	Lava	Shoshoniti
		vu3b	1,59	Pyroclasts	Shoshoniti
		vu2	3,06	Pyroclasts	Shoshoniti
V11-V12	18,67	vu1b	15,7	Lava	Shoshoniti
		vu2	0,76	Pyroclasts	Shoshoniti
		vu3b	2,21	Pyroclasts	Shoshoniti

Table 4.24 – Outcropping source rocks in the different drainage basins (geological map symbols are from De Astis et al., 1994); L/P = lavas + pyroclasts; ha = hectares.

Drainage basin	L + P area (ha)	Lavas (ha)	Pyroclasts (ha)	% LAVAS	% PYROCLASTICS	%TOT	SGI (L)	SGI (P)	SGI Ratio
V1	39,98	7,74	32,24	19,4	80,6	100,0	5,17	1,24	4,17
V2	30,75	10,41	20,34	33,9	66,1	100,0	2,95	1,51	1,95
V4-V5-V7-V8	384,1	32,34	351,76	8,4	91,6	100,0	11,88	1,09	10,88
V6	27,85	22,08	5,77	79,3	20,7	100,0	1,26	4,83	0,26
V9-V10	8,43	3,63	4,8	43,1	56,9	100,0	2,32	1,76	1,32
V11-V12	18,67	15,7	2,97	84,1	15,9	100,0	1,19	6,29	0,19
				TOT %	TOT %				
				44,7	55,3	100,0			

Table 4.25 – Lavas and pyroclastic rocks percentage calculated for each drainage basin and relative SGI values (e.g. Palomares and Arribas, 1993). L = lavas; P = Pyroclastic rocks.; ha = hectares.

4.4.6 – PANAREA ISLAND DRAINAGE BASINS CHARACTERISTICS -

Nine coastal drainage basins were identified and the corresponding beach sands were collected spaced along Panarea coastal perimeter (figs 3.13, 4.119). PN-2, PN-3 and PN-8, PN-9 have been grouped in the same drainage basin respectively (fig. 4.119, tab. 26, 27). In order to evaluate the relationships among source rocks, areal distribution and type of volcanic detritus, source rocks have been described (see 2.1.1f section in chapter 2) and volcanic detritus have been analyzed (see 4.2.1 section in chapter 4). Panarea drainage basins are constituted by a wide range of volcanic products, from basalt to rhyolite (tab. 4.26, fig. 4.119). Among Panarea drainage basins, lavas have an higher areal distribution percentage than pyroclastic rocks (tab 4.26, 4.27, fig. 4.119a,b).

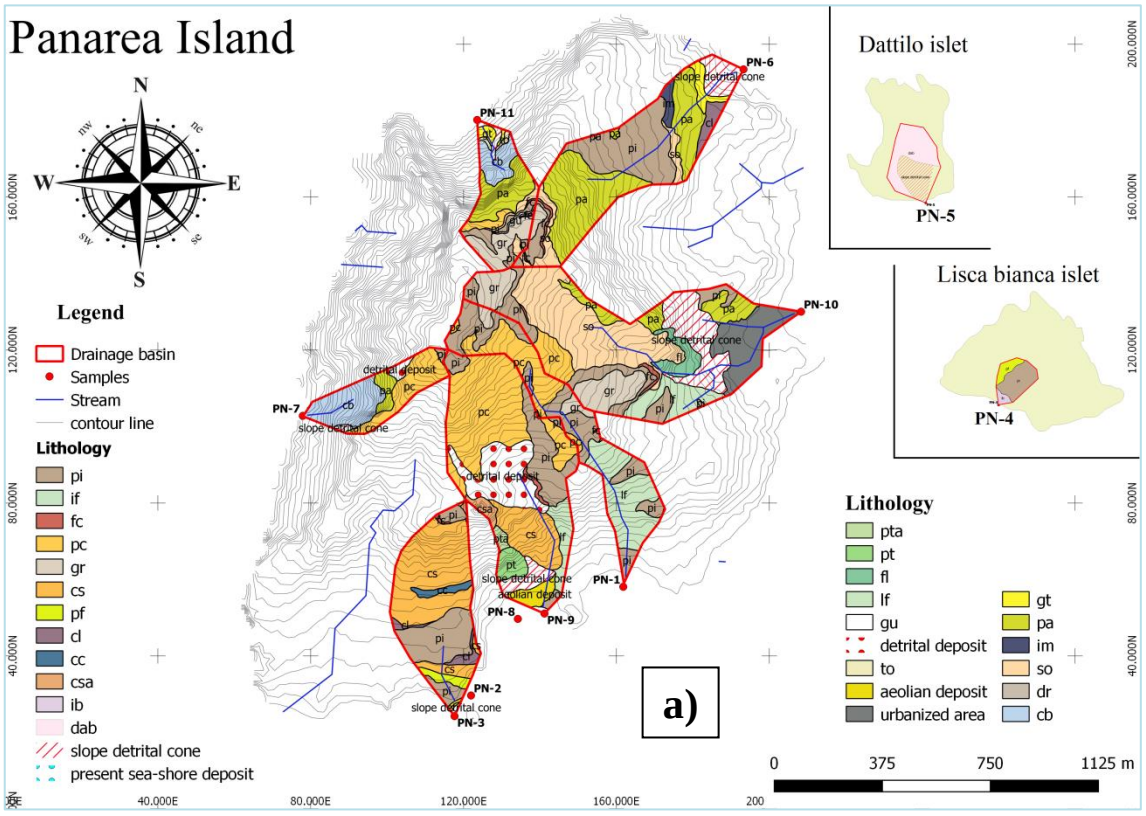

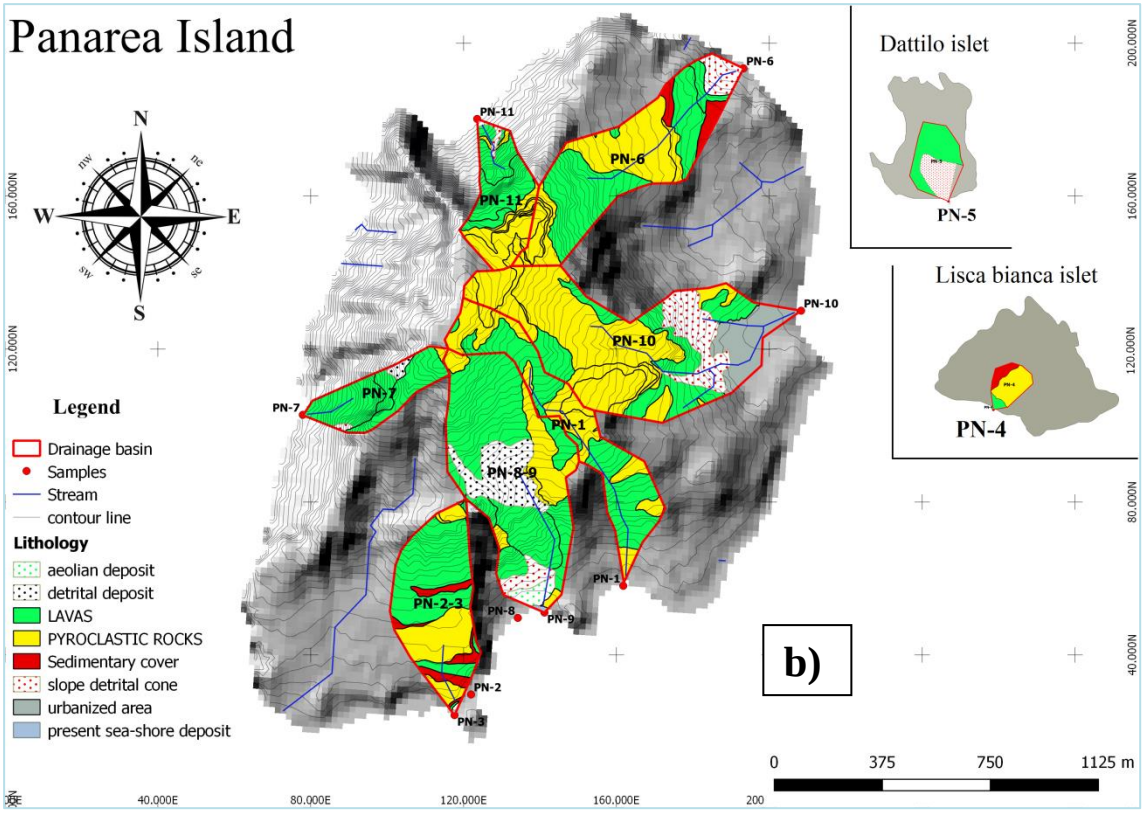

Figure 4.119 – Identified drainage basin (a,b), source rock lithologies (a) and grouped lithologies in lavas and pyroclastic rocks (b).

Drainage Basin	Basin area (ha)	Geological map symble	Outcrop area (ha)	Source rock	Lithology composition
PN-1	14,58	pi	5,5	Pyroclastics	Ca to high-K andesites
		lf	4,87	Lava	High-k dacite
		fc	0,02	Pyroclastics	CA basalts to basaltic andesites
		gr	0,75	Pyroclastics	Latite to rhyolite
		pc	3,44	Lava	High-k dacite to high-k andesite
PN-2-PN-3	15,18	csa	0,08	Lava	High-k dacite
		cs	8,82	Lava	High-k andesite
		pf	0,57	S	/
		pi	4,51	Pyroclastics	Ca to high-K andesites
		cc	0,47	S	/
		pc	0,02	Lava	High-k dacite to high-k andesite
		fc	0,06	Pyroclastics	CA basalts to basaltic andesites
		cl	0,59	S	/
		present sea-shore deposit	0,02	/	/
		slope detrital cone	0,04	/	/
PN-4	0,31	pf	0,07	S	/
		pi	0,21	Pyroclastics	Ca to high-K andesites
		ib	0,03	Lava	High-k andesite to dacite
PN-5	0,66	dab	0,41	Lava	High-k basaltic andesite to high-k dacite
		slope detrital cone	0,25	/	/
PN-6		pa	9,3	Lava	High-k andesite
		pi	6,72	Pyroclastics	Ca to high-K andesites
		so	1,49	Pyroclastics	CA andesite to CA dacite
		gr	0,34	Pyroclastics	Latite to rhyolite
		gt	0,72	Lava	CA andesite to high-k dacite
		fc	0,21	Pyroclastics	CA basalts to basaltic andesites
		cl	0,73	S	/
		im	0,48	S	/
		slope detrital cone	1,46	/	/

Table 4.26 – Outcropping source rocks in the different drainage basins (geological map symbols are from Lucchi et al., 2013); L = lavas; P = Pyroclastic rocks.; L/P = lavas + pyroclasts; S = sedimentary cover; ha = hectares. -(continued)-

Drainage Basin	Basin area (ha)	Geological map symble	Outcrop area (ha)	Source rock	Lithology composition
PN-7	6,9	cb	3,04	Lava	High-k andesite to high-k dacite
		pa	0,67	Lava	High-k andesite
		pi	0,13	Pyroclastics	Ca to high-K andesites
		pc	2,61	Lava	High-k dacite to high-k andesite
		slope detrital cone	0,12	/	/
		detrital deposit	0,33	/	/
PN-8-PN-9	27,18	pi	3,92	Pyroclastics	Ca to high-K andesites
		pc	9,85	Lava	High-k dacite to high-k andesite
		fc	0,21	Pyroclastics	CA basalts to basaltic andesites
		csa	0,51	Lava	High-k dacite
		cs	3,42	Lava	High-k andesite
		lf	1,37	Lava	High-k dacite
		pta	0,29	Pyroclastics	High-k dacite
		pt	0,95	Lava	High-k dacite
		aeolian deposit	0,9	/	/
		detrital deposit	4,57	/	/
		present sea-shore deposit	0,08	/	/
		slope detrital cone	1,11	/	/
PN-10	32,26	pi	4,01	Pyroclastics	Ca to high-K andesites
		gr	3,84	Pyroclastics	Latite to rhyolite
		pa	2,6	Lava	High-k andesite
		fc	0,22	Pyroclastics	CA basalts to basaltic andesites
		so	9,78	Pyroclastics	CA andesite to CA dacite
		fl	1,23	Lava	High-k dacite
		lf	2,27	Lava	High-k dacite
		present sea-shore deposit	0,01	/	/
		urbanized area	4,06	/	/
		slope detrital cone	4,24	/	/
PN-11	8,54	pi	0,9	Pyroclastics	Ca to high-K andesites
		gr	1,79	Pyroclastics	Latite to rhyolite
		fc	0,07	Pyroclastics	CA basalts to basaltic andesites
		so	0,51	Pyroclastics	CA andesite to CA dacite
		gu	0,1	Pyroclastics	Rhyolite
		pc	0,5	Lava	High-k dacite to high-k andesite
		pa	2,56	Lava	High-k andesite
		cb	1,43	Lava	High-k andesite to high-k dacite
		to	0,08	Pyroclastics	altered
		gt	0,33	Lava	CA andesite to high-k dacite
		present sea-shore deposit	0,01	/	/
		slope detrital cone	0,26	/	/

Table 4.26 – Outcropping source rocks in the different drainage basins (geological map symbols are from Lucchi et al., 2013); L = lavas; P = Pyroclastic rocks.; L/P = lavas + pyroclasts; S = sedimentary cover; ha = hectares.

Drainage basin	L + P area (ha)	Lavas (ha)	Pyroclasts (ha)	% LAVAS	% PYROCLASTICS	%TOT	SGI (L)	SGI (P)	SGI Ratio
PN-1	14,58	8,31	6,27	57,0	43,0	100,0	1,75	2,33	0,75
PN-2-PN-3	13,49	8,92	4,57	66,1	33,9	100,0	1,51	2,95	0,51
PN-4	0,24	0,03	0,21	12,5	87,5	100,0	8,00	1,14	7,00
PN-5	0,41	0,41	0	100,0	0,0	100,0	1,00	0,00	0,00
PN-6	18,78	10,02	8,76	53,4	46,6	100,0	1,87	2,14	0,87
PN-7	6,45	6,32	0,13	98,0	2,0	100,0	1,02	49,62	0,02
PN-8-PN-9	20,52	16,10	4,42	78,5	21,5	100,0	1,27	4,64	0,27
PN-10	23,95	6,1	17,85	25,5	74,5	100,0	3,93	1,34	2,93
PN-11	8,27	4,82	3,45	58,3	41,7	100,0	1,72	2,40	0,72
				TOT %	TOT %				
				61,02	38,98	100			

Table 4.27 – Lavas and pyroclastic rocks percentage calculated for each drainage basin and relative SGI values (e.g. Palomares and Arribas, 1993). L = lavas; P = Pyroclastic rocks.; ha = hectares.

4.4.7 – STROMBOLI ISLAND DRAINAGE BASINS CHARACTERISTICS -

Six coastal drainage basins were identified and the corresponding beach sands were collected spaced along Stromboli coastal perimeter (figs 3.15, 4.120). STR-1, STR-2 have been grouped in the same drainage basin respectively (fig. 4.120, tab. 28, 29). In order to evaluate the relationships among source rocks, areal distribution and type of volcanic detritus, source rocks have been described (see 2.1.1g section in chapter 2) and volcanic detritus have been analyzed (see 4.2.1 section in chapter 4). Stromboli drainage basins are predominately constituted by basalts, andesites and shoshonites (tab. 4.28, fig. 4.120). Among Stromboli drainage basins, lavas (59,99 %) have an higher areal distribution percentage than pyroclastic rocks (40,01 %) (tab 4.28, 4.29, fig. 4.120a, b).

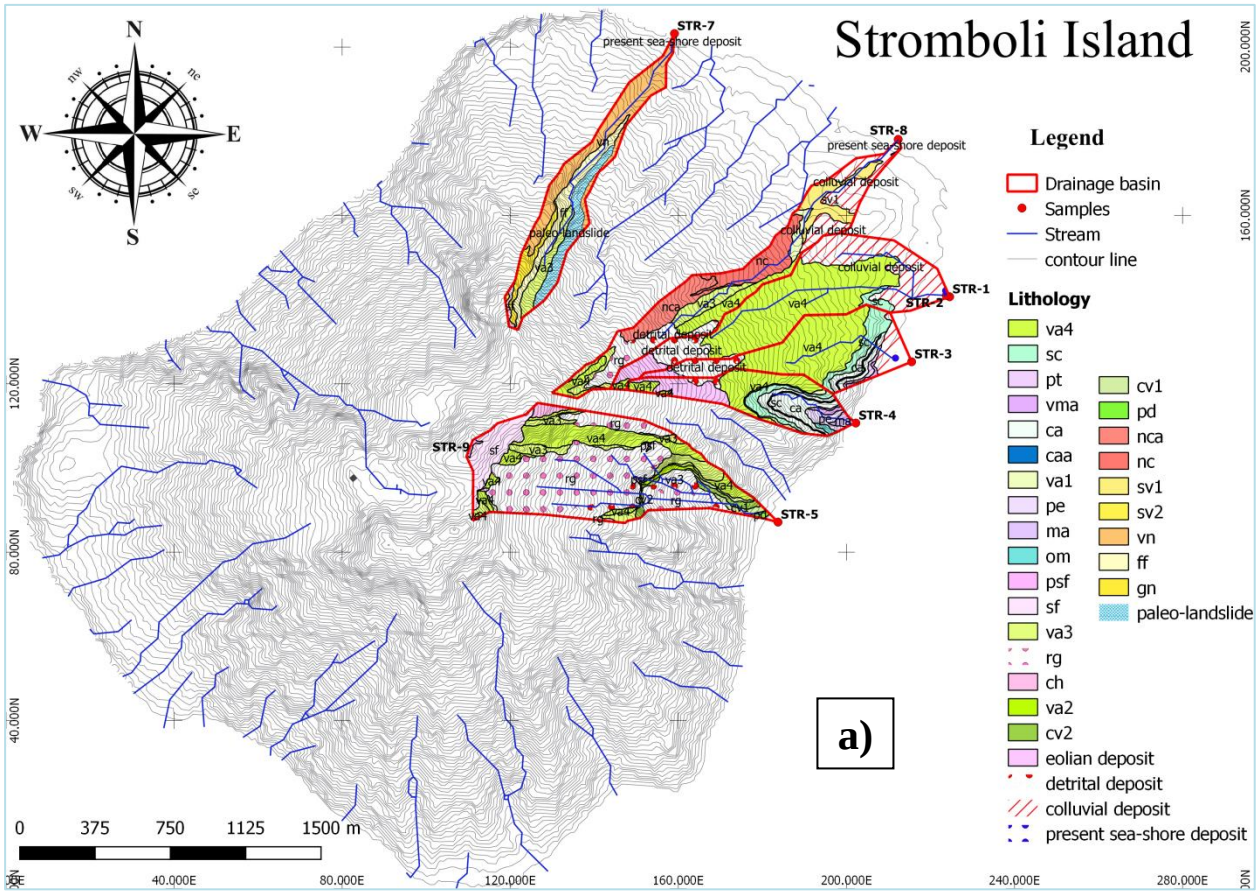

Figure 4.120 – Identified drainage basin (a,b), source rock lithologies (a) and grouped lithologies in lavas and pyroclastic rocks (b) –(continued)-

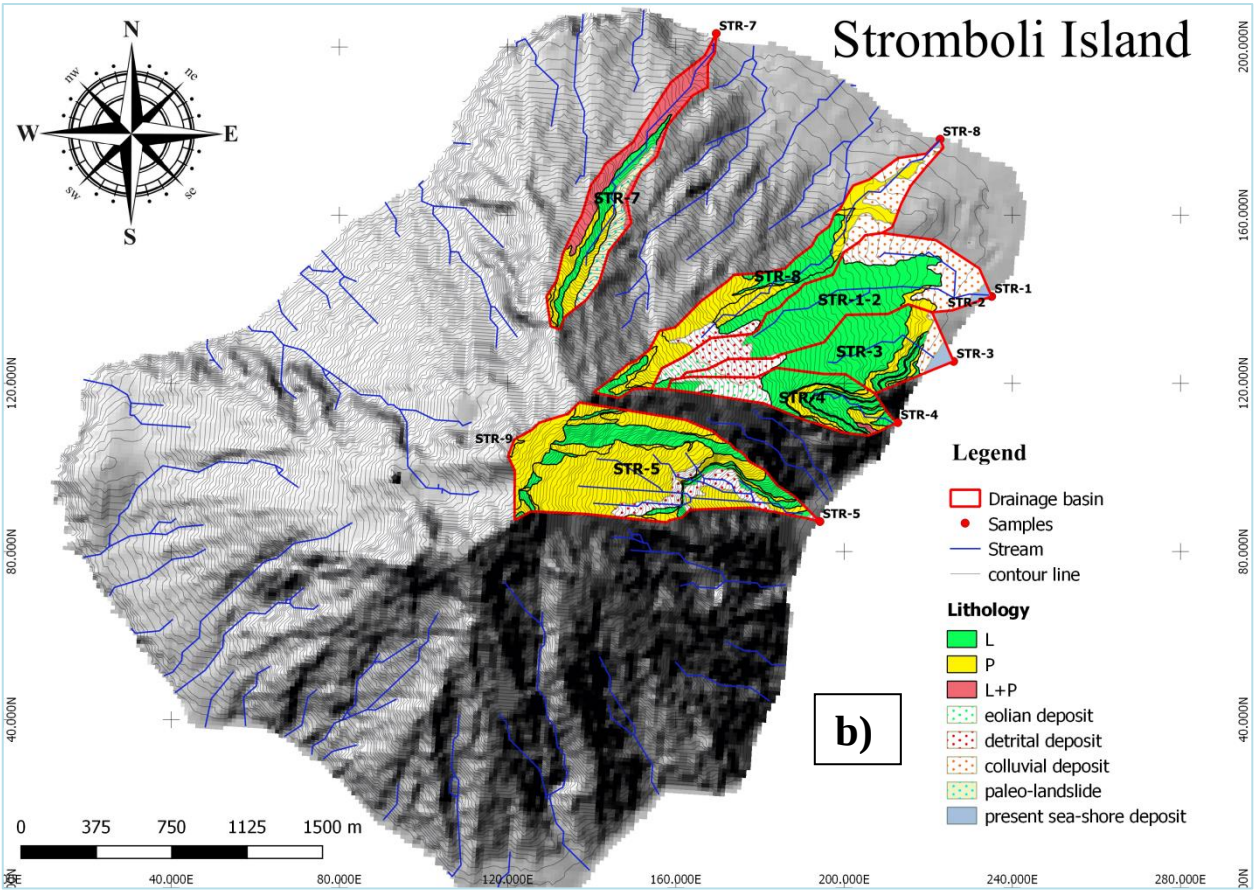

Figure 4.120 – Identified drainage basin (a,b), source rock lithologies (a) and grouped lithologies in lavas and pyroclastic rocks (b).

Drainage Basin	Basin area (ha)	Geological map symble	Outcrop area (ha)	Source rock	Lithology composition
STR-1-2	40,58	sc	0,92	Pyroclastics	High-k basaalts to shoshonite
		va4	22,63	Lava	Latite to trachyte
		detrital deposit	3,17	/	/
		eolian deposit	1,83	/	/
		colluvial deposit	11,48	/	/
		present sea-shore deposit	0,55	/	/
STR-3	24,64	va4	13,35	Lava	Latite to trachyte
		sc	2,8	Pyroclastics	High-k basaalts to shoshonite
		pt	0,43	Pyroclastics	High-k basalts
		vma	0,3	Lava	High-k basaltic andesite
		ca	1,71	Lava	High-k basaltic andesite to shoshonite
		caa	0,23	Pyroclastics	High-k basalt to shoshonitic basalt
		colluvial deposit	1,74	/	/
		eolian deposit	0,61	/	/
		detrital deposit	2,52	/	/
		present sea-shore deposit	0,95	/	/

Table 4.28 – Outcropping source rocks in the different drainage basins (geological map symbols are from Lucchi et al., 2013); L = lavas; P = Pyroclastic rocks.; L/P = lavas + pyroclasts; S = sedimentary cover; ha = hectares. –(continued)-

Drainage Basin	Basin area (ha)	Geological map symble	Outcrop area (ha)	Source rock	Lithology composition
STR-4	18,64	va4	5,7	Lava	Latite to trachyte
		va1	0,65	Pyroclastics	Trachyte
		sc	1,84	Pyroclastics	High-k basaalts to shoshonite
		ca	4,15	Lava	High-k basaltic andesite to shoshonite
		caa	0,34	Pyroclastics	High-k basalt to shoshonitic basalt
		pt	0,09	Pyroclastics	High-k basalts
		vma	0,32	Lava	High-k basaltic andesite
		pe	1,03	Pyroclastics	High-k basaltic andesite to high-k andesite
		ma	0,47	Lava	High-k basaltic andesite to high-k andesite
		om	0,26	L/P	Basaltic andesite to andesite
		eolian deposit	3,21	/	/
		detrital deposit	0,58	/	/
STR-5	58,53	psf	0,38	Pyroclastics	Shosho. basalt to basalt to bas. andesites
		va4	10,32	Lava	Latite to trachyte
		va3	5,35	Pyroclastics	Latite
		va2	0,55	Lava	Latite to trachyte
		va1	0,54	Pyroclastics	Trachyte
		rg	27,2	Pyroclastics	altered
		cv2	1,34	Lava	Shoshonite
		cv1	0,69	Pyroclastics	Shoshonite
		ch	0,77	Pyroclastics	Shoshonite to shoshonitic basalts
		sf	5,26	Pyroclastics	Shosho. basalt to basalt to high-k basalts
		pd	0,22	Lava	High-k basalts to shoshonitic basalts
		detrital deposit	5,87	/	/
		present sea-shore deposit	0,04	/	/
STR-7	24,42	gn	2,15	Pyroclastics	High-k shoshonite
		vn	10,2	L/P	High-k shoshonite
		ff	4,7	Lava	High-k shoshonite
		va3	2,68	Pyroclastics	Latite
		sf	0,38	Pyroclastics	Shosho. basalt to basalt to high-k basalts
		paleo-landslide	4,31	/	/
STR-8	35,07	va4	4,67	Lava	Latite to trachyte
		va3	3,74	Pyroclastics	Latite
		va1	1,11	Pyroclastics	Trachyte
		rg	3,08	Pyroclastics	altered
		nca	4,87	Pyroclastics	High-k shoshonite
		nc	5,23	Lava	High-k shoshonite
		sv1	3,85	Pyroclastics	High-k shoshonite
		sv2	0,03	Lava	High-k shoshonite
		detrital deposit	2,06	/	/
		colluvial deposit	6,25	/	/
		present sea-shore deposit	0,18	/	/

Table 4.28 – Outcropping source rocks in the different drainage basins (geological map symbols are from Lucchi et al., 2013); L = lavas; P = Pyroclastic rocks.; L/P = lavas + pyroclasts; S = sedimentary cover; ha = hectares.

Drainage basin	L + P area (ha)	Lavas (ha)	Pyroclasts (ha)	% LAVAS	% PYROCLASTICS	%TOT	SGI (L)	SGI (P)	SGI Ratio
STR-1-2	23,55	22,63	0,92	96,1	3,9	100,0	1,04	25,60	0,04
STR-3	18,82	15,36	3,46	81,6	18,4	100,0	1,23	5,44	0,23
STR-4	14,85	10,77	4,08	72,5	27,5	100,0	1,38	3,64	0,38
STR-5	52,62	12,43	40,19	23,6	76,4	100,0	4,23	1,31	3,23
STR-7	20,11	9,8	10,31	48,7	51,3	100,0	2,05	1,95	1,05
STR-8	26,58	9,93	16,65	37,4	62,6	100,0	2,68	1,60	1,68
				TOT %	TOT %				
				59,99	40,01	100			

Table 4.29 – Lavas and pyroclastic rocks percentage calculated for each drainage basin and relative SGI values (e.g. Palomares and Arribas, 1993). L = lavas; P = Pyroclastic rocks.; ha = hectares.

-Chapter 5 – Discussion -

In this study we examine aspects of the pre-depositional and pre-burial parameters that affect the composition of volcaniclastic detritus in two different tectonic settings: the Aeolian Islands arc and the Campania magmatic province in southern Italy.

Particular attention has been given to the factors that control the relationships between grain rounding, grain-size, sand composition, texture and source rocks.

- Sand and sources: petrofacies -

The most representative sampling environment were the berms (high-tide and low – tide berm), followed by the swash zone and others. The most representative fraction among all samples from the two studied areas is the medium sand fraction, immediately followed by the fine and then coarse fractions, which were sampled mainly from high-tide berm, low-tide berm and swash zone (tab. 4.11). There is a clear differences between Aeolian Islands costal beach sand and Campania coastal beach sand in terms of detritus maturity. Among 68 Aeolian coastal samples, the 20,6% is represented by gravel (< 2,00 mm), the 10,3% is represented by very coarse sand, the 26,5% is represented by coarse sand, the 32,4% is represented by medium sand, the 10,3% is represented by fine sand; whereas among 72 Campania coastal samples, the 5,8% is represented by gravel, the 10,1% is represented by coarse sand, the 39,1% is represented by medium sand, the 44,9% is represented by fine sand (fig. 4.12). Therefore, it seems that there is some relation between beaches exposure and detritus grain-size among aeolian islands, those sampled on the western islands sides usually have a coarser grain-size probably related with a higher wave/wind energy due to predominant W/NW wind blowing direction, then there is a continuous blocky/gravel clastic supplying from mass-failure processes which are eroded slower then finer detritus by coastal reworking. In fact, the majority of beaches or pocket beaches occur on the eastern aeolian islands sides (fig. 4.59).

Erosion, on the studied areas, can be viewed in terms of a weathering-limited denudation regime (e.g. Carson and Kirkby, 1972). Under this condition, transport rates exceed the rate at which chemical weathering can generate loose and leached material (Johnsson, Ellen and McKittrick, 1993), and thus sandy detritus consists of a varied association of less durable mineral phases, the proportion of which, reflects the composition of the bedrock (e.g. Nesbitt and Young, 1996; Girty et al., 2003).

Especially on the Aeolian Islands high relief drainage basins results in rapid sediment transport and short to no temporary sediment storage and pedogenesis. Thus, chemical weathering appears to be negligible.

In the vicinity to the Volturno river mouth and in a wide open beaches, the strong reworking (wave and river high-energy) play a fundamental role in the mechanical breakage processes from coarser sediment (mainly lithic fragments) to finer sediment (mainly single crystals grain); whereas Pozzuoli bay is a more protected area with a lower-wave energy, in fact Pozzuoli samples show also an higher percentage of coarser sand with respect Volturno-Bacoli coastal stretch.

In Campania beach sands as well as Aeolian beach sands, breakage trend occurs from very coarse to very fine sand fraction, there is a single crystal grains increasing and a lithic grains decreasing from very coarse to very fine sand fraction (figs. 4.16, 4.17, 4.18, 4.19, 4.31, 4.32). For instance, on Stromboli island, "immature" grains (polycrystalline grains) such as lithic fragments become single-crystal grains through mechanical breakage after transportation. The maximum length of stream transportation on Stromboli island is fairly short (3-3.5 km, fig. 4.19). This "immature" to "mature" detritus trend is confirmed by STR-9 crater sample where this trend is less evident with respect beach samples (e.g. STR-1) which are more "mature" than a zero order sand.

Along Campania coastal stretch a significant trend occurs, this trend allow us to understand that sand samples along Volturno-Bacoli coastal stretch are "mature" sands, they are constitute mainly by single crystal grains with lower percentage of lithic fragments (total lithic fragments), whereas going southward to Phlegrean Fields area, there is a single crystal grains decreasing and a lithic fragments increasing (mainly volcanic lithic fragments). Likewise by going away from Phlegrean Fields area towards Portici-Sorrento coastal stretch (southward), again there is to a lesser extent, a lithic fragments decreasing and a single crystal grains increasing (fig. 4.31). Thus, we can affirm that from both Portici-Sorrento coastal stretch and Phlegrean Fields area, sandy detritus had lesser time to become "mature" having a proximal source areas (Vesuvius and Phlegrean Fields volcanoes) with respect Volturno-Bacoli coastal samples which have a distal source areas such as southern Apennines (sedimentary source area) and Roccamonfina volcano (Latium province).

The major components of Aeolian islands and Campania beach sands are monomineralic grains, sedimentary and volcanic lithic fragments with lesser amounts of calcareous bioclasts. Monomineralic grains in Aeolian islands beach samples are

predominantly pyroxene, plagioclase, with lesser olivine, hornblende, opaque minerals, K-feldspar and quartz. Volcanic lithic fragments range in texture from lathwork to microlitic to vitric and felsitic varieties, whereas holocrystalline lithic volcanic grains are minor constituents. Monomineralic components in Campania beaches sand samples are mostly plagioclase, pyroxene, K-feldspar with lesser leucite, nepheline, garnet, hornblende, opaque minerals and biotite. In the Bacoli-Volturno coastal stretch they consist mostly of quartz, plagioclase, calcite and K-feldspar, with except of some placer (e.g. BC-2. VO-2, VO-6) constitute mainly of pyroxene, opaque minerals and lesser garnet, olivine. Lithic fragments are subdivided in two main categories: volcanic lithic fragments, which range in texture from lathwork to microlitic to vitric and felsitic varieties, and sedimentary lithics which are Lss (with siliciclastic composition), and sedimentary lithic fragments with crystalline ($Lsc_{(xx)}$) and micritic ($Lsc_{(micr)}$) carbonate composition (figs. 4.15, 4.21a,b, 4.22, 4.30, 4.33, 4.35, 4.36 4.37, 4.38 and from plate I to plate XIX; appendix A).

Samples from Aeolian islands and Portici Sorrento coastal stretch have an high percentage of volcanic lithic fragments (Lvl > Lvmi> Lvv), whereas samples from Pozzuoli, display an average percentage among Lvl~Lvmi~Lvv.

Campania sand samples have a mixed (dual main source rock) provenance source rocks: sedimentary source rocks and volcanic source rooks; from northern and southern part the volcanic “signal” is influenced by Apennines. The samples from northern coastal stretch with respect to Pozzuoli (toward Volturno river mouth), show a lower percentage of volcanic lithic fragments and, an increasing in sedimentary lithics toward Volturno river mouth. Bacoli series (especially after BC-4 toward north) marks the transition between volcanic and sedimentary petrofacies along the north Campania coastal stretch as a result from clastic supply from Apennines sedimentary source rocks; whereas southward to Portici-Sorrento coastal stretch we mainly found volcanic lithic fragments with exception of Castellammare di Stabia samples (fig. 4.33, 4.34, 4.43). According to “leucite and sanidine signal” in the sandy detritus, it is possible to affirm that Phlegrean Fields products are delimited by Licola to the north and Naples bay to the south, whereas Vesuvius products are delimited by Naples/Portici to the north and Castellammare di Stabia to the south, but also in Sorrento detritus, Vesuvius products have been found until the southernmost promontory immediately after Sorrento village. In this regard, a areal petrofacies-distribution map of the studied Campania coastal stretch has been created according to this study results discriminating among Vesuvian,

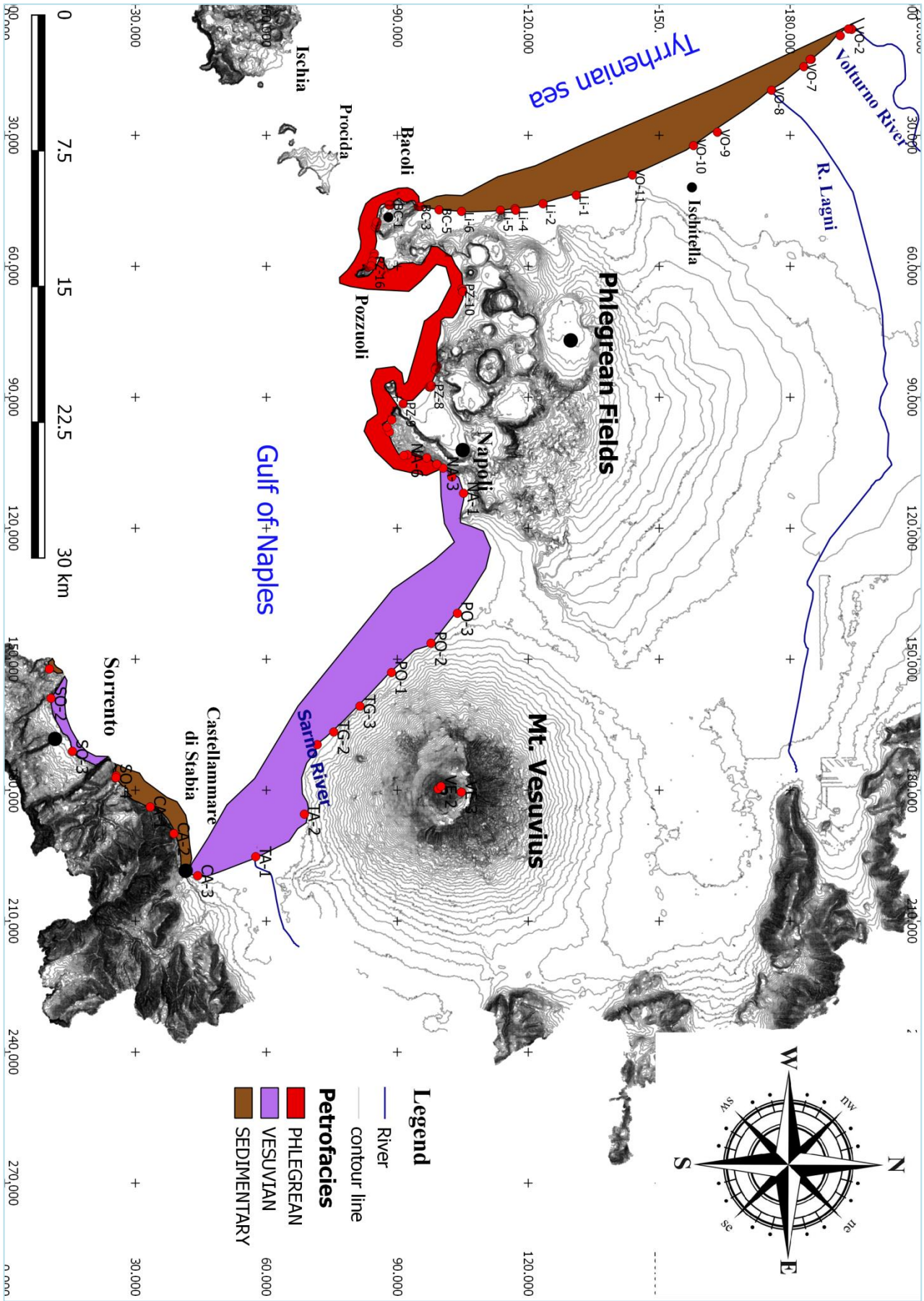

Figure 5.1 - Campania petrofacies distribution based on sand composition along the studied coastal stretch.

Phlegrean and sedimentary petrofacies (figs 4.43, 5.1).

Stromboli, Vulcano, Alicudi and Filicudi sands have a dual basaltic/shoshonitic and andesitic composition "signatures". Panarea, Lipari and Salina sands have a wider range of composition "signatures" ranging from basalts to rhyolites.

The composition of Aeolian beach sand defines, on average, a lithic petrofacies: the medium-grained sands are lithic-rich, whereas from very coarse to very fine sand there is a progressive increase in single crystal grains content (feldspar, olivine, pyroxene, opaque minerals) (fig. 4.15, 4.29 a, b, c).

The sand detrital modes of Aeolian island are immature, are rich in unweathered mafic minerals, glass and bedrock-derived feldspar grains and, moreover, lack pedogenetic particles (e.g. Cleary and Connolly, 1971; Johnsson, Ellen and McKittrick, 1993). The immaturity, both compositional and textural, of the beach sands testifies to the rapidity with which sediment is isolated from soil horizons and pedogenetic processes on the island steep slopes, because of the high mean annual precipitation of 600 mm a^{-1} (ISPRA, 2011) and Mediterranean climate (Arribas et al. 2000; Le Pera et al. 2001; Critelli et al. 2003; Scarciglia et al. 2012). Thus there is evidence that, on Aeolian islands, sand composition does accurately reflect bedrock composition except in the case of source areas dominated by pumice outcrops (e.g. Lipari islands, Morrone et al., 2017).

According to the source rocks, dacitic –rhyolitic "signal" eroded from lavas, which produce Lvl-Lvmi-Lvv (higher amount of Lvv) with colorless and grey groundmass, goes lost in the sandy detritus as well as those eroded from pyroclastic rocks (which produce pumice) after strong reworking and recycle in high-energy environment (wide open beach-environment) such as Licola-Volturno and Portici-Sorrento coastal stretch, whereas in more protected and quite beach-environment such as Pozzuoli bay, this type of volcanic lithic texture (Lvf, pumice, which are associated to more evolved [acid] volcanism and then explosive volcanism) are more preserved (fig. 4.38).

Volcanic lithic with felsitic, colorless and grey groundmass are more preserved in the detritus in more protected and quite beach-environment such as Pozzuoli and Naples bay probably because glassy-rich fragments tend to alter more quickly during sedimentation processes, then during the time it will find basaltic-andesitic-rich sandy detritus overestimating mafic source rocks and underestimating more acid source rocks (fig. 4.37, 4.38, 4.39, 4.40, 4.41).

We have introduced the *Lvlgrgl+Lvmigrgl+Lvvgrgl*, classified as new volcanic lithic compounds, analyzed also through the electron microprobe to characterize geochemistry of this new volcanic lithic types (figs. 4.24, 4.25, 4.26, 4.27 and plate VIII $_{(a, b, c, d)}$).

The new discriminating diagrams (figs. 4.24, 4.25, 4.28, 4.40, 4.41) allow to catch information among the volcanic source rocks ranging from basic to acid composition (SiO_2 ranging from 41% to >77%), they do not discriminate among alkaline series (sodium + potassium content).

Thus, according to source rocks, after hundreds analyzed samples from different source areas (mainly volcanic) it possible to affirm that:

1. *Lvlblgl, Lvmiblgl, Lvvblgl;*
2. *Lvlbrgl, Lvmibrgl, Lvvbrgl*;
3. *Lvlgrgl, Lvmigrgl, Lvvgrgl*;

can be produced not only by basaltic, andesitic and dacitic source rocks but also by source rocks with the same SiO_2 content belonging at different alkaline series (e.g. trachybasalt, shoshonite, latite, trachyandesite, trachydacite, trachyte).

All these diagrams emphasize the textural properties of volcanic lithic granules such as lathwork, microlitic and vitric with different color groundmass, and well display the separation between volcanoclastic sandstone groups derived from different volcanic provinces. This is because volcanic lithic fragments and textures are sensible indicators of the volcanic provinces and volcanic apparatus tectonic setting.

Results show that sandy lithic fragments with different textures such as lathowork, microlitic and vitric are mainly produced by lavas erosion but they can be also produced (in lesser amount) by pyroclastic rocks which tend to produce coarser and/or finer detritus (Morrone et al., 2017).

Furthermore, in a study of andesitic stream sand from humid and semi-arid climate, Mack and Jerzykiewicz (1989) showed that epiclastic–andesitic sands are feldspatholitic, with total feldspar controlled by weathering environment. The plots in figures 4.29, 4, 4.42 clearly show the considerable variation in VFR:ACC:PLG (e.g. Mack and Jerzykiewicz, 1989) percentages versus grain-size as also obtained using more routinely used diagrams such as Q:F:L (e.g. Ingersoll et al., 1984) and Lm:Lv:Ls (e.g. Ingersoll, 1990). Specifically, the conversion from coarse to very fine sand grain-size led to a decrease in polymineralic rock fragments (VFR) and to enrichment into the monomineralic component of the sandy particles, represented by olivine, pyroxene and

opaque (ACC) and plagioclase crystals (PLG). Under the weathering-limited erosion regime of the two studied areas, it is likely that only mechanical breakage of composite rock fragments occurs. For these lithic-rich volcaniclastic sands, boundaries between phenocrysts and glassy groundmass, considered as non-isomineralic interfaces (Heins, 1995), could represent sites of preferential disaggregation, and as the degree of this process intensifies, it controls the conversion from a polymineralic or composite grain to a monomineralic one. Among Aeolian islands, Lipari and Panarea beach sands are similar to the semi-arid examples of Mack and Jerzykiewicz (1989), whereas Stromboli, Alicudi and Filicudi samples are closer to the Hawaiian islands. Amongo Campania coastal stretch, Portici-Sorrento samples comprising Vesuvius crater sands overlap shadow area from Hawaiian Islands, whereas Phlegran fields and Licola-Volturno samples principally overlap semi-arid andesitic source, only few samples are shifted toward ACC apex because they are heavy minerals placer. This may reflect the more mafic, basaltic andesite sources, or just that these two studied areas (as well as Hawaii, e.g. Marsaglia, 1993) are beach environments where dense minerals tend to be concentrated by hydraulic sorting effects (Flores and Shideler, 1978; Komar and Wang, 1984; Frihy, Lotfy and Komar, 1995; Dye and Dickinson, 1996; Garzanti and Andò 2007a; Garzanti, Andò and Vezzoli, 2008, 2009). The grain-size-dependent fractionation between denser and lighter grains results from sea-wave energy (e.g. Marsaglia, 1993; Dye and Dickinson, 1996; Ramalho et al. 2013). The winnowing related to big waves is thus important in a first-cycle modern depositional environment to explain anomalies in the observed suite of minerals and rock fragments. The amount of dense minerals in modern sediments is normally greater than expected from a volcanic source rock (e.g. Morton, 1985; Frihy, Lotfy and Komar, 1995; Dye and Dickinson, 1996; Garzanti et al. 2002; Garzanti and Andò 2007a, b).

The heavy mineral suites of the Campania shoreline (fig. 5.1) reflect the mineralogy of the source rocks, with abundant detrital grains of both opaques (pseudobrookite, pyrite, ilmenite), and transparent species such as diospide, brown and green amphibole, and trace amounts of biotite, garnet, rutile and tourmaline (fig. 4.44, 4.45, 4.46, and tab.4.14). There is no evidence to suggest that chemical weathering processes during sedimentary dispersal have caused any significant decrease in mineral diversity. Both the *magmatic provenance"* of the *Napoli Province* (e.g., Garzanti et al., 2002) and the "*magmatic/sedimentary provenance"* of the *Capua Province* (e.g., Garzanti et al., 2002) shed an heavy minerals assemblage of OPaques+PYroxene+AMPHibole with an

average of $OP_{62}PY_{25}AMPH_{13}$ and of $OP_{48}PY_{28}AMPH_{24}$, respectively for the two sedimentary province. Recycled ultrastable heavy minerals –such as tourmaline and rutile - linked to a provenance from the Apennine thrust belt source rocks are sporadic. Hence, sedimentary provenance lithotypes are diluted and/or unrecognizable using the only HM (Heavy Minerals) approach with respect to the minerals provenance sourced by the potassic volcanic fields of Latium and Campania. Moreover, integrating electron microprobe analysis with standard petrographic procedures has shown that geochemistry of individual members of a mineral group of opaque grains (pseudobrookite, pyrite, ilmenite) provide additional information that constrains the nature of the ultimate source rocks (Le Pera and Morrone 2018).

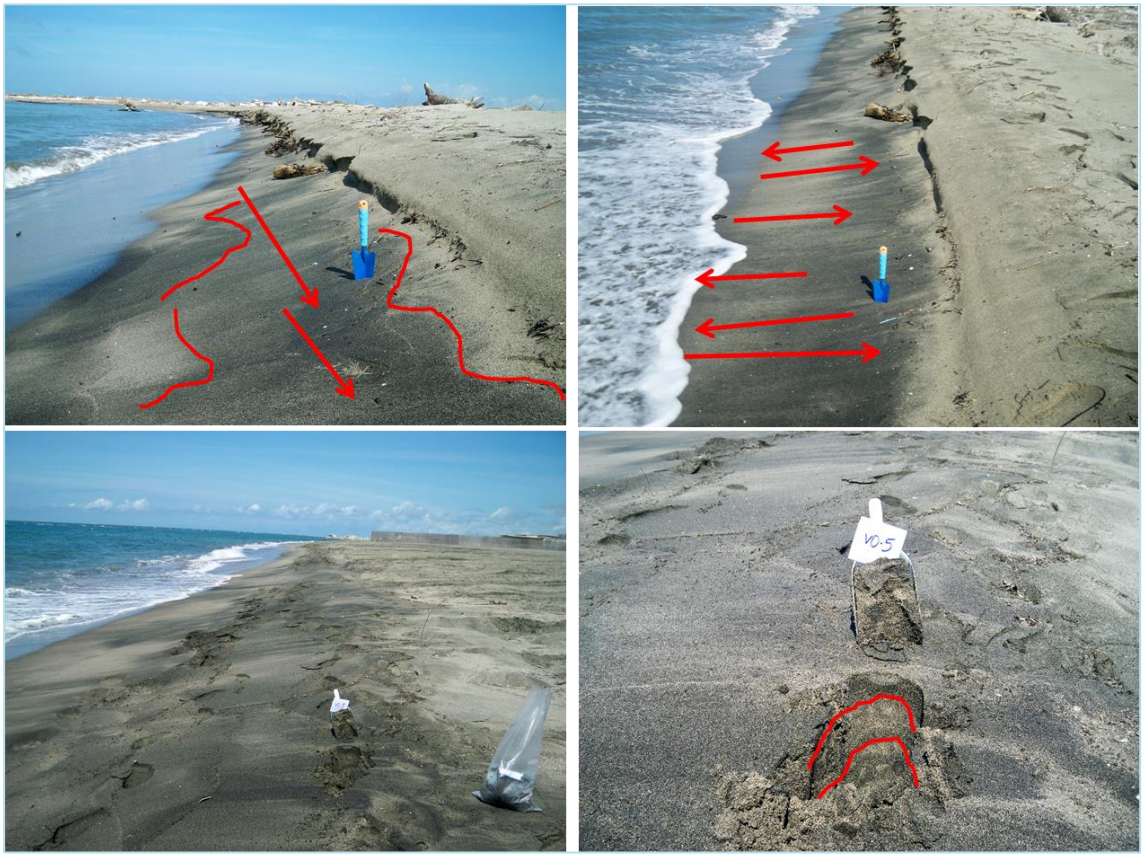

Figure 5.2 - Sites showing heavy minerals "traction carpet" along Campania coastal stretch.

- Roundness of sand grains -

Changes in grain roundness, calculated for both studied areas, were assessed to evaluate grain resistance to transport (stream and marine mechanical transport processes). Variations in mean roundness were determined on medium-sand sized and some test on the five sand fractions were carried out.

The mean roundness was calculated for all grains encountered during point-counting using a slightly modified version of the technique of McBride and Picard (1987). A test

	Lvl grains*						Lvl tot	Lvl Mean	Lvmi grains*						Lvmi tot	Lvmi Mean	Lvv grains*						Lvv tot	Lvv Mean
Sample	1	2	3	4	5	6	grains	Roundness	1	2	3	4	5	6	grains	Roundness	1	2	3	4	5	6	grains	Roundness
PN-1-Vc	89	125	15	0	0	0	229	1,7	0	12	5	0	0	0	17	2,3	1	4	0	0	0	0	5	1,8
PN-1-C	69	129	14	0	0	0	212	1,7	10	26	8	0	0	0	44	2,0	5	3	1	0	0	0	9	1,6
PN-1-m	11	53	8	0	0	0	72	2,0	17	37	9	0	0	0	63	1,9	26	26	12	1	0	0	65	1,8
PN-1-f	11	22	1	0	0	0	34	1,7	20	45	11	0	0	0	76	1,9	32	10	3	12	2	0	59	2,0
PN-1-Vf	2	5	2	0	0	0	9	2,0	10	48	19	0	0	0	77	2,1	36	45	9	1	0	0	91	1,7
PN-2-m	64	85	20	6	2	0	177	1,9	43	79	26	11	3	0	162	2,1	1	1	0	0	0	0	2	1,5
PN-3-m	36	94	26	7	2	0	165	2,1	35	78	34	14	2	0	163	2,2	0	4	0	0	0	0	4	2,0
PN-4-m	13	114	33	0	0	0	160	2,1	6	86	21	4	0	0	117	2,2	5	36	5	0	0	0	46	2,0
PN-5-m	4	63	14	3	0	0	84	2,2	5	62	20	8	0	0	95	2,3	16	66	36	3	4	0	125	2,3
PN-6-m	14	75	16	3	0	0	108	2,1	5	40	11	0	0	0	56	2,1	21	85	24	5	0	0	135	2,1
PN-7-m	29	92	31	13	0	0	165	2,2	4	33	19	8	0	0	64	2,5	5	11	5	0	0	0	21	2,0
PN-8-m	19	61	62	31	6	0	179	2,7	2	38	38	10	10	0	98	2,9	9	2	4	0	6	0	21	2,6
PN-9-m	0	30	48	58	5	0	141	3,3	0	12	52	33	6	0	103	3,3	3	8	6	3	0	0	20	2,5
PN-10-m	2	79	63	19	8	3	174	2,8	3	42	50	12	0	0	107	2,7	7	12	14	4	0	0	37	2,4
PN-11-m	21	54	38	24	7	0	144	2,597	11	41	47	14	3	0	116	2,629	5	12	17	5	1	0	40	2,625
PN-11-m^{30}	7	11	9	3	0	0	30	2,267	1	14	12	3	0	0	30	2,567	4	10	12	3	1	0	30	2,567

$$\Delta AVG_{Lvl} = 0{,}331;\quad \Delta AVG_{Lvmi} = 0{,}063$$
$$\Delta AVG_{Plag} = 0{,}317;\ \Delta AVG_{Lvv} = 0{,}058$$

	Plag grains*						Plag tot	Plag Mean	Py grains*						Py tot	Py Mean	Hb grains*						Hb tot	Hb Mean
Sample#	1	2	3	4	5	6	grains	Roundness	1	2	3	4	5	6	grains	Roundness	1	2	3	4	5	6	grains	Roundness
PN-1-Vc	16	8	0	0	0	0	24	1,3	4	7	0	0	0	0	11	1,6	3	4	0	0	0	0	7	1,6
PN-1-C	36	28	0	0	0	0	64	1,4	12	5	1	0	0	0	18	1,4	11	0	0	0	0	0	11	1,0
PN-1-m	54	25	2	0	0	0	81	1,4	8	18	3	0	0	0	29	1,8	12	6	0	0	0	0	18	1,3
PN-1-f	27	10	2	0	0	0	39	1,4	22	20	7	6	0	0	55	1,9	24	9	0	0	0	0	33	1,3
PN-1-Vf	28	10	3	0	0	0	41	1,4	18	11	5	0	0	0	34	1,6	19	9	0	0	0	0	28	1,3
PN-2-m	10	12	3	0	0	0	25	1,7	2	3	0	0	0	0	5	1,6	3	4	0	0	0	0	7	1,6
PN-3-m	15	14	3	0	0	0	32	1,6	4	11	1	0	0	0	16	1,8	2	6	0	0	0	0	8	1,8
PN-4-m	1	6	2	0	0	0	9	2,1	0	1	0	0	0	0	1	2,0	0	1	0	0	0	0	1	2,0
PN-5-m	15	47	10	0	0	0	72	1,9	0	0	0	0	0	0	0	0,0	0	0	0	0	0	0	0	0,0
PN-6-m	2	13	4	0	0	0	19	2,1	5	2	1	0	0	0	8	1,5	2	0	0	0	0	0	2	1,0
PN-7-m	8	16	0	1	0	0	25	1,8	7	15	3	0	0	0	25	1,8	6	7	0	0	0	0	13	1,5
PN-8-m	7	16	1	1	0	0	25	1,8	1	0	0	0	0	0	1	1,0	2	3	0	0	0	0	5	1,6
PN-9-m	13	19	13	2	0	0	47	2,1	1	17	8	0	0	0	26	2,3	0	10	0	0	0	0	10	2,0
PN-10-m	2	8	5	0	0	0	15	2,2	0	5	4	0	0	0	9	2,4	0	4	0	0	0	0	4	2,0
PN-11-m	10	18	5	2	5	0	40	2,350	1	7	0	1	0	0	9	2,1	1	3	0	0	0	0	4	1,8
PN-11-m^{30}	8	15	5	2	0	0	30	2,033	-	-	-	-	-	-	-	-	-	-	-	-	-	-	-	-

Table 5.1 – Differences between McBride and Picard (1987) and our roundness calculation technique. PN-11: tested sample. Key to grain shape categories. 1 = very angular; 2 = angular; 3 = sub-angular; 4 = sub-rounded; 5 = rounded; 6 = well rounded.

on PN-11-m^{30} was carried out, then the mean roundness was calculated only for the firsts 30 grains, to compare and test their technique (see table below). Thus, by comparing these two techniques, we proved that only in a few cases the values are slightly underestimated (for plagioclase and lathwork texture, tab. 5.1).

The most common roundness category among all grain types from Panarea and Stromboli islands is 2 (angular), followed by 3 (sub-angular), 1 (very angular), 4 (sub-rounded), and then with a very low occurrence of 5 (rounded), and no 6 (well rounded) grains categories whereas, the samples from Alicudi, Filicudi, Salina, Vulcano and Lipari islands show an higher percentage of sub-rounded category (3). The Aeolian Islands central sector (Salina, Lipari, Vulcano) have the most rounded grains and Vulcano has the highest well rounded percentage among all the Aeolian islands (4.48).

This trend is probably attributable to the continuous clastic supply from steep slopes, consistent with a weathering-limited erosion regime of the volcanic edifices (e.g., Morrone et al., 2017).

69351 grains were analyzed under optical microscope and comparing Campania and Aeolian islands mean roundness sand samples, it is evident that the two studied areas have a different roundness degree: Campania samples have an higher percentage of (3), (4), (5) and (6) roundness category, whereas Aeolian islands samples have an higher percentage of (1) and (2) roundness category (fig. 5.3).

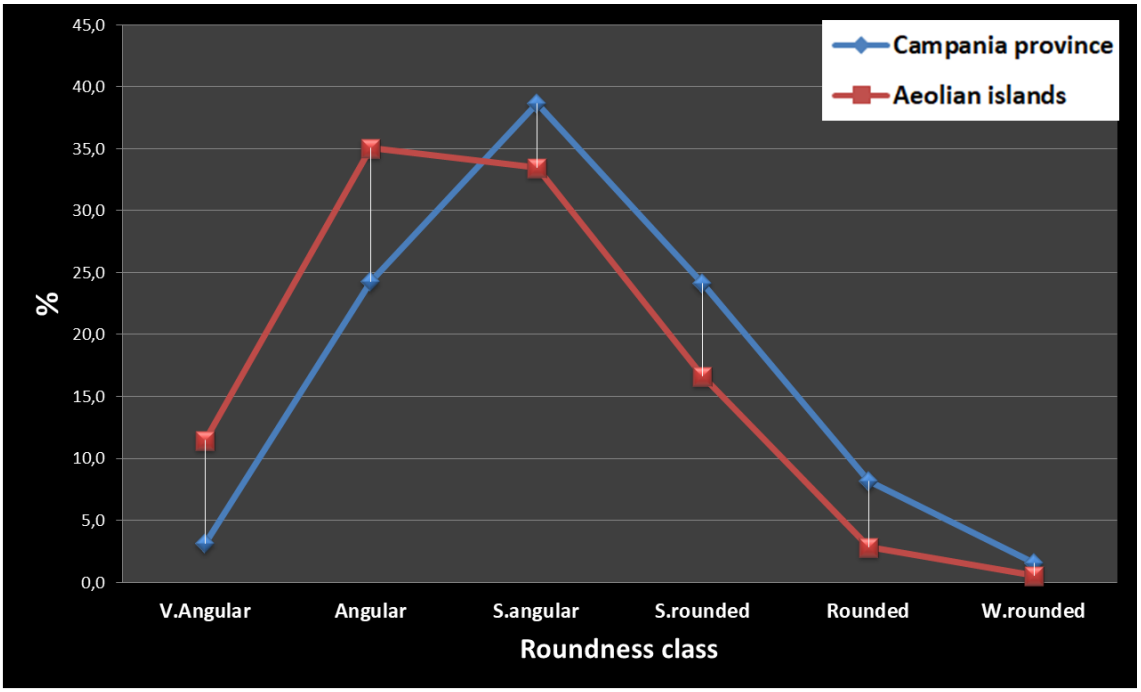

Figure 5.3 – Mean roundness differences among Campania and Aeolian Islands sand samples.

Thus, also roundness study shows that the two studied areas have a different textural maturity degree with Campania samples displaying an higher roundness degree which decrease towards Phlegrean Fields area from north (Volturno river-mouth) to south (figs. 4.48, 4.65, 4.66).

By comparing grain roundness degree and sand composition it was possible to link the transport distance (km) from crater to the coast on Stromboli island (about 3 km transport-distance, fig. 4.49a, 4.50) and from Vesuvius crater to the coast (fig. 4.67, Portici, Torre del Greco, Torre Annunziata, Castellammare di Stabia along about 15 km distance). In both cases there is a roundness category change, from angular to sub-angular for the first, and from sub-angular to sub-rounded for the second. These category changes can be attributed first to stream-setting transportation and then to the

coastal reworking. This suggest also that on Stromboli island there is an higher stream/wave energy which allows to round grains in a shorter distance.

Results show that there is no correlation between beaches area and roundness degree, and there is no correlation between drainage basin size and roundness degree for both, single crystal grains and volcanic lithic fragments (4.51, 4.52, 4.53, 4.54, 4.55, 4.56). Moreover, there is no a strong roundness degree dependence from grain-size, but results showed that very coarse sand fraction tend to round more quickly than fine sand fraction among Campania tested samples, whereas there is a roundness degree increasing from coarser to finer sand fraction among Aeolian islands tested samples.

Among Campania coastal stretch VO-3 (Volturno river-mouth), VO-8 (Regi Lagni river-mouth), VO-11 (Lago di Patria river-mouth) samples which have been sampled from deltaic environment resulted more rounded because of higher environment energy (tab. 3.8, fig. 4.68, 5.1, appendix A, C). Therefore, Campania results showed that sedimentary lithic fragments tend to round more quickly than volcanic lithic fragments (fig. 4.66, 4.68, 4.69) especially from Volturno to Phlegrean Fields coastal stretch where Bacoli samples denote the transition from sedimentary to volcanic petrofacies (fig. 5.1). Among Licola sample series Li-4 is the most rounded probably because it has been sampled from dunal environment (tab. 3.8)

On Aeolian islands, wave energy, decreases from west to east. The mean roundness of all the grain types analysed is considerably greater in the east than the west, and most increase progressively from north-west to east. Therefore, it seems that there is some relation between roundness and geographic location of the beaches. Sand grains round more efficiently under gentler wave action of the eastern side whereas the more angular grains of the north-western beaches are immediately eroded from the nearby cliffs with null or quite minimal reworking (figs. from 4.60 to fig. 4.64).

Mean roundness detailed results of samples from two distinct areas a have allowed to delineate a grain type roundness ranking among various types of volcanic and sedimentary lithic and among single crystal grains, and then a ranking between lithic grains and single crystal grains.

Hence, it has been compared the roundness degree discriminated by sand composition investigating lithic fragments and single crystal grains in detail (figs. from 4.50 to 4.58 and figs. from 4.68 to 4.71). Among the sedimentary lithic grains ($Lsc_{(xx)}$, $Lsc_{(micr)}$, Lss), those with micrite carbonate composition ($Lsc_{(micr)}$) are often more rounded than crystalline carbonate ($Lsc_{(xx)}$) and siliciclastic (Lss) composition. Between

sedimentary lithic and volcanic lithic fragments the first are always more rounded than the second probably because their more labile composition. Volcanic lithic with microlitic texture (Lvmi) are always more rounded then lathwork (Lvl), vitric (Lvv) and felsitic (Lvf) textures with few exceptions. Moreover, along more protected coastal stretch (in depositional environment energy terms) pumice have been found in the sand fraction and they are always well preserved and show a very angular, angular and in a few cases sub-angular roundness category.

Among single crystal grains olivine, leucite and opaque minerals result often (almost always) the most rounded grains in all samples (also in the zero order crater sands, e.g., STR-9, VE-1, VE-2, VE-3) followed by plagioclase and then by pyroxene which have often similar roundness trend. Along Bacoli-Volturno coastal stretch calcite is often the most rounded single crystal grains followed by quartz and k-feldspar single grain.

After these results it is possible to affirm that not always more rounded grains means longer distance transportation or more mature grains, because most likely sometimes the roundness degree could be directly inherited from source rocks and/or directly by crystalline habit (e.g. fig. 5.4).

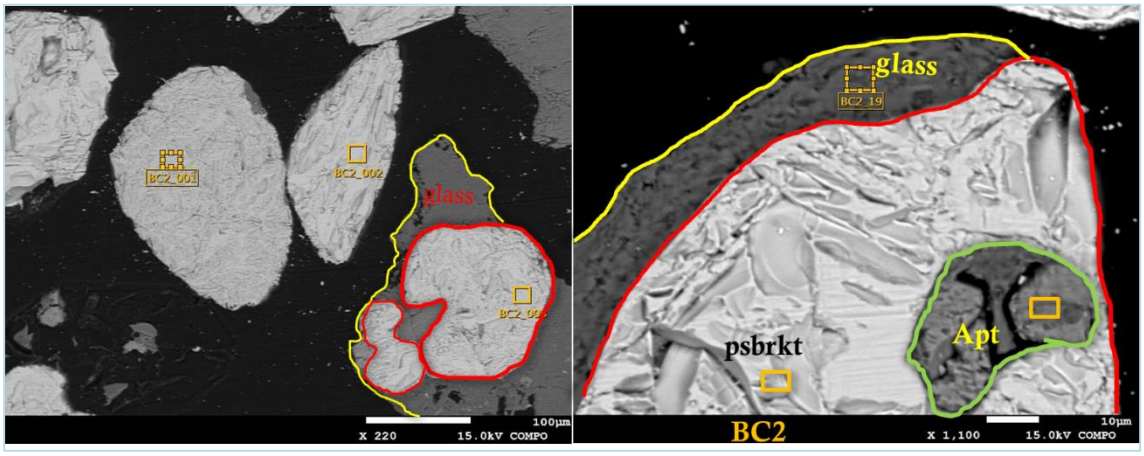

Figure 5.4 – Mean roundness inherited from source rocks/crystalline habit. Pseudobrookite opaque minerals (red boundaries) and intra-crystalline apatite (green boundary). Yellow boundaries = glass. (BC-2, Campania coastal stretch).

Moreover, mean roundness degree has been calculated also with image analysis by scanning thin section and bulk granular sample (fig. 4.73, 4.92, 4.93), data were processed using *ImageJ* software in order to compare the results obtained among these three different roundness calculation methods (optical microscope, scanned thin section, scanned bulk granular sample) so as to obtain the real roundness value as accurate as

possible considering those values which ranging into the same category (figs. from 4.94 to 4.113).

Circularity parameter shows more reliable values than roundness parameter (higher affinity with optical microscope method values) among scanned thin section analysis, especially in the very coarse sand fraction, whereas in the medium sand fraction roundness (scanned thins section) and circularity (bulk sample) shows an higher affinity with the optical microscope method values (figs. from 4.94 to 4.113).

Thus, results often showed that bulk sample methodology tends to overestimate the mean roundness value for both, circularity and roundness parameters, but image acquisition method allows to analyze better among different well-spaced grains avoiding to analyze grains together as unique guy and where sometime non-real grains could be counted during image processing as sometime happen using a scanned thin section method (figs. 4.92, 4.93, 5.5). In future, to improve this methodology (scanned bulk sample method) could be calibrated a new roundness/circularity scale.

In light of these results, it is possible to affirm that image analysis by using *ImageJ* software is a faster tool to calculate roundness category of thousands grains but operator's skills to set this software are really important and it is more difficult to recognize among different grain type (e.g., between quartz and feldspars and between pyroxene and amphibole). Then success of the analysis depends beyond by operator's skills, by also image scanning mode (figs. 4.73, 4.92, 4.93).

Then we can discuss on the pros and cons of both techniques: optical microscope technique (e.g. McBride and Picard, 1987) has more accuracy, then it is possible to make roundness analysis among all the grain typologies (figs. from 4.50 to 4.58 and figs. from 4.68 to 4.71), but it takes a long time and it is influenced by the operator subjectivity using a visual comparator; whereas image analyses is a faster tool to obtain the main roundness class of the whole analyzed sample, it is very difficult to calculate the roundness class by distinguishing among different grain type composition (e.g., between quartz and feldspars), furthermore some grains counted during the roundness calculation are not real such as bubbles or stains (fig. 5.5); even if there is a time(consuming) image analysis method which allows to improve analysis accuracy and to distinguish at least between lithic fragments and single crystals grains by comparing the real scanned image with that returned by the software. At this point, the better way to proceed is to use both techniques, microscope and image analysis in order to obtain best results on roundness and composition analysis.

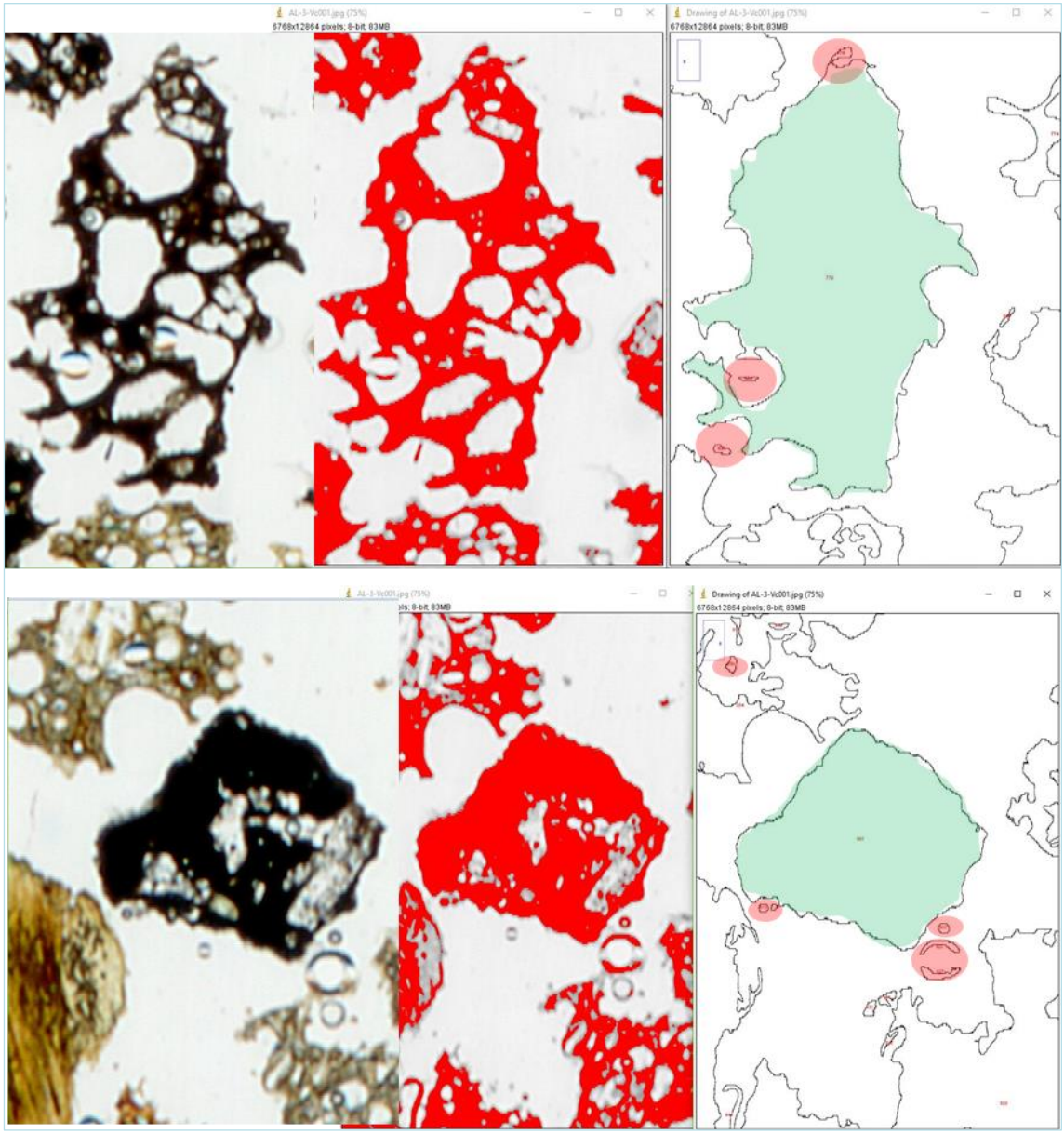

Figure 5.5 – Real grains thin section scanned (on the left); red areas are grains (or grain parts) which have been recognized by the software (middle image); image processed and drawn by the software (on the right); red areas show errors in the roundness evaluation (not real grains), green areas represent the right grains analyzed.

Areal distribution source rocks (lavas and pyroclastic rocks) data results, showed that in those drainage basins predominately constituted by pyroclastic rocks rather than lavas, the corresponding beaches (Aeolian islands) are constituted by immature detritus, namely blocks and gravel with a very low sand amount; whereas in those drainage basins predominately constituted by lavas rather than pyroclastic rocks, the

corresponding beaches are predominately constituted by sandy detritus (figs. from 3.2 to 3.16 and figs. from 4.114 to 4.120; tables from 4.16 to 4.29).

For instance, Gelso beach on Vulcano island (faro localities, V2 drainage basin/sample site) is almost totally constituted by blocks and gravel (fig. 3.12b) and the corresponding drainage basin is predominately constituted by pyroclastic rocks (fig. 4.118; tab.4.25); whereas Vulcanello beaches (e.g. V6, V11, V12) are constituted almost totally by sands and the corresponding drainage basins are predominately constituted by lavas source rocks (e.g. V6, V11-12 drainage basins/sample sites, fig. 3.12a and fig. 4.118; tab. 4.25). Cala degli Zimmari beach (Panarea island) is almost totally constituted by sandy detritus and the corresponding drainage basins are predominately constituted by lavas source rocks (figs. 3.14a, 4.119; tab. 4.27). Also Rinella beach, on Salina island, is totally constituted by sandy detritus and the corresponding drainage basins are constituted by an higher lavas percentage than pyroclastic source rocks (figs 3.6b, 4.116; tab. 4.21). Hence, after these results it possible to affirm that lavas source rocks have an higher propensity to create sandy detritus than pyroclastic source rocks.

Moreover, applying the concept of Sand Generation Index (SGI, first defined by Palomares and Arribas, 1993) important results have been found out for Lipari island sand samples, where felsic to intermediate bedrock association of lavas+pyroclastic rock shows that these lithotypes have different propensities to create detritus, in terms of both grain size and composition. The SGI of lavas is 0.9 to 12.3 times higher than of pyroclastic rocks, even if they constitute a minor outcrop area of the island. Clastic contribution from pyroclastic rock outcrops such as pumice, is not found in the size ranges studied (medium and fine sand), suggesting that these pumiceous source rocks probably only produce gravel or very fine sand and silt (and potentially clay when weathered, Morrone et al., 2017).

-Chapter 6 – Conclusions-

The main factors controlling the chemical and mineralogical composition of siliciclastic sedimentary rocks are the provenance lithotypes (Heins 1995; Arribas and Tortosa, 2003; Heins & Kairo, 2007), climate through chemical weathering (Johnsson et al. 1988), abrasion and sorting during transportation (Nesbitt and Young, 1996), and the tectonic setting (Dickinson and Valloni, 1980).

Analysis of compositional and textural data derived from beach sands of two distinct active volcanic areas in the southern Tyrrhenian sea yields the following conclusions:

There is a clear differences between Aeolian Islands costal beach sand and Campania coastal beach sand in terms of detritus maturity. Grain-size distribution within Aeolian beach sediment show a tendency towards coarser sand fraction to gravel, whereas Campania coastal samples show a tendency towards medium to fine sand fractions; this indicates a varied physical disintegration of the source rocks. Hence, Aeolian islands detritus having a proximal source area reflect their textural immaturity whereas Campania detritus, especially along Licola-Volturno coastal stretch, having a distal source area (more distal with respect Aeolian island beaches) show an higher textural maturity degree.

The major components of Aeolian islands and Campania beach sands are monomineralic grains, sedimentary and volcanic lithic fragments with lesser amounts of calcareous bioclasts. Samples from Aeolian islands and Portici Sorrento coastal stretch have an high percentage of volcanic lithic fragments (Lvl > Lvmi> Lvv), whereas samples from Pozzuoli, display an average percentage among Lvl~Lvmi~Lvv.

Campania sand samples have a mixed provenance source rocks: sedimentary source rocks and volcanic source rooks. Three different petrofacies have been defined along Campania coastal stretch: sedimentary (Apennines), Vesuvian and Phlegrean fields petrofacies.

Stromboli, Vulcano, Alicudi and Filicudi sands have a dual basaltic/shoshonitic and andesitic composition “signatures”. Panarea, Lipari and Salina sands have a wider range of composition “signatures” ranging from basalts to rhyolites.

The bulk composition of a Strombolian sand deposit commonly is similar to the average basalt composition of the crateric area.

Thus there is evidence that, on Aeolian islands, sand composition does accurately reflect bedrock composition except in the case of source areas dominated by pumice outcrops (e.g. Lipari islands, Morrone et al., 2017), whereas in more protected and quite

beach-environment such as Pozzuoli bay, this grain types (pumice, associated to more evolved [acid] volcanism and then explosive volcanism) have been found and resulted to be texturally more preserved.

The heavy mineral suites of the Campania shoreline reflect the mineralogy of the source rocks, with abundant detrital grains of both opaques (pseudobrookite, pyrite, ilmenite), and transparent species such as diospide, brown and green amphibole, and trace amounts of biotite, garnet, rutile and tourmaline.

In the sandy detritus the persistence for the lithic grains is ranked as follows: Lvlblg, Lvmiblgl, Lvvblgl > Lvlbrgl, Lvmibrlgl, Lvvbrgl > Lvlclgl, Lvmiclgl, Lvvclgl > Lvf > Lvlgrgl, Lvmigrgl, Lvvgrgl, pumice. Thus, mafic source rocks will be overestimated and more acid source rocks will be underestimated in the stratigraphic record.

New volcanic lithic compounds have been introduced (*Lvlgrgl*, *Lvmigrgl*, *Lvvgrgl*) then who will study the ancient stratigraphic records will know that the Lvlgrgl means dacitic provenance.

New discriminating diagrams have been introduced which allow to obtain important information among the volcanic source rocks ranging from basic to acid composition.

Lvlblgl, *Lvmiblgl*, *Lvvblgl (1); Lvlbrgl*, *Lvmibrgl*, *Lvvbrgl (2)*; *Lvlgrgl*, *Lvmigrgl*, *Lvvgrgl* (3) can be produced not only by basaltic, andesitic and dacitic source rocks but also by source rocks with the same SiO2 content belonging at different alkaline series (e.g. trachybasalt, shoshonite, latite, trachyandesite, trachydacite, trachyte).

Sandy lithic fragments with different textures such as lathowork, microlitic and vitric are mainly produced by lavas erosion but they can be also produced (in lesser amount) by pyroclastic rocks which tend to produce coarser and/or finer detritus.

This study demonstrates that there is great diversity in the types and abundances of modern volcaniclastic detritus produced in the studied areas. This detritus exhibits considerable diversity with regard to glass and mineral populations and textures of constituent volcanic components as seen in ancient equivalents (Mack and Jerzykiewicz 1989; Cather and Folk, 1991; Critelli and Ingersoll, 1995; Critelli, Marsaglia and Busby, 2002).

Between our and McBride and Picard (1987) roundness calculation techniques, we proved that only in a few cases the values are slightly underestimated.

Salina, Lipari and Vulcano islands (central sector of Aeolian Islands) have the most rounded grains and Vulcano has the highest percentage of the 6th roundness category (well roundned) among all the Aeolian islands. This trend is probably attributable to the

continuous clastic supply from steep slopes, consistent with a weathering-limited erosion regime of the volcanic edifices (e.g., Morrone et al., 2017).

Campania samples displaying an higher roundness degree which decrease towards Phlegrean Fields area from north (Volturno river-mouth) to south and, show an higher percentage of (3), (4), (5) and (6) roundness category, whereas Aeolian islands samples have an higher percentage of (1) and (2) roundness category.

Certain grain types tend to round more quickly in volcano beach environments, such as olivine, leucite and opaque minerals among the single crystal grains and *Lvmi* among the lithic fragments.

Thus, the order of increasing roundness of grains and then increasing rate of abrasion for the lithic grains is ranked as follows: Lvv< Lvl<Lvf<Lvmi for lithic grains and Py ≈ P ≈ K < Ol ≈ Le ≈ Op for monocrystalline grains. Moreover, sedimentary lithic grains tend to round more quickly than volcanic lithic fragments (Lv < Ls) probably because their more labile composition and among sedimentary lithic grains Lss ≈ ($Lsc_{(xx)}$) < $Lsc_{(micr)}$. Furthermore, volcanic lithic fragments tend to round more than single crystal grains. Calcite is always more rounded than monocrystalline quartz and k-feldspar which have similar roundness trend.

There are no significant relationships between mean roundness with the beach size and there are also no significant relationships between mean roundness with different size of drainage basins indicating there is no perceptible rounding of grains transported by short-headed streams, even if there is a roundness category change, from angular to sub-angular in only 3 km of transportation verified on Stromboli island; on the other hand category changes can be attributed first to stream-setting transportation and then to the coastal reworking.

There is a correlation between roundness and geographic location of the Aeolian islands beaches. Sand grains round more efficiently under gentler wave action of the eastern side whereas the more angular grains of the north-western beaches are immediately eroded from the nearby cliffs with null or quite minimal reworking Morrone et al., 2018).

Not always more rounded grains means longer distance transportation or more mature grains, sometimes the roundness degree could be directly inherited from source rocks and/or directly by crystalline habit.

A new methodological and research approach for roundness degree calculation have been tested by conducting image analysis. These results suggest that optical microscope

technique has more accuracy, then it is possible to make roundness analysis among all the grain typologies, but it takes a long time and it is influenced by the operator subjectivity using a visual comparator; whereas image analyses is a faster tool to obtain the main roundness class of the whole analyzed sample, it is very difficult to calculate the roundness class by discriminating among the different grain types (e.g., between quartz and feldspars, pyroxene and amphibole) and the success of analysis also depends on the operator's skill to set software parameters. Best results on roundness and composition analysis could be obtained by using both techniques, microscope and image analysis.

By relating GIS, compositional and textural results, it is possible to affirm that lavas source rocks have an higher propensity to create sandy detritus than pyroclastic source rocks. This finding has implications for the stratigraphic record especially for the sandy pumice clasts which could be underrepresented in older volcaniclastic deposits and overrepresented in other detritus size fractions. This factor, which we relate in this work to a hydrodynamic sorting control in the beach environment, or to a lower sand generation index of the source rocks, in ancient volcaniclastic rocks, has been often attributed to the loss of these clastic particles during diagenetic processes. Instead, this study, suggests also for other factors responsible for its loss formerly, in continental areas, before its entering into burial processes and diagenetic history.

This actualistic study helps in understanding factors controlling siliciclastic sediment composition and texture, in turn, will help in deciphering major controls on ancient volcaniclastic successions, especially those where volcanic terrains have been totally lost by erosion.

- Future work –

- Improving image analysis accuracy for the roundness study by increasing samples dataset;
- Conduct a study which will give quantitative information of debris production starting from a certain volcanic source rocks areal distribution (%) outcropping in a certain drainage basin (e.g. basaltic, dacitic, etc. source rocks among Aeolian islands).

-References-

Andò S., Garzanti E., Padoan M. and Limonta M. (2012) - Corrosion of heavy minerals during weathering and diagenesis: a catalogue for optical analysis. Sedimentary Geology, **280**, 165–178.

Alvarez W., Cocozza T. and Wezel F.C. (1974). Fragmentation of the Alpine orogenic belt by microplate dispersal. Nature, London, **248**, 309-314.

Abramoff M.D., Magalhaes P.J., Ram, S.J. (2004). "Image Processing with ImageJ". Biophotonics International, volume **11**, issue 7, pp. 36-42.

Andronico D., Branca S., Calvari S., Burton M., Caltabiano T., Corsaro R., Del Carlo P., Garfì G., Lodato L., Miraglia L., Murè F., Neri M., Pecora E., Pompilio M.,·Salerno G., Spampinato L. (2005) - A multi-disciplinary study of the 2002–03 Etna eruption: insights into a complex plumbing system. *Bullettin of Volcanol*, **67**, 314–330.

Arribas J., Critelli S., Le Pera E. and Tortosa A. (2000). Composition of modern stream sand derived from a mixture of sedimentary and metamorphic source rocks (Henares River Central Spain). Sedimentary Geology **133**, 27–48.

Armienti P., Barberi F., Bizouard H., Clocchiatti R., Innocenti F., Metrich N., Rosi M., Sbrana A. (1983). The Phlegraean Fields: magma evolution within a shallow chamber. J. Volcanol. Geotherm. Res. **17**:289-311.

Artemieva I. and Meissner R. (2012). Crustal thickness controlled by plate tectonics: A review of crust–mantle interaction processes illustrated by European examples. Tectonophysics, **530**-**531**, 18-49.

Barberi F., Gasparini P., Innocenti F. and Villari L. (1973): Volcanism of the southern Tyrrhenian Sea and its geodynamic implications. Journal of Geophysical Research, **78**: 5221-5232.

Barberi F., Bigi G., Parotto M. and Vezzani L. (1986). Carta Geologica e Gravimetrica dei Campi Flegrei (1:15000).

Bargossi G. M., Campos Venuti M., Gasparotto G. and Rossi P.L. (1989). Petrologia e stratigrafia delle successioni andesitiche l.s. di Lipari, Isole Eolie, Italia. Mineralogica et Petrographica Acta, **22**, 295–326.

Basu A. (1976). Petrology of Holocene fluvial sand derived from plutonic source rocks: implication to paleoclimatic interpretation. *Journal of Sedimentary Petrology*, **46**, 694-709.

Basu A. (1985). Influence of climate and relief on composition of sands released at source areas. In Zuffa G. G., ed., Provenance of Arenites: NATO ASI series 148, Dordrecht, D. Reidel, 1-18.

Basu A. and Molinaroli E. (1989). Provenance characteristics of detrital opaque Fe-Ti oxides minerals. Journal of Sedimentary Petrology **59**, 922–34.

Basu A. and Molinaroli E. (1991). Reliability and application of detrital Fe-Ti oxide minerals in provenance determination. Geological Society, London, Special Publications, **57**, 55–65.

Beccaluva L., Di Girolamo P., Serri G. (1991). Petrogenesis and tectonic setting of the Roman volcanic province, Italy. Lithos. **26**, 191-221.

Bowen N. L. (1922). The reaction principle in petrogenesis. Jour. Geology, **30**, 177-198.

Breyer J. A. and Bart H. A. (1978). The composition of fluvial sands in a temperate semiaris region. Jour. Sed. Petrology, **48**, 1311-1320.

Bruno P.P., Di Fiore V., Ventura G. (2000). Seismic study of the "41st Parallel" fault system offshore the Campanian-Latial continental margin, Italy. Tectonophysics **324**, 37-55.

Bryk K., Kołodziej B. (2014). Assessment of water and air permeability of chernozem supported by image analysis. Soil and Tillage Research **138**, 73-84.

Calanchi N., Peccerillo A. et al. (2002). Petrology and geochemistry of volcanic rocks from the island of Panarea: implications for mantle evolution beneath the Aeolian island arc (southern Tyrrhenian sea).

Journal of Volcanology and Geothermal Research, **115**, 367–395.

Calcagnile G., Panza G. F. (1981). The main characteristics of the lithosphere-asthenosphere system in Italy and surrounding regions. Pure Appl. Geophy. **119**, 865-879.

Cameron K. L. and Blatt H. (1971). Durabilities of sand-sized schist and volcanic rock fragments during fluvial transport, Elk Creek, Black Hills, South Dakota. Jour. Sed. Petrology, **41**, 565-576.

Caracciolo L., Tolosana Delgado R., Le Pera E., Von Eynatten H., Arribas J. and Tarquini S. (2012). Influence of granitoid textural parameters on sediment composition: implications for sediment generation. Sedimentary Geology **280**, 93–107.

Carson M.A. and Kirkby M.J. (1972). Hillslope form and process. *Cambridge University Press*, 3. **viii** + 475 pp.

Cas R. A. F. and Wright .J V. (1987). Volcaniclastic rocks and successions, modern and ancient. (London: Allen and Unwin.).

Cather S. M. and Folk R. L. (1991). Pre-diagenetic sedimentary fractionation of andesitic detritus in a semiarid climate: an example from the Eocene Datil Group, New Mexico. In Sedimentation in Volcanic Settings (eds R. V. Fisher and G. A. Smith), pp. 211–26. Society of Economic Paleontologists and Mineralogists Special Paper **45**.

Cawood P. A. (1985). Accretion and dispersal tectonics of the southern New England Fold Belt, eastern Australia. CircumPacific Council for Energy and Mineral Resources 2008 – Tectonostratigrahic Terranes of the Circum-Pacific Region, Earth Science Series, Number **1**, 1985.

Cawood P. A. (1991). Nature and record of igneous activity in the Tonga Arc, SW Pacific, deduced from the phase chemistry of derived detrital grains. In Developments in Sedimentary Provenance Studies (eds A. C. Morton, S. P. ToddandP. D. W.Haughton), pp. 305–21. Geological Society Special Publication no. **57**.

Cello G., Mazzoli S. (1999). Apennine tectonics in southern Italy. A review. J Geodyn **27:**191-211

Chiarabba C., De Gori P. and Speranza F. (2008). The southern Tyrrhenian subduction zone: deep geometry, magmatism and Plio-Pleistocene evolution. Earth Planetary Science Letters **268**, 408–23.

Cimarelli C., De Rita D., Dolfi D. and Procesi M. (2008). Coeval strombolian and vulcanian-type explosive eruptions at Panarea (Aeolian Islands, Southern Italy). Journal of Volcanology and Geothermal Research, **177**, 797–811.

Cioni R., Marianelli P., Santacroce R. (1997). Thermal and compositional evolution of the shallow magma chambers of Vesuvius: Evidence from pyroxene phenocrysts and melt inclusions. J. Geophys. Res. **103**:18277-18294.

Civetta L., Orsi G., Pappalardo L., Fisher R. V., Heiken G. and Ort M. (1997). Geochemical zoning, mingling, eruptive dynamics and depositional processes - The Campanian Ignimbrite, Campi Flegrei caldera, Italy. Journal of Volcanology and Geothermal Research **75**(3-4):183-219. DOI10.1016/S0377-0273(96)00027-3.

Cleary W. J. and Connolly J. R. (1971). Distribution and genesis of quartz in a piedmont-coastal plain environment. Geological Society of America Bulletin **82**, 2755–66.

Corniello A. (2010). -Idrogeologia ed idrogeochimica della piana compresa tra il M.te Massico ed il F. Volturno (Campania).

Critelli S., De Rosa R., Sonnino M. and Zuffa G. G. (1990). Significato dei depositi vulcanoclastici della Formazione delle Tufiti di Tusa (Miocene inferiore, Lucania meridionale). Bollettino Società Geologica Italiana **109**, 743–62.

Critelli S., Sorriso-Valvo M. and Ventura G. (1993). Relazioni tra attività vulcanica, sedimentazione epiclastica ed evoluzione geomorfologica nell'isola di Salina (Isole Eolie). *Bollettino Società Geologica Italiana* **112**, 447–70.

Critelli S. and Ingersoll R. V. (1995). Interpretation of neovolcanic versus palaeovolcanic sand grains: an example from Miocene deep-marine sandstone of the Topanga Group (southern California). Sedimentology **42**, 783– 804.

Critelli S., Marsaglia K. M. and Busby C. J. (2002). Tectonic history of a Jurassic backarc-basin sequence (the Gran Cañon Formation, Cedros Island, Mexico), based on compositional modes of tuffaceous deposits. *Geological Society of America Bulletin* **114**(5), 515–27.

Critelli S., Arribas J., Le Pera E., Tortosa A., Marsaglia K.M. and LATTER K.K. (2003). The recycled orogenic sand provenance from an uplifted thrust belt, Betic Cordillera, Southern Spain. Journal of Sedimentary Research **73**, 72–81.

Crisci G. M., De rosa R., Esperanza S., Mazzuoli R. and Sonnino M. (1991). Temporal evolution of a threecomponent system: the island of Lipari (Aeolian Arc, south Italy). Bulletin of Volcanology **53**, 207–21.

Crook K. A. W. (1974). Lithogenesis and geotectonics: the significance of compositional variation in flysch arenites (graywakes). In Dott R. H. and Shaver R. H. eds., Modern and ancient geosynclinals sedimentation. Soc. Econ. Paleont. Miner. Spec. Publ., **19**, 304-310.

Damuth J. E. and Fairbridge R. W. (1970). Equatorial Atlantic deep-sea arkosic sands and ice-age aridity in tropical South America. Geol. Soc. Am. Bull., **81**, 189-206.

Davì M., De Rosa R., Donato P., Vetere F., Barca D., Cavallo A. (2009). Magmatic Evolution and plumbing system of ring-fault volcanism: the Vulcanello Peninsula (Aeolian Islands, Italy). Eur. J. Mineral. DOI: 10.1127/0935- 1221/2009/0021-1955.

De Astis, G., La Volpe, L., Peccerillo, A., Civetta, L., (1997). Volcanological and petrological evolution of the Vulcano Island (Aeolian Arc, Southern Tyrrhenian Sea). Journal of Geophysical Research **102**, 8021–8050.

De Astis G., Peccerillo A., Kempton P. D., La Volpe L., Wu T. W. (2000). Transition from calc-alkaline to potassium-rich magmatism in subduction environments: geochemical and Sr, Nd, Pb isotopic constraints from the island of Vulcano (Aeolian arc). Contrib. Mineral. Petrol. **139**:684-703.

De Astis G., Ventura G. and Vilardo G. (2003). Geodynamic significance of the Aeolian volcanism (Southern Tyrrhenian Sea, Italy) in light of structural, seismological, and geochemical data, Tectonics, **22**, 1040, doi:10.1029/2003TC001506.

De Rosa R. and Sheridan M.F. (1983). Evidence for magma mixing in the surge deposits of the Monte Guardia sequence, Lipari. J. Volcanol. Geotherm. Res. **17**:313–328.

De Rosa, R., Zuffa, G., Taira, A., and Leggett, J. (1986). Petrography of trench sands from the Nankai Trough, southwest Japan: Implications for long-distance turbidite transportation. Geological Magazine, **123**(5), 477-486. doi:10.1017/S0016756800035068.

De Rosa R. (1999). Compositional modes in the ash fraction of some modern pyroclastic deposits: their determination and significance. Bulletin of Volcanology **61**, 162–73.

De Rosa R., Giullo, H., Mazzuoli R., Ventura G. (2003). New unspiked K–Ar ages of volcanic rocks of the central and western sector of the Aeolian Island: reconstruction of the volcanic stages. *J. Volcanol. Geoth. Res.*, **120**, 161–178.

De Vivo B., Rolandi G., Gans P. B., Calvert A., Bohrson W. A., Spera F. J. and Belkin H. E. (2001). New constraints on the pyroclastic eruptive history of the Campanian volcanic Plain (Italy). Mineralogy and Petrology, **73**, 47-65.

Dickinson W. R. (1970). Interpreting detrital modes of greywacke and arkose. Journal of Sedimentary Petrology **40**, 695–707.

Dickinson W. R. (1974). Plate tectonics and sedimentation. In Dickinson W. R., ed., Tectonics and sedimentation: Soc. Econ. Paleont. Miner. Spec. Publ. **22**, 1-27.

Dickinson W. R. (1982). Composition of sandstones in circum-Pacific subduction complexes and fore-arc basin. Am. Ass. Petr. Geol. Bull., **66**, 121-137.

Dickinson, W.R. (1985). Provenance Relations from Detrital Modes of Sandstones. In: Zuffa, G.G., Ed., Provenance of Arenites, NATO Advanced Science Institutes Series, C-**148**, 333-362.

Dickinson W. R. and Rich E. I. (1972). Petrologic intervals and petrofacies in the Great Valley Sequence, Sacramento Valley, California. Geol. Soc. Am. Bull., **83**, 3007-3024.

Dickinson W. R. and Suczek C. A. (1979). Plate tectonic and sandstone composition. *American Association of Petroleum Geologists Bulletin* **63**, 2164-2182.

Dickinson W. R. and Valloni R. (1980). Plate settings and provenance of sands in modern ocean basin. Geology, **8**, 82-86.

Dickinson W. R, Beard L. S., Brakenridge G. R., et al., (1983). Provenance of North American Phanerozoic sandstone in relation to tectonic setting. *Geological Society of America Bulletin*, **94**, 222-235.

Di Vito M.A., Isaia R., Orsi G., Southon J., de Vita S., D'Antonio M., Pappalardo L., Piochi M. (1999). "Volcanism and deformation since 12.000 years at the Campi Flegrei caldera (Italy)", J. Volcanol. Geotherm. Res., **91**: 221-246.

Doglioni C., Gueguen E., Harabaglia P. and Mongelli F. (1999). On the origin of W-directed subduction zones and applications to the western Mediterranean. In: The Mediterranean Basins: Tertiary Extension within the Alpine Orogen (B. Durand, L. Jolivet, F. Horvàth and M. Sèranne, eds), *Geological Society of London, Special publication*, pp. 541–561.

Donato P., Behrens H., De Rosa R., Holtz F. and Parat F. (2006). Crystallization conditions in the Upper Pollara magma chamber, Salina Island, Southern Tyrrhenian Sea. Mineralogy and Petrology, **86**, 89-108.

Dutta P. K., Zhou Z. and dos Santos P. R. (1993). A theorethical study of mineralogical maturation of eolian sand. In Johnsson M. J. and Basu A., eds., Processes Controlling the Composition of Clastic Sediments. Geol. Soc. Am. Spec. Paper **284**, 203-209.

Dye T. S. and Dickinson W. R. (1996). Sources of sand tempers in prehistoric Tongan pottery. Geoarchaeology **11**, 141–64.

Ellam, R. M., C. J. Hawkesworth, M. A. Menzies, and N. W. Rogers (1989). The volcanism of southern Italy: Role of subduction and the relationship between potassic and sodic alkaline magmatism, J. Geophys. Res., **94**(B4), 4589–4601, doi:10.1029/JB094iB04p04589.

Enkeboll R. H. (1982). Petrology and provenance of sands and gravels from the Middle America Trench and trench-slope, southwestern Mexico and Guatemala. Initial Reports of the Deep Sea Drilling Project, **66**, 521-530.

Faccenna, C., Becker, T.W., Lucente, F.P., Jolivet, L. and Rossetti, F. (2001). History of subduction and back-arc extension in the central Mediterranean. Geophys. J. Int., **145**, 809–820.

Favalli M., Karatson D., Mazzuoli R., Pareschi M. T. and VENTURA G. (2005). Volcanic geomorphology and tectonics of the Aeolian archipelago (southern Italy) based on integrated DEM data. Bulletin of Volcanology **68**, 157–70.

Fisher R V. (1961). Proposed classification of volcaniclastic sediments and rocks. Geological Society of America Bulletin, Vol. **72**, 1409–1414.

Fisher R V. and Schmincke H U. (1984). Pyroclastic rocks. (Berlin: Springer-Verlag.).

Fisher R V, and Smith G. A. (1991). Volcanism, tectonics and sedimentation, 1–5 in Sedimentation in volcanic settings. SEPM (Society for Sedimentary Geology) Special Publication, No. **45**.

Fisher R.V. and Schmincke H.U. (1994). Volcaniclastic sediment transport and deposition. In: Pye K. (Ed.), Sediment transport and depositional processes. Blackwell scientific publications, 351-388.

Fisher R. V., Heiken G. and Hulen J. B. (1997). Volcanoes: Crucibles of Change. Princeton University Press. ISBN: 069101213X.

Flores R. M. and Shideler G. L. (1978). Factors controlling heavy mineral variations on the South Texas outer continental shelf, Gulf of Mexico. Journal of Sedimentary Petrology **48**, 269–80.

Folk, R. L. 1955. Student operator error in determination of roundness, sphericity and grain size. J. Sediment. Petrol. **25**, 297–301.

Francalanci L., Manetti P. and Peccerillo A. (1989). Volcanological and magmatological evolution of Stromboli volcano (Aeolian islands): the roles of fractional crystallisation, magma mixing, crustal contamination and source heterogeneity. Bulletin of Volcanology, **51**, 355–378.

Francalanci L., Manetti P., Peccerillo A., Keller J. (1993). Magmatological evolution of the Stromboli volcano (Aeolian Arc, Italy): inferences from major and trace element and Sr-isotopic composition of lavas and pyroclastic rocks. Acta Vulcanol **3**:127–151.

Francalanci L., Tommasini S. and Conticelli S. (2004). The volcanic activity of Stromboli in the 1906–1998 A.D. period: mineralogical, geochemical and isotope data relevant to the understanding of plumbing system. Journal of Volcanology and Geothermal Researches, **131**, 179–211.

Francalanci L., Avanzinelli R., Tommasini S. and Heumann A. (2007). A westeast geochemical and isotopic traverse along the subaerial volcanism of the Aeolian Island arc, Southern Tyrrhenian Sea, Italy: Inferences on mantle source processes. In: Beccaluva, L., Bianchini, G. and Wilson, M. (eds) Cenozoic Volcanism in the Mediterranean Area. *Geological Society of America, Special Papers* **418**, 235-263.

Frihy O. E., LotfyM. F. and Komar R, P. (1995). Spatial variations in heavy minerals and patterns of sediment sorting along the Nile delta, Egypt. Sedimentary Geology **97**, 33–41.

Franzinelli E. and Potter P. E. (1983). Petrology, chemistry, and texture of modern river sands, Amazon river system. Jour. Geology, **91**, 23-39.

Fujioka, Kantaro; Furuta, Toshio; Arai, Fusao (1980). Petrography and geochemistry of volcanic glass: Leg 57, Deep Sea Drilling Project. In: Scientific Party, Initial Reports of the Deep Sea Drilling Project, 56/57 (eds.), Initial Reports of the Deep Sea Drilling Project (U.S. Govt. Printing Office), **56-57**, 1049-1066, https://doi.org/10.2973/dsdp.proc.5657.140.1980.

Gasperini D., Blichert Toft J., Bosch D., Del Moro A., Macera P., Albaréde F. (2002). Upwelling of deep mantle material through a plate window: evidence from the geochemistry of Italian basaltic volcanics. J. Geophys. Res. **107**, B12, 2367, doi:10.1029/2001JB000418.

Garzanti E. (1986). Source rock versus sedimentary control on the mineralogy of deltaic volcanic arenites (Upper Triassic, northern Italy). Journal of Sedimentary Petrology **56**, 267–75.

Garzanti E. and Andò S. (2007a). Heavy Mineral Concentration in Modern Sands: Implications for Provenance Interpretation. Developments in Sedimentology **58**, 517–45.

Garzanti E. and Andò S. (2007b). Plate tectonics and heavy minerals suites of modern sands. Developments in Sedimentology **58**, 741–63.

Garzanti E., Andò S. and Vezzoli G. (2008). Settling equivalence of detrital minerals and grain-size dependence of sediment composition. Earth and Planetary Science Letters **273**, 138–51.

Garzanti E., Andò S. and Vezzoli G. (2009). Grain-size dependence of sediment composition and environmental bias in provenance studies. Earth and Planetary Science Letters **277**, 422–32.

Garzanti E., Canclini S., Moretti F. and Petrellan N. (2002). Unravellingmagmatic and orogenic provenances in modern sands: the back-arc side of the Apennine thrust-belt (Italy). Journal of Sedimentary Research **72**, 2–17.

Garzanti E., Resentini A., Andò S., Vezzoli G., Pereira A. and Vermeesch P. (2015) - Physical controls on sand composition and relative durability of detrital minerals during ultra-long distance littoral and aeolian transport (Namibia and southern Angola). Sedimentology, v. **62**, p. 971–996.

Gillespie M. R and Styles M. T. (1999). BGS Rock Classification Scheme. Classification of igneous rocks. *British Geological Survey Research Report*, **1** (2nd edition) RR 99–06.

Gillot P. Y. and Villari L. (1980). K/Ar geochronological data on the Aeolian arc volcanism: a preliminary report. Open File Report, CNR, Italy, 3.

Gioncada A., Mazzuoli R., Milton A. J. (2005). Magma mixing at Lipari (Aeolian Islands, Italy): insights from textural and compositional features of phenocrysts, Journal of Volcanology and Geothermal Research **145**, pp. 97-118.

Girty G. H. (1987). Sandstone provenance, Point Lomo Formation, San Diego, California: evidence for uplift of the Peninsula Ranges during the Laramide orogeny. Jour. Sed. Petrology, **57**, 839-844.

Girty G. H., Mossmann B. J. and Pincus S. D. (1988). Petrology of Holocene sand, Peninsula Ranges, California and Baja Norte, Mexico: implication for provenance discrimination models. Jour. Sed. Petrology, **58**, 881-887.

Girty G. H., Marsh J., Meltzner A., McConnell J. R., Nygren D., Nygren J., Prince G. M., Randall K., Johnson D., Heitman B. and Nielsen J. (2003). Assessing changes in elemental mass as a result of chemical weathering of granodiorite in a Mediterranean (hot summer) climate. Journal of Sedimentary Research **73**(3), 434–43.

Goldich, S. S. (1938). A study in rock-weathering. J. Geol., **46**, 17–58.

Graham J. R., Wrafter J. P., Daly J. S. and Menuge J. F. (1991). A local source for the Ordovician Derryveeny Formation, western Ireland: implication for the Connemara Dalradian. In Morton A. C., Todd S. P. and Haughton P. D. W. (eds.), Developments in sedimentary provenance studies, Geol. Soc. London Spec. Publ., **57**, 199-213.

Grantham J. H. and Velbel M. A. (1988). The influence of climate and topography on rock fragments abundance in modern fluvial sands of the Southern Blue Ridge Mountains, North Carolina. Jour. Sed. Petrology, **58**, 219-227.

Grasso M (2001). The Apenninic-Maghrebian orogen in Southern Italy, Sicily and adjacent areas. In: Vai GB, Martini PI (eds) Anatomy of an Orogen. The Apennines and adjacent Mediterranean basins. Kluwer, Dordrecht, pp 255-286.

Gvirtzman Z. and Nur A. (2001). Residual topography, lithospheric structure and sunken slabs in the central Mediterranean. Earth and Planetary Science Letters **187**, 117–30.

Harrold P. J. and Moore C. (1975). Composition of deep-sea sands from marginal basins of the northwestern Pacific. Initial Reports of the Deep Sea Drilling Project, **31**, 507-514.

Hayes J. R. (1962). Quartz and feldspar content in South Platte, Platte and Missouri River sands. Jour. Sed. Petrology, **32**, 793-800.

Heind W. A. (1995). The use of mineral interfaces in sandsized rock fragments to infer ancient climate. Geological Society of America Bulletin **107**, 113–25.

Heins W. A. and Kairo S. (2007). Predicting sand character with integrated genetic analysis. In, Sedimentary provenance and Petrogenesis: Perspectives from Petrography and Geochemistry (eds J. Arribas, S. Critelli and M. J. Johnsson), pp. 345–79. Geological Society of America Special Paper **420**.

Hjulstrom F. (1935). Studies of the morphological activity of rivers as illustrated by the river Fyris, Inaugural dissertation by; by due permission of the Philosophical Faculty of Upsala, to be publicly discussed in lecture room of the Geographical Institution, May 23th, 1935, at 10 o'clock a. m., for the degree of doctor of philosophy, Uppsala : Almqvist and Wiksells -a.-b.

Hornig-Kjarsgaard I., Keller J., Koberski U., Stadlbauer E., Francalanci L. and Lenhart R. (1993). Geology, stratigraphy and volcanological evolution of the island of Stromboli, Aeolian arc, Italy. Acta Vulcanologica, **3**, 21–68.

Hubert J. f. (1962). A zircon-tourmaline-rutile maturity index and the interdependence of the composition of the heavy minerals assemblages with the gross composition and texture of sandstones. Jour. Sed. Petrology, **32**, 440-450.

Ingersoll R.V. (1990). Actualistic sandstone petrofacies: discriminating modern and ancient source rocks. Geology, **18**, 733-736.

Ingersoll R. V. and Suczek C. A. (1979). Petrology and Provenance of Neogene sand from Nicobar and Bengal Fans, DSDP sites 211 and 218. Jour. Sed. Petrology, **49**, 1217-1228.

Ingersoll R. V., Bullard T. F., Ford R. L., Grim J. P., Pickle J. D. and Sares S. W. (1984). The effect of grain size on detrital modes: a test of the Gazzi-Dickinson point-counting method. Journal of Sedimentary Petrology **54**, 103–16.

Ingersoll R. V., Kretchmer A. G. and Valles P. K. (1993). The effect of sampling scale on actualistic sandstone petrofacies. Sedimentology **40**, 937–53.

Ippolito F., D'Argenio B., Pescatore T., Scandone P. (1975). Structural-stratigraphic units and tectonic framework of Southern Apennines. In: Squyres CH (ed) Geology of Italy. Petrol Expl Soc Libya, Tripoli, pp 317-328.

ISPRA, Istituto Superiore per la Protezione e la Ricerca Ambientale. (2011). Gli indicatori del clima in Italia nel 2010. Anno VI, 152 pp.

Jackson T. A. and Keller W. D. (1970). A comparative study of the role of lichens and “inorganic” processes in the chemical weathering of Recent Hawaiian lava flows. American Journal of Science **269** (5), 446–66.

Jangorzo N. S. and Watteau F., Schwartz C. (2013). Evolution of the pore structure of constructed Technosols during early pedogenesis quantified by image analysis. Geoderma **207-208**, 180-192.

James W. C., Mack G. H. and Suttner L. J. (1981). Relative alteration of microcline and sodic plagioclase in semi-arid and humid climates. Journal of Sedimentary Petrology **51**, 151–64.

James N.P., Jons B., Campbell S.N., Campbell H.J., Titjen J. (2011). Cenozoic temperate and sub-tropical carbonate sedimentation on an oceanic volcano – Chatham Islands, New Zealand. *Sedimentology*, **58**, 4, 1007–1029.

James N. P., Jones B., Nelson C. S., Campbell H. J. and Titjen J. (2011). Cenozoic temperate and sub-tropical carbonate sedimentation on an oceanic volcano – Chatham Islands, New Zealand. Sedimentology, **58**: 1007–1029. doi:10.1111/j.1365-3091.2010.01193.x

Johnsson M. J., Stallard R. F. and Meade R. H. (1988). First-cycle quartz arenites in the Orinoco River basin, Venezuela and Colombia. Journal of Geology **96**, 263–77.

Johnsson M. J. and Stallard R. F. (1989). Phisiographic controls of the composition of fluvial sands derived from volcanic and sedimentary terrains on Barro Colorado island, Panama. Jour. Sed. Petrology, **59**, 768-781.

Johnsson M. J. (1990). Tectonic versus chemical-weathering controls on the composition of fluvial sands in tropical environments. Sedimentology, **37**, 713-726.

Johnsson M. J., Stallard R. F. and Lundberg N. (1991). Controls of composition of fluvial sands frm a tropical weathering environment: sands of the Orinoco River drainage basin, Venezuela and Colombia. Geol. Soc. Am. Bull., **103**, 1622-1647.

Johnsson M. J., Ellen S. D. and M$_C$Kittrick M. A. (1993). Intensity and duration of chemical weathering: an example from soil clays of the southern Koolau Mountains, Oahu, Hawaii. In Processes Controlling the Composition of Clastic Sediments (eds M. J. Johnsson and A. Basu), 1–19. Geological Society of America, Special Paper **284**.

Joron J. L., Metrich N., Rosi M., Santocroce R., Sbrana A. (1987). Chemistry and petrography. In: Santacorce R (ed) Somma-Vesuvius. Quad. Ric. Sci. C.N.R., Rome, **114,** 8: pp 105-174.

Kairo S., Suttner L. J. And Dutta P. K. (1993). Variability in sandstone composition as a function of depositional environment in coarse-grained delta system. . In Johnsson M. J. and Basu A., eds., Processes Controlling the Composition of Clastic Sediments. Geol. Soc. Am. Spec. Paper **284**, 263-282.

Keller J. (1980). The island of Vulcano. Rend. Soc. Italian. Mineral. 35 Petrol., **36**, 369–414.

Keller J. (1982). Mediterranean island arcs. In Andesites (ed. R. S. Thorpe), pp. 307–25 Chichester: Wiley & Sons.

Kelley J. C. and Whetten J. T. (1969). Quantitative statistical analyses of Columbia River sediment samples. Jour. Sed Petrology, **39**, 1167-1173.

King G. M. (2003). Contributions of Atmospheric CO and hydrogen uptake to microbial dynamics on recent Hawaiian volcanic deposits. Applied and Environmental Microbiology **69**(7), 4067–75.

Komar P. D. and Wang C. (1984). Processes of selective grain transport and the formation of placers in beaches. Journal of Geology **92**, 637–55.

Krynine P. D. (1935). Arkose deposit in the humid tropics. A study of sedimentation in southern New Mexico. Am. Jour. Science, **29**, 353-363.

Krynine P. D. (1950). Petrology, stratigraphy and origin of thr Triassic rocks of Connecticut. Connect. Geol. Surv. Bull., **73**, 239 pp.

Kuenen P. H. (1959). Experimental abrasion 3. Fluviatile action on sand. Am. Jour. Science, **257**, 172-190.

Kuenen P. H. (1960). Experimental abrasion 4. Eolian action. Jour. Geology, **68**, 427-449.

Kuenen P. H. (1964). Experimental abrasion 6. Surf action. Sedimentologu, **3**, 29-43.

Le Maitre R. W. and 11 others (editors). (1989). A classification of igneous rocks and glossary of terms. Recommendations of the International Union of Geological Sciences Subcommission on the Systematics of Igneous Rocks. (Oxford, UK: Blackwell Scientific Publications.).

Le Pera E., Arribas J., Critelli S. and Tortosa A. (2001). The effects of source rocks and chemical weathering on the petrogenesis of siliciclastic sand from the Neto River (Calabria, Italy): implications for provenance studies. Sedimentology **48**, 357–78.

Le Pera E. and Morrone C. (2017). Heavy minerals distribution and provenance in modern beach sands of Campania, Italy. Rendiconti Online della Società Geologica Italiana. *In press.*

Leterrier J., Maury C. R., Thonon P., Marchal R. (1982). Clinopyroxene composition as a method of identification of the magmatic affinities of paleo-volcanic series. Earth and Planetary Science Letters **59**(1):139-154 DOI10.1016/0012-821X(82)90122-4.

Locardi E., Nicholich R. (1988). Geodinamica del Tirreno e dell'Appennino centromeridionale: la nuova carta della Moho. Mem Soc. Geol. It. **41**, 121-140.

Lucchi F. R. and Valmori E. (1980). Basin-wide turbidites in a Miocene, over-supplied deep-sea plain: a geometrical analysis. Sedimentology, **27**, 241-270.

Lucchi F., Tranne C.A., Calanchi N., Rossi P.L., (2004). Late Quaternary fossil shorelines in the Aeolian Islands (Southern Tyrrhenian Sea): evaluation of long-term vertical displacements. In: Antonioli, F., Monaco, C. (Eds.), Contribution from the study of ancient shorelines to understanding the recent vertical motions. Field trip across the Messina Straits. Meeting Proceedings. Quaternaria Nova, vol. **VIII**, pp. 115–137.

Lucchi F., Tranne C. A., and Rossi P. L. (2010). Stratigraphic approach to geological mapping of the late Quaternary volcanic island of Lipari (Aeolian archipelago, southern Italy). In Stratigraphy and Geology of Volcanic Areas (eds G. Groppelli & L. Viereck-Goette), pp. 1–32. Geological Society of America Special Paper **464**.

Lucchi F., Peccerillo A., Keller J., Tranne C. A. and Rossi P. L. (2013). The Aeolian Islands Volcanoes. *Geological Society, London, Memoirs*, **37**.

Lucchi R.G., Camerlenghi A., Rebesco M., Colmenero-Hidalgo E., Sierro F.J., Sagnotti L., Urgeles R., Melis R., Morigi C.,. Bárcena M.-A, Giorgetti G., Villa G., Persico D.,. Flores J.-A, Rigual-

Hernández A.S., Pedrosa M.T., Macri P., Caburlotto A. (2013). Postglacial sedimentary processes on the Storfjorden and Kveithola trough mouth fans: Significance of extreme glacimarine sedimentation, In Global and Planetary Change, **111**, Pages 309-326.

Mann W. R. and Cavaroc V. V. (1973). Composition of sands released of three source areas under humid, low-relief weathering in North Carolina piedmont. Jour. Sed. Petrology, **43**, 870-881.

Marsaglia K. M. (1992). Petrography and provenance of volcaniclastic sands recovered from the Izu-Bonin Arc, Leg 126. Proceedings of the Ocean Drilling Program, Scientific Results, **126**, 139–54.

Marsaglia K.M. (1993). Basaltic island sand provenance. In Processes Controlling the Composition of Clastic Sediments (eds M. J. Johnsson and A. Basu), pp. 41–65. Geological Society of America Bulletin, Special Paper **284**.

Marsaglia K. M. and Ingersoll R. V. (1992). A reassessment of magmatic-arc provenance: compositional trends in arc-related, deep-marine sand and sandstone. Geological Society of America Bulletin **104**, 1637–49.

Marsaglia K. M. and Tazaki K. (1992). Diagenetic trend in ODP Leg 126 sandstones. In Proceedings of the Ocean Drilling Program, Scientific Results, vol. **126** (eds B. Taylor, K. Fujioka et al.), pp. 125–38. College Station, TX: Ocean Drilling Program.

Marsaglia, K.M., Garcia y Barragán, J.C., Padilla, I., and Milliken, K.L. (1996). Evolution of the Iberian passive margin as reflected in sand provenance: Proceedings of the Ocean Drilling Program, Scientific Results, v. **149**, p. 269-280.

Marsaglia K. M., Latter K.K., Zahn V. C., R., Comas, M.C., and Klaus, A. (Eds.) (1999). Sand Provenance in the Alboran and Tyrrhenian basins. Proceedings of the Ocean Drilling Program, Scientific Results, Vol. **161**, 37.

Mack G. H. (1981). Composition of modern stream sand in a humid climate derived a low-grade metamorphic and sedimentary foreland fold-thrust belt of north Georgia. Jour. Sed. Petrology, **51** , 1247-1258.

Mack G. H. and Jerzykiewicz T. (1989). Detrital modes of sand and sandstone derived from andesitic rocks as paleoclimatic indicator. Sedimentary Geology **65**, 35–44.

Marcelino V., Cnudde V., Vansteelandt S., Carò F. (2007). An evaluation of 2D-image analysis techniques for measuring soil microporosity. European Journal of Soil Science **58**, 133-140.

Maynard J. B., Valloni R. and Yu H. S. (1982). Composition of modern deep-sea arc-related basin. In Leggett J. K. , ed., Trench-forearc geology, Geol. Soc. London Spec. Publ., **10**, 551-560.

McBride E. F. and Picard M. D. (1987) - Downstream changes in sand composition, roundness, and gravel size in a short-headed high-gradient stream, north-western Italy: Journal of Sedimentary Petrography, v. **57**, p. 1018–1026.

McCoy F. W. and Cornell W. (1990). Volcaniclastic sediments in the Tyrrhenian Basin. In Proceedings of the Ocean Drilling Program, Scientific Results, vol. **107** (eds K. A. Kastens, J. Mascle et al.), pp. 291–305. College Station, TX: Ocean Drilling Program.

Miriello D. and Crisci G. M. (2006). Image analysis and flatbed scanners. A visual procedure in order to study the macro-porosity of the archaeological and historical mortars. Journal of Cultural Heritage **7**, 186-192.

Moore G. F. (1979). Petrography of subduction zone sandstone from Nias Island, Indonesia. Jour. Sed. Petrology, **49**, 71-84.

Morrone C., De Rosa R., Le Pera E. and Marsaglia K. M. (2017) - 'Provenance of volcaniclastic beach sand in a magmatic-arc setting: an example from Lipari island (Aeolian archipelago, Tyrrhenian Sea), Geological Magazine, **154**(4) pp. 804–828. doi: 10.1017/S001675681600042X.

Morrone C., De Rosa R., Le Pera E. and Marsaglia K. M. (2018). Beach sands of Lipari island, Aeolian archipelago: roundness study. Rendiconti Online della Società Geologica Italiana. *In press.*

Morton A. C. (1985). Heavy minerals in provenance study. In Provenance of Arenites (ed. G. G. Zuffa). Dordrecht: Reidel Publishing Company, pp. 249–77. NATO-ASI, series **148**.

Nesbitt H. W., Young G. M., McLennan S. M. and Keays R. R. (1996). Effects of Chemical Weathering and Sorting on the Petrogenesis of Siliciclastic Sediments, with Implications for Provenance Studies The Journal of Geology, **104**, 525-542.

Nicolosi I., Speranza F. and Chiappini M. (2006). Ultrafast oceanic spreading of the Marsili basin, southern Tyrrhenian Sea: evidence from magnetic anomaly analysis. *Geology*, **34**, 717–720.

Ogniben L., Parotto M., Praturlon A. (eds) (1975). Structural model of Italy. Quad Ric Sci CNR, Rome, 90:502 pp.

Orsi G., Civetta L., D'Antonio M., Di Girolamo P., Piochi M. (1995). Step-filling and development of a three-layers magma chamber: the Neapolitan Yellow Tuff case history. J. Volcanol. Geotherm. Res. **67**:291-312.

Orsi G., De Vita S. and Di Vito M. (1996). The restless, resurgent Campi Flegrei nested caldera (Italy): constraints on its evolution and configuration. J. Volcanol. Geotherm. Res. **74**:179-214.

Packer B. M. and Ingersoll R. V. (1986). Provenance and petrology of Deep Sea Drilling Project sands and sandstone from the Japan and Mariana forearc and backarc regions. Sedimentary Geology, **51**, 5-28.

Palomares M. and Arribas J. (1993). Modern stream sands from compound crystalline sources: composition and sand generation index. In Processes Controlling the Composition of Clastic Sediments (eds M. J. Johnsson and A. Basu), 313–22. Geological. Society of America, Special Paper **284**.

Panza G. F., Pontevivo A., Giordano Chimera G., Raykova R. and Abdelkrim Aoudia A. (2003). The lithosphere-asthenosphere: Italy and surroundings. Episodes **26** (3):169-174.

Pappalardo L, Civetta L, D'Antonio M, Deino A, Di Vito MA, Orsi G, Carandente A, De Vita S, Isaia R, Piochi M (1999). Chemical and isotopical evolution of the Phlegraean magmatic system before the Campanian Ignimbrite (37 ka) and the Neapolitan Yellow Tuff (12 ka) eruptions. J Volcanol Geotherm Res **91:**141-166.

Pappalardo L. and Mastrolorenzo G. (2012). Rapid differentiation in a sill-like magma reservoir: a case study from the Campi Flegrei caldera. Nature Scientific Reports, 2012.

Patacca E. and Scandone P. (1989). Post-Tortonian mountain building in the Apennines: the role of the passive sinking of a relic lithospheric slab. In The Lithosphere in Italy: Advances in Earth Science Research (eds A. M. Boriani, M. Bonafede, G. B. Piccardo & G. B. Vai), pp. 157–76. Rome: Accademia Nazionale dei Lincei.

Patacca E., Scandone P. (2001). Late thrust propagation and sedimentary response in the thrust-belt-foredeep system of the southern Apennines (Pliocene-Pleistocene). In: Vai GB, Martini PI (eds) Anatomy of an Orogen. The Apennines and adjacent Mediterranean basins. Kluwer, Dordrecht, pp 401-440.

Peccerillo A. (2001). Geochemical similarities between Vesuvius, Phlegraean Fields and Stromboli volcanoes: petrogenetic, geodynamic and volcanological implications. Miner. Petrol. **73**:93-105.

Peccerillo A. (2005). Plio-Quaternary Volcanism in Italy. Petrology, Geochemistry, Geodynamics. *Springer, Heidelberg*.

Peccerillo A, Taylor S.R. (1976). Geochemistry of Eocene calc-alkaline volcanic rocks of the Kastamonu area, northern Turkey. Contrib Mineral Petrol **58**:63-81.

Peccerillo A. and Wu T.W. (1992). Evolution of calc-alkaline magmas in continental arc volcanoes: evidence from Alicudi, Aeolian arc (Southern Tyrrhenian Sea Italy). J. Petrol. **33**, 1295–1315.

Peccerillo A., Dallai L., Frezzotti M. L. and Kempton P. D. (2004). Sr–Nd–Pb–O isotopic evidence for decreasing crustal contamination with ongoing magma evolution at Alicudi volcano (Aeolian arc, Italy): implications for style of magma-crust in Peccerillo A., De Astis G., Faraone D., Forni F. and Frezzotti M. L. (2013). Compositional variations of magmas in the Aeolian arc: implications for petrogenesis and geodynamics. Geological Society, London, Memoirs. doi: 10.1144/M37.15. Geological Society, London, Memoirs 2013, v.**37**; p491-510.

Peltier L. C., (1950). The geographic cycle in periglacial regions as it is related to climatic geomorphology. Annals of the Association of American Geographers, v. **40**, no. 3, p. 214-236.

Picard M. D. and M$_C$Bride E. F. (1993). Beach sands of Elba Island, Tuscany, Italy: roundness study and evidence of provenance. In Processes Controlling the Composition of Clastic Sediments (eds M. J. Johnsson and A. Basu), pp. 235–45. Geological Society of America, Special Paper **284**.

Pirrie D. (1991). Controls on the petrographic evolution of an active margin sedimentary sequence: the Larsen Basin, Antarctica. In Morton A. C., Todd S. P. and Haughton P. D. W. (eds), Developments in sedimentary provenance studies, Geol. Soc. London Spec. Publ., **57**, 231-249.

Piromallo C., Morelli A. (2003). P wave tomography of the mantle under the Alpine-Mediterranean area. J. Geophys. Res., **108**, B2, 2065, doi: 10.1029/ 2002JB001757.

Pittman E. D. (1969). Destruction of plagioclase twins by stream transport. Journal of Sedimentary Petrology **39**, 1432–7.

Pittman E. D. (1970). Plagioclase feldspar as an indicator of provenance in sedimentary rock. Journal of Sedimentary Petrology **40**, 591–8.

Pollak J. M. (1961). Significance of compositional and textural properties of South Canadian River channel sands, New Mexico, Texas, and Oklahoma. Jour. Sed. Petrology, **31**, 15-37.

Potter P. E. (1978a). Petrology and chemistry of modern big river sand. Jour. Geology, **86**, 423-449.

Powers, M. C. (1953). A new roundness scale for sedimentary particles. J. Sediment. Petrol. **23**, 117–119.

Protz R. and VandenBygaart, A. J. (1998). Towards systematic image analysis in the study of soil micromorphology. Sciences of Soils **3**, 34-44.

QGIS Development Team, (2014). QGIS Geographic Information System. Open Source Geospatial Foundation. URL http://qgis.osgeo.org.

Ramalho R.S., Helffrich, G., Cosca, M., Vance, D., Hoffmann, D., Schmidt, D.N., 2010. Episodic swell growth inferred from variable uplift of the Cape Verde hotspot islands. Nat. Geosci. **3** (11), 774–777.

Ramalho S. R., Quartau R., Trenhaile S. A., Mitchell C. N., Woodroffe D. C. and Ávila P. S. (2013). Coastal evolution on volcanic oceanic islands: a complex interplay between volcanism, erosion, sedimentation, sea-level change and biogenic production. Earth-Science Reviews **127**, 140–70.

Rasband W.S., ImageJ, U. S. National Institutes of Health, Bethesda, Maryland, USA, https://imagej.nih.gov/ij/, 1997-2016.

Rolandi G., Petrosino P., Mc Geehin J. (1998). The interplinian activity at Somma-Vesuvius in the last 3500 years. J. Volcanol. Geotherm. Res. **82**:19-52.

Rosi M., Sbrana A. (eds.) (1987). The Phlegraean Fields. Quad. Ric. Sci. C.N.R. Rome, **114**, 10:175 pp.

Russell R. D. (1937). Mineral composition of Mississipi River sands. Geol. Soc. Am. Bull., **48**, 1307-1348.

Santacorce R .(ed) (1987). Somma-Vesuvius. Quad. Ric. Sci. C.N.R., Rome, **114**, 8: 249 pp.

Santacroce R., Cristofolini R., La Volpe L., Orsi G. and Rosi M. (2003). Italian active volcanoes. Episodes **26**:227-234.

Scandone R., Bellucci F., Lirer L., and Rolandi, G. (1991). The structure of the Campanian Plain and the activity of the Neapolitan volcanoes (Italy). J. Volcanol. Geother. Res. **48**, 1–31. doi: 10.1016/0377-0273(91)90030-4.

Scarciglia F., Le Pera E., Vecchio G. and Critelli S. (2005). The interplay of geomorphic processes and soil development in an upland environment, Calabria, South Italy. Geomorphology **69** (1-4):169-190 DOI10.1016/j.geomorph.2005.01.003.

Scarciglia F., Saporito N., La Russa M. F., Le Pera E., Macchione M., Puntillo D., Crisci G. M. and Pezzino A. (2012). Role of lichens in weathering of granodiorite in the Sila uplands (Calabria, southern Italy). Sedimentary Geology **280**, 119–34.

Schmid R. (1981). Descriptive nomenclature and classification of pyroclastic deposits and fragments: Recommendations of the IUGS Subcommission on the Systematics of Igneous Rocks. Geology, Vol. **9**, 41–43.

Schmincke H.-U. (1981). Ash from vitric muds in deep sea cores from the Mariana Trough and fore-arc region (South Philippine Sea) (Sites 453, 454, 455, 458, 459 and SP), Deep Sea Drilling Project, Leg 60. In Initial Reports of the Deep Sea Drilling Project, **60** (eds D. M. Hussong & S. Uyeda), pp. 473–81. Washington DC: US Government Printing Office.

Schneider C.A., Rasband W.S., Eliceiri K.W. (2012). "NIH Image to ImageJ: 25 years of image analysis". Nature Methods **9**, 671-675.

Schwab F. L. (1975). Framework mineralogy and chemical composition of continental margin-type sandstone. Geology, **3**, 487-490.

Serri G. (1990). Neogene-Quaternary magmatism of the Tyrrhenian region: characterization of the magma sources and geodynamic implications. Mem Geol Soc It **41**, 219-242

Shukis P. S. and Ethridge F. G. (1975). A petrographic reconnaissance of sand-size sediment upper St. Francis River, southeastern Missouri. Jour. Sed. Petrology, **45**, 115-127.

Signorelli S., Vaggelli G., Romano C. (1999). Pre-eruptive volatile (H_2O, F, Cl and S) contents of phonolitic magmas feeding the 3550-year old Avellino eruption from Vesuvius, southern Italy. J. Volcanol. Geotherm. Res **93**:237-256.

Stallard R. F. (1985). River chemistry, geology, geomorphology, and soils in the Amazon and Orinoco basins. In Drever J. I., ed., The Chemistry of Weathering, Dordrecht, D. Reidel, 293-316.

Stallard R. F. (1988). Weathering and erosion in the humid tropics. In Lerman A. and Meybeck M., eds., Physical and Chemical weathering in Geochemical Cycles, Dordrecht, Kluwer, 295-246.

Stallard R. F. and Edmond J. M. (1983). Geochemistry of the Amazon 2. The influence of geology and weathering on the dissolved load. Jour. Geophys. Res., **88**, 9671-9688.

Stallard R. F. and Edmond J. M. (1987). Geochemistry of the Amazon 3. Weathering chemistry and limits to dissolved input. Jour. Geophys. Res., **92**, 8293-8302.

Stallard R. F., Koehnken L. and Johnsson M. J. (1991). Weathering processes and the composition of inorganic material transported through the Orinoco River system Venezuela and Colombia. Geoderma, **51**, 133-165.

Suttner L. J., Basu A. and Mack G. H. (1981). Climate and origin of quartz arenites. Jour. Sed. Petrology, **51**, 1235-1246.

Suttner L. J. and Dutta P. K. (1986). Alluvial sandstone composition and paleoclimate I. Framework mineralogy. Jour. Sed. Petrology, **56**, 329-345.

Swindle, T. D., Spudis, P. D., Taylor, G. J., Korotev, R. L., and Nichols, R. H., Jr (1991). Searching for Crisium Basin ejecta - Chemistry and ages of Luna 20 impact melts. IN: Lunar and Planetary Science Conference, 21st, Houston, TX, Mar. 12-16, 1990, Proceedings (A91-42332 17-91). Houston, TX, Lunar and Planetary Institute, 167-181.

Smith G. A. and Lotosky J. E. (1995). What factors control the composition of andesitic sand? Journal of Sedimentary Research A**65**(1), 91–8.

Tentori D., Marsaglia K.M. and Milli S. (2016) - Sand Compositional Changes As A Support For Sequence-Stratigraphic Interpretation: The Middle Upper Pleistocene To Holocene Deposits of the Roman Basin (Rome, Italy). Journal of Sedimentary Research, DOI: 10.2110/jsr.2016.75.

Todd T. W. (1968). Paleoclimatology and the relative stability of feldspar minerals under atmospheric condition. Jour. Sed. Petrology, **38**, 832-844.

Tranne C.A., Lucchi F., Calanchi N., Lanzafame G., Rossi P.L. (2002). "Geological map of the island of Lipari (Aeolian Islands)". L.A.C., Firenze, scale 1:12.500, Istituto Nazionale di Geofisica e Vulcanologia.

Trua T., Serri G., Marani M. P., Rossi P. L., Gamberi F. and Renzulli A. (2004). Mantle domains beneath the southern Tyrrhenian: constraints from recent seafloor sampling and dynamic implications. *Periodico di Mineralogia*, **73**, 53–73.

Trua T., marani M. P., and Gamberi F. (2011). Magmatic evidence for African mantle propagation into the southern Tyrrhenian backarc region. In Beccaluva L., Bianchini G. and Wilson M (eds), Volcanism and Evolution of the African Lithosphere. Geol. Soc. Am. Boulder. Spec. Paper, **478**, 307-331.

Vai G. B., Martini P.I. (eds.) (2001). Anatomy of an Orogen. The Apennines and adjacent Mediterranean basins. Kluwer, Dordrecht, 632 pp.

Valloni R. (1985). Reading provenance from modern marine sands. In Zuffa G. G., ed., Provenance of Arenites: NATO ASI series **148**, Dordrecht, D. Reidel, 309-332.

Valloni R. and Maynard J. B. (1981). Detrital modes of recent deep-sea sands and their relation to tectonic setting: a first approximation. Sedimentology, **28**, 75-83.

Valloni R. and Mezzadri G. (1984). Compositional suites of terrigenous deep-sea sands of the present continental margin. Sedimentology, **31**, 353-364.

van der Plas L. and Tobi A.C. (1965). A chart for judging the reliability of point counting results. Aerican Journal of Science vol. **263**, 1, 87-90.

Velbel M. A. and Saad M. K. (1991). Paleoweathering or diagenesis as the principal modifier of sandstone framework composition? A case study from some Triassic rift-valley redbeds of eastern North America. In Morton A. C., Todd S. P. and Haughton P. D. W. (eds), Developments in sedimentary provenance studies, Geol. Soc. London Spe. Publ., **57**, 91-99.

Ventura G. (2013). Kinematics of the Aeolian volcanism (Southern Tyrrhenian Sea) from geophysical and geological data. In The Aeolian Islands Volcanoes (eds F. Lucchi, A. Peccerillo, J. Keller, C. A. Tranne & P. L. Rossi), pp. 3–11. Geological Society, London, Memoir **37**.

Ventura G., Giuseppe V., Milano G., Pino N.A. (1999): Relationships among crustal structure, volcanism and strike–slip tectonics in the Lipari–Vulcano Volcanic Complex (Aeolian Islands, Southern Tyrrhenian Sea, Italy). Physics of the Earth and Planetary Interior, **116**, 31–52.

Villari L. (1980). The Island of Alicudi. Rend. Soc. Ital. Mineral. Petrol. **36**, 441–466.

Wadell H. (1933). Sphericity and roundness of rock particles. J. Geol. **40**, 443–451.

Washington H. S. (1906). The Roman Comagmatic Region. Carnegie Inst Washington Publ **57**: 199 pp

Whetten J. T., Kelley J. C. and Hanson L. G. (1969). Characteristics of Columbia River sediment and sediment transport. Jour Sed. Petrology, **39**, 1149-1166.

White J. D. L. and Houghton B. F. (2006). Primary volcaniclastic rocks. Geological Society of America Bulletin, **34**(8), 677–80.

Williams J.R. (1975). Sediment-yield prediction with universal equation using runoff energy factor. In: Present and Prospective Technology for Predicting Sediment Yield and Sources. ARS.S-40, US Gov. Print Office, Washington, D.C., 244-252.

Wilson B. M. (1995). Igneous Petrogenesis. A Global Tectonic Approach. Originally published by Chapman & Hall (first edition 1989).

Yerino L. N. and Maynard J. B. (1984). Petrography of modern marine sands from the Peru-Chile Trench and adjacent areas. Sedimentology, **31**, 83-89.

Zou C. Zhang G., Zhu R., Yuan X., Zhao X., Hou L., Wen B., Wu X. (2013). Volcanic Reservoirs in Petroleum Exploration. http://dx.doi.org/10.1016/B978-0-12-397163-0.00001-4. ISBN: 978-0-12-397163-0. © 2013 Petroleum Industry Press. Published by Elsevier Inc. All rights reserved.

Zuffa G. G. (1985). Optical analyses of arenites: influence of methodology on compositional results. In (ed. G. G. Zuffa), Provenance of Arenites: Dordrecht, Netherlands, D. Reidel, NATO Advanced Study Institute Series, v. **148**, pp. 165–89.

Zuffa G. G. (1987). Unravelling hinterland and offshore paleogeography from deep-water arenites. In, pp. 39–61. Deep-Marine Clastic Sedimentology: Concepts and Case Studies (eds J. K. Leggett and G. G. Zuffa). London: Graham and Trotman.

-Petrographic PLATES-

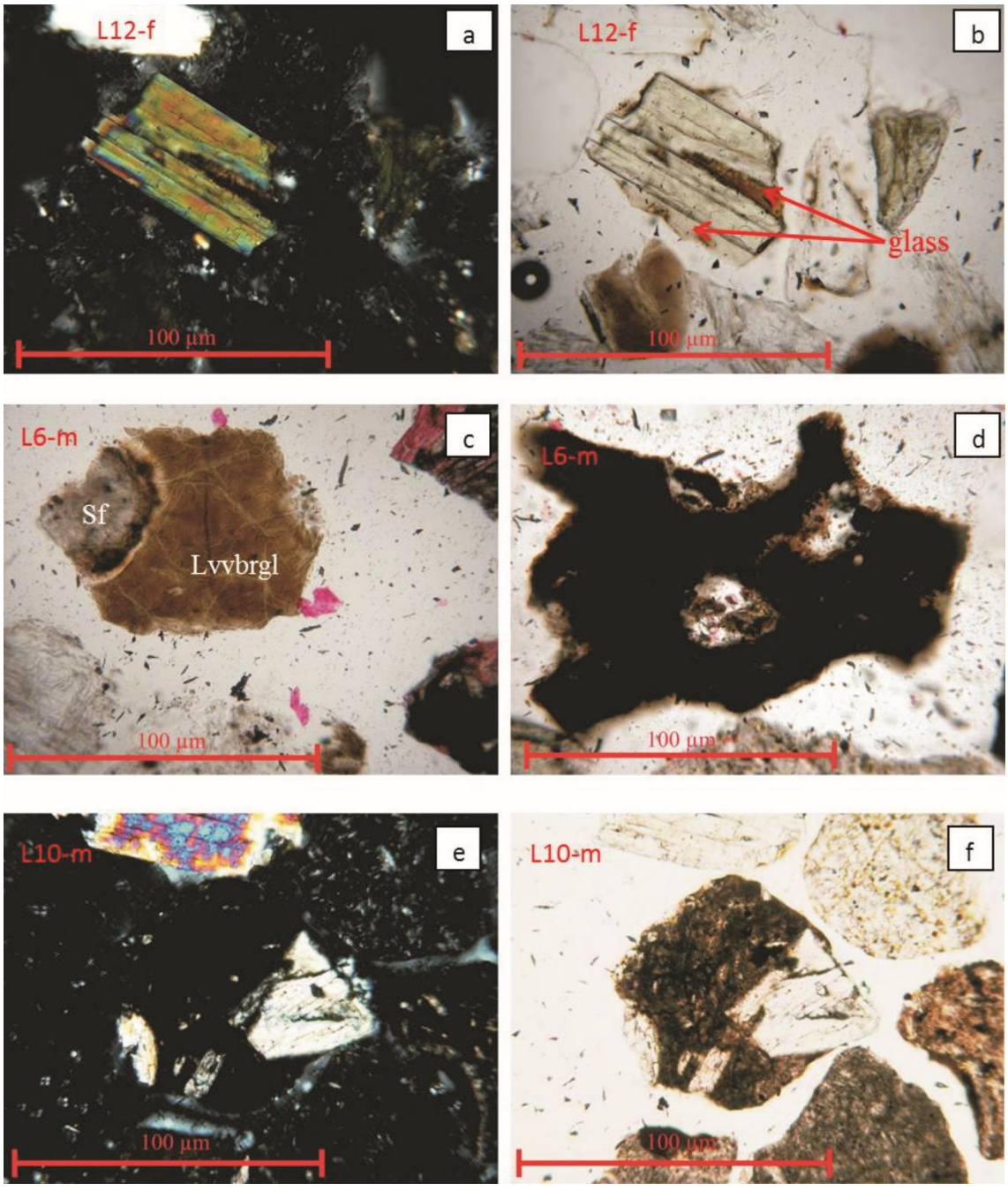

PLATE I - Euhedral monocrystalline clinopyroxene with glassy rim and intracrystalline glass; (a) NX; (b) N//. (c) Lvvbrgl: Vitric volcanic lithic with brown glass; Sf: Devitrification with spherulitic texture (N//). (d) Vesiculated vitric lithic with black glass (Lvvblgl, N//). (e,f) Volcanic lithic with lathwork texture with brown glass (Lvlbrgl). Clearly visible are some phenocrysts of plagioclase (e: NX, f: N//), (modified from Morrone et al., 2017).

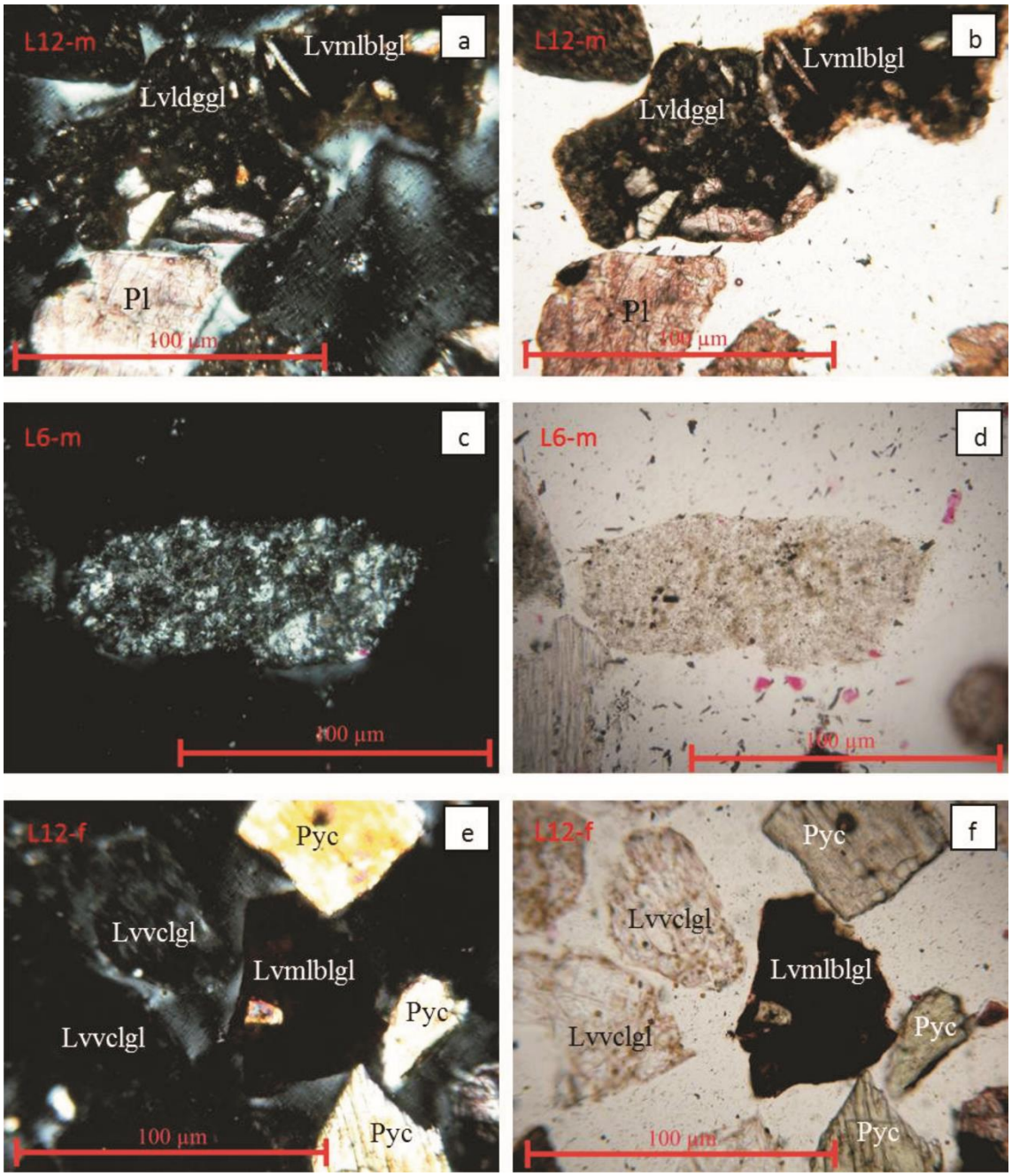

PLATE II - (a,b) Pl: grain of monocrystalline plagioclase; Lvldggl: volcanic lithic fragment with lathwork texture and dark gray glass; Lvmlblgl: volcanic lithic fragment with microlitic texture and black glass (a: NX, b: N//). (c,d) Volcanic lithic fragment with felsitic texture (*Lvf*, c: NX, d: N//). (e,f) Lvmlblgl: volcanic lithic fragment with microlitic texture with black glass; Pyc: angular monocrystalline clinopyroxene grains; Lvvclgl: vitric volcanic lithic colourless glass (e: NX, f: N//), (modified from Morrone et al., 2017).

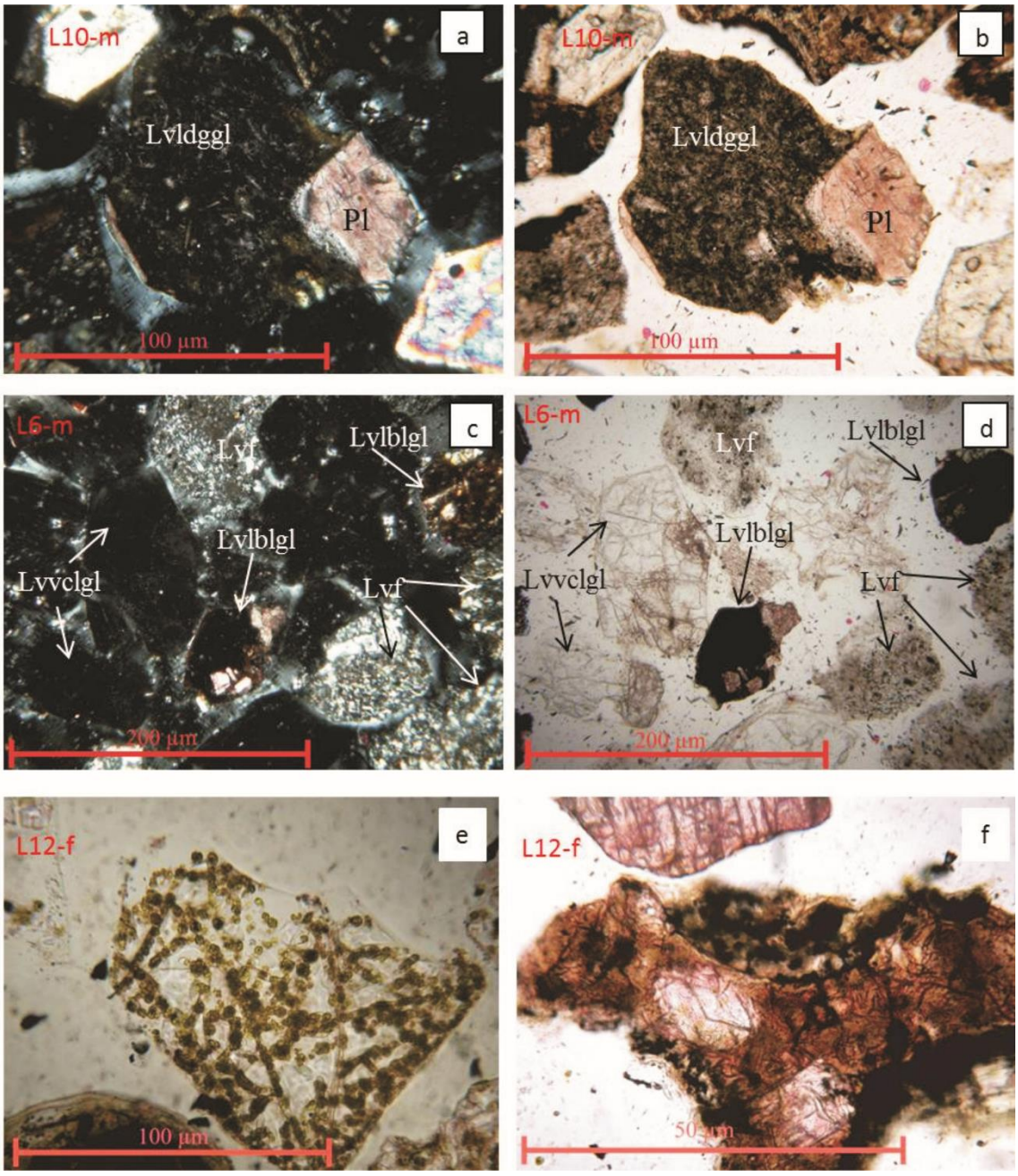

PLATE III - (a,b) Lvldggl: volcanic lithic fragment with lathwork texture with dark grey glass; Pl: plagioclase; (a: NX, b: N//). (c,d) Lvvclgl: vitric volcanic lithic with colourless glass; Lvf: volcanic lithic fragment with felsitic texture; Lvlblgl: volcanic lithic fragment with lathwork texture with black glass (c: NX, d: N//). (e) Potassic fragment of a vitric volcanic lithic colourless glass (*Lvvclgl*) stained with sodium cobaltinitrite (N//). (f) Volcanic lithic fragment with microlitic texture with orange glass (*Lvmlorgl,* N//), (modified from Morrone et al., 2017).

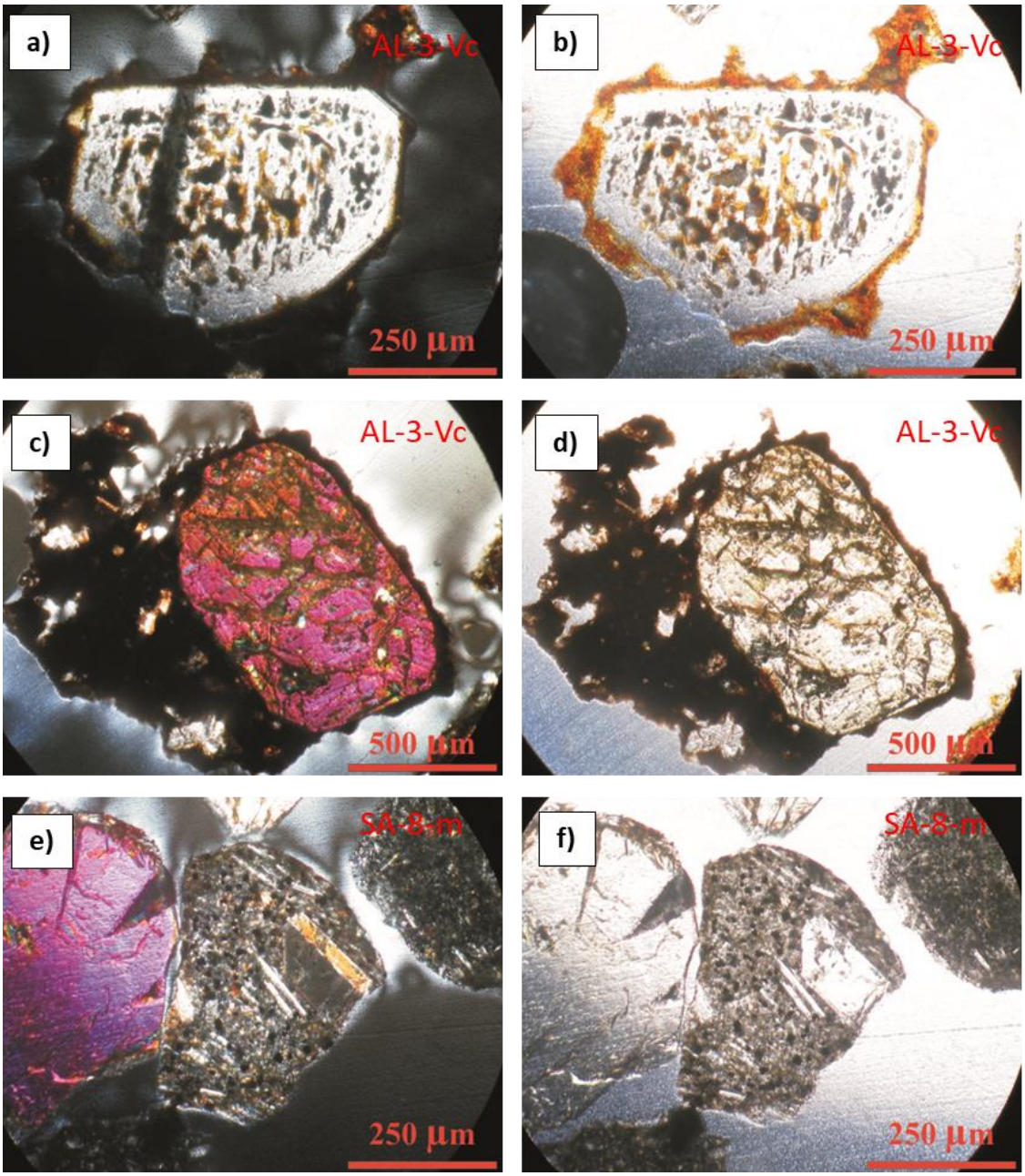

PLATE IV - (a, b): Plagioclase with inter- and intra-crystalline orange glass (*Lvlorgl*, roundness category = 1, a: NX, b: N//); (c, d): euhedral olivine in *Lvlblgl* with roundness category = 2 (c: NX, d: N//); (e, f): *lathwork* volcanic lithic with grey glass (roundness category = 4, e: NX, f: N//).

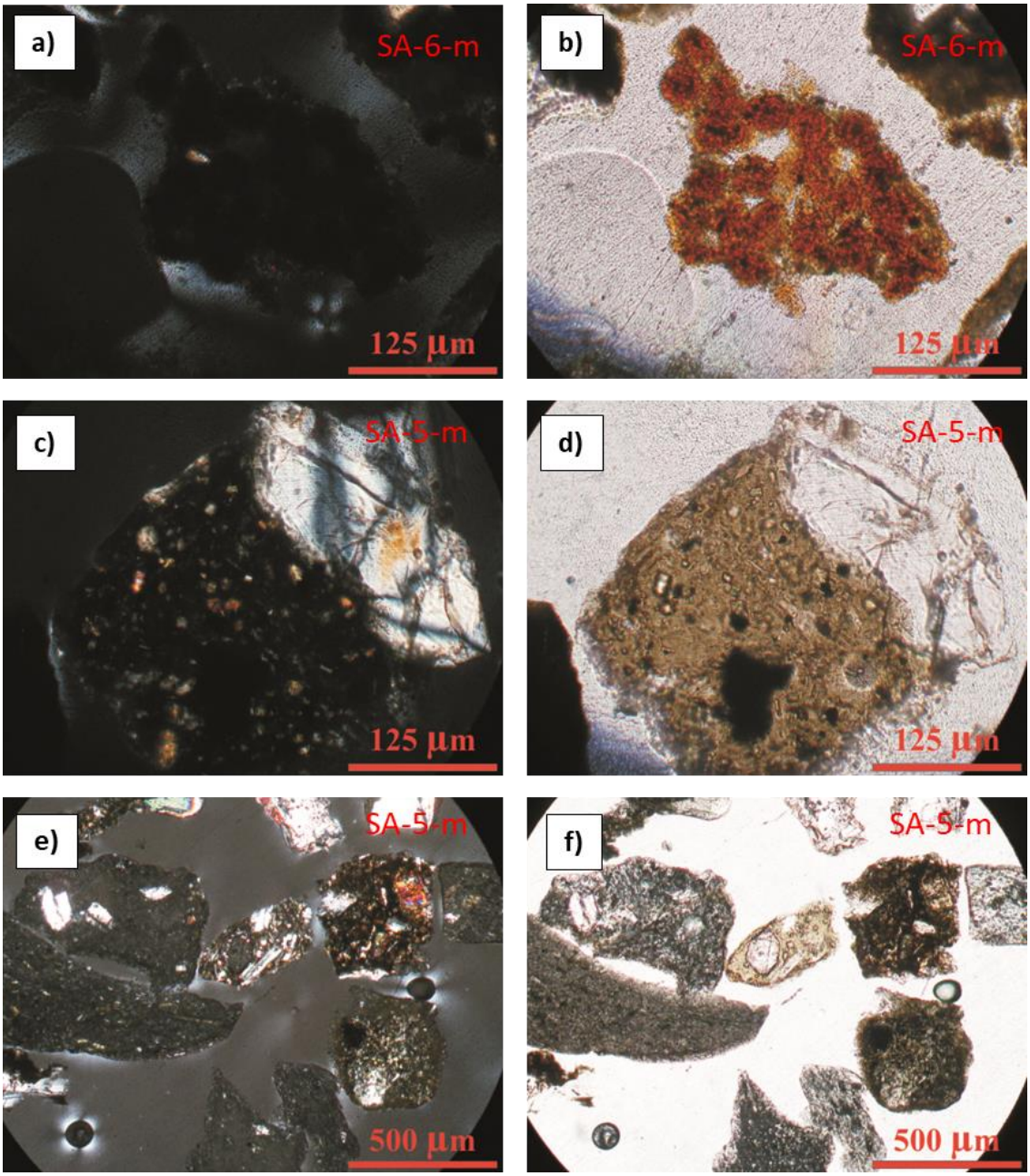

PLATE V - (a, b): *microlitic* volcanic lithic with orange glass (*Lvlorgl*, roundness category = 3, a: NX, b: N//); (c, d): lathwork volcanic lithic with brown glass and plagioclase phenocrysts (*Lvlbrgl* showing an angular (2) roundness category, c: NX, d: N//); (e, f): *lathwork* volcanic lithic with grey (left) and brown (right) glassy groundmass (e: NX, f: N//).

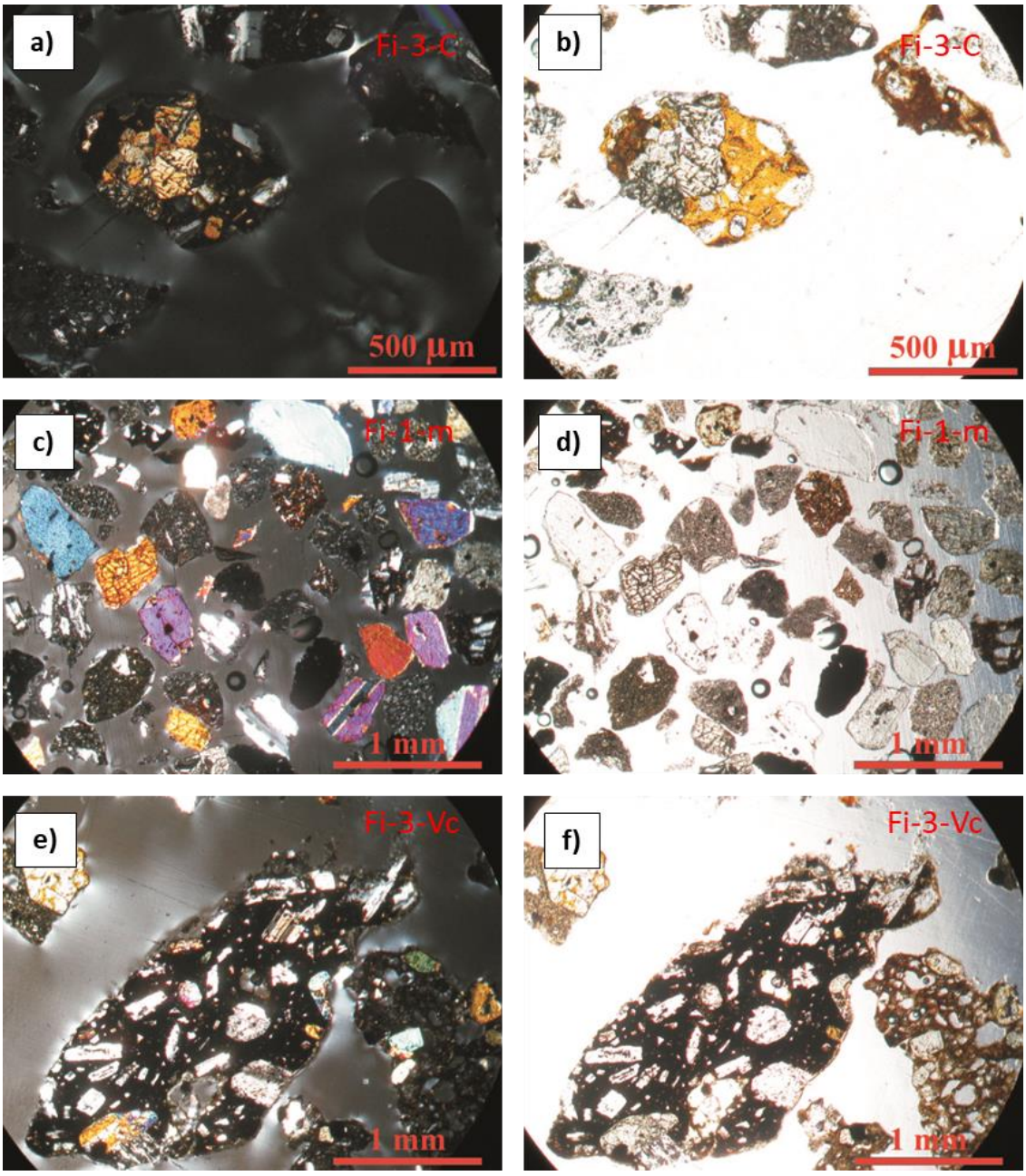

PLATE VI - (a, b): volcanic lithic fragment with lathwork texture with orange glass; and pyroxene phenocrysts Pl: plagioclase; (a: NX, b: N//); (c, d): panoramic view of a Filicudi sand sample showing lithic fragments with *lathwork* texture, plagioclase and pyroxene phenocrysts (c: NX, d: N//); (e, f): volcanic lithic fragment with *lathwork* texture with black (left) and brown (right) glassy groundmass (e: NX, f: N//).

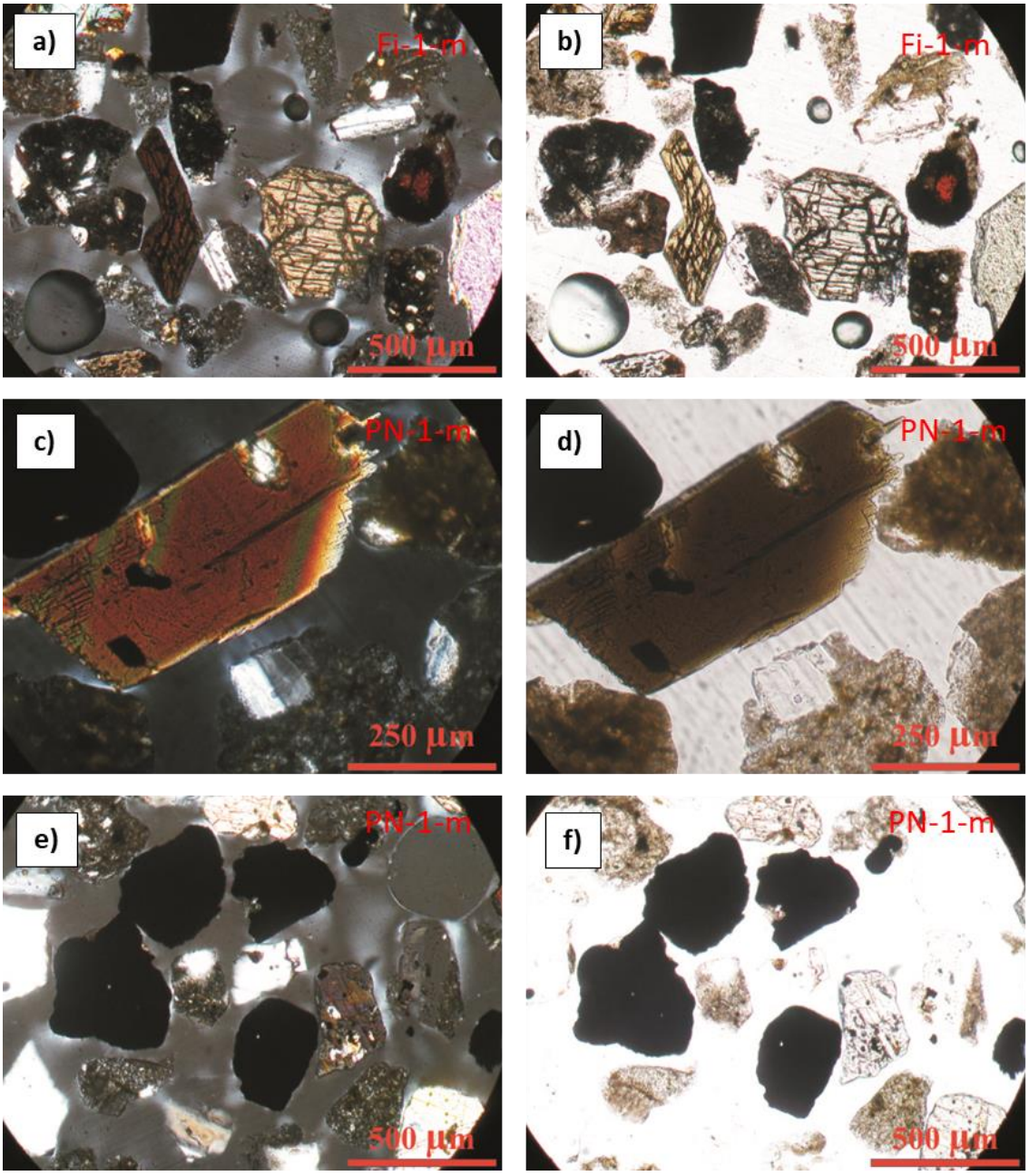

PLATE VII - (a, b): hornblende [001] and pyroxene single crystal grains; iddignsite in a glassy groundmass (right) (a: NX, b: N//); (c, d): very angular (1) biotite [010] single crystal grain (c: NX, d: N//); (e, f): plagioclase and pyroxene single crystal grains; sub-angular (3) to sub-rounded (4) oxides opaque minerals (e: NX, f: N//).

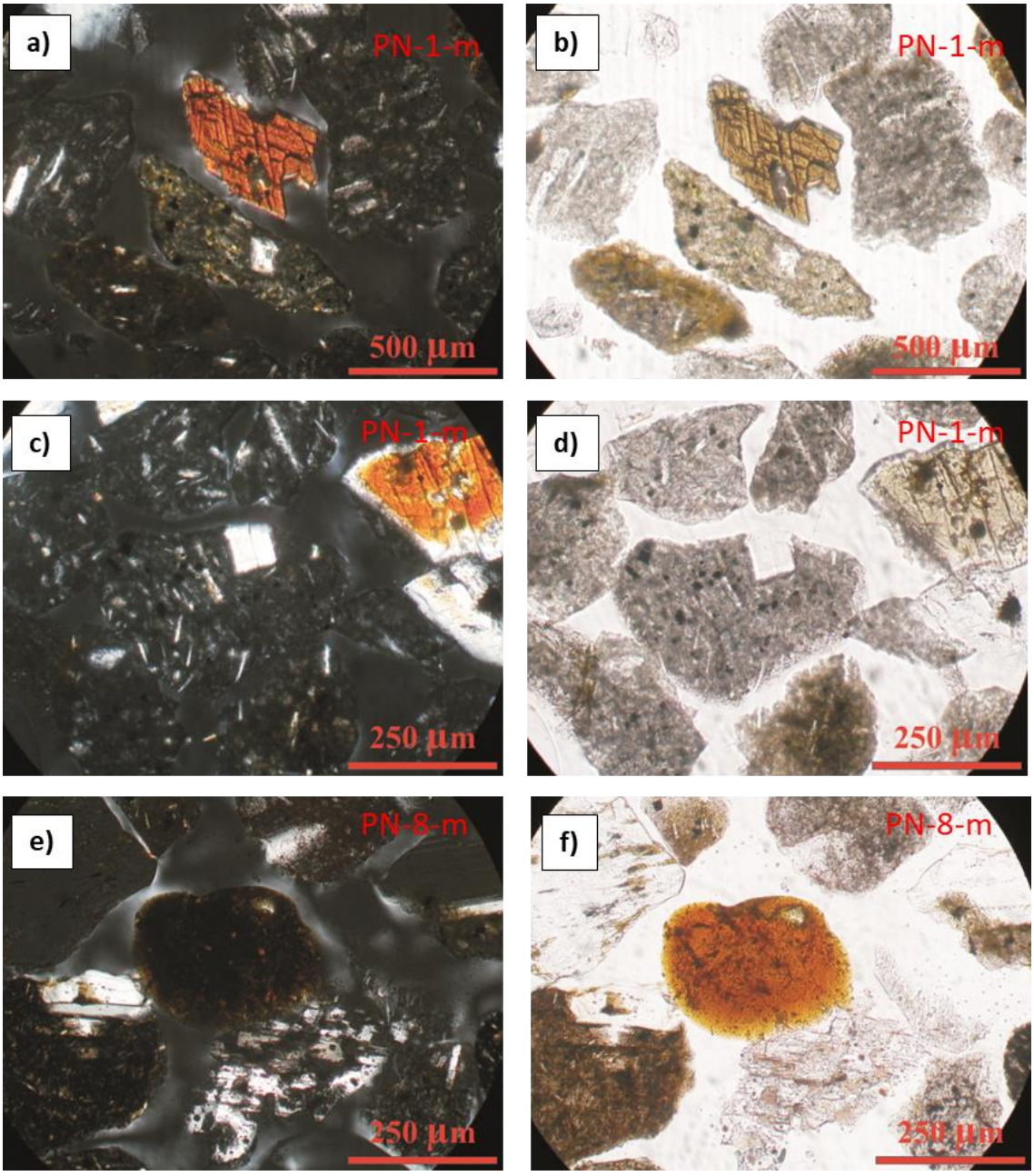

PLATE VIII - (a, b) [001] hornblende with angular roundness category (2) and volcanic lithic fragment with lathwork texture immersed in a grey groundmass *Lvlgrgl* (a: NX, b: N//); (c, d): sub-angular (3) pyroxene single crystal grain (right) and volcanic lithic fragments with *lathwork (grey)* and *microlitic* (brown) textures (c: NX, d: N//); (e, f): volcanic lithic with microlites immersed in an orange groundmass (middle) and lathwork volcanic lithic with brown glass and plagioclase phenocryst (lower left) (e: NX, f: N//).

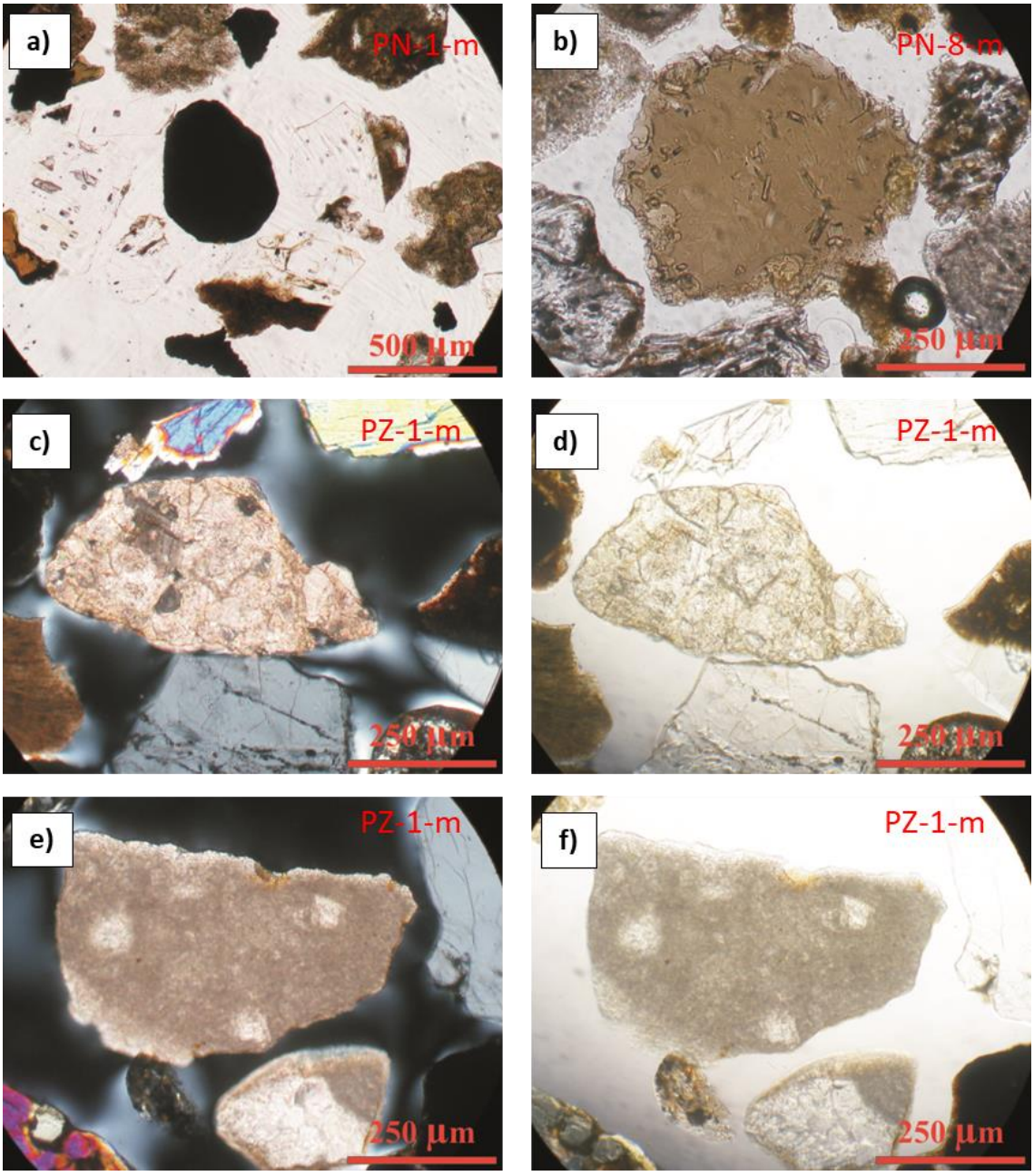

PLATE IX - (a): opaque mineral oxide with a rounded (5) roundness category (N//); (b): microlitic volcanic lithic with brown glass showing a sub-rounded (4) roundness category (N//); (c, d): sparitic limestone [Lsc(xx)] with a sub-rounded (4) roundness category (c: NX, d: N//); (e, f): micritic limestone [Lsc(micr)] showing a sub-angular (3) roundness category (e: NX, f: N//).

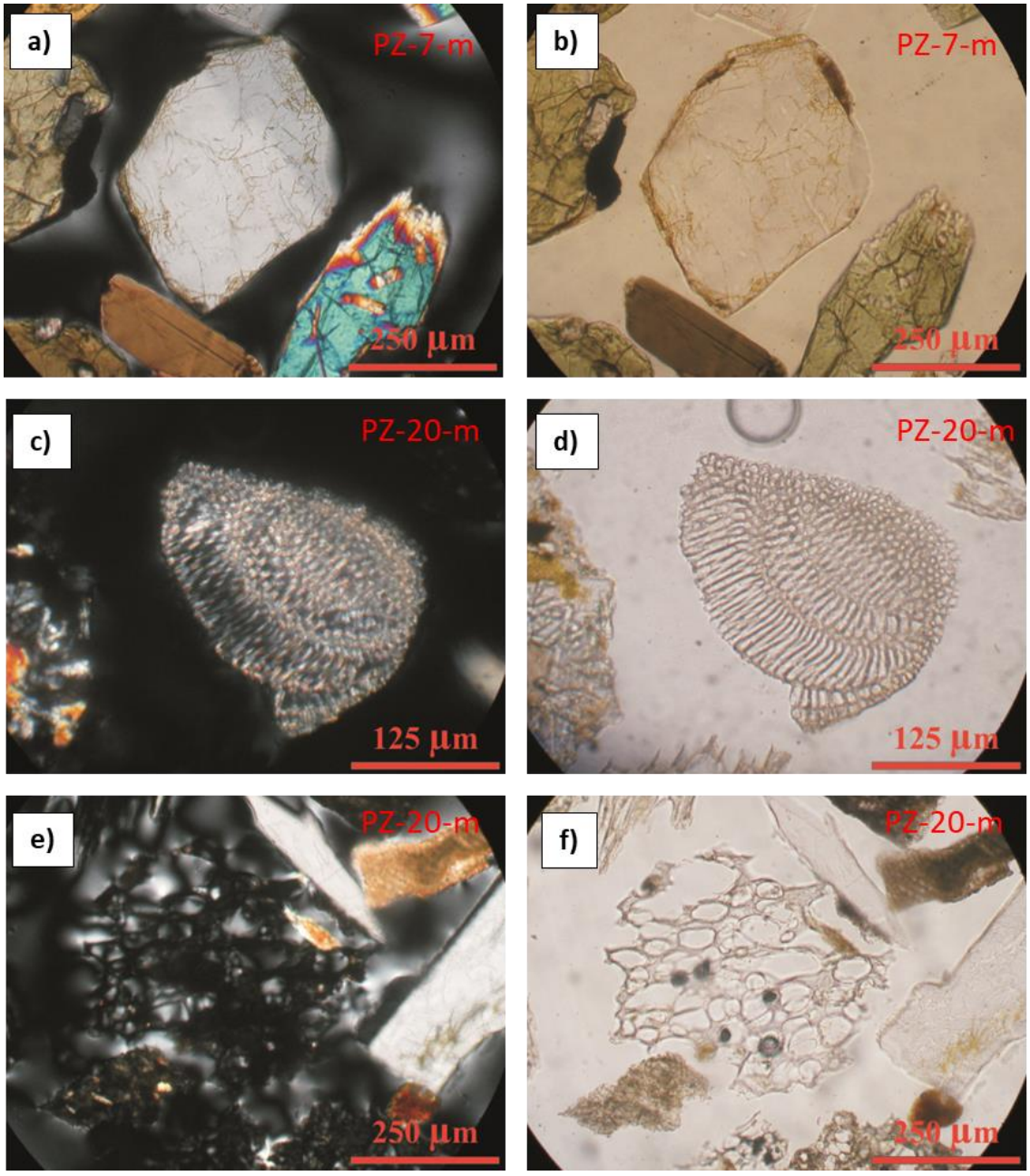

PLATE X - (a, b): Sanidine single crystal grain (stained) which shows a sub-rounded (4) roundness category (a: NX, b: N//); (c, d):calcareous bioclast (c: NX, d: N//); (e, f): very angular (1) well preserved pumice clast (e: NX, f: N//).

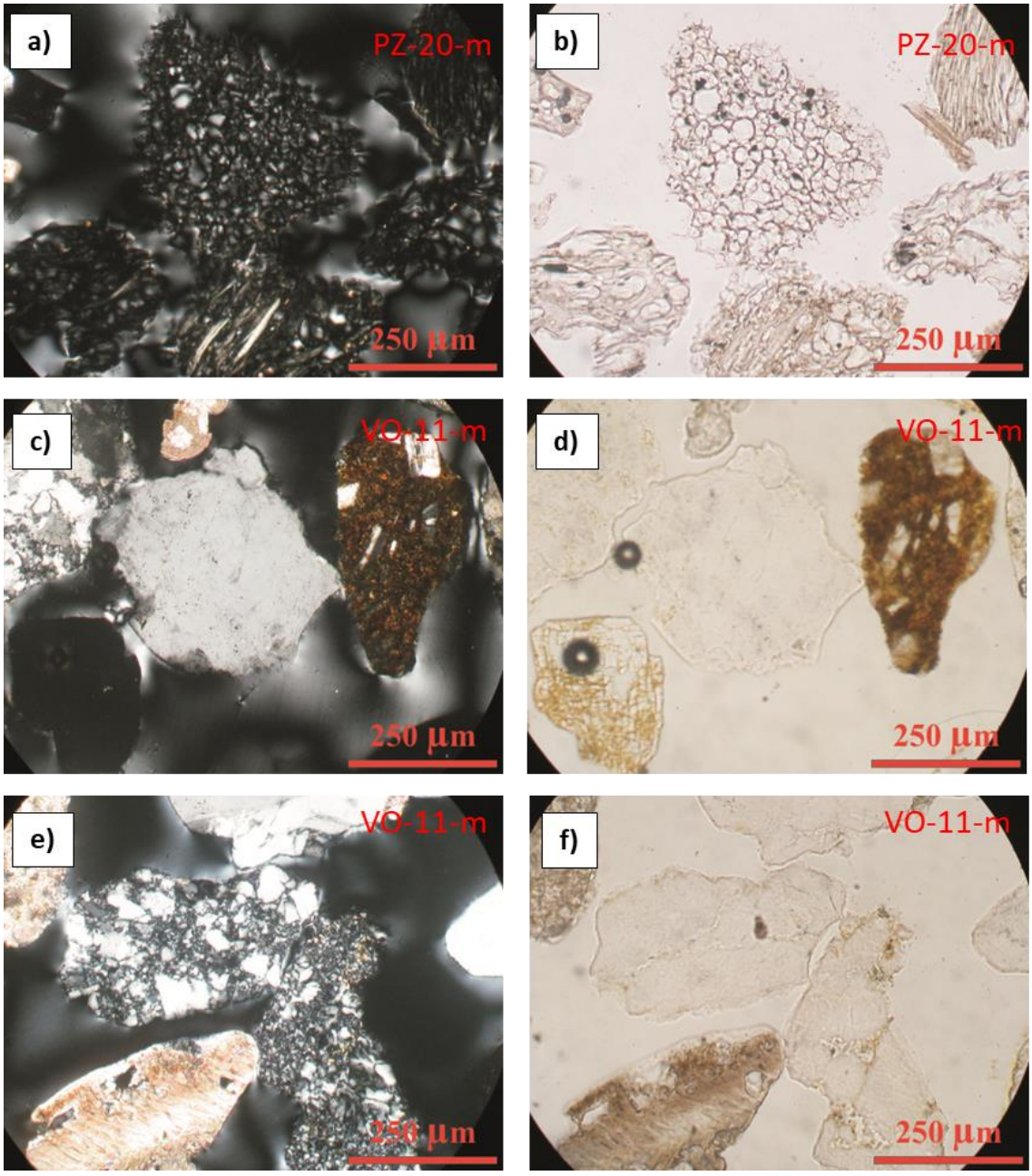

PLATE XI - (a, b): very angular (1) well preserved pumice grains from Torre Fumo like (a: NX, b: N//); (c, d) sub-angular (3) monocrystalline quartz (middle), sanidine single crystal grain (stained, lower left), sub-rounded (4) volcanic lithic with lathwork texture and brown groundmass (right) (c: NX, d: N//); (e, f): polycrystalline quartz and bioclast grains along Volturno-Licola coastal stretch (e: NX, f: N//).

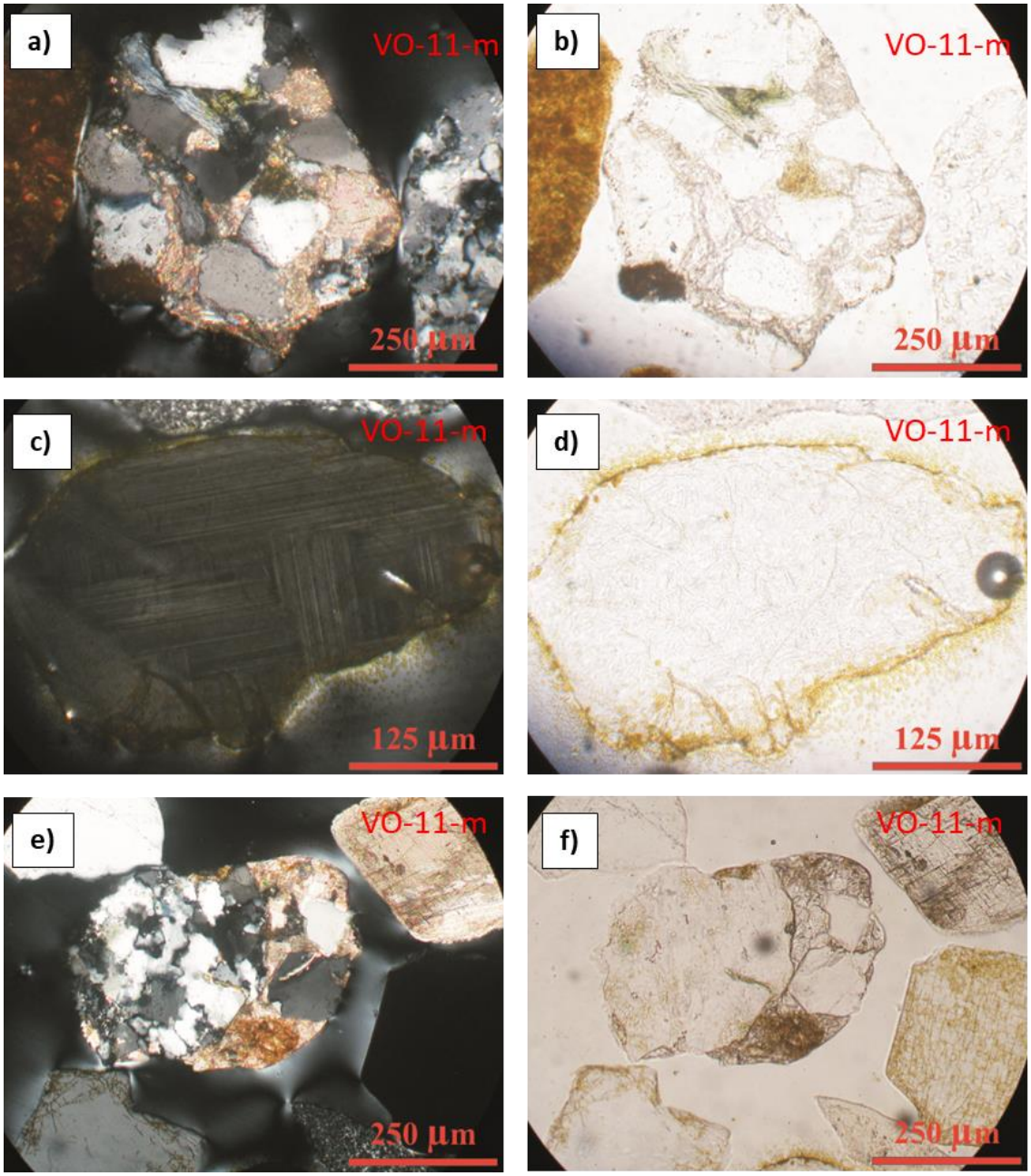

PLATE XII - (a, b): Quartz and calcite in arenite (Rs: sedimentary rock fragments) (Rs (a: NX, b: N//); (c, d): sub-rounded (4) leucite single crystal grain stained with sodium cobaltinitrite (c: NX, d: N//); (e, f): polycrystalline quartz (Qp) and calcite (Ca) in arenite (Rs, fifth roundness category), calcite single crystal grain (upper right) (e: NX, f. N//).

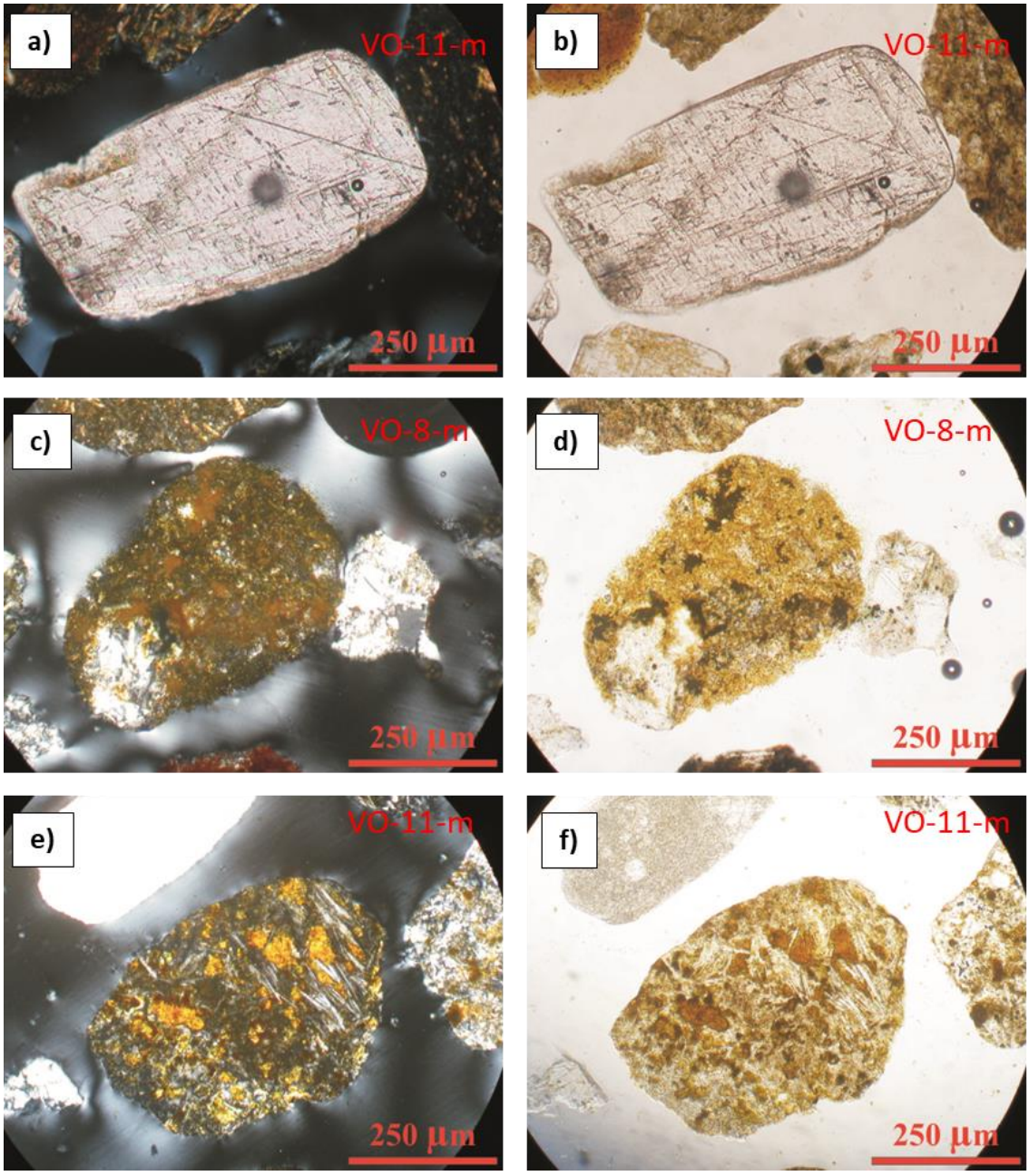

PLATE XIII - (a, b): sub-angular (3) calcite single crystal grain (a: NX, b: N//); (c, d) sub-rounded (4) siliciclastic sedimentary lithic grain (Lss) (c: NX, d: N//); (e, f): altered volcanic lithic fragments (Lv alt) in palagonite and sericite (e: NX, f: N//).

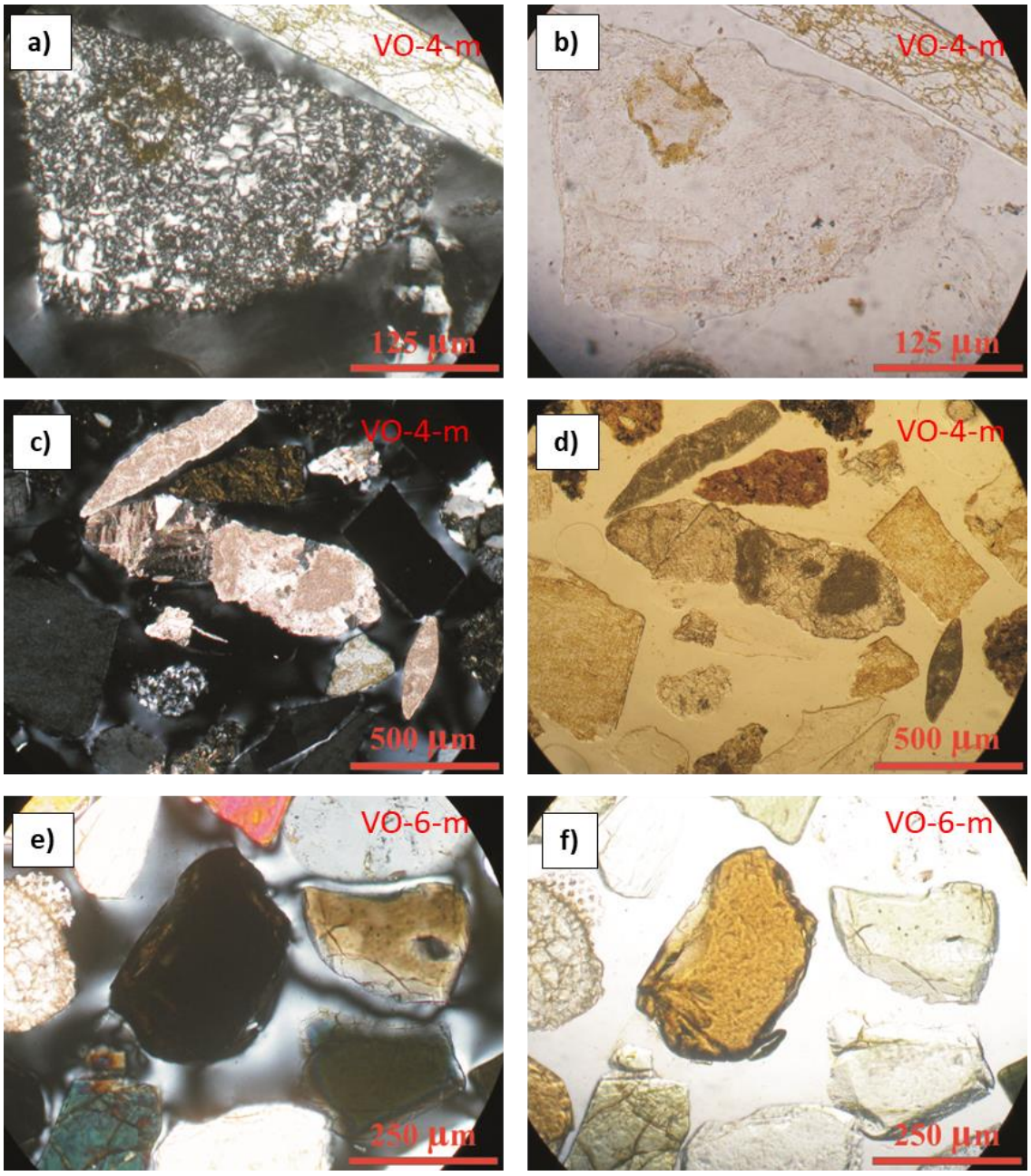

PLATE XIV - (a, b): Chert grain (a: NX, b: N//); (c, d): sedimentary lithic grain with crystalline carbonate composition [Lss(xx)], siliciclastic sedimentary lithic (Lss), sedimentary lithic grain with micritic carbonate composition [Lss(micr)], polycrystalline quartz, angular (2) euhedral sanidine (right) single grain (c: NX, d: N//); (e, f): sub-angular brown garnet single grain (middle) (e: NX, f: N//).

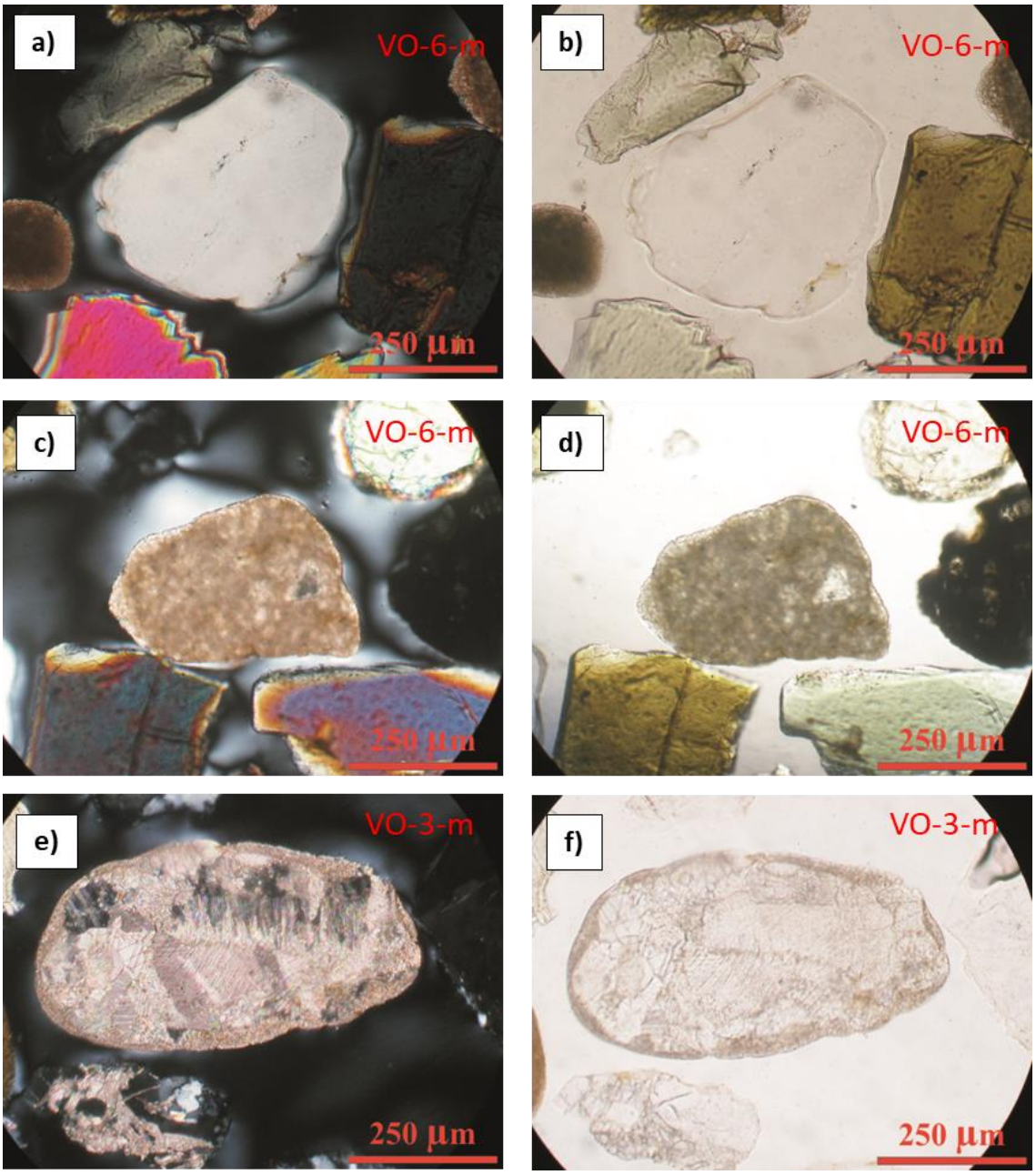

PLATE XV - (a, b): rounded (5) monocrystalline quartz (a: NX, b: N//); (c, d): rounded (5) sedimentary lithic grain with micritic carbonate composition [Lss(micr)] (c: NX, d: N//); (e, f): calcite in a rounded (5) sedimentary rock fragment (Ca in Rs) (e: NX, f: N//).

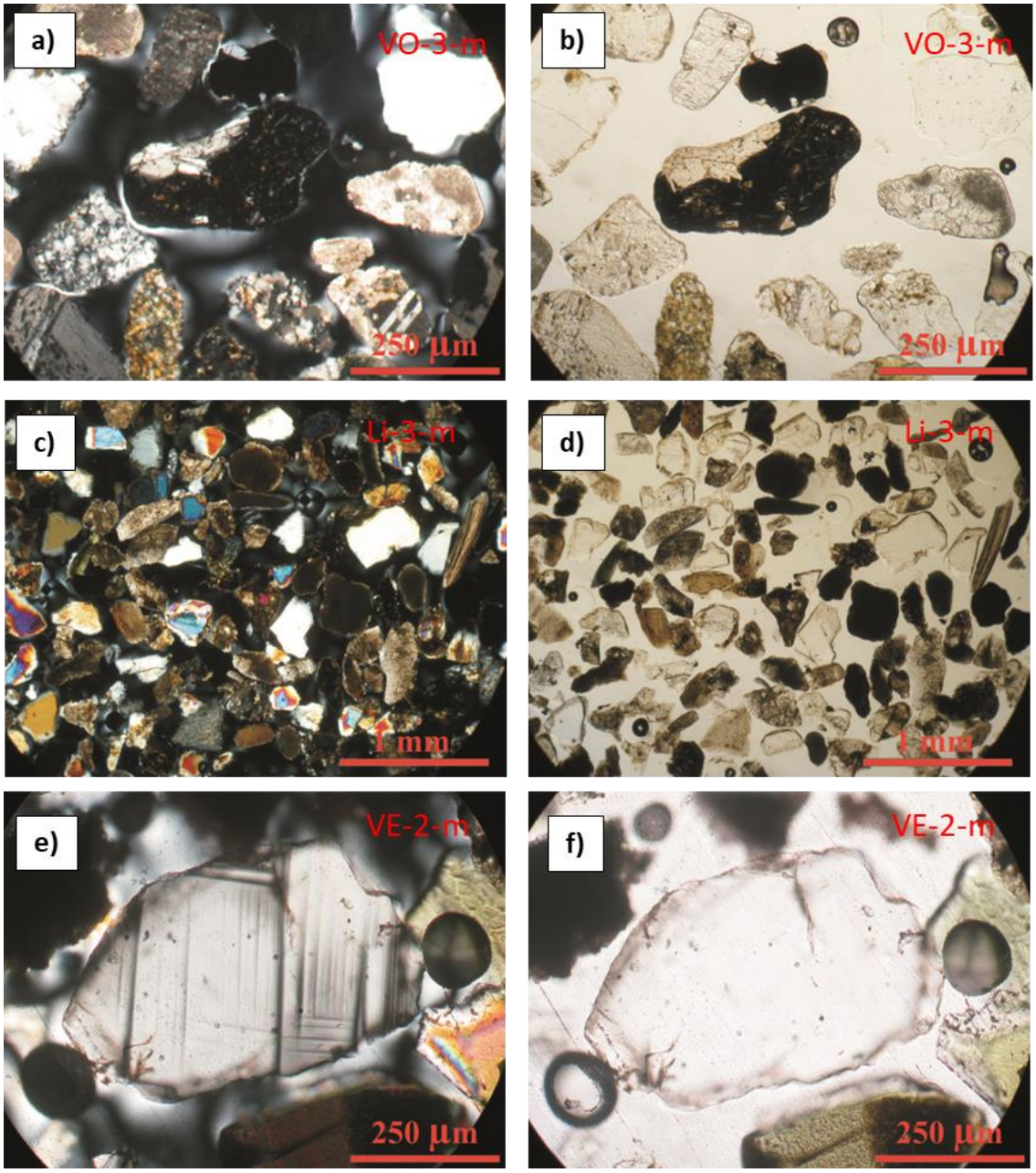

PLATE XVI - (a, b): sub-rounded (4) volcanic lithic fragment with lathwork texture with black glass and plagioclase phenocrysts dispersed among sedimentary grains around Volturno-river mouth (a: NX, b: N//); (c, d): Li-3 sample panoramic view showing an high amount of sedimentary lithic grains (c: NX, d: N//); (e, f): sub-angular leucite single crystal grain in the Vesuvius crater sand (e: NX, f: N//).

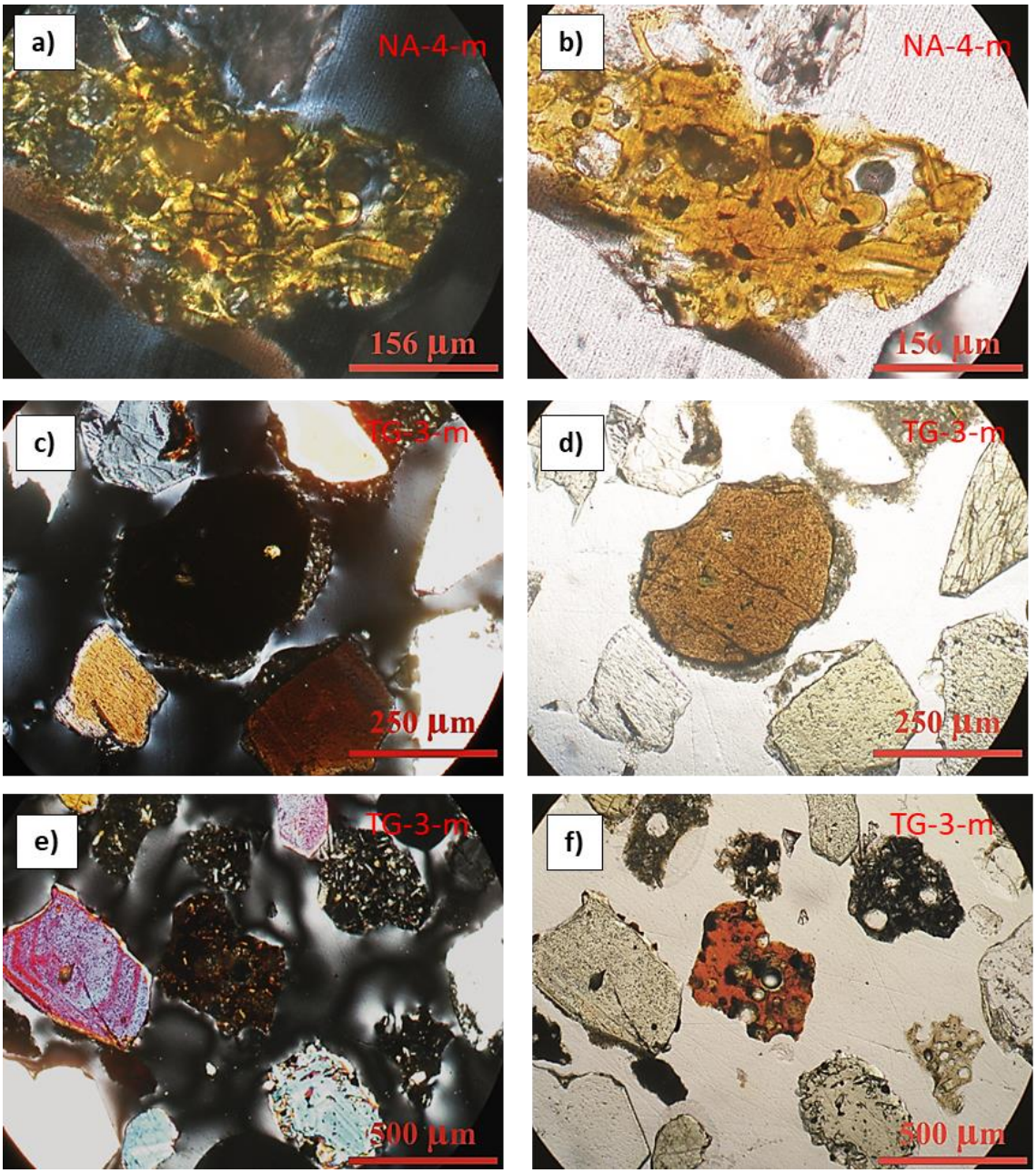

PLATE XVII - (a ,b): Volcanic lithic palagonitization (Lv alt) (a: NX, b: N//); (c, d): brown garnet in volcanic lithic with a brown glassy groundmass (Lvlbrgl) (c: NX, d: N//); (e, f): angular to sub-angular pyroxene single grains and *microlitic* volcanic lithic with orange glass and early plagonitization (middle grain) along Portici-Torre del Greco coastal stretch (e: NX, f: N//).

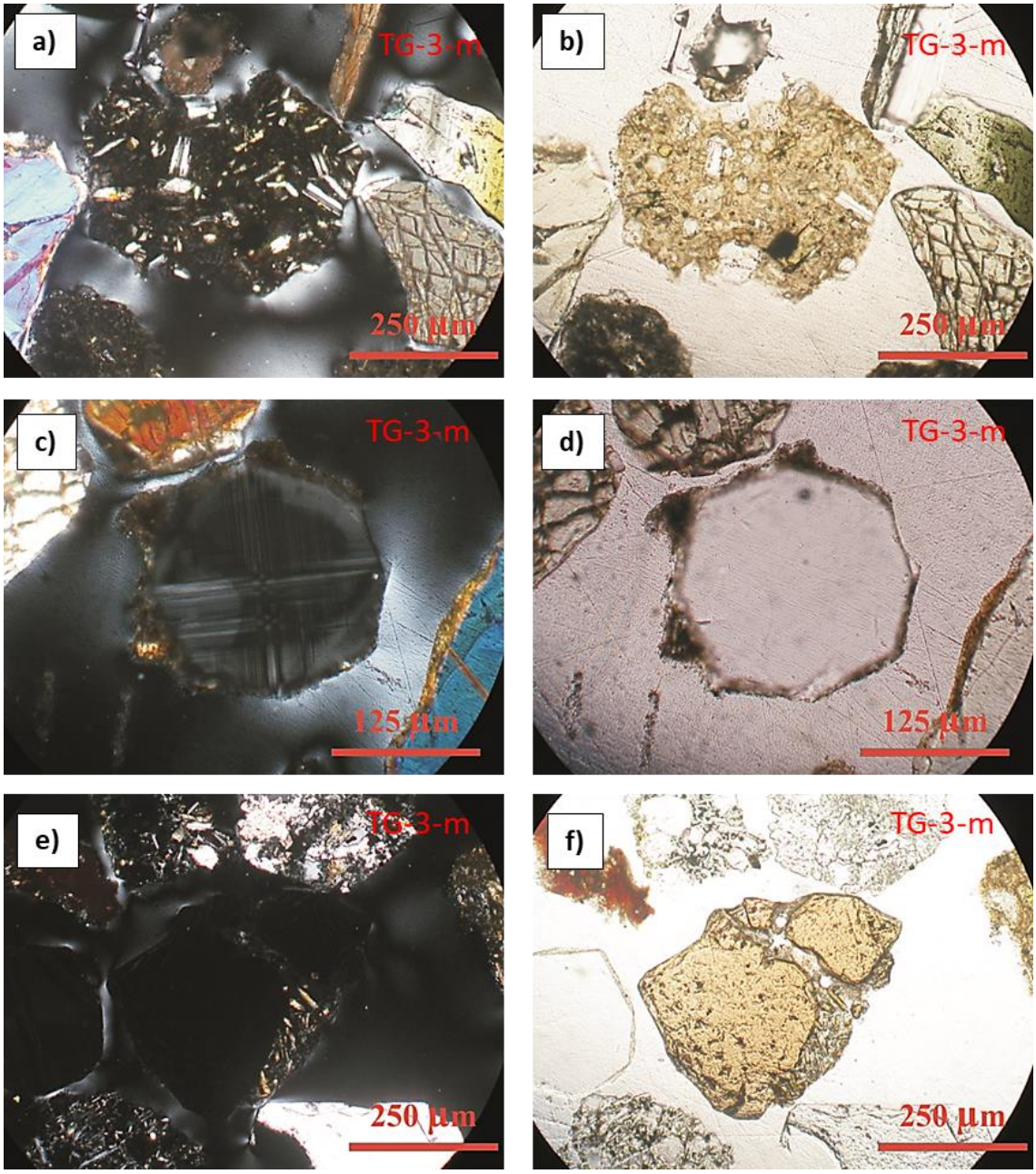

PLATE XVIII - (a ,b): Leucite and plagioclase phenocrysts in a brown glassy groundmass (*Lvlbrgl*) with a sub-angular (3) roundness category (a: NX, b: N//); (c, d): very angular (1) euhedral leucite with a glassy rim (c: NX, d: N//); (e, f): brown garnet in a volcanic lithic with a brown glassy groundmass (Lvlbrgl) (e: NX, f: N//).

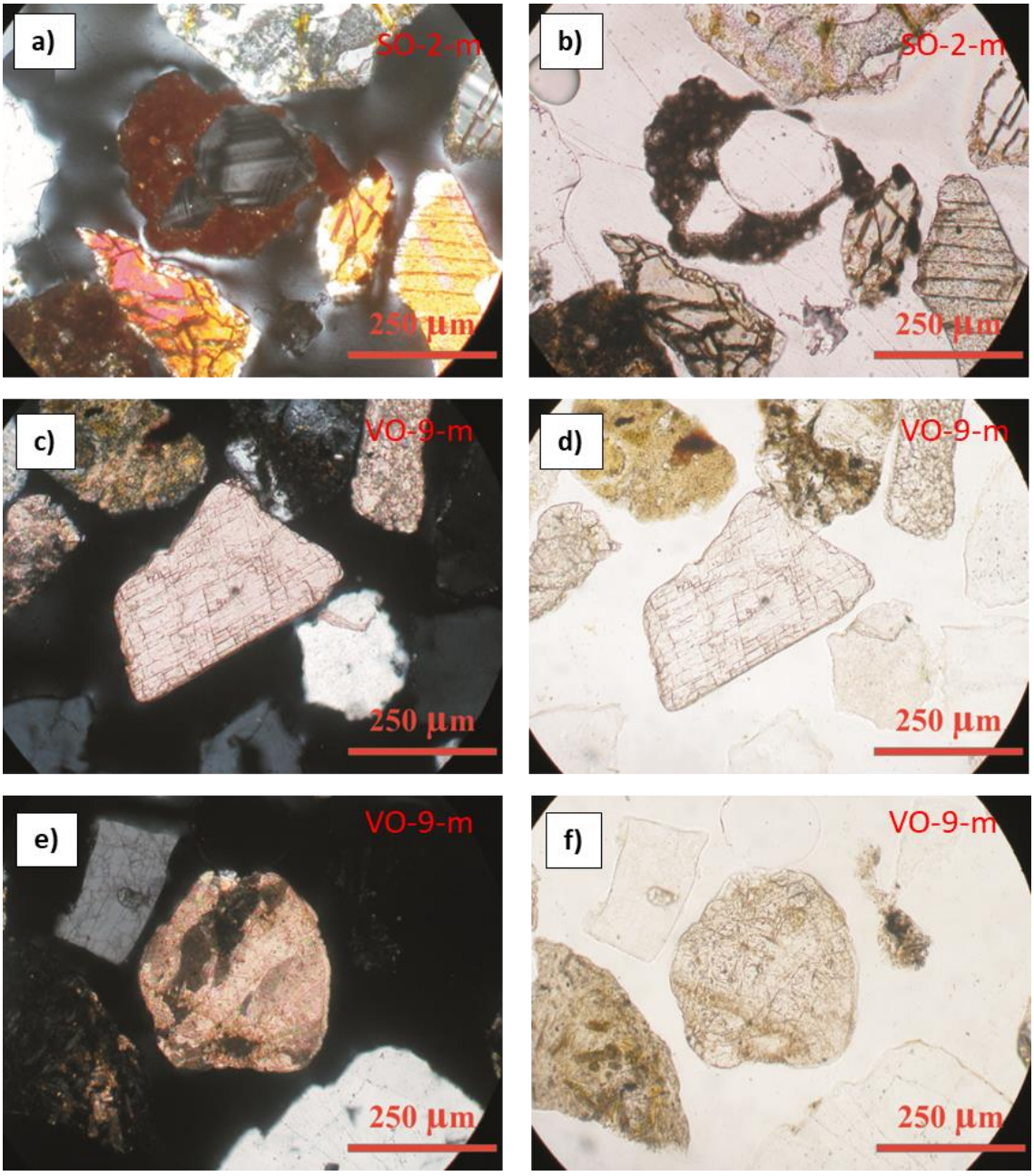

PLATE XIX - (a ,b): Leucite phenocrysts in a black glassy groundmass (*Lvlblgl*) with a sub-angular (3) roundness category from a Sorrento beach (a: NX, b: N//); (c, d): sub-angular (3) calcite single crystal grain (middle), monocrystalline quartz (lower right), siliciclastic sedimentary lithic grain (upper left) and sedimentary lithic grain with crystalline carbonate composition [(upper right, [Lss(xx)] (c: NX, d: N//); (e, f): rounded grain containing calcite mineral (limestone grain) (e: NX, f: N//).

APPENDIX A (point counting raw data)

SALINA ISLAND

SAMPLE	P	P in Lvl	P inLvlblgl	P inLvlbrgl	P inLvlorgl	P inLvlgrgl	P inLvlclgl	P alt	P in Rp	P in Pm	Py	Py in Lvlblgl	Py in Lvlbrgl	Py in Lvlorgl	Py in Lvlgrgl
SA-1-Vc	0	0	28	28	0	37	0	0	0	0	0	22	17	0	19
1	0	0	3	1	0	1	0	0	0	0	0	3	1	0	2
2	0	0	16	12	0	7	0	0	0	0	0	12	8	0	9
3	0	0	6	12	0	15	0	0	0	0	0	7	7	0	7
4	0	0	2	3	0	12	0	0	0	0	0	0	1	0	1
5	0	0	1	0	0	2	0	0	0	0	0	0	0	0	0
6	0	0	0	0	0	0	0	0	0	0	0	0	0	0	0
SA-1-C	16	0	35	20	2	14	0	0	2	0	12	12	7	0	3
1	3	0	4	1	0	1	0	0	0	0	4	2	2	0	0
2	8	0	12	7	0	3	0	0	0	0	7	5	4	0	1
3	4	0	11	8	1	7	0	0	1	0	1	5	1	0	1
4	1	0	8	4	1	3	0	0	1	0	0	0	0	0	1
5	0	0	0	0	0	0	0	0	0	0	0	0	0	0	0
6	0	0	0	0	0	0	0	0	0	0	0	0	0	0	0
SA-1-m	34	0	22	17	5	0	4	7	0	0	30	8	8	0	2
1	3	0	2	1	0	0	0	0	0	0	6	0	0	0	0
2	15	0	6	6	2	0	1	1	0	0	11	5	2	0	1
3	10	0	8	8	2	0	2	2	0	0	8	3	3	0	0
4	6	0	5	2	1	0	1	4	0	0	5	0	3	0	1
5	0	0	1	0	0	0	0	0	0	0	0	0	0	0	0
6	0	0	0	0	0	0	0	0	0	0	0	0	0	0	0
SA-1-f	30	0	4	4	0	0	0	3	0	0	75	2	0	0	4
1	2	0	0	0	0	0	0	0	0	0	15	1	0	0	0
2	10	0	2	2	0	0	0	0	0	0	32	0	0	0	2
3	15	0	1	1	0	0	0	2	0	0	22	1	0	0	1
4	3	0	0	0	0	0	0	1	0	0	6	0	0	0	1
5	0	0	1	1	0	0	0	0	0	0	0	0	0	0	0
6	0	0	0	0	0	0	0	0	0	0	0	0	0	0	0
SA-1-Vf	26	0	0	0	0	0	0	0	0	0	110	0	0	0	0
1	6	0	0	0	0	0	0	0	0	0	15	0	0	0	0
2	16	0	0	0	0	0	0	0	0	0	51	0	0	0	0
3	4	0	0	0	0	0	0	0	0	0	33	0	0	0	0
4	0	0	0	0	0	0	0	0	0	0	9	0	0	0	0
5	0	0	0	0	0	0	0	0	0	0	2	0	0	0	0
6	0	0	0	0	0	0	0	0	0	0	0	0	0	0	0

SAMPLE	Py in Lvlclgl	Py alt	K	K in Lvlblgl	K in Lvlbrgl	K in Lvlorgl	K in Lvlgrgl	K in Lvlclgl	K in Rp	Ol	Ol inLvlblgl	Ol inLvlbrgl	Ol inLvlorgl	Ol inLvlgrgl	Ol alt
SA-1-Vc	0	0	0	0	0	0	0	0	0	0	0	0	0	0	0
1	0	0	0	0	0	0	0	0	0	0	0	0	0	0	0
2	0	0	0	0	0	0	0	0	0	0	0	0	0	0	0
3	0	0	0	0	0	0	0	0	0	0	0	0	0	0	0
4	0	0	0	0	0	0	0	0	0	0	0	0	0	0	0
5	0	0	0	0	0	0	0	0	0	0	0	0	0	0	0
6	0	0	0	0	0	0	0	0	0	0	0	0	0	0	0
SA-1-C	0	0	0	0	0	0	0	0	0	0	0	0	0	0	0
1	0	0	0	0	0	0	0	0	0	0	0	0	0	0	0
2	0	0	0	0	0	0	0	0	0	0	0	0	0	0	0
3	0	0	0	0	0	0	0	0	0	0	0	0	0	0	0
4	0	0	0	0	0	0	0	0	0	0	0	0	0	0	0
5	0	0	0	0	0	0	0	0	0	0	0	0	0	0	0
6	0	0	0	0	0	0	0	0	0	0	0	0	0	0	0
SA-1-m	0	0	7	0	0	0	0	0	0	3	0	0	0	0	0
1	0	0	0	0	0	0	0	0	0	0	0	0	0	0	0
2	0	0	2	0	0	0	0	0	0	0	0	0	0	0	0
3	0	0	3	0	0	0	0	0	0	1	0	0	0	0	0
4	0	0	2	0	0	0	0	0	0	1	0	0	0	0	0
5	0	0	0	0	0	0	0	0	0	1	0	0	0	0	0
6	0	0	0	0	0	0	0	0	0	0	0	0	0	0	0
SA-1-f	0	2	4	0	0	0	0	0	0	4	0	0	0	0	0
1	0	0	0	0	0	0	0	0	0	0	0	0	0	0	0
2	0	0	1	0	0	0	0	0	0	1	0	0	0	0	0
3	0	2	3	0	0	0	0	0	0	2	0	0	0	0	0
4	0	0	0	0	0	0	0	0	0	1	0	0	0	0	0
5	0	0	0	0	0	0	0	0	0	0	0	0	0	0	0
6	0	0	0	0	0	0	0	0	0	0	0	0	0	0	0
SA-1-Vf	0	0	0	0	0	0	0	0	0	6	0	0	0	0	0
1	0	0	0	0	0	0	0	0	0	1	0	0	0	0	0
2	0	0	0	0	0	0	0	0	0	2	0	0	0	0	0
3	0	0	0	0	0	0	0	0	0	1	0	0	0	0	0
4	0	0	0	0	0	0	0	0	0	1	0	0	0	0	0
5	0	0	0	0	0	0	0	0	0	1	0	0	0	0	0
6	0	0	0	0	0	0	0	0	0	0	0	0	0	0	0

Table A-A - *Key to Grain Shape Categories. **1** = very angular; **2** = angular; **3** = sub-angular; **4** = sub-rounded; **5** = rounded; **6** = well rounded; Vc: very coarse sand fraction; C: coarse sand fraction; m: medium sand fraction; f: fine sand fraction; Vf: very fine sand fraction.

SALINA ISLAND (continued)

SAMPLE	Hb	Hbalt	Hb in Lvlblgl	Hb in Lvlbrgl	Hb in Lvlgrgl	Hb in Lvlclgl	Hb in Rp	Gr	Ru	Ru in Lvlblgl	Ru in Lvlbrgl	Op	Op in Lvlbrgl	Op in Pm	Bt
SA-1-Vc	0	0	0	0	2	0	0	0	0	0	0	0	0	0	0
1	0	0	0	0	0	0	0	0	0	0	0	0	0	0	0
2	0	0	0	0	0	0	0	0	0	0	0	0	0	0	0
3	0	0	0	0	0	0	0	0	0	0	0	0	0	0	0
4	0	0	0	0	0	0	0	0	0	0	0	0	0	0	0
5	0	0	0	0	0	0	0	0	0	0	0	0	0	0	0
6	0	0	0	0	0	0	0	0	0	0	0	0	0	0	0
SA-1-C	0	0	0	0	0	0	0	0	0	0	0	0	0	0	0
1	0	0	0	0	0	0	0	0	0	0	0	0	0	0	0
2	0	0	0	0	0	0	0	0	0	0	0	0	0	0	0
3	0	0	0	0	0	0	0	0	0	0	0	0	0	0	0
4	0	0	0	0	0	0	0	0	0	0	0	0	0	0	0
5	0	0	0	0	0	0	0	0	0	0	0	0	0	0	0
6	0	0	0	0	0	0	0	0	0	0	0	0	0	0	0
SA-1-m	0	0	0	0	0	0	0	0	0	0	0	7	0	0	0
1	0	0	0	0	0	0	0	0	0	0	0	1	0	0	0
2	0	0	0	0	0	0	0	0	0	0	0	1	0	0	0
3	0	0	0	0	0	0	0	0	0	0	0	2	0	0	0
4	0	0	0	0	0	0	0	0	0	0	0	3	0	0	0
5	0	0	0	0	0	0	0	0	0	0	0	0	0	0	0
6	0	0	0	0	0	0	0	0	0	0	0	0	0	0	0
SA-1-f	5	0	0	0	0	0	0	0	0	0	0	36	0	0	0
1	1	0	0	0	0	0	0	0	0	0	0	0	0	0	0
2	2	0	0	0	0	0	0	0	0	0	0	7	0	0	0
3	2	0	0	0	0	0	0	0	0	0	0	13	0	0	0
4	0	0	0	0	0	0	0	0	0	0	0	14	0	0	0
5	0	0	0	0	0	0	0	0	0	0	0	2	0	0	0
6	0	0	0	0	0	0	0	0	0	0	0	0	0	0	0
SA-1-Vf	7	0	0	0	0	0	0	0	0	0	0	114	0	0	0
1	1	0	0	0	0	0	0	0	0	0	0	1	0	0	0
2	3	0	0	0	0	0	0	0	0	0	0	14	0	0	0
3	3	0	0	0	0	0	0	0	0	0	0	28	0	0	0
4	0	0	0	0	0	0	0	0	0	0	0	33	0	0	0
5	0	0	0	0	0	0	0	0	0	0	0	26	0	0	0
6	0	0	0	0	0	0	0	0	0	0	0	12	0	0	0

SAMPLE	Bt in Rp	Bt in Rm	Mu	Mu in Rm	Qz-m	Q-p	Q in Rp	Q in Rm	Lvl	Lvlblgl	Lvlbrgl	Lvlorgl	Lvlgrgl	Lvlclgl	Lvlaltgl	Lvmi	Lvmiblgl
SA-1-Vc	2	0	0	0	0	0	2	0	1	38	32	3	46	0	0	2	13
1	0	0	0	0	0	0	0	0	0	3	1	0	1	0	0	0	0
2	0	0	0	0	0	0	0	0	1	19	10	2	15	0	0	1	4
3	1	0	0	0	0	0	1	0	0	13	12	1	16	0	0	0	3
4	1	0	0	0	0	0	1	0	0	3	9	0	14	0	0	1	6
5	0	0	0	0	0	0	0	0	0	0	0	0	0	0	0	0	0
6	0	0	0	0	0	0	0	0	0	0	0	0	0	0	0	0	0
SA-1-C	0	1	1	1	6	2	0	2	0	47	37	0	22	3	26	13	20
1	0	0	0	0	0	0	0	0	0	6	3	0	1	0	1	1	1
2	0	0	0	0	4	1	0	1	0	19	11	0	6	1	6	6	5
3	0	0	1	0	1	1	0	0	0	13	13	0	9	1	10	3	8
4	0	1	0	1	1	0	0	1	0	8	8	0	5	1	6	3	4
5	0	0	0	0	0	0	0	0	0	1	2	0	1	0	3	0	2
6	0	0	0	0	0	0	0	0	0	0	0	0	0	0	0	0	0
SA-1-m	0	0	1	0	5	0	0	1	0	40	28	2	13	9	9	0	31
1	0	0	0	0	0	0	0	0	0	2	0	0	1	0	0	0	1
2	0	0	1	0	2	0	0	0	0	9	4	1	4	3	1	0	7
3	0	0	0	0	3	0	0	1	0	16	8	1	4	4	3	0	9
4	0	0	0	0	0	0	0	0	0	13	16	0	4	2	3	0	12
5	0	0	0	0	0	0	0	0	0	0	0	0	0	0	2	0	2
6	0	0	0	0	0	0	0	0	0	0	0	0	0	0	0	0	0
SA-1-f	0	0	0	0	20	0	0	0	0	12	7	0	0	3	0	0	63
1	0	0	0	0	2	0	0	0	0	0	1	0	0	0	0	0	0
2	0	0	0	0	7	0	0	0	0	4	3	0	0	1	0	0	5
3	0	0	0	0	9	0	0	0	0	7	2	0	0	2	0	0	19
4	0	0	0	0	2	0	0	0	0	1	1	0	0	0	0	0	33
5	0	0	0	0	0	0	0	0	0	0	0	0	0	0	0	0	6
6	0	0	0	0	0	0	0	0	0	0	0	0	0	0	0	0	0
SA-1-Vf	0	0	0	0	9	0	0	0	0	0	0	0	0	0	0	0	21
1	0	0	0	0	0	0	0	0	0	0	0	0	0	0	0	0	0
2	0	0	0	0	5	0	0	0	0	0	0	0	0	0	0	0	2
3	0	0	0	0	4	0	0	0	0	0	0	0	0	0	0	0	5
4	0	0	0	0	0	0	0	0	0	0	0	0	0	0	0	0	14
5	0	0	0	0	0	0	0	0	0	0	0	0	0	0	0	0	0
6	0	0	0	0	0	0	0	0	0	0	0	0	0	0	0	0	0

*Key to Grain Shape Categories. **1** = very angular; **2** = angular; **3** = sub-angular; **4** = sub-rounded; **5** = rounded; **6** = well rounded; Vc: very coarse sand fraction; C: coarse sand fraction; m: medium sand fraction; f: fine sand fraction; Vf: very fine sand fraction.

SALINA ISLAND (continued)

SAMPLE	Lvmibrgl	Lvmiorgl	Lvmigrgl	Lvmiclgl	Lvmialtgl	Lvvblgl	Lvvbrgl	Lvvorgl	Lvvgrgl	Lvvclgl	Lvvalgl	Lvf	Pmcl	Lm	Lp	Lvo	Lsc (crist)	Lsc (micr)	Bio	Unknow	TOT
SA-1-Vc	16	0	12	0	0	15	9	0	8	0	0	0	0	0	0	0	0	0	0	0	350
1	0	0	0	0	0	1	0	0	0	0	0	0	0	0	0	0	0	0	0	0	17
2	3	0	2	0	0	6	3	0	3	0	0	0	0	0	0	0	0	0	0	0	133
3	4	0	4	0	0	6	3	0	3	0	0	0	0	0	0	0	0	0	0	0	121
4	9	0	6	0	0	2	3	0	2	0	0	0	0	0	0	0	0	0	0	0	76
5	0	0	0	0	0	0	0	0	0	0	0	0	0	0	0	0	0	0	0	0	3
6	0	0	0	0	0	0	0	0	0	0	0	0	0	0	0	0	0	0	0	0	0
SA-1-C	21	2	11	0	14	16	6	3	0	0	10	4	7	0	0	0	2	0	0	0	400
1	1	0	0	0	1	5	1	1	0	0	0	0	1	0	0	0	0	0	0	0	40
2	5	0	1	0	3	6	1	2	0	0	2	1	3	0	0	0	0	0	0	0	131
3	6	2	7	0	6	4	3	0	0	0	5	3	3	0	0	0	1	0	0	0	140
4	8	0	3	0	4	1	1	0	0	0	3	0	0	0	0		1	0	0	0	79
5	1	0	0	0	0	0	0	0	0	0	0	0	0	0	0	0	0	0	0	0	10
6	0	0	0	0	0	0	0	0	0	0	0	0	0	0	0	0	0	0	0	0	0
SA-1-m	24	4	7	7	8	27	12	4	0	0	4	0	0	0	0	10	0	0	0	0	400
1	0	0	0	0	0	1	1	0	0	0	0	0	0	0	0	0	0	0	0	0	19
2	6	2	0	1	2	5	3	3	0	0	0	0	0	0	0	1	0	0	0	0	108
3	6	1	3	2	2	12	5	1	0	0	1	0	0	0	0	4	0	0	0	0	138
4	10	1	4	4	4	7	3	0	0	0	3	0	0	0	0	5	0	0	0	0	125
5	2	0	0	0	0	2	0	0	0	0	0	0	0	0	0	0	0	0	0	0	10
6	0	0	0	0	0	0	0	0	0	0	0	0	0	0	0	0	0	0	0	0	0
SA-1-f	24	0	6	0	13	50	17	0	0	3	0	0	0	0	0	0	0	7	2	0	400
1	0	0	0	0	0	9	1	0	0	0	0	0	0	0	0	0	0	0	0	0	32
2	3	0	1	0	1	29	9	0	0	1	0	0	0	0	0	0	0	0	1	0	124
3	8	0	2	0	4	7	6	0	0	2	0	0	0	0	0	0	0	3	1	0	137
4	13	0	3	0	8	5	1	0	0	0	0	0	0	0	0	0	0	4	0	0	97
5	0	0	0	0	0	0	0	0	0	0	0	0	0	0	0	0	0	0	0	0	10
6	0	0	0	0	0	0	0	0	0	0	0	0	0	0	0	0	0	0	0	0	0
SA-1-Vf	8	0	0	0	0	33	23	1	0	7	35	0	0	0	0	0	0	0	0	0	400
1	0	0	0	0	0	3	2	0	0	2	0	0	0	0	0	0	0	0	0	0	31
2	0	0	0	0	0	21	12	1	0	4	8	0	0	0	0	0	0	0	0	0	139
3	3	0	0	0	0	8	7	0	0	1	16	0	0	0	0	0	0	0	0	0	113
4	5	0	0	0	0	1	2	0	0	0	11	0	0	0	0	0	0	0	0	0	76
5	0	0	0	0	0	0	0	0	0	0	0	0	0	0	0	0	0	0	0	0	29
6	0	0	0	0	0	0	0	0	0	0	0	0	0	0	0	0	0	0	0	0	12

SAMPLE	P	P in Lvl	P inLvlblgl	P inLvlbrgl	P inLvlorgl	P inLvlgrgl	P inLvlclgl	P alt	P in Rp	P in Pm	Py	Py in Lvlblgl	Py in Lvlbrgl	Py in Lvlorgl	Py in Lvlgrgl
SA-2-m	42	0	15	18	3	14	0	4	0	0	36	10	5	0	0
1	2	0	0	2	0	1	0	0	0	0	5	0	0	0	0
2	18	0	5	7	2	3	0	1	0	0	14	2	1	0	0
3	17	0	6	6	1	6	0	3	0	0	13	3	3	0	0
4	4	0	4	3	0	4	0	0	0	0	4	3	1	0	0
5	1	0	0	0	0	0	0	0	0	0	0	2	0	0	0
6	0	0	0	0	0	0	0	0	0	0	0	0	0	0	0
SA-3-m	33	0	15	8	0	7	3	1	2	0	92	5	4	0	1
1	1	0	0	0	0	0	0	0	0	0	11	0	0	0	0
2	14	0	4	5	0	3	1	0	1	0	36	2	2	0	0
3	13	0	9	3	0	3	1	1	1	0	28	3	1	0	1
4	4	0	2	0	0	1	1	0	0	0	16	0	1	0	0
5	1	0	0	0	0	0	0	0	0	0	1	0	0	0	0
6	0	0	0	0	0	0	0	0	0	0	0	0	0	0	0
SA-4-m	30	0	21	12	0	0	0	6	0	0	26	0	0	0	0
1	3	0	1	0	0	0	0	0	0	0	3	0	0	0	0
2	15	0	6	5	0	0	0	3	0	0	13	0	0	0	0
3	9	0	11	6	0	0	0	3	0	0	8	0	0	0	0
4	3	0	3	1	0	0	0	0	0	0	2	0	0	0	0
5	0	0	0	0	0	0	0	0	0	0	0	0	0	0	0
6	0	0	0	0	0	0	0	0	0	0	0	0	0	0	0
SA-5-m	23	0	12	6	0	0	0	0	0	10	14	0	0	0	0
1	1	0	0	0	0	0	0	0	0	0	1	0	0	0	0
2	10	0	3	2	0	0	0	0	0	3	6	0	0	0	0
3	8	0	4	3	0	0	0	0	0	4	5	0	0	0	0
4	4	0	5	1	0	0	0	0	0	3	2	0	0	0	0
5	0	0	0	0	0	0	0	0	0	0	0	0	0	0	0
6	0	0	0	0	0	0	0	0	0	0	0	0	0	0	0
SA-6-m	25	0	22	23	0	0	0	3	0	0	10	20	15	0	0
1	0	0	0	0	0	0	0	0	0	0	0	0	0	0	0
2	9	0	3	5	0	0	0	0	0	0	4	11	2	0	0
3	11	0	13	12	0	0	0	1	0	0	5	7	8	0	0
4	5	0	6	6	0	0	0	2	0	0	1	2	5	0	0
5	0	0	0	0	0	0	0	0	0	0	0	0	0	0	0
6	0	0	0	0	0	0	0	0	0	0	0	0	0	0	0

*Key to Grain Shape Categories. **1** = very angular; **2** = angular; **3** = sub-angular; **4** = sub-rounded; **5** = rounded; **6** = well rounded; Vc: very coarse sand fraction; C: coarse sand fraction; m: medium sand fraction; f: fine sand fraction; Vf: very fine sand fraction.

SALINA ISLAND (continued)

SAMPLE	Py in LvlclgI	Py alt	K	K in LvlblgI	K in LvlbrgI	K in LvlorgI	K in LvlgrgI	K in LvlclgI	K in Rp	Ol	Ol inLvlblgI	Ol inLvlbrgI	Ol inLvlorgI	Ol inLvlgrgI	Ol alt
SA-2-m	0	0	4	0	0	0	0	0	0	5	0	3	0	0	0
1	0	0	0	0	0	0	0	0	0		0	0	0	0	0
2	0	0	3	0	0	0	0	0	0	1	0	0	0	0	0
3	0	0	1	0	0	0	0	0	0	2	0	2	0	0	0
4	0	0	0	0	0	0	0	0	0	2	0	1	0	0	0
5	0	0	0	0	0	0	0	0	0	0	0	0	0	0	0
6	0	0	0	0	0	0	0	0	0	0	0	0	0	0	0
SA-3-m	0	0	0	0	0	0	0	0	0	10	0	0	0	0	0
1	0	0	0	0	0	0	0	0	0	0	0	0	0	0	0
2	0	0	0	0	0	0	0	0	0	2	0	0	0	0	0
3	0	0	0	0	0	0	0	0	0	3	0	0	0	0	0
4	0	0	0	0	0	0	0	0	0	4	0	0	0	0	0
5	0	0	0	0	0	0	0	0	0	1	0	0	0	0	0
6	0	0	0	0	0	0	0	0	0	0	0	0	0	0	0
SA-4-m	0	0	0	0	0	0	0	0	0	7	7	0	0	0	4
1	0	0	0	0	0	0	0	0	0	0	1	0	0	0	0
2	0	0	0	0	0	0	0	0	0	2	2	0	0	0	1
3	0	0	0	0	0	0	0	0	0	2	1	0	0	0	2
4	0	0	0	0	0	0	0	0	0	3	3	0	0	0	1
5	0	0	0	0	0	0	0	0	0	0	0	0	0	0	0
6	0	0	0	0	0	0	0	0	0	0	0	0	0	0	0
SA-5-m	0	0	5	0	0	0	4	0	0	0	0	0	0	0	0
1	0	0	0	0	0	0	0	0	0	0	0	0	0	0	0
2	0	0	1	0	0	0	1	0	0	0	0	0	0	0	0
3	0	0	3	0	0	0	2	0	0	0	0	0	0	0	0
4	0	0	1	0	0	0	1	0	0	0	0	0	0	0	0
5	0	0	0	0	0	0	0	0	0	0	0	0	0	0	0
6	0	0	0	0	0	0	0	0	0	0	0	0	0	0	0
SA-6-m	0	0	3	1	0	0	1	0	0	0	2	0	0	0	0
1	0	0	0	0	0	0	0	0	0	0	0	0	0	0	0
2	0	0	0	0	0	0	0	0	0	0	0	0	0	0	0
3	0	0	3	1	0	0	0	0	0	0	2	0	0	0	0
4	0	0	0	0	0	0	1	0	0	0	0	0	0	0	0
5	0	0	0	0	0	0	0	0	0	0	0	0	0	0	0
6	0	0	0	0	0	0	0	0	0	0	0	0	0	0	0

SAMPLE	Hb	Hbalt	Hb in LvlblgI	Hb in LvlbrgI	Hb in LvlgrgI	Hb in LvlclgI	Hb in Rp	Gr	Ru	Ru in LvlblgI	Ru in LvlbrgI	Op	Op in LvlbrgI	Op in Pm	Bt
SA-2-m	0	0	0	0	0	0	0	0	0	0	0	5	0	0	0
1	0	0	0	0	0	0	0	0	0	0	0	0	0	0	0
2	0	0	0	0	0	0	0	0	0	0	0	0	0	0	0
3	0	0	0	0	0	0	0	0	0	0	0	2	0	0	0
4	0	0	0	0	0	0	0	0	0	0	0	3	0	0	0
5	0	0	0	0	0	0	0	0	0	0	0	0	0	0	0
6	0	0	0	0	0	0	0	0	0	0	0	0	0	0	0
SA-3-m	1	0	0	0	0	0	1	0	0	0	0	12	0	0	0
1	0	0	0	0	0	0	0	0	0	0	0	0	0	0	0
2	1	0	0	0	0	0	0	0	0	0	0	3	0	0	0
3	0	0	0	0	0	0	1	0	0	0	0	5	0	0	0
4	0	0	0	0	0	0	0	0	0	0	0	4	0	0	0
5	0	0	0	0	0	0	0	0	0	0	0	0	0	0	0
6	0	0	0	0	0	0	0	0	0	0	0	0	0	0	0
SA-4-m	0	0	0	0	0	0	0	0	0	0	0	7	0	0	4
1	0	0	0	0	0	0	0	0	0	0	0	0	0	0	0
2	0	0	0	0	0	0	0	0	0	0	0	1	0	0	1
3	0	0	0	0	0	0	0	0	0	0	0	2	0	0	2
4	0	0	0	0	0	0	0	0	0	0	0	3	0	0	1
5	0	0	0	0	0	0	0	0	0	0	0	1	0	0	0
6	0	0	0	0	0	0	0	0	0	0	0	0	0	0	0
SA-5-m	4	0	1	0	0	0	0	0	0	0	0	0	0	0	2
1	0	0	0	0	0	0	0	0	0	0	0	0	0	0	0
2	1	0	0	0	0	0	0	0	0	0	0	0	0	0	1
3	2	0	1	0	0	0	0	0	0	0	0	0	0	0	0
4	1	0	0	0	0	0	0	0	0	0	0	0	0	0	1
5	0	0	0	0	0	0	0	0	0	0	0	0	0	0	0
6	0	0	0	0	0	0	0	0	0	0	0	0	0	0	0
SA-6-m	0	0	0	0	0	0	0	1	0	0	0	0	0	0	0
1	0	0	0	0	0	0	0	0	0	0	0	0	0	0	0
2	0	0	0	0	0	0	0	1	0	0	0	0	0	0	0
3	0	0	0	0	0	0	0	0	0	0	0	0	0	0	0
4	0	0	0	0	0	0	0	0	0	0	0	0	0	0	0
5	0	0	0	0	0	0	0	0	0	0	0	0	0	0	0
6	0	0	0	0	0	0	0	0	0	0	0	0	0	0	0

*Key to Grain Shape Categories. **1** = very angular; **2** = angular; **3** = sub-angular; **4** = sub-rounded; **5** = rounded; **6** = well rounded; Vc: very coarse sand fraction; C: coarse sand fraction; m: medium sand fraction; f: fine sand fraction; Vf: very fine sand fraction.

SALINA ISLAND (continued)

SAMPLE	Bt in Rp	Bt in Rm	Mu	Mu in Rm	Qz-m	Q-p	Q in Rp	Q in Rm	Lvl	Lvlblgl	Lvlbrgl	Lvlorgl	Lvlgrgl	Lvlclgl	Lvlaltgl	Lvmi	Lvmiblgl
SA-2-m	0	0	0	0	0	0	1	0	0	31	36	5	15	2	7	0	21
1	0	0	0	0	0	0	0	0	0	2	2	1	0	0	0	0	0
2	0	0	0	0	0	0	0	0	0	4	11	3	3	0	1	0	1
3	0	0	0	0	0	0	0	0	0	15	13	1	6	1	2	0	5
4	0	0	0	0	0	0	1	0	0	9	10	0	6	1	3	0	13
5	0	0	0	0	0	0	0	0	0	1	0	0	0	0	1	0	2
6	0	0	0	0	0	0	0	0	0	0	0	0	0	0	0	0	0
SA-3-m	1	0	0	0	3	0	1	0	0	51	37	0	14	4	3	0	23
1	0	0	0	0	0	0	0	0	0	1	1	0	1	0	0	0	0
2	0	0	0	0	2	0	0	0	0	14	9	0	4	1	1	0	3
3	1	0	0	0	1	0	0	0	0	22	19	0	9	2	2	0	7
4	0	0	0	0	0	0	1	0	0	12	8	0	0	1	0	0	12
5	0	0	0	0	0	0	0	0	0	2	0	0	0	0	0	0	1
6	0	0	0	0	0	0	0	0	0	0	0	0	0	0	0	0	0
SA-4-m	0	0	0	0	0	0	0	0	0	69	33	0	17	0	16	0	43
1	0	0	0	0	0	0	0	0	0	12	4	0	1	0	1	0	2
2	0	0	0	0	0	0	0	0	0	21	9	0	6	0	2	0	11
3	0	0	0	0	0	0	0	0	0	30	16	0	8	0	11	0	13
4	0	0	0	0	0	0	0	0	0	6	4	0	2	0	2	0	17
5	0	0	0	0	0	0	0	0	0	0	0	0	0	0	0	0	0
6	0	0	0	0	0	0	0	0	0	0	0	0	0	0	0	0	0
SA-5-m	0	0	0	0	3	0	0	0	0	46	34	0	24	8	10	0	18
1	0	0	0	0	0	0	0	0	0	0	0	0	0	0	0	0	0
2	0	0	0	0	2	0	0	0	0	7	5	0	5	5	3	0	0
3	0	0	0	0	1	0	0	0	0	19	14	0	12	2	4	0	6
4	0	0	0	0	0	0	0	0	0	20	14	0	7	1	3	0	10
5	0	0	0	0	0	0	0	0	0	0	1	0	0	0	0	0	2
6	0	0	0	0	0	0	0	0	0	0	0	0	0	0	0	0	0
SA-6-m	0	0	0	0	0	0	0	0	0	52	55	13	17	8	0	0	26
1	0	0	0	0	0	0	0	0	0	0	1	0	0	0	0	0	0
2	0	0	0	0	0	0	0	0	0	6	11	5	2	2	0	0	2
3	0	0	0	0	0	0	0	0	0	23	20	5	11	4	0	0	10
4	0	0	0	0	0	0	0	0	0	19	20	3	4	2	0	0	10
5	0	0	0	0	0	0	0	0	0	4	3	0	0	0	0	0	4
6	0	0	0	0	0	0	0	0	0	0	0	0	0	0	0	0	0

SAMPLE	Lvmibrgl	Lvmiorgl	Lvmigrgl	Lvmiclgl	Lvmialtgl	Lvvblgl	Lvvbrgl	Lvvorgl	Lvvgrgl	Lvvclgl	Lvvalgl	Lvf	Pmcl	Lm	Lp	Lvo	Lsc (crist)	Lsc (micr)	Bio	Unknow	TOT
SA-2-m	29	8	3	0	11	21	15	7	0	2	0	0	3	5	0	3	2	6	3	0	400
1	1	0	0	0	0	5	5	3	0	1	0	0	0	1	0	0	0	0	0	0	31
2	5	3	0	0	0	10	7	3	0	1	0	0	1	1	0	0	0	1	0	0	112
3	8	2	1	0	4	5	3	1	0	0	0	0	1	3	0	1	0	3	0	0	140
4	12	3	2	0	5	1	0	0	0	0	0	0	1	0	0	2	0	2	2	0	104
5	3	0	0	0	2	0	0	0	0	0	0	0	0	0	0	0	0	0	1	0	13
6	0	0	0	0	0	0	0	0	0	0	0	0	0	0	0	0	0	0	0	0	0
SA-3-m	21	0	13	0	5	14	8	0	0	0	5	0	0	0	0	0	0	0	0	2	400
1	0	0	0	0	0	1	1	0	0	0	0	0	0	0	0	0	0	0	0	0	17
2	1	0	2	0	0	7	6	0	0	0	1	0	0	0	0	0	0	0	0	0	125
3	8	0	7	0	1	4	1	0	0	0	3	0	0	0	0	0	0	0	0	1	161
4	11	0	4	0	3	2	0	0	0	0	1	0	0	0	0	0	0	0	0	1	89
5	1	0	0	0	1	0	0	0	0	0	0	0	0	0	0	0	0	0	0	0	8
6	0	0	0	0	0	0	0	0	0	0	0	0	0	0	0	0	0	0	0	0	0
SA-4-m	30	0	7	0	7	19	18	0	0	0	7	0	0	1	0	0	0	0	3	6	400
1	1	0	0	0	0	2	2	0	0	0	1	0	0	0	0	0	0	0	0	0	34
2	2	0	1	0	0	11	9	0	0	0	4	0	0	0	0	0	0	0	2	1	128
3	8	0	2	0	3	6	6	0	0	0	2	0	0	1	0	0	0	0	1	3	156
4	16	0	4	0	3	0	1	0	0	0	0	0	0	0	0	0	0	0	0	2	77
5	3	0	0	0	1	0	0	0	0	0	0	0	0	0	0	0	0	0	0	0	5
6	0	0	0	0	0	0	0	0	0	0	0	0	0	0	0	0	0	0	0	0	0
SA-5-m	20	0	25	0	10	22	19	0	0	0	24	0	47	0	0	0	0	0	0	3	400
1	0	0	0	0	0	0	0	0	0	0	1	0	0	0	0	0	0	0	0	0	3
2	1	0	1	0	1	8	9	0	0	0	3	0	7	0	0	0	0	0	0	0	86
3	6	0	7	0	3	9	8	0	0	0	8	0	20	0	0	0	0	0	0	2	155
4	12	0	15	0	6	4	2	0	0	0	10	0	19	0	0	0	0	0	0	1	146
5	1	0	2	0	0	1	0	0	0	0	2	0	1	0	0	0	0	0	0	0	10
6	0	0	0	0	0	0	0	0	0	0	0	0	0	0	0	0	0	0	0	0	0
SA-6-m	26	13	0	0	0	28	23	3	0	0	2	0	1	4	3	0	0	0	0	0	400
1	0	0	0	0	0	5	3	1	0	0	0	0	0	0	0	0	0	0	0	0	10
2	1	1	0	0	0	17	13	2	0	0	0	0	0	2	2	0	0	0	0	0	101
3	11	5	0	0	0	5	5	0	0	0	1	0	1	2	1	0	0	0	0	0	167
4	14	7	0	0	0	1	2	0	0	0	1	0	0	0	0	0	0	0	0	0	111
5	0	0	0	0	0	0	0	0	0	0	0	0	0	0	0	0	0	0	0	0	11
6	0	0	0	0	0	0	0	0	0	0	0	0	0	0	0	0	0	0	0	0	0

*Key to Grain Shape Categories. **1** = very angular; **2** = angular; **3** = sub-angular; **4** = sub-rounded; **5** = rounded; **6** = well rounded; Vc: very coarse sand fraction; C: coarse sand fraction; m: medium sand fraction; f: fine sand fraction; Vf: very fine sand fraction.

SALINA ISLAND (continued)

SAMPLE	P	P in Lvl	P inLvlblgl	P inLvlbrgl	P inLvlorgl	P inLvlgrgl	P inLvlclgl	P alt	P in Rp	P in Pm	Py	Py in Lvlblgl	Py in Lvlbrgl	Py in Lvlorgl	Py in Lvlgrgl
SA-7-m	30	0	46	43	0	0	3	0	0	0	11	4	4	0	0
1	0	0	7	6	0	0	0	0	0	0	1	1	1	0	0
2	8	0	19	18	0	0	0	0	0	0	4	1	1	0	0
3	16	0	18	15	0	0	3	0	0	0	5	2	2	0	0
4	6	0	2	4	0	0	0	0	0	0	1	0	0	0	0
5	0	0	0	0	0	0	0	0	0	0	0	0	0	0	0
6	0	0	0	0	0	0	0	0	0	0	0	0	0	0	0
SA-8-m	33	0	19	13	0	0	0	0	0	0	52	17	8	0	0
1	4	0	1	1	0	0	0	0	0	0	7	1	0	0	0
2	12	0	9	7	0	0	0	0	0	0	21	6	3	0	0
3	13	0	6	5	0	0	0	0	0	0	15	8	4	0	0
4	4	0	3	0	0	0	0	0	0	0	9	2	1	0	0
5	0	0	0	0	0	0	0	0	0	0	0	0	0	0	0
6	0	0	0	0	0	0	0	0	0	0	0	0	0	0	0
SA-9-m	36	0	17	10	0	0	0	0	0	0	48	7	7	0	0
1	2	0	1	0	0	0	0	0	0	0	3	0	0	0	0
2	7	0	6	2	0	0	0	0	0	0	12	2	3	0	0
3	16	0	9	7	0	0	0	0	0	0	23	2	2	0	0
4	7	0	1	1	0	0	0	0	0	0	8	3	2	0	0
5	4	0	0	0	0	0	0	0	0	0	2	0	0	0	0
6	0	0	0	0	0	0	0	0	0	0	0	0	0	0	0
SA-10-m	37	0	11	8	0	0	0	0	0	0	39	7	6	0	0
1	1	0	0	0	0	0	0	0	0	0	3	0	0	0	0
2	12	0	3	3	0	0	0	0	0	0	10	2	3	0	0
3	20	0	6	4	0	0	0	0	0	0	20	5	3	0	0
4	4	0	2	1	0	0	0	0	0	0	6	0	0	0	0
5	0	0	0	0	0	0	0	0	0	0	0	0	0	0	0
6	0	0	0	0	0	0	0	0	0	0	0	0	0	0	0
SA-11-m	36	0	16	9	0	0	0	0	5	0	43	0	1	0	0
1	0	0	1	0	0	0	0	0	0	0	4	0	0	0	0
2	9	0	3	0	0	0	0	0	0	0	17	0	0	0	0
3	22	0	8	6	0	0	0	0	3	0	14	0	1	0	0
4	5	0	3	3	0	0	0	0	2	0	8	0	0	0	0
5	0	0	1	0	0	0	0	0	0	0	0	0	0	0	0
6	0	0	0	0	0	0	0	0	0	0	0	0	0	0	0

SAMPLE	Py in Lvlclgl	Py alt	K	K in Lvlblgl	K in Lvlbrgl	K in Lvlorgl	K in Lvlgrgl	K in Lvlclgl	K in Rp	Ol	Ol inLvlblgl	Ol inLvlbrgl	Ol inLvlorgl	Ol inLvlgrgl	Ol alt
SA-7-m	0	0	0	0	0	0	0	0	0	0	0	0	0	0	0
1	0	0	0	0	0	0	0	0	0	0	0	0	0	0	0
2	0	0	0	0	0	0	0	0	0	0	0	0	0	0	0
3	0	0	0	0	0	0	0	0	0	0	0	0	0	0	0
4	0	0	0	0	0	0	0	0	0	0	0	0	0	0	0
5	0	0	0	0	0	0	0	0	0	0	0	0	0	0	0
6	0	0	0	0	0	0	0	0	0	0	0	0	0	0	0
SA-8-m	0	0	18	0	0	0	0	0	0	5	0	0	0	0	0
1	0	0	0	0	0	0	0	0	0	0	0	0	0	0	0
2	0	0	4	0	0	0	0	0	0	1	0	0	0	0	0
3	0	0	10	0	0	0	0	0	0	1	0	0	0	0	0
4	0	0	4	0	0	0	0	0	0	3	0	0	0	0	0
5	0	0	0	0	0	0	0	0	0	0	0	0	0	0	0
6	0	0	0	0	0	0	0	0	0	0	0	0	0	0	0
SA-9-m	0	0	13	0	0	0	0	0	0	3	0	0	0	0	0
1	0	0	0	0	0	0	0	0	0	0	0	0	0	0	0
2	0	0	2	0	0	0	0	0	0	1	0	0	0	0	0
3	0	0	7	0	0	0	0	0	0	1	0	0	0	0	0
4	0	0	4	0	0	0	0	0	0	1	0	0	0	0	0
5	0	0	0	0	0	0	0	0	0	0	0	0	0	0	0
6	0	0	0	0	0	0	0	0	0	0	0	0	0	0	0
SA-10-m	0	0	8	0	0	0	0	0	0	0	0	0	0	0	0
1	0	0	0	0	0	0	0	0	0	0	0	0	0	0	0
2	0	0	3	0	0	0	0	0	0	0	0	0	0	0	0
3	0	0	3	0	0	0	0	0	0	0	0	0	0	0	0
4	0	0	2	0	0	0	0	0	0	0	0	0	0	0	0
5	0	0	0	0	0	0	0	0	0	0	0	0	0	0	0
6	0	0	0	0	0	0	0	0	0	0	0	0	0	0	0
SA-11-m	0	0	8	5	0	0	0	0	0	0	0	0	0	0	3
1	0	0	0	0	0	0	0	0	0	0	0	0	0	0	0
2	0	0	2	1	0	0	0	0	0	0	0	0	0	0	1
3	0	0	5	2	0	0	0	0	0	0	0	0	0	0	1
4	0	0	1	2	0	0	0	0	0	0	0	0	0	0	1
5	0	0	0	0	0	0	0	0	0	0	0	0	0	0	0
6	0	0	0	0	0	0	0	0	0	0	0	0	0	0	0

*Key to Grain Shape Categories. **1** = very angular; **2** = angular; **3** = sub-angular; **4** = sub-rounded; **5** = rounded; **6** = well rounded; Vc: very coarse sand fraction; C: coarse sand fraction; m: medium sand fraction; f: fine sand fraction; Vf: very fine sand fraction.

SALINA ISLAND (continued)

SAMPLE	Hb	Hbalt	Hb in Lvlblgl	Hb in Lvlbrgl	Hb in Lvlgrgl	Hb in Lvlclgl	Hb in Rp	Gr	Ru	Ru in Lvlblgl	Ru in Lvlbrgl	Op	Op in Lvlbrgl	Op in Pm	Bt
SA-7-m	0	0	0	0	0	0	0	0	0	0	0	0	0	0	0
1	0	0	0	0	0	0	0	0	0	0	0	0	0	0	0
2	0	0	0	0	0	0	0	0	0	0	0	0	0	0	0
3	0	0	0	0	0	0	0	0	0	0	0	0	0	0	0
4	0	0	0	0	0	0	0	0	0	0	0	0	0	0	0
5	0	0	0	0	0	0	0	0	0	0	0	0	0	0	0
6	0	0	0	0	0	0	0	0	0	0	0	0	0	0	0
SA-8-m	0	0	0	0	0	0	0	3	0	0	7	0	0	0	0
1	0	0	0	0	0	0	0	0	0	0	0	0	0	0	0
2	0	0	0	0	0	0	0	0	0	0	1	0	0	0	0
3	0	0	0	0	0	0	0	2	0	0	3	0	0	0	0
4	0	0	0	0	0	0	0	1	0	0	3	0	0	0	0
5	0	0	0	0	0	0	0	0	0	0	0	0	0	0	0
6	0	0	0	0	0	0	0	0	0	0	0	0	0	0	0
SA-9-m	0	0	0	0	0	0	0	0	0	0	0	0	0	0	0
1	0	0	0	0	0	0	0	0	0	0	0	0	0	0	0
2	0	0	0	0	0	0	0	0	0	0	0	0	0	0	0
3	0	0	0	0	0	0	0	0	0	0	0	0	0	0	0
4	0	0	0	0	0	0	0	0	0	0	0	0	0	0	0
5	0	0	0	0	0	0	0	0	0	0	0	0	0	0	0
6	0	0	0	0	0	0	0	0	0	0	0	0	0	0	0
SA-10-m	2	0	0	0	0	0	0	0	0	0	8	0	0	0	10
1	0	0	0	0	0	0	0	0	0	0	0	0	0	0	1
2	0	0	0	0	0	0	0	0	0	0	1	0	0	0	5
3	2	0	0	0	0	0	0	0	0	0	2	0	0	0	3
4	0	0	0	0	0	0	0	0	0	0	4	0	0	0	1
5	0	0	0	0	0	0	0	0	0	0	1	0	0	0	0
6	0	0	0	0	0	0	0	0	0	0	0	0	0	0	0
SA-11-m	3	0	0	0	0	0	0	2	0	0	7	0	0	0	1
1	0	0	0	0	0	0	0	0	0	0	0	0	0	0	0
2	2	0	0	0	0	0	0	1	0	0	1	0	0	0	0
3	1	0	0	0	0	0	0	1	0	0	3	0	0	0	1
4	0	0	0	0	0	0	0	0	0	0	2	0	0	0	0
5	0	0	0	0	0	0	0	0	0	0	1	0	0	0	0
6	0	0	0	0	0	0	0	0	0	0	0	0	0	0	0

SAMPLE	Bt in Rp	Bt in Rm	Mu	Mu in Rm	Qz-m	Q-p	Q in Rp	Q in Rm	Lvl	Lvlblgl	Lvlbrgl	Lvlorgl	Lvlgrgl	Lvlclgl	Lvlaltgl	Lvmi	Lvmiblgl
SA-7-m	0	0	0	0	0	0	0	0	0	80	74	4	3	0	0	0	27
1	0	0	0	0	0	0	0	0	0	8	7	0	0	0	0	0	0
2	0	0	0	0	0	0	0	0	0	38	34	2	0	0	0	0	3
3	0	0	0	0	0	0	0	0	0	25	27	2	3	0	0	0	14
4	0	0	0	0	0	0	0	0	0	7	5	0	0	0	0	0	10
5	0	0	0	0	0	0	0	0	0	2	1	0	0	0	0	0	0
6	0	0	0	0	0	0	0	0	0	0	0	0	0	0	0	0	0
SA-8-m	0	0	0	0	3	0	0	0	0	64	52	5	17	0	0	0	24
1	0	0	0	0	0	0	0	0	0	0	1	1	0	0	0	0	1
2	0	0	0	0	2	0	0	0	0	17	15	2	4	0	0	0	3
3	0	0	0	0	1	0	0	0	0	26	20	1	9	0	0	0	8
4	0	0	0	0	0	0	0	0	0	19	14	1	4	0	0	0	11
5	0	0	0	0	0	0	0	0	0	2	2	0	0	0	0	0	1
6	0	0	0	0	0	0	0	0	0	0	0	0	0	0	0	0	0
SA-9-m	0	0	0	0	0	0	0	0	0	58	51	10	32	0	0	0	22
1	0	0	0	0	0	0	0	0	0	1	7	0	0	0	0	0	0
2	0	0	0	0	0	0	0	0	0	18	24	3	5	0	0	0	3
3	0	0	0	0	0	0	0	0	0	21	14	6	18	0	0	0	5
4	0	0	0	0	0	0	0	0	0	15	6	1	9	0	0	0	12
5	0	0	0	0	0	0	0	0	0	3	0	0	0	0	0	0	2
6	0	0	0	0	0	0	0	0	0	0	0	0	0	0	0	0	0
SA-10-m	0	0	0	0	0	0	0	0	0	54	42	9	25	0	0	0	47
1	0	0	0	0	0	0	0	0	0	2	1	0	1	0	0	0	0
2	0	0	0	0	0	0	0	0	0	9	12	4	6	0	0	0	2
3	0	0	0	0	0	0	0	0	0	32	23	5	14	0	0	0	15
4	0	0	0	0	0	0	0	0	0	9	6	0	4	0	0	0	25
5	0	0	0	0	0	0	0	0	0	2	0	0	0	0	0	0	5
6	0	0	0	0	0	0	0	0	0	0	0	0	0	0	0	0	0
SA-11-m	0	0	0	0	0	0	0	0	0	62	45	4	11	9	0	0	46
1	0	0	0	0	0	0	0	0	0	0	0	0	0	0	0	0	1
2	0	0	0	0	0	0	0	0	0	11	12	0	0	3	0	0	8
3	0	0	0	0	0	0	0	0	0	36	25	3	8	4	0	0	16
4	0	0	0	0	0	0	0	0	0	12	6	1	3	2	0	0	20
5	0	0	0	0	0	0	0	0	0	2	2	0	0	0	0	0	1
6	0	0	0	0	0	0	0	0	0	1	0	0	0	0	0	0	0

*Key to Grain Shape Categories. **1** = very angular; **2** = angular; **3** = sub-angular; **4** = sub-rounded; **5** = rounded; **6** = well rounded; Vc: very coarse sand fraction; C: coarse sand fraction; m: medium sand fraction; f: fine sand fraction; Vf: very fine sand fraction.

SALINA ISLAND (continued)

SAMPLE	Lvmibrgl	Lvmiorgl	Lvmigrgl	Lvmiclgl	Lvmialtgl	Lvvblgl	Lvvbrgl	Lvvorgl	Lvvgrgl	Lvvclgl	Lvvalgl	Lvf	Pmcl	Lm	Lp	Lvo	Lsc (crist)	Lsc (micr)	Bio	Unknow	TOT
SA-7-m	17	0	3	0	0	22	21	2	0	0	6	0	0	0	0	0	0	0	0	0	400
1	0	0	0	0	0	9	7	1	0	0	0	0	0	0	0	0	0	0	0	0	48
2	3	0	0	0	0	11	11	1	0	0	1	0	0	0	0	0	0	0	0	0	155
3	6	0	1	0	0	2	3	0	0	0	2	0	0	0	0	0	0	0	0	0	146
4	8	0	2	0	0	0	0	0	0	0	3	0	0	0	0	0	0	0	0	0	48
5	0	0	0	0	0	0	0	0	0	0	0	0	0	0	0	0	0	0	0	0	3
6	0	0	0	0	0	0	0	0	0	0	0	0	0	0	0	0	0	0	0	0	0
SA-8-m	19	3	11	0	0	13	14	0	0	0	0	0	0	0	0	0	0	0	0	0	400
1	0	0	0	0	0	0	1	0	0	0	0	0	0	0	0	0	0	0	0	0	18
2	5	0	1	0	0	7	8	0	0	0	0	0	0	0	0	0	0	0	0	0	128
3	7	1	5	0	0	5	3	0	0	0	0	0	0	0	0	0	0	0	0	0	153
4	7	2	5	0	0	1	2	0	0	0	0	0	0	0	0	0	0	0	0	0	96
5	0	0	0	0	0	0	0	0	0	0	0	0	0	0	0	0	0	0	0	0	5
6	0	0	0	0	0	0	0	0	0	0	0	0	0	0	0	0	0	0	0	0	0
SA-9-m	15	4	20	0	0	13	23	0	0	2	6	0	3	0	0	0	0	0	0	0	400
1	0	0	0	0	0	2	4	0	0	0	0	0	0	0	0	0	0	0	0	0	20
2	2	0	3	0	0	7	16	0	0	2	2	0	2	0	0	0	0	0	0	0	122
3	4	3	7	0	0	3	3	0	0	0	2	0	1	0	0	0	0	0	0	0	154
4	8	1	9	0	0	1	0	0	0	0	2	0	0	0	0	0	0	0	0	0	91
5	1	0	1	0	0	0	0	0	0	0	0	0	0	0	0	0	0	0	0	0	13
6	0	0	0	0	0	0	0	0	0	0	0	0	0	0	0	0	0	0	0	0	0
SA-10-m	27	0	16	0	0	12	17	6	0	0	9	0	0	0	0	0	0	0	0	0	400
1	0	0	0	0	0	3	3	0	0	0	0	0	0	0	0	0	0	0	0	0	15
2	3	0	0	0	0	7	8	2	0	0	1	0	0	0	0	0	0	0	0	0	96
3	12	0	8	0	0	2	5	3	0	0	4	0	0	0	0	0	0	0	0	0	191
4	11	0	8	0	0	0	1	1	0	0	4	0	0	0	0	0	0	0	0	0	89
5	1	0	0	0	0	0	0	0	0	0	0	0	0	0	0	0	0	0	0	0	9
6	0	0	0	0	0	0	0	0	0	0	0	0	0	0	0	0	0	0	0	0	0
SA-11-m	36	4	7	0	0	21	6	0	0	4	4	0	2	0	0	0	0	0	0	0	400
1	0	0	0	0	0	2	1	0	0	0	0	0	0	0	0	0	0	0	0	0	9
2	3	1	0	0	0	11	4	0	0	3	0	0	1	0	0	0	0	0	0	0	94
3	16	2	1	0	0	6	1	0	0	1	2	0	1	0	0	0	0	0	0	0	190
4	17	1	6	0	0	2	0	0	0	0	2	0	0	0	0	0	0	0	0	0	99
5	0	0	0	0	0	0	0	0	0	0	0	0	0	0	0	0	0	0	0	0	7
6	0	0	0	0	0	0	0	0	0	0	0	0	0	0	0	0	0	0	0	0	1

SAMPLE	P	P in Lvl	P inLvlblgl	P inLvlbrgl	P inLvlorgl	P inLvlgrgl	P inLvlclgl	P alt	P in Rp	P in Pm	Py	Py in Lvlblgl	Py in Lvlbrgl	Py in Lvlorgl	Py in Lvlgrgl
SA-12-m	44	0	10	8	13	0	0	0	3	0	62	4	6	0	0
1	2	0	1	1	2	0	0	0	0	0	6	0	0	0	0
2	11	0	3	2	5	0	0	0	0	0	16	1	2	0	0
3	22	0	4	4	5	0	0	0	3	0	21	2	4	0	0
4	8	0	2	1	1	0	0	0	0	0	17	1	0	0	0
5	1	0	0	0	0	0	0	0	0	0	2	0	0	0	0
6		0	0	0	0	0	0	0	0	0	0	0	0	0	0
SA-13-m	36	0	17	9	0	0	0	0	0	0	40	24	0	0	0
1	1	0	1	0	0	0	0	0	0	0	7	2	0	0	0
2	5	0	3	1	0	0	0	0	0	0	10	6	0	0	0
3	16	0	10	5	0	0	0	0	0	0	10	12	0	0	0
4	13	0	3	2	0	0	0	0	0	0	11	4	0	0	0
5	1	0	0	1	0	0	0	0	0	0	2	0	0	0	0
6	0	0	0	0	0	0	0	0	0	0	0	0	0	0	0
SA-14-m	37	0	19	20	0	0	0	4	0	0	35	7	0	0	0
1	1	0	0	0	0	0	0	0	0	0	3	0	0	0	0
2	7	0	6	4	0	0	0	1	0	0	10	2	0	0	0
3	19	0	10	10	0	0	0	2	0	0	12	4	0	0	0
4	9	0	3	6	0	0	0	1	0	0	10	1	0	0	0
5	1	0	0	0	0	0	0	0	0	0	0	0	0	0	0
6		0	0	0	0	0	0	0	0	0	0	0	0	0	0
SA-15-m	46	0	12	12	0	0	11	0	0	0	7	0	0	0	0
1	2	0	0	1	0	0	0	0	0	0	0	0	0	0	0
2	15	0	4	4	0	0	3	0	0	0	4	0	0	0	0
3	21	0	7	6	0	0	6	0	0	0	3	0	0	0	0
4	7	0	1	1	0	0	2	0	0	0	0	0	0	0	0
5	1	0	0	0	0	0	0	0	0	0	0	0	0	0	0
6	0	0	0	0	0	0	0	0	0	0	0	0	0	0	0

*Key to Grain Shape Categories. **1** = very angular; **2** = angular; **3** = sub-angular; **4** = sub-rounded; **5** = rounded; **6** = well rounded; Vc: very coarse sand fraction; C: coarse sand fraction; m: medium sand fraction; f: fine sand fraction; Vf: very fine sand fraction.

SALINA ISLAND (continued)

SAMPLE	Py in Lvlclgl	Py alt	K	K in Lvlblgl	K in Lvlbrgl	K in Lvlorgl	K in Lvlgrgl	K in Lvlclgl	K in Rp	Ol	Ol inLvlblgl	Ol inLvlbrgl	Ol inLvlorgl	Ol inLvlgrgl	Ol alt
SA-12-m	0	0	8	0	0	0	0	0	4	4	0	0	0	0	0
1	0	0	0	0	0	0	0	0	0	0	0	0	0	0	0
2	0	0	1	0	0	0	0	0	0	0	0	0	0	0	0
3	0	0	2	0	0	0	0	0	3	1	0	0	0	0	0
4	0	0	4	0	0	0	0	0	1	2	0	0	0	0	0
5	0	0	1	0	0	0	0	0	0	1	0	0	0	0	0
6	0	0	0	0	0	0	0	0	0	0	0	0	0	0	0
SA-13-m	0	0	7	0	0	0	0	0	0	5	0	0	0	0	0
1	0	0	0	0	0	0	0	0	0	0	0	0	0	0	0
2	0	0	1	0	0	0	0	0	0	1	0	0	0	0	0
3	0	0	4	0	0	0	0	0	0	3	0	0	0	0	0
4	0	0	2	0	0	0	0	0	0	1	0	0	0	0	0
5	0	0	0	0	0	0	0	0	0	0	0	0	0	0	0
6	0	0	0	0	0	0	0	0	0	0	0	0	0	0	0
SA-14-m	0	0	16	0	0	0	0	0	0	3	0	1	0	0	0
1	0	0	0	0	0	0	0	0	0	0	0	0	0	0	0
2	0	0	3	0	0	0	0	0	0	2	0	0	0	0	0
3	0	0	8	0	0	0	0	0	0	1	0	0	0	0	0
4	0	0	5	0	0	0	0	0	0	0	0	0	0	0	0
5	0	0	0	0	0	0	0	0	0	0	0	0	0	0	0
6	0	0	0	0	0	0	0	0	0	0	0	1	0	0	0
SA-15-m	0	0	0	0	0	0	0	0	0	0	0	0	0	0	0
1	0	0	0	0	0	0	0	0	0	0	0	0	0	0	0
2	0	0	0	0	0	0	0	0	0	0	0	0	0	0	0
3	0	0	0	0	0	0	0	0	0	0	0	0	0	0	0
4	0	0	0	0	0	0	0	0	0	0	0	0	0	0	0
5	0	0	0	0	0	0	0	0	0	0	0	0	0	0	0
6	0	0	0	0	0	0	0	0	0	0	0	0	0	0	0

SAMPLE	Hb	Hbalt	Hb in Lvlblgl	Hb in Lvlbrgl	Hb in Lvlgrgl	Hb in Lvlclgl	Hb in Rp	Gr	Ru	Ru in Lvlblgl	Ru in Lvlbrgl	Op	Op in Lvlbrgl	Op in Pm	Bt
SA-12-m	3	0	0	0	0	0	0	2	0	0	0	4	0	0	0
1	0	0	0	0	0	0	0	0	0	0	0	0	0	0	0
2	1	0	0	0	0	0	0	0	0	0	0	1	0	0	0
3	2	0	0	0	0	0	0	1	0	0	0	1	0	0	0
4	0	0	0	0	0	0	0	1	0	0	0	2	0	0	0
5	0	0	0	0	0	0	0	0	0	0	0	0	0	0	0
6	0	0	0	0	0	0	0	0	0	0	0	0	0	0	0
SA-13-m	0	0	0	0	0	0	0	0	0	0	0	12	0	0	0
1	0	0	0	0	0	0	0	0	0	0	0	0	0	0	0
2	0	0	0	0	0	0	0	0	0	0	0	1	0	0	0
3	0	0	0	0	0	0	0	0	0	0	0	6	0	0	0
4	0	0	0	0	0	0	0	0	0	0	0	5	0	0	0
5	0	0	0	0	0	0	0	0	0	0	0	0	0	0	0
6	0	0	0	0	0	0	0	0	0	0	0	0	0	0	0
SA-14-m	0	0	0	0	0	0	0	0	0	0	0	0	0	0	0
1	0	0	0	0	0	0	0	0	0	0	0	0	0	0	0
2	0	0	0	0	0	0	0	0	0	0	0	0	0	0	0
3	0	0	0	0	0	0	0	0	0	0	0	0	0	0	0
4	0	0	0	0	0	0	0	0	0	0	0	0	0	0	0
5	0	0	0	0	0	0	0	0	0	0	0	0	0	0	0
6	0	0	0	0	0	0	0	0	0	0	0	0	0	0	0
SA-15-m	0	0	0	0	0	0	0	3	0	0	0	0	0	0	0
1	0	0	0	0	0	0	0	0	0	0	0	0	0	0	0
2	0	0	0	0	0	0	0	0	0	0	0	0	0	0	0
3	0	0	0	0	0	0	0	1	0	0	0	0	0	0	0
4	0	0	0	0	0	0	0	1	0	0	0	0	0	0	0
5	0	0	0	0	0	0	0	1	0	0	0	0	0	0	0
6	0	0	0	0	0	0	0	0	0	0	0	0	0	0	0

*Key to Grain Shape Categories. **1** = very angular; **2** = angular; **3** = sub-angular; **4** = sub-rounded; **5** = rounded; **6** = well rounded; Vc: very coarse sand fraction; C: coarse sand fraction; m: medium sand fraction; f: fine sand fraction; Vf: very fine sand fraction.

SALINA ISLAND (continued)

SAMPLE	Bt in Rp	Bt in Rm	Mu	Mu in Rm	Qz-m	Q-p	Q in Rp	Q in Rm	Lvl	Lvlblgl	Lvlbrgl	Lvlorgl	Lvlgrgl	Lvlclgl	Lvlaltgl	Lvmi	Lvmiblgl
SA-12-m	0	0	0	0	0	0	0	4	0	49	40	11	16	0	0	0	51
1	0	0	0	0	0	0	0	0	0	3	2	1	0	0	0	0	4
2	0	0	0	0	0	0	0	0	0	13	6	3	1	0	0	0	8
3	0	0	0	0	0	0	0	3	0	24	23	5	9	0	0	0	17
4	0	0	0	0	0	0	0	1	0	6	8	2	4	0	0	0	20
5	0	0	0	0	0	0	0	0	0	2	1	0	2	0	0	0	2
6	0	0	0	0	0	0	0	0	0	1	0	0	0	0	0	0	0
SA-13-m	0	0	0	0	3	0	0	0	0	68	48	3	5	5	0	0	52
1	0	0	0	0	0	0	0	0	0	4	3	0	0	0	0	0	4
2	0	0	0	0	1	0	0	0	0	20	8	1	1	1	0	0	6
3	0	0	0	0	2	0	0	0	0	30	26	2	3	3	0	0	16
4	0	0	0	0	0	0	0	0	0	10	8	0	1	1	0	0	21
5	0	0	0	0	0	0	0	0	0	3	3	0	0	0	0	0	4
6	0	0	0	0	0	0	0	0	0	1	0	0	0	0	0	0	1
SA-14-m	0	0	0	0	0	0	0	0	0	67	64	0	16	4	0	0	23
1	0	0	0	0	0	0	0	0	0		0	0	0	0	0	0	0
2	0	0	0	0	0	0	0	0	0	8	10	0	5	1	0	0	0
3	0	0	0	0	0	0	0	0	0	36	33	0	7	3	0	0	8
4	0	0	0	0	0	0	0	0	0	22	19	0	4	0	0	0	14
5	0	0	0	0	0	0	0	0	0	1	2	0	0	0	0	0	1
6	0	0	0	0	0	0	0	0	0		0	0	0	0	0	0	0
SA-15-m	0	0	0	0	0	0	0	0	0	40	62	2	28	22	0	0	29
1	0	0	0	0	0	0	0	0	0		1	0	1	1	0	0	0
2	0	0	0	0	0	0	0	0	0	8	15	1	4	5	0	0	1
3	0	0	0	0	0	0	0	0	0	23	32	1	12	12	0	0	6
4	0	0	0	0	0	0	0	0	0	8	13	0	11	4	0	0	16
5	0	0	0	0	0	0	0	0	0	1	1	0	0	0	0	0	6
6	0	0	0	0	0	0	0	0	0	0	0	0	0	0	0	0	0

SAMPLE	Lvmibrgl	Lvmiorgl	Lvmigrgl	Lvmiclgl	Lvmialtgl	Lvvblgl	Lvvbrgl	Lvvorgl	Lvvgrgl	Lvvclgl	Lvvalgl	Lvf	Pmcl	Lm	Lp	Lvo	Lsc (crist)	Lsc (micr)	Bio	Unknow	TOT
SA-12-m	25	5	4	0	0	9	4	0	0	0	0	0	0	2	0	0	4	1	0	0	400
1	1	0	0	0	0	2	0	0	0	0	0	0	0	0	0	0	0	0	0	0	25
2	4	0		0	0	3	3	0	0	0	0	0	0		0	0	0	0	0	0	84
3	9	2	1	0	0	4	1	0	0	0	0	0	0	2	0	0	3	0	0	0	178
4	9	3	3	0	0	0	0	0	0	0	0	0	0	0	0	0	1	1	0	0	98
5	2	0		0	0	0	0	0	0	0	0	0	0	0	0	0	0	0	0	0	14
6	0	0		0	0	0	0	0	0	0	0	0	0	0	0	0	0	0	0	0	1
SA-13-m	38	2	4	0	0	7	2	0	0	0	0	0	9	0	0	0	0	0	0	4	400
1	2	0	0	0	0	0	0	0	0	0	0	0	1	0	0	0	0	0	0	0	25
2	3	0	0	0	0	4	1	0	0	0	0	0	2	0	0	0	0	0	0	1	77
3	12	1	1	0	0	3	1	0	0	0	0	0	5	0	0	0	0	0	0	2	173
4	16	1	3	0	0	0	0	0	0	0	0	0	1	0	0	0	0	0	0	1	104
5	4	0	0	0	0	0	0	0	0	0	0	0		0	0	0	0	0	0	0	18
6	1	0	0	0	0	0	0	0	0	0	0	0		0	0	0	0	0	0	0	3
SA-14-m	28	2	4	0	3	20	7	0	0	0	3	0	5	0	0	0	6	6	0	0	400
1	0	0	0	0	0	1	1	0	0	0	0	0		0	0	0	0	0	0	0	6
2	2	0	0	0	0	11	4	0	0	0	0	0	2	0	0	0	1	1	0	0	80
3	9	2	2	0	2	8	2	0	0	0	2	0	3	0	0	0	2	3	0	0	188
4	15	0	2	0	1	0	0	0	0	0	1	0		0	0	0	3	2	0	0	118
5	2	0	0	0	0	0	0	0	0	0	0	0		0	0	0	0	0	0	0	7
6	0	0	0	0	0	0	0	0	0	0	0	0		0	0	0	0	0	0	0	1
SA-15-m	44	2	19	14	0	12	13	0	0	4	0	0	4	3	0	0	0	6	5	0	400
1	0	0	0	0	0	1	3	0	0	0	0	0	0		0	0	0	0	0	0	10
2	2	0	0	1	0	7	8	0	0	2	0	0	1		0	0	0	1	0	0	86
3	13	1	4	4	0	3	2	0	0	2	0	0	2	2	0	0	0	4	3	0	170
4	22	1	14	8	0	1	0	0	0	0	0	0	1	1	0	0	0	1	2	0	115
5	7	0	1	1	0	0	0	0	0	0	0	0			0	0	0	0	0	0	19
6	0	0	0	0	0	0	0	0	0	0	0	0	0	0	0	0	0	0	0	0	0

*Key to Grain Shape Categories. **1** = very angular; **2** = angular; **3** = sub-angular; **4** = sub-rounded; **5** = rounded; **6** = well rounded; Vc: very coarse sand fraction; C: coarse sand fraction; m: medium sand fraction; f: fine sand fraction; Vf: very fine sand fraction.

FILICUFI ISLAND

SAMPLE	P	P in Lvl	P inLvlblgl	P inLvlbrgl	P inLvlorgl	P inLvlgrgl	P inLvlclgl	P alt	P in Rp	P in Pm	Py	Py in Lvlblgl	Py in Lvlbrgl	Py in Lvlorgl	Py in Lvlgrgl
Fi-1-m	13	0	9	17	0	0	0	0	0	0	87	10	5	0	0
1	0	0	0	0	0	0	0	0	0	0	3	0	0	0	0
2	4	0	3	3	0	0	0	0	0	0	31	0	0	0	0
3	8	0	5	7	0	0	0	0	0	0	32	7	2	0	0
4	1	0	1	6	0	0	0	0	0	0	20	3	3	0	0
5	0	0	0	1	0	0	0	0	0	0	1	0	0	0	0
6	0	0	0	0	0	0	0	0	0	0	0	0	0	0	0
Fi-2-m	32	0	17	29	0	0	0	0	0	0	56	0	19	0	0
1	0	0	0	0	0	0	0	0	0	0	1	0	0	0	0
2	3	0	6	8	0	0	0	0	0	0	14	0	2	0	0
3	14	0	7	11	0	0	0	0	0	0	21	0	12	0	0
4	15	0	2	10	0	0	0	0	0	0	18	0	5	0	0
5	0	0	2	0	0	0	0	0	0	0	2	0	0	0	0
6	0	0	0	0	0	0	0	0	0	0	0	0	0	0	0
Fi-3-Vc	5	0	15	20	0	0	0	0	1	0	9	10	23	0	0
1	0	0	0	2	0	0	0	0	0	0	1	0	0	0	0
2	3	0	7	9	0	0	0	0	0	0	5	5	9	0	0
3	2	0	8	8	0	0	0	0	1	0	3	4	13	0	0
4	0	0	0	1	0	0	0	0	0	0	0	1	1	0	0
5	0	0	0	0	0	0	0	0	0	0	0	0	0	0	0
6	0	0	0	0	0	0	0	0	0	0	0	0	0	0	0
Fi-3-C	19	0	63	49	0	0	0	0	0	0	9	21	15	0	0
1	0	0	4	2	0	0	0	0	0	0	2	0	1	0	0
2	7	0	21	13	0	0	0	0	0	0	3	4	3	0	0
3	9	0	23	18	0	0	0	0	0	0	3	12	7	0	0
4	3	0	14	12	0	0	0	0	0	0	1	4	4	0	0
5	0	0	1	3	0	0	0	0	0	0	0	1	0	0	0
6	0	0	0	1	0	0	0	0	0	0	0	0	0	0	0
Fi-3-m	35	0	52	15	0	0	0	4	0	0	24	10	8	0	0
1	0	0	0	0	0	0	0	0	0	0	0	0	0	0	0
2	4	0	10	5	0	0	0	0	0	0	4	2	4	0	0
3	22	0	32	8	0	0	0	2	0	0	12	4	2	0	0
4	9	0	8	2	0	0	0	2	0	0	8	4	2	0	0
5	0	0	2	0	0	0	0	0	0	0	0	0	0	0	0
6	0	0	0	0	0	0	0	0	0	0	0	0	0	0	0

SAMPLE	Py in Lvlclgl	Py alt	K	K in Lvlblgl	K in Lvlbrgl	K in Lvlorgl	K in Lvlgrgl	K in Lvlclgl	K in Rp	Ol	Ol inLvlblgl	Ol inLvlbrgl	Ol inLvlorgl	Ol inLvlgrgl	Ol alt
Fi-1-m	0	4	0	0	0	0	0	0	0	4	1	2	0	0	0
1	0	0	0	0	0	0	0	0	0	0	0	0	0	0	0
2	0	1	0	0	0	0	0	0	0	1	0	0	0	0	0
3	0	3	0	0	0	0	0	0	0	2	0	1	0	0	0
4	0	0	0	0	0	0	0	0	0	1	0	1	0	0	0
5	0	0	0	0	0	0	0	0	0	0	1	0	0	0	0
6	0	0	0	0	0	0	0	0	0	0	0	0	0	0	0
Fi-2-m	0	0	0	0	0	0	0	0	0	0	0	0	0	0	0
1	0	0	0	0	0	0	0	0	0	0	0	0	0	0	0
2	0	0	0	0	0	0	0	0	0	0	0	0	0	0	0
3	0	0	0	0	0	0	0	0	0	0	0	0	0	0	0
4	0	0	0	0	0	0	0	0	0	0	0	0	0	0	0
5	0	0	0	0	0	0	0	0	0	0	0	0	0	0	0
6	0	0	0	0	0	0	0	0	0	0	0	0	0	0	0
Fi-3-Vc	0	0	0	0	0	0	0	0	0	0	0	0	0	0	0
1	0	0	0	0	0	0	0	0	0	0	0	0	0	0	0
2	0	0	0	0	0	0	0	0	0	0	0	0	0	0	0
3	0	0	0	0	0	0	0	0	0	0	0	0	0	0	0
4	0	0	0	0	0	0	0	0	0	0	0	0	0	0	0
5	0	0	0	0	0	0	0	0	0	0	0	0	0	0	0
6	0	0	0	0	0	0	0	0	0	0	0	0	0	0	0
Fi-3-C	0	0	0	0	0	0	0	0	0	0	1	0	0	0	0
1	0	0	0	0	0	0	0	0	0	0	0	0	0	0	0
2	0	0	0	0	0	0	0	0	0	0	1	0	0	0	0
3	0	0	0	0	0	0	0	0	0	0	0	0	0	0	0
4	0	0	0	0	0	0	0	0	0	0	0	0	0	0	0
5	0	0	0	0	0	0	0	0	0	0	0	0	0	0	0
6	0	0	0	0	0	0	0	0	0	0	0	0	0	0	0
Fi-3-m	0	0	0	0	0	0	0	0	0	0	2	4	0	0	0
1	0	0	0	0	0	0	0	0	0	0	0	0	0	0	0
2	0	0	0	0	0	0	0	0	0	0	0	0	0	0	0
3	0	0	0	0	0	0	0	0	0	0	2	4	0	0	0
4	0	0	0	0	0	0	0	0	0	0	0	0	0	0	0
5	0	0	0	0	0	0	0	0	0	0	0	0	0	0	0
6	0	0	0	0	0	0	0	0	0	0	0	0	0	0	0

*Key to Grain Shape Categories. **1** = very angular; **2** = angular; **3** = sub-angular; **4** = sub-rounded; **5** = rounded; **6** = well rounded; Vc: very coarse sand fraction; C: coarse sand fraction; m: medium sand fraction; f: fine sand fraction; Vf: very fine sand fraction.

FILICUFI ISLAND (continued)

SAMPLE	Hb	Hbalt	Hb in Lvlblgl	Hb in Lvlbrgl	Hb in Lvlgrgl	Hb in Lvlclgl	Hb in Rp	Gr	Ru	Ru in Lvlblgl	Ru in Lvlbrgl	Op	Op in Lvlbrgl	Op in Pm	Bt
Fi-1-m	4	0	0	0	0	0	0	0	0	0	0	14	0	0	0
1	0	0	0	0	0	0	0	0	0	0	0	0	0	0	0
2	3	0	0	0	0	0	0	0	0	0	0	1	0	0	0
3	1	0	0	0	0	0	0	0	0	0	0	7	0	0	0
4	0	0	0	0	0	0	0	0	0	0	0	6	0	0	0
5	0	0	0	0	0	0	0	0	0	0	0	0	0	0	0
6	0	0	0	0	0	0	0	0	0	0	0	0	0	0	0
Fi-2-m	0	0	0	3	0	0	0	0	0	0	0	0	6	3	4
1	0	0	0	0	0	0	0	0	0	0	0	0	0	0	0
2	0	0	0	2	0	0	0	0	0	0	0	0	0	2	2
3	0	0	0	1	0	0	0	0	0	0	0	0	3	1	2
4	0	0	0	0	0	0	0	0	0	0	0	0	1	0	0
5	0	0	0	0	0	0	0	0	0	0	0	0	1	0	0
6	0	0	0	0	0	0	0	0	0	0	0	0	1	0	0
Fi-3-Vc	0	0	0	0	0	0	0	0	0	1	0	0	0	0	0
1	0	0	0	0	0	0	0	0	0	0	0	0	0	0	0
2	0	0	0	0	0	0	0	0	0	0	0	0	0	0	0
3	0	0	0	0	0	0	0	0	0	0	0	0	0	0	0
4	0	0	0	0	0	0	0	0	0	1	0	0	0	0	0
5	0	0	0	0	0	0	0	0	0	0	0	0	0	0	0
6	0	0	0	0	0	0	0	0	0	0	0	0	0	0	0
Fi-3-C	0	0	0	0	0	0	0	0	1	1	2	0	0	0	0
1	0	0	0	0	0	0	0	0	0	0	0	0	0	0	0
2	0	0	0	0	0	0	0	0	0	0	0	0	0	0	0
3	0	0	0	0	0	0	0	0	1	1	2	0	0	0	0
4	0	0	0	0	0	0	0	0	0	0	0	0	0	0	0
5	0	0	0	0	0	0	0	0	0	0	0	0	0	0	0
6	0	0	0	0	0	0	0	0	0	0	0	0	0	0	0
Fi-3-m	0	0	0	0	0	0	0	0	0	0	0	0	0	0	0
1	0	0	0	0	0	0	0	0	0	0	0	0	0	0	0
2	0	0	0	0	0	0	0	0	0	0	0	0	0	0	0
3	0	0	0	0	0	0	0	0	0	0	0	0	0	0	0
4	0	0	0	0	0	0	0	0	0	0	0	0	0	0	0
5	0	0	0	0	0	0	0	0	0	0	0	0	0	0	0
6	0	0	0	0	0	0	0	0	0	0	0	0	0	0	0

SAMPLE	Bt in Rp	Bt in Rm	Mu	Mu in Rm	Qz-m	Q-p	Q in Rp	Q in Rm	Lvl	Lvlblgl	Lvlbrgl	Lvlorgl	Lvlgrgl	Lvlclgl	Lvlaltgl	Lvmi	Lvmiblgl
Fi-1-m	0	0	0	0	0	0	0	2	15	31	39	0	17	12	0	6	31
1	0	0	0	0	0	0	0	0	0	0	0	0	0	0	0	0	0
2	0	0	0	0	0	0	0	0	2	3	4	0	3	1	0	0	1
3	0	0	0	0	0	0	0	1	8	18	16	0	8	6	0	3	16
4	0	0	0	0	0	0	0	1	5	10	18	0	6	3	0	3	14
5	0	0	0	0	0	0	0	0	0	0	1	0	0	2	0	0	0
6	0	0	0	0	0	0	0	0	0	0	0	0	0	0	0	0	0
Fi-2-m	0	0	0	0	0	0	4	0	0	24	77	0	0	7	8	0	25
1	0	0	0	0	0	0	0	0	0	0	0	0	0	0	0	0	0
2	0	0	0	0	0	0	0	0	0	6	8	0	0	3	0	0	1
3	0	0	0	0	0	0	1	0	0	8	32	0	0	2	4	0	9
4	0	0	0	0	0	0	2	0	0	10	31	0	0	2	2	0	13
5	0	0	0	0	0	0	0	0	0	0	6	0	0	0	2	0	2
6	0	0	0	0	0	0	1	0	0	0	0	0	0	0	0	0	0
Fi-3-Vc	0	0	0	0	0	0	0	0	0	59	81	1	0	0	0	0	6
1	0	0	0	0	0	0	0	0	0	2	4	0	0	0	0	0	0
2	0	0	0	0	0	0	0	0	0	30	40	1	0	0	0	0	1
3	0	0	0	0	0	0	0	0	0	24	33	0	0	0	0	0	2
4	0	0	0	0	0	0	0	0	0	3	3	0	0	0	0	0	3
5	0	0	0	0	0	0	0	0	0	0	1	0	0	0	0	0	0
6	0	0	0	0	0	0	0	0	0	0	0	0	0	0	0	0	0
Fi-3-C	0	0	0	0	0	0	0	0	0	69	61	3	13	0	5	0	20
1	0	0	0	0	0	0	0	0	0	4	0	0	1	0	0	0	1
2	0	0	0	0	0	0	0	0	0	15	19	2	3	0	0	0	3
3	0	0	0	0	0	0	0	0	0	30	29	1	7	0	1	0	6
4	0	0	0	0	0	0	0	0	0	19	13	0	2	0	3	0	10
5	0	0	0	0	0	0	0	0	0	1	0	0	0	0	1	0	0
6	0	0	0	0	0	0	0	0	0	0	0	0	0	0	0	0	0
Fi-3-m	0	0	0	0	0	0	0	0	0	54	50	0	0	8	0	0	36
1	0	0	0	0	0	0	0	0	0	2	4	0	0	0	0	0	0
2	0	0	0	0	0	0	0	0	0	18	10	0	0	2	0	0	2
3	0	0	0	0	0	0	0	0	0	18	20	0	0	4	0	0	16
4	0	0	0	0	0	0	0	0	0	14	12	0	0	2	0	0	16
5	0	0	0	0	0	0	0	0	0	2	4	0	0	0	0	0	2
6	0	0	0	0	0	0	0	0	0	0	0	0	0	0	0	0	0

*Key to Grain Shape Categories. **1** = very angular; **2** = angular; **3** = sub-angular; **4** = sub-rounded; **5** = rounded; **6** = well rounded; Vc: very coarse sand fraction; C: coarse sand fraction; m: medium sand fraction; f: fine sand fraction; Vf: very fine sand fraction.

FILICUFI ISLAND (continued) and ALICUDI ISLAND

SAMPLE	Lvmibrgl	Lvmiorgl	Lvmigrgl	Lvmiclgl	Lvmialtgl	Lvvblgl	Lvvbrgl	Lvvorgl	Lvvgrgl	Lvvclgl	Lvvalgl	Lvf	Pmcl	Lm	Lp	Lvo	Lsc (crist)	Lsc (micr)	Bio	Unknow	TOT
Fi-1-m	29	0	10	5	0	14	16	0	0	0	0	0	0	0	0	0	0	0	3	0	400
1	0	0	0	0	0	2	2	0	0	0	0	0	0	0	0	0	0	0	0	0	7
2	0	0	0	0	0	9	8	0	0	0	0	0	0	0	0	0	0	0	0	0	78
3	12	0	4	2	0	3	6	0	0	0	0	0	0	0	0	0	0	0	2	0	180
4	16	0	5	3	0	0	0	0	0	0	0	0	0	0	0	0	0	0	1	0	127
5	1	0	1	0	0	0	0	0	0	0	0	0	0	0	0	0	0	0	0	0	8
6	0	0	0	0	0	0	0	0	0	0	0	0	0	0	0	0	0	0	0	0	0
Fi-2-m	41	6	0	0	0	10	10	0	0	0	0	0	8	4	0	0	0	0	0	0	400
1	0	0	0	0	0	1	1	0	0	0	0	0	0	0	0	0	0	0	0	0	3
2	0	1	0	0	0	6	4	0	0	0	0	0	0	0	0	0	0	0	0	0	72
3	11	3	0	0	0	1	4	0	0	0	0	0	6	2	0	0	0	0	0	0	157
4	23	2	0	0	0	2	1	0	0	0	0	0	2	2	0	0	0	0	0	0	144
5	7	0	0	0	0	0	0	0	0	0	0	0	0	0	0	0	0	0	0	0	22
6	0	0	0	0	0	0	0	0	0	0	0	0	0	0	0	0	0	0	0	0	2
Fi-3-Vc	13	0	0	0	0	0	10	6	0	0	0	0	0	0	0	0	0	0	0	0	260
1	0	0	0	0	0	0	4	3	0	0	0	0	0	0	0	0	0	0	0	0	16
2	0	0	0	0	0	0	6	3	0	0	0	0	0	0	0	0	0	0	0	0	119
3	5	0	0	0	0	0	0	0	0	0	0	0	0	0	0	0	0	0	0	0	103
4	8	0	0	0	0	0	0	0	0	0	0	0	0	0	0	0	0	0	0	0	21
5	0	0	0	0	0	0	0	0	0	0	0	0	0	0	0	0	0	0	0	0	1
6	0	0	0	0	0	0	0	0	0	0	0	0	0	0	0	0	0	0	0	0	0
Fi-3-C	22	0	4	0	0	13	9	0	0	0	0	0	0	0	0	0	0	0	0	0	400
1	1	0	0	0	0	2	3	0	0	0	0	0	0	0	0	0	0	0	0	0	21
2	4	0	1	0	0	9	3	0	0	0	0	0	0	0	0	0	0	0	0	0	111
3	8	0	1	0	0	1	3	0	0	0	0	0	0	0	0	0	0	0	0	0	163
4	9	0	2	0	0	1	0	0	0	0	0	0	0	0	0	0	0	0	0	0	97
5	0	0	0	0	0	0	0	0	0	0	0	0	0	0	0	0	0	0	0	0	7
6	0	0	0	0	0	0	0	0	0	0	0	0	0	0	0	0	0	0	0	0	1
Fi-3-m	51	0	2	0	0	28	17	0	0	0	0	0	0	0	0	0	0	0	0	0	400
1	0	0	0	0	0	6	3	0	0	0	0	0	0	0	0	0	0	0	0	0	15
2	4	0	0	0	0	14	11	0	0	0	0	0	0	0	0	0	0	0	0	0	90
3	23	0	2	0	0	8	3	0	0	0	0	0	0	0	0	0	0	0	0	0	182
4	18	0	0	0	0	0	0	0	0	0	0	0	0	0	0	0	0	0	0	0	97
5	4	0	0	0	0	0	0	0	0	0	0	0	0	0	0	0	0	0	0	0	14
6	2	0	0	0	0	0	0	0	0	0	0	0	0	0	0	0	0	0	0	0	2

SAMPLE	P	P in Lvl	P inLvlblgl	P inLvlbrgl	P inLvlorgl	P inLvlgrgl	P inLvlclgl	P alt	P in Rp	P in Pm	Py	Py in Lvlblgl	Py in Lvlbrgl	Py in Lvlorgl	Py in Lvlgrgl
Fi-3-f	35	0	18	14	0	0	0	0	0	0	26	20	10	0	0
1	3	0	1	0	0	0	0	0	0	0	1	0	0	0	0
2	13	0	6	4	0	0	0	0	0	0	9	6	2	0	0
3	17	0	8	9	0	0	0	0	0	0	10	7	7	0	0
4	2	0	3	1	0	0	0	0	0	0	3	7	1	0	0
5	0	0	0	0	0	0	0	0	0	0	2	0	0	0	0
6	0	0	0	0	0	0	0	0	0	0	1	0	0	0	0
Fi-3-Vf	17	0	0	0	0	0	0	0	0	0	20	0	0	0	0
1	0	0	0	0	0	0	0	0	0	0	1	0	0	0	0
2	4	0	0	0	0	0	0	0	0	0	8	0	0	0	0
3	12	0	0	0	0	0	0	0	0	0	10	0	0	0	0
4	1	0	0	0	0	0	0	0	0	0	1	0	0	0	0
5	0	0	0	0	0	0	0	0	0	0	0	0	0	0	0
6	0	0	0	0	0	0	0	0	0	0	0	0	0	0	0
Fi-4-m	30	7	7	14	0	6	6	0	0	0	32	7	0	0	0
1	1	0	0	1	0	0	0	0	0	0	2	0	0	0	0
2	9	2	2	5	0	2	2	0	0	0	13	2	0	0	0
3	14	5	4	8	0	4	4	0	0	0	15	5	0	0	0
4	6	0	1	0	0	0	0	0	0	0	2	0	0	0	0
5	0	0	0	0	0	0	0	0	0	0	0	0	0	0	0
6	0	0	0	0	0	0	0	0	0	0	0	0	0	0	0
AL-1-m	40	0	24	14	0	0	0	4	0	0	36	7	7	0	0
1	4	0	0	0	0	0	0	0	0	0	1	0	0	0	0
2	9	0	7	3	0	0	0	1	0	0	8	2	2	0	0
3	21	0	12	9	0	0	0	2	0	0	15	4	4	0	0
4	6	0	4	2	0	0	0	1	0	0	11	1	1	0	0
5	0	0	1	0	0	0	0	0	0	0	1	0	0	0	0
6	0	0	0	0	0	0	0	0	0	0	0	0	0	0	0
AL-2-m	50	0	19	18	0	0	0	0	3	0	16	26	29	0	0
1	3	0	0	0	0	0	0	0	0	0	3	2	0	0	0
2	11	0	3	3	0	0	0	0	1	0	4	7	6	0	0
3	23	0	14	14	0	0	0	0	2	0	8	11	16	0	0
4	9	0	2	1	0	0	0	0	0	0	1	4	6	0	0
5	4	0	0	0		0	0	0	0	0	0	2	1	0	0
6	0	0	0	0	0	0	0	0	0	0	0	0	0	0	0

*Key to Grain Shape Categories. **1** = very angular; **2** = angular; **3** = sub-angular; **4** = sub-rounded; **5** = rounded; **6** = well rounded; Vc: very coarse sand fraction; C: coarse sand fraction; m: medium sand fraction; f: fine sand fraction; Vf: very fine sand fraction.

FILICUFI ISLAND (continued) and ALICUDI ISLAND

SAMPLE	Py in Lvlclgl	Py alt	K	K in Lvlblgl	K in Lvlbrgl	K in Lvlorgl	K in Lvlgrgl	K in Lvlclgl	K in Rp	Ol	Ol inLvlblgl	Ol inLvlbrgl	Ol inLvlorgl	Ol inLvlgrgl	Ol alt
Fi-3-f	0	0	0	0	0	0	0	0	0	0	0	0	0	0	0
1	0	0	0	0	0	0	0	0	0	0	0	0	0	0	0
2	0	0	0	0	0	0	0	0	0	0	0	0	0	0	0
3	0	0	0	0	0	0	0	0	0	0	0	0	0	0	0
4	0	0	0	0	0	0	0	0	0	0	0	0	0	0	0
5	0	0	0	0	0	0	0	0	0	0	0	0	0	0	0
6	0	0	0	0	0	0	0	0	0	0	0	0	0	0	0
Fi-3-Vf	0	0	0	0	0	0	0	0	0	0	0	0	0	0	0
1	0	0	0	0	0	0	0	0	0	0	0	0	0	0	0
2	0	0	0	0	0	0	0	0	0	0	0	0	0	0	0
3	0	0	0	0	0	0	0	0	0	0	0	0	0	0	0
4	0	0	0	0	0	0	0	0	0	0	0	0	0	0	0
5	0	0	0	0	0	0	0	0	0	0	0	0	0	0	0
6	0	0	0	0	0	0	0	0	0	0	0	0	0	0	0
Fi-4-m	0	0	0	0	0	0	0	0	0	0	0	0	0	0	0
1	0	0	0	0	0	0	0	0	0	0	0	0	0	0	0
2	0	0	0	0	0	0	0	0	0	0	0	0	0	0	0
3	0	0	0	0	0	0	0	0	0	0	0	0	0	0	0
4	0	0	0	0	0	0	0	0	0	0	0	0	0	0	0
5	0	0	0	0	0	0	0	0	0	0	0	0	0	0	0
6	0	0	0	0	0	0	0	0	0	0	0	0	0	0	0
AL-1-m	0	0	6	0	0	0	0	0	0	6	4	0	0	0	0
1	0	0	0	0	0	0	0	0	0	0	0	0	0	0	0
2	0	0	3	0	0	0	0	0	0	2	1	0	0	0	0
3	0	0	2	0	0	0	0	0	0	1	2	0	0	0	0
4	0	0	1	0	0	0	0	0	0	2	1	0	0	0	0
5	0	0	0	0	0	0	0	0	0	1	0	0	0	0	0
6	0	0	0	0	0	0	0	0	0	0	0	0	0	0	0
AL-2-m	0	0	4	6	6	0	0	0	0	2	8	0	0	0	0
1	0	0	0	0	0	0	0	0	0	0	0	0	0	0	0
2	0	0	1	1	1	0	0	0	0	1	2	0	0	0	0
3	0	0	2	4	4	0	0	0	0	1	3	0	0	0	0
4	0	0	1	1	1	0	0	0	0	0	2	0	0	0	0
5	0	0	0	0	0	0	0	0	0	0	1	0	0	0	0
6	0	0	0	0	0	0	0	0	0	0	0	0	0	0	0

SAMPLE	Hb	Hbalt	Hb in Lvlblgl	Hb in Lvlbrgl	Hb in Lvlgrgl	Hb in Lvlclgl	Hb in Rp	Gr	Ru	Ru in Lvlblgl	Ru in Lvlbrgl	Op	Op in Lvlbrgl	Op in Pm	Bt
Fi-3-f	0	0	0	0	0	0	0	0	3	0	0	0	0	0	0
1	0	0	0	0	0	0	0	0	0	0	0	0	0	0	0
2	0	0	0	0	0	0	0	0	2	0	0	0	0	0	0
3	0	0	0	0	0	0	0	0	1	0	0	0	0	0	0
4	0	0	0	0	0	0	0	0	0	0	0	0	0	0	0
5	0	0	0	0	0	0	0	0	0	0	0	0	0	0	0
6	0	0	0	0	0	0	0	0	0	0	0	0	0	0	0
Fi-3-Vf	0	0	0	0	0	0	0	0	0	0	0	20	0	0	0
1	0	0	0	0	0	0	0	0	0	0	0	1	0	0	0
2	0	0	0	0	0	0	0	0	0	0	0	8	0	0	0
3	0	0	0	0	0	0	0	0	0	0	0	10	0	0	0
4	0	0	0	0	0	0	0	0	0	0	0	1	0	0	0
5	0	0	0	0	0	0	0	0	0	0	0	0	0	0	0
6	0	0	0	0	0	0	0	0	0	0	0	0	0	0	0
Fi-4-m	32	0	0	4	7	0	0	0	0	0	0	22	0	0	0
1	0	0	0	0	0	0	0	0	0	0	0	0	0	0	0
2	14	0	0	2	3	0	0	0	0	0	0	2	0	0	0
3	15	0	0	2	4	0	0	0	0	0	0	7	0	0	0
4	3	0	0	0	0	0	0	0	0	0	0	13	0	0	0
5	0	0	0	0	0	0	0	0	0	0	0	0	0	0	0
6	0	0	0	0	0	0	0	0	0	0	0	0	0	0	0
AL-1-m	0	0	0	0	0	0	0	0	0	0	0	5	0	0	0
1	0	0	0	0	0	0	0	0	0	0	0	0	0	0	0
2	0	0	0	0	0	0	0	0	0	0	0	0	0	0	0
3	0	0	0	0	0	0	0	0	0	0	0	2	0	0	0
4	0	0	0	0	0	0	0	0	0	0	0	3	0	0	0
5	0	0	0	0	0	0	0	0	0	0	0	0	0	0	0
6	0	0	0	0	0	0	0	0	0	0	0	0	0	0	0
AL-2-m	0	0	0	0	0	0	0	0	0	0	0	0	0	0	0
1	0	0	0	0	0	0	0	0	0	0	0	0	0	0	0
2	0	0	0	0	0	0	0	0	0	0	0	0	0	0	0
3	0	0	0	0	0	0	0	0	0	0	0	0	0	0	0
4	0	0	0	0	0	0	0	0	0	0	0	0	0	0	0
5	0	0	0	0	0	0	0	0	0	0	0	0	0	0	0
6	0	0	0	0	0	0	0	0	0	0	0	0	0	0	0

*Key to Grain Shape Categories. **1** = very angular; **2** = angular; **3** = sub-angular; **4** = sub-rounded; **5** = rounded; **6** = well rounded; Vc: very coarse sand fraction; C: coarse sand fraction; m: medium sand fraction; f: fine sand fraction; Vf: very fine sand fraction.

FILICUFI ISLAND (continued) and ALICUDI ISLAND

SAMPLE	Bt in Rp	Bt in Rm	Mu	Mu in Rm	Qz-m	Q-p	Q in Rp	Q in Rm	Lvl	Lvlblgl	Lvlbrgl	Lvlorgl	Lvlgrgl	Lvlclgl	Lvlaltgl	Lvmi	Lvmiblgl
Fi-3-f	0	0	0	0	0	0	0	0	0	48	52	0	0	0	0	0	77
1	0	0	0	0	0	0	0	0	0	8	6	0	0	0	0	0	2
2	0	0	0	0	0	0	0	0	0	4	14	0	0	0	0	0	12
3	0	0	0	0	0	0	0	0	0	23	24	0	0	0	0	0	23
4	0	0	0	0	0	0	0	0	0	12	8	0	0	0	0	0	36
5	0	0	0	0	0	0	0	0	0	1	0	0	0	0	0	0	3
6	0	0	0	0	0	0	0	0	0	0	0	0	0	0	0	0	1
Fi-3-Vf	0	0	0	0	0	0	0	0	0	30	26	0	0	0	0	0	104
1	0	0	0	0	0	0	0	0	0	0	0	0	0	0	0	0	0
2	0	0	0	0	0	0	0	0	0	7	4	0	0	0	0	0	7
3	0	0	0	0	0	0	0	0	0	14	14	0	0	0	0	0	37
4	0	0	0	0	0	0	0	0	0	9	6	0	0	0	0	0	47
5	0	0	0	0	0	0	0	0	0	0	2	0	0	0	0	0	13
6	0	0	0	0	0	0	0	0	0	0	0	0	0	0	0	0	0
Fi-4-m	0	0	0	0	0	0	0	0	0	52	54	0	19	0	0	3	43
1	0	0	0	0	0	0	0	0	0	4	5	0	1	0	0	0	1
2	0	0	0	0	0	0	0	0	0	17	19	0	6	0	0	0	4
3	0	0	0	0	0	0	0	0	0	20	26	0	9	0	0	2	13
4	0	0	0	0	0	0	0	0	0	11	4	0	3	0	0	1	25
5	0	0	0	0	0	0	0	0	0	0	0	0	0	0	0	0	0
6	0	0	0	0	0	0	0	0	0	0	0	0	0	0	0	0	0
AL-1-m	0	0	0	0	5	1	1	0	0	49	42	4	9	0	8	0	38
1	0	0	0	0	0	0	0	0	0	1	1	0	0	0	0	0	0
2	0	0	0	0	2	0	0	0	0	7	5	1	1	0	1	0	0
3	0	0	0	0	3	0	0	0	0	28	23	3	5	0	6	0	11
4	0	0	0	0	0	1	1	0	0	12	13	0	3	0	1	0	25
5	0	0	0	0	0	0	0	0	0	1	0	0	0	0	0	0	2
6	0	0	0	0	0	0	0	0	0	0	0	0	0	0	0	0	0
AL-2-m	0	0	0	0	0	0	0	0	0	56	85	0	0	3	0	0	27
1	0	0	0	0	0	0	0	0	0	4	4	0	0	0	0	0	0
2	0	0	0	0	0	0	0	0	0	11	14	0	0	0	0	0	0
3	0	0	0	0	0	0	0	0	0	35	45	0	0	1	0	0	10
4	0	0	0	0	0	0	0	0	0	5	18	0	0	2	0	0	15
5	0	0	0	0	0	0	0	0	0	1	4	0	0	0	0	0	2
6	0	0	0	0	0	0	0	0	0	0	0	0	0	0	0	0	0

SAMPLE	Lvmibrgl	Lvmiorgl	Lvmigrgl	Lvmiclgl	Lvmialtgl	Lvvblgl	Lvvbrgl	Lvvorgl	Lvvgrgl	Lvvclgl	Lvvalgl	Lvf	Pmcl	Lm	Lp	Lvo	Lsc (crist)	Lsc (micr)	Bio	Unknow	TOT
Fi-3-f	69	0	0	0	0	13	15	0	0	0	0	0	0	0	0	0	0	0	0	0	400
1	1	0	0	0	0	4	3	0	0	0	0	0	0	0	0	0	0	0	0	0	29
2	6	0	0	0	0	6	9	0	0	0	0	0	0	0	0	0	0	0	0	0	93
3	24	0	0	0	0	3	3	0	0	0	0	0	0	0	0	0	0	0	0	0	159
4	32	0	0	0	0	0	0	0	0	0	0	0	0	0	0	0	0	0	0	0	105
5	4	0	0	0	0	0	0	0	0	0	0	0	0	0	0	0	0	0	0	0	10
6	2	0	0	0	0	0	0	0	0	0	0	0	0	0	0	0	0	0	0	0	4
Fi-3-Vf	90	0	0	0	0	55	38	0	0	0	0	0	0	0	0	0	0	0	0	0	400
1		0	0	0	0	7	3	0	0	0	0	0	0	0	0	0	0	0	0	0	12
2	10	0	0	0	0	21	13	0	0	0	0	0	0	0	0	0	0	0	0	0	82
3	32	0	0	0	0	23	18	0	0	0	0	0	0	0	0	0	0	0	0	0	170
4	40	0	0	0	0	4	3	0	0	0	0	0	0	0	0	0	0	0	0	0	112
5	8	0	0	0	0	0	1	0	0	0	0	0	0	0	0	0	0	0	0	0	24
6		0	0	0	0	0	0	0	0	0	0	0	0	0	0	0	0	0	0	0	0
Fi-4-m	30	0	0	0	0	18	7	0	0	0	0	0	0	0	0	0	0	0	0	0	400
1		0	0	0	0	7	2	0	0	0	0	0	0	0	0	0	0	0	0	0	24
2	2	0	0	0	0	8	4	0	0	0	0	0	0	0	0	0	0	0	0	0	118
3	13	0	0	0	0	3	1	0	0	0	0	0	0	0	0	0	0	0	0	0	174
4	14	0	0	0	0	0	0	0	0	0	0	0	0	0	0	0	0	0	0	0	83
5	1	0	0	0	0	0	0	0	0	0	0	0	0	0	0	0	0	0	0	0	1
6		0	0	0	0	0	0	0	0	0	0	0	0	0	0	0	0	0	0	0	0
AL-1-m	22	0	13	0	8	18	11	3	0	0	9	1	0	0	1	1	0	3	0	0	400
1		0	0	0	0	3	1	0	0	0	0	0	0	0	0	0	0	0	0	0	11
2		0	0	0	1	10	7	2	0	0	3	0	0	0	0	0	0	0	0	0	78
3	6	0	3	0	3	5	3	1	0	0	4	1	0	0	0	1	0	1	0	0	181
4	13	0	10	0	4	0	0	0	0	0	2	0	0	0	1	0	0	2	0	0	121
5	3	0	0	0	0	0	0	0	0	0	0	0	0	0	0	0	0	0	0	0	9
6		0	0	0	0	0	0	0	0	0	0	0	0	0	0	0	0	0	0	0	0
AL-2-m	18	0	0	0	8	9	7	0	0	0	0	0	0	0	0	0	0	0	0	0	400
1		0	0	0	0	2	1	0	0	0	0	0	0	0	0	0	0	0	0	0	19
2	1	0	0	0	1	4	4	0	0	0	0	0	0	0	0	0	0	0	0	0	76
3	4	0	0	0	3	1	2	0	0	0	0	0	0	0	0	0	0	0	0	0	203
4	12	0	0	0	4	2	0	0	0	0	0	0	0	0	0	0	0	0	0	0	86
5	1	0	0	0	0	0	0	0	0	0	0	0	0	0	0	0	0	0	0	0	16
6	0	0	0	0	0	0	0	0	0	0	0	0	0	0	0	0	0	0	0	0	0

*Key to Grain Shape Categories. **1** = very angular; **2** = angular; **3** = sub-angular; **4** = sub-rounded; **5** = rounded; **6** = well rounded; Vc: very coarse sand fraction; C: coarse sand fraction; m: medium sand fraction; f: fine sand fraction; Vf: very fine sand fraction.

ALICUDI ISLAND (continued)

SAMPLE	P	P in Lvl	P inLvlblgl	P inLvlbrgl	P inLvlorgl	P inLvlgrgl	P inLvlclgl	P alt	P in Rp	P in Pm	Py	Py in Lvlblgl	Py in Lvlbrgl	Py in Lvlorgl	Py in Lvlgrgl
AL-3-Vc	12	0	25	19	3	0	0	0	0	0	5	23	17	0	0
1	1	0	2	3	0	0	0	0	0	0	0	2	2	0	0
2	4	0	8	6	2	0	0	0	0	0	3	10	8	0	0
3	7	0	13	9	1	0	0	0	0	0	2	8	7	0	0
4	0	0	2	1	0	0	0	0	0	0	0	3	0	0	0
5	0	0	0	0	0	0	0	0	0	0	0	0	0	0	0
6	0	0	0	0	0	0	0	0	0	0	0	0	0	0	0
AL-3-C	14	0	36	23	10	0	0	0	0	0	25	19	10	0	0
1	2	0	6	2	3	0	0	0	0	0	3	1	1	0	0
2	6	0	14	11	5	0	0	0	0	0	11	6	6	0	0
3	5	0	15	10	2	0	0	0	0	0	9	9	2	0	0
4	1	0	1	0	0	0	0	0	0	0	2	3	1	0	0
5	0	0	0	0	0	0	0	0	0	0	0	0	0	0	0
6	0	0	0	0	0	0	0	0	0	0	0	0	0	0	0
AL-3-m	36	0	16	22	0	0	0	0	0	0	39	16	14	0	0
1	1	0	1	1	0	0	0	0	0	0	4	1	1	0	0
2	12	0	3	4	0	0	0	0	0	0	17	4	4	0	0
3	21	0	11	12	0	0	0	0	0	0	15	10	8	0	0
4	2	0	1	5	0	0	0	0	0	0	3	1	1	0	0
5	0	0	0	0	0	0	0	0	0	0	0	0	0	0	0
6	0	0	0	0	0	0	0	0	0	0	0	0	0	0	0
AL-3-f	45	0	22	9	6	0	0	0	0	0	53	9	13	0	0
1	3	0	0	0	0	0	0	0	0	0	3	0	0	0	0
2	17	0	7	3	1	0	0	0	0	0	18	1	4	0	0
3	21	0	13	6	3	0	0	0	0	0	26	5	7	0	0
4	4	0	2	0	1	0	0	0	0	0	4	3	2	0	0
5	0	0	0	0	0	0	0	0	0	0	2	0	0	0	0
6	0	0	0	0	1	0	0	0	0	0	0	0	0	0	0
AL-3-Vf	60	0	7	0	0	0	0	0	0	0	72	0	0	0	0
1	0	0	0	0	0	0	0	0	0	0	1	0	0	0	0
2	24	0	1	0	0	0	0	0	0	0	28	0	0	0	0
3	34	0	4	0	0	0	0	0	0	0	39	0	0	0	0
4	2	0	2	0	0	0	0	0	0	0	4	0	0	0	0
5	0	0	0	0	0	0	0	0	0	0	0	0	0	0	0
6	0	0	0	0	0	0	0	0	0	0	0	0	0	0	0

SAMPLE	Py in Lvlclgl	Py alt	K	K in Lvlblgl	K in Lvlbrgl	K in Lvlorgl	K in Lvlgrgl	K in Lvlclgl	K in Rp	Ol	Ol inLvlblgl	Ol inLvlbrgl	Ol inLvlorgl	Ol inLvlgrgl	Ol alt
AL-3-Vc	0	0	3	0	0	0	0	0	0	0	3	0	0	0	0
1	0	0	0	0	0	0	0	0	0	0	0	0	0	0	0
2	0	0	0	0	0	0	0	0	0	0	2	0	0	0	0
3	0	0	2	0	0	0	0	0	0	0	1	0	0	0	0
4	0	0	1	0	0	0	0	0	0	0	0	0	0	0	0
5	0	0	0	0	0	0	0	0	0	0	0	0	0	0	0
6	0	0	0	0	0	0	0	0	0	0	0	0	0	0	0
AL-3-C	0	0	4	0	0	0	0	0	0	0	8	7	0	0	0
1	0	0	0	0	0	0	0	0	0	0	3	0	0	0	0
2	0	0	1	0	0	0	0	0	0	0	3	2	0	0	0
3	0	0	3	0	0	0	0	0	0	0	2	4	0	0	0
4	0	0	0	0	0	0	0	0	0	0	0	1	0	0	0
5	0	0	0	0	0	0	0	0	0	0	0	0	0	0	0
6	0	0	0	0	0	0	0	0	0	0	0	0	0	0	0
AL-3-m	0	0	16	0	0	0	0	0	0	5	3	2	0	0	0
1	0	0	1	0	0	0	0	0	0	0	0	0	0	0	0
2	0	0	3	0	0	0	0	0	0	0	3	2	0	0	0
3	0	0	10	0	0	0	0	0	0	0	2	1	1	0	0
4	0	0	2	0	0	0	0	0	0	0	0	0	1	0	0
5	0	0	0	0	0	0	0	0	0	0	0	0	0	0	0
6	0	0	0	0	0	0	0	0	0	0	0	0	0	0	0
AL-3-f	0	0	11	0	0	0	0	0	0	6	0	0	0	0	0
1	0	0	0	0	0	0	0	0	0	0	0	0	0	0	0
2	0	0	3	0	0	0	0	0	0	1	0	0	0	0	0
3	0	0	7	0	0	0	0	0	0	2	0	0	0	0	0
4	0	0	1	0	0	0	0	0	0	3	0	0	0	0	0
5	0	0	0	0	0	0	0	0	0	0	0	0	0	0	0
6	0	0	0	0	0	0	0	0	0	0	0	0	0	0	0
AL-3-Vf	0	0	0	0	0	0	0	0	0	17	0	0	0	0	0
1	0	0	0	0	0	0	0	0	0	0	0	0	0	0	0
2	0	0	0	0	0	0	0	0	0	6	0	0	0	0	0
3	0	0	0	0	0	0	0	0	0	6	0	0	0	0	0
4	0	0	0	0	0	0	0	0	0	4	0	0	0	0	0
5	0	0	0	0	0	0	0	0	0	1	0	0	0	0	0
6	0	0	0	0	0	0	0	0	0	0	0	0	0	0	0

*Key to Grain Shape Categories. **1** = very angular; **2** = angular; **3** = sub-angular; **4** = sub-rounded; **5** = rounded; **6** = well rounded; Vc: very coarse sand fraction; C: coarse sand fraction; m: medium sand fraction; f: fine sand fraction; Vf: very fine sand fraction.

ALICUDI ISLAND (continued)

SAMPLE	Hb	Hbalt	Hb in Lvlblgl	Hb in Lvlbrgl	Hb in Lvlgrgl	Hb in Lvlclgl	Hb in Rp	Gr	Ru	Ru in Lvlblgl	Ru in Lvlbrgl	Op	Op in Lvlbrgl	Op in Pm	Bt
AL-3-Vc	0	0	0	0	0	0	0	0	0	0	0	0	0	0	0
1	0	0	0	0	0	0	0	0	0	0	0	0	0	0	0
2	0	0	0	0	0	0	0	0	0	0	0	0	0	0	0
3	0	0	0	0	0	0	0	0	0	0	0	0	0	0	0
4	0	0	0	0	0	0	0	0	0	0	0	0	0	0	0
5	0	0	0	0	0	0	0	0	0	0	0	0	0	0	0
6	0	0	0	0	0	0	0	0	0	0	0	0	0	0	0
AL-3-C	0	0	0	0	0	0	0	0	0	0	0	0	0	0	0
1	0	0	0	0	0	0	0	0	0	0	0	0	0	0	0
2	0	0	0	0	0	0	0	0	0	0	0	0	0	0	0
3	0	0	0	0	0	0	0	0	0	0	0	0	0	0	0
4	0	0	0	0	0	0	0	0	0	0	0	0	0	0	0
5	0	0	0	0	0	0	0	0	0	0	0	0	0	0	0
6	0	0	0	0	0	0	0	0	0	0	0	0	0	0	0
AL-3-m	0	0	0	0	0	0	0	0	0	0	0	4	0	0	0
1	0	0	0	0	0	0	0	0	0	0	0	0	0	0	0
2	0	0	0	0	0	0	0	0	0	0	0	1	0	0	0
3	0	0	0	0	0	0	0	0	0	0	0	3	0	0	0
4	0	0	0	0	0	0	0	0	0	0	0	0	0	0	0
5	0	0	0	0	0	0	0	0	0	0	0	0	0	0	0
6	0	0	0	0	0	0	0	0	0	0	0	0	0	0	0
AL-3-f	0	0	0	0	0	0	0	0	0	0	0	0	0	0	0
1	0	0	0	0	0	0	0	0	0	0	0	0	0	0	0
2	0	0	0	0	0	0	0	0	0	0	0	0	0	0	0
3	0	0	0	0	0	0	0	0	0	0	0	0	0	0	0
4	0	0	0	0	0	0	0	0	0	0	0	0	0	0	0
5	0	0	0	0	0	0	0	0	0	0	0	0	0	0	0
6	0	0	0	0	0	0	0	0	0	0	0	0	0	0	0
AL-3-Vf	0	0	0	0	0	0	0	0	0	0	0	0	0	0	1
1	0	0	0	0	0	0	0	0	0	0	0	0	0	0	0
2	0	0	0	0	0	0	0	0	0	0	0	0	0	0	0
3	0	0	0	0	0	0	0	0	0	0	0	0	0	0	1
4	0	0	0	0	0	0	0	0	0	0	0	0	0	0	0
5	0	0	0	0	0	0	0	0	0	0	0	0	0	0	0
6	0	0	0	0	0	0	0	0	0	0	0	0	0	0	0

SAMPLE	Bt in Rp	Bt in Rm	Mu	Mu in Rm	Qz-m	Q-p	Q in Rp	Q in Rm	Lvl	Lvlblgl	Lvlbrgl	Lvlorgl	Lvlgrgl	Lvlclgl	Lvlaltgl	Lvmi	Lvmiblgl
AL-3-Vc	0	0	0	0	0	0	0	0	0	45	34	15	0	0	0	0	8
1	0	0	0	0	0	0	0	0	0	8	10	3	0	0	0	0	0
2	0	0	0	0	0	0	0	0	0	19	15	6	0	0	0	0	2
3	0	0	0	0	0	0	0	0	0	16	9	5	0	0	0	0	3
4	0	0	0	0	0	0	0	0	0	2	0	1	0	0	0	0	3
5	0	0	0	0	0	0	0	0	0	0	0	0	0	0	0	0	0
6	0	0	0	0	0	0	0	0	0	0	0	0	0	0	0	0	0
AL-3-C	0	0	0	0	0	0	0	0	0	79	55	13	0	0	0	0	28
1	0	0	0	0	0	0	0	0	0	9	8	3	0	0	0	0	1
2	0	0	0	0	0	0	0	0	0	28	18	6	0	0	0	0	9
3	0	0	0	0	0	0	0	0	0	39	28	4	0	0	0	0	15
4	0	0	0	0	0	0	0	0	0	3	1	0	0	0	0	0	3
5	0	0	0	0	0	0	0	0	0	0	0	0	0	0	0	0	0
6	0	0	0	0	0	0	0	0	0	0	0	0	0	0	0	0	0
AL-3-m	0	0	0	0	0	0	0	0	3	46	28	8	0	0	0	0	40
1	0	0	0	0	0	0	0	0	0	4	1	1	0	0	0	0	2
2	0	0	0	0	0	0	0	0	0	11	10	3	0	0	0	0	9
3	0	0	0	0	0	0	0	0	2	22	14	4	0	0	0	0	20
4	0	0	0	0	0	0	0	0	1	8	3	0	0	0	0	0	8
5	0	0	0	0	0	0	0	0	0	1	0	0	0	0	0	0	1
6	0	0	0	0	0	0	0	0	0	0	0	0	0	0	0	0	0
AL-3-f	0	0	0	0	0	0	0	0	0	29	20	0	0	0	0	0	68
1	0	0	0	0	0	0	0	0	0	0	2	0	0	0	0	0	2
2	0	0	0	0	0	0	0	0	0	5	4	0	0	0	0	0	15
3	0	0	0	0	0	0	0	0	0	18	12	0	0	0	0	0	33
4	0	0	0	0	0	0	0	0	0	6	2	0	0	0	0	0	17
5	0	0	0	0	0	0	0	0	0	0	0	0	0	0	0	0	1
6	0	0	0	0	0	0	0	0	0	0	0	0	0	0	0	0	0
AL-3-Vf	0	0	0	0	0	0	0	0	0	18	14	0	0	0	0	0	63
1	0	0	0	0	0	0	0	0	0	0	0	0	0	0	0	0	1
2	0	0	0	0	0	0	0	0	0	5	4	0	0	0	0	0	10
3	0	0	0	0	0	0	0	0	0	11	10	0	0	0	0	0	34
4	0	0	0	0	0	0	0	0	0	2	0	0	0	0	0	0	18
5	0	0	0	0	0	0	0	0	0	0	0	0	0	0	0	0	0
6	0	0	0	0	0	0	0	0	0	0	0	0	0	0	0	0	0

*Key to Grain Shape Categories. **1** = very angular; **2** = angular; **3** = sub-angular; **4** = sub-rounded; **5** = rounded; **6** = well rounded; Vc: very coarse sand fraction; C: coarse sand fraction; m: medium sand fraction; f: fine sand fraction; Vf: very fine sand fraction.

ALICUDI ISLAND (continued)

SAMPLE	Lvmibrgl	Lvmiorgl	Lvmigrgl	Lvmiclgl	Lvmialtgl	Lvvblgl	Lvvbrgl	Lvvorgl	Lvvgrgl	Lvvclgl	Lvvalgl	Lvf	Pmcl	Lm	Lp	Lvo	Lsc (crist)	Lsc (micr)	Bio	Unknow	TOT
AL-3-Vc	7	4	0	0	0	11	9	6	0	0	0	0	0	1		0	0	0	0	0	250
1	0	0	0	0	0	5	5	4	0	0	0	0	0	0		0	0	0	0	0	45
2	1	3	0	0	0	6	3	2	0	0	0	0	0	0		0	0	0	0	0	100
3	4	1	0	0	0	0	1	0	0	0	0	0	0	1		0	0	0	0	0	90
4	2	0	0	0	0	0	0	0	0	0	0	0	0	0		0	0	0	0	0	15
5	0	0	0	0	0	0	0	0	0	0	0	0	0	0		0	0	0	0	0	0
6	0	0	0	0	0	0	0	0	0	0	0	0	0	0		0	0	0	0	0	0
AL-3-C	20	11	0	0	0	22	16	0	0	0	0	0	0	0		0	0	0	0	0	400
1	2	1	0	0	0	9	4	0	0	0	0	0	0	0		0	0	0	0	0	58
2	6	3	0	0	0	7	6	0	0	0	0	0	0	0		0	0	0	0	0	148
3	9	5	0	0	0	5	3	0	0	0	0	0	0	0		0	0	0	0	0	169
4	3	2	0	0	0	1	3	0	0	0	0	0	0	0		0	0	0	0	0	25
5	0	0	0	0	0	0	0	0	0	0	0	0	0	0		0	0	0	0	0	0
6	0	0	0	0	0	0	0	0	0	0	0	0	0	0		0	0	0	0	0	0
AL-3-m	34	0	0	0	0	38	30	0	0	0	0	0	0	0		0	0	0	0	0	400
1	3	0	0	0	0	10	6	0	0	0	0	0	0	0		0	0	0	0	0	37
2	6	0	0	0	0	21	17	0	0	0	0	0	0	0		0	0	0	0	0	130
3	17	0	0	0	0	7	7	0	0	0	0	0	0	0		0	0	0	0	0	187
4	7	0	0	0	0	0	0	0	0	0	0	0	0	0		0	0	0	0	0	43
5	1	0	0	0	0	0	0	0	0	0	0	0	0	0		0	0	0	0	0	3
6	0	0	0	0	0	0	0	0	0	0	0	0	0	0		0	0	0	0	0	0
AL-3-f	54	5	0	0	0	26	24	0	0	0	0	0	0	0		0	0	0	0	0	400
1	2	0	0	0	0	10	7	0	0	0	0	0	0	0		0	0	0	0	0	29
2	11	1	0	0	0	12	10	0	0	0	0	0	0	0		0	0	0	0	0	113
3	29	3	0	0	0	4	6	0	0	0	0	0	0	0		0	0	0	0	0	195
4	12	1	0	0	0	0	1	0	0	0	0	0	0	0		0	0	0	0	0	59
5	0	0	0	0	0	0		0	0	0	0	0	0	0		0	0	0	0	0	3
6	0	0	0	0	0	0		0	0	0	0	0	0	0		0	0	0	0	0	1
AL-3-Vf	51	13	0	0	0	46	30	8	0	0	0	0	0	0		0	0	0	0	0	400
1	0	0	0	0	0	4	4	0	0	0	0	0	0	0		0	0	0	0	0	10
2	6	1	0	0	0	28	20	5	0	0	0	0	0	0		0	0	0	0	0	138
3	24	7	0	0	0	12	6	3	0	0	0	0	0	0		0	0	0	0	0	191
4	20	5	0	0	0	1		0	0	0	0	0	0	0		0	0	0	0	0	58
5	1	0	0	0	0	1	0	0	0	0	0	0	0	0	0	0	0	0	0	0	3
6	0	0	0	0	0	0	0	0	0	0	0	0	0	0	0	0	0	0	0	0	0

SAMPLE	P	P in Lvl	P inLvlblgl	P inLvlbrgl	P inLvlorgl	P inLvlgrgl	P inLvlclgl	P alt	P in Rp	P in Pm	Py	Py in Lvlblgl	Py in Lvlbrgl	Py in Lvlorgl	Py in Lvlgrgl
AL-4-C	12	0	48	33	0	0	0	0	0	0	19	19	13	0	0
1	1	0	3	1	0	0	0	0	0	0	0	0	0	0	0
2	3	0	8	7	0	0	0	0	0	0	6	8	3	0	0
3	8	0	24	19	0	0	0	0	0	0	13	10	10	0	0
4	0	0	9	6	0	0	0	0	0	0	0	1	0	0	0
5	0	0	4	0	0	0	0	0	0	0	0	0	0	0	0
6	0	0	0	0	0	0	0	0	0	0	0	0	0	0	0
AL-5-m	33	0	41	28	8	0	0	0	0	0	35	25	19	7	0
1	2	0	1	0	1	0	0	0	0	0	3	2	3	1	0
2	10	0	11	9	3	0	0	0	0	0	17	5	8	3	0
3	13	0	19	16	4	0	0	0	0	0	10	14	7	2	0
4	4	0	8	3	0	0	0	0	0	0	3	4	1	1	0
5	4	0	2	0	0	0	0	0	0	0	2	0	0	0	0
6	0	0	0	0	0	0	0	0	0	0	0	0	0	0	0
AL-6-m	22	0	33	30	0	0	0	0	0	0	43	15	12	0	0
1	1	0	0	1	0	0	0	0	0	0	4	1	1	0	0
2	7	0	8	9	0	0	0	0	0	0	11	3	2	0	0
3	12	0	20	14	0	0	0	0	0	0	19	9	7	0	0
4	2	0	4	4	0	0	0	0	0	0	7	2	2	0	0
5	0	0	1	2	0	0	0	0	0	0	2	0	0	0	0
6	0	0	0	0	0	0	0	0	0	0	0	0	0	0	0
AL-7-m	27	0	23	20	0	0	0	0	0	0	61	23	19	0	0
1	1	0	2	2	0	0	0	0	0	0	4	1	0	0	0
2	6	0	4	5	0	0	0	0	0	0	27	6	4	0	0
3	16	0	14	12	0	0	0	0	0	0	22	12	13	0	0
4	3	0	3	1	0	0	0	0	0	0	7	4	2	0	0
5	1	0	0	0	0	0	0	0	0	0	1	0	0	0	0
6	0	0	0	0	0	0	0	0	0	0	0	0	0	0	0

*Key to Grain Shape Categories. **1** = very angular; **2** = angular; **3** = sub-angular; **4** = sub-rounded; **5** = rounded; **6** = well rounded; Vc: very coarse sand fraction; C: coarse sand fraction; m: medium sand fraction; f: fine sand fraction; Vf: very fine sand fraction.

ALICUDI ISLAND (continued)

SAMPLE	Py in Lvlclgl	Py alt	K	K in Lvlblgl	K in Lvlbrgl	K in Lvlorgl	K in Lvlgrgl	K in Lvlclgl	K in Rp	Ol	Ol inLvlblgl	Ol inLvlbrgl	Ol inLvlorgl	Ol inLvlgrgl	Ol alt
AL-4-C	0	0	0	0	0	0	0	0	0	0	0	0	0	0	0
1	0	0	0	0	0	0	0	0	0	0	0	0	0	0	0
2	0	0	0	0	0	0	0	0	0	0	0	0	0	0	0
3	0	0	0	0	0	0	0	0	0	0	0	0	0	0	0
4	0	0	0	0	0	0	0	0	0	0	0	0	0	0	0
5	0	0	0	0	0	0	0	0	0	0	0	0	0	0	0
6	0	0	0	0	0	0	0	0	0	0	0	0	0	0	0
AL-5-m	0	0	0	0	0	0	0	0	0	9	5	0	0	0	0
1	0	0	0	0	0	0	0	0	0	0	0	0	0	0	0
2	0	0	0	0	0	0	0	0	0	2	2	0	0	0	0
3	0	0	0	0	0	0	0	0	0	3	3	0	0	0	0
4	0	0	0	0	0	0	0	0	0	2	0	0	0	0	0
5	0	0	0	0	0	0	0	0	0	2	0	0	0	0	0
6	0	0	0	0	0	0	0	0	0	0	0	0	0	0	0
AL-6-m	0	0	0	0	0	0	0	0	0	2	0	0	0	0	0
1	0	0	0	0	0	0	0	0	0	0	0	0	0	0	0
2	0	0	0	0	0	0	0	0	0	0	0	0	0	0	0
3	0	0	0	0	0	0	0	0	0	0	0	0	0	0	0
4	0	0	0	0	0	0	0	0	0	1	0	0	0	0	0
5	0	0	0	0	0	0	0	0	0	1	0	0	0	0	0
6	0	0	0	0	0	0	0	0	0	0	0	0	0	0	0
AL-7-m	0	0	0	0	0	0	0	0	0	8	0	0	0	0	0
1	0	0	0	0	0	0	0	0	0	0	0	0	0	0	0
2	0	0	0	0	0	0	0	0	0	2	0	0	0	0	0
3	0	0	0	0	0	0	0	0	0	4	0	0	0	0	0
4	0	0	0	0	0	0	0	0	0	2	0	0	0	0	0
5	0	0	0	0	0	0	0	0	0	0	0	0	0	0	0
6	0	0	0	0	0	0	0	0	0	0	0	0	0	0	0

SAMPLE	Hb	Hbalt	Hb in Lvlblgl	Hb in Lvlbrgl	Hb in Lvlgrgl	Hb in Lvlclgl	Hb in Rp	Gr	Ru	Ru in Lvlblgl	Ru in Lvlbrgl	Op	Op in Lvlbrgl	Op in Pm	Bt
AL-4-C	0	0	0	0	0	0	0	0	0	0	0	0	0	0	0
1	0	0	0	0	0	0	0	0	0	0	0	0	0	0	0
2	0	0	0	0	0	0	0	0	0	0	0	0	0	0	0
3	0	0	0	0	0	0	0	0	0	0	0	0	0	0	0
4	0	0	0	0	0	0	0	0	0	0	0	0	0	0	0
5	0	0	0	0	0	0	0	0	0	0	0	0	0	0	0
6	0	0	0	0	0	0	0	0	0	0	0	0	0	0	0
AL-5-m	0	0	0	0	0	0	0	0	0	0	0	0	0	0	0
1	0	0	0	0	0	0	0	0	0	0	0	0	0	0	0
2	0	0	0	0	0	0	0	0	0	0	0	0	0	0	0
3	0	0	0	0	0	0	0	0	0	0	0	0	0	0	0
4	0	0	0	0	0	0	0	0	0	0	0	0	0	0	0
5	0	0	0	0	0	0	0	0	0	0	0	0	0	0	0
6	0	0	0	0	0	0	0	0	0	0	0	0	0	0	0
AL-6-m	0	0	0	0	0	0	0	0	0	0	0	0	0	0	1
1	0	0	0	0	0	0	0	0	0	0	0	0	0	0	0
2	0	0	0	0	0	0	0	0	0	0	0	0	0	0	0
3	0	0	0	0	0	0	0	0	0	0	0	0	0	0	1
4	0	0	0	0	0	0	0	0	0	0	0	0	0	0	0
5	0	0	0	0	0	0	0	0	0	0	0	0	0	0	0
6	0	0	0	0	0	0	0	0	0	0	0	0	0	0	0
AL-7-m	0	0	0	0	0	0	0	0	0	0	0	0	0	0	0
1	0	0	0	0	0	0	0	0	0	0	0	0	0	0	0
2	0	0	0	0	0	0	0	0	0	0	0	0	0	0	0
3	0	0	0	0	0	0	0	0	0	0	0	0	0	0	0
4	0	0	0	0	0	0	0	0	0	0	0	0	0	0	0
5	0	0	0	0	0	0	0	0	0	0	0	0	0	0	0
6	0	0	0	0	0	0	0	0	0	0	0	0	0	0	0

*Key to Grain Shape Categories. **1** = very angular; **2** = angular; **3** = sub-angular; **4** = sub-rounded; **5** = rounded; **6** = well rounded; Vc: very coarse sand fraction; C: coarse sand fraction; m: medium sand fraction; f: fine sand fraction; Vf: very fine sand fraction.

ALICUDI ISLAND (continued)

SAMPLE	Bt in Rp	Bt in Rm	Mu	Mu in Rm	Qz-m	Q-p	Q in Rp	Q in Rm	Lvl	Lvlblgl	Lvlbrgl	Lvlorgl	Lvlgrgl	Lvlclgl	Lvlaltgl	Lvmi	Lvmiblgl
AL-4-C	0	0	0	0	0	0	0	0	0	69	63	0	0	0	0	0	42
1	0	0	0	0	0	0	0	0	0	8	4	0	0	0	0	0	0
2	0	0	0	0	0	0	0	0	0	23	23	0	0	0	0	0	10
3	0	0	0	0	0	0	0	0	0	24	27	0	0	0	0	0	22
4	0	0	0	0	0	0	0	0	0	11	7	0	0	0	0	0	10
5	0	0	0	0	0	0	0	0	0	3	2	0	0	0	0	0	0
6	0	0	0	0	0	0	0	0	0	0	0	0	0	0	0	0	0
AL-5-m	0	0	0	0	0	0	0	0	0	55	30	11	0	0	0	0	30
1	0	0	0	0	0	0	0	0	0	3	3	2	0	0	0	0	0
2	0	0	0	0	0	0	0	0	0	10	8	4	0	0	0	0	3
3	0	0	0	0	0	0	0	0	0	30	19	5	0	0	0	0	20
4	0	0	0	0	0	0	0	0	0	9	0	0	0	0	0	0	7
5	0	0	0	0	0	0	0	0	0	3	0	0	0	0	0	0	0
6	0	0	0	0	0	0	0	0	0	0	0	0	0	0	0	0	0
AL-6-m	0	0	0	0	0	0	0	0	0	64	50	6	11	0	0	0	40
1	0	0	0	0	0	0	0	0	0	7	2	0	1	0	0	0	0
2	0	0	0	0	0	0	0	0	0	14	14	1	2	0	0	0	3
3	0	0	0	0	0	0	0	0	0	24	26	4	7	0	0	0	14
4	0	0	0	0	0	0	0	0	0	12	6	1	1	0	0	0	23
5	0	0	0	0	0	0	0	0	0	7	2	0	0	0	0	0	0
6	0	0	0	0	0	0	0	0	0	0	0	0	0	0	0	0	0
AL-7-m	0	0	0	0	0	0	0	0	0	66	43	6	8	0	0	0	32
1	0	0	0	0	0	0	0	0	0	6	2	0	1	0	0	0	0
2	0	0	0	0	0	0	0	0	0	20	13	3	4	0	0	0	2
3	0	0	0	0	0	0	0	0	0	29	23	3	2	0	0	0	13
4	0	0	0	0	0	0	0	0	0	9	4	0	1	0	0	0	15
5	0	0	0	0	0	0	0	0	0	2	1	0	0	0	0	0	2
6	0	0	0	0	0	0	0	0	0	0	0	0	0	0	0	0	0

SAMPLE	Lvmibrgl	Lvmiorgl	Lvmigrgl	Lvmiclgl	Lvmialtgl	Lvvblgl	Lvvbrgl	Lvvorgl	Lvvgrgl	Lvvclgl	Lvvalgl	Lvf	Pmcl	Lm	Lp	Lvo	Lsc (crist)	Lsc (micr)	Bio	Unknow	TOT
AL-4-C	31	0	0	0	0	28	23	0	0	0	0	0	0	0	0	0	0	0	0	0	400
1	0	0	0	0	0	8	3	0	0	0	0	0	0	0	0	0	0	0	0	0	28
2	5	0	0	0	0	12	10	0	0	0	0	0	0	0	0	0	0	0	0	0	118
3	13	0	0	0	0	8	9	0	0	0	0	0	0	0	0	0	0	0	0	0	187
4	13	0	0	0	0	0	1	0	0	0	0	0	0	0	0	0	0	0	0	0	58
5	0	0	0	0	0	0	0	0	0	0	0	0	0	0	0	0	0	0	0	0	9
6	0	0	0	0	0	0	0	0	0	0	0	0	0	0	0	0	0	0	0	0	0
AL-5-m	14	0	0	0	0	29	13	8	0	0	0	0	0	0	0	0	0	0	0	0	400
1	0	0	0	0	0	5	3	1	0	0	0	0	0	0	0	0	0	0	0	0	30
2	2	0	0	0	0	17	9	4	0	0	0	0	0	0	0	0	0	0	0	0	127
3	7	0	0	0	0	6	1	3	0	0	0	0	0	0	0	0	0	0	0	0	182
4	5	0	0	0	0	1	0	0	0	0	0	0	0	0	0	0	0	0	0	0	48
5	0	0	0	0	0	0	0	0	0	0	0	0	0	0	0	0	0	0	0	0	13
6	0	0	0	0	0	0	0	0	0	0	0	0	0	0	0	0	0	0	0	0	0
AL-6-m	33	0	6	0	0	19	9	4	0	0	0	0	0	0	0	0	0	0	0	0	400
1	0	0	0	0	0	1	1	0	0	0	0	0	0	0	0	0	0	0	0	0	20
2	4	0	0	0	0	11	3	3	0	0	0	0	0	0	0	0	0	0	0	0	95
3	9	0	2	0	0	6	4	1	0	0	0	0	0	0	0	0	0	0	0	0	179
4	20	0	4	0	0	1	1	0	0	0	0	0	0	0	0	0	0	0	0	0	91
5	0	0	0	0	0	0	0	0	0	0	0	0	0	0	0	0	0	0	0	0	15
6	0	0	0	0	0	0	0	0	0	0	0	0	0	0	0	0	0	0	0	0	0
AL-7-m	22	0	4	0	0	20	13	5	0	0	0	0	0	0	0	0	0	0	0	0	400
1	0	0	0	0	0	3	4	1	0	0	0	0	0	0	0	0	0	0	0	0	27
2	2	0	1	0	0	12	7	3	0	0	0	0	0	0	0	0	0	0	0	0	121
3	4	0	1	0	0	5	2	1	0	0	0	0	0	0	0	0	0	0	0	0	176
4	13	0	2	0	0	0	0	0	0	0	0	0	0	0	0	0	0	0	0	0	66
5	3	0	0	0	0	0	0	0	0	0	0	0	0	0	0	0	0	0	0	0	10
6	0	0	0	0	0	0	0	0	0	0	0	0	0	0	0	0	0	0	0	0	0

*Key to Grain Shape Categories. **1** = very angular; **2** = angular; **3** = sub-angular; **4** = sub-rounded; **5** = rounded; **6** = well rounded; Vc: very coarse sand fraction; C: coarse sand fraction; m: medium sand fraction; f: fine sand fraction; Vf: very fine sand fraction.

PANAREA ISLAND

SAMPLE	P	P inLvlblgl	P inLvlbrgl	P inLvlgrgl	P inLvlclgl	P alt	Py	Py in Lvlblgl	Py in Lvlbrgl	Py in Lvlorgl	Py in Lvlgrgl	Py in Lvlclgl	Py alt	K	K in Lvlblgl	K in Lvlbrgl
PN-1-Vc	24	40	0	0	0	0	11	0	0	0	0	0	0	0	0	0
1	16	22	0	0	0	0	4	0	0	0	0	0	0	0	0	0
2	8	18	0	0	0	0	7	0	0	0	0	0	0	0	0	0
3	0	0	0	0	0	0	0	0	0	0	0	0	0	0	0	0
4	0	0	0	0	0	0	0	0	0	0	0	0	0	0	0	0
5	0	0	0	0	0	0	0	0	0	0	0	0	0	0	0	0
6	0	0	0	0	0	0	0	0	0	0	0	0	0	0	0	0
PN-1-C	62	3	29	0	0	2	18	1	2	0	0	0	0	0	0	0
1	36	2	7	0	0	0	12	0	1	0	0	0	0	0	0	0
2	26	0	22	0	0	2	5	1	0	0	0	0	0	0	0	0
3	0	1	0	0	0	0	1	0	1	0	0	0	0	0	0	0
4	0	0	0	0	0	0	0	0	0	0	0	0	0	0	0	0
5	0	0	0	0	0	0	0	0	0	0	0	0	0	0	0	0
6	0	0	0	0	0	0	0	0	0	0	0	0	0	0	0	0
PN-1-m	81	2	5	0	2	0	29	0	2	0	0	0	0	2	0	0
1	54	0	0	0	0	0	8	0	0	0	0	0	0	0	0	0
2	25	2	5	0	2	0	18	0	2	0	0	0	0	2	0	0
3	2	0	0	0	0	0	3	0	0	0	0	0	0	0	0	0
4	0	0	0	0	0	0	0	0	0	0	0	0	0	0	0	0
5	0	0	0	0	0	0	0	0	0	0	0	0	0	0	0	0
6	0	0	0	0	0	0	0	0	0	0	0	0	0	0	0	0
PN-1-f	39	2	4	0	6	0	54	0	0	0	0	0	1	6	0	0
1	27	1	1	0	0	0	22	0	0	0	0	0	0	0	0	0
2	10	1	3	0	6	0	20	0	0	0	0	0	0	6	0	0
3	2	0	0	0	0	0	6	0	0	0	0	0	1	0	0	0
4	0	0	0	0	0	0	6	0	0	0	0	0	0	0	0	0
5	0	0	0	0	0	0	0	0	0	0	0	0	0	0	0	0
6	0	0	0	0	0	0	0	0	0	0	0	0	0	0	0	0
PN-1-Vf	41	0	0	0	0	0	34	0	0	0	0	0	0	11	0	0
1	28	0	0	0	0	0	18	0	0	0	0	0	0	4	0	0
2	10	0	0	0	0	0	11	0	0	0	0	0	0	7	0	0
3	3	0	0	0	0	0	5	0	0	0	0	0	0	0	0	0
4	0	0	0	0	0	0	0	0	0	0	0	0	0	0	0	0
5	0	0	0	0	0	0	0	0	0	0	0	0	0	0	0	0
6	0	0	0	0	0	0	0	0	0	0	0	0	0	0	0	0

SAMPLE	K in Lvlgrgl	K in Lvlclgl	Ol	Hb	Hbalt	Hb in Lvlblgl	Hb in Lvlbrgl	Hb in Lvlgrgl	Hb in Lvlclgl	Op	Op in Lvlbrgl	Bt	Bt in Lvlbrgl	Bt in Lvlclgl	Ca	Zeo/Dev	Qzm	Qp
PN-1-Vc	0	0	0	7	0	1	19	0	0	0	0	0	12	0	0	0	0	0
1	0	0	0	3	0	1	1	0	0	0	0	0	12	0	0	0	0	0
2	0	0	0	4	0	0	18	0	0	0	0	0	0	0	0	0	0	0
3	0	0	0	0	0	0	0	0	0	0	0	0	0	0	0	0	0	0
4	0	0	0	0	0	0	0	0	0	0	0	0	0	0	0	0	0	0
5	0	0	0	0	0	0	0	0	0	0	0	0	0	0	0	0	0	0
6	0	0	0	0	0	0	0	0	0	0	0	0	0	0	0	0	0	0
PN-1-C	0	0	0	11	0	0	5	0	0	3	3	18	5	5	0	4	0	0
1	0	0	0	11	0	0	0	0	0	0	3	16	0	0	0	0	0	0
2	0	0	0	0	0	0	5	0	0	0	0	0	5	5	0	4	0	0
3	0	0	0	0	0	0	0	0	0	0	0	2	0	0	0	0	0	0
4	0	0	0	0	0	0	0	0	0	3	0	0	0	0	0	0	0	0
5	0	0	0	0	0	0	0	0	0	0	0	0	0	0	0	0	0	0
6	0	0	0	0	0	0	0	0	0	0	0	0	0	0	0	0	0	0
PN-1-m	0	0	1	18	0	2	0	0	0	28	0	18	0	0	0	0	0	0
1	0	0	0	12	0	0	0	0	0	0	0	10	0	0	0	0	0	0
2	0	0	1	6	0	2	0	0	0	10	0	8	0	0	0	0	0	0
3	0	0	0	0	0	0	0	0	0	14	0	0	0	0	0	0	0	0
4	0	0	0	0	0	0	0	0	0	4	0	0	0	0	0	0	0	0
5	0	0	0	0	0	0	0	0	0	0	0	0	0	0	0	0	0	0
6	0	0	0	0	0	0	0	0	0	0	0	0	0	0	0	0	0	0
PN-1-f	0	0	0	33	0	0	2	0	1	37	0	35	1	0	0	0	0	0
1	0	0	0	24	0	0	0	0	1	0	0	26	0	0	0	0	0	0
2	0	0	0	9	0	0	2	0	0	15	0	8	1	0	0	0	0	0
3	0	0	0	0	0	0	0	0	0	19	0	1	0	0	0	0	0	0
4	0	0	0	0	0	0	0	0	0	3	0	0	0	0	0	0	0	0
5	0	0	0	0	0	0	0	0	0	0	0	0	0	0	0	0	0	0
6	0	0	0	0	0	0	0	0	0	0	0	0	0	0	0	0	0	0
PN-1-Vf	0	0	0	28	0	0	0	0	0	53	0	34	0	0	0	0	0	0
1	0	0	0	19	0	0	0	0	0	1	0	24	0	0	0	0	0	0
2	0	0	0	9	0	0	0	0	0	7	0	10	0	0	0	0	0	0
3	0	0	0	0	0	0	0	0	0	14	0	0	0	0	0	0	0	0
4	0	0	0	0	0	0	0	0	0	17	0	0	0	0	0	0	0	0
5	0	0	0	0	0	0	0	0	0	14	0	0	0	0	0	0	0	0
6	0	0	0	0	0	0	0	0	0	0	0	0	0	0	0	0	0	0

*Key to Grain Shape Categories. **1** = very angular; **2** = angular; **3** = sub-angular; **4** = sub-rounded; **5** = rounded; **6** = well rounded; Vc: very coarse sand fraction; C: coarse sand fraction; m: medium sand fraction; f: fine sand fraction; Vf: very fine sand fraction.

PANAREA ISLAND (continued)

SAMPLE	Chert	Lvl	Lvlblgl	Lvlbrgl	Lvlgrgl	Lvlclgl	Lvlaltgl	Lvmi	Lvmiblgl	Lvmibrgl	Lvmigrgl	Lvmiclgl	Lvmialtgl
PN-1-Vc	0	0	15	123	4	0	15	0	0	17	0	0	0
1	0	0	10	43	0	0	0	0	0	0	0	0	0
2	0	0	5	65	4	0	15	0	0	12	0	0	0
3	0	0	0	15	0	0	0	0	0	5	0	0	0
4	0	0	0	0	0	0	0	0	0	0	0	0	0
5	0	0	0	0	0	0	0	0	0	0	0	0	0
6	0	0	0	0	0	0	0	0	0	0	0	0	0
PN-1-C	0	1	9	117	2	14	16	0	0	42	0	1	1
1	0	0	3	47	0	6	0	0	0	9	0	1	0
2	0	0	6	59	2	8	16	0	0	25	0	0	1
3	0	1	0	11	0	0	0	0	0	8	0	0	0
4	0	0	0	0	0	0	0	0	0	0	0	0	0
5	0	0	0	0	0	0	0	0	0	0	0	0	0
6	0	0	0	0	0	0	0	0	0	0	0	0	0
PN-1-m	2	0	12	15	0	13	19	0	27	4	0	17	15
1	0	0	1	1	0	9	0	0	10	4	0	3	0
2	2	0	7	10	0	4	19	0	12	0	0	14	11
3	0	0	4	4	0	0	0	0	5	0	0	0	4
4	0	0	0	0	0	0	0	0	0	0	0	0	0
5	0	0	0	0	0	0	0	0	0	0	0	0	0
6	0	0	0	0	0	0	0	0	0	0	0	0	0
PN-1-f	0	0	3	4	0	7	4	0	19	14	0	11	32
1	0	0	1	1	0	6	0	0	9	2	0	0	9
2	0	0	2	2	0	1	4	0	8	7	0	11	19
3	0	0	0	1	0	0	0	0	2	5	0	0	4
4	0	0	0	0	0	0	0	0	0	0	0	0	0
5	0	0	0	0	0	0	0	0	0	0	0	0	0
6	0	0	0	0	0	0	0	0	0	0	0	0	0
PN-1-Vf	0	0	5	4	0	0	0	0	5	6	0	27	39
1	0	0	1	1	0	0	0	0	0	2	0	2	6
2	0	0	3	2	0	0	0	0	4	4	0	24	16
3	0	0	1	1	0	0	0	0	1	0	0	1	17
4	0	0	0	0	0	0	0	0	0	0	0	0	0
5	0	0	0	0	0	0	0	0	0	0	0	0	0
6	0	0	0	0	0	0	0	0	0	0	0	0	0

SAMPLE	Lvvblgl	Lvvbrgl	Lvvorgl	Lvvgrgl	Lvvclgl	Lvvalgl	Lvf	Pmcl	Lm	Lp	Lvo	Lsc (crist)	Lsc (micr)	Xe	Unk	TOT
PN-1-Vc	2	2	0	0	1	0	6	0	0	0	0	1	0	0	0	300
1	0	0	0	0	1	0	0	0	0	0	0	0	0	0	0	113
2	2	2	0	0	0	0	6	0	0	0	0	1	0	0	0	167
3	0	0	0	0	0	0	0	0	0	0	0	0	0	0	0	20
4	0	0	0	0	0	0	0	0	0	0	0	0	0	0	0	0
5	0	0	0	0	0	0	0	0	0	0	0	0	0	0	0	0
6	0	0	0	0	0	0	0	0	0	0	0	0	0	0	0	0
PN-1-C	2	5	0	0	2	0	15	0	0	0	0	0	1	0	1	400
1	1	2	0	0	2	0	0	0	0	0	0	0	0	0	0	159
2	1	2	0	0	0	0	12	0	0	0	0	0	1	0	1	209
3	0	1	0	0	0	0	3	0	0	0	0	0	0	0	0	29
4	0	0	0	0	0	0	0	0	0	0	0	0	0	0	0	3
5	0	0	0	0	0	0	0	0	0	0	0	0	0	0	0	0
6	0	0	0	0	0	0	0	0	0	0	0	0	0	0	0	0
PN-1-m	40	16	0	0	8	1	18	3	0	0	0	0	0	0	0	400
1	17	4	0	0	5	0	5	2	0	0	0	0	0	0	0	145
2	14	8	0	0	3	1	13	1	0	0	0	0	0	0	0	202
3	8	4	0	0	0	0	0	0	0	0	0	0	0	0	0	48
4	1	0	0	0	0	0	0	0	0	0	0	0	0	0	0	5
5	0	0	0	0	0	0	0	0	0	0	0	0	0	0	0	0
6	0	0	0	0	0	0	0	0	0	0	0	0	0	0	0	0
PN-1-f	53	0	0	0	0	6	15	0	0	0	0	0	0	0	0	400
1	32	0	0	0	0	0	5	0	0	0	0	0	0	0	0	167
2	10	0	0	0	0	0	10	0	0	0	0	0	0	0	0	164
3	3	0	0	0	0	0	0	0	0	0	0	0	0	0	0	46
4	8	0	0	0	0	4	0	0	0	0	0	0	0	0	0	21
5	0	0	0	0	0	2	0	0	0	0	0	0	0	0	0	2
6	0	0	0	0	0	0	0	0	0	0	0	0	0	0	0	0
PN-1-Vf	45	10	0	0	34	2	11	0	0	0	0	0	0	0	11	400
1	21	3	0	0	12	0	2	0	0	0	0	0	0	0	5	149
2	15	6	0	0	22	2	9	0	0	0	0	0	0	0	6	167
3	8	1	0	0	0	0	0	0	0	0	0	0	0	0	0	52
4	1	0	0	0	0	0	0	0	0	0	0	0	0	0	0	18
5	0	0	0	0	0	0	0	0	0	0	0	0	0	0	0	14
6	0	0	0	0	0	0	0	0	0	0	0	0	0	0	0	0

*Key to Grain Shape Categories. **1** = very angular; **2** = angular; **3** = sub-angular; **4** = sub-rounded; **5** = rounded; **6** = well rounded; Vc: very coarse sand fraction; C: coarse sand fraction; m: medium sand fraction; f: fine sand fraction; Vf: very fine sand fraction.

PANAREA ISLAND (continued)

SAMPLE	P	P inLvlblgl	P inLvlbrgl	P inLvlgrgl	P inLvlclgl	P alt	Py	Py in Lvlblgl	Py in Lvlbrgl	Py in Lvlorgl	Py in Lvlgrgl	Py in Lvlclgl	Py alt	K	K in Lvlblgl	K in Lvlbrgl
PN-2-m	25	0	0	5	0	0	5	0	0	0	0	0	0	7	0	0
1	10	0	0	0	0	0	2	0	0	0	0	0	0	2	0	0
2	12	0	0	5	0	0	3	0	0	0	0	0	0	5	0	0
3	3	0	0	0	0	0	0	0	0	0	0	0	0	0	0	0
4	0	0	0	0	0	0	0	0	0	0	0	0	0	0	0	0
5	0	0	0	0	0	0	0	0	0	0	0	0	0	0	0	0
6	0	0	0	0	0	0	0	0	0	0	0	0	0	0	0	0
PN-3-m	32	0	1	5	0	0	16	0	0	0	1	2	0	1	0	0
1	15	0	1	1	0	0	4	0	0	0	1	0	0	0	0	0
2	14	0	0	4	0	0	11	0	0	0	0	2	0	1	0	0
3	3	0	0	0	0	0	1	0	0	0	0	0	0	0	0	0
4	0	0	0	0	0	0	0	0	0	0	0	0	0	0	0	0
5	0	0	0	0	0	0	0	0	0	0	0	0	0	0	0	0
6	0	0	0	0	0	0	0	0	0	0	0	0	0	0	0	0
PN-4-m	9	0	0	1	0	0	0	0	0	0	0	0	1	3	1	0
1	1	0	0	0	0	0	0	0	0	0	0	0	0	0	0	0
2	6	0	0	1	0	0	0	0	0	0	0	0	1	3	1	0
3	2	0	0	0	0	0	0	0	0	0	0	0	0	0	0	0
4	0	0	0	0	0	0	0	0	0	0	0	0	0	0	0	0
5	0	0	0	0	0	0	0	0	0	0	0	0	0	0	0	0
6	0	0	0	0	0	0	0	0	0	0	0	0	0	0	0	0
PN-5-m	14	0	0	0	0	58	0	0	0	0	0	0	0	2	0	0
1	5	0	0	0	0	10	0	0	0	0	0	0	0	2	0	0
2	9	0	0	0	0	38	0	0	0	0	0	0	0	0	0	0
3	0	0	0	0	0	10	0	0	0	0	0	0	0	0	0	0
4	0	0	0	0	0	0	0	0	0	0	0	0	0	0	0	0
5	0	0	0	0	0	0	0	0	0	0	0	0	0	0	0	0
6	0	0	0	0	0	0	0	0	0	0	0	0	0	0	0	0
PN-6-m	17	0	1	0	0	2	8	0	0	0	0	0	0	12	0	0
1	2	0	0	0	0	0	5	0	0	0	0	0	0	4	0	0
2	11	0	1	0	0	2	2	0	0	0	0	0	0	8	0	0
3	4	0	0	0	0	0	1	0	0	0	0	0	0	0	0	0
4	0	0	0	0	0	0	0	0	0	0	0	0	0	0	0	0
5	0	0	0	0	0	0	0	0	0	0	0	0	0	0	0	0
6	0	0	0	0	0	0	0	0	0	0	0	0	0	0	0	0

SAMPLE	K in Lvlgrgl	K in Lvlclgl	Ol	Hb	Hbalt	Hb in Lvlblgl	Hb in Lvlbrgl	Hb in Lvlgrgl	Hb in Lvlclgl	Op	Op in Lvlbrgl	Bt	Bt in Lvlbrgl	Bt in Lvlclgl	Ca	Zeo/Dev	Qzm	Qp
PN-2-m	0	0	0	7	0	0	0	0	0	0	0	0	0	0	0	0	11	2
1	0	0	0	3	0	0	0	0	0	0	0	0	0	0	0	0	0	0
2	0	0	0	4	0	0	0	0	0	0	0	0	0	0	0	0	9	0
3	0	0	0	0	0	0	0	0	0	0	0	0	0	0	0	0	2	2
4	0	0	0	0	0	0	0	0	0	0	0	0	0	0	0	0	0	0
5	0	0	0	0	0	0	0	0	0	0	0	0	0	0	0	0	0	0
6	0	0	0	0	0	0	0	0	0	0	0	0	0	0	0	0	0	0
PN-3-m	0	0	0	8	0	0	0	0	0	2	0	1	0	0	0	0	5	1
1	0	0	0	2	0	0	0	0	0	0	0	0	0	0	0	0	0	0
2	0	0	0	6	0	0	0	0	0	2	0	1	0	0	0	0	5	0
3	0	0	0	0	0	0	0	0	0	0	0	0	0	0	0	0	0	1
4	0	0	0	0	0	0	0	0	0	0	0	0	0	0	0	0	0	0
5	0	0	0	0	0	0	0	0	0	0	0	0	0	0	0	0	0	0
6	0	0	0	0	0	0	0	0	0	0	0	0	0	0	0	0	0	0
PN-4-m	0	0	0	1	0	0	0	0	0	0	0	0	0	0	0	0	2	0
1	0	0	0	0	0	0	0	0	0	0	0	0	0	0	0	0	0	0
2	0	0	0	1	0	0	0	0	0	0	0	0	0	0	0	0	2	0
3	0	0	0	0	0	0	0	0	0	0	0	0	0	0	0	0	0	0
4	0	0	0	0	0	0	0	0	0	0	0	0	0	0	0	0	0	0
5	0	0	0	0	0	0	0	0	0	0	0	0	0	0	0	0	0	0
6	0	0	0	0	0	0	0	0	0	0	0	0	0	0	0	0	0	0
PN-5-m	0	0	0	0	0	0	0	0	0	0	0	0	0	0	0	0	2	0
1	0	0	0	0	0	0	0	0	0	0	0	0	0	0	0	0	0	0
2	0	0	0	0	0	0	0	0	0	0	0	0	0	0	0	0	2	0
3	0	0	0	0	0	0	0	0	0	0	0	0	0	0	0	0	0	0
4	0	0	0	0	0	0	0	0	0	0	0	0	0	0	0	0	0	0
5	0	0	0	0	0	0	0	0	0	0	0	0	0	0	0	0	0	0
6	0	0	0	0	0	0	0	0	0	0	0	0	0	0	0	0	0	0
PN-6-m	0	0	0	2	0	0	0	0	0	0	0	0	0	1	0	0	14	0
1	0	0	0	2	0	0	0	0	0	0	0	0	0	0	0	0	0	0
2	0	0	0	0	0	0	0	0	0	0	0	0	0	1	0	0	11	0
3	0	0	0	0	0	0	0	0	0	0	0	0	0	0	0	0	3	0
4	0	0	0	0	0	0	0	0	0	0	0	0	0	0	0	0	0	0
5	0	0	0	0	0	0	0	0	0	0	0	0	0	0	0	0	0	0
6	0	0	0	0	0	0	0	0	0	0	0	0	0	0	0	0	0	0

*Key to Grain Shape Categories. **1** = very angular; **2** = angular; **3** = sub-angular; **4** = sub-rounded; **5** = rounded; **6** = well rounded; Vc: very coarse sand fraction; C: coarse sand fraction; m: medium sand fraction; f: fine sand fraction; Vf: very fine sand fraction.

PANAREA ISLAND (continued)

SAMPLE	Chert	Lvl	Lvlblgl	Lvlbrgl	Lvlgrgl	Lvlclgl	Lvlaltgl	Lvmi	Lvmiblgl	Lvmibrgl	Lvmigrgl	Lvmiclgl	Lvmialtgl
PN-2-m	0	0	13	29	89	40	1	0	7	29	90	36	0
1	0	0	2	7	34	21	0	0	1	3	21	18	0
2	0	0	7	18	35	19	1	0	5	18	39	17	0
3	0	0	4	4	12	0	0	0	1	8	16	1	0
4	0	0	0	0	6	0	0	0	0	0	11	0	0
5	0	0	0	0	2	0	0	0	0	0	3	0	0
6	0	0	0	0	0	0	0	0	0	0	0	0	0
PN-3-m	0	0	16	24	89	21	6	0	12	22	51	18	60
1	0	0	3	1	24	5	0	0	3	0	15	4	13
2	0	0	9	15	42	16	6	0	4	12	20	14	28
3	0	0	2	8	16	0	0	0	1	10	10	0	13
4	0	0	2	0	5	0	0	0	4	0	5	0	5
5	0	0	0	0	2	0	0	0	0	0	1	0	1
6	0	0	0	0	0	0	0	0	0	0	0	0	0
PN-4-m	31	0	10	33	58	13	42	0	8	18	34	4	53
1	0	0	0	2	9	1	1	0	1	1	4	0	0
2	17	0	8	17	38	12	35	0	6	11	23	3	43
3	9	0	2	14	11	0	6	0	1	6	7	1	6
4	5	0	0	0	0	0	0	0	0	0	0	0	4
5	0	0	0	0	0	0	0	0	0	0	0	0	0
6	0	0	0	0	0	0	0	0	0	0	0	0	0
PN-5-m	6	0	5	16	10	8	45	0	6	12	7	4	66
1	0	0	1	1	2	0	0	0	1	1	1	0	2
2	6	0	4	12	8	8	31	0	2	6	6	4	44
3	0	0	0	3	0	0	11	0	3	5	0	0	12
4	0	0	0	0	0	0	3	0	0	0	0	0	8
5	0	0	0	0	0	0	0	0	0	0	0	0	0
6	0	0	0	0	0	0	0	0	0	0	0	0	0
PN-6-m	6	0	10	16	26	5	47	0	0	14	14	7	21
1	0	0	2	0	2	0	10	0	0	2	2	0	1
2	6	0	7	13	18	5	28	0	0	7	10	7	16
3	0	0	1	3	6	0	6	0	0	5	2	0	4
4	0	0	0	0	0	0	3	0	0	0	0	0	0
5	0	0	0	0	0	0	0	0	0	0	0	0	0
6	0	0	0	0	0	0	0	0	0	0	0	0	0

SAMPLE	Lvvblgl	Lvvbrgl	Lvvorgl	Lvvgrgl	Lvvclgl	Lvvalgl	Lvf	Pmcl	Lm	Lp	Lvo	Lsc (crist)	Lsc (micr)	Xe	Unk	TOT
PN-2-m	0	0	0	0	2	0	0	0	0		0	0	0	2	0	400
1	0	0	0	0	1	0	0	0	0		0	0	0	0	0	125
2	0	0	0	0	1	0	0	0	0		0	0	0	2	0	200
3	0	0	0	0	0	0	0	0	0		0	0	0	0	0	53
4	0	0	0	0	0	0	0	0	0		0	0	0	0	0	17
5	0	0	0	0	0	0	0	0	0		0	0	0	0	0	5
6	0	0	0	0	0	0	0	0	0		0	0	0	0	0	0
PN-3-m	0	0	0	2	2	0	0	1	0		0	0	0	1	0	400
1	0	0	0	0	0	0	0	0	0		0	0	0	0	0	92
2	0	0	0	2	2	0	0	1	0		0	0	0	0	0	217
3	0	0	0	0	0	0	0	0	0		0	0	0	1	0	66
4	0	0	0	0	0	0	0	0	0		0	0	0	0	0	21
5	0	0	0	0	0	0	0	0	0		0	0	0	0	0	4
6	0	0	0	0	0	0	0	0	0		0	0	0	0	0	0
PN-4-m	0	5	0	0	9	32	15	0	0		0	0	0	4	6	400
1	0	0	0	0	2	3	0	0	0		0	0	0	0	0	25
2	0	5	0	0	7	24	15	0	0		0	0	0	4	6	296
3	0	0	0	0	0	5	0	0	0		0	0	0	0	0	70
4	0	0	0	0	0	0	0	0	0		0	0	0	0	0	9
5	0	0	0	0	0	0	0	0	0		0	0	0	0	0	0
6	0	0	0	0	0	0	0	0	0		0	0	0	0	0	0
PN-5-m	26	0	0	0	2	97	4	0	0		0	0	1	0	5	400
1	8	0	0	0	0	8	0	0	0		0	0	0	0	0	42
2	14	0	0	0	2	50	4	0	0		0	0	0	0	3	257
3	4	0	0	0	0	32	0	0	0		0	0	1	0	2	83
4	0	0	0	0	0	3	0	0	0		0	0	0	0	0	14
5	0	0	0	0	0	4	0	0	0		0	0	0	0	0	4
6	0	0	0	0	0	0	0	0	0		0	0	0	0	0	0
PN-6-m	18	14	0	2	37	64	11	24	0	2	0	0	0	1	0	400
1	5	0	0	0	8	8	0	0	0		0	0	0	0	0	53
2	13	10	0	2	25	35	11	16	0	2	0	0	0	1	0	272
3	0	4	0	0	4	16	0	8	0		0	0	0	0	0	67
4	0	0	0	0	0	5	0	0	0		0	0	0	0	0	8
5	0	0	0	0	0	0	0	0	0		0	0	0	0	0	0
6	0	0	0	0	0	0	0	0	0		0	0	0	0	0	0

*Key to Grain Shape Categories. **1** = very angular; **2** = angular; **3** = sub-angular; **4** = sub-rounded; **5** = rounded; **6** = well rounded; Vc: very coarse sand fraction; C: coarse sand fraction; m: medium sand fraction; f: fine sand fraction; Vf: very fine sand fraction.

PANAREA ISLAND (continued)

SAMPLE	P	P inLvlblgl	P inLvlbrgl	P inLvlgrgl	P inLvlclgl	P alt	Py	Py in Lvlblgl	Py in Lvlbrgl	Py in Lvlorgl	Py in Lvlgrgl	Py in Lvlclgl	Py alt	K	K in Lvlblgl	K in Lvlbrgl
PN-7-m	23	0	2	5	1	2	25	0	2	0	2	0	0	13	1	0
1	8	0	0	0	0	0	7	0	0	0	0	0	0	3	0	0
2	14	0	2	5	1	2	15	0	2	0	2	0	0	10	1	0
3	0	0	0	0	0	0	3	0	0	0	0	0	0	0	0	0
4	1	0	0	0	0	0	0	0	0	0	0	0	0	0	0	0
5	0	0	0	0	0	0	0	0	0	0	0	0	0	0	0	0
6	0	0	0	0	0	0	0	0	0	0	0	0	0	0	0	0
PN-8-m	24	0	3	0	0	1	1	2	1	0	0	0	0	26	0	3
1	7	0	0	0	0	0	1	0	0	0	0	0	0	4	0	0
2	15	0	3	0	0	1	0	2	1	0	0	0	0	18	0	2
3	1	0	0	0	0	0	0	0	0	0	0	0	0	4	0	0
4	1	0	0	0	0	0	0	0	0	0	0	0	0	0	0	1
5	0	0	0	0	0	0	0	0	0	0	0	0	0	0	0	0
6	0	0	0	0	0	0	0	0	0	0	0	0	0	0	0	0
PN-9-m	47	5	6	0	0	0	26	0	0	0	1	0	0	17	0	1
1	13	0	0	0	0	0	1	0	0	0	0	0	0	0	0	0
2	19	3	1	0	0	0	17	0	0	0	0	0	0	9	0	0
3	13	2	3	0	0	0	8	0	0	0	0	0	0	5	0	1
4	2	0	0	0	0	0	0	0	0	0	1	0	0	3	0	0
5	0	0	2	0	0	0	0	0	0	0	0	0	0	0	0	0
6	0	0	0	0	0	0	0	0	0	0	0	0	0	0	0	0
PN-10-m	15	0	2	1	0	0	9	0	0	0	0	0	0	10	0	0
1	2	0	0	0	0	0	0	0	0	0	0	0	0	0	0	0
2	8	0	0	0	0	0	5	0	0	0	0	0	0	7	0	0
3	5	0	2	0	0	0	4	0	0	0	0	0	0	3	0	0
4	0	0	0	1	0	0	0	0	0	0	0	0	0	0	0	0
5	0	0	0	0	0	0	0	0	0	0	0	0	0	0	0	0
6	0	0	0	0	0	0	0	0	0	0	0	0	0	0	0	0
PN-11-m	38	0	0	0	0	2	9	2	0	0	0	0	0	12	0	0
1	10	0	0	0	0	0	1	0	0	0	0	0	0	3	0	0
2	18	0	0	0	0	0	7	2	0	0	0	0	0	6	0	0
3	3	0	0	0	0	2	0	0	0	0	0	0	0	3	0	0
4	2	0	0	0	0	0	1	0	0	0	0	0	0	0	0	0
5	5	0	0	0	0	0	0	0	0	0	0	0	0	0	0	0
6	0	0	0	0	0	0	0	0	0	0	0	0	0	0	0	0

SAMPLE	K in Lvlgrgl	K in Lvlclgl	Ol	Hb	Hbalt	Hb in Lvlblgl	Hb in Lvlbrgl	Hb in Lvlgrgl	Hb in Lvlclgl	Op	Op in Lvlbrgl	Bt	Bt in Lvlbrgl	Bt in Lvlclgl	Ca	Zeo/Dev	Qzm	Qp
PN-7-m	1	0	0	13	0	4	0	7	0	7	0	1	0	0	0	0	12	0
1	0	0	0	6	0	0	0	0	0	0	0	1	0	0	0	0	4	0
2	1	0	0	7	0	4	0	7	0	3	0	0	0	0	0	0	8	0
3	0	0	0	0	0	0	0	0	0	4	0	0	0	0	0	0	0	0
4	0	0	0	0	0	0	0	0	0	0	0	0	0	0	0	0	0	0
5	0	0	0	0	0	0	0	0	0	0	0	0	0	0	0	0	0	0
6	0	0	0	0	0	0	0	0	0	0	0	0	0	0	0	0	0	0
PN-8-m	0	0	0	5	0	0	0	0	0	0	0	0	0	0	0	0	21	0
1	0	0	0	2	0	0	0	0	0	0	0	0	0	0	0	0	4	0
2	0	0	0	3	0	0	0	0	0	0	0	0	0	0	0	0	13	0
3	0	0	0	0	0	0	0	0	0	0	0	0	0	0	0	0	3	0
4	0	0	0	0	0	0	0	0	0	0	0	0	0	0	0	0	1	0
5	0	0	0	0	0	0	0	0	0	0	0	0	0	0	0	0	0	0
6	0	0	0	0	0	0	0	0	0	0	0	0	0	0	0	0	0	0
PN-9-m	0	0	0	10	0	0	3	0	0	1	0	2	0	0	0	0	18	0
1	0	0	0	0	0	0	0	0	0	0	0	0	0	0	0	0	0	0
2	0	0	0	10	0	0	0	0	0	1	0	2	0	0	0	0	9	0
3	0	0	0	0	0	0	3	0	0	0	0	0	0	0	0	0	7	0
4	0	0	0	0	0	0	0	0	0	0	0	0	0	0	0	0	2	0
5	0	0	0	0	0	0	0	0	0	0	0	0	0	0	0	0	0	0
6	0	0	0	0	0	0	0	0	0	0	0	0	0	0	0	0	0	0
PN-10-m	0	0	0	4	0	0	0	0	0	0	0	4	0	0	2	0	9	0
1	0	0	0	0	0	0	0	0	0	0	0	0	0	0	0	0	0	0
2	0	0	0	4	0	0	0	0	0	0	0	0	0	0	2	0	7	0
3	0	0	0	0	0	0	0	0	0	0	0	4	0	0	0	0	2	0
4	0	0	0	0	0	0	0	0	0	0	0	0	0	0	0	0	0	0
5	0	0	0	0	0	0	0	0	0	0	0	0	0	0	0	0	0	0
6	0	0	0	0	0	0	0	0	0	0	0	0	0	0	0	0	0	0
PN-11-m	0	0	1	4	0	0	0	0	0	0	0	0	0	0	0	0	13	0
1	0	0	0	1	0	0	0	0	0	0	0	0	0	0	0	0	0	0
2	0	0	0	3	0	0	0	0	0	0	0	0	0	0	0	0	8	0
3	0	0	0	0	0	0	0	0	0	0	0	0	0	0	0	0	5	0
4	0	0	0	0	0	0	0	0	0	0	0	0	0	0	0	0	0	0
5	0	0	1	0	0	0	0	0	0	0	0	0	0	0	0	0	0	0
6	0	0	0	0	0	0	0	0	0	0	0	0	0	0	0	0	0	0

*Key to Grain Shape Categories. **1** = very angular; **2** = angular; **3** = sub-angular; **4** = sub-rounded; **5** = rounded; **6** = well rounded; Vc: very coarse sand fraction; C: coarse sand fraction; m: medium sand fraction; f: fine sand fraction; Vf: very fine sand fraction.

PANAREA ISLAND (continued)

SAMPLE	Chert	Lvl	Lvlblgl	Lvlbrgl	Lvlgrgl	Lvlclgl	Lvlaltgl	Lvmi	Lvmiblgl	Lvmibrgl	Lvmigrgl	Lvmiclgl	Lvmialtgl
PN-7-m	0	0	22	20	81	12	5	0	14	8	34	6	2
1	0	0	7	6	14	0	2	0	0	0	4	0	0
2	0	0	11	8	33	12	3	0	6	4	15	6	2
3	0	0	4	6	21	0	0	0	4	4	11	0	0
4	0	0	0	0	13	0	0	0	4	0	4	0	0
5	0	0	0	0	0	0	0	0	0	0	0	0	0
6	0	0	0	0	0	0	0	0	0	0	0	0	0
PN-8-m	0	0	17	89	49	15	0	0	16	48	17	16	1
1	0	0	3	9	7	0	0	0	1	1	0	0	0
2	0	0	5	24	17	7	0	0	9	13	5	11	0
3	0	0	9	33	12	8	0	0	6	20	7	4	1
4	0	0	0	23	7	0	0	0	0	5	5	0	0
5	0	0	0	0	6	0	0	0	0	9	0	1	0
6	0	0	0	0	0	0	0	0	0	0	0	0	0
PN-9-m	0	0	12	68	27	11	7	0	18	55	23	4	3
1	0	0	0	0	0	0	0	0	0	0	0	0	0
2	0	0	2	11	6	7	0	0	3	5	1	3	0
3	0	0	4	20	4	4	7	0	15	24	9	1	3
4	0	0	5	37	15	0	0	0	0	24	9	0	0
5	0	0	1	0	2	0	0	0	0	2	4	0	0
6	0	0	0	0	0	0	0	0	0	0	0	0	0
PN-10-m	1	0	21	59	76	14	1	0	21	49	31	6	0
1	0	0	0	1	1	0	0	0	1	2	0	0	0
2	1	0	9	23	32	14	1	0	7	19	11	5	0
3	0	0	12	19	30	0	0	0	9	22	18	1	0
4	0	0	0	10	8	0	0	0	4	6	2	0	0
5	0	0	0	3	5	0	0	0	0	0	0	0	0
6	0	0	0	3	0	0	0	0	0	0	0	0	0
PN-11-m	0	0	15	24	96	4	3	13	16	0	73	5	9
1	0	0	3	5	13	0	0	0	1	0	10	0	0
2	0	0	3	7	35	4	3	6	5	0	24	5	1
3	0	0	3	8	27	0	0	6	9	0	28	0	4
4	0	0	6	3	15	0	0	1	1	0	8	0	4
5	0	0	0	1	6	0	0	0	0	0	3	0	0
6	0	0	0	0	0	0	0	0	0	0	0	0	0

SAMPLE	Lvvblgl	Lvvbrgl	Lvvorgl	Lvvgrgl	Lvvclgl	Lvvalgl	Lvf	Pmcl	Lm	Lp	Lvo	Lsc (crist)	Lsc (micr)	Xe	Unk	TOT
PN-7-m	15	0	0	0	0	6	49	0	1	1	0	2	0	1	0	400
1	3	0	0	0	0	2	13	0	0	0	0	0	0	0	0	80
2	7	0	0	0	0	4	24	0	0	1	0	0	0	0	0	220
3	5	0	0	0	0	0	8	0	1	0	0	0	0	0	0	71
4	0	0	0	0	0	0	4	0	0	0	0	2	0	1	0	29
5	0	0	0	0	0	0	0	0	0	0	0	0	0	0	0	0
6	0	0	0	0	0	0	0	0	0	0	0	0	0	0	0	0
PN-8-m	3	4	1	0	12	1	22	1	0	0	0	0	0	1	0	400
1	0	0	0	0	9	0	2	0	0	0	0	0	0	0	0	50
2	2	0	0	0	0	0	11	1	0	0	0	0	0	1	0	164
3	1	0	1	0	2	0	8	0	0	0	0	0	0	0	0	120
4	0	0	0	0	0	0	1	0	0	0	0	0	0	0	0	44
5	0	4	0	0	1	1	0	0	0	0	0	0	0	0	0	22
6	0	0	0	0	0	0	0	0	0	0	0	0	0	0	0	0
PN-9-m	12	1	0	0	7	0	6	4	0	0	0	0	0	0	5	400
1	0	0	0	0	3	0	0	0	0	0	0	0	0	0	0	17
2	4	0	0	0	4	0	3	4	0	0	0	0	0	0	0	124
3	6	0	0	0	0	0	3	0	0	0	0	0	0	0	0	142
4	2	1	0	0	0	0	0	0	0	0	0	0	0	0	5	106
5	0	0	0	0	0	0	0	0	0	0	0	0	0	0	0	11
6	0	0	0	0	0	0	0	0	0	0	0	0	0	0	0	0
PN-10-m	12	0	1	1	18	5	10	8	1	2	0	5	2	0	0	400
1	2	0	0	0	5	0	0	0	0	0	0	0	0	0	0	14
2	3	0	1	0	8	0	6	6	0	2	0	5	0	0	0	186
3	4	0	0	1	4	5	4	2	0	0	0	0	2	0	0	153
4	3	0	0	0	1	0	0	0	1	0	0	0	0	0	0	36
5	0	0	0	0	0	0	0	0	0	0	0	0	0	0	0	8
6	0	0	0	0	0	0	0	0	0	0	0	0	0	0	0	3
PN-11-m	29	3	0	2	3	3	4	16	0	0	0	0	0	1	0	400
1	3	0	0	0	1	1	0	0	0	0	0	0	0	0	0	52
2	8	2	0	0	2	0	2	6	0	0	0	0	0	0	0	157
3	12	1	0	2	0	2	0	6	0	0	0	0	0	1	0	122
4	5	0	0	0	0	0	2	4	0	0	0	0	0	0	0	52
5	1	0	0	0	0	0	0	0	0	0	0	0	0	0	0	17
6	0	0	0	0	0	0	0	0	0	0	0	0	0	0	0	0

*Key to Grain Shape Categories. **1** = very angular; **2** = angular; **3** = sub-angular; **4** = sub-rounded; **5** = rounded; **6** = well rounded; Vc: very coarse sand fraction; C: coarse sand fraction; m: medium sand fraction; f: fine sand fraction; Vf: very fine sand fraction.

STROMBOLI ISLAND

SAMPLE	P	P inLvlblgl	P inLvlbrgl	P inLvlorgl	P inLvlgrgl	P inLvlclgl	P alt	Py	Py in Lvlblgl	Py in Lvlbrgl	Py in Lvlorgl	Py in Lvlgrgl
STR-1-Vc	4	78	9	0	2	0	0	23	13	3	0	0
1	0	18	1	0	0	0	0	2	3	0	0	0
2	3	32	6	0	0	0	0	9	5	2	0	0
3	1	20	2	0	0	0	0	7	3	1	0	0
4	0	8	0	0	1	0	0	5	2	0	0	0
5	0	0	0	0	1	0	0	0	0	0	0	0
6	0	0	0	0	0	0	0	0	0	0	0	0
STR-1-C	6	81	2	0	0	0	0	48	33	1	0	0
1	0	3	0	0	0	0	0	8	0	0	0	0
2	5	57	2	0	0	0	0	33	28	1	0	0
3	1	16	0	0	0	0	0	7	5	0	0	0
4	0	5	0	0	0	0	0	0	0	0	0	0
5	0	0	0	0	0	0	0	0	0	0	0	0
6	0	0	0	0	0	0	0	0	0	0	0	0
STR-1-m	11	36	2	0	0	0	0	46	9	3	0	0
1	0	0	0	0	0	0	0	1	0	0	0	0
2	7	15	0	0	0	0	0	26	5	1	0	0
3	4	12	2	0	0	0	0	12	2	0	0	0
4	0	8	0	0	0	0	0	5	2	1	0	0
5	0	1	0	0	0	0	0	2	0	1	0	0
6	0	0	0		0	0	0	0	0	0	0	0
STR-1-f	38	30	4	0	0	0	0	72	5	0	0	0
1	4	1	0	0	0	0	0	8	0	0	0	0
2	31	14	4	0	0	0	0	58	4	0	0	0
3	3	13	0	0	0	0	0	6	1	0	0	0
4	0	2	0	0	0	0	0	0	0	0	0	0
5	0	0	0	0	0	0	0	0	0	0	0	0
6	0	0	0	0	0	0	0	0	0	0	0	0
STR-1-Vf	54	2	0	0	0	0	0	128	0	0	0	0
1	15	0	0	0	0	0	0	37	0	0	0	0
2	31	1	0	0	0	0	0	79	0	0	0	0
3	5	1	0	0	0	0	0	12	0	0	0	0
4	3	0	0	0	0	0	0	0	0	0	0	0
5	0	0	0	0	0	0	0	0	0	0	0	0
6	0	0	0	0	0	0	0	0	0	0	0	0

SAMPLE	Py alt	K	K in Lvlblgl	K in Lvlbrgl	K in Lvlorgl	Ol	Ol inLvlblgl	Ol inLvlbrgl	Ol inLvlorgl	Ol inLvlgrgl	Ol alt	Lvl	Lvlblgl
STR-1-Vc	0	1	9	0	0	6	22	2	0	0	0	0	87
1	0	0	1	0	0	0	4	0	0	0	0	0	20
2	0	0	3	0	0	2	10	0	0	0	0	0	30
3	0	1	3	0	0	1	6	2	0	0	0	0	23
4	0	0	2	0	0	3	2	0	0	0	0	0	10
5	0	0	0	0	0	0	0	0	0	0	0	0	3
6	0	0	0	0	0	0	0	0	0	0	0	0	1
STR-1-C	0	2	10	0	0	5	16	3	0	0	0	0	128
1	0	0	0	0	0	1	0	0	0	0	0	0	10
2	0	2	8	0	0	3	7	2	0	0	0	0	66
3	0	0	2	0	0	0	3	0	0	0	0	0	40
4	0	0	0	0	0	1	6	1	0	0	0	0	9
5	0	0	0	0	0	0	0	0	0	0	0	0	3
6	0	0	0	0	0	0	0	0	0	0	0	0	0
STR-1-m	0	0	6	16	0	28	11	3	0	0	0	0	73
1	0	0	0	0	0	1	0	0	0	0	0	0	2
2	0	0	3	3	0	17	2	1	0	0	0	0	27
3	0	0	2	9	0	7	6	2	0	0	0	0	18
4	0	0	1	4	0	2	2	0	0	0	0	0	22
5	0	0	0	0	0	1	1	0	0	0	0	0	4
6	0	0	0	0	0	0	0	0	0	0	0	0	0
STR-1-f	0	12	0	0	0	19	3	0	0	0	0	0	48
1	0	0	0	0	0	2	0	0	0	0	0	0	0
2	0	9	0	0	0	13	2	0	0	0	0	0	35
3	0	3	0	0	0	3	1	0	0	0	0	0	12
4	0	0	0	0	0	1	0	0	0	0	0	0	1
5	0	0	0	0	0	0	0	0	0	0	0	0	0
6	0	0	0	0	0	0	0	0	0	0	0	0	0
STR-1-Vf	0	15	0	0	0	52	2	1	0	0	0	0	14
1	0	1	0	0	0	19	0	0	0	0	0	0	2
2	0	9	0	0	0	22	1	1	0	0	0	0	8
3	0	5	0	0	0	7	1	0	0	0	0	0	4
4	0	0	0	0	0	4	0	0	0	0	0	0	0
5	0	0	0	0	0	0	0	0	0	0	0	0	0
6	0	0	0	0	0	0	0	0	0	0	0	0	0

*Key to Grain Shape Categories. **1** = very angular; **2** = angular; **3** = sub-angular; **4** = sub-rounded; **5** = rounded; **6** = well rounded; Vc: very coarse sand fraction; C: coarse sand fraction; m: medium sand fraction; f: fine sand fraction; Vf: very fine sand fraction.

STROMBOLI ISLAND (continued)

SAMPLE	Lvlbrgl	Lvlorgl	Lvlgrgl	Lvlclgl	Lvlalt	Lvmi	Lvmiblgl	Lvmibrgl	Lvmiorgl	Lvmigrgl	Lvmiclgl	Lvmialt	Lvvblgl
STR-1-Vc	11	0	7	0	0	2	0	0	0	0	0	0	8
1	2	0	1	0	0	0	0	0	0	0	0	0	0
2	5	0	4	0	0	1	0	0	0	0	0	0	5
3	3	0	1	0	0	1	0	0	0	0	0	0	1
4	0	0	1	0	0	0	0	0	0	0	0	0	2
5	1	0	0	0	0	0	0	0	0	0	0	0	0
6	0	0	0	0	0	0	0	0	0	0	0	0	0
STR-1-C	13	0	5	1	0	0	23	2	0	1	0	0	20
1	4	0	0	0	0	0	4	0	0	0	0	0	1
2	6	0	3	1	0	0	12	2	0	1	0	0	13
3	3	0	2	0	0	0	7	0	0	0	0	0	6
4	0	0	0	0	0	0	0	0	0	0	0	0	0
5	0	0	0	0	0	0	0	0	0	0	0	0	0
6	0	0	0	0	0	0	0	0	0	0	0	0	0
STR-1-m	9	0	3	0	1	0	58	7	0	9	0	0	60
1	0	0	0	0	0	0	0	0	0	0	0	0	3
2	4	0	0	0	0	0	17	1	0	0	0	0	20
3	2	0	1	0	1	0	18	3	0	1	0	0	17
4	1	0	1	0	0	0	18	2	0	3	0	0	13
5	2	0	1	0	0	0	5	1	0	5	0	0	7
6	0	0	0	0	0	0	0	0	0	0	0	0	0
STR-1-f	7	0	1	0	0	0	75	13	0	7	0	0	60
1	0	0	0	0	0	0	6	0	0	0	0	0	15
2	4	0	1	0	0	0	38	11	0	4	0	0	29
3	3	0	0	0	0	0	20	2	0	2	0	0	14
4	0	0	0	0	0	0	11	0	0	1	0	0	2
5	0	0	0	0	0	0	0	0	0	0	0	0	0
6	0	0	0	0	0	0	0	0	0	0	0	0	0
STR-1-Vf	0	0	0	0	0	0	48	21	0	2	0	0	47
1	0	0	0	0	0	0	6	1	0	0	0	0	15
2	0	0	0	0	0	0	27	15	0	2	0	0	24
3	0	0	0	0	0	0	13	5	0	0	0	0	7
4	0	0	0	0	0	0	2	0	0	0	0	0	1
5	0	0	0	0	0	0	0	0	0	0	0	0	0
6	0	0	0	0	0	0	0	0	0	0	0	0	0

SAMPLE	Lvvbrgl	Lvvorgl	Lvvgrgl	Lvvclgl	Lvvalgl	Lvf	Pm	Lvo	Lsc (crist)	Lsc (micr)	Hb	Op	Unknown	TOT
STR-1-Vc	0	0	0	0	0	0	0	0	0	0	0	0	0	287
1	0	0	0	0	0	0	0	0	0	0	0	0	0	52
2	0	0	0	0	0	0	0	0	0	0	0	0	0	117
3	0	0	0	0	0	0	0	0	0	0	0	0	0	76
4	0	0	0	0	0	0	0	0	0	0	0	0	0	36
5	0	0	0	0	0	0	0	0	0	0	0	0	0	5
6	0	0	0	0	0	0	0	0	0	0	0	0	0	1
STR-1-C	0	0	0	0	0	0	0	0	0	0	0	0	0	400
1	0	0	0	0	0	0	0	0	0	0	0	0	0	31
2	0	0	0	0	0	0	0	0	0	0	0	0	0	252
3	0	0	0	0	0	0	0	0	0	0	0	0	0	92
4	0	0	0	0	0	0	0	0	0	0	0	0	0	22
5	0	0	0	0	0	0	0	0	0	0	0	0	0	3
6	0	0	0	0	0	0	0	0	0	0	0	0	0	0
STR-1-m	0	0	1	2	0	2	0	0	2	1	1	0	0	400
1	0	0	0	0	0	0	0	0	0	0	0	0	0	7
2	0	0	1	2	0	1	0	0	1	0	1	0	0	155
3	0	0	0	0	0	1	0	0	0	0	0	0	0	120
4	0	0	0	0	0	0	0	0	1	1	0	0	0	87
5	0	0	0	0	0	0	0	0	0	0	0	0	0	31
6	0	0	0	0	0	0	0	0	0	0	0	0	0	0
STR-1-f	1	0	1	0	0	0	1	0	0	0	0	3	0	400
1	1	0	0	0	0	0	0	0	0	0	0	0	0	37
2	0	0	1	0	0	0	0	0	0	0	0	3	0	261
3	0	0	0	0	0	0	1	0	0	0	0	0	0	84
4	0	0	0	0	0	0	0	0	0	0	0	0	0	18
5	0	0	0	0	0	0	0	0	0	0	0	0	0	0
6	0	0	0	0	0	0	0	0	0	0	0	0	0	0
STR-1-Vf	5	1	0	1	0	1	1	0	0	0	2	3	0	400
1	1	0	0	0	0	0	1	0	0	0	0	0	0	98
2	4	1	0	1	0	1	0	0	0	0	2	0	0	229
3	0	0	0	0	0	0	0	0	0	0	0	3	0	63
4	0	0	0	0	0	0	0	0	0	0	0	0	0	10
5	0	0	0	0	0	0	0	0	0	0	0	0	0	0
6	0	0	0	0	0	0	0	0	0	0	0	0	0	0

*Key to Grain Shape Categories. **1** = very angular; **2** = angular; **3** = sub-angular; **4** = sub-rounded; **5** = rounded; **6** = well rounded; Vc: very coarse sand fraction; C: coarse sand fraction; m: medium sand fraction; f: fine sand fraction; Vf: very fine sand fraction.

STROMBOLI ISLAND (continued)

SAMPLE	P	P inLvlblgl	P inLvlbrgl	P inLvlorgl	P inLvlgrgl	P inLvlclgl	P alt	Py	Py in Lvlblgl	Py in Lvlbrgl	Py in Lvlorgl	Py in Lvlgrgl
STR-2-m	3	9	3	0	0	0	0	189	21	1	0	0
1	0	0	0	0	0	0	0	3	0	0	0	0
2	2	5	1	0	0	0	0	86	1	0	0	0
3	1	3	2	0	0	0	0	58	19	1	0	0
4	0	1	0	0	0	0	0	40	1	0	0	0
5	0	0	0	0	0	0	0	2	0	0	0	0
6	0	0	0	0	0	0	0	0	0	0	0	0
STR-3-m	15	57	8	0	8	0	2	50	12	1	1	0
1	0	2	0	0	0	0	0	2	0	0	0	0
2	10	22	6	0	0	0	0	22	5	0	1	0
3	5	24	2	0	6	0	0	18	7	1	0	0
4	0	9	0	0	2	0	2	8	0	0	0	0
5	0	0	0	0	0	0	0	0	0	0	0	0
6	0	0	0	0	0	0	0	0	0	0	0	0
STR-4-m	14	49	15	0	6	1	1	62	13	1	0	1
1	3	0	0	0	0	0	0	0	0	0	0	0
2	10	26	11	0	1	0	0	32	6	1	0	0
3	1	18	4	0	5	1	0	25	5	0	0	0
4	0	5	0	0	0	0	1	5	2	0	0	1
5	0	0	0	0	0	0	0	0	0	0	0	0
6	0	0	0	0	0	0	0	0	0	0	0	0
STR-5-m	16	47	15	0	4	0	0	44	23	2	0	0
1	1	1	0	0	0	0	0	6	0	2	0	0
2	11	14	10	0	1	0	0	17	12	0	0	0
3	3	26	5	0	2	0	0	16	9	0	0	0
4	1	6	0	0	1	0	0	5	2	0	0	0
5	0	0	0	0	0	0	0	0	0	0	0	0
6	0	0	0	0	0	0	0	0	0	0	0	0

SAMPLE	Py alt	K	K in Lvlblgl	K in Lvlbrgl	K in Lvlorgl	Ol	Ol inLvlblgl	Ol inLvlbrgl	Ol inLvlorgl	Ol inLvlgrgl	Ol alt	Lvl	Lvlblgl
STR-2-m	0	0	0	0	0	70	28	7	0	0	0	0	33
1	0	0	0	0	0	0	0	0	0	0	0	0	0
2	0	0	0	0	0	16	3	0	0	0	0	0	15
3	0	0	0	0	0	8	3	0	0	0	0	0	5
4	0	0	0	0	0	29	10	5	0	0	0	0	7
5	0	0	0	0	0	17	12	2	0	0	0	0	6
6	0	0	0	0	0	0	0	0	0	0	0	0	0
STR-3-m	2	5	1	0	0	4	1	0	0	0	0	6	112
1	0	0	0	0	0	0	0	0	0	0	0	0	0
2	0	0	1	0	0	3	0	0	0	0	0	1	33
3	2	5	0	0	0	0	1	0	0	0	0	1	50
4	0	0	0	0	0	1	0	0	0	0	0	4	22
5	0	0	0	0	0	0	0	0	0	0	0	0	7
6	0	0	0	0	0	0	0	0	0	0	0	0	0
STR-4-m	0	6	0	0	0	2	2	0	0	0	1	4	86
1	0	0	0	0	0	0	0	0	0	0	0	0	0
2	0	4	0	0	0	2	1	0	0	0	0	4	43
3	0	2	0	0	0	0	1	0	0	0	0	0	32
4	0	0	0	0	0	0	0	0	0	0	1	0	10
5	0	0	0	0	0	0	0	0	0	0	0	0	1
6	0	0	0	0	0	0	0	0	0	0	0	0	0
STR-5-m	0	6	2	0	0	10	11	4	0	0	1	0	79
1	0	0	0	0	0	2	0	2	0	0	0	0	2
2	0	3	2	0	0	6	6	1	0	0	0	0	30
3	0	3	0	0	0	1	3	1	0	0	0	0	31
4	0	0	0	0	0	0	1	0	0	0	1	0	16
5	0	0	0	0	0	1	1	0	0	0	0	0	0
6	0	0	0	0	0	0	0	0	0	0	0	0	0

*Key to Grain Shape Categories. **1** = very angular; **2** = angular; **3** = sub-angular; **4** = sub-rounded; **5** = rounded; **6** = well rounded; Vc: very coarse sand fraction; C: coarse sand fraction; m: medium sand fraction; f: fine sand fraction; Vf: very fine sand fraction.

STROMBOLI ISLAND (continued)

SAMPLE	Lvlbrgl	Lvlorgl	Lvlgrgl	Lvlclgl	Lvlalt	Lvmi	Lvmiblgl	Lvmibrgl	Lvmiorgl	Lvmigrgl	Lvmiclgl	Lvmialt	Lvvblgl
STR-2-m	3	0	3	0	0	0	10	4	0	2	0	0	10
1	0	0	0	0	0	0	0	0	0	0	0	0	0
2	0	0	0	0	0	0	2	0	0	2	0	0	2
3	3	0	3	0	0	0	3	4	0	0	0	0	3
4	0	0	0	0	0	0	5	0	0	0	0	0	1
5	0	0	0	0	0	0	0	0	0	0	0	0	4
6	0	0	0	0	0	0	0	0	0	0	0	0	0
STR-3-m	25	1	17	2	0	2	56	3	0	2	0	0	7
1	0	0	0	0	0	0	0	0	0	0	0	0	0
2	10	1	5	0	0	0	18	0	0	0	0	0	5
3	12	0	9	2	0	2	32	3	0	1	0	0	1
4	3	0	3	0	0	0	6	0	0	1	0	0	1
5	0	0	0	0	0	0	0	0	0	0	0	0	0
6	0	0	0	0	0	0	0	0	0	0	0	0	0
STR-4-m	29	0	23	0	0	2	49	8	0	2	0	0	20
1	0	0	0	0	0	0	0	0	0	0	0	0	0
2	10	0	4	0	0	0	21	4	0	2	0	0	13
3	16	0	14	0	0	2	23	4	0	0	0	0	6
4	3	0	5	0	0	0	5	0	0	0	0	0	1
5	0	0	0	0	0	0	0	0	0	0	0	0	0
6	0	0	0	0	0	0	0	0	0	0	0	0	0
STR-5-m	12	0	9	0	3	0	52	11	0	7	0	0	36
1	2	0	0	0	0	0	2	0	0	0	0	0	1
2	6	0	1	0	0	0	15	5	0	1	0	0	10
3	2	0	6	0	1	0	24	6	0	6	0	0	16
4	2	0	2	0	2	0	11	0	0	0	0	0	9
5	0	0	0	0	0	0	0	0	0	0	0	0	0
6	0	0	0	0	0	0	0	0	0	0	0	0	0

SAMPLE	Lvvbrgl	Lvvorgl	Lvvgrgl	Lvvclgl	Lvvalgl	Lvf	Pm	Lvo	Lsc (crist)	Lsc (micr)	Hb	Op	Unknown	TOT
STR-2-m	0	0	0	1	0	0	0	0	0	0	0	3	0	400
1	0	0	0	0	0	0	0	0	0	0	0	0	0	3
2	0	0	0	1	0	0	0	0	0	0	0	0	0	136
3	0	0	0	0	0	0	0	0	0	0	0	0	0	116
4	0	0	0	0	0	0	0	0	0	0	0	3	0	102
5	0	0	0	0	0	0	0	0	0	0	0	0	0	43
6	0	0	0	0	0	0	0	0	0	0	0	0	0	0
STR-3-m	0	0	0	0	0	0	0	0	0	0	0	0	0	400
1	0	0	0	0	0	0	0	0	0	0	0	0	0	4
2	0	0	0	0	0	0	0	0	0	0	0	0	0	143
3	0	0	0	0	0	0	0	0	0	0	0	0	0	184
4	0	0	0	0	0	0	0	0	0	0	0	0	0	62
5	0	0	0	0	0	0	0	0	0	0	0	0	0	7
6	0	0	0	0	0	0	0	0	0	0	0	0	0	0
STR-4-m	3	0	0	0	0	0	0	0	0	0	0	0	0	400
1	0	0	0	0	0	0	0	0	0	0	0	0	0	3
2	2	0	0	0	0	0	0	0	0	0	0	0	0	197
3	1	0	0	0	0	0	0	0	0	0	0	0	0	160
4	0	0	0	0	0	0	0	0	0	0	0	0	0	39
5	0	0	0	0	0	0	0	0	0	0	0	0	0	1
6	0	0	0	0	0	0	0	0	0	0	0	0	0	0
STR-5-m	3	0	0	0	0	0	0	0	0	0	0	0	3	400
1	1	0	0	0	0	0	0	0	0	0	0	0	0	22
2	0	0	0	0	0	0	0	0	0	0	0	0	3	154
3	0	0	0	0	0	0	0	0	0	0	0	0	0	161
4	2	0	0	0	0	0	0	0	0	0	0	0	0	61
5	0	0	0	0	0	0	0	0	0	0	0	0	0	2
6	0	0	0	0	0	0	0	0	0	0	0	0	0	0

*Key to Grain Shape Categories. **1** = very angular; **2** = angular; **3** = sub-angular; **4** = sub-rounded; **5** = rounded; **6** = well rounded; Vc: very coarse sand fraction; C: coarse sand fraction; m: medium sand fraction; f: fine sand fraction; Vf: very fine sand fraction.

STROMBOLI ISLAND (continued)

SAMPLE	P	P inLvlblgl	P inLvlbrgl	P inLvlorgl	P inLvlgrgl	P inLvlclgl	P alt	Py	Py in Lvlblgl	Py in Lvlbrgl	Py in Lvlorgl	Py in Lvlgrgl
STR-7-m	18	55	15	0	6	0	0	39	13	1	0	0
1	3	3	0	0	0	0	0	6	0	0	0	0
2	9	30	13	0	2	0	0	27	9	1	0	0
3	6	19	2	0	3	0	0	6	4	0	0	0
4	0	3	0	0	1	0	0	0	0	0	0	0
5	0	0	0	0	0	0	0	0	0	0	0	0
6	0	0	0	0	0	0	0	0	0	0	0	0
STR-8-m	10	32	18	1	2	0	0	90	17	6	0	0
1	3	3	1	0	0	0	0	16	0	0	0	0
2	5	17	12	1	1	0	0	53	14	2	0	0
3	2	9	5	0	1	0	0	18	3	3	0	0
4	0	2	0	0	0	0	0	3	0	1	0	0
5	0	1	0	0	0	0	0	0	0	0	0	0
6	0	0	0	0	0	0	0	0	0	0	0	0
STR-9-Vc	0	28	49	3	0	0	0	9	15	22	7	0
1	0	15	36	2	0	0	0	7	8	21	5	0
2	0	8	13	1	0	0	0	2	7	1	2	0
3	0	4	0	0	0	0	0	0	0	0	0	0
4	0	1	0	0	0	0	0	0	0	0	0	0
5	0	0	0	0	0	0	0	0	0	0	0	0
6	0	0	0	0	0	0	0	0	0	0	0	0
STR-9-C	1	91	64	3	0	0	1	6	6	4	0	0
1	0	44	40	2	0	0		3	2	0	0	0
2	1	35	14	1	0	0	0	3	2	3	0	0
3	0	11	9	0	0	0	1	0	2	1	0	0
4	0	1	1	0	0	0	0	0	0	0	0	0
5	0	0	0	0	0	0	0	0	0	0	0	0
6	0	0	0	0	0	0	0	0	0	0	0	0

SAMPLE	Py alt	K	K in Lvlblgl	K in Lvlbrgl	K in Lvlorgl	Ol	Ol inLvlblgl	Ol inLvlbrgl	Ol inLvlorgl	Ol inLvlgrgl	Ol alt	Lvl	Lvlblgl
STR-7-m	1	2	2	0	0	4	14	1	0	0	1	0	76
1	0	0	0	0	0	0	0	0	0	0	0	0	0
2	0	1	2	0	0	3	7	1	0	0	0	0	44
3	1	1	0	0	0	1	7	0	0	0	1	0	24
4	0	0	0	0	0	0	0	0	0	0	0	0	8
5	0	0	0	0	0	0	0	0	0	0	0	0	0
6	0	0	0	0	0	0	0	0	0	0	0	0	0
STR-8-m	0	5	5	2	0	8	5	2	0	1	1	0	76
1	0	0	0	0	0	2	0	0	0	0	0	0	4
2	0	4	5	2	0	6	3	2	0	1	0	0	33
3	0	1	0	0	0	0	1	0	0	0	0	0	26
4	0	0	0	0	0	0	1	0	0	0	1	0	12
5	0	0	0	0	0	0	0	0	0	0	0	0	1
6	0	0	0	0	0	0	0	0	0	0	0	0	0
STR-9-Vc	0	0	0	4	1	0	1	11	0	0	0	0	39
1	0	0	0	1	1	0	1	11	0	0	0	0	32
2	0	0	0	3	0	0	0	0	0	0	0	0	7
3	0	0	0	0	0	0	0	0	0	0	0	0	0
4	0	0	0	0	0	0	0	0	0	0	0	0	0
5	0	0	0	0	0	0	0	0	0	0	0	0	0
6	0	0	0	0	0	0	0	0	0	0	0	0	0
STR-9-C	0	0	4	1	0	1	4	6	0	0	0	0	90
1	0	0	3	1	0	0	4	4	0	0	0	0	45
2	0	0	1	0	0	1	0	1	0	0	0	0	26
3	0	0	0	0	0	0	0	0	0	0	0	0	14
4	0	0	0	0	0	0	0	1	0	0	0	0	4
5	0	0	0	0	0	0	0	0	0	0	0	0	1
6	0	0	0	0	0	0	0	0	0	0	0	0	0

*Key to Grain Shape Categories. **1** = very angular; **2** = angular; **3** = sub-angular; **4** = sub-rounded; **5** = rounded; **6** = well rounded; Vc: very coarse sand fraction; C: coarse sand fraction; m: medium sand fraction; f: fine sand fraction; Vf: very fine sand fraction.

STROMBOLI ISLAND (continued)

SAMPLE	Lvlbrgl	Lvlorgl	Lvlgrgl	Lvlclgl	Lvlalt	Lvmi	Lvmiblgl	Lvmibrgl	Lvmiorgl	Lvmigrgl	Lvmiclgl	Lvmialt	Lvvblgl
STR-7-m	29	1	10	0	0	0	48	18	0	15	2	1	22
1	0	0	0	0	0	0	2	0	0	0	0	0	2
2	17	1	4	0	0	0	22	9	0	8	2	1	13
3	10	0	3	0	0	0	21	7	0	7	0	0	6
4	2	0	3	0	0	0	3	2	0	0	0	0	1
5	0	0	0	0	0	0	0	0	0	0	0	0	0
6	0	0	0	0	0	0	0	0	0	0	0	0	0
STR-8-m	38	0	14	0	0	0	36	8	0	3	0	0	18
1	0	0	0	0	0	0	2	0	0	0	0	0	5
2	15	0	10	0	0	0	18	5	0	3	0	0	10
3	15	0	3	0	0	0	15	3	0	0	0	0	3
4	7	0	1	0	0	0	1	0	0	0	0	0	0
5	1	0	0	0	0	0	0	0	0	0	0	0	0
6	0	0	0	0	0	0	0	0	0	0	0	0	0
STR-9-Vc	76	5	0	0	0	0	3	10	1	0	0	0	3
1	58	5	0	0	0	0	3	5	0	0	0	0	2
2	18	0	0	0	0	0	0	4	1	0	0	0	1
3	0	0	0	0	0	0	0	1	0	0	0	0	0
4	0	0	0	0	0	0	0	0	0	0	0	0	0
5	0	0	0	0	0	0	0	0	0	0	0	0	0
6	0	0	0	0	0	0	0	0	0	0	0	0	0
STR-9-C	52	7	0	0	0	0	18	12	0	0	0	0	21
1	27	5	0	0	0	0	10	6	0	0	0	0	19
2	19	2	0	0	0	0	7	5	0	0	0	0	2
3	5	0	0	0	0	0	1	1	0	0	0	0	0
4	1	0	0	0	0	0	0	0	0	0	0	0	0
5	0	0	0	0	0	0	0	0	0	0	0	0	0
6	0	0	0	0	0	0	0	0	0	0	0	0	0

SAMPLE	Lvvbrgl	Lvvorgl	Lvvgrgl	Lvvclgl	Lvvalgl	Lvf	Pm	Lvo	Lsc (crist)	Lsc (micr)	Hb	Op	Unknown	TOT
STR-7-m	1	0	0	0	0	0	0	4	0	0	0	0	1	400
1	0	0	0	0	0	0	0	0	0	0	0	0	0	16
2	0	0	0	0	0	0	0	2	0	0	0	0	1	229
3	1	0	0	0	0	0	0	2	0	0	0	0	0	132
4	0	0	0	0	0	0	0	0	0	0	0	0	0	23
5	0	0	0	0	0	0	0	0	0	0	0	0	0	0
6	0	0	0	0	0	0	0	0	0	0	0	0	0	0
STR-8-m	2	0	0	0	0	0	0	0	0	0	0	0	0	400
1	0	0	0	0	0	0	0	0	0	0	0	0	0	36
2	1	0	0	0	0	0	0	0	0	0	0	0	0	223
3	1	0	0	0	0	0	0	0	0	0	0	0	0	109
4	0	0	0	0	0	0	0	0	0	0	0	0	0	29
5	0	0	0	0	0	0	0	0	0	0	0	0	0	3
6	0	0	0	0	0	0	0	0	0	0	0	0	0	0
STR-9-Vc	13	0	0	0	0	0	0	0	0	0	0	0	0	300
1	9	0	0	0	0	0	0	0	0	0	0	0	0	222
2	4	0	0	0	0	0	0	0	0	0	0	0	0	72
3	0	0	0	0	0	0	0	0	0	0	0	0	0	5
4	0	0	0	0	0	0	0	0	0	0	0	0	0	1
5	0	0	0	0	0	0	0	0	0	0	0	0	0	0
6	0	0	0	0	0	0	0	0	0	0	0	0	0	0
STR-9-C	8	0	0	0	0	0	0	0	0	0	0	0	0	400
1	5	0	0	0	0	0	0	0	0	0	0	0	0	220
2	3	0	0	0	0	0	0	0	0	0	0	0	0	126
3	0	0	0	0	0	0	0	0	0	0	0	0	0	45
4	0	0	0	0	0	0	0	0	0	0	0	0	0	8
5	0	0	0	0	0	0	0	0	0	0	0	0	0	1
6	0	0	0	0	0	0	0	0	0	0	0	0	0	0

*Key to Grain Shape Categories. **1** = very angular; **2** = angular; **3** = sub-angular; **4** = sub-rounded; **5** = rounded; **6** = well rounded; Vc: very coarse sand fraction; C: coarse sand fraction; m: medium sand fraction; f: fine sand fraction; Vf: very fine sand fraction.

STROMBOLI ISLAND (continued)

SAMPLE	P	P inLvlblgl	P inLvlbrgl	P inLvlorgl	P inLvlgrgl	P inLvlclgl	P alt	Py	Py in Lvlblgl	Py in Lvlbrgl	Py in Lvlorgl	Py in Lvlgrgl
STR-9-m	19	62	29	4	1	0	1	15	8	3	1	0
1	1	9	10	1	0	0	0	1	1	2	0	0
2	15	28	19	1	1	0	0	10	6	0	1	0
3	3	23	0	2	0	0	1	3	1	1	0	0
4	0	2	0	0	0	0	0	1	0	0	0	0
5	0	0	0	0	0	0	0	0	0	0	0	0
6	0	0	0	0	0	0	0	0	0	0	0	0
STR-9-f	31	38	21	1	0	0	1	27	7	0	0	0
1	6	6	3	1	0	0	0	9	0	0	0	0
2	20	16	18	0	0	0	1	16	4	0	0	0
3	5	15	0	0	0	0	0	2	3	0	0	0
4	0	1	0	0	0	0	0	0	0	0	0	0
5	0	0	0	0	0	0	0	0	0	0	0	0
6	0	0	0	0	0	0	0	0	0	0	0	0
STR-9-Vf	30	10	9	0	0	0	4	21	1	0	0	0
1	3	1	1	0	0	0	0	0	0	0	0	0
2	23	6	8	0	0	0	4	19	1	0	0	0
3	4	3	0	0	0	0	0	2	0	0	0	0
4	0	0	0	0	0	0	0	0	0	0	0	0
5	0	0	0	0	0	0	0	0	0	0	0	0
6	0	0	0	0	0	0	0	0	0	0	0	0

SAMPLE	Py alt	K	K in Lvlblgl	K in Lvlbrgl	K in Lvlorgl	Ol	Ol inLvlblgl	Ol inLvlbrgl	Ol inLvlorgl	Ol inLvlgrgl	Ol alt	Lvl	Lvlblgl
STR-9-m	0	2	3	2	1	4	0	3	1	0	0	0	83
1	0	0	0	0	1	1	0	0	1	0	0	0	19
2	0	2	3	2	0	2	0	3	0	0	0	0	36
3	0	0	0	0	0	0	0	0	0	0	0	0	26
4	0	0	0	0	0	1	0	0	0	0	0	0	2
5	0	0	0	0	0	0	0	0	0	0	0	0	0
6	0	0	0	0	0	0	0	0	0	0	0	0	0
STR-9-f	0	6	2	0	0	6	2	0	0	0	2	0	42
1	0	1	0	0	0	3	0	0	0	0	0	0	5
2	0	3	2	0	0	3	2	0	0	0	0	0	31
3	0	2	0	0	0	0	0	0	0	0	2	0	6
4	0	0	0	0	0	0	0	0	0	0	0	0	0
5	0	0	0	0	0	0	0	0	0	0	0	0	0
6	0	0	0	0	0	0	0	0	0	0	0	0	0
STR-9-Vf	0	4	0	0	0	9	1	0	0	0	0	0	10
1	0	0	0	0	0	3	0	0	0	0	0	0	0
2	0	2	0	0	0	4	1	0	0	0	0	0	6
3	0	2	0	0	0	2	0	0	0	0	0	0	3
4	0	0	0	0	0	0	0	0	0	0	0	0	1
5	0	0	0	0	0	0	0	0	0	0	0	0	0
6	0	0	0	0	0	0	0	0	0	0	0	0	0

*Key to Grain Shape Categories. **1** = very angular; **2** = angular; **3** = sub-angular; **4** = sub-rounded; **5** = rounded; **6** = well rounded; Vc: very coarse sand fraction; C: coarse sand fraction; m: medium sand fraction; f: fine sand fraction; Vf: very fine sand fraction.

STROMBOLI ISLAND (continued)

SAMPLE	Lvlbrgl	Lvlorgl	Lvlgrgl	Lvlclgl	Lvlalt	Lvmi	Lvmiblgl	Lvmibrgl	Lvmiorgl	Lvmigrgl	Lvmiclgl	Lvmialt	Lvvblgl
STR-9-m	37	2	0	0	0	0	44	23	1	0	0	1	34
1	8	2	0	0	0	0	10	6	0	0	0	0	11
2	21	0	0	0	0	0	26	12	1	0	0	0	18
3	7	0	0	0	0	0	7	5	0	0	0	1	5
4	1	0	0	0	0	0	1	0	0	0	0	0	0
5	0	0	0	0	0	0	0	0	0	0	0	0	0
6	0	0	0	0	0	0	0	0	0	0	0	0	0
STR-9-f	31	2	0	0	1	0	69	35	3	0	0	0	51
1	7	0	0	0	0	0	28	13	2	0	0	0	26
2	22	2	0	0	0	0	32	15	1	0	0	0	20
3	2	0	0	0	1	0	9	7	0	0	0	0	5
4	0	0	0	0	0	0	0	0	0	0	0	0	0
5	0	0	0	0	0	0	0	0	0	0	0	0	0
6	0	0	0	0	0	0	0	0	0	0	0	0	0
STR-9-Vf	11	3	0	0	0	0	49	35	4	0	0	0	114
1	2	0	0	0	0	0	15	8	3	0	0	0	42
2	8	3	0	0	0	0	29	20	1	0	0	0	60
3	1	0	0	0	0	0	5	7	0	0	0	0	12
4	0	0	0	0	0	0	0	0	0	0	0	0	0
5	0	0	0	0	0	0	0	0	0	0	0	0	0
6	0	0	0	0	0	0	0	0	0	0	0	0	0

SAMPLE	Lvvbrgl	Lvvorgl	Lvvgrgl	Lvvclgl	Lvvalgl	Lvf	Pm	Lvo	Lsc (crist)	Lsc (micr)	Hb	Op	Unknown	TOT
STR-9-m	14	2	0	0	0	0	0	0	0	0	0	0	0	400
1	5	2	0	0	0	0	0	0	0	0	0	0	0	91
2	8	0	0	0	0	0	0	0	0	0	0	0	0	215
3	1	0	0	0	0	0	0	0	0	0	0	0	0	86
4	0	0	0	0	0	0	0	0	0	0	0	0	0	8
5	0	0	0	0	0	0	0	0	0	0	0	0	0	0
6	0	0	0	0	0	0	0	0	0	0	0	0	0	0
STR-9-f	19	3	0	0	0	0	0	0	0	0	0	0	0	400
1	9	2	0	0	0	0	0	0	0	0	0	0	0	121
2	7	1	0	0	0	0	0	0	0	0	0	0	0	216
3	3	0	0	0	0	0	0	0	0	0	0	0	0	62
4	0	0	0	0	0	0	0	0	0	0	0	0	0	1
5	0	0	0	0	0	0	0	0	0	0	0	0	0	0
6	0	0	0	0	0	0	0	0	0	0	0	0	0	0
STR-9-Vf	61	13	0	2	4	0	0	0	0	0	0	0	5	400
1	24	5	0	0	0	0	0	0	0	0	0	0	3	110
2	26	4	0	2	0	0	0	0	0	0	0	0	2	229
3	11	4	0	0	4	0	0	0	0	0	0	0	0	60
4	0	0	0	0	0	0	0	0	0	0	0	0	0	1
5	0	0	0	0	0	0	0	0	0	0	0	0	0	0
6	0	0	0	0	0	0	0	0	0	0	0	0	0	0

*Key to Grain Shape Categories. **1** = very angular; **2** = angular; **3** = sub-angular; **4** = sub-rounded; **5** = rounded; **6** = well rounded; Vc: very coarse sand fraction; C: coarse sand fraction; m: medium sand fraction; f: fine sand fraction; Vf: very fine sand fraction.

VULCANO ISLAND

Samples	Qm	Qp	P	K	Pyc	Pyo	Ol	Op	Lvvbrgl	Lvvblgl	Lvvclgl	Lvvalt	Lvvorgl	Lvvgrgl	Lvmibrgl	Lvmiblgl	Lvmiclgl	Lvmialt
V1-m	1	0	34	0	138	17	8	1	1	10	0	0	0	0	7	24	0	0
V1-f	0	0	66	0	167	14	15	19	4	8	0	3	1	0	14	23	0	7
V2-m	0	0	33	0	82	10	7	3	0	4	0	1	2	0	6	25	0	1
V2-f	0	0	79	0	113	5	31	16	1	22	0	4	2	0	11	43	0	0
V4-m	0	0	45	2	85	3	3	6	0	2	0	4	0	0	27	29	21	0
V4-f	0	0	50	8	106	7	9	6	4	12	1	2	5	0	27	30	33	0
V5-m	0	0	38	2	23	0	5	0	3	10	0	1	1	0	18	59	8	0
V5-f	0	0	45	3	36	0	23	0	1	9	1	0	0	0	25	83	14	0
V6-m	0	0	47	1	15	0	3	0	9	10	0	0	3	0	20	48	10	0
V6-f	0	0	36	3	40	0	1	0	1	12	0	0	0	0	34	88	30	0
V7-m	4	4	36	7	92	7	4	0	7	8	0	0	1	0	9	32	12	0
V7-f	2	2	44	0	96	6	15	6	2	7	0	3	2	0	16	70	12	0
V8-m	0	0	24	4	50	0	1	0	2	1	7	8	0	0	16	47	12	0
V8-f	0	0	54	11	54	2	17	0	1	5	0	12	2	0	20	81	7	0
V9-m	0	0	28	3	132	10	16	6	1	2	0	0	1	0	8	34	1	0
V9-f	0	0	34	10	98	0	13	12	2	15	0	0	0	0	11	111	3	0
V10-m	0	0	45	2	72	0	9	0	0	1	0	0	0	0	8	32	1	0
V10-f	0	0	42	2	98	0	9	1	0	2	0	0	1	0	12	107	6	0
V11-m	0	0	50	3	83	3	21	1	2	14	0	0	0	0	13	70	3	0
V11-f	0	0	51	2	81	6	12	0	0	0	0	0	0	0	7	114	14	0
V12-m	0	0	40	2	184	7	13	24	0	7	0	0	0	0	3	23	3	0
V12-f	0	0	15	1	205	9	43	34	0	1	0	1	0	0	3	23	2	0

Samples	Lvmiorgl	Lvmigrgl	Lvlbrgl	Lvlblgl	Lvlorgl	Lvlgrgl	Lvlclgl	Lvlalt	Lvf	Lvo	Ls	Bio	Lmt	Bt	Zeo	Tourm	Lvha	TOT
V1-m	6	2	31	88	24	6	0	0	0	1	1	0	0	0	0	0	0	400
V1-f	0	3	21	22	10	2	0	0	1	0	0	0	0	0	0	0	0	400
V2-m	3	10	20	145	16	19	1	2	0	10	0	0	0	0	0	0	0	400
V2-f	4	4	7	42	9	4	0	0	0	3	0	0	0	0	0	0	0	400
V4-m	3	0	44	30	15	0	37	0	17	3	8	0	0	0	0	0	16	400
V4-f	8	0	13	26	8	0	15	0	4	0	14	0	0	0	0	0	12	400
V5-m	13	4	37	114	13	5	27	0	3	6	4	0	0	0	0	0	6	400
V5-f	8	8	28	73	9	2	18	0	0	4	5	0	0	0	0	0	5	400
V6-m	18	8	42	106	17	9	19	0	7	0	4	0	0	0	0	0	4	400
V6-f	14	5	15	91	5	1	19	0	2	2	1	0	0	0	0	0	0	400
V7-m	4	2	33	78	4	3	28	0	5	2	9	0	0	0	0	0	9	400
V7-f	15	4	22	49	15	0	8	0	0	0	3	0	1	0	0	0	0	400
V8-m	14	5	42	99	8	4	25	0	2	5	24	0	0	0	0	0	0	400
V8-f	20	3	18	57	3	6	12	0	0	1	14	0	0	0	0	0	0	400
V9-m	1	1	15	134	5	0	2	0	0	0	0	0	0	0	0	0	0	400
V9-f	4	1	12	70	1	0	3	0	0	0	0	0	0	0	0	0	0	400
V10-m	1	2	25	166	2	17	14	0	0	0	3	0	0	0	0	0	0	400
V10-f	5	3	19	81	2	2	6	0	0	1	1	0	0	0	0	0	0	400
V11-m	4	5	40	70	10	3	5	0	0	0	0	0	0	0	0	0	0	400
V11-f	10	2	12	75	2	1	10	0	0	0	1	0	0	0	0	0	0	400
V12-m	3	4	7	57	12	2	9	0	0	0	0	0	0	0	0	0	0	400
V12-f	3	2	6	37	9	2	4	0	0	0	0	0	0	0	0	0	0	400

Composition raw data. Vc: very coarse sand fraction; C: coarse sand fraction; m: medium sand fraction; f: fine sand fraction; Vf: very fine sand fraction.

VULCANO ISLAND (continued)

SAMPLE	P	Py	K	Ol	Op	Lvl	Lvmi	Lvv	Lvf	TOT
V1-m	40	158	0	8	0	144	39	11	0	400
1	2	17	0	0	0	17	0	4	0	40
2	16	77	0	0	0	28	5	7	0	133
3	17	60	0	3	0	68	14	0	0	162
4	4	4	0	4	0	26	15	0	0	53
5	1	0	0	1	0	5	3	0	0	10
6	0	0	0	0	0	0	2	0	0	2
V2-m	32	98	0	7	4	194	52	13	0	400
1	1	9	0	0	0	21	0	5	0	36
2	12	57	0	0	0	40	4	8	0	121
3	18	27	0	3	1	90	22	0	0	161
4	1	5	0	4	3	36	20	0	0	69
5	0	0	0	0	0	5	3	0	0	8
6	0	0	0	0	0	2	3	0	0	5
V4-m	43	77	5	6	9	137	99	6	18	400
1	2	11	0	0	0	4	0	2	0	19
2	12	22	2	0	0	23	11	4	3	77
3	21	33	3	1	2	59	47	0	6	172
4	7	9	0	3	3	37	41	0	7	107
5	1	2	0	2	4	8	0	0	2	19
6	0	0	0	0	0	6	0	0	0	6
V5-m	41	52	4	7	2	161	104	29	0	400
1	6	11	0	0	0	26	2	15	0	60
2	22	32	0	0	0	69	21	12	0	156
3	12	9	3	3	0	46	29	2	0	104
4	1	0	1	3	2	16	35	0	0	58
5	0	0	0	1	0	3	11	0	0	15
6	0	0	0	0	0	1	6	0	0	7
V6-m	47	44	3	3	2	184	88	23	6	400
1	8	12	0	0	0	29	3	12	0	64
2	27	17	2	1	0	78	21	11	3	160
3	10	15	1	1	1	51	28	0	2	109
4	2	0	0	1	1	15	20	0	1	40
5	0	0	0	0	0	7	9	0	0	16
6	0	0	0	0	0	4	7	0	0	11
V7-m	39	92	6	7	0	133	97	22	4	400
1	1	17	1	0	0	8	0	9	0	36
2	8	29	2	1	0	28	2	8	1	79
3	15	44	2	2	0	55	34	5	2	159
4	13	2	1	2	0	29	41	0	1	89
5	2	0	0	1	0	12	12	0	0	27
6	0	0	0	1	0	1	8	0	0	10

SAMPLE	P	Py	K	Ol	Op	Lvl	Lvmi	Lvv	Lvf	TOT
V9-m	40	145	9	18	13	92	60	23	0	400
1	0	28	0	0	0	0	0	7	0	35
2	4	58	4	0	1	19	0	9	0	95
3	15	48	3	3	2	25	15	5	0	116
4	17	9	2	7	5	32	28	2	0	102
5	4	2	0	6	4	11	17	0	0	44
6	0	0	0	2	1	5	0	0	0	8
V10-m	55	80	13	12	3	162	58	17	0	400
1	5	16	1	0	0	9	0	8	0	39
2	12	24	4	1	0	29	2	9	0	81
3	15	21	5	3	0	50	12	0	0	106
4	19	19	2	3	2	47	19	0	0	111
5	4	0	1	3	1	20	14	0		43
6	0	0	0	2	0	7	11	0	0	20
V11-m	51	83	6	15	5	125	98	15	2	400
1	9	25	1			17	2	6	0	60
2	19	32	2	0	0	29	11	8	0	101
3	15	24	2	4	1	35	29	1	1	112
4	8	2	1	5	2	31	35	0	1	85
5	0	0	0	4	2	11	16	0	0	33
6	0	0	0	2	0	2	5	0	0	9
V12-m	50	200	7	14	20	55	47	7	0	400
1	7	28	0	0	0	2	0	4	0	41
2	17	84	4	0	3	15	2	3	0	128
3	19	74	2	4	5	19	14	0	0	137
4	7	14	1	5	6	14	17	0	0	64
5	0	0	0	3	4	5	9	0	0	21
6	0	0	0	2	2	0	5	0	0	9
V8-m	44	55	3	4	3	165	101	20	5	400
1	1	7	0	0	0	7	0	9	0	24
2	12	24	1		0	38	9	11	1	96
3	14	19	1	1	1	64	28	0	2	130
4	15	5	1	2	1	40	31	0	1	96
5	2	0		1	1	14	22	0	1	41
6	0	0	0	0	0	2	11	0	0	13

Roundness raw data; m: medium sand fraction.

For Lipari raw data (modal composition and roundness) see Morrone et al., 2017 and Morrone et al., 2018.

VOLTURNO-LICOLA COASTAL STRETCH

SAMPLE	P	P in Lvl	P in Lvl bigl	P in Lvl orgl	P alt	Py	Py in Lvl bigl	Py in Lvl brgl	Py in Lvl	Py in PM	Py alt	K Ort	San San in Rs	Micr K in Ar	Ort in Ar	K in Lvl
Vo-1-m	6	-	2	-	3	133	3	-	-	-	1	13	-	-	-	-
1	-	-	-	-	13	-	-	-	-	-	-	-	-	-	-	-
2	3	-	-	-	1	57	-	-	-	1	5	-	-	-	-	-
3	3	-	1	-	2	45	3	-	-	-	5	-	-	-	-	-
4	-	-	1	-	0	16	-	-	-	-	3	-	-	-	-	-
5	-	-	-	-	0	2	-	-	-	-	-	-	-	-	-	-
6	-	-	-	-	-	-	-	-	-	-	-	-	-	-	-	-
Vo-2-m	4	-	-	-	6	169	2	-	-	-	9	-	-	-	-	-
1	1	-	-	-	1	56	-	-	-	-	1	-	-	-	-	-
2	1	-	-	-	2	70	2	-	-	-	5	-	-	-	-	-
3	2	-	-	-	3	34	-	-	-	-	2	-	-	-	-	-
4	-	-	-	-	-	3	-	-	-	-	1	-	-	-	-	-
5	-	-	-	-	-	-	-	-	-	-	-	-	-	-	-	-
6	-	-	-	-	-	-	-	-	-	-	-	-	-	-	-	-
Vo-3-m	13	-	-	-	11	23	-	-	-	-	45	-	-	6	-	-
1	-	-	-	-	-	-	-	-	-	-	-	-	-	-	-	-
2	6	-	-	-	0	7	-	-	-	-	11	-	-	1	-	-
3	3	-	-	-	4	9	-	-	-	-	19	-	-	3	-	-
4	4	-	-	-	7	7	-	-	-	-	11	-	-	2	-	-
5	-	-	-	-	-	-	-	-	-	-	4	-	-	-	-	-
6	-	-	-	-	-	-	-	-	-	-	-	-	-	-	-	-
Vo-4-m	19	-	4	-	17	8	-	2	-	-	54	-	-	9	-	-
1	-	-	-	-	1	-	-	-	-	-	5	-	-	-	-	-
2	5	-	-	-	1	2	-	1	-	-	24	-	-	2	-	-
3	11	-	3	-	8	4	-	1	-	-	19	-	-	4	-	-
4	3	-	1	-	8	1	-	-	-	-	5	-	-	3	-	-
5	-	-	-	-	-	-	-	-	-	-	1	-	-	-	-	-
6	-	-	-	-	-	-	-	-	-	-	-	-	-	-	-	-
Vo-5-m	20	-	-	-	8	168	-	3	3	-	13	-	-	1	-	-
1	-	-	-	-	8	-	-	-	-	-	-	-	-	-	-	-
2	4	-	-	-	3	52	-	1	-	-	7	-	-	-	-	-
3	14	-	-	-	3	65	-	2	2	-	5	-	-	1	-	-
4	2	-	-	-	2	42	-	-	1	-	1	-	-	-	-	-
5	-	-	-	-	-	1	-	-	-	-	-	-	-	-	-	-
6	-	-	-	-	-	-	-	-	-	-	-	-	-	-	-	-
Vo-6-m	2	-	-	4	208	2	-	-	-	-	7	-	-	-	-	-
1	-	-	-	-	16	-	-	-	-	-	-	-	-	-	-	-
2	1	-	-	-	65	-	-	-	-	-	2	-	-	-	-	-
3	1	-	-	-	2	86	2	-	-	-	4	-	-	-	-	-
4	-	-	-	-	2	35	-	-	-	-	1	-	-	-	-	-
5	-	-	-	-	-	6	-	-	-	-	-	-	-	-	-	-
6	-	-	-	-	-	-	-	-	-	-	-	-	-	-	-	-

*Key to Grain Shape Categories. **1** = very angular; **2** = angular; **3** = sub-angular; **4** = sub-rounded; **5** = rounded; **6** = well rounded; Vc: very coarse sand fraction; C: coarse sand fraction; m: medium sand fraction; f: fine sand fraction; Vf: very fine sand fraction.

VOLTURNO-LICOLA COASTAL STRETCH (continued)

SAMPLE	K in Rm	K in Rp	K in Rs	K alt Ol	Le Gr	Grbr	Hb Op	Bt Ca	CC in Ar	Ca in Ar	Qzm Qz	in Ar Qp	in Ar Qp	Qzp-tf	Qz in Rm	Qz in Rs	Qz in Rp	Ch Lvl	Lvlblgl	Lvlbrgl
Vo-1-m	-	-	5	-	3	-	9	27	12	2	28	-	17	60	6	-	11	2	-	-	-	1	1	4	-
1	-	-	-	-	-	-	-	1	-	-	-	-	2	5	-	-	-	-	-	-	-	-	-	-	-
2	-	-	1	-	2	-	3	11	2	1	4	-	2	19	-	-	3	-	-	-	-	-	-	-	-
3	-	-	3	-	1	-	4	8	7	1	11	-	7	25	2	-	7	1	-	-	-	1	-	3	-
4	-	-	1	-	-	-	2	7	3	-	8	-	6	9	3	-	1	1	-	-	-	-	1	-	-
5	-	-	-	-	-	-	-	-	-	-	4	-	2	2	1	-	-	-	-	-	-	-	-	1	-
6	-	-	-	-	-	-	-	-	-	-	1	-	-	-	-	-	-	-	-	-	-	-	-	-	-
Vo-2-m	-	-	2	21	-	23	-	43	57	5	13	-	21	2	-	1	-	-	-	3	-	-	-	-	-
1	-	-	-	-	-	-	-	1	-	-	-	-	1	-	-	-	-	-	-	-	-	-	-	-	-
2	-	-	-	7	-	10	-	21	9	1	-	-	4	-	-	-	-	-	-	-	-	-	-	-	-
3	-	-	1	9	-	9	-	18	22	2	9	-	8	1	-	-	1	-	-	1	-	-	-	-	-
4	-	-	1	5	-	3	-	3	19	2	4	-	4	1	-	-	-	-	-	2	-	-	-	-	-
5	-	-	-	-	-	-	-	6	-	-	-	-	4	-	-	-	-	-	-	-	-	-	-	-	-
6	-	-	-	-	-	-	-	-	1	-	-	-	-	-	-	-	-	-	-	-	-	-	-	-	-
Vo-3-m	-	-	13	-	1	-	3	-	-	32	11	-	78	11	-	20	5	-	-	5	10	4	-	-	-
1	-	-	-	-	-	-	-	-	-	-	-	-	-	-	-	-	-	-	-	-	-	-	-	-	-
2	-	-	1	-	-	-	3	-	-	1	-	-	22	-	-	1	1	-	-	-	1	-	-	-	-
3	-	-	6	-	1	-	-	-	-	7	4	-	29	6	-	11	3	-	-	2	6	1	-	-	-
4	-	-	6	-	-	-	-	-	-	13	5	-	24	5	-	6	1	-	-	3	3	2	-	-	-
5	-	-	-	-	-	-	-	-	-	11	2	-	3	-	-	2	-	-	-	-	-	1	-	-	-
6	-	-	-	-	-	-	-	-	-	-	-	-	-	-	-	-	-	-	-	-	-	-	-	-	-
Vo-4-m	-	-	17	-	8	-	-	-	2	28	-	6	62	14	-	29	8	5	-	-	3	4	10	5	-
1	-	-	-	-	-	-	-	-	-	-	-	-	4	-	-	-	-	-	-	-	-	-	-	-	-
2	-	-	1	-	4	-	-	-	-	1	-	1	22	1	-	7	2	1	-	-	1	-	2	-	2
3	-	-	9	-	2	-	-	-	-	6	-	3	25	4	-	13	4	3	-	-	2	3	5	3	3
4	-	-	6	-	2	-	-	-	1	13	-	2	8	8	-	8	2	1	-	-	-	1	2	-	-
5	-	-	1	-	-	-	-	-	1	5	-	-	3	1	-	1	-	-	-	-	-	-	1	-	-
6	-	-	-	-	-	-	-	-	-	3	-	-	-	-	-	-	-	-	-	-	-	-	-	1	-
Vo-5-m	-	-	6	-	5	-	12	2	1	21	-	8	49	8	-	9	3	-	-	3	5	4	-	-	-
1	-	-	-	-	-	-	-	-	-	-	-	-	-	-	-	-	-	-	-	-	-	-	-	-	-
2	-	-	-	-	1	-	4	-	-	-	-	-	13	1	-	2	-	-	-	-	-	-	-	-	-
3	-	-	2	-	2	-	7	1	1	7	-	3	25	5	-	4	2	-	-	-	2	3	2	-	-
4	-	-	3	-	2	-	1	1	-	10	-	4	8	2	-	3	1	-	-	-	1	2	1	-	-
5	-	-	1	-	-	-	-	-	-	3	-	1	2	-	-	-	-	-	-	-	-	-	1	-	-
6	-	-	-	-	-	-	-	-	-	1	-	-	1	-	-	-	-	-	-	-	-	-	-	-	-
Vo-6-m	-	-	-	1	-	18	-	28	15	3	12	-	49	3	-	6	-	-	-	-	-	-	-	2	-
1	-	-	-	-	-	2	-	1	-	-	-	-	2	-	-	-	-	-	-	-	-	-	-	-	-
2	-	-	-	-	-	6	-	10	1	-	-	-	10	1	-	1	-	-	-	-	-	-	-	1	-
3	-	-	-	1	-	9	-	11	5	2	7	-	24	2	-	4	-	-	-	-	-	-	-	1	-
4	-	-	-	-	-	1	-	6	6	1	5	-	12	-	-	1	-	-	-	-	-	-	-	-	-
5	-	-	-	-	-	-	-	-	3	-	-	-	1	-	-	-	-	-	-	-	-	-	-	-	-
6	-	-	-	-	-	-	-	-	-	-	-	-	-	-	-	-	-	-	-	-	-	-	-	-	-

*Key to Grain Shape Categories. **1** = very angular; **2** = angular; **3** = sub-angular; **4** = sub-rounded; **5** = rounded; **6** = well rounded; Vc: very coarse sand fraction; C: coarse sand fraction; m: medium sand fraction; f: fine sand fraction; Vf: very fine sand fraction.

VOLTURNO-LICOLA COASTAL STRETCH (continued)

SAMPLE	Lvlgrgl	Lvlaltgl	Lvmi	Lvmiblgl	Lvmibrgl	Lvmigrgl	Lvmialt	Lvvblgl	Lvvbrgl	Lvvclgl	Lvvalgl	Lvf	PMcl	Lm	Lp	Lvo	Lsc(crist)	Lsc(micr)	Lss	Bio	Biomic	Tourm	Unk	TOT
Vo-1-m	-	-	-	-	-	-	1	-	-	4	1	-	5	-	-	13	19	1	2	-	-	2	-	400
1	-	-	-	-	-	-	-	-	-	-	-	-	-	-	-	-	-	-	-	-	-	-	-	19
2	-	-	-	-	-	-	-	-	-	1	-	-	1	-	-	2	2	-	-	-	-	-	-	121
3	-	1	-	2	-	-	-	-	-	2	-	-	4	-	-	5	8	-	-	-	-	1	1	163
4	-	-	-	-	-	-	1	-	-	1	-	-	-	-	-	5	9	1	1	-	-	1	1	81
5	-	-	-	-	-	-	-	-	-	-	1	-	-	-	-	1	-	1	1	-	-	-	-	15
6	-	-	-	-	-	-	-	-	-	-	-	-	-	-	-	-	-	-	-	-	-	-	-	1
Vo-2-m	-	1	-	-	-	-	-	-	-	-	-	2	-	-	-	3	6	-	5	-	-	2	2	400
1	-	-	-	-	-	-	-	-	-	-	-	1	-	-	-	-	-	-	1	-	-	-	-	10
2	-	-	-	-	-	-	-	-	-	-	-	-	-	-	-	-	-	-	-	-	-	-	-	113
3	-	1	-	-	-	-	-	-	-	-	-	1	-	-	-	-	1	-	1	-	-	-	2	168
4	-	-	-	-	-	-	-	-	-	-	-	-	-	-	-	3	4	-	3	-	-	-	-	93
5	-	-	-	-	-	-	-	-	-	-	-	-	-	-	-	-	1	-	-	-	-	-	-	15
6	-	-	-	-	-	-	-	-	-	-	-	-	-	-	-	-	-	-	-	-	-	-	-	1
Vo-3-m	-	17	-	3	-	-	2	-	-	2	-	6	-	-	-	23	28	21	4	-	-	3	3	400
1	-	-	-	-	-	-	-	-	-	-	-	-	-	-	-	-	-	-	-	-	-	-	-	0
2	-	1	-	1	-	-	-	-	-	-	-	1	-	-	-	-	-	1	-	-	-	-	1	60
3	-	7	-	-	-	-	2	-	-	-	-	4	-	-	-	4	3	4	2	-	-	1	1	141
4	-	9	-	1	-	-	-	-	-	1	-	1	-	-	-	13	16	12	1	-	-	1	1	154
5	-	-	-	1	-	-	-	-	-	1	-	-	-	-	-	6	9	4	1	-	-	-	-	45
6	-	-	-	-	-	-	-	-	-	-	-	-	-	-	-	-	-	-	-	-	-	-	-	0
Vo-4-m	1	15	-	2	-	-	4	-	-	-	-	9	-	-	-	11	17	18	5	-	-	4	4	400
1	-	-	-	-	-	-	-	-	-	-	-	-	-	-	-	-	-	-	-	-	-	-	-	10
2	-	1	-	1	-	-	1	-	-	-	-	2	-	-	-	-	-	-	-	-	-	1	1	86
3	1	6	-	-	-	-	2	-	-	-	-	5	-	-	-	2	2	6	-	-	-	-	3	159
4	-	6	-	1	-	-	1	-	-	-	-	2	-	-	-	6	8	6	1	-	-	-	-	106
5	-	1	-	-	-	-	-	-	-	-	-	-	-	-	-	3	7	4	3	-	-	-	-	31
6	-	1	-	-	-	-	-	-	-	-	-	-	-	-	-	-	-	2	1	-	-	-	-	8
Vo-5-m	-	0	-	-	-	-	-	-	-	-	1	-	7	-	-	21	8	7	1	-	-	-	3	400
1	-	-	-	-	-	-	-	-	-	-	-	-	-	-	-	-	-	1	-	-	-	-	-	9
2	-	-	-	-	-	-	-	-	-	-	-	-	1	-	-	2	-	2	-	-	-	-	1	94
3	-	-	-	-	-	-	-	-	-	-	1	-	4	-	-	4	1	3	-	-	-	-	1	172
4	-	-	-	-	-	-	-	-	-	-	-	-	2	-	-	7	3	1	-	-	-	-	1	101
5	-	-	-	-	-	-	-	-	-	-	-	-	-	-	-	5	2	-	1	-	-	-	-	17
6	-	-	-	-	-	-	-	-	-	-	-	-	-	-	-	3	2	-	-	-	-	-	-	7
Vo-6-m	-	4	-	-	-	-	1	-	-	-	1	-	-	-	-	5	22	2	-	-	-	3	2	400
1	-	-	-	-	-	-	-	-	-	-	-	-	-	-	-	-	-	-	-	-	-	-	-	21
2	-	1	-	-	-	-	-	-	-	-	-	-	-	-	-	1	-	1	-	-	-	1	-	102
3	-	2	-	-	-	-	1	-	-	-	-	-	-	-	-	3	5	1	-	-	-	2	1	176
4	-	1	-	-	-	-	-	-	-	-	1	-	-	-	-	1	10	-	-	-	-	-	1	84
5	-	-	-	-	-	-	-	-	-	-	-	-	-	-	-	-	6	-	-	-	-	-	-	16
6	-	-	-	-	-	-	-	-	-	-	-	-	-	-	-	-	1	-	-	-	-	-	-	1

*Key to Grain Shape Categories. **1** = very angular; **2** = angular; **3** = sub-angular; **4** = sub-rounded; **5** = rounded; **6** = well rounded; Vc: very coarse sand fraction; C: coarse sand fraction; m: medium sand fraction; f: fine sand fraction; Vf: very fine sand fraction.

VOLTURNO-LICOLA COASTAL STRETCH (continued)

SAMPLE	P	P inLvl	P inLvlblgl	P inLvlorgl	P alt	Py	Py in Lvlblgl	Py in Lvlbrgl	Py in Lvl	Py in PM	Py alt	K	Ort	San	San in Rs	Micr K in Ar	Ort in Ar	K in Lvl
Vo-7-m	13	-	7	1	7	16	-	-	-	-	-	43	-	-	-	7	-	-
1	-	-	-	-	1	-	-	-	-	-	-	-	-	-	-	-	-	-
2	4	-	2	1	-	7	1	-	-	-	-	19	-	-	-	-	-	-
3	5	-	-	-	4	5	1	-	-	-	-	15	-	-	-	4	-	-
4	3	-	3	-	3	3	-	-	-	-	-	8	-	-	-	3	-	-
5	1	-	2	-	-	-	-	-	-	-	-	1	-	-	-	-	-	-
6	-	-	-	-	-	-	-	-	-	-	-	-	-	-	-	-	-	-
Vo-8-m	15	-	2	-	1	36	-	-	-	-	-	19	18	-	6	-	3	-
1	-	-	-	-	-	-	-	-	-	-	-	-	1	-	-	-	-	-
2	5	-	-	-	1	14	-	-	-	-	-	1	12	-	1	-	-	-
3	7	-	-	-	-	17	-	-	-	-	-	7	5	-	2	-	1	-
4	3	-	1	-	-	5	-	-	-	-	-	9	-	-	2	-	2	-
5	-	-	1	-	-	-	-	-	-	-	-	2	-	-	1	-	-	-
6	-	-	-	-	-	-	-	-	-	-	-	-	-	-	-	-	-	-
Vo-9-m	13	2	2	-	4	11	-	-	2	-	-	20	29	-	15	1	-	-
1	-	-	-	-	-	-	-	-	-	-	-	-	3	-	-	-	-	-
2	7	-	-	-	1	4	-	-	2	-	-	1	17	-	2	-	-	-
3	4	1	1	-	1	5	-	-	-	-	-	7	7	-	6	-	-	-
4	2	1	1	-	2	2	-	-	-	-	-	12	2	-	7	1	-	-
5	-	-	-	-	-	-	-	-	-	-	-	-	-	-	-	-	-	-
6	-	-	-	-	-	-	-	-	-	-	-	-	-	-	-	-	-	-
Vo-10-m	19	-	3	-	10	5	-	-	-	-	-	17	32	3	15	-	-	-
1	-	-	-	-	-	1	-	-	-	-	-	-	2	-	-	-	-	-
2	7	-	1	-	-	3	-	-	-	-	-	1	22	-	1	-	-	-
3	7	-	2	-	5	1	-	-	-	-	-	9	6	-	6	-	-	-
4	5	-	-	-	5	-	-	-	-	-	-	7	2	1	7	-	-	-
5	-	-	-	-	-	-	-	-	-	-	-	-	-	-	1	-	-	-
6	-	-	-	-	-	-	-	-	-	-	-	-	-	-	-	-	-	-
Vo-11-m	12	-	-	-	11	-	-	-	-	-	-	3	60	-	8	-	-	2
1	-	-	-	-	-	-	-	-	-	-	-	-	-	-	-	-	-	-
2	6	-	-	-	3	-	-	-	-	-	-	-	29	-	1	-	-	-
3	5	-	-	-	7	-	-	-	-	-	-	1	22	-	4	-	-	1
4	1	-	-	-	1	-	-	-	-	-	-	2	9	-	3	-	-	1
5	-	-	-	-	-	-	-	-	-	-	-	-	-	-	-	-	-	-
6	-	-	-	-	-	-	-	-	-	-	-	-	-	-	-	-	-	-

*Key to Grain Shape Categories. **1** = very angular; **2** = angular; **3** = sub-angular; **4** = sub-rounded; **5** = rounded; **6** = well rounded; Vc: very coarse sand fraction; C: coarse sand fraction; m: medium sand fraction; f: fine sand fraction; Vf: very fine sand fraction.

VOLTURNO-LICOLA COASTAL STRETCH (continued)

SAMPLE	K in Rm	K in Rp	K in Rs	K alt	Ol	Le	Gr	Grbr	Hb	Op	Bt	Ca	CC in Ar	Ca in Ar	Qzm	Qz in Ar	Qp in Ar	Qp	Qzp-tf	Qz in Rm	Qz in Rs	Qz in Rp	Ch	Lvl	Lvlblgl	Lvlbrgl
Vo-7-m	-	-	-	11	-	-	-	-	-	-	37	-	9	94	-	11	18	-	-	-	-	4	9	8	-	-
1	-	-	-	-	-	-	-	-	-	-	-	-	2	2	-	1	-	-	-	-	-	-	-	-	-	-
2	-	-	-	2	-	-	-	-	-	-	3	-	2	34	-	3	5	-	-	-	-	1	1	2	-	-
3	-	-	-	5	-	-	-	-	-	-	10	-	4	34	-	3	9	-	-	-	-	2	3	5	-	-
4	-	-	-	4	-	-	-	-	-	-	15	-	3	21	-	4	4	-	-	-	-	1	5	1	-	-
5	-	-	-	-	-	-	-	-	-	-	8	-	-	3	-	-	-	-	-	-	-	-	-	-	-	-
6	-	-	-	-	-	-	-	-	-	-	1	-	-	-	-	-	-	-	-	-	-	-	-	-	-	-
Vo-8-m	-	-	-	6	-	2	-	-	-	-	17	-	9	97	8	-	9	6	-	-	-	2	7	4	-	-
1	-	-	-	-	-	-	-	-	-	-	-	-	-	2	-	-	-	-	-	-	-	-	-	-	-	-
2	-	-	-	-	-	1	-	-	-	-	-	-	-	32	-	-	-	1	-	-	-	2	1	1	-	-
3	-	-	-	2	-	-	-	-	-	-	2	-	2	43	5	-	7	5	-	-	-	-	3	2	-	-
4	-	-	-	4	-	1	-	-	-	-	9	-	4	16	3	-	2	-	-	-	-	-	2	1	-	-
5	-	-	-	-	-	-	-	-	-	-	6	-	3	4	-	-	-	-	-	-	-	-	1	-	-	-
6	-	-	-	-	-	-	-	-	-	-	-	-	-	-	-	-	-	-	-	-	-	-	-	-	-	-
Vo-9-m	-	-	-	4	-	2	-	-	-	-	10	-	3	117	10	-	17	5	-	-	-	1	12	2	-	-
1	-	-	-	-	-	-	-	-	-	-	-	-	-	6	-	-	-	-	-	-	-	-	-	-	-	-
2	-	-	-	-	-	-	-	-	-	-	-	-	-	36	2	-	2	-	-	-	-	-	1	-	-	-
3	-	-	-	1	-	1	-	-	-	-	4	-	1	43	1	-	8	3	-	-	-	1	6	1	-	-
4	-	-	-	3	-	1	-	-	-	1	4	-	2	28	5	-	5	2	-	-	-	-	5	1	-	-
5	-	-	-	-	-	-	-	-	-	-	2	-	-	4	2	-	2	-	-	-	-	-	-	-	-	-
6	-	-	-	-	-	-	-	-	-	-	-	-	-	-	-	-	-	-	-	-	-	-	-	-	-	-
Vo-10-m	1	-	-	3	-	4	-	-	-	-	5	15	-	5	83	3	-	16	6	-	5	6	7	19	5	-
1	-	-	-	-	-	-	-	-	-	-	-	-	-	5	-	-	-	-	-	-	-	-	-	-	-	-
2	-	-	-	-	-	1	-	-	-	-	-	-	-	28	-	-	-	1	1	-	-	1	-	-	-	-
3	1	-	-	1	-	2	-	-	-	-	2	3	-	30	2	-	-	8	3	-	2	1	4	3	1	-
4	-	-	-	2	-	1	-	-	-	-	3	9	-	15	1	-	7	2	-	-	3	3	3	11	3	-
5	-	-	-	-	-	-	-	-	-	-	3	-	-	5	-	-	-	-	-	-	-	1	-	5	1	-
6	-	-	-	-	-	-	-	-	-	-	-	-	-	-	-	-	-	-	-	-	-	-	-	-	-	-
Vo-11-m	-	-	-	-	-	-	-	-	-	-	5	3	-	4	49	25	-	17	4	-	-	-	9	14	16	5	-
1	-	-	-	-	-	-	-	-	-	-	-	-	-	-	1	-	-	-	-	-	-	-	-	-	-	-
2	-	-	-	-	-	-	-	-	-	-	-	-	-	-	9	2	-	1	-	-	-	-	-	2	-	-
3	-	-	-	1	-	-	-	-	-	-	2	3	-	1	29	9	-	8	3	-	-	1	5	8	1	-
4	-	-	-	-	-	4	-	-	-	-	-	-	-	-	8	11	-	8	1	-	-	-	-	5	3	-
5	-	-	-	1	-	5	-	-	-	-	3	-	-	1	2	3	-	-	-	-	-	5	4	10	1	-
6	-	-	-	-	-	-	-	-	-	-	-	-	-	2	2	-	-	-	-	-	-	3	-	1	-	-

*Key to Grain Shape Categories. **1** = very angular; **2** = angular; **3** = sub-angular; **4** = sub-rounded; **5** = rounded; **6** = well rounded; Vc: very coarse sand fraction; C: coarse sand fraction; m: medium sand fraction; f: fine sand fraction; Vf: very fine sand fraction.

VOLTURNO-LICOLA COASTAL STRETCH (continued)

SAMPLE	Lvlgrgl	Lvlaltgl	Lvmi	Lvmiblgl	Lvmibrgl	Lvmigrgl	Lvmialt	Lvvblgl	Lvvbrgl	Lvvclgl	Lvvalgl	Lvf	PMcl	Lm	Lp	Lvo	Lsc (crist)	Lsc (micr)	Lss	Bio	Biomicr	Tourm	Unk	TOT
Vo-7-m	1	6	-	5	-	5	3	-	-	-	-	1	14	-	-	-	15	26	14	7	-	-	4	400
1	-	-	-	-	-	-	-	-	-	-	-	-	-	-	-	-	-	-	-	-	-	-	-	4
2	1	-	-	2	-	1	-	-	-	-	-	1	3	-	-	-	-	-	1	-	-	-	-	96
3	-	3	-	2	-	2	1	-	-	1	-	-	6	-	-	-	3	6	4	3	-	-	2	142
4	-	3	-	1	-	2	1	-	-	1	-	-	5	-	-	-	8	9	4	2	-	-	2	119
5	-	-	-	-	-	-	1	-	-	-	-	-	-	-	-	-	4	9	2	1	-	-	-	32
6	-	-	-	-	-	-	-	-	-	-	-	-	-	-	-	-	-	2	3	1	-	-	-	7
Vo-8-m	-	4	2	-	1	4	-	-	-	-	4	-	19	-	-	-	41	36	12	2	3	-	3	400
1	-	-	-	-	-	-	-	-	-	-	-	-	1	-	-	-	-	1	1	-	-	-	-	3
2	-	1	-	-	-	-	-	-	-	-	-	-	1	-	-	-	-	1	1	-	-	-	-	76
3	-	-	2	2	-	1	-	-	-	-	-	1	8	-	-	-	15	5	2	-	1	-	1	151
4	-	1	-	-	-	2	-	-	-	-	-	3	7	-	-	-	18	11	6	1	2	-	2	118
5	-	-	-	-	-	-	-	-	-	-	-	-	3	-	-	-	6	17	3	1	-	-	-	48
6	-	-	-	-	-	-	-	-	-	-	-	-	-	-	-	-	2	2	-	-	-	-	-	4
Vo-9-m	-	-	1	1	1	4	2	-	-	-	-	5	6	-	-	-	59	30	-	4	-	-	3	400
1	-	-	-	-	-	-	-	-	-	-	-	-	-	-	-	-	-	-	-	-	-	-	-	9
2	-	-	-	-	1	-	-	-	-	-	-	1	1	-	-	-	1	2	-	1	-	-	-	82
3	-	-	1	-	-	1	2	-	-	-	-	3	4	-	-	-	16	2	-	1	-	-	2	136
4	-	-	-	-	-	3	-	-	-	-	1	-	1	-	-	-	34	15	-	2	-	-	1	144
5	-	-	-	-	-	-	-	-	-	-	-	-	-	-	-	-	6	8	-	-	-	-	-	24
6	-	-	-	-	-	-	-	-	-	-	-	-	-	-	-	-	2	3	-	-	-	-	-	5
Vo-10-m	-	10	-	3	4	-	2	-	-	-	-	-	4	-	4	37	20	24	1	-	-	4	400
1	-	-	-	-	-	-	-	-	-	-	-	-	-	-	-	-	-	-	-	-	-	-	8	
2	-	-	-	-	-	-	-	-	-	-	-	-	-	1	-	2	-	-	-	-	-	-	70	
3	-	2	-	1	1	-	1	-	-	-	-	-	1	-	2	11	1	3	-	-	-	2	129	
4	-	6	-	2	3	-	1	-	-	-	-	-	3	-	1	19	7	13	1	-	-	2	150	
5	-	2	-	-	-	-	-	-	-	-	-	-	-	-	-	4	8	7	-	-	-	-	37	
6	-	-	-	-	-	-	-	-	-	-	-	-	-	-	-	1	4	1	-	-	-	-	6	
Vo-11-m	-	8	3	-	3	-	5	-	1	-	-	-	1	-	-	14	28	69	4	-	-	-	400	
1	-	-	-	-	-	-	-	-	-	-	-	-	-	-	-	-	-	-	-	-	-	-	1	
2	-	1	-	-	-	-	-	-	-	-	-	-	-	-	-	1	-	8	-	-	-	-	65	
3	-	3	1	-	2	-	2	-	1	-	-	-	-	-	-	4	8	13	1	-	-	-	153	
4	-	4	2	-	1	-	3	-	-	-	-	-	1	-	-	8	13	27	2	-	-	-	139	
5	-	-	-	-	-	-	-	-	-	-	-	-	-	-	-	1	7	16	1	-	-	-	37	
6	-	-	-	-	-	-	-	-	-	-	-	-	-	-	-	-	-	5	-	-	-	-	5	

*Key to Grain Shape Categories. **1** = very angular; **2** = angular; **3** = sub-angular; **4** = sub-rounded; **5** = rounded; **6** = well rounded; Vc: very coarse sand fraction; C: coarse sand fraction; m: medium sand fraction; f: fine sand fraction; Vf: very fine sand fraction.

VOLTURNO-LICOLA COASTAL STRETCH (continued)

SAMPLE	P	P in Ar	P alt	Py	Py in Lvlblgl	Py in Lvlbrgl	K	K in Ar	K alt	Le	Hb	Bt	Ca	CC in Ar	Ca in Ar	Qzm	Qz in Ar	Qp
Li-1-m	14	9	8	2	-	-	52	13	16	6	2	6	37	7	21	62	23	17
1	-	-	-	-	-	-	2	-	-	-	-	-	7	-	-	3	1	-
2	3	3	1	1	-	-	21	5	5	1	-	2	17	2	4	25	4	4
3	9	5	3	-	-	-	17	7	8	4	1	3	13	3	14	21	14	10
4	2	1	4	1	-	-	12	1	3	1	1	1	-	2	3	12	4	3
5	-	-	-	-	-	-	-	-	-	-	-	-	-	-	-	1	-	-
6	-	-	-	-	-	-	-	-	-	-	-	-	-	-	-	-	-	-
Li-2-m	13	-	12	5	-	-	30	10	22	-	6	42	-	10	48	15	16	1
1	-	-	-	-	-	-	-	-	-	-	-	12	-	-	-	-	-	1
2	4	-	2	4	-	-	15	2	7	-	2	18	-	2	20	3	7	7
3	8	-	7	1	-	-	12	6	13	-	3	10	-	6	18	10	7	1
4	1	-	2	-	-	-	3	2	2	-	1	2	-	2	10	2	1	-
5	-	-	1	-	-	-	-	-	-	-	-	-	-	-	-	-	-	-
6	-	-	-	-	-	-	-	-	-	-	-	-	-	-	-	-	-	-
Li-3-m	8	-	4	4	1	3	34	0	23	-	7	48	-	-	54	-	18	1
1	-	-	-	-	-	-	1	-	1	-	-	1	-	-	3	-	1	-
2	3	-	3	2	-	2	13	-	4	-	4	15	-	-	16	-	7	1
3	4	-	1	1	1	1	17	-	8	-	2	22	-	-	23	-	9	1
4	1	-	-	1	-	3	3	-	10	-	1	9	-	-	7	-	1	-
5	-	-	-	-	-	-	-	-	-	-	-	1	-	-	4	-	-	-
6	-	-	-	-	-	-	-	-	-	-	-	-	-	-	1	-	-	-
Li-4-m	36	-	4	-	-	30	-	6	-	-	8	62	-	8	59	6	35	4
1	3	-	-	-	-	1	-	-	-	-	-	1	-	-	1	-	4	4
2	14	-	1	-	-	10	-	1	-	-	3	23	-	3	13	1	9	9
3	18	-	3	-	-	15	-	4	-	-	4	22	-	4	23	4	17	17
4	1	-	-	-	-	3	-	1	-	-	1	14	-	1	16	1	4	4
5	-	-	-	-	-	1	-	-	-	-	-	2	-	-	6	-	1	1
6	-	-	-	-	-	-	-	-	-	-	-	-	-	-	-	-	-	-
Li-5-m	39	-	10	-	-	29	-	-	-	5	7	52	-	10	55	13	14	14
1	1	-	-	-	-	2	-	-	-	-	-	1	-	1	1	1	-	-
2	16	-	6	-	-	12	-	-	-	3	3	14	-	3	23	3	4	4
3	18	-	3	-	-	11	-	-	2	3	3	22	-	4	20	7	8	8
4	4	-	1	-	-	4	-	-	-	1	1	14	-	1	9	3	2	2
5	-	-	-	-	-	-	-	-	-	-	-	1	-	1	2	-	-	-
6	-	-	-	-	-	-	-	-	-	-	-	-	-	-	-	-	-	-
Li-6-m	37	-	4	-	-	67	9	13	-	9	45	-	13	50	14	16	16	16
1	2	-	-	-	-	7	-	-	-	-	-	-	-	-	9	-	-	-
2	13	-	3	-	-	23	3	3	-	-	3	12	-	4	15	4	3	3
3	19	-	1	-	-	33	5	7	-	-	4	23	-	8	21	8	9	9
4	3	-	-	-	-	4	1	3	-	-	2	9	-	1	4	2	3	3
5	-	-	-	-	-	-	-	-	-	-	-	1	-	-	1	-	1	1
6	-	-	-	-	-	-	-	-	-	-	-	-	-	-	-	-	-	-

*Key to Grain Shape Categories. **1** = very angular; **2** = angular; **3** = sub-angular; **4** = sub-rounded; **5** = rounded; **6** = well rounded; Vc: very coarse sand fraction; C: coarse sand fraction; m: medium sand fraction; f: fine sand fraction; Vf: very fine sand fraction.

VOLTURNO-LICOLA COASTAL STRETCH (continued)

SAMPLE	Ch	Lvl	Lvlblgl	Lvlbrgl	Lvlaltgl	Lvmi	Lvmiblgl	Lvmibrgl	Lvmiclgl	Lvmialtgl	Lvvclgl	Lvvalgl	Lvf	Lsc (crist)	Lsc (micr)	Lss	Bio	Unk	TOT
Li-1-m	7	12	9	-	9	1	1	-	1	4	1	9	-	12	16	18	5	-	400
1	-	-	-	-	-	-	-	-	-	-	-	-	-	-	-	-	-	-	13
2	2	2	2	-	1	-	-	-	-	-	-	3	-	1	-	2	1	-	112
3	4	8	5	-	4	1	1	-	-	2	-	5	-	7	6	8	3	-	186
4	1	2	2	-	4	-	-	-	1	2	1	1	-	4	8	6	1	-	84
5	-	-	-	-	-	-	-	-	-	-	-	-	-	-	2	2	-	-	5
6	-	-	-	-	-	-	-	-	-	-	-	-	-	-	-	-	-	-	0
Li-2-m	5	8	7	-	17	4	-	-	-	7	2	9	-	37	29	36	6	4	400
1	-	-	-	-	-	-	-	-	-	-	-	-	-	-	-	-	-	-	13
2	2	2	1	-	7	2	-	-	-	2	1	3	-	12	7	12	1	1	139
3	3	4	6	-	9	1	-	-	-	3	1	4	-	17	12	16	4	3	184
4	-	2	-	-	1	1	-	-	-	1	-	1	-	6	9	7	1	-	57
5	-	-	-	-	-	-	-	-	-	1	-	1	-	2	1	1	-	-	7
6	-	-	-	-	-	-	-	-	-	-	-	-	-	-	-	-	-	-	0
Li-3-m	13	-	7	7	11	-	4	4	-	9	-	17	-	22	55	47	-	-	400
1	-	-	-	-	-	-	-	-	-	-	-	-	-	-	1	2	-	-	10
2	3	-	1	2	3	-	1	1	-	3	-	2	-	6	16	7	-	-	114
3	9	-	4	4	6	-	2	3	-	4	-	12	-	14	22	17	-	-	186
4	1	-	2	1	2	-	1	-	-	2	-	2	-	2	11	12	-	-	69
5	-	-	-	-	-	-	-	-	-	-	-	1	-	-	3	8	-	-	17
6	-	-	-	-	-	-	-	-	-	-	-	-	-	-	2	1	-	-	4
Li-4-m	15	-	11	-	11	-	3	-	-	3	-	10	4	19	33	27	10	-	400
1	-	-	-	-	-	-	-	-	-	-	-	-	-	1	1	1	-	-	13
2	4	-	2	-	4	-	1	-	-	1	-	3	1	2	4	4	3	-	107
3	9	-	8	-	6	-	2	-	-	2	-	3	3	9	9	17	4	-	186
4	2	-	1	-	1	-	-	-	-	-	-	3	-	6	12	4	3	-	74
5	-	-	-	-	-	-	-	-	-	-	-	1	-	1	4	1	-	-	17
6	-	-	-	-	-	-	-	-	-	-	-	-	-	-	3	-	-	-	3
Li-5-m	7	-	9	2	6	6	2	-	-	3	-	6	-	10	71	44	-	-	400
1	-	-	-	-	-	-	-	-	-	-	-	-	-	-	4	3	-	-	13
2	2	-	1	1	2	2	-	-	-	1	-	1	-	2	15	10	-	-	124
3	4	-	7	1	3	3	2	-	-	2	-	4	-	7	25	14	-	-	170
4	1	-	1	-	1	1	-	-	-	-	-	1	-	1	18	8	-	-	71
5	-	-	-	-	-	-	-	-	-	-	-	-	-	-	6	6	-	-	16
6	-	-	-	-	-	-	-	-	-	-	-	-	-	-	3	3	-	-	6
Li-6-m	-	-	10	1	3	-	3	-	-	2	1	4	-	21	26	33	8	11	400
1	-	-	-	-	-	-	-	-	-	-	-	-	-	-	-	-	-	-	18
2	-	-	2	-	2	1	-	-	-	-	1	1	-	4	4	8	2	3	115
3	-	-	6	-	1	2	-	-	-	2	-	2	-	10	14	20	4	5	204
4	-	-	2	-	-	-	-	-	-	-	-	1	-	4	4	2	2	2	49
5	-	-	-	-	-	-	-	-	-	-	-	-	-	2	3	2	-	1	11
6	-	-	-	-	-	-	-	-	-	-	-	-	-	1	1	1	-	-	3

*Key to Grain Shape Categories. **1** = very angular; **2** = angular; **3** = sub-angular; **4** = sub-rounded; **5** = rounded; **6** = well rounded; Vc: very coarse sand fraction; C: coarse sand fraction; m: medium sand fraction; f: fine sand fraction; Vf: very fine sand fraction.

BACOLI-POZZUOLI COASTAL STRETCH

SAMPLE	P	P inLvl	P inLvlblgl	P inLvlbrgl	P inLvldggl	P inLvlclgl	P in Ar	P in PM	P alt	Py	Py in Lvlblgl	Py in Lvlbrgl	Py in Lvlclgl	K	K in Ar	K in Lvl	K in Lvlblgl	K in Lvlbrgl	K in Lvlgrgl
BC-1-Vc	62	-	-	9	-	-	-	-	1	6	8	-	9	-	-	-	-	-	-
1	-	-	-	-	-	-	-	-	-	-	-	-	-	-	-	-	-	-	-
2	13	-	-	-	-	-	-	-	-	-	-	-	4	-	-	-	-	-	-
3	27	-	-	-	-	-	-	-	1	2	-	-	5	-	-	-	-	-	-
4	19	-	3	3	-	-	-	-	-	4	5	-	-	-	-	-	-	-	-
5	3	-	4	6	-	-	-	-	-	-	3	-	-	-	-	-	-	-	-
6	-	-	-	-	-	-	-	-	-	-	-	-	-	-	-	-	-	-	-
BC-1-C	50	-	6	4	2	1	-	-	4	4	4	-	43	-	-	2	5	-	-
1	3	-	-	-	-	-	-	-	-	-	-	-	-	-	-	-	-	-	-
2	19	-	2	2	1	1	-	-	3	3	1	-	19	-	-	-	1	-	-
3	19	-	3	2	1	-	-	-	1	1	3	-	16	-	-	1	3	-	-
4	9	-	-	-	-	-	-	-	-	-	-	-	8	-	-	1	-	-	-
5	-	-	1	-	-	-	-	-	-	-	-	-	-	-	-	-	1	-	-
6	-	-	-	-	-	-	-	-	-	-	-	-	-	-	-	-	-	-	-
BC-1-m	24	38	3	3	3	2	-	1	5	2	-	-	25	-	15	-	-	-	-
1	1	6	-	-	-	-	-	-	-	-	-	-	2	-	2	-	-	-	-
2	9	13	1	1	1	2	-	-	-	2	-	-	12	-	4	-	-	-	-
3	8	13	2	2	2	-	-	-	1	-	-	-	6	-	9	-	-	-	-
4	6	6	-	-	-	-	-	1	4	-	-	-	5	-	-	-	-	-	-
5	-	-	-	-	-	-	-	-	-	-	-	-	-	-	-	-	-	-	-
6	-	-	-	-	-	-	-	-	-	-	-	-	-	-	-	-	-	-	-
BC-1-f	12	-	3	2	-	-	-	-	14	8	-	-	26	-	3	1	-	-	-
1	-	-	-	-	-	-	-	-	-	-	-	-	-	-	-	-	-	-	-
2	3	-	-	-	-	-	-	-	3	3	-	-	6	-	1	-	-	-	-
3	4	-	1	1	-	-	-	-	6	3	-	-	11	-	2	1	-	-	-
4	4	-	2	1	-	-	-	-	5	2	-	-	8	-	-	-	-	-	-
5	1	-	-	-	-	-	-	-	-	-	-	-	1	-	-	-	-	-	-
6	-	-	-	-	-	-	-	-	-	-	-	-	-	-	-	-	-	-	-
BC-1-Vf	15	-	-	1	-	-	-	-	2	119	-	-	9	1	-	-	-	-	1
1	-	-	-	-	-	-	-	-	-	13	-	-	-	-	-	-	-	-	-
2	8	-	-	-	-	-	-	-	-	59	-	-	5	-	-	-	-	-	-
3	6	-	-	1	-	-	-	-	1	30	-	-	3	1	-	-	-	-	1
4	1	-	-	-	-	-	-	-	1	14	-	-	1	-	-	-	-	-	-
5	-	-	-	-	-	-	-	-	-	3	-	-	-	-	-	-	-	-	-
6	-	-	-	-	-	-	-	-	-	-	-	-	-	-	-	-	-	-	-
BC-2-m	35	-	5	1	-	1	-	-	2	121	4	-	7	-	-	-	-	-	-
1	3	-	-	-	-	-	-	-	-	11	-	-	-	-	-	-	-	-	-
2	17	-	2	-	-	1	-	-	-	61	1	-	5	-	-	-	-	-	-
3	8	-	3	1	-	-	-	-	1	24	1	-	2	-	-	-	-	-	-
4	7	-	-	-	-	-	-	-	1	24	2	-	-	-	-	-	-	-	-
5	-	-	-	-	-	-	-	-	-	-	-	-	-	-	-	-	-	-	-
6	-	-	-	-	-	-	-	-	-	1	-	-	-	-	-	-	-	-	-

*Key to Grain Shape Categories. **1** = very angular; **2** = angular; **3** = sub-angular; **4** = sub-rounded; **5** = rounded; **6** = well rounded; Vc: very coarse sand fraction; C: coarse sand fraction; m: medium sand fraction; f: fine sand fraction; Vf: very fine sand fraction.

BACOLI-POZZUOLI COASTAL STRETCH (continued)

SAMPLE	K alt	Ol	Ne	Le	Gr	Hb	Op	Bt	Bt in Lvlbrgl	Bt in Lvlclgl	Bt alt	Mu	Ti	Ca CC in Ar	Ca in Ar	Ca in Lvl	Zeo/Dev	Qzm	Qz in Ar	Qp	Qzptf	Ch	Lvl	Lvlblgl	Lvlbrgl	Lvlgrgl	Lvlclgl	Lvlaltgl	Lvmi
BC-1-Vc	-	-	-	-	-	-	-	-	-	-	-	-	-	-	-	-	-	1	-	-	-	-	-	77	61	25	-	3	-
1	-	-	-	-	-	-	-	-	-	-	-	-	-	-	-	-	-	-	-	-	-	-	-	-	-	-	-	-	-
2	-	-	-	-	-	-	-	-	-	-	-	-	-	-	-	-	-	-	-	-	-	-	6	4	-	-	-	-	-
3	-	-	-	-	-	-	-	-	-	-	-	-	-	-	-	-	-	-	-	-	-	-	28	26	10	-	3	-	-
4	-	-	-	-	-	-	-	-	-	-	-	-	-	-	-	-	-	1	-	-	-	-	32	18	10	-	-	-	-
5	-	-	-	-	-	-	-	-	-	-	-	-	-	-	-	-	-	-	-	-	-	-	9	12	4	-	-	-	-
6	-	-	-	-	-	-	-	-	-	-	-	-	-	-	-	-	-	-	-	-	-	-	2	1	1	-	-	-	-
BC-1-C	-	-	1	-	-	-	2	-	1	-	-	-	2	-	-	-	-	5	-	-	-	2	27	28	18	10	8	-	-
1	-	-	-	-	-	-	-	-	-	-	-	-	-	-	-	-	-	-	-	-	-	-	1	-	-	-	-	-	-
2	-	-	1	-	-	-	2	-	-	-	-	-	1	-	-	-	-	2	-	-	-	-	10	5	3	4	1	-	-
3	-	-	-	-	-	-	-	-	1	-	-	-	-	-	-	-	-	3	-	-	1	9	17	9	6	3	-	-	-
4	-	-	-	-	-	-	-	-	-	-	-	-	-	-	-	-	-	-	-	-	1	4	5	5	-	3	-	-	-
5	-	-	-	-	-	-	-	-	-	-	-	-	-	-	-	-	-	-	-	-	-	3	1	1	-	1	-	-	-
6	-	-	-	-	-	-	-	-	-	-	-	-	1	-	-	-	-	-	-	-	-	-	-	-	-	-	-	-	-
BC-1-m	4	-	5	3	1	1	-	-	-	-	-	2	5	-	-	2	1	7	-	12	-	3	30	13	18	9	10	8	5
1	-	-	-	-	-	-	-	-	-	-	-	-	-	-	-	-	-	-	-	-	-	2	2	1	1	1	1	-	-
2	-	-	2	3	-	1	-	-	-	-	-	-	1	-	-	-	-	5	-	5	-	1	14	3	7	3	4	4	1
3	1	-	3	-	1	-	-	-	-	-	-	2	1	-	-	1	1	2	-	4	-	1	12	7	6	4	5	3	2
4	3	-	-	-	-	-	-	-	-	-	-	-	3	-	-	1	-	-	-	3	-	1	2	-	4	1	-	1	2
5	-	-	-	-	-	-	-	-	-	-	-	-	-	-	-	-	-	-	-	-	-	-	-	1	-	-	-	-	-
6	-	-	-	-	-	-	-	-	-	-	-	-	-	-	-	-	-	-	-	-	-	-	-	-	-	-	-	-	-
BC-1-f	8	-	7	4	-	4	-	-	-	-	-	1	1	58	-	-	-	83	-	19	-	8	-	-	-	-	-	3	6
1	-	-	-	-	-	-	-	-	-	-	-	-	-	-	-	-	-	4	-	-	-	-	-	-	-	-	-	-	-
2	1	-	3	-	-	2	-	-	-	-	-	-	-	11	-	-	-	25	-	3	-	-	1	-	-	-	-	-	1
3	5	-	3	1	-	1	-	-	-	-	-	1	1	18	-	-	-	27	-	10	-	2	-	-	-	-	-	1	3
4	2	-	1	3	-	1	-	-	-	-	-	-	-	17	-	-	-	18	-	5	-	5	-	-	-	-	-	1	2
5	-	-	-	-	-	-	-	-	-	-	-	-	-	10	-	-	-	8	-	1	-	-	-	-	-	-	-	1	-
6	-	-	-	-	-	-	-	-	-	-	-	-	-	2	-	-	-	1	-	-	-	-	-	-	-	-	-	-	-
BC-1-Vf	-	-	3	9	-	9	35	-	-	-	-	3	18	-	25	-	-	33	-	8	-	-	-	-	-	-	-	-	8
1	-	-	-	-	-	2	-	-	-	-	-	1	1	-	-	-	-	1	-	-	-	-	-	-	-	-	-	-	-
2	-	-	2	5	-	3	14	-	-	-	-	1	8	-	8	-	-	15	-	-	-	-	-	-	-	-	-	-	2
3	-	-	1	4	-	3	13	-	-	-	-	1	6	-	12	-	-	10	-	2	-	-	-	-	-	-	-	-	3
4	-	-	-	-	-	2	4	-	-	-	-	-	3	-	4	-	-	6	-	3	-	-	-	-	-	-	-	-	3
5	-	-	-	-	-	1	1	-	-	-	-	-	-	-	1	-	-	1	-	1	-	-	-	-	-	-	-	-	-
6	-	-	-	-	-	1	-	-	-	-	-	-	-	-	-	-	-	-	-	2	-	-	-	-	-	-	-	-	-
BC-2-m	-	12	7	3	-	12	97	1	-	-	-	-	-	-	-	-	3	6	-	1	-	5	9	4	6	5	6	-
1	-	-	1	-	-	5	-	-	-	-	-	-	-	-	-	1	-	-	-	-	-	-	-	-	-	-	-	-	-
2	-	4	3	2	-	4	23	1	-	-	-	-	-	-	-	1	5	-	-	-	-	1	4	1	3	3	3	-	-
3	-	2	2	1	-	4	33	-	-	-	-	-	-	-	-	1	1	-	-	-	-	3	3	2	3	1	1	-	-
4	-	3	1	-	-	4	25	-	-	-	-	-	-	-	-	-	-	-	-	1	-	1	2	1	-	-	2	-	-
5	-	3	-	-	-	8	-	-	-	-	-	-	-	-	-	-	-	-	-	-	-	-	-	-	-	-	-	-	-
6	-	-	-	-	-	3	-	-	-	-	-	-	-	-	-	-	-	-	-	-	-	-	-	-	-	-	-	-	-

*Key to Grain Shape Categories. **1** = very angular; **2** = angular; **3** = sub-angular; **4** = sub-rounded; **5** = rounded; **6** = well rounded; Vc: very coarse sand fraction; C: coarse sand fraction; m: medium sand fraction; f: fine sand fraction; Vf: very fine sand fraction.

BACOLI-POZZUOLI COASTAL STRETCH (continued)

SAMPLE	Lvmiblgl	Lvmibrgl	Lvmidggl	Lvmiclgl	Lvmialtgl	Lvvblgl	Lvvbrgl	Lvvclgl	Lvvalgl	Lvf	PMcl	PMclxx	PMbr	PMbrxx	PMalt	Lm	Lvo	Lsc (crist)	Lsc (micr)	Lss	Bio	Unk	TOT
BC-1-Vc	5	9	-	-	4	2	8	8	5	32	1	-	1	-	-	-	-	3	1	2	-	-	350
1	-	-	-	-	-	-	-	-	-	-	-	-	-	-	-	-	-	-	-	-	-	-	0
2	-	-	-	-	2	1	3	3	-	1	-	-	-	-	-	-	-	-	-	-	-	-	34
3	5	2	-	-	1	1	4	4	4	9	-	-	-	-	-	-	-	-	1	-	-	-	133
4	-	7	-	-	1	-	1	1	1	14	-	-	1	-	-	-	-	3	-	1	-	-	125
5	-	-	-	-	-	-	3	-	-	8	1	-	-	-	-	-	-	-	-	1	-	-	54
6	-	-	-	-	-	-	-	-	-	-	-	-	-	-	-	-	-	-	-	-	-	-	4
BC-1-C	8	6	5	1	6	6	6	4	10	32	18	-	10	-	-	-	20	9	9	10	8	3	400
1	-	-	-	-	-	-	-	-	-	-	5	-	-	-	-	-	-	-	-	-	-	-	9
2	5	2	1	-	1	3	2	3	1	6	7	-	7	-	-	-	6	3	-	1	3	-	132
3	2	2	4	1	2	2	4	1	5	13	3	-	3	-	-	-	9	2	5	4	3	1	165
4	1	2	-	-	3	1	-	-	4	11	3	-	-	-	-	-	5	2	2	4	2	1	77
5	-	-	-	-	-	-	-	-	-	2	-	-	-	-	-	-	-	1	2	1	-	1	15
6	-	-	-	-	-	-	-	-	-	-	-	-	-	-	-	-	-	1	-	-	-	-	2
BC-1-m	3	21	3	6	9	-	7	11	4	14	10	6	-	4	4	-	8	10	7	8	3	400
1	-	1	-	-	0	-	-	2	-	0	1	-	-	-	-	-	-	0	1	-	-	24
2	2	6	1	3	1	-	4	4	1	4	6	5	-	2	2	-	1	0	4	1	1	148
3	1	9	2	2	3	-	2	2	3	7	2	1	-	1	1	-	3	2	0	-	1	141
4	-	3	-	1	4	-	1	3	-	3	1	-	-	1	1	-	4	6	1	5	-	77
5	-	2	-	-	1	-	-	-	-	-	-	-	-	-	-	-	-	2	1	2	1	10
6	-	-	-	-	-	-	-	-	-	-	-	-	-	-	-	-	-	-	-	-	-	-	0
BC-1-f	4	1	-	4	8	1	1	10	8	-	1	-	-	-	-	-	16	25	33	11	5	400
1	-	-	-	-	-	-	-	1	-	-	-	-	-	-	-	-	-	-	-	-	-	5
2	-	-	-	-	2	-	-	5	2	-	-	-	-	-	-	-	1	-	1	1	1	77
3	2	1	-	1	2	1	1	4	2	-	1	-	-	-	-	-	5	7	8	4	3	144
4	1	-	-	2	3	-	-	-	3	-	-	-	-	-	-	-	7	12	12	4	1	122
5	1	-	-	1	1	-	-	-	1	-	-	-	-	-	-	-	3	5	11	2	-	47
6	-	-	-	-	-	-	-	-	-	-	-	-	-	-	-	-	-	1	1	1	-	5
BC-1-Vf	-	3	-	9	3	-	-	6	3	5	1	-	-	-	-	5	-	29	9	16	9	3	400
1	-	-	-	-	-	-	-	-	-	-	-	-	-	-	-	-	-	-	-	-	-	-	18
2	-	-	-	4	1	-	-	2	1	1	1	-	-	-	-	2	-	3	-	2	2	1	151
3	-	1	-	3	1	-	-	2	-	3	-	-	-	-	-	3	-	11	3	8	3	1	138
4	-	2	-	2	1	-	-	2	2	1	-	-	-	-	-	-	-	13	4	4	2	1	74
5	-	-	-	-	-	-	-	-	-	-	-	-	-	-	-	-	-	2	2	2	1	-	15
6	-	-	-	-	-	-	-	-	-	-	-	-	-	-	-	-	-	-	-	-	1	-	4
BC-2-m	10	8	1	2	5	-	-	-	9	-	-	-	-	-	-	-	-	-	-	9	-	3	400
1	-	-	-	-	-	-	-	-	-	-	-	-	-	-	-	-	-	-	-	-	-	-	21
2	4	2	-	1	1	-	-	-	1	-	-	-	-	-	-	-	-	-	-	3	-	1	158
3	3	4	1	1	2	-	-	-	4	-	-	-	-	-	-	-	-	-	-	2	-	2	116
4	3	1	-	-	2	-	-	-	3	-	-	-	-	-	-	-	-	-	-	3	-	-	87
5	-	1	-	-	-	-	-	-	1	-	-	-	-	-	-	-	-	-	-	1	-	-	14
6	-	-	-	-	-	-	-	-	-	-	-	-	-	-	-	-	-	-	-	-	-	-	4

*Key to Grain Shape Categories. **1** = very angular; **2** = angular; **3** = sub-angular; **4** = sub-rounded; **5** = rounded; **6** = well rounded; Vc: very coarse sand fraction; C: coarse sand fraction; m: medium sand fraction; f: fine sand fraction; Vf: very fine sand fraction.

BACOLI-POZZUOLI COASTAL STRETCH (continued)

SAMPLE	P	P inLvl	P inLvlblgl	P inLvlbrgl	P inLvldggl	P inLvlclgl	P in Ar	P in PM	P alt	Py	Py in Lvlblgl	Py in Lvlbrgl	Py in Lvlclgl	K	K in Ar	K in Lvl	K in Lvlblgl	K in Lvlbrgl	K in Lvlgrgl
BC-3-m	19	11	3	-	3	3	7	-	3	-	1	-	40	11	5	-	-	-	-
1	2	1	-	-	-	-	-	-	-	-	-	-	2	-	-	-	-	-	-
2	10	5	-	-	2	2	2	-	1	-	1	-	18	1	1	-	-	-	-
3	5	4	1	-	1	1	4	-	2	-	-	-	14	3	3	-	-	-	-
4	2	1	2	-	-	-	1	-	-	-	-	-	5	3	1	-	-	-	-
5	-	-	-	-	-	-	-	-	-	-	-	-	1	4	-	-	-	-	-
6	-	-	-	-	-	-	-	-	-	-	-	-	-	-	-	-	-	-	-
BC-4-m	19	8	-	-	-	-	-	-	-	-	-	-	40	4	-	-	-	-	-
1	1	1	-	-	-	-	-	-	-	-	-	-	5	-	-	-	-	-	-
2	9	4	-	-	-	-	-	-	4	1	-	-	16	1	-	-	-	-	-
3	6	2	-	-	-	-	-	-	3	2	-	-	14	2	-	-	-	-	-
4	2	1	-	-	-	-	-	-	2	1	-	-	4	1	-	-	-	-	-
5	1	-	-	-	-	-	-	-	-	-	-	-	1	-	-	-	-	-	-
6	-	-	-	-	-	-	-	-	-	-	-	-	-	-	-	-	-	-	-
BC-5-m	15	-	6	-	-	-	-	3	7	-	-	-	39	11	-	-	-	-	-
1	-	-	-	-	-	-	-	-	-	-	-	-	5	-	-	-	-	-	-
2	8	-	2	-	-	-	-	1	5	-	-	-	18	5	-	-	-	-	-
3	5	-	3	-	-	-	-	2	2	-	-	-	12	4	-	-	-	-	-
4	1	-	1	-	-	-	-	-	-	-	-	-	4	2	-	-	-	-	-
5	-	-	-	-	-	-	-	-	-	-	-	-	-	-	-	-	-	-	-
6	-	-	-	-	-	-	-	-	-	-	-	-	-	-	-	-	-	-	-

SAMPLE	K alt	Ol	Ne	Le	Gr	Hb	Op	Bt	Bt in Lvlbrgl	Bt in Lvlclgl	Bt alt	Mu	Ti	Ca	CC in Ar	Ca in Ar	Ca in Lvl	Zeo/Dev	Qzm	Qz in Ar	Qp	Qzptf	Ch	Lvl	Lvlblgl	Lvlbrgl	Lvlgrgl	Lvlclgl	Lvlaltgl	Lvmi
BC-3-m	1	-	1	-	-	-	-	11	1	-	3	-	-	15	8	15	-	20	17	9	1	7	15	4	-	3	4	21	9
1	-	-	-	-	-	-	-	-	-	-	-	-	-	-	-	-	-	2	-	-	-	-	-	-	-	-	-	-	-	-
2	-	-	1	-	-	-	-	2	-	-	-	-	-	5	-	5	-	7	3	2	-	1	4	1	-	-	2	4	3	-
3	1	-	-	-	-	-	-	2	1	-	-	-	-	5	3	6	-	8	9	5	1	4	7	3	-	2	2	9	4	-
4	-	-	-	-	-	-	-	5	-	-	-	-	-	5	4	4	-	2	5	2	-	2	4	-	-	1	-	6	2	-
5	-	-	-	-	-	-	-	2	-	-	1	-	-	4	1	-	-	1	-	-	-	-	-	-	-	-	-	2	-	-
6	-	-	-	-	-	-	-	-	-	-	2	-	-	-	-	-	-	-	-	-	-	-	-	-	-	-	-	-	-	-
BC-4-m	-	-	7	-	1	-	9	-	-	-	-	-	-	52	1	5	-	5	41	8	22	-	6	7	12	4	3	1	9	3
1	-	-	-	-	-	-	-	-	-	-	-	-	-	1	-	-	-	6	-	2	-	-	-	-	-	-	-	-	-	-
2	-	-	3	-	1	-	6	-	-	-	-	-	-	19	-	1	-	2	19	1	6	-	2	3	2	1	2	1	3	2
3	-	-	3	-	-	-	2	-	-	-	-	-	-	18	1	3	-	2	11	3	9	-	3	3	6	3	1	-	2	1
4	-	-	1	-	-	-	1	-	-	-	-	-	-	13	-	1	-	1	4	4	3	-	1	1	4	-	-	-	4	-
5	-	-	-	-	-	-	-	-	-	-	-	-	-	1	-	-	-	-	1	-	1	-	-	-	-	-	-	-	-	-
6	-	-	-	-	-	-	-	-	-	-	-	-	-	-	-	-	-	-	-	-	1	-	-	-	-	-	-	-	-	-
BC-5-m	16	-	-	6	-	4	-	11	-	-	-	-	-	32	8	16	-	-	32	16	18	1	2	10	4	-	-	-	10	4
1	-	-	-	-	-	1	-	-	-	-	-	-	-	1	-	1	-	-	8	-	-	-	-	-	-	-	-	-	-	-
2	4	-	-	3	-	2	-	6	-	-	-	-	-	8	2	5	-	-	12	5	5	1	-	3	2	-	-	-	1	1
3	8	-	-	3	-	1	-	3	-	-	-	-	-	12	5	6	-	-	10	6	10	-	2	5	2	-	-	-	4	2
4	3	-	-	-	-	-	-	2	-	-	-	-	-	6	1	3	-	-	2	4	3	-	-	2	-	-	-	-	3	1
5	1	-	-	-	-	-	-	-	-	-	-	-	-	4	-	1	-	-	-	1	-	-	-	-	-	-	-	-	2	-
6	-	-	-	-	-	-	-	-	-	-	-	-	-	1	-	-	-	-	-	-	-	-	-	-	-	-	-	-	-	-

*Key to Grain Shape Categories. **1** = very angular; **2** = angular; **3** = sub-angular; **4** = sub-rounded; **5** = rounded; **6** = well rounded; Vc: very coarse sand fraction; C: coarse sand fraction; m: medium sand fraction; f: fine sand fraction; Vf: very fine sand fraction.

BACOLI-POZZUOLI COASTAL STRETCH (continued)

SAMPLE	Lvmiblgl	Lvmibrgl	Lvmidggl	Lvmiclgl	Lvmiaktgl	Lvvblgl	Lvvbrgl	Lvvdgl	Lvvalgl	Lvf	PMd	PMdxx	PMbr	PMbrxx	PMalt	Lm	Lvo	Lsc (crist)	Lsc (micr)	Lss	Bio	Unk	TOT
BC-3-m	7	6	3	-	5	-	-	8	8	9	4	-	-	3	-	-	-	11	19	25	16	5	400
1	-	-	-	-	-	-	-	-	-	-	-	-	-	-	-	-	-	-	-	-	1	-	8
2	1	2	-	-	1	-	-	5	3	3	1	-	-	1	-	-	-	2	3	3	3	1	112
3	5	1	2	-	2	-	-	2	3	4	2	-	-	2	-	-	-	5	4	7	5	3	157
4	1	3	1	-	2	-	-	1	2	2	1	-	-	-	-	-	-	4	8	9	6	1	99
5	-	-	-	-	-	-	-	-	-	-	-	-	-	-	-	-	-	-	2	4	1	-	20
6	-	-	-	-	-	-	-	-	-	-	-	-	-	-	-	-	-	-	2	2	-	-	4
BC-4-m	9	1	-	5	2	-	-	2	2	11	-	-	-	-	-	3	-	23	23	30	8	1	400
1	-	-	-	-	-	-	-	-	-	1	-	-	-	-	-	-	-	-	-	-	-	-	17
2	1	1	-	-	-	-	-	-	3	-	-	-	-	-	-	1	-	5	2	8	4	-	134
3	5	-	-	3	1	-	-	-	1	5	-	-	-	-	-	2	-	11	8	10	3	1	150
4	2	-	-	1	1	-	-	1	1	2	-	-	-	-	-	-	-	7	9	8	1	-	82
5	1	-	-	1	-	-	-	1	-	-	-	-	-	-	-	-	-	-	3	3	-	-	14
6	-	-	-	-	-	-	-	-	-	-	-	-	-	-	-	-	-	-	1	1	-	-	3
BC-5-m	1	1	-	10	-	-	-	5	10	5	-	-	-	-	-	-	-	28	28	30	10	1	400
1	-	-	-	-	-	-	-	-	1	-	-	-	-	-	-	-	-	-	-	-	-	-	18
2	-	1	-	1	-	-	-	3	4	2	-	-	-	-	-	-	-	7	5	6	2	-	130
3	1	-	-	4	-	-	-	2	3	3	-	-	-	-	-	-	-	11	11	10	4	1	157
4	-	-	-	3	-	-	-	-	2	-	-	-	-	-	-	-	-	9	8	7	2	-	69
5	-	-	-	2	-	-	-	-	-	-	-	-	-	-	-	-	-	1	4	3	2	-	21
6	-	-	-	-	-	-	-	-	-	-	-	-	-	-	-	-	-	-	-	4	-	-	5

SAMPLE	P	P inLvlblgl	P inLvlbrgl	P inLvlorgl	P inLvlclgl	P in PM	P alt	Py	Py in Lvlblgl	Py in Lvlbrgl	Py in Lvldggl	Py in Lvlclgl	Py in PM	Py alt	K	K in Lvlblgl	K in Lvlbrgl	K in Lvlorgl	K in Lvlgrgl
PZ-1-m	40	0	2	0	0	0	69	0	2	0	0	0	0	21	0	1	0	0	0
1																			
2	18						24						9			1			
3	17		1				32		1				7						
4	5						13		1				5						
5			1																
6																			
PZ-2-m	7	0	0	0	0	0	58	2	0	0	0	0	0	0	0	0	0	0	0
1																			
2								16											
3	3							28	2										
4	4							14											
5																			
6																			
PZ-3-m	66	1	2	0	0	0	80	0	0	0	0	1	0	6	0	0	0	0	0
1	5						5												
2	29						48												
3	27	1	2				18						4						
4	5						7					1	2						
5							2												
6																			

*Key to Grain Shape Categories. **1** = very angular; **2** = angular; **3** = sub-angular; **4** = sub-rounded; **5** = rounded; **6** = well rounded; Vc: very coarse sand fraction; C: coarse sand fraction; m: medium sand fraction; f: fine sand fraction; Vf: very fine sand fraction.

BACOLI-POZZUOLI COASTAL STRETCH (continued)

SAMPLE	K in Pm	Ol	Ne	Le	Hb	Op	Op in Lvlcigl	Bt	Bt in Lvlbrgl	Ca	Zeo/Dev	Qzm	Qp	Qzptf	Ch	Lvl	Lvlblgl	Lvlbrgl	Lvlorgl	Lvlgrgl	Lvlcigl	Lvlaltgl	Lvmi	Lvmiblgl	Lvmibrgl	Lvmiorgl	Lvmigrgl	Lvmicigl	Lvmialtgl
PZ-1-m	0	20	0	8	0	0	0	0	0	2	0	12	0	0	0	0	9	9	5	2	8	9	0	19	16	2	0	0	0
1																													
2		14			4							4					1	2				2		1					
3		6			4					1		8					8	5	4	2	4			14	6	2				
4																		2	1		4	7		4	3					
5										1															6					
6																									1					
PZ-2-m	0	0	0	164	0	6	0	0	0	0	0	0	0	0	0	0	61	0	0	0	0	0	0	26	0	0	0	0	0
1																													
2				40													19							9					
3				49			3										31							17					
4				44			3										11							0					
5				16																									
6				15																									
PZ-3-m	0	4	1	8	0	2	0	1	0	4	0	1	1	0	0	0	6	10	4	0	3	5	0	7	19	0	0	3	0
1																													
2		3	1	5		1												2						2					
3		1		2		1				4		1					3	8	4			3		3	16			2	
4														1			3					5			3			1	
5				1																				2					
6																													

SAMPLE	Lvvblgl	Lvvbrgl	Lvvorgl	Lvvgrgl	Lvvclgl	Lvvalgl	Lvf	PMcl	PMcixx	PMbr	PMbrxx	PMalt	Lp	Lvo	Lsc (xx)	Lsc (micr)	Lss	Bio	Unk	TOT
PZ-1-m	14	10	0	0	3	0	25	11	0			0	0	33	8	7	28	5	400	
1																	0		0	
2	5					6	6							3	2	1	8		111	
3	5	5				17	5							22	3	6	15		200	
4	3	5			2	2								5	3		5	5	75	
5					1									3					12	
6	1																		2	
PZ-2-m	57	4	2	0	0	0	0	0	0			0	0	9	1	1	2	0	400	
1																			0	
2	24													6	1	1	1		117	
3	26	4	2											3			1		169	
4	7																		83	
5																			16	
6																			15	
PZ-3-m	11	8	0	0	6	15	17	26		0			0	2	44	13	8	10	6	400
1																			10	
2	4	1			2	4	5	9						13	6		5		140	
3	7	3			1	6	10	17					2	20	7	5	5	4	192	
4		4			3	4								5		3		2	44	
5						1	2							6					14	
6																			0	

*Key to Grain Shape Categories. **1** = very angular; **2** = angular; **3** = sub-angular; **4** = sub-rounded; **5** = rounded; **6** = well rounded; Vc: very coarse sand fraction; C: coarse sand fraction; m: medium sand fraction; f: fine sand fraction; Vf: very fine sand fraction.

BACOLI-POZZUOLI COASTAL STRETCH (continued)

SAMPLE	P	P in Lvlblgl	P in Lvlbrgl	P in Lvlorgl	P in Lvlclgl	P in PM	P alt	Py	Py in Lvlblgl	Py in Lvlbrgl	Py in Lvldggl	Py in Lvlclgl	Py in PM	Py alt	K	K in Lvlblgl	K in Lvlbrgl	K in Lvlorgl	K in Lvlgrgl
PZ-4-m	44	1	1	0	0	0	0	25	0	0	0	0	0	38	0	3	0	0	0
1																			
2	20							12						10					
3	19		1					10						20		3			
4	5	1						3						8					
5																			
6																			
PZ-5-m	35	0	0	1	0	1	0	13	11	0	0	3	0	60	0	1	1	0	
1	10							1						7					
2	13					1		5	7					23		1			
3	9							5	4			3		23					
4	3							2						7					
5				1													1		
6																			
PZ-6-m	20	0	1	0	0	0	0	12	0	0	0	0	0	40	2	0	0	0	
1																			
2	8							2						15	1				
3	9							10						22	1				
4	3													3	1				
5			1																
6																			
PZ-7-m	19	0	0	0	0	0	0	185	0	0	0	0	0	19	0	0	0	0	0
1	7							12											
2	11							50						4					
3	1							80						13					
4								41						2					
5								2											
6																			
PZ-8-Vc	9	1	0	0	1	0	0	2	0	0	0	0	0	4	0	0	0	0	0
1																			
2	1													1					
3	3							2						3					
4	3																		
5	2				1														
6		1																	
PZ-8-C	37	1	0	3	0	0	6	0	0	0	0	0	0	27	0	0	0	1	0
1														1					
2	12			1										2					
3	20	1					5							14					
4	5			2			1							10				1	
5																			
6																			
PZ-8-m	61	8	2	0	1	0	4	28	0	0	1	0	0	54	3	0	0	0	0
1																			
2	35							12						30					
3	23	4			1		4	14			1			24	3				
4	3	4	1					2											
5			1																
6																			

*Key to Grain Shape Categories. **1** = very angular; **2** = angular; **3** = sub-angular; **4** = sub-rounded; **5** = rounded; **6** = well rounded; Vc: very coarse sand fraction; C: coarse sand fraction; m: medium sand fraction; f: fine sand fraction; Vf: very fine sand fraction.

BACOLI-POZZUOLI COASTAL STRETCH (continued)

SAMPLE	K in Pm	Ol	Ne	Le	Hb	Op	Op in Lvlclgl	Bt	Bt in Lvlbrgl	Ca	Zeo/Dev	Qzm	Qp	Qzptf	Ch	Lvl	Lvlblgl	Lvlbrgl	Lvlorgl	Lvlgrgl	Lvlclgl	Lvlaltgl	Lvmi	Lvmiblgl	Lvmibrgl	Lvmiorgl	Lvmigrgl	Lvmiclgl	Lvmialtgl
PZ-4-m																													
1		0	7	2	0	0	0	1	0	5	0	0	0	0	0	0	9	0	10	0	9	2	0	13	2	10	0	0	0
2																	3												
3								1		3							6		10		9	1		9	1	8			
4			4	2						2												1		1	1	2			
5																													
6																													
PZ-5-m																													
1		0	5	0	0	0	0	3	0	2	0	1	0	0	1	8	7	14	0	8	1	0	8	28	0	0	2		
2			4					3		2		1				4	3	7					4	1	6				
3			1												1	4	2	6			8		3	16	9			2	
4																	1						1	8	3				
5																	1	1											
6																								3					
PZ-6-m																													
1		0	24	0	0	1	0	7	0	0	0	6	0	0	1	17	15	7	0	2	5	0	40	24	6	0	0	16	
2			15			1		6				4				6							11					1	
3			9					1				2				11	4	7			2	5	19	22	6			15	
4															1		11						8	2					
5																							2						
6																													
PZ-7-m																													
1		28	0	0	16	55	0	0	0	0	0	1	0	0	0	21	1	0	0	0	0	0	7	0	0	0	0	0	
2		3														3													
3		2			4	7										12							1						
4		5			5	22						1											6						
5		10			3	16										6	1												
6		8			4	10																							
PZ-8-Vc																													
1		0	2	0	0	0	0	0	0	0	0	0	0	0	29	35	47	4	24	6	28	0	0	9	1	0	0	0	
2																	3			1	2								
3		2													3	10	7	2	3		7					1			
4															14	8	18		10	5	8			2					
5															12	14	14		11		11			6					
6																3	5	2						1					
PZ-8-C																													
1		0	2	0	0	0	0	2	0	0	3	5	0	4	17	18	28	26	6	13	1	0	7	18	20	0	0	0	
2								2				4			1		3						2		1				
3			2									1			2	6	5	10	12	6	8		5	11	10				
4											3				2	5	3	9	12		5	1		7	8				
5															5	10	6	6	2						1				
6																													
PZ-8-m																													
1		0	8	0	1	0	0	3	0	0	0	9	0	0	0	17	4	0	5	2	7	0	21	22	2	1	2	13	
2		5					3					8			5	2				1				1					
3		3		1								1			8	1			5	1	7		14	19	1	1		11	
4															4								6	2				2	
5																1							1						
6																													

*Key to Grain Shape Categories. **1** = very angular; **2** = angular; **3** = sub-angular; **4** = sub-rounded; **5** = rounded; **6** = well rounded; Vc: very coarse sand fraction; C: coarse sand fraction; m: medium sand fraction; f: fine sand fraction; Vf: very fine sand fraction.

BACOLI-POZZUOLI COASTAL STRETCH (continued)

SAMPLE	Lvvblgl	Lvvbrgl	Lvvorgl	Lvvgrgl	Lvvclgl	Lvvalgl	Lvf	PMcl	PMclxx	PMbr	PMbrxx	PMalt	Lp	Lvo	Lsc (xx)	Lsc (micr)	Lss	Bio	Unk	TOT
PZ-4-m	17	16	0	0	19	3	39	38		0			0	0	55	10	6	14	1	400
1																				0
2	5	4			4		13	17							16	6		5	1	126
3	8	12			10	3	18	21							30	4	3	9		223
4	4				5		5								6		3			45
5							3								3					6
6																				0
PZ-5-m	9	12	7	0	17	0	53	13		0			0	0	25	0	5	26	1	400
1							5											3		26
2	4		5		4		22	5							12		3	11		151
3	3	8			7		22	8							10		2	9	1	166
4	1		2		6		1								3			1		40
5	1	4					3											2		14
6																				3
PZ-6-m	34	14	2	0	7	4	17	57		0		10	0	0	1	0	4	1	3	400
1																				0
2	7	4			2		5	31												118
3	14	6	1		3	1	10	20				10			1		3	1	2	217
4	10	4	1		2		2	6									1		1	56
5	3																			4
6						3														5
PZ-7-m	25	3	0	0	4	0	7	3		0			0	0	4	0	0	2	0	400
1																				22
2	3						2	1												87
3	8	2			2		5	2										2		161
4	9	1			2										4					101
5	5																			29
6																				0
PZ-8-Vc	0	2	5	0	2	0	68	17		0			0	0	0	0	4	0	0	300
1																				0
2							2	3												13
3		2			1		8	8												62
4			2		1		20													91
5			3				28	6									2			110
6							10										2			24
PZ-8-C	7	3	0	0	14	0	55	69		0			0	0	0	0	7	0	0	400
1								4												5
2					5		6	18												57
3		3			5		16	29									4			175
4	5				4		25	13									3			124
5	2						6	5												37
6							2													2
PZ-8-m	29	24	2	0	7	3	24	16		0			0	0	1	0	6	0	9	400
1								1												1
2	6				3		8	9											1	130
3	20	16	2		4	2	13	6							1		4		8	222
4	3	8					3										2			43
5						1														4
6																				0

*Key to Grain Shape Categories. **1** = very angular; **2** = angular; **3** = sub-angular; **4** = sub-rounded; **5** = rounded; **6** = well rounded; Vc: very coarse sand fraction; C: coarse sand fraction; m: medium sand fraction; f: fine sand fraction; Vf: very fine sand fraction.

BACOLI-POZZUOLI COASTAL STRETCH (continued)

SAMPLE	P	P inLvlblgl	P inLvlbrgl	P inLvlorgl	P inLvlclgl	P in PM	P alt	Py	Py in Lvlblgl	Py in Lvlbrgl	Py in Lvldggl	Py in Lvlclgl	Py in PM	Py alt	K	K in Lvlblgl	K in Lvlbrgl	K in Lvlorgl	K in Lvlgrgl
PZ-8-f	44	0	0	0	0	0	10	51	0	0	0	0	0	59	0	0	0	0	0
1	7							4						33					
2	18						6	20						22					
3	13						4	16						4					
4	6							9											
5								2											
6																			
PZ-8-Vf	29	0	0	0	0	0	4	68	0	0	0	0	0	7	21	0	0	0	0
1																			
2	11							31						3	7				
3	14						4	27						4	13				
4	4							8							1				
5								2											
6																			
PZ-9-m	0	0	0	0	0	0	0	1	0	0	0	0	0	3	0	0	0	0	0
1																			
2								1						2					
3														1					
4																			
5																			
6																			
PZ-10-m	7	1	0	0	0	1	0	0	0	0	0	0	0	37	0	0	0	0	0
1														8					
2	5					1								24					
3	2	1												4					
4														1					
5																			
6																			
PZ-11-m	34	0	0	1	0	3	2	15	0	0	0	1	1	0	71	0	4	0	0
1	5					2							1		11				
2	19			1		1	2	11				1			38		4		
3	9							3							22				
4								1											
5	1																		
6																			
PZ-12-m	70	1	1	0	0	0	14	127	0	0	0	0	4	1	24	0	0	0	0
1	8							19							1				
2	30						5	57						1	16				
3	22	1	1				9	33							7				
4	9							13					4						
5	1							5											
6																			
PZ-13-m	7	0	0	0	0	1	13	0	0	0	0	0	0	0	24	0	1	0	0
1					1														
2	3						5								14				
3	4						8								10				
4																	1		
5																			
6																			

*Key to Grain Shape Categories. **1** = very angular; **2** = angular; **3** = sub-angular; **4** = sub-rounded; **5** = rounded; **6** = well rounded; Vc: very coarse sand fraction; C: coarse sand fraction; m: medium sand fraction; f: fine sand fraction; Vf: very fine sand fraction.

BACOLI-POZZUOLI COASTAL STRETCH (continued)

SAMPLE	K in	Pm	Ol	Ne	Le	Hb	Op	Op in	Lvlclgl	Bt	Bt in	Lvlbrgl	Ca	Zeo/Dev	Qzm	Qp	Qzptf	Ch	Lvl	Lvlblgl	Lvlbrgl	Lvlorgl	Lvlgrgl	Lvlclgl	Lvlaltgl	Lvmi	Lvmiblgl	Lvmibrgl	Lvmiorgl	Lvmigrgl	Lvmiclgl	Lvmialtgl
PZ-8-f	0	7	0	1	21	0	4	6	0	0	0	0	0	0	0	0	0	0	16	12	0	0	1	6	0	28	22	0	0	0	4
1																															
2			1		1	7				4	4								4	3						7	2				
3			6			2					2								7	9				5		10	14				4
4						3													5				1	1		11	6				
5						6																									
6						3																									
PZ-8-Vf	4	0	0	3	25	0	2	0	0	0	0	0	0	6	0	0	0	0	9	0	0	0	0	0	0	20	12	0	0	0	0
1																															
2					6				2					4																	
3		4		1	13									2					6							7	5				
4				2	4														3							13	7				
5					2																										
6																															
PZ-9-m	0	0	0	0	3	0	7	0	0	0	0	0	0	0	0	0	0	0	8	2	7	0	0	4	0	29	11	18	0	2	8
1							1																								
2					3		3			3									3							5	3	4			
3							3			3									5	2	6			4		13	8	11		2	8
4																					1					5		3			
5																										6					
6																															
PZ-10-m	1	0	14	0	0	3	0	5	0	0	0	0	0	0	0	0	0	0	14	26	0	2	2	10	0	14	11	3	2	5	14
1																															
2	1		9			3		5											5	8				4		4					
3			5																8	18		2	2	6		8	7	3	2	2	7
4																			1							2	4				6
5																															1
6																															
PZ-11-m	0	8	0	0	0	0	0	7	0	0	0	0	0	4	0	0	0	0	13	15	0	0	11	0	0	22	34	8	2	8	7
1								2																							
2			6					5						1					5	4				6		5	10	3		3	3
3			2											2					8	11				5		10	21	5	2	4	4
4														1												6	3			1	
5																										1					
6																															
PZ-12-m	4	5	0	2	10	6	6	0	0	0	0	0	0	12	0	0	0	0	31	11	0	0	0	0	0	7	13	0	0	1	4
1																															
2		4		2	3	2	3							3					8	1						1	1				
3			4	1			7							5					22	9						4	8		1		4
4														2					1	1						2	3				
5																															
6								4						2													1				
PZ-13-m	0	0	0	0	0	0	0	9	0	0	0	0	0	8	0		6	1	35	29	2	1	11	3	0	46	18	2	3	0	16
1																															
2								7						3			3		15	10	1		4			10	2	2			
3								2						5			3		19	19	1	1	1	1		20	12		2		10
4																	1		1				6	2		8	4		1		6
5																										8					
6																															

*Key to Grain Shape Categories. **1** = very angular; **2** = angular; **3** = sub-angular; **4** = sub-rounded; **5** = rounded; **6** = well rounded; Vc: very coarse sand fraction; C: coarse sand fraction; m: medium sand fraction; f: fine sand fraction; Vf: very fine sand fraction.

BACOLI-POZZUOLI COASTAL STRETCH (continued)

SAMPLE	Lvvblgl	Lvvbrgl	Lvvorgl	Lvvgrgl	Lvvclgl	Lvvalgl	Lvf	PMcl	PMclxx	PMbr	PMbrxx	PMalt	Lp	Lvo	Lsc (xx)	Lsc (micr)	Lss	Bio	Unk	TOT
PZ-8-f	43	10	0	0	9	4	26	12		0			0	0	2	0	1	1	0	400
1																				44
2	10				2		8	3												122
3	19	7			7		10	8							2		1			150
4	3	3					7	1										1		57
5	7					4	1													20
6	4																			7
PZ-8-Vf	106	9	0	0	41	1	9	20		0		0	0	0	0	0	1	0	3	400
1	10							13												23
2	42				15	1	6	7											1	136
3	42	9			21		3										1		2	178
4	8				5															55
5	4																			8
6																				0
PZ-9-m	55	14	10	0	6	63	13	126		0		10	0	0	0	0	0	0	0	400
1								24												25
2	8	1	2		2	10	3	44												94
3	20	11	5		4	40	7	32				10								192
4	18	2	3			13	3	17												65
5	6							9												21
6	3																			3
PZ-10-m	30	18	4	0	8	25	5	37	71	11	17	0	0	0	0	0	0	2	0	400
1	6						1	15	45											75
2	9	3	4		5	7		18	19	10	15									169
3	12	6			3	14	2	3	6	1	2									125
4	3	9				4	2	1	1									2		31
5																				0
6																				0
PZ-11-m	17	12	1	0	13	15	10	15	39	0		0	0	0	2	0	1	2	2	400
1					2		1	7	13											44
2	4	1	1		7	3	4	6	17									2		173
3	9	11			4	8	5	2	9						1				2	159
4	3					4									1					20
5	1																1			4
6																				0
PZ-12-m	3	6	0	0	11	0	4	0	9	0		0	0	2	11	0	0	0	0	400
1																				28
2		1			4		1		6						2					151
3	3	5			6		3		3					1	6					167
4					1									1	3					41
5																				13
6																				0
PZ-13-m	15	12	0	0	12	15	13	46		28		9	0	0	3	0	0	4	7	400
1					4			5		11										21
2	7				6		2	22		10		4							3	133
3	8	7			2	9	9	17		7		5			2			1	4	189
4		5				4	2	2							1			3		47
5						2														10
6																				0

*Key to Grain Shape Categories. **1** = very angular; **2** = angular; **3** = sub-angular; **4** = sub-rounded; **5** = rounded; **6** = well rounded; Vc: very coarse sand fraction; C: coarse sand fraction; m: medium sand fraction; f: fine sand fraction; Vf: very fine sand fraction.

BACOLI-POZZUOLI COASTAL STRETCH (continued)

SAMPLE	P	P intLvlblgl	P intLvlbrgl	P intLvlorgl	P intLvlclgl	P in PM	P alt	Py	Py in Lvlblgl	Py in Lvlbrgl	Py in Lvlclggl	Py in Lvlclgl	Py in PM	Py alt	K	K in Lvlblgl	K in Lvlbrgl	K in Lvlorgl	K in Lvlgrgl
PZ-14-Vc	13	1	0	0	0	0	2	3	0	0	0	1	0	5	0	0	0	0	0
1																			
2	3						2							1					
3	8							3				1		4					
4	2	1																	
5																			
6																			
PZ-14-C	13	7	2	0	0	0	2	1	0	0	0	0	0	52	1	5	0	4	
1																			
2	7													20					
3	5	4					1	1						25					
4	1	3	1				1							7		5		4	
5															1				
6			1																
PZ-14-m	10	0	2	0	0	0	2	0	0	0	0	0	0	10	1	2	0	0	
1														1					
2	5		1				1							4	1				
3	5		1				1							5		1			
4																			
5																1			
6																			
PZ-14-f	24	0	0	0	0	0	0	0	0	0	0	0	0	38	0	0	0	0	0
1																			
2	12													15					
3	11													20					
4	1													3					
5																			
6																			
PZ-14-Vf	32	0	0	0	0	0	76	0	0	0	0	0	0	25	0	0	0	0	0
1							1												
2	5						33							5					
3	15						21							18					
4	12						12							2					
5							9												
6																			
PZ-15-m	32	0	0	0	0	0	3	1	0	0	0	0	0	68	4	2	0	0	0
1														3					
2	12						1							30					
3	15						2	1						31	2	1			
4	5													4	1	1			
5															1	1			
6																			

*Key to Grain Shape Categories. **1** = very angular; **2** = angular; **3** = sub-angular; **4** = sub-rounded; **5** = rounded; **6** = well rounded; Vc: very coarse sand fraction; C: coarse sand fraction; m: medium sand fraction; f: fine sand fraction; Vf: very fine sand fraction.

BACOLI-POZZUOLI COASTAL STRETCH (continued)

SAMPLE	K in Pm	Ol	Ne	Le	Hb	Op	Op in Lvlclgl	Bt	Bt in Lvlbrgl	Ca	Zeo/Dev	Qzm	Qp	Qzptf	Ch	Lvl	Lvlblgl	Lvlbrgl	Lvlorgl	Lvlgrgl	Lvlclgl	Lvlaltgl	Lvmi	Lvmiblgl	Lvmibrgl	Lvmiorgl	Lvmigrgl	Lvmiclgl	Lvmialtgl
PZ-14-Vc		0	0	0	0	0	0	0	0	0	0	4	0	0	0	0	42	22	0	4	6	0	0	1	4	0	0	1	0
1																													
2												3					1	2											
3												1					21	6			2					2			1
4																	10	8		1	4			1					
5																	6	6		1						2			
6																	4												
PZ-14-C		0	0	0	0	0	0	5	1	0	0	3	2	0	0	40	41	4	8	17	0	0	23	25	5	1	4	0
1																													
2								4	1			1				4	4	1		6			3		1			1	
3								1				1				12	18	3	4	8			13	17	4	1		3	
4												1	2			16	15		2	3			5	8					
5																8	4		2				1						
6																							1						
PZ-14-m		0	0	0	0	0	0	7	0	0	0	6	1	1	0	21	34	2	14	18	0	0	19	26	2	11	3	0
1												4																
2								5				2	1			4	4	1	3	6			5	1	1	4	1		
3								2								13	14		7	7			13	17	1	5	2		
4															1	4	15	1	4	5			1	8		2			
5																1													
6																													
PZ-14-f		0	0	0	0	0	0	5	0	12	0	69	21	9	0	17	4	0	2	0	0	0	27	28	1	7	8	0
1																													
2										3		28	5			2	1						3	1	1	3	4		
3								1		5		30	6	2		9	3		2				15	15		4	3		
4								3		4		5	8	4		3							5	6			1		
5								1				6	2	3		3							4	6					
6																													
PZ-14-Vf		0	0	0	14	1	0	0	0	4	0	107	6	4	4	0	5	0	0	2	0	0	9	4	0	0	0	2
1																													
2				7	1					2		25		1						1								1	
3				6						1		48	4	2	2					1			6	4				1	
4				1						1		27	2	2	1		2						3						
5												7																	
6																													
PZ-15-m		0	3	0	0	0	0	3	0	2	0	13	0	0	2	0	37	32	1	11	9	0	0	21	21	2	13	7	0
1																													
2			1					1		1		1				1	8	8		3	5					1	3		
3			1					2		1		8			1	23	19	1	7	4			18	15	2	3	3		
4			1									4			1	6	4		1				1	6		4	1		
5																	1						2			5			
6																													

*Key to Grain Shape Categories. **1** = very angular; **2** = angular; **3** = sub-angular; **4** = sub-rounded; **5** = rounded; **6** = well rounded; Vc: very coarse sand fraction; C: coarse sand fraction; m: medium sand fraction; f: fine sand fraction; Vf: very fine sand fraction.

BACOLI-POZZUOLI COASTAL STRETCH (continued)

SAMPLE	Lvvblgl	Lvvbrgl	Lvvorgl	Lvvgrgl	Lvvclgl	Lvvalgl	Lvf	PMcl	PMclxx	PMbr	PMbrxx	PMalt	Lp	Lvo	Lsc (xx)	Lsc (micr)	Lss	Bio	Unk	TOT
PZ-14-Vc	7	8	0	2	0	0	12	1		0		0	1	0	3	1	4	2	0	150
1																				0
2		1		1			1											1		17
3		3					4	1												58
4	1	4		1			2										1			36
5	6						5						1		3	1	3	1		35
6																				4
PZ-14-C	13	10	0	0	16	0	12	46		23			0	0	0	1	3	10	0	400
1								6												6
2	1	3			1			20		7								4		89
3	5	6			10		5	13		9								4		173
4	5	1			5		3	7		7							3	2		107
5	1						4									1				22
6	1																			3
PZ-14-m	15	16	0	0	35	0	26	70	0	30	0	3	3	0	0	1	3	3	3	400
1							1	16		15			2							39
2	3	9			12		6	34		10		1	1				2	1	1	130
3	9	5			19		13	20		4		2					1	2	2	171
4	3	2			4		4			1										55
5							2									1				5
6																				0
PZ-14-f	9	10	0	0	13	0	22	9	0	0	0	0	0	0	18	12	24	4	7	400
1								3												3
2					4		2	5							3	1	7	1		101
3	1	6			7		13	1							9	5	8	1	2	179
4	7	3			2		4								6	4	8	2	5	84
5	1	1					3									2	1			33
6																				0
PZ-14-Vf	11	2	0	0	3	6	4	0	0	0	0	0	0	0	50	13	11	0	5	400
1																				1
2	2	1				1	1								2					88
3	9	1			3	1	3								20	9	8		3	189
4						1									21	3	2		1	93
5						3									4	1	1		1	26
6															3					3
PZ-15-m	16	20	2	0	7	1	20	18	0	14	0	0	0	0	7	4	1	3	0	400
1								3												6
2	3	4			2		2	11		8								1		107
3	13	6	1		4	1	11	4		5					5	3		2		214
4		8	1		1		4			1					2	1	1			58
5		2					3													15
6																				0

*Key to Grain Shape Categories. **1** = very angular; **2** = angular; **3** = sub-angular; **4** = sub-rounded; **5** = rounded; **6** = well rounded; Vc: very coarse sand fraction; C: coarse sand fraction; m: medium sand fraction; f: fine sand fraction; Vf: very fine sand fraction.

BACOLI-POZZUOLI COASTAL STRETCH (continued)

SAMPLE	P	P in Lv lbgl	P in Lv lbrgl	P in Lv lorgl	P in Lv lcgl	P in PM	P alt	Py	Py in Lv lbgl	Py in Lv lbrgl	Py in Lv ldggl	Py in Lv lcgl	Py in PM	Py alt	K	K in Lv lbgl	K in Lv lbrgl	K in Lv lorgl	K in Lv lgrgl
PZ-16-m	37	0	0	0	0	0	7	0	0	0	0	0	0	0	63	0	0	0	0
1															5				
2	5							2							15				
3	17							5							34				
4	15														8				
5															1				
6																			
PZ-17-m	44	0	3	0	1	0	6	3	0	1	0	0	0	0	21	0	2	0	0
1															1				
2	19					4	1			1					9	1			
3	21		2		1	2	2								9	1			
4	4		1												2				
5																			
6																			
PZ-18-m	5	5	1	0	0	0	3	6	0	0	0	0	0	0	14	1	0	0	0
1								4							7				
2	1	1						2							7				
3	1	3					2												
4	3	1	1				1												
5																1			
6																			
PZ-19-m	17	0	0	0	0	0	0	0	0	0	0	0	0	0	40	2	0	0	0
1															5				
2	10					2									26				
3	7					4									8	1			
4															1	1			
5																			
6																			

SAMPLE	K in Pm	Ol	Ne	Le	Hb	Op	Op in Lv lcgl	Bt	Bt in Lv lbrgl	Ca Zeo/Dev	Qzm	Qp	Qz ptf	Ch	Lvl	Lv lbgl	Lv lbrgl	Lv lorgl	Lv lgrgl	Lv lcgl	Lv lalt gl	Lvmi	Lvmi bgl	Lvmi brgl	Lvmi orgl	Lvmi grgl	Lvmi cgl	Lvmi alt gl
PZ-16-m	0	3	0	0	0	0	0	6	0	0	18	3	0	3	0	42	25	0	18	8	0	0	23	27	0	15	0	0
1																												
2		1					4				5					10	6		5	4			5			4		
3		2					2				8	1		1		22	19		9	1			11	20		6		
4											3	2		1		10			4	3			7	7		5		
5											2			1														
6																												
PZ-17-m	0	6	0	0	0	0	9	0	0	0	25	0	0	5	0	14	17	2	2	15	0	0	33	21	5	9	5	0
1																							1					
2	4						2				8			1	1	3	3			2			6	1	1	3	1	
3	2						2				8			3	7	11	1	1	2	7			21	10		5	2	
4							3				6			1	6	3	1			6			4	8	2	1	2	
5							2				3												2	1	2			
6																												
PZ-18-m	0	0	0	2	5	0	1	0	0	0	0	0	0	0	0	18	12	0	17	6	9	0	18	15	5	30	10	29
1																												
2			1													6	8		6	1			8	1		10	2	6
3				2												7	4		7	2	9		7	13		8	4	15
4			1	1			1									5			4	3			2	2	4	9	4	8
5				2																			1			3		
6																												
PZ-19-m	0	0	0	0	1	0	1	0	2	0	1	0	0	0	0	26	30	1	18	3	1	0	22	33	0	17	5	5
1																											2	
2							1		1							5	9		2				4	5		4	1	2
3									1							11	17		10	2	1		8	12		8	2	1
4				1							1					10	4	1	6	1			8	12		4		2
5																							2	4		1		
6																												

*Key to Grain Shape Categories. **1** = very angular; **2** = angular; **3** = sub-angular; **4** = sub-rounded; **5** = rounded; **6** = well rounded; Vc: very coarse sand fraction; C: coarse sand fraction; m: medium sand fraction; f: fine sand fraction; Vf: very fine sand fraction.

BACOLI-POZZUOLI COASTAL STRETCH (continued)

SAMPLE	Lvvblgl	Lvvbrgl	Lvvorgl	Lvvgrgl	Lvvclgl	Lvvalgl	Lvf	PMcl	PMclxx	PMbr	PMbrxx	PMalt	Lp	Lvo	Lsc (xx)	Lsc (micr)	Lss	Bio	Unk	TOT
PZ-16-m	8	22	0	0	14	4	7	20	0	5	0	0	1	1	10	5	0	2	3	400
1								5												10
2	1	5			7		2	13		2					1	1			1	99
3	4	11			4	1	5	2		2			1	1	7	1			1	198
4	3	5			1	1				1					2	3		1	1	83
5		1			2	2												1		10
6																				0
PZ-17-m	5	16	0	0	26	0	39	13	0	12	0	0	0	6	8	4	14	4	4	400
1								1												3
2	1	6			11		9	9		7				2	1		2		3	119
3	4	7			10		18	3		5				3	4	3	7	1	1	185
4		3			5		9							1	3	1	3	3		78
5							3										1			14
6																	1			1
PZ-18-m	24	18	0	12	19	45	20	40	0	6	0	0	0	3	0	0	0	0	1	400
1								12												12
2	6	4			10	10	4	13		4				1						114
3	10	8		6	7	18	9	10		2				2						163
4	3	4		6	2	10	6	5												87
5	2	2				7	1												1	21
6	3																			3
PZ-19-m	4	18	0	0	26	4	17	61	0	10	0	0	0	0	17	5	0	7	0	400
1					9			12		1										29
2	1	3			9		4	31		3					3			2		128
3	3	7			7	4	9	14		6					8	2		2		155
4		8			1		4	4							6	3				78
5																		2		9
6																		1		1

SAMPLE	P	K	Op	Bt	Qzm	Qp	Lvlblgl	Lvlbrgl	Lvlclgl	Lvmiblgl	Lvmibrgl
PZ-20-m	2	5	14	20	3	1	7	9	10	8	10
1			1	6							
2	1	3	5	11	2	1	1	3	9	2	
3	1	2	4	3	1		4	6	1	6	10
4			4				2				
5											
6											

SAMPLE	Lvmiclgl	Lvmialtgl	Lvvblgl	Lvvbrgl	Lvvclgl	Lvvalgl	Lvf	PMcl	PMbr	Lsc (crist)	Bio	TOT
PZ-20-m	7	4	10	12	25	12	5	157	46	4	29	400
1					2			57	10		1	77
2	3		7	7	11	7	1	78	28	1	10	191
3	4	4	3	4	9	2	4	19	8	1	11	107
4				1	3	1		3		2	5	21
5						2					2	4
6												0

*Key to Grain Shape Categories. **1** = very angular; **2** = angular; **3** = sub-angular; **4** = sub-rounded; **5** = rounded; **6** = well rounded; Vc: very coarse sand fraction; C: coarse sand fraction; m: medium sand fraction; f: fine sand fraction; Vf: very fine sand fraction.

NAPOLI-SORRENTO COASTAL STRETCH

SAMPLE	P	P intvl	P intvlblgl	P intvlbrgl	P inPMcl	P in PMbr	P alt	Py	Py in Lvlblgl	Py in Lvlbrgl	Py in PMcl	Py in PMbr	Py alt	Ort	San	Micr	San in Lvlblgl	San in Lvlbrgl	K in Rp	K in Rs	K alt	Ol	Ol inLvlblgl	Ne
Ve-1-m	0	0	3	0	0	0	43	51	0	0		0	0	0	0	0	0	0	0	0	3	12	0	
1							2	2																
2			1				19	15														2		
3			2				18	25												1	5			
4							4	9												2	4			
5																					1			
6																								
Ve-2-m	4	0	7	0	0	0	38	40	0	0		3	0	0	0	0	0	0	0	0	8	15	0	
1							3	5																
2	2		2				12	11				1									1	1		
3	2		4				17	20				2									3	7		
4			1				5	3													3	4		
5							1	1													1	2		
6																						1		
Ve-3-m	11	0	12	0	0	0	30	24	0	0		0	0	1	0	0	0	0	0	0	8	14	0	
1	3		2				4	3																
2	3		3				7	11													2	3		
3	5		4				13	7						1							3	7		
4			3				5	3													3	4		
5							1																	
6																								
NA-6-m	28	0	0	2	0	0	5	53	7	0		0	5	41	5	4		0	1	0	0	5	0	0
1	1						4							4										
2	7					1	12	1					1	10	1	1								
3	13			1		2	19	3					2	14	3	1					2			
4	6			1		2	14	3					2	9	1	2			1		3			
5	1						4							3										
6														1										
TG-2	4	0	9	0	0	0	180	15	6	0		0	0	12	0	0		0	0	0	2	9	2	0
1							8							6										
2	1		1				60	3						5							1	1	1	
3	3		6				54	8	4					5							1	3	1	
4			2				34	4	2					1								3		
5							20															3		
6							4															2		
PO-3-m	20	0	10	0	0	0	37	2	0	0		0	0	8	0	3		0	0	0	0	4	0	0
1	1						1							1										
2	7					1	7							3	1									
3	8		3			3	15	1						3		1						1		
4	4		5			4	13	1						3		1						2		
5			2			1	1							1		1						1		
6																								
PO-1-m	17	0	10	0	0	0	50	21	0	0		2	0	6	0	0		0	0	0	0	4	4	0
1							2																	
2	4		2				13	4						3								1		
3	10		5			1	25	7						2								3		
4	3		3			1	10	9						1									1	
5								1															1	
6																							2	

*Key to Grain Shape Categories. **1** = very angular; **2** = angular; **3** = sub-angular; **4** = sub-rounded; **5** = rounded; **6** = well rounded; Vc: very coarse sand fraction; C: coarse sand fraction; m: medium sand fraction; f: fine sand fraction; Vf: very fine sand fraction.

NAPOLI-SORRENTO COASTAL STRETCH (continued)

SAMPLE	Le	Le in Lvlbgl	Le in Lvlbrgl	Gr	Grbr	Grbr in Lvlbr	Hb	Op	Op in PMcl	Bt	Bt in Lvlbrgl	Bt in PMcl	Mu	Ca	Ca in Ar	Zeo/Dev	Qzm	Q in Ar	Qp	Qzptf	Q in Rm	Q in Rs	Q in Rp	Lvl	Lvlbgl	Lvlbrgl	Lvlgrgl	Lvlcgl
Ve-1-m	42	32		0	0		0	2		0	0		0	0	0	0	0	0	0	0	0	0	0	2				
1	1	1																										
2	5	7																						11				
3	18	18					1																	27				
4	16	5					1																	11				
5	2	1																						1				
6																								1				
Ve-2-m	43	26		0	0		0	8		0	0		0	0	0	0	0	0	0	0	0	0	0	4	53	0	0	0
1	3																							4				
2	4	6					1																	17				
3	14	12					4																	28				
4	20	4					3																	4				
5	4	1																										
6	1																											
Ve-3-m	74	50		0	0		0	0		0	0		0	0	0	0	0	0	0	0	0	0	0	8	53	0	0	0
1	4	4																						8				
2	15	12																						10				
3	20	25																						20				
4	26	8																						9				
5	8	1																						4				
6	1																							2				
NA-6-m	10			1	4		3	2		5	0		0	6	0	0	6	0	1	0	0	0	0	7	22	3	0	1
1							1																					
2	1				1		1			1							2							1	3			
3	2						1			2			1				2							4	9	2		1
4	6			1	3			1		2			4				2	1						2	9	1		
5	1							1					1												1			
6																												
TG-2	28			0	0		8	3		5	0		0	0	0	0	0	0	0	0	0	0	5	46	4	6	0
1																												
2	2						2			1							1							4	1			
3	10						5	1		2														1	22	1	2	
4	14						1	2		2														3	17	2	3	
5	2																							1	3		1	
6																												
PO-3-m	22	2		0	0		2	7		5	0		0	1	0	0	4	0	0	1	0	0	0	3	70	8	0	0
1																										1		
2	1						1										1							8	1			
3	7	1						2		2							2							1	22	3		
4	9	1					1	3		2			1				1			1				2	24	3		
5	4							1		1															14			
6	1							1																	2			
PO-1-m	36	5		0	0		9	6		5	0		4	0	0	0	5	0	0	0	0	0	0	78	5	0	0
1							1																	2				
2							4			1			1				1							10				
3	12	2					3	2		3			3				2							25				
4	16	2					1	3		1							2							21	5			
5	8							1																20				
6																												

*Key to Grain Shape Categories. **1** = very angular; **2** = angular; **3** = sub-angular; **4** = sub-rounded; **5** = rounded; **6** = well rounded; Vc: very coarse sand fraction; C: coarse sand fraction; m: medium sand fraction; f: fine sand fraction; Vf: very fine sand fraction.

NAPOLI-SORRENTO COASTAL STRETCH (continued)

SAMPLE	Lvlaltgl	Lvmi	Lvmiblgl	Lvmibrgl	Lvmialtgl	Lvvblgl	Lvvbrgl	Lvvclgl	Lvvalgl	LV alt	Lvf	PMcl	PMclxx	PMbr/gr	PMbrxx	PMalt	Lm	Lp	Lsc (crist)	Lsc (micr)	Lss	Bio	Tourm	Ru	Unk	TOT
Ve-1-m	0	0	60	0	0	99	0	0	0	0	0	0	0	0	0	0	0	0	0	0	0	0	0	0	0	400
1			2			31																				41
2			3			39																				102
3			20			20																				155
4			29			6																				87
5			5			3																				13
6			1																							2
Ve-2-m	0	0	77	0	0	75	0	0	0	0	0	0	0	0	0	0	0	0	0	0	0	0	0	3	0	400
1			2			20																				37
2			7			35																		2		102
3			30			12																		1		156
4			33			5																				85
5			4			3																				17
6			1																							3
Ve-3-m	0	0	64	0	0	59	0	0	0	0	0	0	0	0	0	0	0	0	0	0	0	0	0	0	0	400
1			4			15																				47
2			8			20																				94
3			15			15																				135
4			20			6																				87
5			10			2																				26
6			7			1																				11
NA-6-m	7	0	21	4	14	10	2	0	11	0	11	1	9	0	0	4	0	22	33	7	8	3	6	400		
1						2			1				1													14
2			2		1	4	1		2		4	1	3						1			2		2		67
3	3		4	1	2	3	1		3		4		4			2		6	7	3	3	1		1		132
4	3		9	3	3	1			2		3		1			2		8	9	3	3			3		129
5	1		4		6				3									4	10	1	2					43
6			2		2													4	6							15
TG-2	8	1	23	0	5	7	0	0	0	0	0	0	0	0	0	0	0	1	1	2	0	7	1	400		
1	1					4																				8
2	1					3																1				87
3	3		2		1																	5				141
4	3	1	6		4													1	1	1		1		1		111
5	1		13																	1						45
6			2																							8
PO-3-m	12	0	62	7	19	19	0	0	8	0	1	0	0	0	0	0	1	5	34	7	5	0	2	400		
1						2																				5
2			1		1	3			1		1															35
3	3		9	2	4	7			2								1									107
4	4		21	3	7	3			4									4	7	3	3			2		142
5	5		22	2	6	2			1									1	16	2	1					85
6			9		1	2													9	1						26
PO-1-m	12	0	46	1	25	11	0	0	10	0	0	0	0	0	0	0	0	10	14	0	2	0	2	400		
1			2		3																					10
2			3		1	4			2																	55
3	8		8		3	4			3									3	2					1		137
4	2		15		6				3									4	4		2			1		116
5	2		13	1	11				2									3	7							70
6			5		4														1							12

*Key to Grain Shape Categories. **1** = very angular; **2** = angular; **3** = sub-angular; **4** = sub-rounded; **5** = rounded; **6** = well rounded; Vc: very coarse sand fraction; C: coarse sand fraction; m: medium sand fraction; f: fine sand fraction; Vf: very fine sand fraction.

NAPOLI-SORRENTO COASTAL STRETCH (continued)

SAMPLE	P	P intvl	P intvlblgl	P intvlbrgl	P inPMcl	P in PMbr	P alt	Py	Py in Lvlblgl	Py in Lvlbrgl	Py in PMcl	Py in PMbr	Py alt	Ort	San	Micr	San in Lvlblgl	San in Lvlbrgl	K in Rp	K in Rs	K alt	Ol	Ol inLvlblgl	Ne
TA-1-m	25	0	16	0	0	0	5	13	2	0	0	0	0	2	13	0	0	0	0	4	4	0	0	0
1	1						1							2										
2	5						7							8						1				
3	14		5			2	4	1						3						2	1			
4	3		9			3	1	1												1	2			
5	2		2																		1			
6																								
TA-2-m	20	0	19	0	0	0	61	6	0	0	0	5	0	4	0	0	0	0	0	0	0	0	0	0
1																								
2	4		3				15							2										
3	13		6				28	1				2		1										
4	3		10				13	4				3		1										
5							5	1																
6																								
CO-1-m	17	0	3	1	0	2	15	0	0	0	0	0	0	30	0	9	0	0	0	15	0	0	0	0
1	1													2										
2	5						3							8		2				2				
3	9		1			1	10							13		5				8				
4	2		1			1	2							7		2				4				
5				1																1				
6																								
MC-1-m	35	0	9	4	0	7	39	4	0	0		2	0	33	0	5	4	0	0	6	0	0	0	0
1	1					4								2										
2	11					2	13	2						10										
3	15		3	3		2	15	2				1		13		3		1		3				
4	6		4	1		2	7					1		8		2		3		3				
5	2		2			1																		
6																								
GA-1-m	30	12	9	10	0	5	36	5	10	10		5	0	37	0	6	5	2	0	6	0	0	0	0
1	1					3			1					2										
2	9	4	1	2		1	12		3			1		14		1								
3	14	6	3	6		3	16	4	5			3		16		3	3		2					
4	6	2	4	2		1	5	1	2			1		5		1	1	1						
5			1													1	1	1						
6																								
NA-3-m	33	0	7	10	6	3	5	19	1	2	6	0	0	29	0	3	6	0	0	8	0	0	0	0
1							1				1			3										
2	11		1	1	3	1	2	5		1	3			9			3			1				
3	19		3	5	3	2	3	9	1		2			13		2				3				
4	3		3	3			3			1				4		1				4				
5			1				1																	
6																								

*Key to Grain Shape Categories. **1** = very angular; **2** = angular; **3** = sub-angular; **4** = sub-rounded; **5** = rounded; **6** = well rounded; Vc: very coarse sand fraction; C: coarse sand fraction; m: medium sand fraction; f: fine sand fraction; Vf: very fine sand fraction.

NAPOLI-SORRENTO COASTAL STRETCH (continued)

SAMPLE	Le	Le in Lvlblgl	Le in Lvlbrgl	Gr	Grbr	Grbr in Lvlbr	Hb	Op	Op in PMcl	Bt	Bt in Lvlbrgl	Bt in PMcl	Mu	Ca	Ca in Ar	Zeo/Dev	Qzm	Q in Ar	Qp	Qzptf	Q in Rm	Q in Rs	Q in Rp	Lvl	Lvlblgl	Lvlbrgl	Lvlgrgl	Lvlclgl
TA-1-m	31	5		0	0		0	16		10	0		0	0	0	0	3	0	0	0	0	0	0	56	5	0	0	
1										1																		
2										2																		
3	9	2						4		5							2							20	3			
4	14	3						6		2							1							25	1			
5	8							6																9				
6																								2				
TA-2-m	52	14		0	0		3	5		8	0		0	0	0	0	0	0	0	0	0	0	0	64	0	0	0	
1																								2				
2	5						1			1														4				
3	21	10					2	2		5														20				
4	15	4						3		2														25				
5	7																							10				
6	4																							3				
CO-1-m	1			0	0		4	0		5	0		0	0	0	0	0	0	1	0	0	0	0	5	15	3	0	0
1										1																		
2							2			2														3				
3							2			1													4	8	2			
4	1									1								1					1	4	1			
5																												
6																												
MC-1-m	2			5	25		3	0		3	0		0	0	0	0	1	0	0	0	0	0	0	25	9	0	0	
1																												
2				2	5		1			1															2			
3				3	7		1			2														9	3			
4	1				6		1										1							11	4			
5	1				4																			5				
6					3																							
GA-1-m	1			0	0		0	12	6	2	0	6	0	0	0	1	0	0	0	0	0	0	7	27	10	0	0	
1							1			1		3												4	5			
2							3	3	3	1		3											3	15	4			
3							3	5															2	7	1			
4	1						5	3								1							1	1				
5							2																1					
6							1																					
NA-3-m	0			0	6		0	0		7	0		0	0	0	0	0	0	0	0	0	0	0	33	37	0	0	
1																								1				
2				3						4														12	13			
3				2						3														14	15			
4				1																				6	9			
5																												
6																												

*Key to Grain Shape Categories. **1** = very angular; **2** = angular; **3** = sub-angular; **4** = sub-rounded; **5** = rounded; **6** = well rounded; Vc: very coarse sand fraction; C: coarse sand fraction; m: medium sand fraction; f: fine sand fraction; Vf: very fine sand fraction.

NAPOLI-SORRENTO COASTAL STRETCH (continued)

SAMPLE	Lvlaltgl	Lvmi	Lvmiblgl	Lvmibrgl	Lvmialtgl	Lvvblgl	Lvvbrgl	Lvvclgl	Lvvalgl	LV alt	Lvf	PMcl	PMclxx	PMbr/gr	PMbrxx	PMalt	Lm	Lp	Lsc (crist)	Lsc (micr)	Lss	Bio	Tourm	Ru	Unk	TOT
TA-1-m	13	0	58	3	27	29	0	0	11	0	0	0	0	0	0	0	0	2	10	28	3	0	4	1	3	400
1						2																				7
2			2			8			2														2		1	39
3	2		14	1	2	9			2								1						2		1	111
4	5		18	1	10	8			7								1								1	143
5	6		21	1	15	2												1	7	11	2			1		93
6			3																3	15	1					7
TA-2-m	16	0	58	0	22	24	6	0	12	0	0	0	0	0	0	0	0	0	0	2	0	0	1	0	0	400
1						1	1																			4
2		1				9	3		1																	49
3	3		5		2	3	2		4													1				131
4	10		22		7	3			7																	132
5	3		25		13	4																				68
6			5			4																				16
CO-1-m	0	0	0	0	0	13	14	0	0	114	0	21	20	20	14	32	0	0	4	9	6	5	0		2	400
1						4	3			3																14
2						5	9			28		7	7	12	4	10					1					110
3						3	2			43		12	10	8	7	13			2	1	2	2			2	171
4						1				26		2	3		3	9			2	3	2	2				81
5										11										2	2					17
6										3										3						7
MC-1-m	0	0	14	7	0	9	8	0	0	46	0	0	0	4	9	3	2	0	24	14	0	36	1	2	400
1						1	2																			10
2						3	4			1				2	5	2						5		1	72	
3		2	2			4	2			9				2	4	1	2		3	1		5	1	1	125	
4		5	2			1				17									8	3		13			110	
5		7	3							18									11	6		9			69	
6										1									2	4		4			14	
GA-1-m	0	0	9	5	0	6	12	0	0	38	0	10	5	11	0	12	0	0	11	8	0	7	0	6	400
1							3																			10
2		1	1			3	7			5		4	2	7		2								1	102	
3		2	2			2	2			22		4	3	3		8			4			2		3	180	
4		4	2			1				10		2		1		2			6	3		1		2	89	
5		2								1									1	4		1			16	
6																				1					3	
NA-3-m	0	0	21	15	0	7	16	0	0	67	0	18	0	3	0	9	0	0	9	5	0	9	0	0	400
1						1	5			2		2													16	
2		1				3	7			11		8		2		3						1			109	
3		4				3	4			23		5		1		2			2	1		3			156	
4		14								21		3				4			3	3		4			94	
5		3								9									3	1		1			23	
6										1									1						2	

*Key to Grain Shape Categories. **1** = very angular; **2** = angular; **3** = sub-angular; **4** = sub-rounded; **5** = rounded; **6** = well rounded; Vc: very coarse sand fraction; C: coarse sand fraction; m: medium sand fraction; f: fine sand fraction; Vf: very fine sand fraction.

NAPOLI-SORRENTO COASTAL STRETCH (continued)

SAMPLE	P	P inLvl	P inLvlblgl	P inLvlbrgl	P inPMcl	P in PMbr	P alt	Py	Py in Lvlblgl	Py in Lvlbrgl	Py in PMcl	Py in PMbr	Py alt	Ort	San	Micr	San in Lvlblgl	San in Lvlbrgl	K in Rp	K in Rs	K alt	Ol	Ol inLvlblgl	Ne
CA-2B-m	7	0	0	0	0	0	10	156	2	3	0	0	0	6	0	0	0	0	0	0	9	0	0	0
1																								
2	1						50			2				1								1		
3	4						45	2		1				3								3		
4	2						29							2								4		
5							19															1		
6							3																	
NA-2-m	28	0	10	4	0	0	27	0	6	0		0	0	28	0	2	4	0	0	6	1	0	0	
1																								
2	14			2			11		4					6										
3	12		4			6	13		2					12			2				2			
4	2		2	2		2	3							10		2	2				4			
5			4			2															1			
6																								
NA-1-m	23	0	7	2	0	0	9	0	0	0		0	0	17	0	0	0	0	0	8	0	0	0	
1														1										
2	11						1							4						1				
3	9		2	2			4							9						3				
4	3		3			3	4							3						3				
5			2																	1				
6																								
PO-2-m	6	0	11	0	0	0	202	11	1	0		0	0	4	0	0	0	0	0	0	6	0	0	
1							1																	
2	1	2					35							3										
3	4	4					61	7						1							1			
4	1	5					75	4													2			
5							26			1											2			
6							4														1			
SO-3-m	40	0	2	0	0	10	100	5	1	0		6	0	42	0	0	0	0	0	11	7	0	0	
1														1										
2	10						11					2		11						2				
3	15					4	33	1		1				16						4	1			
4	13			2		5	34	3				4		12						5	4			
5	2					1	15	1						2							2			
6							7																	
SO-1-m	12	0	0	0	0	14	134	0	0	0		17	10	7	0	0	0	0	0	0	2	0	0	
1							1																	
2	2						25						2											
3	6					5	40					6	7	3							1			
4	4					7	46					10	3	2							1			
5						2	22					1												
6																								

*Key to Grain Shape Categories. **1** = very angular; **2** = angular; **3** = sub-angular; **4** = sub-rounded; **5** = rounded; **6** = well rounded; Vc: very coarse sand fraction; C: coarse sand fraction; m: medium sand fraction; f: fine sand fraction; Vf: very fine sand fraction.

NAPOLI-SORRENTO COASTAL STRETCH (continued)

SAMPLE	Le	Le in Lvlbgl	Le in Lvlbrgl	Gr	Grbr	Grbr in Lvlbr	Hb	Op	Op in PMcl	Bt	Bt in Lvlbrgl	Bt in PMcl	Mu	Ca	Ca in Ar	Zeo/Dev	Qzm	Q in Ar	Qp	Qzptf	Q in Rm	Q in Rs	Q in Rp	Lvl	Lvlbgl	Lvlbrgl	Lvlgrgl	Lvlclgl
CA-2B-m	3			0	3		7	12		0	0		0	10	6	0	0	0	0	0	0	0	0	18	0	0	0
1																												
2						3																						
3	1					3	2						4	2										3				
4	2				2	1	4						5	4										9				
5				1	2		3						1											5				
6					1		3																	1				
NA-2-m	4			5	3		0	0		2	1	1	3	0	0	0	0	1	0	0	0	0	0	22	7	0	2
1																												
2									2				1	1											2		
3	1			2	1						1			1				1						6	1		
4	3			3	1							1		1										10	4		2
5				1																				6			
6																											
NA-1-m	4			0	3		0	0		6	0		0	0	0	0	1	0	0	0	0	0	2	37	2	0	5
1									1																		
2					1				3														2	5			2
3	2				2				2								1							13	1		3
4	1																							15	1		
5	1																							2			
6																								2			
PO-2-m	5			0	5		9	7		0	0		0	0	0	0	0	0	0	0	0	0	5	64	3	0	0
1																											
2						1																	1	1			
3	1				2	5	2																2	21	1		
4	3	1			3	3	4																2	27	2		
5	1						1																	11			
6																								4			
SO-3-m	3			0	1		5	22		2	0		0	2	0	0	3	0	5	0	1	1	0	0	45	2	0	0
1																											
2							1	1									1							5			
3							2	4					1											14			
4	2				1		2	8		1			1				2		3		1		1	20		2	
5								7		1									1					5			
6	1							2																1			
SO-1-m	16			1	1		3	3		0	0		0	3	5	0	37	0	10	3	4	4	5	0	20	2	0	0
1																	5										
2																											
3	4					1							1	3			12		4	2	3	3	2	4	1		
4	8				1		2	1					2	2			15		5	1	1	1	3	11			
5	3							2									4		1					4	1		
6	1																1							1			

*Key to Grain Shape Categories. **1** = very angular; **2** = angular; **3** = sub-angular; **4** = sub-rounded; **5** = rounded; **6** = well rounded; Vc: very coarse sand fraction; C: coarse sand fraction; m: medium sand fraction; f: fine sand fraction; Vf: very fine sand fraction.

NAPOLI-SORRENTO COASTAL STRETCH (continued)

SAMPLE	Lvlaltgl	Lvmi	Lvmiblgl	Lvmibrgl	Lvmialtgl	Lvvblgl	Lvvbrgl	Lvvclgl	Lvvalgl	LV alt	Lvf	PMcl	PMclxx	PMbr/gr	PMbrxx	PMalt	Lm	Lp	Lsc (crist)	Lsc (micr)	Lss	Bio	Tourm	Ru	Unk	TOT
CA-2B-m	3	0	12	0	4	0	0	0	0	0	0	0	0	0	0	0	0	65	58	11	0	2	3	400		
1																									10	
2																		10	2	1		1			72	
3			1															23	6	5		1		2	111	
4	2		3		2													22	10	4			1	108		
5	1		5		2													9	20	1				68		
6			3															1	20					31		
NA-2-m	8	0	34	10	12	18	16	10	0	29	0	35	17	18	0	1	0	5	8	0	1	0	0	400		
1						4	2					2												8		
2						12	12	6		2		12	4	6										97		
3	2		2			2	2	4		10		15	6	8		1			1					120		
4	4		16	4	5					10		8	5	4				3	1	1		1		115		
5	2		12	6	7					7								2	4					54		
6			4																2					6		
NA-1-m	0	0	47	4	0	38	4	6	0	68	0	21	22	17	7	10	0	0	7	5	0	8	0	5	400	
1						1	2	2				2	1	2		1								1	14	
2			1			10	2	3		1		8	8	8	5	2						3		2	83	
3			8			12		1		15		7	9	4	2	3			2	1		3		1	122	
4			17	3		9				23		4	4	3		4			3	1		2		1	111	
5			15	1		4				21									2	2					51	
6			6			2				8										1					19	
PO-2-m	0	0	31	2	0	7	3	1	0	2	0	0	0	0	0	0	0	5	8	0	0	2	0	400		
1																								1		
2						5	2	1																52		
3			4			1	1					1											1	120		
4			16	2		1				1								3	2			1		158		
5			11															2	3					58		
6																			3					12		
SO-3-m	0	0	23	0	0	25	0	0	0	9	0	0	0	0	0	5	0	7	13	0	0	0	2	400		
1						1																		2		
2						11																		52		
3			3			8				2						2		1					1	117		
4			7			4				6						3		4	2				1	153		
5			9			1				1								2	8					58		
6			4																3					18		
SO-1-m	0	0	9	0	0	5	0	0	0	0	0	0	0	0	0	18	7	20	23	0	5	0	0	400		
1						3										1								4		
2						2										8	5	1			1			37		
3																9	2	10	6		2			123		
4			3															7	13		1			158		
5			4															2	4		1			66		
6			2																					12		

*Key to Grain Shape Categories. **1** = very angular; **2** = angular; **3** = sub-angular; **4** = sub-rounded; **5** = rounded; **6** = well rounded; Vc: very coarse sand fraction; C: coarse sand fraction; m: medium sand fraction; f: fine sand fraction; Vf: very fine sand fraction.

NAPOLI-SORRENTO COASTAL STRETCH (continued)

SAMPLE	P	P intvl	P intvlblgl	P intvlbrgl	P inPMcl	P in PMbr	P alt	Py	Py in Lvlblgl	Py in Lvlbrgl	Py in PMcl	Py in PMbr	Py alt	Ort San	Micr San in Lvlblgl	San in Lvlbrgl	K in Rp	K in Rs	K alt	Ol	Ol inLvlblgl	Ne
SO-5-m	18	0	13	0	0	0	95	11	4	0	4	0	4	21	0	1	0	0	0	4	4	0
1	1						4															
2	6		1				26	1	1		3			6								
3	7		8				31	3	2				3	11					1	1	1	
4	3		4				27	6	1		1		1	4		1			3	2	2	
5	1						7	1												1		
6																						
CA-3-m	42	0	10	0	0	0	15	12	4	0	0	0	0	25	0	0	0	0	0	0	0	0
1																						
2	10					2	5							8								
3	15		3			5	7	2						13								
4	12		5			5		2						4								
5	5		2			3																
6																						
SO-2-m	26	0	7	6	0	12	34	10	7	0		0	7	22	0	0	0	0	0	1	0	
1				2		2																
2	10			2			5		1					5								
3	11		2	2		5	11	5	3				4	10							1	
4	5		5	2		7	15	4	3				3	5								
5						1	1							2								
6																						
CA-2-m	22	0	3	0	0	0	82	0	0	0		0	0	11	0	0	0	0	0	0	0	0
1							2															
2	5						22							2								
3	12		1				32							5								
4	5		2				19							4								
5							7															
6																						
SO-4-m	16	0	3	2	0	0	30	0	0	0		0	0	33	0	0	0	0	0	0	0	0
1							9							7								
2	3																					
3	7		1	1			12							14								
4	5		2	1			8							10								
5	1						1							2								
6																						
TG-3-m	21	0	9	0	0	0	38	7	0	0		0	0	16	0	4	0	0	0	6	0	0
1																						
2	2						16	2						3								
3	12		5				13	3						7		2				1		
4	4		4				7	2						4		2				3		
5	3						2							2						2		
6																						

*Key to Grain Shape Categories. **1** = very angular; **2** = angular; **3** = sub-angular; **4** = sub-rounded; **5** = rounded; **6** = well rounded; Vc: very coarse sand fraction; C: coarse sand fraction; m: medium sand fraction; f: fine sand fraction; Vf: very fine sand fraction.

NAPOLI-SORRENTO COASTAL STRETCH (continued)

SAMPLE	Le	Le in Lvlbgl	Le in Lvlbrgl	Gr	Grbr	Grbr in Lvlbr	Hb	Op	Op in PMcl	Bt	Bt in Lvlbrgl	Bt in PMcl	Mu	Ca	Ca in Ar	Zeo/Dev	Qzm	Q in Ar	Qp	Qzptf	Q in Rm	Q in Rs	Q in Rp	Lvl	Lvlbgl	Lvlbrgl	Lvlgrgl	Lvlclgl
SO-5-m	22	6		0	2		1	0		0	0		0	5	0	0	6	0	1	0	0	0	0	5	46	7	1	0
1																								1				
2				1		1											1							2				
3	5	1		1									3				4						1	18	3	1		
4	11	4											2				1		1				3	20	3			
5	6	1																					1	5	1			
6																												
CA-3-m	24			0	0		3	12		13	0		0	5	0	0	0	0	0	0	0	0	0	51	21	0	0	
1														1										1				
2							2		5				1											10	2			
3	6						1	1	3				3											18	10			
4	14							6	2				1											14	7			
5	4							5	3															6	2			
6																								2				
SO-2-m	29	5	4	0	1		5	18	4	0		0	0	0	0	1	2	6	3	0	0	0	7	0	33	27	0	3
1																												
2	2		1				3		1															4	4	4		
3	8	2	2				2	4	2								1	3	1			3		10	13			2
4	13	2	1		1			8	1							1	1	3	2			4		15	9			1
5	5	1						6																3	1			
6	1																							1				
CA-2-m	0		0	3		0	11	0	0	0		0	8	13	2	27	0	0	0	0	0	0	0	34	4	0	0	
1																												
2							1									1								5				
3				1			5						3	5		10								11	1			
4				1			4						5	7	1	13								14	2			
5				1			1							1	1	3								4	1			
6																												
SO-4-m	21		0	4		0	0	0	0	0		0	1	0	0	3	0	4	0	0	0	0	0	50	16	0	0	
1																												
2	3															1								4	3			
3	6			3												1								12	9			
4	10			1									1			1		2						22	3			
5	2															1		2						11	1			
6																								1				
TG-3-m	33	8		0	0	1	7	17	9	0		0	0	0	0	0	0	0	0	0	0	0	5	58	24	0	0	
1																								2				
2	2						3		3															7	6			
3	13	4				1	2	3	4														2	16	2			
4	8	4					2	7	2														3	18	10			
5	6							6																12	4			
6	4							1																3	2			

*Key to Grain Shape Categories. **1** = very angular; **2** = angular; **3** = sub-angular; **4** = sub-rounded; **5** = rounded; **6** = well rounded; Vc: very coarse sand fraction; C: coarse sand fraction; m: medium sand fraction; f: fine sand fraction; Vf: very fine sand fraction.

NAPOLI-SORRENTO COASTAL STRETCH (continued)

SAMPLE	Lvlaltgl	Lvmi	Lvmiblgl	Lvmibrgl	Lvmialtgl	Lvvblgl	Lvvbrgl	Lvvclgl	Lvvalgl	LV alt	Lvf	PMcl	PMclxx	PMbr/gr	PMbrxx	PMalt	Lm	Lp	Lsc (crist)	Lsc (micr)	Lss	Bio	Tourm	Ru	Unk	TOT
SO-5-m	0	0	30	2	0	19	2	0	0	5	0	4	0	0	0	0	0	0	23	32	0	0	2	0	0	400
1						2																			8	
2						12	1					2													64	
3		3				5	1			1		1							8	3		1			127	
4		10	1							3		1							13	9		1			136	
5		16	1							1									1	15					58	
6		1																	1	5					7	
CA-3-m	0	0	50	24	0	15	6	0	0	14	0	9	0	0	0	0	0	0	12	33	0	0	0	0	400	
1																									1	
2		3				10	3					2													63	
3		8	4			5	3			4		5							3	8					127	
4		13	12							7		2							7	12					125	
5		20	8							3									2	8					71	
6		6																		5					13	
SO-2-m	0	0	17	9	0	11	5	0	0	20	0	0	0	0	0	0	7	11	17	5	13	1	0	4	400	
1																	1	1			1				2	
2						5	3										3	5	4					1	49	
3		1	2			3	2			4							3	3	8	1	2			1	134	
4		7	5			2				11							3	3	8	1	7			3	161	
5		9	2			1				5								2	4	3	3				49	
6																			1	1	1				5	
CA-2-m	0	0	7	1	0	2	2	0	0	0	0	0	0	0	0	0	0	0	99	64	0	5	0	0	400	
1																									2	
2						1	2												5			2			46	
3						1													27	7		3			124	
4		3	1																33	30					144	
5		4																	26	20					69	
6																			8	7					15	
SO-4-m	0	0	36	17	0	21	16	0	0	0	0	1	0	0	0	0	0	0	45	73	0	6	0	2	400	
1				4	3	4	3																		7	
2				7	8	7	5					1							12	9		4		1	113	
3		5	3																16	31	2			1	144	
4		17	8			3													13	22					76	
5		14	6																4	11					16	
6																										
TG-3-m	0	0	54	28	0	20	10	0	0	3	1	0	0	0	0	0	0	0	7	6	0	8	0	0	400	
1				1		5	2																		9	
2				1		9	3															2			59	
3		12		2		4	4			1									1			3			117	
4		14		11		2	1			2	1								4	1		3			119	
5		16		12															1	4					70	
6		12		2															1	1					26	

*Key to Grain Shape Categories. **1** = very angular; **2** = angular; **3** = sub-angular; **4** = sub-rounded; **5** = rounded; **6** = well rounded; Vc: very coarse sand fraction; C: coarse sand fraction; m: medium sand fraction; f: fine sand fraction; Vf: very fine sand fraction.

NAPOLI-SORRENTO COASTAL STRETCH (continued)

SAMPLE	P	P inLvl	P inLvlblgl	P inLvlbrgl	P inPMcl	P in PMbr	P alt	Py	Py in Lvlblgl	Py in Lvlbrgl	Py in PMcl	Py in PMbr	Py alt	Ort	San Micr	San in Lvlblgl	San in Lvlbrgl	K in Rp	K in Rs	K alt	Ol	Ol inLvlblgl	Ne
CA-1-m	4	0	0	0	0	0	0	98	0	0	0	12	0	5	0	0	0	0	0	1	0	0	0
1								6															
2	1							23						2									
3	2							35				6		3									
4	1							25				5								1			
5								9				1											
6																							
TG-1-m	27	0	6	0	0	0	3	106	6	0	0	4	0	16	0	0	0	0	0	4	2	0	0
1								7															
2	6							27	3					7						1			
3	13		2				1	32	2			2		6						2			
4	7		3				2	28	1			2		3						1	1		
5	1		1					11													1		
6								1															
NA-4-m	38	0	3	4	3	0	5	16	3	0	6	0	0	22	0	0	0	0	2	0	0	0	0
1																							
2	9			2							3			7					1				
3	17		2	1	1		2	7	2		2			9									
4	9		1	1	2		2	6	1		1			6					1				
5	3																						
6																							
NA-5-m	42	0	8	0	5	0	0	96	0	2	0	0	0	22	0	0	0	0	0	0	2	0	0
1	1																						
2	13		1					24						11									
3	20		2		3			38		1				9									
4	8		4		2			25		1				2							1		
5			1					9													1		
6																							
NA-7-m	35	0	9	3	1	0	5	17	6	2	0	0	0	25	0	0	0	0	0	0	0	0	0
1																							
2	9		2				6							8									
3	18		3		1	3	8	1		1				13									
4	7		4	2		2	3	3		1				4									
5	1			1				1															
6								1															

*Key to Grain Shape Categories. **1** = very angular; **2** = angular; **3** = sub-angular; **4** = sub-rounded; **5** = rounded; **6** = well rounded; Vc: very coarse sand fraction; C: coarse sand fraction; m: medium sand fraction; f: fine sand fraction; Vf: very fine sand fraction.

NAPOLI-SORRENTO COASTAL STRETCH (continued)

SAMPLE	Le	Le in Lvlbgl	Le in Lvlbrgl	Gr	Grbr	Grbr in Lvlbr	Hb	Op	Op in PMcl	Bt	Bt in Lvlbrgl	Bt in PMcl	Mu	Ca	Ca in Ar	Zeo/Dev	Qzm	Q in Ar	Qp	Qzptf	Q in Rm	Q in Rs	Q in Rp	Lvl	Lvlbgl	Lvlbrgl	Lvlgrgl	Lvlclgl
CA-1-m	5		0	5			7	10		0	0		0	13	14	0	0	0	0	0	0	0	0	21	0	0	0
1														1														
2							4	1						5	5									2				
3	2			1			2	2						7	8									11				
4	3			3			1	3							1									7				
5				1				4																1				
6																												
TG-1-m	22	2																										
1																												
2	2						1	1		1														8	3			
3	6	1					2	3		1														19	7	2		
4	7	1		1			1	4																24	3	1		
5	7							3																9	3			
6																								1				
NA-4-m	0		0	8			0	3		7	0		0	0	0	0	0	2	0	0	0	0	0	26	12	0	0	
1																												
2				1						2														3	4			
3				3				1		3		1												11	4			
4				4				2		2		2						2						9	3			
5																								3	1			
6																												
NA-5-m	3		0	7		1	25	2	2	0			0	0	0	0	0	0	0	0	0	0	0	34	12	0	0	
1									1																			
2																								3				
3	1			3		1	8	1	1															16	6			
4	2			4			14	1																12	4			
5							3																	3	2			
6																												
NA-7-m	0		0	2		0	3		9	0			0	0	0	0	0	0	0	0	0	0	0	40	5	0	0	
1									4																			
2									2															6				
3				1			1		2															14	3			
4				1			2		3															17	2			
5																								3				
6																												

*Key to Grain Shape Categories. **1** = very angular; **2** = angular; **3** = sub-angular; **4** = sub-rounded; **5** = rounded; **6** = well rounded; Vc: very coarse sand fraction; C: coarse sand fraction; m: medium sand fraction; f: fine sand fraction; Vf: very fine sand fraction.

NAPOLI-SORRENTO COASTAL STRETCH (continued)

SAMPLE	Lvlaltgl	Lvmi	Lvmiblgl	Lvmibrgl	Lvmialtgl	Lvvblgl	Lvvbrgl	Lvvclgl	Lvvalgl	LV alt	Lvf	PMcl	PMclxx	PMbr/gr	PMbrxx	PMalt	Lm	Lp	Lsc (crist)	Lsc (micr)	Lss	Bio	Tourm	Ru	Unk	TOT
CA-1-m	0	0	0	0	0	0	0	0	0	1	0	0	0	0	0	0	0	0	71	123	0	10	0	0	0	400
1																			7	6	1					6
2																			26	28	4					48
3																			26	54	5					132
4																			9	26						149
5										1									3	9						53
6																										12
TG-1-m	0	0	52	14	0	22	8	0	0	8	0	0	0	0	0	0	0	0	0	0	0	0	0	0	0	400
1						1																				8
2		2				12	3			1																78
3		16	3			9	4			3																136
4		18	7				1			3																119
5		12	4							1																53
6		4																								6
NA-4-m	0	0	24	8	0	13	19	0	0	20	1	34	20	21	5	14	0	0	17	13	17	7	0	7	7	400
1						3	3							1												7
2						8	12			2		8	6	7		1										79
3		6	1			2	4			5		16	9	8	3	5			4	3	3	2		4	3	142
4		8	2							9	1	8	4	4	2	7			11	6	11	3		3	3	133
5		10	5							4		2	1	1		1			2	3	1	2				39
6																				1	2					3
NA-5-m	0	0	19	9	0	7	10	0	0	6	0	18	11	11	0	0	0	0	16	15	3	10	0	2	2	400
1																									1	1
2					6	6						4	6	2								3			1	80
3		1	1		1	3				2		7	3	4					5	2	1	2			1	142
4		6	3			1				3		7	2	4					8	4	1	4		2	2	125
5		9	5							1				1					3	7	1	1				47
6		3																		2						5
NA-7-m	0	0	30	20	0	16	16	0	0	14	0	45	9	13	14	0	0	0	28	24	0	9	0	0	0	400
1					2	4						4														10
2					12	9				1		16	2	1	6				2			3				87
3		2	1		2	3				4		19	3	4	6				12	4		3				132
4		9	7							7		6	4	8	2				10	9		3				116
5		15	5							2									4	7						39
6		4	7																	4						16

*Key to Grain Shape Categories. **1** = very angular; **2** = angular; **3** = sub-angular; **4** = sub-rounded; **5** = rounded; **6** = well rounded; Vc: very coarse sand fraction; C: coarse sand fraction; m: medium sand fraction; f: fine sand fraction; Vf: very fine sand fraction.

APPENDIX B (recalculated petrographic parameters)

Sample	Qt (%)	F (%)	L (%)
STR-1-Vc	0	2	98
STR-1-C	0	2	98
STR-1-m	0	5	95
STR-1-f	0	16	84
STR-1-Vf	0	32	68
STR-2-m	0	2	98
STR-3-m	0	6	94
STR-4-m	0	6	94
STR-5-m	0	6	94
STR-7-m	0	6	94
STR-8-m	0	5	95
STR-9-Vc	0	0	100
STR-9-C	0	1	99
STR-9-m	0	6	94
STR-9-f	0	10	90
STR-9-Vf	0	10	90
PN-1-Vc	0	9	91
PN-1-C	0	19	81
PN-1-m	0	27	73
PN-1-f	0	19	81
PN-1-Vf	0	22	78
PN-2-m	3	8	88
PN-3-m	2	9	90
PN-4-m	1	3	96
PN-5-m	1	19	81
PN-6-m	4	8	88
PN-7-m	3	11	86
PN-8-m	5	13	82
PN-9-m	5	18	77
PN-10-m	2	7	91
PN-11-m	3	14	83
V1-m	0	14	85
V1-f	0	36	64
V2-m	0	11	89
V2-f	0	34	66
V4-m	0	16	84
V4-f	0	21	79
V5-m	0	11	89
V5-f	0	14	86
V6-m	0	13	87
V6-f	0	11	89
V7-m	3	14	83
V7-f	1	16	83
V8-m	0	8	92
V8-f	0	20	80
V9-m	0	13	87
V9-f	0	16	84
V10-m	0	15	85
V10-f	0	15	85
V11-m	0	18	82
V11-f	0	18	82
V12-m	0	24	76
V12-f	0	15	85
L1-m	0	6	94
L1-f	0	27	73
L2-m	0	6	94
L2-f	0	22	78

Sample	Qt (%)	F (%)	L (%)
L4-m	0	11	89
L4-f	0	17	83
L5-m	1	4	95
L5-f	1	13	86
L6-m	0	3	97
L6-f	1	8	91
L7-m	0	3	97
L7-f	0	4	95
L8-m	0	2	98
L8-f	1	11	89
L9-m	0	16	84
L9-f	0	30	70
L10-m	0	25	75
L10-f	2	30	68
L11-m	1	24	74
L11-f	3	36	61
L12-m	1	12	87
L12-f	3	14	83
L13-m	2	2	97
L13-f	0	3	97
SA-1-Vc	0	1	99
SA-1-C	2	5	93
SA-1-m	1	14	85
SA-1-f	7	13	79
SA-1-Vf	6	16	79
SA-2-m	0	15	85
SA-3-m	1	13	86
SA-4-m	0	10	90
SA-5-m	1	7	92
SA-6-m	0	8	92
SA-7-m	0	8	92
SA-8-m	1	15	84
SA-9-m	0	14	86
SA-10-m	0	13	87
SA-11-m	0	14	86
SA-12-m	0	19	81
SA-13-m	1	13	86
SA-14-m	0	16	84
SA-15-m	0	12	88
Fi-1-m	0	5	95
Fi-2-m	0	11	89
Fi-3-Vc	0	2	98
Fi-3-C	0	5	95
Fi-3-m	0	10	90
Fi-3-f	0	9	91
Fi-3-Vf	0	5	95
Fi-4-m	0	10	90
AL-1-m	2	14	84
AL-2-m	0	15	85
AL-3-Vc	0	6	94
AL-3-C	0	5	95
AL-3-m	0	15	85
AL-3-f	0	16	84
AL-3-Vf	0	19	81
AL-4-C	0	3	97
AL-5-m	0	9	91
AL-6-m	0	6	94
AL-7-m	0	8	92

Sample	Qt (%)	F (%)	L (%)
PZ-1-m	4	23	73
PZ-2-m	0	4	96
PZ-3-m	1	25	74
PZ-4-m	0	24	76
PZ-5-m	0	27	73
PZ-6-m	2	17	81
PZ-7-m	1	33	66
PZ-8-Vc	0	4	96
PZ-8-C	1	17	82
PZ-8-m	3	34	64
PZ-8-f	0	36	64
PZ-8-Vf	2	19	79
PZ-9-m	0	1	99
PZ-10-m	0	12	88
PZ-11-m	1	29	70
PZ-12-m	5	44	51
PZ-13-m	2	12	86
PZ-14-Vc	3	12	85
PZ-14-C	1	17	82
PZ-14-m	2	5	93
PZ-14-f	24	17	59
PZ-14-Vf	38	19	43
PZ-15-m	3	26	71
PZ-16-m	6	26	68
PZ-17-m	7	19	74
PZ-18-m	0	6	94
PZ-19-m	0	16	84
PZ-20-m	1	2	97
BC-1-Vc	0	20	79
BC-1-C	1	24	74
BC-1-m	5	15	80
BC-1-f	35	18	47
BC-1-Vf	21	14	65
BC-2-m	5	31	64
BC-3-m	9	18	73
BC-4-m	21	22	57
BC-5-m	17	19	64
Li-1-m	26	24	50
Li-2-m	21	18	60
Li-3-m	23	14	63
Li-4-m	31	23	47
Li-5-m	22	22	56
Li-6-m	22	36	42
Vo-1-m	42	13	45
Vo-2-m	38	33	29
Vo-3-m	32	22	46
Vo-4-m	29	29	41
Vo-5-m	34	24	43
Vo-6-m	51	12	36
Vo-7-m	36	20	44
Vo-8-m	34	17	50
Vo-9-m	40	19	41
Vo-10-m	29	23	47
Vo-11-m	20	26	54
NA-1-m	0	15	85
NA-2-m	0	20	79
NA-3-m	0	21	79
NA-4-m	1	18	81

Sample	Qt (%)	F (%)	L (%)
NA-5-m	0	25	75
NA-6-m	2	29	69
NA-7-m	0	18	82
CO-1-m	0	17	82
GA-1-m	0	24	76
MC-1-m	0	29	71
PO-1-m	2	8	90
PO-2-m	0	6	94
PO-3-m	1	12	87
Ve-1-m	0	0	100
Ve-2-m	0	1	99
Ve-3-m	0	4	96
TG-1-m	0	20	80
TG-2-m	0	11	89
TG-3-m	0	13	87
TA-1-m	1	15	84
TA-2-m	0	9	91
CA-1-m	0	4	96
CA-2-m	9	11	79
CA-2B-m	0	7	93
CA-3-m	0	25	75
SO-1-m	23	25	52
SO-2-m	2	24	74
SO-3-m	3	42	55
SO-4-m	2	15	83
SO-5-m	3	16	81

Table A-B -1- **Qt**: total quartz; **F**: feldspars; **L**: lithic fragments; Vc: very coarse sand fraction; C: coarse sand fraction; m: medium sand fraction; f: fine sand fraction; Vf: very fine sand fraction.

Sample	Lm (%)	Ls (%)	Lv (%)	Sample	Lm (%)	Ls (%)	Lv (%)	Sample	Lm (%)	Ls (%)	Lv (%)
PZ-1-m	0	27	73	V8-m	0	7	93	SA-1-C	0	1	99
PZ-2-m	0	7	93	V8-f	0	5	95	SA-1-m	0	0	100
PZ-3-m	0	36	64	V9-m	0	0	100	SA-1-f	0	3	97
PZ-4-m	0	32	68	V9-f	0	0	100	SA-1-Vf	0	0	100
PZ-5-m	0	13	87	V10-m	0	1	99	SA-2-m	2	3	94
PZ-6-m	0	2	98	V10-f	0	0	100	SA-3-m	0	0	100
PZ-7-m	0	6	94	V11-m	0	0	100	SA-4-m	0	0	100
PZ-8-Vc	0	2	98	V11-f	0	0	100	SA-5-m	0	0	100
PZ-8-C	0	3	97	V12-m	0	0	100	SA-6-m	1	0	99
PZ-8-m	0	4	96	V12-f	0	0	100	SA-7-m	0	0	100
PZ-8-f	0	2	98	L1-m	0	1	99	SA-8-m	0	0	100
PZ-8-Vf	0	0	100	L1-f	0	6	94	SA-9-m	0	0	100
PZ-9-m	0	0	100	L2-m	0	2	98	SA-10-m	0	0	100
PZ-10-m	0	0	100	L2-f	0	0	100	SA-11-m	0	0	100
PZ-11-m	0	2	98	L4-m	0	0	99	SA-12-m	1	2	97
PZ-12-m	0	11	89	L4-f	0	1	99	SA-13-m	0	0	100
PZ-13-m	0	1	99	L5-m	0	1	98	SA-14-m	0	5	95
PZ-14-Vc	0	7	93	L5-f	0	0	100	SA-15-m	1	2	97
PZ-14-C	0	2	98	L6-m	0	2	98	Fi-1-m	0	0	100
PZ-14-m	0	2	98	L6-f	0	1	99	Fi-2-m	2	0	98
PZ-14-f	0	27	73	L7-m	0	0	100	Fi-3-Vc	0	0	100
PZ-14-Vf	0	61	39	L7-f	0	0	100	Fi-3-C	0	0	100
PZ-15-m	0	5	95	L8-m	0	1	99	Fi-3-m	0	0	100
PZ-16-m	0	7	93	L8-f	0	3	97	Fi-3-f	0	0	100
PZ-17-m	0	11	89	L9-m	0	0	100	Fi-3-Vf	0	0	100
PZ-18-m	0	0	100	L9-f	0	0	100	Fi-4-m	0	0	100
PZ-19-m	0	9	91	L10-m	0	0	100	AL-1-m	0	1	99
PZ-20-m	0	3	97	L10-f	0	0	100	AL-2-m	0	0	100
BC-1-Vc	0	2	98	L11-m	0	1	99	AL-3-Vc	1	0	99
BC-1-C	0	12	88	L11-f	1	0	99	AL-3-C	0	0	100
BC-1-m	2	13	86	L12-m	1	1	99	AL-3-m	0	0	100
BC-1-f	0	58	42	L12-f	0	1	98	AL-3-f	0	0	100
BC-1-Vf	5	56	39	L13-m	2	2	96	AL-3-Vf	0	0	100
BC-2-m	0	11	89	L13-f	1	26	73	AL-4-C	0	0	100
BC-3-m	0	35	65	PN-1-Vc	0	1	99	AL-5-m	0	0	100
BC-4-m	2	51	47	PN-1-C	0	0	100	AL-6-m	0	0	100
BC-5-m	0	59	41	PN-1-m	0	0	100	AL-7-m	0	0	100
Li-1-m	0	49	51	PN-1-f	0	0	100	NA-1-m	0	15	85
Li-2-m	0	65	35	PN-1-Vf	0	0	100	NA-2-m	0	20	79
Li-3-m	0	68	32	PN-2-m	0	0	100	NA-3-m	0	21	79
Li-4-m	0	65	35	PN-3-m	0	0	100	NA-4-m	1	18	81
Li-5-m	0	79	21	PN-4-m	2	0	98	NA-5-m	0	25	75
Li-6-m	0	77	23	PN-5-m	1	0	98	NA-6-m	2	29	69
Vo-1-m	10	63	27	PN-6-m	1	0	99	NA-7-m	0	18	82
Vo-2-m	0	69	31	PN-7-m	0	1	99	CO-1-m	0	17	82
Vo-3-m	5	62	33	PN-8-m	0	0	100	GA-1-m	0	24	76
Vo-4-m	9	48	43	PN-9-m	0	0	100	MC-1-m	0	29	71
Vo-5-m	13	68	19	PN-10-m	0	2	98	PO-1-m	2	8	90
Vo-6-m	0	78	22	PN-11-m	0	0	100	PO-2-m	0	6	94
Vo-7-m	13	51	36	STR-1-Vc	0	0	100	PO-3-m	1	12	87
Vo-8-m	14	66	19	STR-1-C	0	0	100	Ve-1-m	0	0	100
Vo-9-m	5	72	23	STR-1-m	0	1	99	Ve-2-m	0	1	99
Vo-10-m	3	61	36	STR-1-f	0	0	100	Ve-3-m	0	4	96
Vo-11-m	0	73	27	STR-1-Vf	0	0	100	TG-1-m	0	20	80
V1-m	0	0	100	STR-2-m	0	0	100	TG-2-m	0	11	89
V1-f	0	0	100	STR-3-m	0	0	100	TG-3-m	0	13	87
V2-m	0	0	100	STR-4-m	0	0	100	TA-1-m	1	15	84
V2-f	0	0	100	STR-5-m	0	0	100	TA-2-m	0	9	91
V4-m	0	3	97	STR-7-m	0	0	100	CA-1-m	0	4	96
V4-f	0	7	93	STR-8-m	0	0	100	CA-2-m	9	11	79
V5-m	0	1	99	STR-9-Vc	0	0	100	CA-2B-m	0	7	93
V5-f	0	2	98	STR-9-C	0	0	100	CA-3-m	0	25	75
V6-m	0	1	99	STR-9-m	0	0	100	SO-1-m	23	25	52
V6-f	0	0	100	STR-9-f	0	0	100	SO-2-m	2	24	74
V7-m	0	4	96	STR-9-Vf	0	0	100	SO-3-m	3	42	55
V7-f	0	1	98	SA-1-Vc	0	0	100	SO-4-m	2	15	83
								SO-5-m	3	16	81

Table A-B -2- **Lm**: metamorphic lithics; **Ls**: sedimentary lithichs; **Lv**: volcanic lithics. Vc: very coarse sand fraction; C: coarse sand fraction; m: medium sand fraction; f: fine sand fraction; Vf: very fine sand fraction.

Sample	Lvl (%)	Lvmi (%)	Lvv (%)
PZ-1-m	42	33	24
PZ-2-m	41	17	41
PZ-3-m	32	29	40
PZ-4-m	30	22	48
PZ-5-m	36	36	29
PZ-6-m	25	44	31
PZ-7-m	36	11	52
PZ-8-m	28	35	37
PZ-9-m	9	29	62
PZ-10-m	29	26	45
PZ-11-m	24	44	32
PZ-12-m	53	26	21
PZ-13-m	37	38	24
PZ-14-m	43	28	30
PZ-15-m	47	31	22
PZ-16-m	45	32	23
PZ-17-m	32	41	27
PZ-18-m	23	36	40
PZ-19-m	38	38	24
PZ-20-m	23	25	52
BC-1-m	63	25	12
BC-2-m	64	36	0
BC-3-m	58	28	15
BC-4-m	60	30	10
BC-5-m	49	26	25
Li-1-m	64	15	21
Li-2-m	59	20	20
Li-3-m	46	27	27
Li-4-m	58	16	26
Li-5-m	50	32	18
Li-6-m	58	21	21
Vo-1-m	58	16	26
Vo-2-m	100	0	0
Vo-3-m	82	13	5
Vo-4-m	87	13	0
Vo-5-m	100	0	0
Vo-6-m	80	10	10
Vo-7-m	69	20	10
Vo-8-m	54	46	0
Vo-9-m	64	28	8
Vo-10-m	80	20	0
Vo-11-m	72	26	2
NA-1-m	36	33	31
NA-2-m	40	34	27
NA-3-m	63	23	15
NA-4-m	43	29	29
NA-5-m	55	28	17
NA-6-m	46	34	20
NA-7-m	44	34	22
CO-1-m	57	0	43
GA-1-m	76	11	14
MC-1-m	61	21	17
PO-1-m	59	32	9
PO-2-m	68	24	8
PO-3-m	49	39	12
Ve-1-m	49	19	32
Ve-2-m	48	26	26
Ve-3-m	55	23	21
TG-1-m	49	35	16
TG-2-m	74	21	5
TG-3-m	51	36	13
TA-1-m	43	39	18
TA-2-m	49	33	17
CA-1-m	100	0	0

Sample	Lvl (%)	Lvmi (%)	Lvv (%)
CA-2-m	77	15	8
CA-2B-m	62	38	0
CA-3-m	48	41	12
SO-1-m	61	25	14
SO-2-m	71	18	11
SO-3-m	53	22	24
SO-4-m	44	33	23
SO-5-m	65	21	14
SA-1-m	57	27	16
SA-2-m	58	26	16
SA-3-m	63	26	11
SA-4-m	57	28	14
SA-5-m	50	27	22
SA-6-m	65	19	16
SA-7-m	73	13	14
SA-8-m	70	20	10
SA-9-m	65	21	15
SA-10-m	55	30	15
SA-11-m	56	32	12
SA-12-m	62	33	5
SA-13-m	63	34	3
SA-14-m	69	21	10
SA-15-m	53	37	10
Fi-1-m	59	30	11
Fi-2-m	58	33	9
Fi-3-m	60	26	13
Fi-4-m	64	27	9
AL-1-m	58	28	14
AL-2-m	79	16	5
AL-3-m	53	25	23
AL-4-C	66	20	14
AL-5-m	71	14	15
AL-6-m	67	24	10
AL-7-m	68	19	13
PN-1-m	36	32	33
PN-2-m	52	48	1
PN-3-m	50	49	1
PN-4-m	50	36	14
PN-5-m	28	31	41
PN-6-m	36	19	45
PN-7-m	66	26	8
PN-8-m	60	33	7
PN-9-m	53	39	8
PN-10-m	55	34	12
PN-11-m	48	39	13
STR-1-m	56	24	20
STR-2-m	80	12	8
STR-3-m	78	20	2
STR-4-m	73	19	7
STR-5-m	66	22	12
STR-7-m	68	25	7
STR-8-m	77	16	7
STR-9-m	67	19	14
L1-m	70	22	8
L2-m	67	27	7
L4-m	52	38	11
L5-m	38	21	41
L6-m	38	23	39
L7-m	78	12	10
L8-m	49	19	32
L9-m	55	27	18
L10-m	64	30	6
L11-m	42	21	37
L12-m	27	28	45

Sample	Lvl (%)	Lvmi (%)	Lvv (%)
L13-m	18	29	53
V1-m	75	20	6
V2-m	80	18	3
V4-m	59	38	3
V5-m	63	36	1
V6-m	65	33	3
V7-m	71	27	2
V8-m	64	32	3
V9-m	76	22	2
V10-m	83	16	0
V11-m	55	42	3
V12-m	67	28	5

Sample	Lvl (%)	Lvmi (%)	Lvv (%)
SA-1-Vc	78	12	9
SA-1-C	66	24	10
SA-1-m	57	27	16
SA-1-f	17	50	33
SA-1-Vf	0	23	77
Fi-3-Vc	86	8	7
Fi-3-C	82	13	6
Fi-3-m	60	26	13
Fi-3-f	36	53	10
Fi-3-Vf	16	57	27
AL-3-Vc	80	8	11
AL-3-C	70	16	14
AL-3-m	53	25	23
AL-3-f	38	45	18
AL-3-Vf	16	51	34
PN-1-Vc	91	7	2
PN-1-C	80	17	3
PN-1-m	36	32	33
PN-1-f	20	45	35
PN-1-Vf	5	44	51
STR-1-Vc	96	1	3
STR-1-C	86	8	6
STR-1-m	56	24	20
STR-1-f	38	37	25
STR-1-Vf	13	49	38
STR-9-Vc	84	7	8
STR-9-C	85	8	7
STR-9-m	67	19	14
STR-9-f	45	33	22
STR-9-Vf	14	27	59

Sample	Lvl (%)	Lvmi (%)	Lvv (%)
PZ-8-Vc	90	5	5
PZ-8-C	62	25	13
PZ-8-m	28	35	37
PZ-8-f	25	34	41
PZ-8-Vf	5	16	79
PZ-14-Vc	77	6	17
PZ-14-C	57	25	17
PZ-14-m	43	28	30
PZ-14-f	18	56	25
PZ-14-Vf	16	34	50
BC-1-Vc	0	2	98
BC-1-C	0	12	88
BC-1-m	63	25	12
BC-1-f	0	58	42
BC-1-Vf	5	56	39

Table A-B -3- **Lvl**: lathwork texture; **Lvmi**: microlitic texture; **Lvv**: vitric texture. Vc: very coarse sand fraction; C: coarse sand fraction; m: medium sand fraction; f: fine sand fraction; Vf: very fine sand fraction.

Sample	Lvf (%)	Lvmi (%)	Lvl (%)
PN-1-Vc	2	7	91
PN-1-C	6	16	78
PN-1-m	12	41	47
PN-1-f	12	61	27
PN-1-Vf	11	79	9
PN-2-m	0	48	52
PN-3-m	0	50	50
PN-4-m	5	40	54
PN-5-m	2	52	46
PN-6-m	6	32	62
PN-7-m	18	23	59
PN-8-m	7	33	60
PN-9-m	2	41	56
PN-10-m	3	37	60
PN-11-m	2	44	55
STR-1-Vc	0	1	99
STR-1-C	0	8	92
STR-1-m	1	31	69
STR-1-f	0	49	51
STR-1-Vf	1	78	21
STR-2-m	0	13	87
STR-3-m	0	20	80
STR-4-m	0	21	79
STR-5-m	0	25	75
STR-7-m	0	27	73
STR-8-m	0	18	82
STR-9-Vc	0	5	95
STR-9-C	0	8	92
STR-9-m	0	22	78
STR-9-f	0	42	58
STR-9-Vf	0	66	34
SA-1-Vc	0	14	86
SA-1-C	1	26	73
SA-1-m	0	33	67
SA-1-f	0	75	25
SA-1-Vf	0	100	0
SA-2-m	0	31	69
SA-3-m	0	29	71
SA-4-m	0	33	67
SA-5-m	0	35	65
SA-6-m	0	22	78
SA-7-m	0	15	85
SA-8-m	0	23	77
SA-9-m	0	24	76
SA-10-m	0	36	64
SA-11-m	0	36	64
SA-12-m	0	35	65
SA-13-m	0	35	65
SA-14-m	0	23	77
SA-15-m	0	36	64
Fi-1-m	0	34	66
Fi-2-m	0	27	73
Fi-3-Vc	0	8	92
Fi-3-C	0	13	87
AL-2-m	0	17	83
AL-3-Vc	0	9	91
AL-3-C	0	18	82
AL-3-f	0	54	46
AL-3-Vf	0	77	23
AL-4-C	0	23	77
AL-5-m	0	16	84
AL-6-m	0	26	74
AL-7-m	0	22	78
V1-m	0	21	79
V1-f	1	46	53
V2-m	0	18	82
V2-f	0	50	50
V4-m	8	36	57
V4-f	2	60	38
V5-m	1	34	65
V5-f	0	51	49
V6-m	2	34	63
V6-f	1	56	43
V7-m	2	28	70
V7-f	0	55	45
V8-m	1	34	65
V8-f	0	58	42
V9-m	0	22	78
V9-f	0	60	40
V10-m	0	16	84
V10-f	0	55	45
V11-m	0	43	57
V11-f	0	60	40
V12-m	0	29	71
V12-f	0	36	64
L1-m	2	13	86
L1-f	0	58	42
L2-m	13	20	68
L2-f	9	51	40
L4-m	2	44	54
L4-f	0	60	40
L5-m	27	31	42
L5-f	12	56	31
L6-m	51	18	31
L6-f	42	25	32
L7-m	9	7	85
L7-f	31	33	35
L8-m	16	26	58
L8-f	19	54	27
L9-m	9	28	63
L9-f	4	55	42
L10-m	14	21	65
L10-f	13	43	44
L11-m	15	26	59
L11-f	13	39	48
L12-m	9	39	52
L12-f	10	42	48
L13-m	11	48	42
L13-f	0	94	6
Fi-3-m	0	30	70
Fi-3-f	0	47	53
Fi-3-Vf	0	78	22
Fi-4-m	0	29	71
AL-1-m	0	32	67
AL-3-m	0	32	68
PZ-1-m	23	34	43
PZ-2-m	0	29	71
PZ-3-m	22	37	41
PZ-4-m	39	25	35
PZ-5-m	32	34	34
PZ-6-m	11	56	33
PZ-7-m	19	19	61
PZ-8-Vc	27	4	69
PZ-8-C	26	21	53
PZ-8-m	18	45	37
PZ-8-f	21	45	34
PZ-8-Vf	18	64	18
PZ-9-m	13	67	21
PZ-10-m	5	45	50
PZ-11-m	7	60	33
PZ-12-m	5	32	63
PZ-13-m	7	47	46
PZ-14-Vc	12	6	81
PZ-14-C	6	29	65
PZ-14-m	14	34	52
PZ-14-f	19	61	20
PZ-14-Vf	15	58	27
PZ-15-m	11	35	54
PZ-16-m	4	39	56
PZ-17-m	23	43	34
PZ-18-m	10	55	35
PZ-19-m	9	46	45
PZ-20-m	8	48	43
BC-1-Vc	13	7	80
BC-1-C	18	14	68
BC-1-m	7	22	72
BC-1-f	0	52	48
BC-1-Vf	17	77	7
BC-2-m	11	32	57
BC-3-m	8	27	65
BC-4-m	15	25	60
BC-5-m	10	31	59
Li-1-m	0	19	81
Li-2-m	0	26	74
Li-3-m	0	37	63
Li-4-m	13	19	69
Li-5-m	0	39	61
Li-6-m	0	26	74
Vo-1-m	0	21	79
Vo-2-m	0	0	100
Vo-3-m	0	14	86
Vo-4-m	0	13	87
Vo-5-m	6	0	94
Vo-6-m	0	11	89
Vo-7-m	0	23	77
Vo-8-m	14	39	46
Vo-9-m	17	23	60
Vo-10-m	0	20	80
Vo-11-m	0	26	74
NA-1-m	0	53	47
NA-2-m	0	59	41
NA-3-m	0	34	66
NA-4-m	1	45	54
NA-5-m	0	38	62
NA-6-m	0	49	51
NA-7-m	0	53	47
CO-1-m	0	0	100
GA-1-m	0	24	76
MC-1-m	0	38	62
PO-1-m	0	43	57
PO-2-m	0	31	69
PO-3-m	0	49	51
Ve-1-m	0	53	47
Ve-2-m	0	59	41
Ve-3-m	0	55	45
TG-1-m	0	45	55
TG-2-m	0	30	70
TG-3-m	1	48	51
TA-1-m	0	54	46
TA-2-m	0	50	50
CA-1-m	0	0	100
CA-2-m	0	17	83
CA-2B-m	0	43	57
CA-3-m	0	51	49
SO-1-m	0	29	71
SO-2-m	0	29	71
SO-3-m	0	33	67
SO-4-m	0	45	55
SO-5-m	0	35	65

Table A-B -4 - **Lvf:** felsitic texture; **Lvmi**: microlitic texture; **Lvl**: lathwork texture. Vc: very coarse sand fraction; C: coarse sand fraction; m: medium sand fraction; f: fine sand fraction; Vf: very fine sand fraction.

Sample	Pm	Lvl	Lvmi
PZ-1-m	12	49	39
PZ-2-m	0	71	29
PZ-3-m	30	37	33
PZ-4-m	39	36	26
PZ-5-m	11	44	44
PZ-6-m	33	25	42
PZ-7-m	9	69	22
PZ-8-Vc	8	87	5
PZ-8-C	30	50	20
PZ-8-m	13	39	48
PZ-8-f	11	38	50
PZ-8-Vf	33	15	52
PZ-9-m	60	9	30
PZ-10-m	57	23	20
PZ-11-m	32	24	44
PZ-12-m	15	57	28
PZ-13-m	33	33	34
PZ-14-Vc	1	92	7
PZ-14-C	27	51	22
PZ-14-m	40	36	24
PZ-14-f	9	22	69
PZ-14-Vf	0	32	68
PZ-15-m	17	50	33
PZ-16-m	14	51	36
PZ-17-m	16	37	47
PZ-18-m	21	31	48
PZ-19-m	30	35	35
PZ-20-m	79	10	11
BC-1-Vc	1	91	8
BC-1-C	16	69	15
BC-1-m	9	70	21
BC-1-f	2	47	51
BC-1-Vf	4	8	88
BC-2-m	0	64	36
BC-3-m	6	67	27
BC-4-m	0	71	29
BC-5-m	0	65	35
Li-1-m	0	81	19
Li-2-m	0	74	26
Li-3-m	0	63	37
Li-4-m	0	79	21
Li-5-m	0	61	39
Li-6-m	0	74	26
Vo-1-m	0	79	21
Vo-2-m	25	75	0
Vo-3-m	0	86	14
Vo-4-m	0	87	13
Vo-5-m	0	100	0
Vo-6-m	0	89	11
Vo-7-m	2	76	22
Vo-8-m	0	54	46
Vo-9-m	7	67	26
Vo-10-m	0	80	20
Vo-11-m	0	74	26

Sample	Pm	Lvl	Lvmi
NA-1-m	42	30	28
NA-2-m	37	34	29
NA-3-m	25	55	20
NA-4-m	56	26	17
NA-5-m	36	43	21
NA-6-m	19	47	35
NA-7-m	42	33	25
CO-1-m	75	25	0
GA-1-m	34	58	8
MC-1-m	16	62	22
PO-1-m	0	65	35
PO-2-m	0	74	26
PO-3-m	1	55	44
Ve-1-m	0	72	28
Ve-2-m	0	65	35
Ve-3-m	0	71	29
TG-1-m	0	59	41
TG-2-m	0	78	22
TG-3-m	0	59	41
TA-1-m	0	52	48
TA-2-m	0	60	40
CA-1-m	0	100	0
CA-2-m	0	84	16
CA-2B-m	0	62	38
CA-3-m	5	51	44
SO-1-m	0	71	29
SO-2-m	0	80	20
SO-3-m	0	71	29
SO-4-m	1	57	42
SO-5-m	6	71	23

Sample	Lvvclgl	Lvvblgl	Lvvbrgl
PZ-1-m	11	52	37
PZ-2-m	0	93	7
PZ-3-m	24	44	32
PZ-4-m	37	33	31
PZ-5-m	45	24	32
PZ-6-m	13	62	25
PZ-7-m	13	78	9
PZ-8-Vc	50	0	50
PZ-8-C	58	29	13
PZ-8-m	12	48	40
PZ-8-f	15	69	16
PZ-8-Vf	26	68	6
PZ-9-m	8	73	19
PZ-10-m	14	54	32
PZ-11-m	31	40	29
PZ-12-m	55	15	30
PZ-13-m	31	38	31
PZ-14-Vc	0	47	53
PZ-14-C	41	33	26
PZ-14-m	53	23	24
PZ-14-f	41	28	31
PZ-14-Vf	19	69	13
PZ-15-m	16	37	47
PZ-16-m	32	18	50
PZ-17-m	55	11	34
PZ-18-m	31	39	30
PZ-19-m	54	8	38
PZ-20-m	53	21	26
BC-1-Vc	44	11	44
BC-1-C	25	38	38
BC-1-m	61	0	39
BC-1-f	83	8	8
BC-1-Vf	100	0	0
BC-2-m	0	0	0
BC-3-m	100	0	0
BC-4-m	50	50	0
BC-5-m	100	0	0
Li-1-m	100	0	0
Li-2-m	100	0	0
Li-3-m	0	0	0
Li-4-m	0	0	0
Li-5-m	0	0	0
Li-6-m	100	0	0
Vo-1-m	100	0	0
Vo-2-m	0	0	0
Vo-3-m	0	0	0
Vo-4-m	0	0	0
Vo-5-m	0	0	0
Vo-6-m	0	0	0
Vo-7-m	0	100	0
Vo-8-m	0	0	0
Vo-9-m	0	100	0
Vo-10-m	0	0	0
Vo-11-m	0	0	100

Sample	Lvvclgl	Lvvblgl	Lvvbrgl
PO-1-m	0	100	0
PO-2-m	9	64	27
PO-3-m	0	100	0
Ve-1-m	0	100	0
Ve-2-m	0	100	0
Ve-3-m	0	100	0
TG-1-m	0	73	27
TG-2-m	0	100	0
TG-3-m	0	67	33
TA-1-m	0	100	0
TA-2-m	0	80	20
CA-1-m	0	0	0
CA-2-m	0	50	50
CA-2B-m	0	0	0
CA-3-m	0	71	29
SO-1-m	0	100	0
SO-2-m	0	69	31
SO-3-m	0	100	0
SO-4-m	0	57	43
SO-5-m	0	90	10
NA-1-m	13	79	8
NA-2-m	23	41	36
NA-3-m	0	30	70
NA-4-m	0	41	59
NA-5-m	0	41	59
NA-6-m	0	83	17
NA-7-m	0	50	50
CO-1-m	0	48	52
GA-1-m	0	33	67
MC-1-m	0	53	47

Table A-B -5 - **Pm**: pumice grains; **Lvl**: lathwork texture; **Lvmi**: microlitic texture. **Lvvbrgl**: brown vitric texture; **Lvvblgl**: black vitric texture; **Lvvclgl**: colorless vitric texture. Vc: very coarse sand fraction; C: coarse sand fraction; m: medium sand fraction; f: fine sand fraction; Vf: very fine sand fraction. (Values are expressed as %).

Samples	Lvvbrgl (%)	Lvvblgl (%)	Lvvclgl (%)
V1-m	9	91	0
V1-f	33	67	0
V2-m	0	100	0
V2-f	4	96	0
V4-m	0	100	0
V4-f	24	71	6
V5-m	23	77	0
V5-f	9	82	9
V6-m	47	53	0
V6-f	8	92	0
V7-m	47	53	0
V7-f	22	78	0
V8-m	20	10	70
V8-f	17	83	0
V9-m	33	67	0
V9-f	12	88	0
V10-m	0	100	0
V10-f	0	100	0
V11-m	13	88	0
V11-f	0	0	0
V12-m	0	100	0
V12-f	0	100	0
L1-m	0	50	50
L1-f	0	80	20
L2-m	8	0	92
L2-f	0	79	21
L4-m	0	0	100
L4-f	0	4	96
L5-m	2	0	98
L5-f	0	17	83
L6-m	24	3	73
L6-f	2	16	82
L7-m	0	8	92
L7-f	2	4	95
L8-m	2	2	96
L8-f	1	3	96
L9-m	0	6	94
L9-f	0	4	96
L10-m	0	38	62
L10-f	8	46	46
L11-m	4	18	78
L11-f	4	43	54
L12-m	1	8	91
L12-f	8	15	78
L13-m	1	9	90
L13-f	13	64	23
STR-1-Vc	0	100	0
STR-1-C	0	100	0
STR-1-m	0	97	3
STR-1-f	2	98	0
STR-1-Vf	9	89	2
STR-2-m	0	91	9
STR-3-m	0	100	0
AL-3-Vf	39	61	0
AL-4-C	45	55	0
AL-5-m	31	69	0
AL-6-m	32	68	0
AL-7-m	39	61	0

Samples	Lvvbrgl (%)	Lvvblgl (%)	Lvvclgl (%)
STR-4-m	13	87	0
STR-5-m	8	92	0
STR-7-m	4	96	0
STR-8-m	10	90	0
STR-9-Vc	81	19	0
STR-9-C	28	72	0
STR-9-m	29	71	0
STR-9-f	27	73	0
STR-9-Vf	34	64	1
PN-1-Vc	40	40	20
PN-1-C	56	22	22
PN-1-m	25	63	13
PN-1-f	0	100	0
PN-1-Vf	11	51	38
PN-2-m	0	0	100
PN-3-m	0	0	100
PN-4-m	36	0	64
PN-5-m	0	93	7
PN-6-m	20	26	54
PN-7-m	0	100	0
PN-8-m	21	16	63
PN-9-m	5	60	35
PN-10-m	0	40	60
PN-11-m	9	83	9
SA-1-Vc	38	63	0
SA-1-C	27	73	0
SA-1-m	31	69	0
SA-1-f	24	71	4
SA-1-Vf	37	52	11
SA-2-m	39	55	5
SA-3-m	36	64	0
SA-4-m	49	51	0
SA-5-m	46	54	0
SA-6-m	45	55	0
SA-7-m	49	51	0
SA-8-m	52	48	0
SA-9-m	61	34	5
SA-10-m	59	41	0
SA-11-m	19	68	13
SA-12-m	31	69	0
SA-13-m	22	78	0
SA-14-m	26	74	0
SA-15-m	45	41	14
Fi-1-m	53	47	0
Fi-2-m	50	50	0
Fi-3-Vc	100	0	0
Fi-3-C	41	59	0
Fi-3-m	38	62	0
Fi-3-f	54	46	0
Fi-3-Vf	41	59	0
Fi-4-m	28	72	0
AL-1-m	38	62	0
AL-2-m	44	56	0
AL-3-Vc	45	55	0
AL-3-C	42	58	0
AL-3-m	44	56	0
AL-3-f	48	52	0

Sample	BAS & AND	ALT	RIO & DAC
PN-1-Vc	92	6	2
PN-1-C	84	6	9
PN-1-m	63	18	20
PN-1-f	60	25	15
PN-1-Vf	42	23	34
PN-2-m	23	0	77
PN-3-m	23	20	58
PN-4-m	23	40	37
PN-5-m	21	68	10
PN-6-m	24	44	31
PN-7-m	35	5	60
PN-8-m	62	1	37
PN-9-m	69	4	28
PN-10-m	52	2	46
PN-11-m	31	5	64
STR-1-Vc	96	3	1
STR-1-C	98	0	2
STR-1-m	95	0	5
STR-1-f	96	0	4
STR-1-Vf	97	1	2
STR-2-m	96	0	4
STR-3-m	90	1	9
STR-4-m	89	0	11
STR-5-m	93	1	6
STR-7-m	89	1	10
STR-8-m	93	0	7
STR-9-Vc	95	5	0
STR-9-C	97	3	0
STR-9-m	96	4	0
STR-9-f	97	3	0
STR-9-Vf	92	7	1
SA-1-Vc	64	1	36
SA-1-C	67	17	16
SA-1-m	74	12	14
SA-1-f	86	6	8
SA-1-Vf	66	28	5
SA-2-m	73	15	13
SA-3-m	77	5	17
SA-4-m	82	10	8
SA-5-m	62	15	23
SA-6-m	84	9	7
SA-7-m	94	3	3
SA-8-m	87	3	10
SA-9-m	75	7	18
SA-10-m	78	8	14
SA-11-m	85	4	11
SA-12-m	81	11	8
SA-13-m	93	2	5
SA-14-m	89	3	8
SA-15-m	69	1	30
Fi-1-m	82	0	18
Fi-2-m	93	5	2
Fi-3-Vc	97	3	0
Fi-3-C	93	2	5
Fi-3-m	97	0	3
Fi-3-f	100	0	0
Fi-3-Vf	100	0	0
Fi-4-m	86	0	14

Sample	BAS & AND	ALT	RIO & DAC
AL-1-m	81	11	8
AL-2-m	97	2	1
AL-3-Vc	88	12	0
AL-3-C	90	10	0
AL-3-m	97	3	0
AL-3-f	96	4	0
AL-3-Vf	92	8	0
AL-4-C	100	0	0
AL-5-m	89	11	0
AL-6-m	92	3	5
AL-7-m	92	4	4
V1-m	81	15	4
V1-f	78	18	4
V2-m	78	10	12
V2-f	82	12	5
V4-m	62	10	27
V4-f	61	13	27
V5-m	77	9	14
V5-f	78	6	15
V6-m	71	14	15
V6-f	77	6	17
V7-m	74	5	20
V7-f	74	16	11
V8-m	74	10	16
V8-f	74	15	11
V9-m	95	3	2
V9-f	95	2	3
V10-m	86	1	13
V10-f	90	3	7
V11-m	87	6	7
V11-f	84	5	11
V12-m	75	12	14
V12-f	75	14	11
L1-m	81	7	12
L1-f	84	4	12
L2-m	77	3	20
L2-f	75	4	21
L4-m	49	3	48
L4-f	61	4	36
L5-m	56	4	40
L5-f	72	2	26
L6-m	58	6	35
L6-f	61	5	34
L7-m	73	8	20
L7-f	39	2	58
L8-m	47	3	50
L8-f	47	1	52
L9-m	71	5	24
L9-f	67	6	28
L10-m	82	3	15
L10-f	76	14	11
L11-m	56	15	29
L11-f	58	21	20
L12-m	28	9	62
L12-f	45	12	43
L13-m	22	16	62
L13-f	85	9	6

Table A-B -6 - **Lvvbrgl**: brown vitric texture; **Lvvblgl**: black vitric texture; **Lvvclgl**: colorless vitric texture. BAS & AND: basaltic and andesitic provenance; ALT: altered volcanic grains; RIO & Dac: rhyolitic and dacitic provenance. Vc: very coarse sand fraction; C: coarse sand fraction; m: medium sand fraction; f: fine sand fraction; Vf: very fine sand fraction. (Values are expressed as %).

Sample	BasProv	AndProv	DacProv
PN-1-Vc	19	80	2
PN-1-C	9	90	1
PN-1-m	59	41	0
PN-1-f	58	42	0
PN-1-Vf	44	56	0
PN-2-m	5	23	72
PN-3-m	11	22	67
PN-4-m	15	30	55
PN-5-m	26	46	28
PN-6-m	7	41	53
PN-7-m	13	17	70
PN-8-m	17	57	26
PN-9-m	18	59	23
PN-10-m	13	44	43
PN-11-m	17	10	73
STR-1-Vc	89	11	1
STR-1-C	92	7	2
STR-1-m	85	10	5
STR-1-f	83	12	4
STR-1-Vf	73	24	2
STR-2-m	81	15	4
STR-3-m	79	12	9
STR-4-m	70	19	11
STR-5-m	77	16	7
STR-7-m	69	21	10
STR-8-m	65	28	8
STR-9-Vc	35	65	0
STR-9-C	61	39	0
STR-9-m	67	33	0
STR-9-f	65	35	0
STR-9-Vf	56	44	0
SA-1-Vc	33	30	37
SA-1-C	46	34	20
SA-1-m	51	39	11
SA-1-f	64	28	8
SA-1-Vf	72	28	0
SA-2-m	39	46	16
SA-3-m	47	35	18
SA-4-m	59	31	10
SA-5-m	41	32	28
SA-6-m	47	46	7
SA-7-m	52	46	2
SA-8-m	51	38	11
SA-9-m	44	35	22
SA-10-m	49	34	17
SA-11-m	54	38	8
SA-12-m	54	37	9
SA-13-m	61	36	3
SA-14-m	47	45	8
SA-15-m	33	48	19
Fi-1-m	41	46	13
Fi-2-m	27	73	0
Fi-3-Vc	40	60	0
Fi-3-C	51	44	5
Fi-3-m	54	45	1
Fi-3-f	53	47	0
Fi-3-Vf	54	46	0
Fi-4-m	45	42	13
AL-1-m	53	37	10
AL-2-m	48	52	0
AL-3-Vc	57	43	0
AL-3-C	60	40	0
AL-3-m	55	45	0
AL-3-f	57	43	0
AL-3-Vf	58	42	0
AL-4-C	56	44	0
AL-5-m	63	37	0
AL-6-m	52	43	6
AL-7-m	55	40	5
V1-m	71	24	5
V1-f	53	41	6
V2-m	76	12	13
V2-f	77	16	7

Sample	BasProv	AndProv	DacProv
V9-f	88	11	0
V10-m	79	13	8
V10-f	84	14	2
V11-m	71	25	4
V11-f	90	9	1
V12-m	83	10	6
V12-f	82	12	5
L1-m	77	13	10
L1-f	80	9	11
L2-m	69	20	11
L2-f	81	4	16
L4-m	75	12	13
L4-f	75	19	5
L5-m	82	16	3
L5-f	77	13	10
L6-m	71	25	4
L6-f	84	12	4
L7-m	85	14	1
L7-f	90	10	0
L8-m	78	15	7
L8-f	89	10	1
L9-m	81	13	6
L9-f	75	15	9
L10-m	62	32	6
L10-f	46	51	3
L11-m	67	30	3
L11-f	57	43	0
L12-m	57	43	0
L12-f	70	30	0
L13-m	82	18	0
L13-f	10	90	0
V4-m	45	55	0
V4-f	58	42	0
V5-m	73	24	4
V5-f	71	24	5
V6-m	67	26	7
V6-f	76	21	3
V7-m	70	27	3
V7-f	74	24	2
V8-m	70	26	4
V8-f	75	21	5
V9-m	88	12	1

Sample	BasProv	AndProv	DacProv
PZ-1-m	44	42	14
PZ-2-m	97	3	0
PZ-3-m	32	51	17
PZ-4-m	44	24	31
PZ-5-m	32	43	25
PZ-6-m	60	35	6
PZ-7-m	87	7	7
PZ-8-Vc	28	46	26
PZ-8-C	29	43	29
PZ-8-m	52	35	13
PZ-8-f	59	34	7
PZ-8-Vf	69	11	21
PZ-9-m	72	21	6
PZ-10-m	44	41	14
PZ-11-m	34	43	23
PZ-12-m	46	34	20
PZ-13-m	52	33	15
PZ-14-Vc	53	33	14
PZ-14-C	39	38	23
PZ-14-m	26	37	37
PZ-14-f	42	34	24
PZ-14-Vf	69	17	14
PZ-15-m	39	37	23
PZ-16-m	36	37	27
PZ-17-m	31	35	34
PZ-18-m	32	22	46
PZ-19-m	26	40	34
PZ-20-m	26	32	43

Sample	BasProv	AndProv	DacProv
Vo-9-m	78	11	11
Vo-10-m	73	27	0
Vo-11-m	56	44	0
BC-1-Vc	43	42	15
BC-1-C	36	36	28
BC-1-m	17	43	40
BC-1-f	32	14	54
BC-1-Vf	0	20	80
BC-2-m	50	23	27
BC-3-m	30	17	52
BC-4-m	68	15	18
BC-5-m	65	6	29
Li-1-m	83	0	17
Li-2-m	78	0	22
Li-3-m	46	54	0
Li-4-m	100	0	0
Li-5-m	85	15	0
Li-6-m	87	7	7
Vo-1-m	73	0	27
Vo-2-m	100	0	0
Vo-3-m	100	0	0
Vo-4-m	67	29	4
Vo-5-m	57	43	0
Vo-6-m	100	0	0
Vo-7-m	96	0	4
Vo-8-m	89	0	11
NA-1-m	93	7	0
NA-2-m	77	23	0
NA-3-m	51	49	0
NA-4-m	71	29	0
NA-5-m	72	28	0
NA-6-m	86	14	0
NA-7-m	74	26	0
CO-1-m	83	17	0
GA-1-m	71	29	0
MC-1-m	71	29	0
PO-1-m	95	5	0
PO-2-m	95	5	0
PO-3-m	90	10	0
Ve-1-m	100	0	0
Ve-2-m	100	0	0
Ve-3-m	100	0	0
TG-1-m	77	21	2
TG-2-m	87	5	8
TG-3-m	68	32	0
TA-1-m	93	7	0
TA-2-m	100	0	0
CA-1-m	100	0	0
CA-2-m	89	11	0
CA-2B-m	100	0	0
CA-3-m	69	31	0
SO-1-m	94	6	0
SO-2-m	58	42	0
SO-3-m	97	3	0
SO-4-m	72	28	0
SO-5-m	88	10	1

Sample	BAS & AND	ALT	RIO & DAC
PZ-1-m	59	12	29
PZ-2-m	99	1	0
PZ-3-m	54	21	25
PZ-4-m	38	17	45
PZ-5-m	38	22	41
PZ-6-m	69	19	12
PZ-7-m	84	0	16
PZ-8-Vc	40	16	43
PZ-8-C	38	22	41
PZ-8-m	63	15	22
PZ-8-f	72	8	20
PZ-8-Vf	75	0	24
PZ-9-m	48	44	8
PZ-10-m	59	29	12
PZ-11-m	60	16	23

Sample	BAS & AND	ALT	RIO & DAC
PZ-12-m	78	4	18
PZ-13-m	67	16	17
PZ-14-Vc	77	0	23
PZ-14-C	69	4	26
PZ-14-m	54	2	44
PZ-14-f	64	1	35
PZ-14-Vf	65	17	19
PZ-15-m	67	3	30
PZ-16-m	69	2	29
PZ-17-m	51	3	46
PZ-18-m	34	29	37
PZ-19-m	58	5	37
PZ-20-m	47	13	39
BC-1-Vc	68	5	27
BC-1-C	46	14	40
BC-1-m	46	15	39
BC-1-f	18	48	35
BC-1-Vf	10	21	69
BC-2-m	48	17	35
BC-3-m	22	44	35
BC-4-m	46	26	28
BC-5-m	13	65	22
Li-1-m	29	65	6
Li-2-m	17	79	5
Li-3-m	37	63	0
Li-4-m	33	57	10
Li-5-m	46	54	0
Li-6-m	58	38	4
Vo-1-m	46	23	31
Vo-2-m	75	25	0
Vo-3-m	25	75	0
Vo-4-m	46	51	3
Vo-5-m	80	0	20
Vo-6-m	25	75	0
Vo-7-m	53	43	3
Vo-8-m	40	27	33
Vo-9-m	38	25	38
Vo-10-m	50	50	0
Vo-11-m	41	59	0

Sample	BAS & AND	ALT	RIO & DAC
NA-1-m	63	32	5
NA-2-m	64	29	7
NA-3-m	66	34	0
NA-4-m	83	16	1
NA-5-m	94	6	0
NA-6-m	65	34	1
NA-7-m	90	10	0
CO-1-m	28	72	0
GA-1-m	64	36	0
MC-1-m	61	39	0
PO-1-m	75	25	0
PO-2-m	97	2	1
PO-3-m	81	19	0
Ve-1-m	100	0	0
Ve-2-m	100	0	0
Ve-3-m	100	0	0
TG-1-m	94	4	2
TG-2-m	81	13	6
TG-3-m	98	2	1
TA-1-m	75	25	0
TA-2-m	75	25	0
CA-1-m	95	5	0
CA-2-m	100	0	0
CA-2B-m	81	19	0
CA-3-m	92	8	0
SO-1-m	100	0	0
SO-2-m	82	16	2
SO-3-m	91	9	0
SO-4-m	100	0	0
SO-5-m	95	4	1

Table A-B -7- **Bas_{Prov}**: basaltic provenance; **And_{Prov}:** andesitic provenance; **Dac_{Prov}:** dacitic provenance. BAS & AND: basaltic and andesitic provenance; ALT: altered volcanic grains; RIO & Dac: rhyolitic and dacitic provenance. Vc: very coarse sand fraction; C: coarse sand fraction; m: medium sand fraction; f: fine sand fraction; Vf: very fine sand fraction. (Values are expressed as %).

Sample	VFR	ACC	PLG
PZ-1-m	63	25	13
PZ-2-m	42	57	2
PZ-3-m	58	24	18
PZ-4-m	79	8	13
PZ-5-m	84	4	12
PZ-6-m	90	4	6
PZ-7-m	20	75	5
PZ-8-Vc	96	1	3
PZ-8-C	88	2	10
PZ-8-m	70	9	21
PZ-8-f	61	22	16
PZ-8-Vf	62	29	9
PZ-9-m	99	1	0
PZ-10-m	97	1	2
PZ-11-m	83	5	12
PZ-12-m	35	41	24
PZ-13-m	94	0	6
PZ-14-Vc	89	1	9
PZ-14-C	95	1	4
PZ-14-m	97	1	3
PZ-14-f	90	0	10
PZ-14-Vf	50	37	13
PZ-15-m	89	1	10
PZ-16-m	85	2	12
PZ-17-m	84	1	15
PZ-18-m	95	3	2
PZ-19-m	93	0	7
PZ-20-m	95	4	1
BC-1-Vc	81	0	18
BC-1-C	84	1	15
BC-1-m	90	1	9
BC-1-f	79	7	15
BC-1-Vf	41	53	6
BC-2-m	24	66	10
BC-3-m	92	1	7
BC-4-m	84	2	13
BC-5-m	88	5	8
Li-1-m	86	2	11
Li-2-m	86	2	11
Li-3-m	89	5	6
Li-4-m	77	0	23
Li-5-m	77	6	17
Li-6-m	77	0	23
Vo-1-m	31	66	3
Vo-2-m	6	91	3
Vo-3-m	74	13	12
Vo-4-m	76	4	20
Vo-5-m	27	64	10
Vo-6-m	14	84	2
Vo-7-m	80	9	11
Vo-8-m	75	17	8
Vo-9-m	84	6	10
Vo-10-m	82	3	15
Vo-11-m	90	0	10

Sample	VFR	ACC	PLG
NA-1-m	89	3	8
NA-2-m	81	8	11
NA-3-m	83	6	11
NA-4-m	82	5	12
NA-5-m	53	35	12
NA-6-m	68	21	11
NA-7-m	83	6	11
CO-1-m	89	6	6
GA-1-m	74	16	10
MC-1-m	70	15	15
PO-1-m	74	21	5
PO-2-m	40	58	2
PO-3-m	78	14	8
Ve-1-m	87	13	0
Ve-2-m	83	16	1
Ve-3-m	85	12	3
TG-1-m	56	36	8

Sample	VFR	ACC	PLG
TG-2-m	41	58	1
TG-3-m	73	20	6
TA-1-m	81	10	9
TA-2-m	72	22	6
CA-1-m	64	35	1
CA-2-m	67	27	6
CA-2B-m	49	49	2
CA-3-m	75	8	17
SO-1-m	40	51	8
SO-2-m	71	17	12
SO-3-m	42	43	15
SO-4-m	86	9	5
SO-5-m	65	30	5

Sample	VFR	ACC	PLG
SA-1-Vc	100	0	0
SA-1-C	93	4	3
SA-1-m	79	11	10
SA-1-f	58	9	33
SA-1-Vf	33	7	61
SA-2-m	76	12	12
SA-3-m	62	9	29
SA-4-m	79	9	11
SA-5-m	89	6	5
SA-6-m	90	7	3
SA-7-m	90	8	3
SA-8-m	74	9	17
SA-9-m	78	9	13
SA-10-m	77	10	13
SA-11-m	76	9	15
SA-12-m	69	12	20
SA-13-m	76	9	15
SA-14-m	79	11	10
SA-15-m	86	12	2
Fi-1-m	68	3	29

Sample	VFR	ACC	PLG
Fi-2-m	77	8	15
Fi-3-Vc	95	2	3
Fi-3-C	93	5	3
Fi-3-m	84	10	6
Fi-3-f	84	9	7
Fi-3-Vf	86	4	10
Fi-4-m	71	8	22
AL-1-m	76	11	12
AL-2-m	83	13	5
AL-3-Vc	93	5	2
AL-3-C	90	4	6
AL-3-m	78	9	13
AL-3-f	73	12	15
AL-3-Vf	63	15	22
AL-4-C	92	3	5
AL-5-m	81	8	11
AL-6-m	83	6	11
AL-7-m	76	7	17

Sample	VFR	ACC	PLG
PN-1-Vc	7	84	9
PN-1-C	9	74	17
PN-1-m	20	58	22
PN-1-f	35	54	11
PN-1-Vf	33	55	12
PN-2-m	3	90	7
PN-3-m	7	85	8
PN-4-m	1	97	3
PN-5-m	0	81	19
PN-6-m	3	92	5
PN-7-m	12	81	7
PN-8-m	2	91	7
PN-9-m	10	76	13
PN-10-m	4	92	4
PN-11-m	4	86	11
STR-1-Vc	10	88	1
STR-1-C	13	85	2
STR-1-m	19	78	3
STR-1-f	24	66	10
STR-1-Vf	48	38	14
STR-2-m	66	34	1
STR-3-m	14	82	4
STR-4-m	16	80	4
STR-5-m	14	82	4
STR-7-m	11	84	5
STR-8-m	25	72	3
STR-9-Vc	3	97	0
STR-9-C	2	98	1
STR-9-m	5	90	5
STR-9-f	9	83	8
STR-9-Vf	8	84	9

Table A-B – 8 - **VFR**: volcanic rock fragments with all texture typologies accessory minerals; **ACC**: single grains of olivine, pyroxene, opaque; **PLG**: plagioclase. (Values are expressed as %).

APPENDIX C (roundness recalculated parameters [optical microscope])

	Lvl grains*						Lvl tot	Lvl Mean	Lvmi grains*						Lvmi tot	Lvmi Mean	Lvv grains*						Lvv tot	Lvv Mean
Sample	1	2	3	4	5	6	grains	Roundness	1	2	3	4	5	6	grains	Roundness	1	2	3	4	5	6	grains	Roundness
STR-1-Vc	50	97	64	26	5	1	243	2,3	0	1	1	0	0	0	2	2,5	0	5	1	2	0	0	8	2,6
STR-1-C	17	181	71	21	3	0	293	2,4	4	15	7	0	0	0	26	2,1	1	13	6	0	0	0	20	2,3
STR-1-m	2	61	57	42	10	0	172	3,0	0	18	22	23	11	0	74	3,4	3	23	17	13	7	0	63	3,0
STR-1-f	1	64	30	3	0	0	98	2,4	6	53	24	12	0	0	95	2,4	16	30	15	2	0	0	63	2,0
STR-1-Vf	2	11	6	0	0	0	19	2,2	7	44	18	2	0	0	71	2,2	17	30	7	1	0	0	55	1,9
STR-2-m	0	25	39	24	20	0	108	3,4	0	4	7	5	0	0	16	3,1	0	3	3	1	4	0	11	3,5
STR-3-m	2	85	115	43	7	0	252	2,9	0	18	38	7	0	0	63	2,8	0	5	1	1	0	0	7	2,4
STR-4-m	0	107	96	26	1	0	230	2,7	0	27	29	5	0	0	61	2,6	0	15	7	1	0	0	23	2,4
STR-5-m	9	83	86	32	1	0	211	2,7	2	21	36	11	0	0	70	2,8	2	10	16	11	0	0	39	2,9
STR-7-m	3	131	72	17	0	0	223	2,5	2	42	35	5	0	0	84	2,5	2	13	7	1	0	0	23	2,3
STR-8-m	8	118	66	24	3	0	219	2,5	2	26	18	1	0	0	47	2,4	5	11	4	0	0	0	20	2,0
STR-9-Vc	96	60	4	1	0	0	161	1,4	8	5	1	0	0	0	14	1,5	11	5	0	0	0	0	16	1,3
STR-9-C	177	104	42	8	1	0	332	1,7	16	12	2	0	0	0	30	1,5	24	5	0	0	0	0	29	1,2
STR-9-m	54	121	60	5	0	0	240	2,1	16	39	13	1	0	0	69	2,0	18	26	6	0	0	0	50	1,8
STR-9-f	22	97	27	1	0	0	147	2,0	43	48	16	0	0	0	107	1,7	37	28	8	0	0	0	73	1,6
STR-9-Vf	4	33	7	1	0	0	45	2,1	26	50	12	0	0	0	88	1,8	71	92	31	0	0	0	194	1,8

	Plag grains*						Plag tot	Plag Mean	Py grains*						Py tot	Py Mean	Ol grains*						Ol tot	Ol Mean
Sample	1	2	3	4	5	6	grains	Roundness	1	2	3	4	5	6	grains	Roundness	1	2	3	4	5	6	grains	Roundness
STR-1-Vc	0	3	1	0	0	0	4	2,3	2	9	7	5	0	0	23	2,7	0	2	1	3	0	0	6	3,2
STR-1-C	0	5	1	0	0	0	6	2,2	8	33	7	0	0	0	48	2,0	1	3	0	1	0	0	5	2,2
STR-1-m	0	7	4	0	0	0	11	2,4	1	26	12	5	2	0	46	2,6	1	17	7	2	1	0	28	2,5
STR-1-f	4	31	3	0	0	0	38	2,0	8	58	6	0	0	0	72	2,0	2	13	3	1	0	0	19	2,2
STR-1-Vf	15	31	5	3	0	0	54	1,9	37	79	12	0	0	0	128	1,8	19	22	7	4	0	0	52	1,9
STR-2-m	0	2	1	0	0	0	3	2,3	3	86	58	40	2	0	189	2,7	0	16	8	29	#	0	70	3,7
STR-3-m	0	10	5	0	0	0	15	2,3	2	22	18	0	0	0	42	2,6	0	3	0	1	0	0	4	2,5
STR-4-m	3	10	1	0	0	0	14	1,9	0	32	25	5	0	0	62	2,6	0	2	0	0	0	0	2	2,0
STR-5-m	1	11	3	1	0	0	16	2,3	6	17	16	5	0	0	44	2,5	2	6	1	0	1	0	10	2,2
STR-7-m	3	9	6	0	0	0	18	2,2	6	27	6	0	0	0	39	2,0	0	3	1	0	0	0	4	2,3
STR-8-m	3	5	2	0	0	0	10	1,9	16	53	18	3	0	0	90	2,1	2	6	0	0	0	0	8	1,8
STR-9-Vc	0	0	0	0	0	0	0	0,0	7	2	0	0	0	0	9	1,2	0	0	0	0	0	0	0	0,0
STR-9-C	0	1	0	0	0	0	1	2,0	3	3	0	0	0	0	6	1,5	0	1	0	0	0	0	1	2,0
STR-9-m	1	15	3	0	0	0	19	2,1	1	10	3	1	0	0	15	2,3	1	2	0	1	0	0	4	2,3
STR-9-f	6	20	5	0	0	0	31	2,0	9	16	2	0	0	0	27	1,7	3	3	0	0	0	0	6	1,5
STR-9-Vf	3	23	4	0	0	0	30	2,0	0	19	2	0	0	0	21	2,1	3	4	2	0	0	0	9	1,9

	Lvl grains*						Lvl tot	Lvl Mean	Lvmi grains*						Lvmi tot	Lvmi Mean	Lvv grains*						Lvv tot	Lvv Mean
Sample	1	2	3	4	5	6	grains	Roundness	1	2	3	4	5	6	grains	Roundness	1	2	3	4	5	6	grains	Roundness
PN-1-Vc	89	125	15	0	0	0	229	1,7	0	12	5	0	0	0	17	2,3	1	4	0	0	0	0	5	1,8
PN-1-C	69	129	14	0	0	0	212	1,7	10	26	8	0	0	0	44	2,0	5	3	1	0	0	0	9	1,6
PN-1-m	11	53	8	0	0	0	72	2,0	17	37	9	0	0	0	63	1,9	26	26	12	1	0	0	65	1,8
PN-1-f	11	22	1	0	0	0	34	1,7	20	45	11	0	0	0	76	1,9	32	10	3	12	2	0	59	2,0
PN-1-Vf	2	5	2	0	0	0	9	2,0	10	48	19	0	0	0	77	2,1	36	45	9	1	0	0	91	1,7
PN-2-m	64	85	20	6	2	0	177	1,9	43	79	26	11	3	0	162	2,1	1	1	0	0	0	0	2	1,5
PN-3-m	36	94	26	7	2	0	165	2,1	35	78	34	14	2	0	163	2,2	0	4	0	0	0	0	4	2,0
PN-4-m	13	114	33	0	0	0	160	2,1	6	86	21	4	0	0	117	2,2	5	36	5	0	0	0	46	2,0
PN-5-m	4	63	14	3	0	0	84	2,2	5	62	20	8	0	0	95	2,3	16	66	36	3	4	0	125	2,3
PN-6-m	14	75	16	3	0	0	108	2,1	5	40	11	0	0	0	56	2,1	21	85	24	5	0	0	135	2,1
PN-7-m	29	92	31	13	0	0	165	2,2	4	33	19	8	0	0	64	2,5	5	11	5	0	0	0	21	2,0
PN-8-m	19	61	62	31	6	0	179	2,7	2	38	38	10	10	0	98	2,9	9	2	4	0	6	0	21	2,6
PN-9-m	0	30	48	58	5	0	141	3,3	0	12	52	33	6	0	103	3,3	3	8	6	3	0	0	20	2,5
PN-10-m	2	79	63	19	8	3	174	2,8	3	42	50	12	0	0	107	2,7	7	12	14	4	0	0	37	2,4
PN-11-m	21	54	38	24	7	0	144	2,597	11	41	47	14	3	0	116	2,629	5	12	17	5	1	0	40	2,625
PN-11-m[30]	7	11	9	3	0	0	30	2,267	1	14	12	3	0	0	30	2,567	4	10	12	3	1	0	30	2,567

	Plag grains*						Plag tot	Plag Mean	Py grains*						Py tot	Py Mean	Hb grains*						Hb tot	Hb Mean
Sample	1	2	3	4	5	6	grains	Roundness	1	2	3	4	5	6	grains	Roundness	1	2	3	4	5	6	grains	Roundness
PN-1-Vc	16	8	0	0	0	0	24	1,3	4	7	0	0	0	0	11	1,6	3	4	0	0	0	0	7	1,6
PN-1-C	36	28	0	0	0	0	64	1,4	12	5	1	0	0	0	18	1,4	11	0	0	0	0	0	11	1,0
PN-1-m	54	25	2	0	0	0	81	1,4	8	18	3	0	0	0	29	1,8	12	6	0	0	0	0	18	1,3
PN-1-f	27	10	2	0	0	0	39	1,4	22	20	7	6	0	0	55	1,9	24	9	0	0	0	0	33	1,3
PN-1-Vf	28	10	3	0	0	0	41	1,4	18	11	5	0	0	0	34	1,6	19	9	0	0	0	0	28	1,3
PN-2-m	10	12	3	0	0	0	25	1,7	2	3	0	0	0	0	5	1,6	3	4	0	0	0	0	7	1,6
PN-3-m	15	14	3	0	0	0	32	1,6	4	11	1	0	0	0	16	1,8	2	6	0	0	0	0	8	1,8
PN-4-m	1	6	2	0	0	0	9	2,1	0	1	0	0	0	0	1	2,0	0	1	0	0	0	0	1	2,0
PN-5-m	15	47	10	0	0	0	72	1,9	0	0	0	0	0	0	0	0,0	0	0	0	0	0	0	0	0,0
PN-6-m	2	13	4	0	0	0	19	2,1	5	2	1	0	0	0	8	1,5	2	0	0	0	0	0	2	1,0
PN-7-m	8	16	0	1	0	0	25	1,8	7	15	3	0	0	0	25	1,8	6	7	0	0	0	0	13	1,5
PN-8-m	7	16	1	1	0	0	25	1,8	1	0	0	0	0	0	1	1,0	2	3	0	0	0	0	5	1,6
PN-9-m	13	19	13	2	0	0	47	2,1	1	17	8	0	0	0	26	2,3	0	10	0	0	0	0	10	2,0
PN-10-m	2	8	5	0	0	0	15	2,2	0	5	4	0	0	0	9	2,4	0	4	0	0	0	0	4	2,0
PN-11-m	10	18	5	2	5	0	40	2,350	1	7	0	1	0	0	9	2,1	1	3	0	0	0	0	4	1,8
PN-11-m[30]	8	15	5	2	0	0	30	2,033	-	-	-	-	-	-	-	-	-	-	-	-	-	-	-	-

	Lvl grains*						Lvl tot	Lvl Mean	Lvmi grains*						Lvmi tot	Lvmi Mean	Lvv grains*						Lvv tot	Lvv Mean
Sample#	1	2	3	4	5	6	grains	Roundness	1	2	3	4	5	6	grains	Roundness	1	2	3	4	5	6	grains	Roundness
L1-m	9	49	98	35	3	0	194	2,9	0	6	26	25	4	0	61	3,4	6	11	5	1	0	0	23	2,0
L2-m	11	43	98	27	8	1	188	2,9	0	10	17	40	6	2	75	3,6	0	1	1	10	6	1	19	4,3
L4-m	32	93	41	2	0	0	168	2,1	3	30	58	32	0	0	123	3,0	11	17	6	1	0	0	35	1,9
L5-m	14	41	53	11	1	0	120	2,5	3	19	21	23	0	0	66	3,0	35	55	23	16	0	0	129	2,2
L6-m	9	25	33	13	2	0	82	2,7	1	6	21	19	2	0	49	3,3	23	28	20	10	2	0	83	2,3
L7-m	0	32	63	19	4	1	119	3,0	0	0	12	6	0	0	18	3,3	6	8	2	0	0	0	16	1,8
L8-m	7	48	68	30	1	0	154	2,8	0	9	27	25	0	0	61	3,3	11	43	32	14	1	0	101	2,5
L9-m	6	28	69	35	8	2	148	3,1	2	14	19	24	12	1	72	3,5	3	16	18	10	2	0	49	2,8
L10-m	4	24	71	32	10	4	145	3,2	1	12	22	21	8	5	69	3,6	3	4	7	0	0	0	14	2,3
L11-m	0	8	32	36	4	0	80	3,5	1	4	6	13	13	3	40	4,1	2	11	17	25	11	3	69	3,6
L12-m	0	10	39	31	8	1	89	3,4	2	15	26	31	15	5	94	3,6	9	46	50	36	6	4	151	3,0
L13-m	3	9	37	9	5	2	65	3,2	10	18	33	35	6	6	108	3,3	24	77	62	24	6	3	196	2,6

	Lvf grains*						Lvf tot	Lvf Mean	Plag grains*						Plag tot	Plag Mean	Py grains*						Py tot	Py Mean
Sample#	1	2	3	4	5	6	grains	Roundness	1	2	3	4	5	6	grains	Roundness	1	2	3	4	5	6	grains	Roundness
L1-m	0	5	16	6	0	0	27	3,0	11	18	3	1	0	0	33	1,8	29	22	10	1	0	0	62	1,7
L2-m	6	11	25	6	2	0	50	2,7	4	12	4	1	0	0	21	2,1	12	21	7	2	0	0	42	2,0
L4-m	2	6	2	0	0	0	10	2,0	22	16	3	0	0	0	41	1,5	13	7	2	0	0	0	22	1,5
L5-m	1	11	35	9	2	1	59	2,9	3	8	0	0	0	0	11	1,7	7	8	0	0	0	0	15	1,5
L6-m	0	17	53	31	3	0	104	3,2	6	7	8	0	0	0	21	2,1	8	8	2	1	0	0	19	1,8
L7-m	0	4	10	2	0	0	16	2,9	1	4	2	1	0	0	8	2,4	52	91	61	19	0	0	223	2,2
L8-m	0	9	21	10	3	0	43	3,2	1	3	3	1	0	0	8	2,5	7	14	8	1	0	0	30	2,1
L9-m	0	3	10	5	0	0	18	3,1	12	23	16	10	1	0	62	2,4	4	14	11	14	1	0	44	2,9
L10-m	0	5	10	6	1	0	22	3,1	13	36	22	10	2	0	83	2,4	9	25	12	11	6	0	63	2,7
L11-m	1	2	13	9	1	0	26	3,3	1	17	14	20	6	3	61	3,4	1	23	25	21	4	1	75	3,1
L12-m	0	1	9	3	0	0	13	3,2	0	7	21	6	3	1	38	3,2	0	3	3	1	0	0	7	2,7
L13-m	0	3	9	2	3	2	19	3,6	0	0	2	1	1	0	4	3,8	0	1	0	0	1	0	2	3,5

	Lvl grains*						Lvl tot	Lvl Mean	Lvmi grains*						Lvmi tot	Lvmi Mean	Lvv grains*						Lvv tot	Lvv Mean
Sample	1	2	3	4	5	6	grains	Roundness	1	2	3	4	5	6	grains	Roundness	1	2	3	4	5	6	grains	Roundness
V1-m	144	17	28	68	26	5	288	2,4	39	0	5	14	15	3	76	2,7	11	4	7	0	0	0	22	1,8
V2-m	21	40	90	36	5	2	194	2,8	0	4	22	20	3	3	52	3,6	5	8	0	0	0	0	13	1,6
V4-m	4	23	59	37	8	6	137	3,3	0	11	47	41	0	0	99	3,3	2	4	0	0	0	0	6	1,7
V5-m	26	69	46	16	3	1	161	2,4	2	21	29	35	11	6	104	3,5	15	12	2	0	0	0	29	1,6
V6-m	29	78	51	15	7	4	184	2,5	3	21	28	20	9	7	88	3,4	12	11	0	0	0	0	23	1,5
V7-m	8	28	55	29	12	1	133	3,1	0	2	34	41	12	8	97	3,9	9	8	5	0	0	0	22	1,8
V8-m	7	38	64	40	14	2	165	3,1	0	9	28	31	22	11	101	4,0	9	11	0	0	0	0	20	1,6
V9-m	0	19	25	32	11	5	92	3,5	0	0	15	28	17	0	60	4,0	7	9	5	2	0	0	23	2,1
V10-m	9	29	50	47	20	7	162	3,4	0	2	12	19	14	11	58	4,3	8	9	0	0	0	0	17	1,5
V11-m	17	29	35	31	11	2	125	3,0	2	11	29	35	16	5	98	3,7	6	8	1	0	0	0	15	1,7
V12-m	2	15	19	14	5	0	55	3,1	0	2	14	17	9	5	47	4,0	4	3	0	0	0	0	7	1,4

	Ol grains*						Ol tot	Ol Mean	Plag grains*						Plag tot	Plag Mean	Py grains*						Py tot	Py Mean
Sample	1	2	3	4	5	6	grains	Roundness	1	2	3	4	5	6	grains	Roundness	1	2	3	4	5	6	grains	Roundness
V1-m	0	0	3	4	1	0	8	3,7	40	2	16	17	4	1	80	2,3	158	17	77	60	4	0	316	2,2
V2-m	0	0	3	4	0	0	7	3,6	1	12	18	1	0	0	32	2,6	9	57	27	5	0	0	98	2,3
V4-m	0	0	1	3	2		6	4,2	2	12	21	7	1	0	43	2,8	11	22	33	9	2	0	77	2,6
V5-m	0	0	3	3	1	0	7	3,7	6	22	12	1	0	0	41	2,2	11	32	9	0	0	0	52	2,0
V6-m	0	1	1	1	0	0	3	3,0	8	27	10	2	0	0	47	2,1	12	17	15	0	0	0	44	2,1
V7-m	0	1	2	2	1	1	7	3,8	1	8	15	13	2	0	39	3,2	17	29	44	2	0	0	92	2,3
V8-m	0	0	1	2	1	0	4	4,0	1	12	14	15	2	0	44	3,1	7	24	19	5	0	0	55	2,4
V9-m	0	0	3	7	6	2	18	4,4	0	4	15	17	4	0	40	3,5	28	58	48	9	2	0	145	2,3
V10-m	0	1	3	3	3	2	12	4,2	5	12	15	19	4	0	55	3,1	16	24	21	19	0	0	80	2,5
V11-m	0	0	4	5	4	2	15	4,3	9	19	15	8	0	0	51	2,4	25	32	24	2	0	0	83	2,0
V12-m	0	0	4	5	3	2	14	4,2	7	17	19	7	0	0	50	2,5	28	84	74	14	0	0	200	2,4

Table A-C -1 – Key to grain shape categories. **1** = very angular; **2** = angular; **3** = sub-angular; **4** = sub-rounded; **5** = rounded; **6** = well rounded. **Lvl** = volcanic lithic with lathwork texture, **Lvmi** = volcanic lithic with microlitic texture, **Lvv** = volcanic lithic with vitric texture, **Lvf** = volcanic lithic with felsitic texture, **Plag** = plagioclase, **Py** = pyroxene; **Ol** = Olivine; **Hb** = hornblende (Lipari data are from Morrone et al., 2018).

	Lvl grains*						Lvl tot	Lvl Mean	Lvmi grains*						Lvmi tot	Lvmi Mean	Lvv grains*						Lvv tot	Lvv Mean
Sample	1	2	3	4	5	6	grains	Roundness	1	2	3	4	5	6	grains	Roundness	1	2	3	4	5	6	grains	Roundness
SA-1-Vc	16	111	96	45	3	0	271	2,7	0	10	11	22	0	0	43	3,3	1	12	12	7	0	0	32	2,8
SA-1-C	21	75	80	45	7	0	228	2,7	4	20	32	22	3	0	81	3,0	7	11	12	5	0	0	35	2,4
SA-1-m	6	45	62	51	3	0	167	3,0	1	18	23	35	4	0	81	3,3	2	11	19	13	2	0	47	3,0
SA-1-f	2	14	15	3	2	0	36	2,7	0	10	33	57	6	0	106	3,6	10	39	15	6	0	0	70	2,2
SA-1-Vf	0	0	0	0	0	0	0	0,0	0	2	8	19	0	0	29	3,6	7	46	32	14	0	0	99	2,5
SA-2-m	8	42	65	45	4	0	164	3,0	1	9	20	35	7	0	72	3,5	14	21	9	1	0	0	45	1,9
SA-3-m	3	46	75	26	2	0	152	2,9	0	6	23	30	3	0	62	3,5	2	14	8	3	0	0	27	2,4
SA-4-m	20	51	83	21	0	0	175	2,6	3	14	26	40	4	0	87	3,3	5	24	14	1	0	0	44	2,3
SA-5-m	0	31	61	52	1	0	145	3,2	0	4	24	46	5	0	79	3,7	1	20	25	16	3	0	65	3,0
SA-6-m	1	47	106	68	7	0	229	3,1	0	4	26	31	4	0	65	3,5	9	32	11	4	0	0	56	2,2
SA-7-m	30	113	97	18	3	0	261	2,4	0	6	21	20	0	0	47	3,3	17	24	7	3	0	0	51	1,9
SA-8-m	5	63	79	44	4	0	195	2,9	1	9	21	25	1	0	57	3,3	1	15	8	3	0	0	27	2,5
SA-9-m	9	63	79	38	3	0	192	2,8	0	8	19	30	4	0	61	3,5	6	27	8	3	0	0	44	2,2
SA-10-m	4	42	92	22	2	0	162	2,9	0	5	35	44	6	0	90	3,6	6	18	14	6	0	0	44	2,5
SA-11-m	1	30	93	32	5	1	162	3,1	1	12	35	44	1	0	93	3,3	3	18	10	4	0	0	35	2,4
SA-12-m	10	36	80	25	5	1	157	2,9	5	12	29	35	4	0	85	3,2	2	6	5	0	0	0	13	2,2
SA-13-m	10	41	91	29	7	1	179	2,9	6	9	30	41	8	2	96	3,4	0	5	4	0	0	0	9	2,4
SA-14-m	0	36	103	55	3	1	198	3,1	0	2	23	32	3	0	60	3,6	2	15	12	1	0	0	30	2,4
SA-15-m	3	33	80	36	2	0	154	3,0	0	4	28	61	15	0	108	3,8	4	17	7	1	0	0	29	2,2

	Plag grains*						Plag tot	Plag Mean	Py grains*						Py tot	Py Mean	Op grains*						Op tot	Op Mean
Sample	1	2	3	4	5	6	grains	Roundness	1	2	3	4	5	6	grains	Roundness	1	2	3	4	5	6	grains	Roundness
SA-1-Vc	0	0	0	0	0	0	0	0,0	0	0	0	0	0	0	0	0,0	0	0	0	0	0	0	0	0,0
SA-1-C	3	8	4	1	0	0	16	2,2	4	7	1	0	0	0	12	1,8	0	0	0	0	0	0	0	0,0
SA-1-m	3	16	12	10	0	0	41	2,7	6	11	8	5	0	0	30	2,4	1	1	2	3	0	0	7	3,0
SA-1-f	2	10	17	4	0	0	33	2,7	15	32	24	6	0	0	77	2,3	0	7	13	14	2	0	36	3,3
SA-1-Vf	6	16	4	0	0	0	26	1,9	15	51	33	9	2	0	110	2,4	1	14	28	33	26	12	114	3,9
SA-2-m	2	19	20	4	1	0	46	2,6	5	14	13	4	0	0	36	2,4	0	0	2	3	0	0	5	3,6
SA-3-m	1	14	14	4	1	0	34	2,7	11	36	28	16	1	0	92	2,6	0	3	5	4	0	0	12	3,1
SA-4-m	3	18	12	3	0	0	36	2,4	3	13	8	2	0	0	26	2,3	0	1	2	3	1	0	7	3,5
SA-5-m	1	10	8	4	0	0	23	2,7	1	6	5	2	0	0	14	2,6	0	0	0	0	0	0	0	0,0
SA-6-m	0	9	12	7	0	0	28	2,9	0	4	5	1	0	0	10	2,7	0	0	0	0	0	0	0	0,0
SA-7-m	0	8	16	6	0	0	30	2,9	1	4	5	1	0	0	11	2,5	0	0	0	0	0	0	0	0,0
SA-8-m	4	12	13	4	0	0	33	2,5	7	21	15	9	0	0	52	2,5	0	1	3	3	0	0	7	3,3
SA-9-m	2	7	16	7	4	0	36	3,1	3	12	23	8	2	0	48	2,9	0	0	0	0	0	0	0	0,0
SA-10-m	1	12	20	4	0	0	37	2,8	3	10	20	6	0	0	39	2,7	0	1	2	4	1	0	8	3,6
SA-11-m	0	9	22	5	0	0	36	2,9	4	17	14	8	0	0	43	2,6	0	1	3	2	1	0	7	3,4
SA-12-m	2	11	22	8	1	0	44	2,9	6	16	21	17	2	0	62	2,9	0	1	1	2	0	0	4	3,3
SA-13-m	1	5	16	13	1	0	36	3,2	7	10	10	11	2	0	40	2,8	0	1	6	5	0	0	12	3,3
SA-14-m	1	8	21	10	1	0	41	3,0	3	10	12	10	0	0	35	2,8	0	0	0	0	0	0	0	0,0
SA-15-m	2	15	21	7	1	0	46	2,8	0	4	3	0	0	0	7	2,4	0	0	0	0	0	0	0	0,0

	Lvl grains*						Lvl tot	Lvl Mean	Lvmi grains*						Lvmi tot	Lvmi Mean	Lvv grains*						Lvv tot	Lvv Mean
Sample	1	2	3	4	5	6	grains	Roundness	1	2	3	4	5	6	grains	Roundness	1	2	3	4	5	6	grains	Roundness
Fi-1-m	0	19	78	56	5	0	158	3,3	0	1	37	41	2	0	81	3,5	4	17	9	0	0	0	30	2,2
Fi-2-m	0	19	50	46	9	1	125	3,4	0	2	23	38	9	0	72	3,8	2	10	5	3	0	0	20	2,5
Fi-3-Vc	8	101	90	10	1	0	210	2,5	0	1	7	11	0	0	19	3,5	7	9	0	0	0	0	16	1,6
Fi-3-C	12	81	128	71	7	1	300	2,9	2	8	15	21	0	0	46	3,2	5	12	4	1	0	0	22	2,0
Fi-3-m	6	51	94	44	8	0	203	3,0	0	6	41	34	6	2	89	3,5	9	25	11	0	0	0	45	2,0
Fi-3-f	14	18	47	20	1	0	100	2,8	3	18	47	68	7	3	146	3,5	7	15	6	0	0	0	28	2,0
Fi-3-Vf	0	11	28	15	2	0	56	3,1	0	17	69	87	21	0	194	3,6	10	34	41	7	1	0	93	2,5
Fi-4-m	11	62	91	19	0	0	183	2,6	1	6	28	40	1	0	76	3,4	9	12	4	0	0	0	25	1,8

	Plag grains*						Plag tot	Plag Mean	Py grains*						Py tot	Py Mean	Op grains*						Op tot	Op Mean
Sample	1	2	3	4	5	6	grains	Roundness	1	2	3	4	5	6	grains	Roundness	1	2	3	4	5	6	grains	Roundness
Fi-1-m	0	4	8	1	0	0	13	2,8	3	32	35	20	1	0	91	2,8	0	1	7	6	0	0	14	3,4
Fi-2-m	0	3	14	15	0	0	32	3,4	1	14	21	18	2	0	56	3,1	0	0	0	0	0	0	0	0,0
Fi-3-Vc	0	3	2	0	0	0	5	2,4	1	5	3	0	0	0	9	2,2	0	0	0	0	0	0	0	0,0
Fi-3-C	0	7	9	3	0	0	19	2,8	2	3	3	1	0	0	9	2,3	0	0	0	0	0	0	0	0,0
Fi-3-m	0	4	24	11	0	0	39	3,2	0	4	12	8	0	0	24	3,2	0	0	0	0	0	0	0	0,0
Fi-3-f	3	13	17	2	0	0	35	2,5	1	9	10	3	2	1	26	3,0	0	0	0	0	0	0	0	0,0
Fi-3-Vf	0	4	12	1	0	0	17	2,8	1	8	10	1	0	0	20	2,6	1	8	10	1	0	0	20	2,6
Fi-4-m	1	9	14	6	0	0	30	2,8	2	13	15	2	0	0	32	2,5	0	2	7	13	0	0	22	3,5

Table A-C -2 – Key to grain shape categories. **1** = very angular; **2** = angular; **3** = sub-angular; **4** = sub-rounded; **5** = rounded; **6** = well rounded. **Lvl** = volcanic lithic with lathwork texture, **Lvmi** = volcanic lithic with microlitic texture, **Lvv** = volcanic lithic with vitric texture, **Lvf** = volcanic lithic with felsitic texture, **Plag** = plagioclase, **Py** = pyroxene; **Ol** = Olivine; **Hb** = hornblende (Lipari data are from Morrone et al., 2018).

	Lvl grains*						Lvl tot	Lvl Mean	Lvmi grains*						Lvmi tot	Lvmi Mean	Lvv grains*						Lvv tot	Lvv Mean
Sample	1	2	3	4	5	6	grains	Roundness	1	2	3	4	5	6	grains	Roundness	1	2	3	4	5	6	grains	Roundness
AL-1-m	2	30	96	38	2	0	168	3,0	0	1	23	52	5	0	81	3,8	4	22	13	2	0	0	41	2,3
AL-2-m	10	48	147	42	9	0	256	3,0	0	2	17	31	3	53	3,66	3,0	3	8	3	2	0	0	16	3,3
AL-3-Vc	30	76	69	9	0	0	184	2,3	0	6	8	5	0	0	19	2,9	14	11	1	0	0	0	26	1,5
AL-3-C	36	99	115	10	0	0	260	2,4	4	18	29	8	0	0	59	2,7	17	22	10	1	0	0	50	1,9
AL-3-m	10	41	85	21	1	0	158	2,8	5	15	37	15	2	0	74	2,9	16	38	14	0	0	0	68	2,0
AL-3-f	2	25	64	16	0	1	108	2,9	4	27	65	30	1	0	127	3,0	17	22	10	1	0	0	50	1,9
AL-3-Vf	0	10	25	4	0	0	39	2,8	1	17	65	43	1	0	127	3,2	8	53	21	1	1	0	84	2,2
AL-4-C	16	72	114	34	9	0	275	2,8	0	15	35	23	0	0	73	3,1	11	22	17	1	0	0	51	2,2
AL-5-m	16	63	119	26	5	0	229	2,7	0	5	27	12	0	0	44	3,2	9	30	10	1	0	0	50	2,1
AL-6-m	13	53	111	32	12	0	221	2,9	0	7	25	47	0	0	79	3,5	2	17	11	2	0	0	32	2,4
AL-7-m	14	59	108	24	3	0	208	2,7	0	5	18	30	5	0	58	3,6	8	22	8	0	0	0	38	2,0

	Plag grains*						Plag tot	Plag Mean	Py grains*						Py tot	Py Mean	Ol grains*						Ol tot	Ol Mean
Sample	1	2	3	4	5	6	grains	Roundness	1	2	3	4	5	6	grains	Roundness	1	2	3	4	5	6	grains	Roundness
AL-1-m	4	10	23	7	0	0	44	2,8	1	8	15	11	1	0	36	3,1	0	2	1	2	1	0	6	3,3
AL-2-m	3	11	23	9	4	0	50	3,0	3	4	8	1	0	0	16	2,4	0	1	1	0	0	0	2	2,5
AL-3-Vc	1	4	7	0	0	0	12	2,5	0	3	2	0	0	0	5	2,4	0	0	0	0	0	0	0	0,0
AL-3-C	2	6	5	1	0	0	14	2,4	3	11	9	2	0	0	25	2,4	0	0	0	0	0	0	0	0,0
AL-3-m	1	12	21	2	0	0	36	2,7	4	17	15	3	0	0	39	2,4	0	3	2	0	0	0	5	2,4
AL-3-f	3	17	21	4	0	0	45	2,6	3	18	26	4	2	0	53	2,7	0	1	2	3	0	0	6	3,3
AL-3-Vf	0	24	34	2	0	0	60	2,6	1	28	39	4	0	0	72	2,6	0	6	6	4	1	0	17	3,0
AL-4-C	1	3	8	0	0	0	12	2,6	0	6	13	0	0	0	19	2,7	0	0	0	0	0	0	0	0,0
AL-5-m	2	10	13	4	4	0	33	2,9	3	17	10	3	2	0	35	2,5	0	2	3	2	2	0	9	3,4
AL-6-m	1	7	12	2	0	0	22	2,7	4	11	19	7	2	0	43	2,8	0	0	0	1	1	0	2	4,5
AL-7-m	1	6	16	3	1	0	27	2,9	4	27	22	7	1	0	61	2,6	0	2	4	2	0	0	8	3,0

	Pm grains*						Pm tot	Pm Mean	K grains*						K tot	K Mean	Plag grains*						Plag tot	Plag Mean
Sample	1	2	3	4	5	6	grains	Roundness	1	2	3	4	5	6	grains	Roundness	1	2	3	4	5	6	grains	Roundness
PZ-1-m	0	6	5	0	0	0	11	2,5	0	9	7	5	0	0	21	2,8	0	18	17	5	0	0	40	2,7
PZ-2-m	0	0	0	0	0	0	0	0,0	0	0	0	0	0	0	0	0,0	0	0	3	4	0	0	7	3,6
PZ-3-m	0	9	17	0	0	0	26	2,6	0	0	4	2	0	0	6	3,3	5	29	27	5	0	0	66	2,8
PZ-4-m	0	17	21	0	0	0	38	2,6	0	10	20	8	0	0	38	2,9	0	20	19	5	0	0	44	2,7
PZ-5-m	0	5	8	0	0	0	13	2,6	7	23	23	7	0	0	0	2,5	10	13	9	3	0	0	0	2,1
PZ-6-m	0	31	30	6	0	0	67	2,6	0	15	22	3	0	0	40	2,7	0	8	9	3	0	0	20	2,8
PZ-7-m	0	1	2	0	0	0	3	2,7	0	4	13	2	0	0	19	2,9	7	11	1	0	0	0	19	1,7
PZ-8-Vc	0	3	8	0	6	0	17	3,5	4	0	1	3	0	0	8	2,4	0	1	3	3	2	0	9	3,7
PZ-8-C	4	18	29	13	5	0	69	3,0	1	2	14	10	0	0	27	3,2	0	12	20	5	0	0	37	2,8
PZ-8-m	1	9	6	0	0	0	16	2,3	0	30	24	0	0	0	54	2,4	0	35	27	3	0	0	65	2,5
PZ-8-f	0	3	8	1	0	0	12	2,8	59	33	22	4	0	0	118	1,8	7	24	17	6	0	0	54	2,4
PZ-8-Vf	13	7	0	0	0	0	20	1,4	0	7	13	1	0	0	21	2,7	0	11	18	4	0	0	33	2,8
PZ-9-m	24	44	42	17	9	0	136	2,6	0	2	1	0	0	0	3	2,3	0	0	0	0	0	0	0	0,0
PZ-10-m	60	62	12	2	0	0	136	1,7	8	24	4	1	0	0	37	1,9	0	5	2	0	0	0	7	2,3
PZ-11-m	20	23	11	0	0	0	54	1,8	11	38	22	0	0	0	71	2,2	5	21	9	0	1	0	36	2,2
PZ-12-m	0	6	3	0	0	0	9	2,3	1	16	7	0	0	0	24	2,3	8	35	31	9	1	0	84	2,5
PZ-13-m	16	0	0	0	0	0	16	1,0	0	14	10	0	0	0	24	2,4	0	8	12	0	0	0	20	2,6
PZ-14-Vc	0	0	1	0	0	0	1	3,0	0	1	4	0	0	0	5	2,8	0	3	8	2	0	0	13	2,9
PZ-14-C	6	27	22	14	0	0	69	2,6	0	20	25	7	0	0	52	2,8	0	7	5	1	0	0	13	2,5
PZ-14-m	31	45	26	1	0	0	103	2,0	1	4	5	0	0	0	10	2,4	0	5	5	0	0	0	10	2,5
PZ-14-f	3	5	1	0	0	0	9	1,8	0	15	20	3	0	0	38	2,7	0	12	11	1	0	0	24	2,5
PZ-14-Vf	0	5	18	2	0	0	25	2,9	0	5	18	2	0	0	25	2,9	0	5	15	12	0	0	32	3,2
PZ-15-m	3	19	9	1	0	0	32	2,3	3	30	31	4	0	0	68	2,5	0	12	15	5	0	0	32	2,8
PZ-16-m	5	15	4	1	0	0	25	2,0	5	15	34	8	1	0	63	2,8	0	5	17	15	0	0	37	3,3
PZ-17-m	1	16	8	0	0	0	25	2,3	1	9	9	2	0	0	21	2,6	0	23	23	4	0	0	50	2,6
PZ-18-m	12	17	12	5	0	0	46	2,2	0	7	7	0	0	0	14	2,5	0	1	1	5	1	0	8	3,8
PZ-19-m	13	34	20	4	0	0	71	2,2	5	26	8	1	0	0	40	2,1	0	12	11	0	0	0	23	2,5
PZ-20-m	67	106	27	3	0	0	203	1,8	0	3	2	0	0	0	5	2,4	0	1	1	0	0	0	2	2,5
BC-1-Vc	0	0	0	0	1	0	1	5,0	0	4	5	0	0	0	9	2,6	0	13	27	19	3	0	62	3,2
BC-1-C	5	14	6	3	0	0	28	2,3	0	19	16	8	0	0	43	2,7	3	19	19	9	0	0	50	2,6
BC-1-m	1	13	4	2	0	0	20	2,4	2	12	7	8	0	0	29	2,7	1	9	9	10	0	0	29	3,0
BC-1-f	0	0	1	0	0	0	1	3,0	0	7	16	10	1	0	32	3,1	0	6	10	9	1	0	26	3,2
BC-1-Vf	0	1	0	0	0	0	0	2,0	0	5	3	1	0	0	9	2,6	0	8	7	2	0	0	17	2,6
BC-2-m	0	0	0	0	0	0	0	0,0	0	5	2	0	0	0	2,28	3,0	3	17	9	8	0	0	37	2,6
BC-3-m	0	2	4	1	0	0	7	2,9	2	18	15	5	1	0	41	2,6	2	10	5	2	0	0	19	2,4
BC-4-m	0	0	0	0	0	0	0	0,0	5	16	14	4	1	0	40	2,5	1	13	9	4	1	0	28	2,7

Table A-C -3 – Key to grain shape categories. **1** = very angular; **2** = angular; **3** = sub-angular; **4** = sub-rounded; **5** = rounded; **6** = well rounded. **Lvl** = volcanic lithic with lathwork texture, **Lvmi** = volcanic lithic with microlitic texture, **Lvv** = volcanic lithic with vitric texture, **Lvf** = volcanic lithic with felsitic texture, **Pm**: pumice grain; **Plag** = plagioclase, **Py** = pyroxene; **K** = k-feldspar.

	Lvl grains*						Lvl tot	Lvl Mean	Lvmi grains*						Lvmi tot	Lvmi Mean	Lvv grains*						Lvv tot	Lvv Mean	Lvf grains*						Lvf tot	Lvf Mean
Sample	1	2	3	4	5	6	grains	Roundness	1	2	3	4	5	6	grains	Roundness	1	2	3	4	5	6	grains	Roundness	1	2	3	4	5	6	grains	Roundness
PZ-1-m	0	6	25	15	1	0	47	3,2	0	1	22	7	6	1	37	3,6	0	5	10	10	1	1	27	3,4	0	6	17	2	0	0	25	2,8
PZ-2-m	0	19	33	11	0	0	63	2,9	0	9	17	0	0	0	26	2,7	0	24	32	7	0	0	63	2,7	0	0	0	0	0	0	0	0,0
PZ-3-m	0	2	26	4	0	0	32	3,1	0	2	21	4	2	0	29	3,2	0	11	17	11	1	0	40	3,1	0	5	10	0	2	0	17	2,9
PZ-4-m	0	6	30	2	0	2	40	3,1	0	3	18	4	0	0	25	3,0	0	13	33	9	0	0	55	2,9	0	13	18	5	3	0	39	2,9
PZ-5-m	0	22	28	2	3	0	55	2,7	0	11	30	12	0	3	56	3,2	0	13	18	9	5	0	45	3,1	5	22	22	1	3	0	53	2,5
PZ-6-m	0	6	30	13	1	0	50	3,2	0	12	62	10	0	2	86	3,0	0	13	25	17	3	3	61	3,3	0	5	10	2	0	0	17	2,8
PZ-7-m	0	3	12	7	0	0	22	3,2	0	0	1	6	0	0	7	3,9	0	13	12	12	5	0	32	3,6	0	2	5	0	0	0	7	2,7
PZ-8-Vc	0	6	32	63	63	11	175	4,2	0	0	1	2	6	1	10	4,7	0	0	3	3	3	0	9	4,0	0	2	8	20	28	10	68	4,5
PZ-8-C	0	5	48	38	23	0	114	3,7	0	3	26	15	1	0	45	3,3	0	5	8	9	2	0	24	3,3	0	6	16	25	6	2	55	3,7
PZ-8-m	0	8	28	12	2	0	50	3,2	0	2	48	10	1	0	61	3,2	0	9	44	11	1	0	65	3,1	0	8	13	3	0	0	24	2,8
PZ-8-f	0	11	23	7	0	0	41	2,9	0	9	28	17	0	0	54	3,1	0	12	33	6	11	4	66	3,4	0	8	10	7	1	0	26	3,0
PZ-8-Vf	0	0	6	3	0	0	9	3,3	0	0	12	20	0	0	32	3,6	10	58	72	13	4	0	157	2,6	0	6	3	0	0	0	9	2,3
PZ-9-m	0	3	17	1	0	0	21	2,9	0	12	42	8	6	0	68	3,1	0	23	80	36	6	3	148	3,2	0	3	7	3	0	0	13	3,0
PZ-10-m	0	17	37	1	0	0	55	2,7	0	14	28	7	0	0	49	2,9	6	28	35	16	0	0	85	2,7	1	0	2	2	0	0	5	3,0
PZ-11-m	36	13	0	0	39	0	88	2,9	0	24	46	10	1	0	81	2,9	2	16	32	7	1	0	58	2,8	1	4	5	0	0	0	10	2,4
PZ-12-m	0	9	33	2	0	0	44	2,8	0	2	17	5	1	0	25	3,2	0	5	14	1	0	0	20	2,8	0	1	3	0	0	0	4	2,8
PZ-13-m	0	30	42	11	0	0	83	2,8	0	14	44	19	8	0	85	3,2	4	13	26	9	2	0	54	2,9	0	2	9	2	0	0	13	3,0
PZ-14-Vc	0	3	35	24	13	4	79	3,7	0	1	2	1	2	0	6	3,7	0	2	3	6	6	0	17	3,9	0	1	4	2	5	0	12	3,9
PZ-14-C	0	5	48	38	23	0	114	3,7	0	5	38	13	1	1	58	3,2	0	5	21	11	1	1	39	3,3	0	0	5	3	4	0	12	3,9
PZ-14-m	0	20	43	29	2	0	94	3,1	0	12	38	11	0	0	61	3,0	0	24	33	9	0	0	66	2,8	1	6	13	4	2	0	26	3,0
PZ-14-f	0	3	14	3	3	0	23	3,3	0	12	37	12	10	0	71	3,3	0	4	14	12	2	0	32	3,4	0	2	13	4	3	0	22	3,4
PZ-14-Vf	0	1	4	2	0	0	7	3,1	0	1	11	3	0	0	15	3,1	0	4	14	1	3	0	22	2,8	0	1	3	0	0	0	4	2,8
PZ-15-m	0	24	56	13	3	0	96	2,9	0	4	41	12	7	0	64	3,3	0	9	25	10	2	0	46	3,1	0	2	11	4	3	0	20	3,4
PZ-16-m	0	25	51	17	0	0	93	2,9	0	9	37	19	0	0	65	3,2	0	13	20	10	5	0	48	3,1	0	2	5	0	0	0	7	2,7
PZ-17-m	0	8	32	17	0	0	57	3,2	1	12	38	17	5	0	73	3,2	0	18	21	8	0	0	47	2,8	0	9	18	9	3	0	39	3,2
PZ-18-m	0	22	32	14	1	0	69	2,9	0	27	47	29	4	0	107	3,1	0	30	49	25	11	3	118	3,2	0	4	9	6	1	0	20	3,2
PZ-19-m	0	16	42	23	0	0	81	3,1	2	16	31	26	7	0	82	3,2	9	13	21	9	0	0	52	2,6	0	4	9	4	0	0	17	3,0
PZ-20-m	0	13	11	2	0	0	26	2,6	0	5	24	0	0	0	29	2,0	2	32	18	5	2	0	59	2,5	0	1	4	0	0	0	5	2,8
BC-1-Vc	0	10	69	75	38	4	196	3,8	0	2	8	8	0	0	18	3,3	0	4	13	3	3	0	23	3,2	0	1	9	14	8	0	32	3,9
BC-1-C	1	34	59	19	8	0	121	3,0	0	9	11	6	0	0	26	2,9	0	9	12	5	0	0	26	2,8	0	6	13	11	2	0	32	3,28
BC-1-m	16	58	66	15	1	0	156	2,5	1	14	19	10	3	0	47	3,0	2	9	7	4	0	0	22	2,59	0	4	7	3	0	0	14	2,92
BC-1-f	0	3	8	9	1	0	21	3,4	0	3	9	8	3	0	23	3,5	1	7	8	3	1	0	20	2,8	0	0	0	0	0	0	0	0
BC-1-Vf	0	0	2	0	0	0	2	3,0	0	8	9	6	0	0	23	2,9	0	3	2	4	0	0	9	3,1	0	1	3	1	0	0	5	3
BC-2-m	0	19	18	9	0	0	46	2,8	0	8	11	6	1	0	26	3,0	0	0	0	0	0	0	0	0,0	0	1	4	3	1	0	9	3,4
BC-3-m	1	22	34	15	2	0	74	2,9	0	7	14	9	0	0	30	0,0	0	8	5	3	0	0	16	2,7	0	3	4	2	0	0	9	2,9
BC-4-m	1	16	17	10	0	0	44	2,8	0	4	9	3	2	0	18	3,2	0	0	2	3	1	0	6	3,8	1	3	5	2	0	0	11	2,7

Table A-C - 4 – Key to grain shape categories. **1** = very angular; **2** = angular; **3** = sub-angular; **4** = sub-rounded; **5** = rounded; **6** = well rounded. **Lvl** = volcanic lithic with lathwork texture, **Lvmi** = volcanic lithic with microlitic texture, **Lvv** = volcanic lithic with vitric texture, **Lvf** = volcanic lithic with felsitic texture, **Pm**: pumice grain; **Plag** = plagioclase, **Py** = pyroxene; **Ol** = olivine.

	Lss grains*						Lss tot	Lss Mean	Lsc(xx) grains*						Lsc(xx)tot	Lsc(xx) Mean	Lsc(micr) grains*						Lsc(micr) tot	Lsc(micr) Mean
Sample	1	2	3	4	5	6	grains	Roundness	1	2	3	4	5	6	grains	Roundness	1	2	3	4	5	6	grains	Roundness
BC-5-m	0	6	10	7	3	4	30	3,4	0	7	11	9	1	0	28	3,1	0	5	11	8	4	0	30	3,6
Li-1-m	1	20	51	17	2	0	91	3,0	0	1	7	4	0	0	12	3,3	0	0	6	8	2	0	16	3,8
Li-2-m	0	19	38	13	1	0	71	2,9	0	12	17	6	2	0	37	2,9	0	7	12	9	1	0	29	3,1
Li-3-m	2	7	17	12	8	1	47	3,4	0	6	14	2	0	0	22	2,8	1	16	22	11	3	2	55	3,1
Li-4-m	1	8	25	6	1	0	41	3,0	1	2	9	6	1	0	19	3,2	1	4	9	12	4	3	33	3,7
Li-5-m	4	16	25	12	7	3	67	3,2	0	2	7	1	0	0	10	2,9	4	15	25	18	6	3	71	3,2
Li-6-m	0	19	41	6	2	1	69	2,9	0	4	10	4	2	1	21	3,3	0	4	14	4	3	1	26	3,3
Vo-1-m	0	0	0	1	1	0	2	4,5	0	2	5	5	1	0	13	3,4	0	2	8	9	0	0	19	3,4
Vo-2-m	0	0	0	0	0	0	0	0,0	0	0	0	3	0	0	3	4,0	0	0	1	4	1	0	6	4,0
Vo-3-m	0	1	4	12	4	0	21	3,9	0	0	4	13	6	0	23	4,1	0	0	3	16	9	0	28	4,2
Vo-4-m	0	0	6	6	4	2	18	4,1	0	0	2	6	3	0	11	4,1	0	0	2	8	7	0	17	4,3
Vo-5-m	1	2	3	1	0	0	7	2,6	0	2	4	7	5	3	21	4,1	0	0	1	3	2	2	8	4,6
Vo-6-m	0	1	1	0	0	0	2	2,5	0	1	3	1	0	0	5	3,0	0	0	5	10	6	1	22	4,1
Vo-7-m	0	1	4	4	2	3	14	4,1	0	0	3	8	4	0	15	4,1	0	0	6	9	9	2	26	4,3
Vo-8-m	0	1	2	6	3	0	12	3,9	0	0	15	18	6	2	41	3,9	0	1	5	11	17	2	36	4,4
Vo-9-m	0	0	0	0	0	0	0	0,0	0	1	16	34	6	2	59	3,9	0	2	2	15	8	3	30	4,3
Vo-10-m	0	0	3	13	7	1	24	4,3	0	2	11	19	4	1	37	3,8	0	0	1	7	8	4	20	4,8
Vo-11-m	0	8	13	27	16	5	69	4,0	0	1	4	8	1	0	14	3,6	0	0	8	13	7	0	28	4,0

	K grains*						K tot	K Mean	Qzm grains*						Qzm tot	Qzm Mean	Ca grains*						Ca tot	Ca Mean
Sample	1	2	3	4	5	6	grains	Roundness	1	2	3	4	5	6	grains	Roundness	1	2	3	4	5	6	grains	Roundness
BC-5-m	55	5	22	20	7	1	110	2,3	8	12	10	2	0	0	32	2,2	0	2	5	1	0	0	8	2,9
Li-1-m	2	26	25	15	0	0	68	2,8	3	25	21	12	1	0	62	2,7	7	17	13	0	0	0	37	2,2
Li-2-m	0	22	25	5	0	0	52	2,7	0	20	18	10	0	0	48	2,8	12	18	10	2	0	0	42	2,0
Li-3-m	2	17	25	13	0	0	57	2,9	3	16	23	7	4	1	54	2,9	1	15	22	9	1	0	48	2,9
Li-4-m	1	11	19	4	1	0	36	2,8	1	13	23	16	6	0	59	3,2	1	23	22	14	2	0	62	2,9
Li-5-m	2	12	11	4	0	0	29	2,6	1	23	20	9	2	0	55	2,8	1	14	22	14	1	0	52	3,0
Li-6-m	7	26	40	7	0	0	80	2,6	9	15	21	4	1	0	50	2,5	0	12	23	9	1	0	45	3,0
Vo-1-m	0	6	8	4	0	0	18	2,9	5	19	25	9	2	0	60	2,7	0	4	11	8	4	1	28	3,5
Vo-2-m	0	1	6	3	1	0	11	3,4	1	4	8	4	4	0	21	3,3	0	0	9	4	0	0	13	3,3
Vo-3-m	0	12	25	17	4	0	58	3,2	0	22	29	24	3	0	78	3,1	0	1	7	13	11	0	32	4,1
Vo-4-m	5	25	28	11	2	0	71	2,7	4	22	25	8	3	0	62	2,7	0	1	6	13	5	3	28	4,1
Vo-5-m	0	7	7	4	1	0	19	2,9	0	13	25	8	2	1	49	3,0	0	0	7	10	3	1	21	3,9
Vo-6-m	0	2	4	1	0	0	7	2,9	2	10	24	12	1	0	49	3,0	0	0	7	5	0	0	12	3,4
Vo-7-m	0	21	20	12	1	0	54	2,9	2	34	34	21	3	0	94	2,9	0	3	10	15	8	1	37	3,8
Vo-8-m	1	14	16	15	3	0	49	3,1	2	32	43	16	4	0	97	2,9	0	0	2	9	6	0	17	4,2
Vo-9-m	3	18	15	17	0	0	53	2,9	6	36	43	28	4	0	117	2,8	0	0	4	4	2	0	10	3,8
Vo-10-m	2	24	22	18	1	0	67	2,9	5	28	30	15	5	0	83	2,8	0	0	3	9	3	0	15	4,0
Vo-11-m	0	30	27	14	0	0	71	2,8	1	9	29	8	2	0	49	3,0	0	0	3	0	0	0	3	3,0

Table A-C -5 – Key to grain shape categories. 1 = very angular; 2 = angular; 3 = sub-angular; 4 = sub-rounded; 5 = rounded; 6 = well rounded. Lss = siliciclastic sedimentary lithic; Lsc(xx) = crystalline carbonate sedimentary lithic; Lsc(micr) = micritic carbonate sedimentary lithic; Qm: monocrystalline quartz grain; Ca = calcite grain; K = K-feldspar.

	Py grains*						Py tot	Py Mean	K grains*						K tot	K Mean	Plag grains*						Plag tot	Plag Mean
Sample	1	2	3	4	5	6	grains	Roundness	1	2	3	4	5	6	grains	Roundness	1	2	3	4	5	6	grains	Roundness
CO-1-m	0	3	10	2	0	0	15	2,9	2	10	21	11	1	0	45	3,0	1	5	10	3	0	0	19	2,8
MC-1-m	4	13	16	8	0	0	41	2,7	2	10	16	11	0	0	39	2,9	1	13	17	8	3	0	42	3,0
GA-1-m	3	13	19	6	0	0	41	2,7	2	15	19	7	0	0	43	2,7	1	10	17	7	0	0	35	2,9
NA-1-m	0	1	4	4	0	0	9	3,3	1	5	12	6	1	0	25	3,0	0	11	11	6	0	0	28	2,8
NA-2-m	0	11	13	3	0	0	27	2,7	0	6	14	14	0	0	34	3,2	0	14	18	4	2	0	38	2,8
NA-3-m	1	5	9	3	1	0	19	2,9	3	10	16	8	0	0	37	2,8	0	13	22	3	0	0	38	2,7
NA-4-m	0	3	7	6	0	0	16	3,2	0	7	9	6	0	0	22	3,0	0	10	19	11	3	0	43	3,2
NA-5-m	0	24	38	25	9	0	96	3,2	0	11	9	2	0	0	22	2,6	1	13	20	8	0	0	42	2,8
NA-6-m	4	12	19	14	4	0	53	3,0	4	12	19	12	3	1	51	3,0	1	8	15	8	1	0	33	3,0
NA-7-m	0	6	8	3	0	0	17	2,8	0	8	13	4	0	0	25	2,8	0	9	21	9	1	0	40	3,1

Table A-C -6 – Key to grain shape categories. **1** = very angular; **2** = angular; **3** = sub-angular; **4** = sub-rounded; **5** = rounded; **6** = well rounded. **Plag** = plagioclase, **Py** = pyroxene; **K** = k-feldspar.

	Lvl grains*						Lvl tot	Lvl Mean	Lvmi grains*						Lvmi tot	Lvmi Mean	Lvv grains*						Lvv tot	Lvv Mean	Pm grains*						Pm tot	Pm Mean
Sample	1	2	3	4	5	6	grains	Roundness	1	2	3	4	5	6	grains	Roundness	1	2	3	4	5	6	grains	Roundness	1	2	3	4	5	6	grains	Roundness
CO-1-m	0	5	20	9	1	1	36	3,3	0	0	0	0	0	0	0	0,0	7	14	5	1	0	0	27	2,0	0	40	50	17	0	0	107	2,8
MC-1-m	0	2	22	25	7	0	56	3,7	0	0	4	7	10	0	21	4,3	3	7	6	1	0	0	17	2,3	0	9	7	0	0	0	16	2,4
GA-1-m	0	20	48	22	5	1	96	3,2	0	2	4	6	2	0	14	3,6	3	10	4	1	0	0	18	2,2	1	21	25	7	0	0	54	2,7
NA-1-m	0	9	21	19	4	2	55	3,4	0	1	8	20	16	6	51	4,4	5	15	13	9	4	2	48	3,0	6	31	25	15	0	0	77	2,6
NA-2-m	0	8	17	28	12	0	65	3,7	0	0	2	25	25	4	56	4,6	6	30	8	0	0	0	44	2,0	2	22	30	18	0	0	72	2,9
NA-3-m	1	28	34	16	0	0	79	2,8	0	1	9	19	7	0	36	3,9	6	10	7	0	0	0	23	2,0	3	20	15	7	0	0	45	2,6
NA-4-m	0	9	20	15	4	0	48	3,3	0	0	7	10	15	0	32	4,3	6	20	6	0	0	0	32	2,0	1	25	45	30	5	0	106	3,1
NA-5-m	0	4	25	21	6	0	56	3,5	0	0	2	9	14	3	28	4,6	0	12	4	1	0	0	17	2,4	0	12	18	16	1	0	47	3,1
NA-6-m	0	6	24	21	2	0	53	3,4	0	3	7	15	10	4	39	4,1	3	7	7	3	3	0	23	2,8	1	8	8	4	0	0	21	2,7
NA-7-m	45	2	11	27	21	4	110	2,9	0	0	3	16	20	11	50	4,8	6	21	5	0	0	0	32	2,0	4	25	33	20	0	0	82	2,8

	Lvl grains*						Lvl tot	Lvl Mean	Lvmi grains*						Lvmi tot	Lvmi Mean	Lsc(xx) grains*						Lsc(xx)tot	Lsc(xx) Mean	Lsc(micr) grains*						Lsc(micr) tot	Lsc(micr) Mean
Sample	1	2	3	4	5	6	grains	Roundness	1	2	3	4	5	6	grains	Roundness	1	2	3	4	5	6	grains	Roundness	1	2	3	4	5	6	grains	Roundness
CA-1-m	0	2	11	7	1	0	21	3,3	0	0	0	0	0	0	0	0,0	0	7	26	26	9	3	71	3,6	0	6	28	54	26	9	123	4,0
CA-2-m	0	5	13	18	5	0	41	3,6	0	0	0	4	4	0	8	4,5	0	5	27	33	26	8	99	4,1	0	0	7	30	20	7	64	4,4
CA-2B-m	0	2	4	11	6	1	24	4,0	0	0	1	5	7	3	16	4,8	0	10	23	22	9	1	65	3,5	0	2	6	10	20	20	58	4,9
CA-3-m	1	12	33	28	10	2	86	3,5	0	3	12	25	28	6	74	4,3	0	0	3	7	2	0	12	3,9	0	0	8	12	8	5	33	4,3

	Plag grains*						Plag tot	Plag Mean	Py grains*						Py tot	Py Mean	Op grains*						Op tot	Op Mean
Sample	1	2	3	4	5	6	grains	Roundness	1	2	3	4	5	6	grains	Roundness	1	2	3	4	5	6	grains	Roundness
CA-1-m	0	1	2	1	0	0	4	3,0	6	23	41	30	10	0	110	3,1	0	1	2	3	4	0	10	4,0
CA-2-m	0	5	12	5	0	0	22	3,0	2	22	32	19	7	0	82	3,1	0	1	5	4	1	0	11	3,5
CA-2B-m	0	1	4	2	0	0	7	3,1	10	50	45	29	19	3	156	3,0	0	0	2	4	3	3	12	4,5
CA-3-m	0	12	20	17	8	0	57	3,4	0	5	7	0	0	0	12	2,6	0	0	1	6	5	0	12	4,3

	Lvl grains*						Lvl tot	Lvl Mean	Lvmi grains*						Lvmi tot	Lvmi Mean	Lvv grains*						Lvv tot	Lvv Mean
Sample	1	2	3	4	5	6	grains	Roundness	1	2	3	4	5	6	grains	Roundness	1	2	3	4	5	6	grains	Roundness
PO-1-m	2	17	47	43	24	2	135	3,6	2	4	11	21	25	9	72	4,3	3	6	7	3	2	0	21	2,8
PO-2-m	0	4	35	41	11	4	95	3,7	0	0	4	18	11	0	33	4,2	0	8	2	1	0	0	11	2,4
PO-3-m	1	9	35	41	22	2	110	3,7	0	2	15	31	30	10	88	4,4	2	4	9	7	3	2	27	3,4
TG-1-m	0	14	33	33	13	1	94	3,5	0	2	19	25	16	4	66	4,0	1	15	13	1	0	0	30	2,5
TG-2-m	0	10	47	36	6	0	99	3,4	0	0	3	11	13	2	29	4,5	0	4	3	0	0	0	7	2,4
TG-3-m	2	15	34	43	16	5	115	3,6	0	1	14	25	28	14	82	4,5	7	12	8	3	0	0	30	2,2
TA-1-m	0	1	33	44	17	2	97	3,9	0	2	17	29	37	3	88	4,3	2	10	11	15	2	0	40	3,1
TA-2-m	2	7	40	53	14	3	119	3,7	0	1	7	29	38	5	80	4,5	2	13	9	10	4	4	42	3,3
SO-1-m	0	0	5	11	5	1	22	4,1	0	0	0	3	4	2	9	4,9	3	2	0	0	0	0	5	1,5
SO-2-m	0	12	42	42	6	1	103	3,4	0	0	3	12	11	0	26	4,3	0	8	5	2	1	0	16	2,8
SO-3-m	0	5	16	27	6	1	55	3,7	0	0	3	7	9	4	23	4,6	1	11	8	4	1	0	25	2,7
SO-4-m	0	7	23	28	12	1	71	3,7	0	0	8	25	20	0	53	4,2	7	15	12	3	0	0	37	2,3
SO-5-m	1	5	37	40	9	0	92	3,6	0	0	3	11	17	1	32	4,5	2	13	6	0	0	0	21	2,2

	Le grains*						Le tot	Le Mean	Py grains*						Py tot	Py Mean	K grains*						K tot	K Mean	Plag grains*						Plag tot	Plag Mean
Sample	1	2	3	4	5	6	grains	Roundness	1	2	3	4	5	6	grains	Roundness	1	2	3	4	5	6	grains	Roundness	1	2	3	4	5	6	grains	Roundness
PO-1-m	0	0	12	16	8	0	36	3,9	2	13	26	11	0	0	52	2,9	0	3	2	1	0	0	6	2,7	0	4	10	3	0	0	17	2,9
PO-2-m	0	0	1	3	1	0	5	4,0	1	35	61	75	26	4	202	3,5	0	3	1	0	0	0	4	2,3	0	1	4	1	0	0	6	3,0
PO-3-m	0	1	7	9	4	1	22	3,9	1	7	15	13	1	0	37	3,2	0	1	3	3	1	0	8	3,5	1	8	11	8	1	0	29	3,0
TG-1-m	0	2	6	7	7	0	22	3,9	7	27	34	30	11	1	110	3,1	0	8	8	4	0	0	80	2,8	0	6	14	9	1	0	30	3,2
TG-2-m	0	2	10	14	2	0	28	3,6	8	60	54	34	20	4	180	3,1	0	6	6	2	0	0	14	2,7	0	1	3	0	0	0	4	2,8
TG-3-m	0	2	13	8	6	4	33	3,9	0	16	13	7	2	0	38	2,9	0	3	7	4	2	0	16	3,3	0	2	12	4	3	0	21	3,4
TA-1-m	0	0	9	14	8	0	31	4,0	1	7	4	1	0	0	13	2,4	2	9	5	1	0	0	17	2,3	1	5	16	6	2	0	30	3,1
TA-2-m	0	5	21	15	7	4	52	3,7	0	15	30	16	5	0	66	3,2	0	2	1	1	0	0	4	2,8	0	4	13	3	0	0	20	3,0
SO-1-m	0	0	4	8	3	1	16	4,1	1	25	46	56	23	0	151	3,5	0	2	10	5	0	0	17	3,2	0	2	11	11	2	0	26	3,5
SO-2-m	0	2	8	13	5	1	29	3,8	2	5	11	15	1	0	34	3,2	0	5	14	8	2	0	29	3,2	0	10	16	12	0	0	38	3,1
SO-3-m	0	0	0	2	0	1	3	4,7	0	11	35	38	15	7	106	3,7	1	13	20	17	2	0	53	3,1	0	10	19	18	3	0	50	3,3
SO-4-m	0	3	6	10	2	0	21	3,5	0	9	12	8	1	0	30	3,,0	0	7	14	10	2	0	33	3,2	0	3	7	5	1	0	16	3,3
SO-5-m	0	0	5	11	6	0	22	4,0	4	26	31	27	7	0	95	3,1	0	6	14	5	0	0	25	3,0	1	6	7	3	1	0	18	2,8

	Lvl grains*						Lvl tot	Lvl Mean	Lvmi grains*						Lvmi tot	Lvmi Mean	Lvv grains*						Lvv tot	Lvv Mean
Sample	1	2	3	4	5	6	grains	Roundness	1	2	3	4	5	6	grains	Roundness	1	2	3	4	5	6	grains	Roundness
VE-1-m	5	36	77	29	3	1	151	2,9	2	3	20	29	5	1	60	3,6	31	39	20	6	3	0	99	2,1
VE-2-m	12	37	71	16	4	1	141	2,8	2	7	30	33	4	1	77	3,4	20	35	12	5	3	0	75	2,1
VE-3-m	12	22	45	17	5	0	101	2,8	4	8	15	20	10	0	57	3,4	15	20	15	6	2	0	58	2,3

	Le grains*						Le tot	Le Mean	Ol grains*						Ol tot	Ol Mean	Py grains*						Py tot	Py Mean
Sample	1	2	3	4	5	6	grains	Roundness	1	2	3	4	5	6	grains	Roundness	1	2	3	4	5	6	grains	Roundness
VE-1-m	1	5	18	16	2	0	42	3,3	0	0	1	2	0	0	3	3,7	2	19	18	4	0	0	43	2,6
VE-2-m	0	4	14	20	4	1	43	3,6	0	1	3	3	1	0	8	3,5	3	13	19	5	1	0	41	2,7
VE-3-m	4	15	20	26	8	0	73	3,3	0	2	3	3	0	0	8	3,1	4	7	13	5	1	0	30	2,7

Table A-C – 7 – Key to grain shape categories. **1** = very angular; **2** = angular; **3** = sub-angular; **4** = sub-rounded; **5** = rounded; **6** = well rounded. **Lvl** = volcanic lithic with lathwork texture, **Lvmi** = volcanic lithic with microlitic texture, **Lvv** = volcanic lithic with vitric texture, **Lvf** = volcanic lithic with felsitic texture, **Pm**: pumice grain; **Plag** = plagioclase, **Py** = pyroxene; **K** = k-feldspar. **Le** = leucite.